> Rockfall and protection forests – models, experiments and reality

Habilitationsschrift von Dr. Lucas Karel Agnes (Luuk) Dorren

Bundesamt für Umwelt BAFU
Abt. Gefahrenprävention, Sektion Rutschungen Lawinen und Schutzwald
Bern, Schweiz

Universität für Bodenkultur
Wien, Österreich



November 2008

im wissenschaftlichen Fach:

Alpine Naturgefahren und Schutzwaldbewirtschaftung
(Mountain risk engineering and protection forest management)

The work presented in this habilitation is the fruit of working with, sharing with, and living with many people. I would like to thank all those who contributed in one way or another. Special thanks go to: Frédéric Berger and his family, Bernhard Maier, Ger Bergkamp, Joris de Vente, Karl Kleemayr, Philippe Cozic, Pascal Tardif, Eric Mermin, Uif Putters, André Wehrli, Harry Seijmonsbergen, Anton Imeson, Markus Stoffel, Roderick Kühne, Franck Bourrier, Jean-Baptiste Moulin, Michel Jaboyedoff, Peter Brang, Manfred Lexer, Hubert Hasenauer, Xavier Gauquelin, Roland Métral, Caterina Allegra, Gerard Heuvelink, Axel Volkwein, Raphael Schwitter, Barbara Polanšek, Mitja Skudnik, Alexia Stokes, Thierry Fourcaud, Michael Mölk, Simone Perret, Hans Kienholz, Kaspar Zürcher, Jean-Jacques Thormann, Federico Agliardi, Thomas Lerch, Markus Wick, Hubert Malin, Iris Voyat, Alain Soutrenon, Sanneke van Asselen, Christopher Dich, Mark van Wijk, Renzo Motta, Arthur Sandri, Bernard Loup, Marc Hanewinkel, Roderich von Detten, Jean-Louis Gay, Jacques Fay, Claude Lebahy, Jerôme Liévois, Oliver Jancke, Christophe Bigot, Cas Dorren, Youp Dorren and not to forget, my love Claske Dijkema.

> Content

Chapter		Page
1.	Framework of this habilitation	3
2.	Schutzwaldmanagement in den Alpen	23
3.	A review of rockfall mechanics and modelling approaches	39
4.	Comparison of three rockfall models at a regional scale	59
5.	Field assessment and modeling of rockfall in a protection forest	77
6.	On the accuracy of the 3D rockfall model RockyFor	95
7.	Full scale rockfall experiments	111
8.	Energy dissipation by trees during rockfall impacts	125
9.	Comparing experimental and simulated results	135
10.	Evaluating Swiss rockfall protection forests using RockyFor	145
11.	Principles of a simple rockfall – forest assessment tool	157
12.	State of the art in rockfall – forest interactions	167
13.	Laser scanning for characterising mountain forests	183
Other publications		203
Summary / Zusammenfassung / Résumé / Samenvatting		289
Publication list		297
Lebenslauf (German C.V. of Luuk Dorren)		307

> Chapter 1

Framework of this habilitation



> Rockfall and protection forests – models, experiments and reality

Introduction

Natural hazards, especially floods and rapid mass movements such as avalanches, rockfall and landslides, form an inherent part of living in mountainous areas like the Alps (e.g., BUWAL 1999; Rudolf-Miklau et al. 2006; Bezzola and Hegg 2007). Their impact on Alpine livelihoods can, however, be disastrous. Therefore, prevention of those hazards is an important issue in Alpine countries. A large part of hazard prevention is done firstly by using hazard zone maps (e.g, Rickli and Banzer 1996; Hubert 2003; Loat 2006; Rudolf-Miklau et al. 2007) and consequent building restrictions, and secondly by protective measures. In the alpine countries, a wide range of protective measures can be identified, varying from forests to many different civil engineering structures. If the willingness exists to make use, as much as possible, of the potential of mountain forests to protect against natural hazards in hazard prevention, it is critical to be able to quantify the protective function of a forest stand (cf. Fitze 2005). This is because, firstly, it has to be decided which forests require silvicultural interventions to prevent a degradation of the forests partly due to the consequences of the natural hazard the forest should protect against. Due to the natural evolution of forest stands, the protective capacity against natural hazards of a forest changes over time (Mayer and Ott 1976; Brang 2001; Dorren et al. 2004). Systematic and well-planned silvicultural interventions can prevent being overtaken by events and therefore constantly treating the urgent cases only. Secondly, it allows identifying required investments in natural hazard protection and the required intervention: forest engineering, civil engineering, or a mix of those. Thirdly, a quantification of the protective potential of a forest stand help to targets additional, detailed site investigations on a local natural hazard.

In my research, I focused on protection forests and natural hazards, being mainly rockfall, but also avalanches and landslides. The large goal of the last 10 years of research has been to develop methods and tools for calculating the rockfall hazard at a given site taking into account the protective effect of forests. Having the capability to include the effect of forests, these tools allow quantifying the protective function of a forest stand against rockfall. This work, which is reflected by the articles presented in this habilitation, is a combination of field observations, simulation models and rockfall experiments. In general, two general approaches can be identified. The first one is a rockfall-based approach, meaning that the method of analysis focuses on the rockfall process, and the mechanisms behind it, where the forest is considered as a process constraint in

the sense that the rockfall hazard is reduced. The second approach is a forest-based approach, which means that the method of analysis focuses on forest characteristics and translates those either into a quantitative energy dissipative capacity or into a more general, qualitative, protective capacity.

The wider context

In the French Alps it is told that, in the 14th century, one risked a punishment, varying from having his hands being cut off to the death penalty, if cutting a tree in a protection forest upslope from an alpine village in the Savoy. Fortunately, the death penalty never has been sentenced for this offence, but the example shows that the protection against natural hazards provided by mountain forests has been recognised since centuries. These days, many Alpine livelihoods heavily rely on mountain forests for protection against hazards such as rockfall, snow avalanches, floods and shallow landslides (cf. Lebensministerium 2008). This is also stated in the first paragraph of the Mountain Forest Protocol of the Alpine Convention, which mentions that mountain forests provide the most effective, the least expensive and the most aesthetic protection against natural hazards. Switzerland, for example, invested the last 5 years on average 65 million Euros yearly to maintain or improve the protection provided by mountain forests (Sandri 2008).

Traditionally, mountain forests have been exploited intensively for their timber and non-timber products, with the exception of forests on slopes above residential areas where natural hazards, mostly snow avalanches and rockfall, have been active. The latter type of forests were often put under a logging ban (*Bannwald* in German, or *forêt mise à ban* in French), which means that the forest was classified as a reserved forest where tree felling was only allowed under strict, locally defined rules.

At present, mostly the term protection forest (*Schutzwald* in German, *forêt de protection* in French, *forêt protectrice* in Swiss-French and *foreste/bosco di protezione* in Italian) is being used, which are forests that particularly provide a protective function for objects of value (Schönenberger 2000). This function implies that people, buildings, and infrastructure (the so-called damage potential) are directly protected against the impact of natural hazards such as snow avalanches and rockfall (Brang 2001). At the same time, those forests provide a site-protective function, which is actually a prerequisite for the direct protective function. Site-protection is important, since a forest stand

needs to protect its site against processes such as excessive soil erosion. If the site-protective function is impaired, the forest site erodes, resulting in a loss of the forest ecosystem as a whole (Dorren et al. 2004).

With the diversification of Alpine economies, which have evolved from agricultural to tourism-based economies, the population densities and the economic value of the main alpine valleys have increased significantly since the sixties. Consequently, the risk related to natural hazards increased and hazard prevention / mitigation therefore gained importance. During this process, great trust has been put into technical protective works (e.g. engineered structures), partly due to the residual risk of protection forests and partly to the lack of quantitative data on the efficacy of protection forests. In that sense, forests became, and still are, subordinate to technical structures in the field of mountain risk engineering. This accounts especially for France, but also, although to a lesser extent, for Switzerland and Austria, where investments per ha protection forest are significantly higher. This "secondary" role of protection forests is despite the recognition of their protective function in the practice (both hazard and forest management), as well as in scientific literature (e.g., Kautz 1912; Moor 1954; Mayer and Ott 1976, Kienholz and Mani 1994).

Forest practitioners and researchers are still in the process of refining the definition of optimal characteristics of protection forests. Scientific evidence is limited due to the slow reaction of mountain forests in comparison to the rapid environmental and socio-economic changes that have occurred in the Alps during the last century. Nevertheless, there has been considerable progress in research on mountain forests and their protective effect (see for example Couvreur 1982; Ott and Schönbächler 1986; Berger and Renaud 1994; Gsteiger 1993; Motta and Haudemand 2000; Bebi et al. 2001; Margreth 2004; Brauner et al. 2005; Dorren et al. 2005; Amman 2006; Brang et al. 2006; Dorren and Berger 2006; Kalberer 2006; Berger and Dorren 2007; Dorren et al. 2007; Woltjer et al. 2008). In parallel, practitioners have gained enormous experience by managing and observing protection forests, but also by setting up (inter-)national networks (e.g., Ziegner 2006; Gauquelin et al. 2008), in which monitoring sites on the effects of silvicultural operations have been installed. Mutual exchange between science and practice has led to the development of very detailed management recommendations and guidelines for protection forests (Wasser and Frehner 1996; Frehner et al. 2005; Gauquelin et al. 2005; Beretti et al. 2006).

The knowledge and tools obtained from research during the last decades have now enabled a quantitative assessment of how different mountain forests perform their protective function.

This allows searching for effective and cost-efficient solutions for natural risk prevention using forest management/engineering (eco-engineering), civil engineering, or a mix of both (cf. Holub and Hübl 2008). For example, the last five years, the Swiss state invests yearly, on average, 153 million Euros in protection against rapid mass movements (snow avalanches, rockfall, debris flows and landslides). From this total sum, 42% is invested in protection forests and 58% in the construction and maintenance of technical (civil engineering) protective structures (Sandri 2008). Knowing that investment costs per ha in protection forests are up to 15 times cheaper than those of technical protective structures, it is clear that their protective effects are relevant for much larger areas throughout Switzerland compared to those of technical structures. The Austrian project ISDW (Initiative Schutz durch Wald, cf. Perzl and Kleemayr 2007; Schima et al. 2008) is another good example of making optimal use of the protective role of forests in hazard prevention and management. I believe that research, which focuses on both protection forests and natural hazards, similar to the studies presented in this habilitation, can contribute to finding solutions that incorporate the protective effect of forests where the potential is available, which are cost-efficient, though effective.

> Chapters in this habilitation

Protection forest management in the Alps

The following chapter (Chapter 2) gives a general introduction in protection forests in the Alps. It shows that many Alpine forests protect residential areas and infrastructures from natural hazards and how knowledge on these forests and their protective capacity increases continuously. In the Alps, there are currently several projects being conducted which aim to harmonise methods for assessing the natural hazard potential, the damage potential and resulting classifications of protection forests. It is the objective to develop funding schemes so as to invest in protection forests where needed in order to prevent damage from natural hazards in a cost efficient manner. The article concludes that, currently, there is a need for improving 1) protection forest monitoring using advanced technology, such as laser scanning, 2) linking inventory data from different sources, 3) simulation models that allow estimating the long-term benefits of measures in protection forests, and 4) transnational collaboration. The article has been written by a European group of authors who decided to publish an overview of different facets of protection forest management at the International workshop 'Protection forests: science and practice', organised by myself and Frédéric Berger in 2005 in Vaujany, France. The article is not a

pure scientific review, but presents general viewpoints on protection forests of applied forest research institutes, as well as governmental and management organisations. André Wehrli kindly took up the role as lead author.

A review of rockfall mechanics and modelling approaches

Chapter 3 subsequently introduces the subject of rockfall by presenting a review of literature, which has been published until the year 2001, on the rockfall process and rockfall modelling approaches. The objective of the review was to investigate if models could be useful tools to assess the risk posed by rockfall throughout relatively large mountainous areas (>500 km^2) for improving protection of endangered residential areas and infrastructure. Therefore the article summarises rockfall models that existed at the time and proposes modifications to make them suitable for predicting rockfall at a regional scale. In this chapter, firstly, the basic mechanics of rockfall are summarized, including knowledge of the main modes of motion: falling, bouncing and rolling. Secondly, existing models are divided in three groups: (1) empirical or statistical models, (2) process-based models and (3) Geographical Information System (GIS) based models. For each model type the basic principles and its ability to predict rockfall runout zones are summarised. The final part discusses how a model for predicting rockfall runout zones at a regional scale could be developed. A GIS-based distributed model is suggested, which combines a detailed process-based model and a GIS. Potential rockfall source areas and trajectories are calculated by the GIS component of the model and the rockfall runout zones are calculated by the process-based component. In addition to such a model, methods for the estimation of model parameter values at a regional scale have to be developed

Comparison of three rockfall models at a regional scale

The study presented in Chapter four builds further on the review of chapter 3 and evaluates the capacity of two GIS-based models and a spatially distributed, process-based model called Rocky3, developed by myself. Site-specific information about the level of protection that mountain forests provide is often not available for large regions. Information regarding rockfall is especially scarce. The most efficient way to obtain information about rockfall activity and the efficacy of protection forests at a regional scale is to use a simulation model. At the time of the study, which was carried out in 2000, forest parameters were rarely incorporated in such models. Therefore, the purpose of this study was to test and evaluate a model for rockfall assessment at a regional

scale in which simple forest stand parameters, such as the number of trees per hectare and the diameter at breast height, are incorporated. Therefore, the newly developed model Rocky3 was compared with two existing rockfall models. The developed model is the only model that calculates the rockfall velocity on the basis of energy loss due to collisions with trees and rebounds on the soil surface. The two existing models calculate energy loss due to a frictional force applied to the distance between two cell centres. This force is dependent on the land cover and/or slope characteristics. Rocky3 calculates multiple rebounds within a raster cell. The patterns of rockfall runout zones produced by the three models are compared with patterns of rockfall deposits derived from geomorphological field maps. Furthermore, the rockfall velocities modelled by the three models are compared. It is found that the models produced rockfall runout zone maps with rather similar accuracies, if considered for the whole study region. However, the developed model performs best on forested slopes and it also produces velocities that match best with field estimates on both forested and non-forested slopes irrespective of the slope gradient.

Field assessment and modelling of rockfall at the scale of a protection forest

To study the effect of the forest parameters and the slope characteristics on the rockfall process more in detail, we applied a combined approach in Chapter 5, using field techniques and a new simulation model called RockyFor. The main goal was to assess the determining factors for rockfall source areas, rockfall tracks and rockfall runout zones on a forested slope in mountainous terrain. This main goal was translated into three specific objectives. The first one was to understand why rockfall occurs in the study area. The second one was to translate the knowledge obtained in the field into model algorithms to obtain more realistic simulations of rockfall dynamics on a forested slope as compared to the Rocky3 model in Chapter 4. The third objective was to assess which slope characteristics primarily determine the distribution of active rockfall tracks. To achieve these objectives, we measured the major discontinuity planes in the bedrock that are exposed in the rockfall source areas and we made a geomorphological map of the whole study area. Furthermore, a test site for simulation modelling within the larger study area was defined in which both a forest and a slope inventory were carried out. The available data and the developed rockfall simulation model RockyFor allowed us to assess the slope characteristics that mainly determine the distribution of zones affected by rockfall. We found that, in decreasing order of importance, both standing and felled trees, the surface roughness and rockfall resistant shrubs primarily determine the distribution of rockfall-affected zones in the test site. Simulation tests without a forest cover produced similar rockfall runout zones as fossil

rockfall events identified in the field. We believe that the combined field and modelling approach is a prerequisite for understanding how forests can protect against rockfall.

On the accuracy of the 3D rockfall model RockyFor

To go back to a regional scale, we investigated in Chapter 6 whether the new version of Rockyfor, which was further developed for rockfall assessment at slope scale and therefore using input data with a support (defined as the largest area treated as homogenous such that an average value of the property of interest is known but not the variation within; in a raster dataset this equals the raster resolution or the cell size) of 2.5m × 2.5m, could be used for rockfall assessment at the regional scale, using input data with a support of 25m × 25m (thus of poorer quality). We anticipated that in the latter case the model error would increase. A definition of support is the largest area treated as homogenous such that an average value of the property of interest is known but not the variation within. For raster data it often corresponds to the resolution or cell size. Three types of simulations were applied to the same model and the outcomes were validated with field data. The first simulation used input data with a support of 2.5m × 2.5m and aggregated the output to a support of 25m × 25m. The second simulation used the same input data as in the first simulation, but these data were aggregated to a support of 25m × 25m before running the model. The third simulation used input data of poorer quality obtained at a support of 25m × 25m. The results show that simulating the maximum extent of rockfall runout zones with a distributed model using data with a support of 25m × 25m is realistic and feasible. This is also true for data with poorer quality as the third simulation resulted in a slightly larger mean squared error than the first simulation. Surprisingly it also gave a smaller error than the second simulation. We investigated the cause of the large error produced by the second simulation and concluded that this was mainly caused by the combination of a high-quality digital elevation model and the loss of spatial structure in the input data due to spatial aggregation.

Full scale rockfall experiments

The last chapters showed us that rockfall modelling, taking into account the effect of trees, seems to work, based on terrain observations of rockfall deposits. What was missing were data from real rockfall events. Simultaneously, there was, and still is, also a lack of experimentally gained, quantitative data (runout distances, energies, rebound heights) on full scale or real size rockfall events both on forested and non-forested slopes. Therefore, the first objective of the study

presented in Chapter 7 was to carry out real size rockfall experiments and quantify the velocities, rebound heights as well as the residual hazard of rockfall on a forested and a non-forested slope. The second objective was to evaluate existing rockfall protection forest management guidelines, as well as the underlying criteria. We carried out and analysed 100 real size rockfall experiments at a non-forested site (Site 1) and 102 identical experiments at a forested site (Site 2) on the same slope. We compared the obtained results with literature data on rockfall protection forests. At the non-forested site, results show that the mean maximum velocity is 15.4 m s^{-1}, compared to 11.7 m s^{-1} at the forested site. The maximum rebound height decreases from 8 m (Site 1) to 2 m (Site 2) and the number of rocks that surpass the 223.5 m slope distance decreases from 95 out of 100 (Site 1) to 35 out of 102 (Site 2). A major effect of rockfall on a forested slope is the development of a treeless rockfall path or *couloir*, which had evolved after releasing 78 rocks at Site 2. The effect of such a *couloir* can be mitigated by cutting trees on both sides into the *couloir* and leaving the trunks on the slope, diagonally to the slope direction. This is a known and effective technique to reduce the effect of gaps in protection forests. During our experiments, none of the rocks attained their maximal velocity within the first 40 m. They did, however, attain destructive velocities (11 – 15 m s^{-1}) within that distance. We propose a maximum gap size in the slope direction of 1.3 times the mean tree height, with a maximum of 40 m, to have sufficient light in created regeneration gaps. Further, we present various findings that have direct implications for the management of rockfall protection forests. Finally, the results proved that forests can provide effective protection against rockfall.

Energy dissipation by trees during rockfall impacts

Another important step in the development of a rockfall model that accounts for the effects of trees, apart from good validation data, was the description of the capacity of individual trees to dissipate the energy imposed by rockfall. At the time of our real size rockfall experiments, some data was available from static tree-pulling tests or from dynamic impact tests on wood samples. We anticipated that these data were not representative for the maximum amount of energy that can be dissipated by living trees at rockfall impacts. Therefore, we used the results from the real size rockfall experiments on a forested slope in the French Alps to come up with a function that describes the capacity of individual trees to dissipate the energy of rockfall impacts. Such impacts against trees were captured on digital films, and allowed calculating the energies of falling rocks before and after the impact. Nine impacts that caused an instantaneous breakage of *Abies alba* Mill. trees could be analysed in detail using the film recordings. We obtained an exponential

relationship between the stem diameter at breast height (DBH) of *Abies alba* trees and the maximum amount of energy they can dissipate, which highly correlates with our experimental data. We transferred this relationship to other tree species by using literature data on fracture energies. The obtained relationships for *Cedrus spp.*, *Fagus sylvatica* L. and *Picea abies* (L.) Karst. significantly correlated with data from other dynamic impact tests in the field and maximum bending moments obtained with tree-pulling experiments. Finally, multiple linear regressions on our experimental data revealed that the impact height influences the energy that will be dissipated by an *Abies alba* tree, especially for trees with a DBH up to 15 cm. However, for trees with a larger DBH the data suggested hat the effect is minimal for impact heights ranging from 50 – 100 cm. We expect that the energy dissipation decreases with increasing impact height on the tree stem, but our results did not allow the development of accurate energy dissipation versus height function. We found a strong relationship between the amount of energy that is dissipated by a tree and the horizontal distance between the impact centre and the vertical central tree axis.

Comparing experimental and simulated results

Having implements the developed energy dissipation function for trees, it was time to compare the simulation results of the RockyFor model with the data obtained from the real size rockfall experiments. In addition, the objective of the study presented in Chapter 9 was to improve the generic rockfall simulation model RockyFor, by developing a clear method for quantifying and modelling slope surface characteristics based on the quantitative field data. On the basis of a polygon map representing different diameter classes of the material covering the slope, we determine the mean obstacle height (MOH) for each homogeneous unit at the experimental sites. We proposed an algorithm for calculating the tangential coefficient of restitution using the MOH. Comparing the simulated and observed data from the real-size rockfall experiments showed that the 3D combined deterministic - probabilistic rockfall simulation model RockyFor accurately predicted rockfall events on a non-forested (Root Mean Square Error = 17%) and a forested site (Root Mean Square Error = 12%). We conclude that for further improvement of rockfall-forest simulation on different slope types more quantitative data is required on (1) the energy dissipative capacity of shrubs and bushes (e.g., in coppice stands), (2) the effect of the slope material, (3) the rock shape as well as the rock size, and (4) the tangential and normal coefficient of restitution. Based on the presented results we can state that the RockyFor model could contribute to better taking into account the mitigating effect of the existing forest cover when planning protective measures.

Evaluating Swiss rockfall protection forests using RockyFor

Chapter 10 presents three additional tests with the improved RockyFor model. We compared the simulation results with empirical data on tree impacts from three different mountain forests in Switzerland. Even though we used model input data with different resolutions at the study sites, RockyFor accurately predicted the spatial distribution of trajectory frequencies at all sites. In contrast, RockyFor underestimated mean impact heights observed on trees at the two sites where high- and medium-resolution input data were available and overestimated them at the site where input data with the lowest resolution data were used. By comparing the results of the simulation scenarios "current forest cover" and "non-forested slope", we assessed the protective effect of the current stands at all three sites. The number of rocks reaching the bottom parts of the study sites would, on average, almost triple if the "current forest cover" were absent. We therefore conclude that RockyFor is able to predict the spatial distribution of rockfall trajectories on forested slopes accurately, based on input data with a resolution of at least 5 m × 5 m. With the increasing availability of high-resolution data, it provides a useful tool for assessing the protective effect of mountain forests against rockfall.

Principles of a simple rockfall – forest assessment tool

In parallel to the development of the RockyFor model, Frédéric Berger (Cemagref Grenoble) and myself worked a long time on a tool that determines the optimal density and mean DBH of a rockfall protection forest, taking into account given forest and site characteristics, as well as the size and energy of the falling rock, and which quantifies the protective capacity of the given forest in parallel. At the time of development, clear rules for doing the above did not exist. The tool was baptised Rockfor^{NET} (www.rockfor.net). Chapter 11 explains the underlying principles as well as the calculation methods used. In addition, it presents case studies that served for validation. Additional conditions, mainly given by foresters working in the daily practice of protection forest management, were that the tool allows an easy and rapid assessment. This implies the calculation of the protective capacity of a forest stand using a small dataset, formalised in a user-friendly tool. The input data should give a global representation of reality and should be easy to acquire, for example, at the scale of the slope or the forest stand.

State of the art in rockfall – forest interactions

After 10 years of research on rockfall and forest, it was again time to make a balance of the unknowns and knowns in this field. Therefore, together with a group of colleagues who all work on rockfall from a different angle, a review was written to set the state of the art. The specific objective of this Chapter was to give an overview of the current scientific knowledge and methods that are applied by practitioners who deal with rockfall and forests protecting against it. Efficient ways to derive information on the probable magnitude and frequency of future rockfall events from the source and deposit area are described. Subsequently, the scientific knowledge on the energy absorption capacity of single trees and the presently available knowledge on the protective function of forests stand against rockfall is presented. Then easy-to-use tools and simulation models for rockfall hazard assessment on forested slopes are described. Finally, this paper identifies the most important challenges to be tackled in the field of integrated rockfall-forest research.

Laser scanning for characterising mountain forests

Chapter 13 takes up one of the research challenges mentioned in the previous review. Since not only the description of slope characteristics influences the outcomes of rockfall-forest simulation models, the representation of forest characteristics needs to be as precise as possible, given the scale of analysis. Before the availability of methods for retrieving forest structural data from LiDAR (Light Detection And Ranging, or laserscanning) this meant precisely digitising high resolution orhophotos, combined with a detailed forest inventory in the study area. If such orthophotos were not available, it was also required to make a forest stand type map. All this is labour-intensive. LiDAR (Light Detection And Ranging) offers new, labour-extensive ways for describing forest structure in 3D. However, mountain forest structures are complex and creative methods are therefore needed to extract reliable structural information from LiDAR. The objective of this study was to investigate if the application of landscape metrics to a normalised canopy model (nCM) allows an automatic characterisation of forest structure. We used a generic automated approach that created height class patches based on a segmented nCM. Two multi-resolution segmentations were carried out: level 1 objects represented tree crowns and collectives of tree crowns, level 2 objects represented forest stands. Level 1 objects were classified into four height classes and subsequently overlaid with level 2 stands in order to calculate the metrics 1) canopy density and vertical layering of the forest, 2) forest gap distribution and 3) canopy

roughness using the Division Index (DIVI). Canopy density values of each height class allowed the classification of the vertical layering. Distinguishing between single- and multi-layered stands, 82% of all the sample plots were correctly classified. The DIVI calculated on gaps proved to be sufficient to describe the spatial arrangement of patches and distinguish between stands with many small gaps from stands with only a few but larger gaps. Canopy roughness could not satisfactorily be described using the DIVI based on the validation plots. With the approach presented, the structure of forest stands can be assessed quite easy.

Other publications

The chapter 'Other publications' presents a selection of articles that describe different types of research in rockfall or in mountain forests and give an additional background in the subject. These articles, however, were not considered the 'core' of this habilitation.

> Conclusions from 10 years research

It is, to some extent, redundant to write an extensive scientific conclusion on what has been achieved in this field of research and what still needs to be done, as this has been done in chapter 12. However, a major conclusion from the work presented in this habilitation, is that mountain forests play a very important role in protection against rockfall. In my opinion, their protective effect should therefore be taken into account in all rockfall hazard analyses that are being carried out on forested slopes. Another personal conclusion, which becomes less apparent after reading the scientific papers, is that the exchange with practitioners in the field has been vital for my work. Firstly, it allowed defining the gaps in knowledge and the accompanying research questions. Secondly, it allowed testing developed theories and research findings.

In the following part of this chapter, I wrote down general conclusive remarks, also on topics that have not been highlighted as much in the included papers. When I started working on rockfall, I searched for general information on the rockfall process, especially regarding the modes of motion on different slope gradients. The best generalising figure on this subject was published by Ritchie (1963), shown in chapter 3. However, the mean slope gradient values shown in this figure are rather optimistic in the sense that bouncing occurs on slopes that are much less steep than 45° and falling / flying of rocks also occurs on slopes less steep than 70°. Based on the observations I made in the field and during the full scale rockfall experiments, as well as on

the basis of data from Jahn (1988) and Gerber (1992, 1998), I would like to propose a relationship between the modes of motion of falling rocks and the mean slope gradient as presented in Figure 1. One of my goals the coming years is to complete this figure with field data.

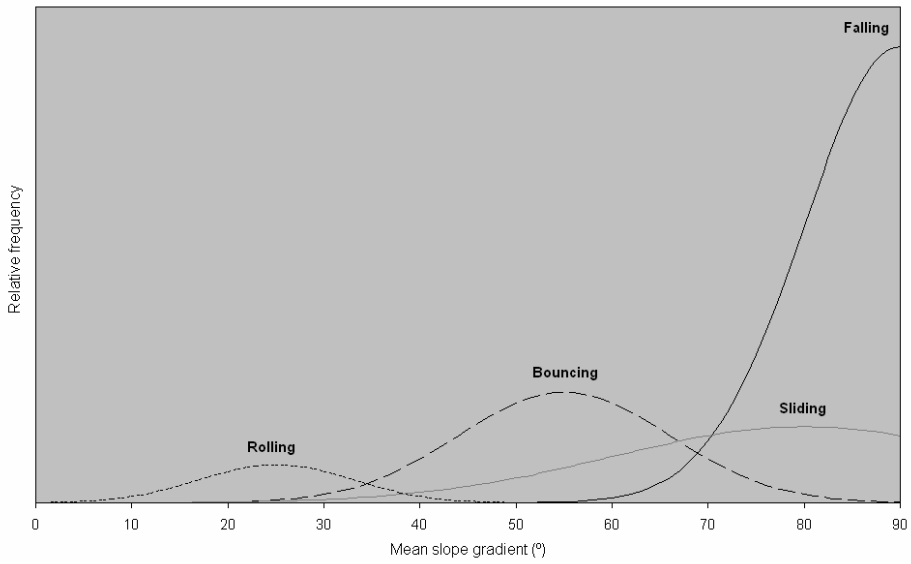


Fig. 1. Proposed relationship between the main modes of motion of falling rocks and the mean slope gradient.

With regards to rockfall simulation models, I considered two aspects very important. The first one is the realistic integration of trees in 3D models. The full scale experiments allowed developing a realistic and practical relationship between the tree diameter and the energy dissipative capacity for different tree species. The work of Jonsson (2008) and his colleagues in the WSL team confirmed the range of energy values that can be absorbed by trees and presented moreover the effect of the height of the rockfall impact on the tree stem on the energy absorption. These relationships, which all have been, or will be, published in Tree Physiology (e.g., Dorren and Berger 2005, Lundström et al. 2008), enabled a realistic integration of trees as rockfall obstacles in simulation models.

The second aspect is the development of a representative and useful algorithm that calculates the rebound of a falling rock. Here, useful is meant as an algorithm that allows for a repeatable and reproducible estimation of the required parameters in the field. Carrying out and observing the full scale rockfall experiments has been very helpful for the development of the algorithm presented in chapter 9. But still, more work has to be done and personally I suppose that different stochastic algorithms for different soil types based on data from real size and half-scale experiments might bring a solution (cf. Bourrier et al. 2008). Nevertheless, it is already satisfying

to see that the current generation of 3D models, which take into account the effect of forests, are already capable of predicting rockfall runout zones, energies and passing heights on forested and non forested slopes within an error range of -15% to +15% (Guzetti et al 2002; Agliardi and Crosta 2004; Rammer et al. 2007; cf. Berger and Dorren, 2006).

A lot of progress has been made in the detail of silvicultural guidelines for rockfall protection forests (e.g., Frehner et al. 2005, Gauquelin et al. 2006, Berreti et al. 2006), which is the fruit of a close cooperation between scientists and practitioners (e.g., as in the GWG – Schweizerische Gebirgswaldpflege-Gruppe or between the French research institute Cemagref and the Office National des Forêts). What is still needed is a better definition of the maximal gap length measured in the steepest downslope direction in such forests, in relation to the mean slope gradient. Currently, most guidelines mention one single maximum gap length, whereas a gap length on a flatter slope probably can be larger than the one on a steep slope, without increasing the rockfall risk below the forested slope. These gap lengths currently restrict fellings using cable cranes in rockfall protection forests. In this context, it should be investigated to what extent, and for which time period, high tree stumps and diagonally lying trees can compensate larger openings in these forests.

The study presented in the last chapter shows that forest structure types can be automatically retrieved from LiDAR data. In addition, many studies showed that recognition of individual tree crowns of dominant and co-dominant trees is very well possible using such data (Persson et al. 2002; Koch et al. 2006; Solberg et al. 2006). Combining automatic forest structure type determination and single tree mapping using LiDAR data with inventory data allows for excellent protection forest assessments. For local natural hazard assessments, which include the protective effect of forests, a detailed inventory could be carried out by collecting data in a representative inventory point in each automatically derived forest structure type. With these data, a DBH - tree height relationship can be established, which serves for attributing DBH values to LiDAR retrieved tree point data (x, y, tree height). The combinations of the field assessed stand densities, tree heights and DBH distributions allow validating the LiDAR based tree points and forest structure types. One can subsequently decide if these tree points are directly fed into the model, or that the model generates single trees, based on the LiDAR based forest structure types and the DBH data from the field inventory. The main advantage of LiDAR based data, which is having a precise spatial definition of forested and non-forested patches, as well as rockfall couloirs that are extremely important for the protective function, remains.

It is my intention to further investigate the use of LiDAR data, and similar high resolution terrain and canopy data, for integrated rockfall - forest studies. In addition, I hope to continue tackling the future challenges in rockfall forest research listed in the final part of chapter 12 using the combination of developing the 3D rockfall model (presently called Rockyfor3D) based on field observations, conducting rockfall experiments and analysing rockfall events in the field. Looking back at 10 years of research on rockfall and protection forests I conclude that this combination has been an excellent approach for studying rockfall and protection forests. Without this combination, significant progress in the realistic integration of trees in 3D models, the development of a representative and useful rockfall rebound algorithm, the further development of silvicultural guidelines for rockfall protection forests, and an improvement of the knowledge on the modes of motion on different slope gradients, would not have been possible.

> References

Ammann, M., 2006. Schutzwirkung abgestorbener Bäume gegen Naturgefahren. ETH PhD Thesis Nr. 16 638, Zürich: 228 pp.

Agliardi, F., Crosta, G., 2003. High resolution three-dimensional numerical modelling of rockfalls, Int. J. Rock Mechanics and Mining Sci. 40: 455–471.

Bebi, P., Kienast, F., Schönenberger, W., 2001. Assessing structures in mountain forests as a basis for investigating the forests' dynamics and protective function. Forest Ecology and Management 145(1): 3-14.

Berger, F., Dorren, L.K.A., 2006. Objective comparison of rockfall models using real size experimental data. In: Marui, H. et al. (Eds.), Disaster mitigation of debris flows, slope failures and landslides, Universal Academy Press, Inc., Tokyo (JP): pp. 245-252.

Berger, F., Dorren, L.K.A., 2007. Principles of the tool Rockfor.NET for quantifying the rockfall hazard below a protection forest. Schweizerische Zeitschrift für Forstwesen 158(6): 157-165.

Berger, F., Renaud, J.-P., 1994. Stabilité et fonction de protection des forêts de montagne dans les Alpes du Nord. L'exemple de la forêt domaniale de Rioupéroux. Revue Forestière Française 46(4): 359-374.

Berretti, R., Caffo, L., Camerino, P., De Ferrari, F., Domaine, A., Dotta, A., Gottero, F., Haudemand, J.C., Letey, C., Meloni, F., Motta, R., Terzuolo, P., 2006. Selvicoltura nelle

foreste di protezione. Esperienze ed indirizzi gestionali in Piemonte e Valle d'Aosta. Compagnia delle foreste, Arezzo: 224 pp.

Bezzola, G.-R., Hegg, C., 2007. Ereignisanalyse Hochwasser 2005. Teil 1 – Prozesse, Schäden und erste Einordnung. Bundesamt für Umwelt BAFU, Bern und der Eidgenössischen Forschungsanstalt für Wald, Schnee und Landschaft WSL, Birmensdorf: 215 pp.

Brang, P., 2001. Resistance and elasticity: promising concepts for the management of protection forests in the European Alps. Forest Ecology and Management 145(1): 107-117.

Brang, P., Schönenberger, W., Frehner, M., Schwitter, R., Thormann, J., Wasser, B., 2006. Management of protection forests in the European Alps: an overview. Forest Snow and Landscape Research. 80(1): 23–44.

Brauner, M., Weinmeister, W., Agner, P., Vospernik, S., Hoesle, B., 2005. Forest management decision support for evaluating forest protection effects against rockfall. Forest Ecology and Management 207(1-2): 75-85.

Bourrier, F., Dorren, L.K.A., Nicot, F., Berger, F., Darve, 2008. Towards objective rockfall trajectory modelling using a stochastic rebound algorithm. Geomorphology (submitted).

BUWAL, 1999. Leben mit dem Lawinenrisiko- Die Lehren aus dem Lawinenwinter 1999. Bundeamt für Umwelt, Wald und Landschaft (BUWAL), Bern: 27 pp.

Couvreur, S. 1982. Les forêts de protection contre les risques naturels. École Nationale du Génie Rural des Eaux et Forêts (ENGREF): 89 pp.

Dorren, L.K.A., Berger, F., Imeson, A.C., Maier, B., Rey, F., 2004. Integrity, stability and management of protection forests in the European Alps. Forest Ecology and Management 195(1-2): 165-176.

Dorren, L.K.A., Berger, F. 2005. Stem breakage of trees and energy dissipation during rockfall impacts. Tree Physiology 26: 63-71.

Dorren, L.K.A., Berger, F., Le Hir, C., Mermin, E., Tardif, P., 2005. Mechanisms, effects and management implications of rockfall in forests. Forest Ecology and Management 215(1-3): 183-195.

Dorren, L.K.A., Berger, F., Jonnson, M., Krautblatter, M., Moelk, M., Stoffel, M., Wehrli, A., 2007. State of the art in rockfall - forest interactions. Schweizerische Zeitschrift für Forstwesen 158(6): 128-141.

Fitze, U., 2005. Schutzwald: Bund kauft Schutzleistungen ein. Umwelt 3/05: 20 - 22.

Frehner, M., Wasser B., Schwitter, R., 2005. Nachhaltigkeit und Erfolgskontrolle im Schutzwald. Wegleitung für Pflegemassnahmen in Wäldern mit Schutzfunktion. Bundesamt für Umwelt, Wald und Landschaft (BUWAL), Bern. 564 pp.

Gauquelin X., Courbaud B., Ancelin P., Barthelon C., Berger F., Cardew M., Chauvin C., Descroix L., Dorren L.K.A., Fay J., Gaudry P., Genin J.-R., Joud D., Loho P., Mermin E., Plancheron F., Prochasson A., Rey F., Rubeaud D., Wlérick L. 2006. Guide des sylvicultures de montagne. Cemagref/CRPF Rhône-Alpes/ONF, France: 289 pp.

Gauquelin, X., Courbaud, B., Fay, J., Berger, F., Mermin, E., 2008. Conduite de peuplements mélangés en forêts de montagne : exemple d'une collaboration chercheurs-gestionnaires. Revue Forestiere Francaise 60(2): 207 - 214.

Gerber, W., 1992. Teilbereich: Steinschlag. Unterlagen Fortbildungsveranstaltung 1992, Berner Oberland. Forstl. Arbeitsg. Wildbach-, Hang- und Runsenverbau. WSL Verbauwesen: 17 pp.

Gerber, W., 1998. Waldwirkungen und Steinschlag. Unterlagen GWG/FAN-Kurs 1998, Engelberg. WSL Verbauwesen: 12 pp.

Gsteiger, P., 1993. Steinschlagschutzwald. Ein Beitrag zur Abgrenzung, Beurteilung und Bewirtschaftung. Schweizerische Zeitschrift für Forstwesen 144: 115-132.

Guzzetti, F., Crosta, G., Detti, R., Agliardi, F., 2002. STONE: a computer program for the three-dimensional simulation of rock-falls. Computers & Geosciences 28(9): 1079-1093.

Holub, M., Hübl, J., 2008. Local protection against mountain hazards – state of the art and future needs. Natural Hazards and Earth System Sciences 8: 81–99.

Hubert, T., 2003. Les Plans de Prévention des Risques naturels PPR. Ministère de l'Ecologie et du Développement durable, Direction de la Prévention des Pollutions et des Risques. 8 p.

Jahn, J., 1988. Entwaldung und Steinschlag, Interpraevent, Graz. Tagungspubl. Bd.1: pp. 185-198.

Jonsson, M., 2007. Energy absorption of trees in a rockfall protection forest. PhD Thesis ETH. http://e-collection.ethbib.ethz.ch/view/eth:29858.

Kalberer, M., 2007. Quantifizierung und Optimierung der Schutzwaldleistung gegenüber Steinschlag. PhD Thesis Albert-Ludwigs-Universität, Freiburg i. Brsg.: 221 pp.

Kautz, H., 1912 Schutzwald: Forst- und wasserwirtschaftliche Gedanken. Berlin, Springer, 74 pp.

Kienholz, H., Mani, P.J., 1994. Assessment of Geomorphic Hazards and Priorities for Forest Management on the Rigi North Face, Switzerland. Mountain Research and Development 14(4): 321-328.

Koch, B., Heyder, U., Weinacker, H., 2006. Detection of individual tree crowns in airborne LiDAR data. Photogrammetric Engineering & Remote Sensing 72(4): 357-364.

Lebensministerium, 2008. Sustainable Forest Management in Austria 2008. Austrian Forest Report. Prem, J. (Ed.). Bundesministerium für Land- und Forstwirtschaft, Umwelt und Wasserwirtschaft. Wien: 136 pp.

Loat R., 2006. Hazard maps. Colour insert with PCP Forum No. 8/2006: 14–21. [http://www.bevoelkerungsschutz.admin.ch/internet/bs/en/home/themen/kgs/publikationen_kgs/forum.html].

Lundström, T., Jonsson, M.J., Volkwein, A., 2008. Reactions and energy absorption of trees subject to rockfall: a detailed assessment using a new experimental method. Tree Physiology (accepted).

Margreth, S., 2004. Die Wirkung des Waldes bei Lawinen. Forum für Wissen 2004, WSL: 21-26.

Mayer, H., Ott, E., 1976. Gebirgswaldbau - Schutzwaldpflege. Stuttgart: 436 pp.

Moor, M. 1954. Fichtenwälder im Schweizer Jura. Plant Ecology 5-6 (1): 542-552.

Motta, R., Haudemand, J.C., 2000. Protective forests and silvicultural stability - An example of planning in the Aosta Valley. Mountain Research and Development 20(2): 180-187.

Ott E., Schönbächler, D., 1986. Die Stabilitsbeurteilung im Gebirgswald als Voraussetzung für die Schutzwald-Überwachung und –Pflege. Schweizerische Zeitschrift für Forstwesen 137(9): 725-738.

Persson, A., Holmgren, J., Söderman, U., 2002. Detecting and measuring individual trees using an airborne laserscanner. Photogrammetric Engineering & Remote Sensing 68(9): 925–932.

Perzl, F., Kleemayr, K., 2007. Wie gut schützt Wald. Forstzeitung 07/2007: 44 – 45.

Rammer, W., Brauner, M., Dorren, L.K.A., Berger, F., Lexer, M.J. 2007. Validation of an integrated 3D forest - rockfall model. EGU General Assembly, 15 - 20 April 2007, Wien (AT).

Rickli C., Banzer E., 1996. Hazard mapping in the principality of Liechtenstein. Interpraevent, Garmisch-Partenkirchen. Tagungspubl. Bd.3: pp. 183-192.

Ritchie, A.M., 1963. Evaluation of rockfall and its control. Highway Research Board. Highway Research Records 17: 13–28.

Rudolf-Miklau, F., Ellmer, A., Gruber, H., Hübl, J., Kleemayr, K., Lang, E., Markart, G., Scheuringer, E., Schmid, F., Schnetzer, I., Weber, C., Wöhrer-Alge, M., 2006. Hochwasser 2005 - Ereignisdokumentation. Bundesministerium für Land- und Forstwirtschaft, Umwelt und Wasserwirtschaft, Sektion Forst, Abteilung Wildbach- und Lawinenverbauung, Wien: 126 pp.

Rudolf-Miklau F., Leitgeb M., Schmidt R., Weber C., Daschek F., Roßnagl F., 2007. Wildbach- und Lawinenverbauung in Österreich. Bundesministerium für Land- und Forstwirtschaft, Umwelt und Wasserwirtschaft, Sektion Forstwesen, Wien: 13 pp.

Sandri, A., 2008. Bundesausgaben Naturgefahren im Bereich Rutschungen, Lawinen und Schutzwald. Internal financial report of the Section Landslides Avalanches and Protection Forest, Bundesamt für Umwelt (BAFU), Bern.

Schima J., Keller M., Kiessling J., Starsich A., 2008. Initiative Schutz Durch Wald. Broschüre ISDW (www.isdw.at), Bundesministerium für Land- und Forstwirtschaft, Umwelt und Wasserwirtschaft, Wien: 8 pp.

Schönenberger, W., 2000. Silvicultural problems in subalpine forests in the Alps. In: M.F. Price and N. Butt (Eds.), Forests in sustainable mountain development: a state of knowledge report for 2000. IUFRO Research Series 5. CABI Publishing, Wallingford, UK: pp. 197-203.

Solberg, S., Naesset, E., Bollandsas, O. M., 2006. Single Tree Segmentation Using Airborne Laser Scanner Data in a Structurally Heterogeneous Spruce Forest. Photogrammetric Engineering and Remote Sensing 72(12): 1369-1378.

Wasser B., Frehner M., 1996. Minimale Pflegesmassnahmen für Wälder mit Schutzfunktion. Wegleitung. Bundesamt für Umwelt, Wald und Landscahft (BUWAL), Bern.

Woltjer, M., Rammer, W., Brauner, M., Seidl, R., Mohren, G.M.J., Lexer, M.J., 2008. Coupling a 3D patch model and a rockfall module to assess rockfall protection in mountain forests. Journal of Environmental management 87: 373-388.

Ziegner, K., 2006. NMF - Gemeinsame Strategie für die europäischen Bergwälder. Tiroler Forstdienst 49: 5 – 6.

> Chapter 2

Schutzwaldmanagement in den Alpen



Schutzwaldmanagement in den Alpen – eine Übersicht

André Wehrli Bundesamt für Umwelt, Abteilung Gefahrenprävention (CH)*
Peter Brang Eidgenössische Forschungsanstalt WSL (CH)
Bernhard Maier Stand Montafon Forstfonds (AT)
Philippe Duc Eidgenössische Forschungsanstalt WSL (CH)
Franz Binder Bayerische Landesanstalt für Wald und Forstwirtschaft (DE)
Emanuele Lingua Università degli Studi di Torino, Dept. AGROSELVITER (IT)
Kurt Ziegner Landesforstdirektion Tirol (AT)
Karl Kleemayr BFW, Institut für Naturgefahren und Waldgrenzregionen (AT)
Luuk Dorren Cemagref Grenoble (FR)

Management of protection forests in the Alps – an overview

Many mountain forests in the Alps protect residential areas and infrastructures from natural hazards. They are described as protection forests and their management aims to permanently provide a high protective effect. The maintenance and management of these forests are continuously improved and have reached a high standard. There is now a better understanding of the protective effects of the forest against natural hazards. In the Alps, there are currently several projects being conducted which aim to harmonize the assessment of natural hazards, damage potential and a resulting classification of protection forests. It is the objective to apply funding where needed in order to prevent damage from natural hazards. Currently, there is a need for improvement in the area of monitoring with advanced technology, such as Laser-Scanning (LIDAR), in linking inventory data from different sources, in simulation modeling to better estimate the long-term benefit of measures in the protection forest, and in transboundary collaboration.

Keywords: protection forest, natural hazards, forest management, monitoring
doi: 10.3188/szf.2007.0142

* CH-3003 Bern, E-Mail andre.wehrli@bafu.admin.ch

Viele Gebirgswälder schützen Siedlungen und Verkehrswege vor Naturgefahren wie Steinschlag, Lawinen, Erosion, Rutschungen, Wildbächen, Murgängen und Überflutung (Brang et al 2001). Diese Naturgefahrenprozesse treten im Alpenraum vergleichsweise häufig auf. Der hohe Schutzwaldanteil in diesen Regionen ist daher nicht erstaunlich: So weisen nach dem Schweizerischen Landesforstinventar 37% der Aufnahmeflächen in Gebirgswäldern Hinweise auf Schneebewegungen auf, 31% der Flächen Spuren von Steinschlag und 16% Spuren von Erosion (Mahrer et al 1988). Basierend auf Zahlen aus den Kantonen und dem Projekt SilvaProtect-CH geht das Bundesamt für Umwelt BAFU aktuell davon aus, dass zirka 40–60% des Schweizer Waldes eine Schutzfunktion gegen Naturgefahren haben. In Frankreich schützt der Gebirgswald, der sich zu 90% im Besitz der Kommunen und des Staates befindet, vor den Prozessen Erosion im Gerinnebereich (auf 65% der Fläche), Lawinen (14%), Steinschlag (10.5%) und Rutschungen (10.5%; Sonnier 1991). In den Bayerischen Alpen im Südosten von Deutschland sind ungefähr 60% des Waldes Schutzwald nach dem Bayerischen Waldgesetz (Brosinger 2004). Im Bayerischen Hochgebirge, das etwa 5300 km² des gesamten Alpenraumes abdeckt, schützen schätzungsweise 63% der Wälder gegen Erosion und Murgang, 42% gegen Lawinen und 64% gegen Überflutung (Plochmann 1985). In Österreich sind etwa 31% der gesamten Waldfläche mit einer Schutzfunktion belegt (BMLUFW 2006). Der Anteil an Schutzwald im alpinen Raum liegt deutlich höher, beispielsweise in Tirol bei mehr als 66% (ca. 330000 ha; Amt Tiroler Landesregierung 2005). In der Autonomen Region des Aostatals in Italien haben ungefähr 80% der Wälder eine Schutzfunktion (Meloni et al 2006).

Trotz offensichtlicher Unterschiede in der Methodik der Datenerhebung zeigen die Zahlen die Bedeutung der Schutzwälder im Alpenraum deutlich auf. In den letzten Jahrzehnten hat deren Bedeutung noch zugenommen: Gebiete, welche früher im Winter gemieden wurden, sind heute ganzjährig für die Touristen zugänglich. Gegenden werden besiedelt,

die von unseren Vorfahren noch als unsicher eingeschätzt wurden. Der Transport von Personen und Gütern durch die Alpen hat massiv zugenommen (BUWAL 2001). Einige Kennzahlen aus den Bayerischen Alpen machen deutlich, wie stark die Veränderung im Alpenraum ist: So hat sich die Bevölkerung in den letzten 150 Jahren vervierfacht und erreicht nun eine Dichte von über 400 Bewohnern pro km² besiedelbarer Fläche (BayStMELF 2000). Darüber hinaus wird die Region von mehr als 4.5 Millionen Touristen pro Jahr besucht (Bayerischer Landtag 2006). In Tirol verbringen jährlich rund 8 Millionen Gäste ihre Sommer- und Winterferien und erhöhen damit die Einwohnerzahl saisonal auf mehr als 800 Bewohner pro km².

Angesichts solcher Zahlen kann der starke Anstieg des Schadenpotenzials in vielen Regionen des Alpenraumes nicht verwundern. Dies wiederum macht grosse Investitionen in Schutzmassnahmen nötig. Die Schweiz investierte beispielsweise während den letzten Jahrzehnten zwischen 120–150 Millionen CHF an Bundesgeldern pro Jahr für «Schutzaktivitäten im Waldbereich» (Schärer 2004). Ungefähr 60% der Geldmittel (d.h. rund 70–94 Millionen CHF) wurden benötigt für den «Schutz durch Wald», das heisst für Schutzwaldpflege, Verjüngung und Behebung von Waldschäden, forstliche Planungsgrundlagen, Erschliessungsanlagen und Investitionskredite (Schärer 2004). In Österreich fliessen ungefähr 120 Millionen Euro pro Jahr in technische Schutzmassnahmen zur Wildbach- und Lawinenverbauung und in das präventive Schutzwaldmanagement. Allein im Bundesland Vorarlberg wurden im Jahr 2006 zirka 2.5 Millionen Euro in die Schutzwaldpflege und -erhaltung investiert. Umgelegt auf die gesamte Schutzwaldfläche entspricht dies rund 48 Euro pro Hektare. In Tirol liegt dieser Wert sogar bei 80 Euro pro Hektare und Jahr (Amt Tiroler Landesregierung 2005). In der Region Piemont in Italien werden im Zeitraum von 2006–2008 Beiträge von bis zu 80 Euro pro Hektare für Schutzwälder ausgegeben, mit dem Ziel, deren ökologische und physische Stabilität zu erhalten oder zu fördern und die Nachteile, welche den Eigentümern durch die Bewirtschaftung entstehen, teilweise auszugleichen (Massnahme I Aktion 7 des «Piano di Sviluppo Rurale» – D.G.R. 26-3081 gemäss EC-Verordnung No. 1257/1999). In Bayern wurden seit Beginn des Schutzwaldsanierungsprogrammes im Jahre 1986 rund 60 Mio Euro in die Sanierung der Schutzwälder investiert (BayStMLF 2006). Das entspricht rund 250 Euro pro Hektare und Jahr im Schnitt der letzten 20 Jahre. Im Gegensatz dazu sind in Frankreich momentan keine strukturellen Finanzmittel für das Schutzwaldmanagement verfügbar. Auf Antrag werden lokal begrenzte Massnahmen im Rahmen des Schutzwaldmanagements geprüft und fallweise genehmigt. Auf diese Weise investiert die französische Regierung jährlich zwischen 500000 und 800000 Euro in das Schutzwaldmanagement (ONF, persönliche Mitteilung). In absehbarer Zukunft ist auch in Frankreich die Errichtung von strukturellen Finanzmitteln für das Schutzwaldmanagement vorgesehen.

Die oben genannten Zahlen belegen den ökonomischen Wert und die Bedeutung des Schutzwaldes. Der vorliegende Aufsatz gibt einen Überblick über den aktuellen Stand des Wissens beim Schutzwaldmanagement in den Alpen. Einleitend wird der Begriff «Schutzwald» definiert und die potenzielle Schutzwirkung von Wäldern gegen verschiedene Naturgefahren erklärt. An Beispielen aus mehreren Ländern werden sodann die Abgrenzung und Ausscheidung, die Pflege und das Monitoring solcher Wälder thematisiert. Schliesslich werden Forschungsbedürfnisse sowie Schritte zur Verbesserung des Schutzwaldmanagements formuliert.

Definition von Schutzwäldern und ihrer Wirkung gegen Naturgefahren

Die Hauptfunktion eines Schutzwaldes ist der Schutz von Menschen, Gütern und Infrastrukturen vor Naturgefahren (Brang et al 2006). Ein Schutzwald bedingt das Vorhandensein (1) eines Gefahrenpotenzials (z.B. eine instabile Felswand), (2) eines Schadenpotenzials (z.B. eine Siedlung oder ein Verkehrsweg) und (3) eines Waldes, welcher eine Schutzwirkung gegen die Naturgefahr entfalten kann (Brang et al 2001).

Schutzwälder können in Wälder unterteilt werden, welche eine direkte Schutzwirkung bieten und solche mit indirekter Schutzwirkung (Brang et al 2006). Eine direkte Schutzwirkung ist gegeben, wenn die Wirkung von der Anwesenheit eines Waldes an einem bestimmten Ort, in der Regel oberhalb des Schadenpotenzials, abhängt. Ein typisches Beispiel hierfür ist ein Lawinenschutzwald oberhalb einer Siedlung. Die indirekte Schutzwirkung hängt hingegen von der Anwesenheit eines bestimmten Waldanteiles auf der Landschaftsskala ab und nicht von der genauen Lage eines Waldes. Dieser Umstand macht es schwierig, die Schutzwirkung eines solchen Waldes in Bezug zum Schadenpotenzial zu setzen. Beispiele für Wälder mit indirekter Schutzwirkung finden sich häufig in Einzugsgebieten von Wasserläufen, wo sie zur Reduktion von Erosionsprozessen oder Überflutungen beitragen können (Hamilton 1992).

Wälder können gegenüber Lawinen, Steinschlag, flachgründigen Rutschungen, Murgang, Erosionsprozessen und Überflutung Schutzwirkung entfalten (Brang et al 2006). Diese hängt dabei stark vom Naturgefahrenprozess ab. Sie kann die Prozesse verhindern oder vermindern. Lawinenschutzwald wirkt beispielsweise eher vorbeugend als abschwä-

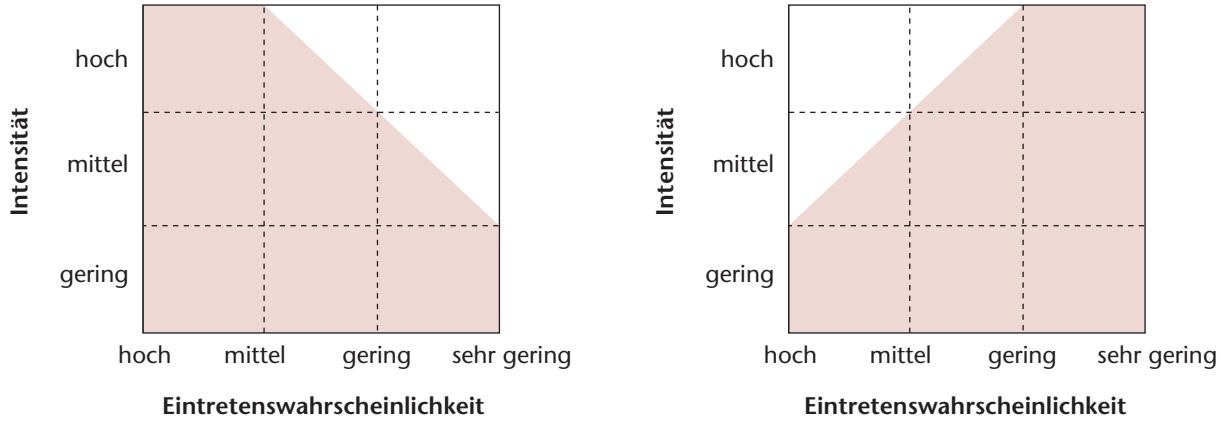


Abb 1 *Mögliche Schutzwirkung von Waldbeständen gegen Lawinen (links) und Steinschlag (rechts). Die Schattierung gibt die Bereiche der Intensität und Eintretenswahrscheinlichkeit von Naturgefahren wieder, bei denen ein Wald eine gute Schutzwirkung entfalten kann (nach Sandri 2006).*

chend. Die Intensität von Lawinen gemessen in Volumen und Energien übersteigt oft die Möglichkeiten eines Waldes zur Minderung des Prozesses (Berger 1996, Bartelt & Stöckli 2001, Margreth 2004). Baumkronen, vor allem von immergrünen Nadelbäumen, wirken durch Schneeinterzeption und durch den aus den Kronen herabfallenden Schnee dem Aufbau einer homogenen Schneeschicht entgegen, welche damit nicht mehr als kompaktes Paket abgleiten kann (In der Gand 1978). Auf diese Weise kann die Auslösung einer Lawine verhindert werden (Margreth 2004).

Bei Steinschlagereignissen mit einem Volumen < 5 m^3 (Berger et al 2002) kann ein Wald abschwächend wirken. Bäume und sogar tote, liegende Stämme können den Steinschlagprozess wirksam abdämpfen, indem sie die Energie der Steine verringern oder die Steine gar ganz stoppen (Couvreur 1982, Jahn 1988, Gsteiger 1993, Lafortune et al 1997, Dorren et al 2005). Die Schutzwirkung eines Waldes hängt einerseits primär von der Grösse und der kinetischen Energie eines Steines ab und andererseits von der Kombination der Hindernisse in der Transitstrecke wie zum Beispiel Geländeunebenheiten, Bäume, Strünke und tote, liegende Stämme (Schönenberger et al 2005, siehe auch Dorren et al 2007). Für einen optimalen Steinschlagschutz sind nicht allein Bäume mit grossem Durchmesser nötig. Ein gut strukturierter Bestand mit einer breiten Durchmesserverteilung und einem Mosaik von verschiedenen Entwicklungsstufen kann unter Umständen weitaus besser gegen Steine schützen (Dorren et al 2007).

Baumwurzeln können flachgründige Rutschungen durch mechanische Verstärkung des Bodens verhindern oder zumindest deren Ausmass verkleinern (Hamilton 1992, Rickli et al 2001), indem sie die mechanischen Bodeneigenschaften durch Aggregatbildung respektive Aggregatstabilisierung erhöhen (Böll & Graf 2001). Insbesondere in Böden mit einer mässigen Durchlässigkeit erhöhen sie darüber hinaus das im Boden verfügbare Wasser-Speichervolumen (Hegg et al 2005). Zudem können Wälder auf Erosions- und hydrologische Prozesse einwirken, indem sie beispielsweise durch permanenten Streueintrag die Oberflächenerosion reduzieren oder durch Aufbau einer organischen Auflage die Wasserrückhaltekapazität erhöhen (Hamilton 1992). Weiter wirken sich Bäume positiv auf die Interzeption von Niederschlägen und die Evapotranspirationsbilanz aus, was wiederum zu einer verbesserten Wasserbilanz des Bodens führen kann (Rickli et al 2004, Frehner et al 2005).

Die Schutzwirkung eines Waldes hängt wie bereits erwähnt von der Art der Naturgefahr ab, insbesondere von deren Auftretenswahrscheinlichkeit und deren Intensität, sowie vom Zustand des Waldes selbst. Schutzwälder können kaum je einen hundertprozentigen Schutz bieten, aber sie können die vom Prozess ausgehende Gefahr und somit das Restrisiko beträchtlich reduzieren (Abbildung 1). Für den Fall, dass das Risiko trotz der Schutzwirkung des Waldes noch zu hoch ist, kann die Schutzwirkung des Waldes durch zusätzliche technische Abwehrmassnahmen wie Steinschlagschutznetze oder Lawinenverbauungen ergänzt werden.

Obwohl die Schutzwirkung unter bestimmten Bedingungen ergänzt werden muss, sind Wälder im Allgemeinen ein sehr wirksames Mittel im Rahmen des integralen Risikomanagements (Planat 2005). Sie können auf grossen Flächen gleichzeitig Schutz gegen verschiedene Naturgefahren bieten. Eine solche Überlagerung von mehreren Gefahrenprozessen kommt recht häufig vor. Daher haben Schutzwälder einen klaren Vorteil gegenüber technischen Massnahmen, welche oft nur gegen einzelne Naturgefahren wirksam sind (z.B. gegen Lawinen oder Steinschlag, aber nicht gegen beide Naturgefahren). Darüber hinaus ist die Schutzwaldpflege fünf bis zehn Mal kostengünstiger als technische Massnahmen (Sandri 2006).

Abgrenzung und Ausscheidung von Schutzwäldern

Schutzwälder liegen oft an Gebirgshängen, da viele relevante Naturgefahren schwerkraftabhängige Massenbewegungen sind. Schutzwälder können aber auch im Talgrund oder auf Sedimentkegeln wachsen, wo sie eine Schutzwirkung gegen Überflutung und Oberflächenerosion haben (Wilford et al 2003). Bislang gibt es im Alpenraum keine einheitliche Methodik, um Schutzwälder abzugrenzen und auszuscheiden, da die Definition der Schutzwälder per se bereits einige Schwierigkeiten aufwirft: So kann einerseits die potenzielle Schutzwirkung eines Waldes gegen bestimmte Naturgefahren aufgrund eines fehlenden Prozessverständnisses oder fehlender Informationen zu den Prozessfrequenzen und -intensitäten nicht immer klar abgeschätzt werden. Andererseits hängt die Definition eines Schutzwaldes auch von der Definition des (relevanten) Schadenpotenzials ab, wobei eine nicht einheitliche Definition des Schadenpotenzials eben auch zu Abgrenzungs- und Ausscheidungsschwierigkeiten führt. Diese Schwierigkeiten sind in den verschiedenen Ansätzen zur Schutzwaldausscheidung im Alpenraum zu erkennen: In Italien existiert beispielsweise keine Ausscheidung von Schutzwäldern auf nationaler Ebene. Die Kompetenz für das Waldmanagement wurde in den späten 70er-Jahren von der nationalen zu den regionalen Verwaltungen delegiert, wobei bislang keine einzige Region ihre Schutzwälder umfassend ausgeschieden hat. Schutzwald-Ausscheidungen wurden nur für einzelne Talschaften oder Gemeinden und oftmals nach ganz verschiedenen Methoden gemacht (Lingua et al 2003, Zampa et al 2004). In der Autonomen Region Aostatal wurden die Schutzwälder beispielsweise im Rahmen des INTERREG III A-Projekts «Gestion durable des forêts de montagne à fonction de protection» halbautomatisiert aufgrund der Analyse eines digitalen Geländemodells (DGM) ausgeschieden (Meloni et al 2005). Die Genauigkeit dieser Methode hängt hauptsächlich von der Verfügbarkeit von aktuellen Geo-Daten zur Bodenbedeckung (Wald) und zum Schadenpotenzial ab. Diese müssen in einer hohen Auflösung vorliegen.

In Bayern sind nach dem Waldgesetz für den Schutzwald von Amts wegen Schutzwaldverzeichnisse anzulegen. Die Kriterien für die Ausscheidung von Schutzwäldern sind in einer Bekanntmachung des Bayerischen Staatsministeriums für Ernährung, Landwirtschaft und Forste aus dem Jahr 1977 spezifiziert (Zerle et al 2006). Sie enthalten verschiedene Aspekte bezüglich Naturgefahren und Gelände, so zum Beispiel Informationen zur orographischen und geographischen Lage und Hangneigung. Für viele Wälder bildete auch die Hanglabilitätskartierung von Laatsch & Grottenthaler (1973) die Grundlage. Die Ausscheidung erfolgte durch verbeamtete Forstleute. Dieses Vorgehen führte in Bayern zu einer ziemlich präzisen und flächenscharfen Ausscheidung von Schutzwäldern.

In Österreich unterscheidet das Forstgesetz zwischen Standortschutzwald, Objektschutzwald und Bannwald und definiert die Abgrenzungskriterien für jede Kategorie innerhalb des Gesetzes. Ein Standortschutzwald ist ein Wald, dessen Standort durch die erosiv wirkenden Kräfte von Wind, Wasser und Schwerkraft bedroht ist. Der Wald ist somit selbst das eigentliche Schadenpotenzial. Ein Objektschutzwald schützt dagegen Siedlungen, Verkehrswege und andere Infrastrukturen sowie Kulturland gegen Naturgefahren. In beiden Kategorien sind spezielle Pflegemassnahmen vorgesehen (§ 21 Par. 2 Österreichisches Forstgesetz 1975).[1] Ein Bannwald wird per Bescheid ausgeschieden, und seine Ausscheidung verpflichtet die direkten Nutzniesser zur Erhaltung der Schutzwirkung. Die Umsetzung des Forstgesetzes sowie die Ausscheidung der Schutzwälder obliegt der Landesforstverwaltung in Zusammenarbeit mit den Bezirksforstämtern. Diese Verwaltungseinheiten scheiden verschiedene Waldfunktionen wie die Schutzfunktion in Waldentwicklungsplänen aus. Gemäss den neuen Richtlinien für Waldentwicklungspläne (BMLUFW 2006) werden Objektschutzwälder nicht explizit abgegrenzt, sondern nur deren Anteil an der Waldfläche geschätzt. Basierend auf den Waldentwicklungsplänen wird der Schutzwaldanteil auf nationaler Ebene momentan auf 19.3% der Waldfläche geschätzt, das heisst auf rund 755 000 ha. Die Bundesländer verfügen darüber hinaus über präzisere Angaben zu den Schutzwäldern, zum Beispiel Gefahrenzonenpläne, welche auf flächigen Gutachten zu den Naturgefahren Wildbach, Lawinen und Erosionen basieren, die in der Regel durch Experten des Forsttechnischen Dienstes für Wildbach- und Lawinenverbauung erstellt werden. Diese zusätzlichen Angaben erlauben eine präzisere Ausscheidung von Schutzwäldern, können aber auch als Grundlage zur Planung von konkreten organisatorischen (z.B. Zonenpläne) oder technischen (z.B. Verbauungen) Massnahmen gebraucht werden.

2007 lancierte die österreichische Bundesregierung die Initiative «Schutz durch Wald» (ISDW). Damit sollen einerseits die Massnahmen im Schutzwald durch zusätzliche finanzielle Anreize erhöht und andererseits die Informationen über den derzeitigen Zustand und die Entwicklung verbessert werden. Das ISDW-Programm gliedert sich in zwei Abschnitte. Im ersten wurden von Vertretern der Forstbezirksbehörden und der Wildbach- und Lawinenverbauung auf regionaler Ebene Flächen für ganz Österreich ausgeschieden, in denen Bergwäl-

[1] www.lebensministerium.at (3. April 2007)

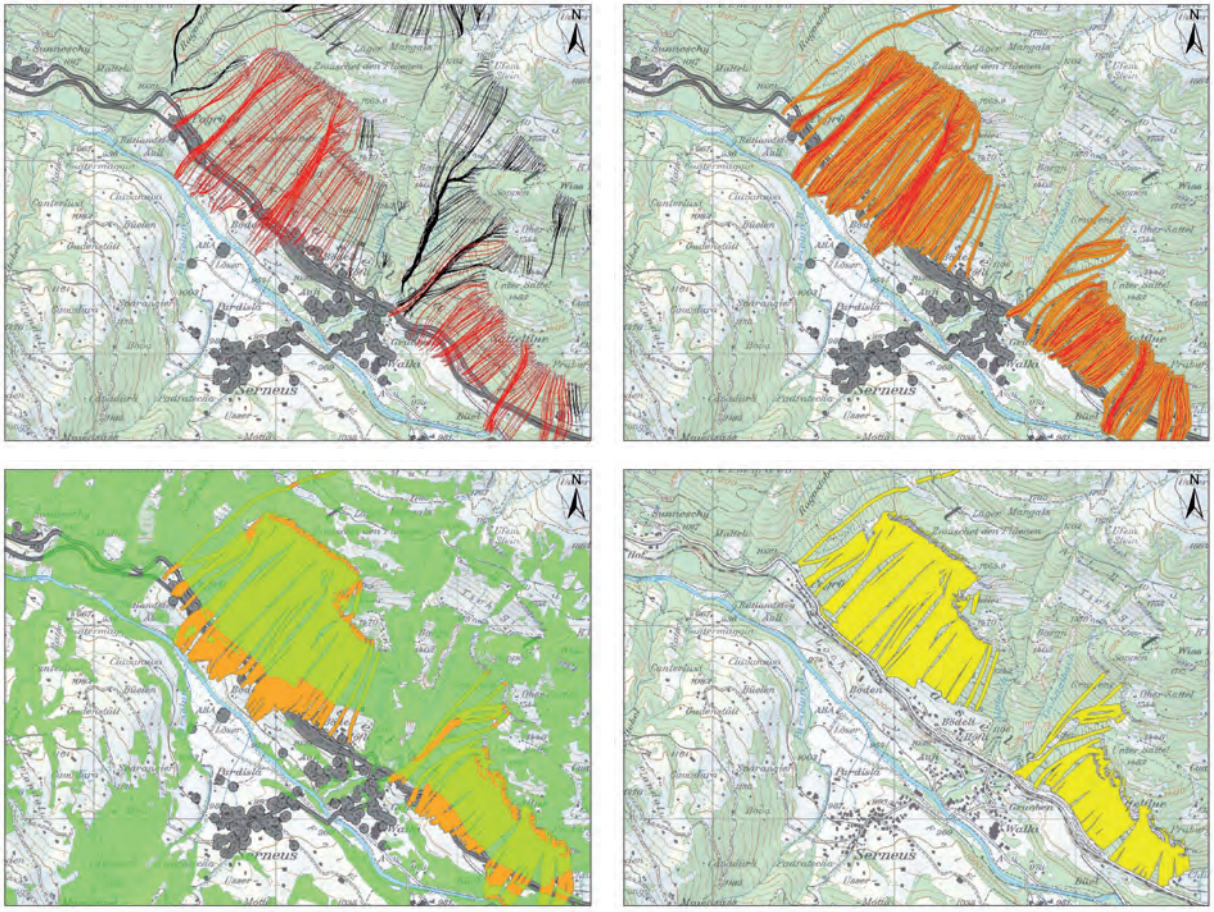


Abb 2 *Bestimmung der schadenrelevanten Prozessflächen im Wald gemäss SilvaProtect-CH am Beispiel des Prozesses Steinschlag. Landeskarte 1:25 000 reproduziert mit Bewilligung von swisstopo (BA071178). Schritt 1: Selektion der Steinschlagtrajektorien (rot), welche auf ein Schadenpotenzial (grau) treffen (schwarz: restliche Trajektorien). Schritt 2: Pufferung der selektierten Steinschlagtrajektorien (rot) mit einem zweiseitigen Puffer (orange). Schritt 3: Verschnitt der vereinigten Pufferfläche (orange) mit der Waldfläche (grün). Schritt 4: Freistellung der schadenrelevanten Prozessflächen im Wald (gelb).*

der mit Objektschutzcharakter bekannt sind (Rahmenpläne). Innerhalb dieser ausgewiesenen Flächen können im zweiten Abschnitt für waldbauliche Massnahmen, die der Verbesserung und Nachhaltigkeit der Schutzfunktion dienen, Fördermittel beantragt werden. Bei der Vergabe der Fördermittel kommt ein Entscheidungsunterstützungssystem zum Einsatz, das die Beurteilung der Gefahr (Unterscheidung nach Grösse und Frequenz für jeden Gefahrentyp) und des Waldes (Unterscheidung zwischen gegenwärtigem Zustand und Entwicklungsdynamik) mit wenigen Parametern verbindet. Diese Daten werden in einer Entscheidungsmatrix verarbeitet und für die spätere Evaluation und Effizienzkontrolle archiviert.

In der Schweiz existiert gegenwärtig noch keine einheitliche Schutzwaldausscheidung, obwohl Massnahmen zum Schutzwaldmanagement bereits seit mehr als 30 Jahren unterstützt werden. Zwar haben praktisch alle Kantone die Schutzwälder gemäss den Vorgaben des Bundes ausgeschieden, aber diese Vorgaben waren vergleichsweise unscharf und erlaubten den Kantonen eine grosszügige Auslegung. Aus diesem Grund ist das Bundesamt für Umwelt (BAFU) in Zusammenarbeit mit den Kantonen momentan daran, die Kriterien zur Schutzwaldausscheidung zu harmonisieren.[2] Dazu wurden über die ganze Schweiz die bedeutsamen Naturgefahrenprozesse mit Hilfe von dynamischen Modellen erhoben. Die resultierenden Gefahrenprozessräume wurden sodann mit dem Waldperimeter und dem relevanten Schadenpotenzial in einem geographischen Informationssystem (GIS) verschnitten (Abbildung 2). Die Resultate dieses Verschnitts, die «schadenrelevanten Prozessflächen im Wald», wurden anschliessend mit den aktuellen kantonalen Schutzwaldperimetern verglichen. Diese Vergleiche dienen nun als Basis für die Vereinheitlichung der Kriterien zur Schutzwaldausscheidung. Die Kriterien sollen bis Ende 2011 in den kantonalen Schutzwaldausscheidungen berücksichtigt werden.

[2] siehe auch www.bafu.admin.ch/naturgefahren (27. April 2007)

Schutzwaldpflege

Walddynamik und Schutzwirkung

Ein Wald ist ein dynamisches System, welches nicht über längere Zeit in einem bestimmten Zustand gehalten werden kann (Brang 2001). Die Bestandesstruktur, welche die Schutzwirkung eines Waldes massgebend beeinflusst, verändert sich andauernd. Damit ändert sich auch laufend die Schutzwirkung eines Bestandes. So können beispielsweise Bestände mit hohen Stammzahlen, welche einen sehr wirksamen Schutz gegen Steinschlag bieten (Omura & Marumo 1988, Cattiau et al 1995), langfristig nicht erhalten werden: Solche Bestände sind normalerweise anfällig für Sturmschäden (Rottmann 1986) und Schneebruch (Rottmann 1985, Oliver & Larsen 1990) und verhindern zudem durch ihre Struktur eine ausreichende Verjüngung. Gerade in Schutzwäldern ist aber ein Mindestmass an Verjüngung von entscheidender Bedeutung, da nur so eine dauerhafte Bestockung gesichert werden kann und damit eine langfristige Schutzwirkung erst ermöglicht wird. In Gebirgswäldern kann sich ein Verjüngungsmangel besonders gravierend auswirken, da sich infolge des langsamen Baumwachstums in grossen Höhenlagen (Ott et al 1997) ein allfälliges Defizit erst nach Jahrzehnten auf die Schutzwirkung auswirkt und daher leicht zu spät entdeckt wird (Wehrli 2005).

Normalerweise sind ungleichförmige, vielschichtige Bestände mit einem Mosaik von Bäumen verschiedener Grösse und verschiedenen Alters am besten für den Schutz vor Naturgefahren geeignet (Ott et al 1997, Motta & Haudemand 2000, O'Hara 2006). Derartig reich strukturierte Bestände bieten oftmals Schutz gegen verschiedene Naturgefahrenprozesse. Sie scheinen zudem weniger anfällig gegen natürliche Störungen zu sein und zeigen eine höhere Elastizität nach Störungen wie Windwürfen (Brang et al 2006). Leider sind momentan viele Bestände im Alpenraum eher gleichförmig und einschichtig. Solche Bestände weisen oft ein Verjüngungsdefizit auf. Das stellt ihre langfristige Schutzwirkung in Frage. Beispiele hierzu finden sich in den Fichtendominierten Gebirgswäldern der Schweiz, welche momentan vielerorts eher gleichförmig, dicht und arm an Verjüngung sind (siehe auch Brang & Duc 2002). Aber auch in Österreich weist die nationale Waldinventur (ÖWI) ein deutliches Verjüngungsdefizit aus: So verfügen gemäss ÖWI bloss 30% der Waldfläche über genügend Verjüngung (BMLUFW 2006). Nicht anders sieht es in Bayern aus. Auf nur 21% der über 80 Jahre alten Schutzwaldbestände hat sich die Vorausverjüngung eingefunden (Bayerische Landesanstalt für Wald und Forstwirtschaft 2005).

Neben homogenen Beständen mit Verjüngungsmangel gibt es weitere Faktoren, welche die zukünftige Schutzwirkung von Wäldern in Frage stellen können, so zum Beispiel Bestandeslücken, Bestandesüberalterung, Windwurf, Borkenkäfer oder hoher Verbissdruck durch Schalenwild und Weidevieh. Diese Faktoren haben dazu geführt, dass vielerorts die Schutzfunktion der Wälder beeinträchtigt ist: So wird in Bayern die Schutzwirkung von mehr als 12 000 ha des Schutzwaldes momentan als ungenügend eingeschätzt (BayStMLF 2005), im Tirol gar von rund 85 000 Hektaren (Amt Tiroler Landesregierung 2006).

Schutzwaldpflege in den Alpen

Um die Schutzwirkung der Wälder langfristig und nachhaltig sicherzustellen, müssen Schutzwälder oft gepflegt werden. Dabei macht man sich die Tatsache zu Nutze, dass die Dynamik von Gebirgswäldern und somit auch deren Schutzwirkung durch waldbauliche Massnahmen beeinflusst werden kann (Schönenberger & Brang 2004). Die Massnahmen zielen oft darauf ab, ein kleinräumiges Mosaik von Waldstrukturen in verschiedenen Entwicklungsstufen zu generieren. Dazu wird der homogene und dichte Bestand mittels schlitzförmiger Öffnungen in kleinere Einheiten unterteilt. Sobald sich die Verjüngung in diesen Schlitzen etabliert hat, wird der Mosaikbildungsprozess durch weitere Schlitze fortgesetzt. Dieses Vorgehen sollte über den gesamten Entwicklungszyklus eines Bestandes weitergeführt werden, damit schliesslich phasenverschobene Mosaikstrukturen entstehen (Dorren et al 2004). Solche waldbauliche Eingriffe sind zwar oft Erfolg versprechend, aber auch ziemlich teuer.

Der Bedarf an Schutzwaldpflege in einzelnen Schutzwäldern ist oftmals schwierig abzuschätzen. Einige neuere Studien deuten darauf hin, dass Wälder unter bestimmten Bedingungen für eine gewisse Zeit auch ohne waldbauliche Massnahmen eine gute Schutzwirkung leisten können (siehe z.B. Frey & Thee 2002, Kupferschmid Albisetti 2003, Kupferschmid Albisetti 2004, Schönenberger et al 2005). Allerdings können aus diesen Studien noch keine allgemein gültigen Regeln abgeleitet werden, da die Datengrundlage zu dünn ist. Solange nicht ausreichende Datenreihen vorhanden sind, welche die Entwicklung von Schutzwäldern ohne waldbauliche Eingriffe über längere Zeiträume dokumentieren, scheint die aktive Schutzwaldpflege gemäss fachlich abgestützten Richtlinien die bessere Option zu sein als ein Verzicht auf Schutzwaldpflege.

In vielen Alpenländern wurde in den letzten Jahrzehnten das Schutzwaldmanagement optimiert, indem spezielle Richtlinien zur Schutzwaldpflege ausgearbeitet und angewendet wurden. So existieren in Bayern waldbauliche Richtlinien für die Staatswälder im Hochgebirge bereits seit 1982 (BayStMELF 1982). Darüber hinaus wurde ein Handbuch zur Schutzwaldsanierung erstellt (BayStMELF 1997). Ziel der beiden

Ort	potenzieller Beitrag des Waldes	minimale Anforderungen aufgrund der Naturgefahr	ideale Anforderungen aufgrund der Naturgefahr
Entstehungsgebiet	**mittel**	**Stabilitätsträger** keine instabilen, schweren Bäume	
Transitgebiet	**gross** Steine bis 0.05 m³ (Durchmesser etwa 40 cm)	**Gefüge horizontal** mind. 400 Bäume/ha mit BHD > 12 cm	**Gefüge horizontal** mind. 600 Bäume/ha mit BHD > 12 cm
		evtl. auch Stockausschläge	
		Gefüge vertikal Zieldurchmesser[1] angepasst	
	Steine 0.05 bis 0.20 m³ (Durchmesser etwa 40 bis 60 cm)	**Gefüge horizontal** mind. 300 Bäume/ha mit BHD > 24 cm	**Gefüge horizontal** mind. 400 Bäume/ha mit BHD > 24 cm
		Gefüge vertikal Zieldurchmesser[1] angepasst	
	Steine 0.20 bis 5.00 m³ (Durchmesser etwa 60 bis 180 cm)	**Gefüge horizontal** mind. 150 Bäume/ha mit BHD > 36 cm	**Gefüge horizontal** mind. 200 Bäume/ha mit BHD > 36 cm
	zusätzlich für alle Steingrössen	**Gefüge horizontal** bei Öffnungen[2] in der Falllinie Stammabstand < 20 m liegendes Holz und hohe Stöcke: als Ergänzung zu stehenden Bäumen, falls keine Sturzgefahr	
		minimale Anforderungen aufgrund des Standortstyps erfüllt	ideale Anforderungen aufgrund des Standortstyps erfüllt
Auslauf- und Ablagerungsgebiet	**gross** Der wirksame Mindestdurchmesser der Bäume ist deutlich geringer als im Transitgebiet und liegendes Holz ist immer wirksam.	**Gefüge horizontal** mind. 400 Bäume/ha mit BHD > 12 cm	**Gefüge horizontal** mind. 600 Bäume/ha mit BHD > 12 cm
		Gefüge horizontal bei Öffnungen[2] in der Falllinie Stammabstand < 20 m evtl. auch Stockausschläge	
		Gefüge vertikal Zieldurchmesser[1] angepasst liegendes Holz und hohe Stöcke: als Ergänzung zu stehenden Bäumen	
		minimale Anforderungen aufgrund des Standortstyps erfüllt	ideale Anforderungen aufgrund des Standortstyps erfüllt

Tab 1 *Anforderungsprofil des Waldes bezüglich Steinschlag (aus Frehner et al 2005). [1] Zieldurchmesser angepasst: Der Zieldurchmesser ist so zu wählen, dass die erforderliche Stammzahl mit dem wirksamen Mindestdurchmesser nachhaltig möglich wird. [2] Öffnungen: Öffnung von Stamm zu Stamm im Stangenholz und Baumholz.*

Richtlinien ist es, möglichst naturnahe, in aller Regel gemischte, vielschichtige Bestände zu erhalten oder zu schaffen. In Tirol wird derzeit im Rahmen des INTERREG IIII B-Projektes «Naturpotenziale alpiner Berggebiete» (NAB) eine flächige Waldtypenkarte mit Beschreibung und ein Waldbauhandbuch erstellt. Dieses neue Werkzeug bietet die Grundlage für die langfristige Schutzwaldbehandlung.

In Italien wurden die wichtigen Schutzwälder während langer Zeit mit einem Bann belegt, d.h. die meisten Massnahmen in Schutzwäldern wie Holzeinschläge wurden untersagt. In letzter Zeit wird aber auch hier vermehrt aktiv in den Schutzwald eingegriffen. Fortbildungsmassnahmen sollen dafür ein Bewusstsein schaffen. So werden beispielsweise in den Regionen Piemont und Aostatal im Rahmen eines INTERREG-Projektes Kurse zu minimalen Pflegemassnahmen in Schutzwäldern für Waldfachleute angeboten. Darüber hinaus wurde 2001 ein Netz von permanenten Aufnahmeflächen eingerichtet, welches erlaubt, die Auswirkungen von waldbaulichen Eingriffen über längere Zeit zu verfolgen. Auf diesen Flächen wurden die aktuelle Schutzwirkung der Wälder gegen die wichtigsten Naturgefahren auf Grundlage des Schutzwaldhandbuchs von der Autonomen Region Valle d'Aosta – Regione Piemonte (2006) erhoben und notwendige Massnahmen zur langfristigen Verbesserung der Schutzwirkung abgeleitet.

In Frankreich wurde letztes Jahr eine sehr detaillierte Richtlinie als Basis für die Schutzwaldpflege unter dem Titel «Guide des sylvicultures de montagne» (Gauquelin et al 2006) veröffentlicht. Ähnlich wie die italienische basiert auch die französische Richtlinie teilweise auf der im Jahr 2005 in der Schweiz erschienenen Wegleitung «Nachhaltigkeit und Erfolgskontrolle im Schutzwald» (NaiS, Frehner et al 2005). Aufgrund der Prioritätensetzung wurden in den Richtlinien beider Länder spezifische, zusätzliche Schwerpunkte gesetzt. In der französischen Richtlinie wird beispielsweise die Schutzwirkung gegen Steinschlag deutlich ausführlicher behandelt als in der Wegleitung NaiS. Die Wegleitung NaiS listet sieben Grundsätze für eine effiziente Schutzwaldpflege auf:

1. Auf das Schutzziel ausgerichtet: Pflegemassnahmen in Schutzwäldern dienen ausschliesslich der Verminderung von Naturgefahren.
2. Am richtigen Ort: Pflegemassnahmen werden dort ausgeführt, wo der Wald die Wirkung von Naturgefahren auf Menschen oder Sachwerte verhindern oder verringern kann.
3. Zur richtigen Zeit: Pflegemassnahmen werden dann ausgeführt, wenn eine optimale Wirkung mit minimalem Aufwand erzielt werden kann.
4. Im Einklang mit den natürlichen Lebensabläufen: Pflegemassnahmen sind auf die Standortverhältnisse abgestimmt. So lassen sich die Kräfte der natürlichen Waldentwicklung nutzen.
5. Objektbezogen, transparent, nachvollziehbar und kontrollierbar: Pflegemassnahmen werden durch Fachleute an Ort und Stelle festgelegt. Damit wird man den kleinräumig wechselnden Verhältnissen gerecht. Der Entscheidungsprozess verläuft immer gleich. Er wird dokumentiert und damit transparent, nachvollziehbar und kontrollierbar gemacht.
6. Wirksam: Pflegemassnahmen führen mit hoher Wahrscheinlichkeit zum Ziel.
7. Ziel mit verhältnismässigem Aufwand erreichbar: Pflegemassnahmen stehen in einem angemessenen Kosten-Nutzen-Verhältnis.

Das Konzept von NaiS beruht auf einem Vergleich des aktuellen Zustands des Bestandes mit Anforderungsprofilen für Naturgefahren und Standortstypen (siehe Frehner et al 2005). Die Anforderungsprofile für Naturgefahren beschreiben dabei eine Bestandesstruktur, welche verschiedene strukturelle Elemente (beispielsweise Stammzahl oder Lückengrösse) berücksichtigt. Diese Struktur bietet gemäss heutigem Wissen eine ausreichende Schutzwirkung gegen eine bestimmte Naturgefahr. Die Anforderungsprofile für Standortstypen fokussieren sich auf die langfristige Sicherstellung der Schutzwirkung, indem beispielsweise für jeden Standort Angaben zur optimalen Durchmischung und Verjüngung gemacht werden. Um nun langfristig die Schutzwirkung sicherstellen zu können, müssen beide Anforderungsprofile erfüllt sein. Beispiele für die beiden Profile finden sich in den Tabellen 1 und 2.

Entscheidungen bezüglich Pflegemassnahmen werden auf lokaler Ebene mit Hilfe eines standardisierten Verfahrens gefällt. Dazu werden Einzugsgebiete in Perimeter mit identischen Anforderungsprofilen bezüglich Naturgefahr und Standort unterteilt. Diese Einteilung in so genannte Zieltypen basiert auf Informationen zu den relevanten Naturgefahrenprozessen sowie auf einer Standortskartierung. Innerhalb der Zieltypen werden dann die Bestände mit einer ähnlichen Bestandesstruktur zu so genannten Behandlungstypen zusammengefasst. Für jeden Behandlungstyp werden die notwendigen Pflegemassnahmen schliesslich auf einer zirka 1 Hektar grossen Weiserfläche, die für den jeweiligen Behandlungstyp repräsentativ ist, bestimmt. Dabei werden der heutige Bestandeszustand sowie dessen erwartete Entwicklung in 10 und 50 Jahren mit den Anforderungsprofilen in einer Checkliste verglichen (Tabelle 3).

Tab 2 Anforderungsprofil bezüglich Standort am Beispiel des Hochstauden-Fichtenwaldes (aus Frehner et al 2005).

60 Typischer Hochstauden-Fichtenwald 60A Hochstauden-Fichtenwald mit Alpenwaldfarn		
Bestandes- und Einzelbaummerkmale	**minimale Anforderungen**	**ideale Anforderungen**
Mischung Art und Grad	Fichte 70–100% Vogelbeere, Grünerle Samenbäume – 30%	Fichte 90–95% Vogelbeere, Grünerle 10%
Gefüge BHD-Streuung	genügend entwicklungsfähige Bäume in mind. 2 verschiedenen Durchmesserklassen pro ha	genügend entwicklungsfähige Bäume in mind. 3 verschiedenen Durchmesserklassen pro ha
horizontal	Rotten, allenfalls Einzelbäume	Rotten, allenfalls Einzelbäume Schlussgrad locker–räumig
Stabilitätsträger Kronen	Kronenlänge mind. 2/3	Kronen bis zum Boden
Stand/Verankerung	meistens lotrechte Stämme mit guter Verankerung, nur vereinzelt starke Hänger	lotrechte Stämme mit guter Verankerung, keine starken Hänger
Verjüngung Keimbett	alle 10 m (100 Stellen/ha) Moderholz vorhanden	alle 8 m (150 Stellen/ha) Moderholz vorhanden
Anwuchs (10 cm bis 40 cm Höhe)	an mind. 1/3 der verjüngungsgünstigen Stellen Fichte und Vogelbeere vorhanden	an mind. 1/2 der verjüngungsgünstigen Stellen Fichte und Vogelbeere vorhanden
Aufwuchs (bis und mit Dickung, 40 cm Höhe bis 12 cm BHD)	mindestens 70 Verjüngungsansätze/ha (durchschnittlich alle 12 m) Mischung zielgerecht	mindestens 100 Verjüngungsansätze/ha (durchschnittlich alle 10 m) Mischung zielgerecht

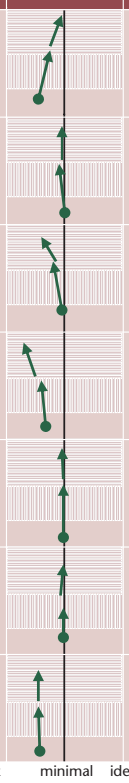
Gemeinde / Ort: Amden / Oberer Sitenwald	Weiserfl. Nr. 5		Datum: 17.4.02	BearbeiterIn: Ehrbar, Schwitter, Frehner, Wasser

1. Standortstyp: 25C Turinermeister-Lindenwald mit Schmerwurz (9 Platterbsen-Buchenwald)

2. Naturgefahr + Wirksamkeit: Steinschlag - Transitgebiet ca. 75%, massgebende Steingrösse Durchmesser 0 bis 50 cm, Pot. Beitrag gross

3. Zustand, Entwicklungstendenz und Massnahmen

Bestandes- und Einzelbaummerkmale	Minimalprofil (inkl. Naturgefahren)	Zustand 2002	Zustand heute Entwicklung in 10, in 50 Jahren	wirksame Massnahmen	verhältnismässig	**6. Etappenziel** Wird in 10 Jahren (2012) überprüft.
Mischung Art und Grad	Li, Ah, Es, Ei, Ki, Mb andere Laubbäume 90–100 % Nadelbäume 0–10%	Li, Ah, Es, BUl, Div., SFö, Lä, Fi Lbb 60 % Fi 15%, SFö,Lä 25% Haselsträucher				Li, Ah, Es, BUl, Div., SFö, Lä, Fi Lbb 75 % Fi 10%, SFö,Lä 15% Haselsträucher
Gefüge (vertikal) BHD Streuung	genügend entwicklungsfähige Bäume in zwei BHD-Klassen, nur vereinzelt Bäume > 50 cm	BHD-Klassen 20 - 40 cm gut vertreten 45 Ndb/ha > 52 cm 9 Lbb/ha > 52 cm				BHD-Klassen 20 - 40 cm gut vertreten
Gefüge (horizontal) DG, Stammzahl Lückenlänge	Öffnungen in Falllinie < 20m Stz. > 24 mind. 300/ha in Öffnungen lieg. Holz	Einzelbäume, grosse Alters-differenzierung Stz . > 24 ca. 320/ha Lothar-Lücken m. lieg. Bäumen				BHD-Klasse > 50 reduziert Stz. > 24 mind. 300/ha
Stabilitätsträger Kronenentwicklung Schlankheitsgrad Zieldurchmesser	mind. die Hälfte der Kronen gleichm. geformt, meistens Stämme mit guter Verankerung nur vereinzelt starke Hänger	viele deformierte Kronen Fichte nicht stabil vereinzelte Hänger		extreme Hänger und schwere Bäume entfernen	x	keine extremen, dicken Hänger
Verjüngung **Keimbett**	vor Schuttbewegung ge-schützte Kleinstandorte vorh. Fläche mit starker Veg.-Konkur. für Es kleiner 1/3	nur geringe Vegetations-konkurrenz		Holz aus Schlag 2003 schräg im Hang liegend (z.T. Ndh-Trämel mit Heli entfernen)		
Anwuchs (10 cm bis 40 cm)	Anwuchs in Lücken vorhanden	flächendeckend vereinzelte Pflanzen vorhanden		Öffnungen 20x25m, (auch für Stockausschläge) Kontrollzaun	x	Anwuchs unter Schirm auf 1/2 der Fläche, Mischung zielgerecht (Anteil Li und Bah mind. 30%)
Aufwuchs (40 cm Höhe – 12 cm BHD)	pro ha mind 2 Trupps (2–5a, durchschnittlich alle 75 m) oder Deckungsgrad mind. 4% Mischung zielgerecht	nur einzelne unterdrückte Lbb - Bäumchen				Aufwuchs in Öffnungen ca. 1.5 m. Mischung gemäss Ziel



4. Handlungsbedarf: ja x nein

5. Dringlichkeit: klein mittel x gross

Tab 3 Beispiel einer ausgefüllten Checkliste zur Herleitung des Handlungsbedarfes und der Pflegemassnahmen (aus Frehner et al 2005).

Falls der in 50 Jahren erwartete Waldzustand die Anforderungsprofile nicht erfüllt, aber waldbauliche Massnahmen die Waldentwicklung positiv, d.h. in Richtung der Anforderungsprofile beeinflussen können, sollen diese ergriffen werden. In einigen Fällen kann aber auch eine gezielte Unterlassung (kein Eingriff) optimal sein. Dies ist zum Beispiel dann der Fall, wenn sich der Bestand selbständig, dank der natürlichen Walddynamik, mit grosser Wahrscheinlichkeit über die geforderten Anforderungsprofile hinaus entwickelt. Solche Fälle können mit Hilfe der standardisierten Entscheidungsfindung eindeutig identifiziert werden.

Die standardisierte Entscheidungsfindung ist zudem sehr wichtig für die Erfolgskontrolle. Diese wiederum ist unerlässlich für eine weitere Entwicklung und Verbesserung der Schutzwaldpflege durch adaptives Management (Walthers 1986). Die Erfolgskontrolle beinhaltet die vier Schritte:

1. Vollzugskontrolle: Sind die Massnahmen am richtigen Ort und fachgerecht ausgeführt worden?

2. Wirkungsanalyse: Wie ist die Wirkung der Massnahmen?

3. Zielerreichungsanalyse: Inwieweit entspricht der Waldzustand den Anforderungsprofilen?

4. Zielanalyse: Sind die Anforderungsprofile zweckmässig oder müssen sie revidiert werden?

Während die ersten beiden Schritte kleinräumig kontrolliert werden (Weiserflächen in den Beständen), werden die Schritte 3 und 4 lokal bis regional überprüft.

Um die Konzeption NaiS im Alpenraum bekannt zu machen, wird in Kürze im Rahmen des INTERREG III C-Projektes Network Mountain Forest (NMF) eine englische Übersetzung der wichtigsten Teile der Wegleitung NaiS erscheinen.

Schutzwaldmonitoring

Für ein effizientes und erfolgreiches Schutzwaldmanagement sind verlässliche und aktuelle Informationen über den Zustand und die Entwicklung der Schutzwälder unerlässlich. Solche Informationen können durch Inventuren und andere Monitoringsysteme erhoben werden. Dabei werden der aktuelle Zustand sowie dessen Veränderungen erfasst. Dies erlaubt schliesslich, die Zusammenhänge zwischen verschiedenen Waldfunktionen unter Einbezug der verschiedenen ökologischen, ökonomischen und sozialen Faktoren zu analysieren. Auf diese Weise stehen objektive Grundlagen für die Entscheidungsfindung zur Verfügung.

Monitoring-Techniken zur objektiven Priorisierung im Schutzwaldmanagement

Bislang gibt es kein allgemein gültiges Monitoring-System im Alpenraum, welches explizit auf Schutzwälder zugeschnitten ist. Das Monitoring in Schutzwäldern wird jedoch durch verschiedene nationale und regionale Inventuren und verschiedene Monitoring-Systeme abgedeckt, welche Informationen zum Zustand dieser Wälder liefern und so beispielsweise zur Priorisierung von Pflegemassnahmen herangezogen werden können.

In Österreich liefern dazu die nationale Waldinventur (ÖWI), der Waldentwicklungsplan (WEP), die Landesschutzwaldkonzepte (LSK) sowie zahlreiche Inventuren von Unternehmen oder Kontrollsysteme relevante Informationen zum Zustand der Schutzwälder. Im Rahmen der ÖWI werden forstliche Kennzahlen durch regelmässige Feldaufnahmen auf einem Stichprobennetz erhoben. Ab 1971 wurden dabei auch spezielle Informationen zum Schutzwald aufgenommen. Beschränkten sich diese Erhebungen anfangs nur auf Schutzwald im Ertrag, wurden ab der Aufnahme 1992/96 auch die nichtproduktiven Schutzwälder berücksichtigt. Der Schutzwaldbegriff laut ÖWI umfasst jedoch ausschliesslich Standortschutzwald. Die Kategorie Objektschutzwald wurde erst im Jahr 2002 durch eine Ergänzung des Forstgesetzes eingeführt und wird somit erst in der gegenwärtigen Inventurperiode berücksichtigt (BMLUFW 2005). Die stetige Zunahme des Detaillierungsgrades beim Aufnahmekatalog zum Schutzwald wiederspiegelt dabei gewissermassen die steigende Bedeutung der Schutzwälder im öffentlichen Bewusstsein. Der Waldentwicklungsplan (WEP) ist Teil der forstlichen Raumplanung, wie sie im Österreichischen Forstgesetz festgehalten ist. Er deckt die gesamten Wälder von Österreich ab und ist momentan das wichtigste Werkzeug, um die Waldfunktionen abzugrenzen. Diese «nationale Waldkarte» gewichtet die Bedeutung der verschiedenen Waldfunktionen (Nutz-, Schutz-, Erholungs- und Wohlfahrtsfunktion). Ein gut fundierter und transparenter Vergleich zwischen der aktuellen und der gewünschten Waldfunktion erlaubt es, die nötigen Massnahmen sowie deren Dringlichkeit und Kosten abzuschätzen. Gemäss diesem Plan hat der Schutz vor Naturgefahren auf rund 26.4% der gesamten Waldfläche Vorrangfunktion. Der Waldentwicklungsplan wird zunehmend für die Aufgaben der generellen Raumplanung genutzt.

Die Landesschutzwaldkonzepte (LSK) werden in Kooperation zwischen den lokalen Forstbehörden und dem Forsttechnischen Dienst für Wildbach- und Lawinenverbauung erstellt. Diese Pläne bilden die Grundlage für die regionalen Schutzwaldprojekte und so genannten flächenwirtschaftlichen Projekte. Anlässlich einer kürzlich durchgeführten Revision der LSK wurde die Unterscheidung zwischen Standort- und Objektschutzwald eingeführt. Gemäss dieser LSK ist in etwa 7.2% der Österreichischen Wälder die Wiederherstellung ihrer Schutzwirkung dringend (Mauser 2006).

Neben der nationalen Waldinventur gibt es in Österreich verschiedene Steuerungs- und Kontrollsysteme, welche in den einzelnen Schutzwaldprojekten angewendet werden. Hauptziel dieser Systeme ist es, die durch Projektmassnahmen angestrebte qualitative und quantitative Verbesserung des Zustandes der Wälder zu erfassen und überwachen. Diese Erhebung erfolgt mit terrestrischen Inventuren, welche im Fünfjahresturnus während der 20-jährigenProjektlaufzeit durchgeführt werden. Die Evaluation gibt nicht nur Auskunft über den Fortschritt der Arbeiten und deren Auswirkungen auf das Gesamtsystem Schutzwald, sondern beinhaltet zusätzlich eine Langzeit-Dokumentation des Projektes. Im Tirol wird diese Art von Überwachung seit 1996 bereits bei etwa 100 Projekten angewendet.

Während die ÖWI detaillierte Informationen zu Artenzusammensetzung, Verjüngung, Totholz und Bestandesstabilität von Schutzwäldern liefert, sind der WEP und die LSK für die Priorisierung von Massnahmen im Schutzwald sowie die zielgerichtete Mittelzuteilung hilfreich. Die oben erwähnten Inventur- und Monitoringsysteme verfolgen verschiedene Ziele und weisen teilweise unterschiedliche Definitionen von Schutzwald auf. Darüber hinaus arbeiten sie auf verschiedenen räumlichen Skalen. Daher ist es zwar möglich, durch den Zusammenzug der verschiedenen Systeme einige generelle Schlüsse zu ziehen, die Inkonsistenz in Terminologie, Definitionen und insbesondere in der Aufnahmemethodik lassen aber eine fundierte, übergreifende Analyse nicht zu. Um dem entgegenzuwirken, schlägt Mauser (2006) vor, die zukünftigen Datenerhebungen zu harmonisieren. Auf diese Weise sollte es möglich sein, die Wirkung des Schutzwaldmanagements auf einheitliche Art zu erheben und so die Basis für ein integratives Schutzwaldmonitoring zu schaffen.

Im Bayerischen Staatswald werden im Abstand von zirka 10 bis 15 Jahren Stichprobeninventuren in den Hochgebirgsforstämtern (seit 2005 Forstbetriebe genannt) durchgeführt. Diese liefern unter anderem Aussagen zum Altersaufbau der Bestände, zur Baumartenzusammensetzung und zur Verjüngungssituation. Im Unterschied zu den Bundeswaldinventuren der Jahre 1987 und 2002 erfolgten die Aufnahmen nicht alle im gleichen Zeitraum. Sie sind damit nicht ohne weiteres auf den ganzen Bayerischen Alpenraum übertragbar. Der Erfolg der Sanierungsmassnahmen wird hingegen intensiv kontrolliert. Auf ausgewählten Sanierungsflächen wurden Dauerbeobachtungsflächen eingerichtet. Mit Hilfe eines Stichprobenverfahrens werden Daten über Pflanzenzahl, Mischungsverhältnis, Wuchsleistung und Schäden erhoben und ausgewertet. Durch Fol-

geaufnahmen, die im 5-jährigen Turnus wiederkehren, werden fundierte Einblicke in die Entwicklung der Verjüngung gewonnen. Langfristig sollen mit diesem Verfahren rund 10% der gesamten Sanierungsfläche erfasst werden (BayStMELF 2000). Neben dieser Stichprobeninventur werden alle Sanierungsflächen jährlich von verbeamteten Forstleuten nach einem einheitlichen Schema beurteilt.

Integrativer Monitoring-Ansatz

Monitoring- und Planungsmassnahmen sind zu koordinieren und zu vereinheitlichen. Dazu sind entsprechende Werkzeuge nötig. Diese Werkzeuge sollen helfen, wichtige Schutzwaldparameter wie zum Beispiel Durchmesserverteilung, Bestandesdichte, -struktur und -lücken durch quantitative Methoden zu erfassen. Um die Werkzeuge inventurübergreifend nutzen zu können, sind die Schutzwaldparameter einheitlich oder zumindest durchgängig zu definieren. Die Parameter müssen so gewählt werden, dass sie einerseits für den Schutzwald und seinen Zustand repräsentativ sind und andererseits auf einfache und kostengünstige Weise erhoben werden können. Die Methodik der Datenaufnahme muss transparent sein, damit die Daten, welche auf verschiedenen Skalen erhoben wurden, vergleichbar sind. Da sich das Management von Schutzwäldern mit sehr langsam ablaufenden natürlichen Prozessen konfrontiert sieht, müssen diese Instrumente zudem in der Lage sein, Veränderungen über lange Zeiträume zu erfassen.

In der Schweiz wird momentan unter der Führung des BAFU ein integrativer Monitoringansatz entwickelt. So wurde in enger Zusammenarbeit zwischen dem Schweizerischen Landesforstinventar (LFI) und den Autoren der Wegleitung NaiS (Frehner et al 2005, siehe oben) eine gemeinsame Definition der relevanten Schutzwaldparameter erarbeitet. Zu diesen Parametern gehören neben Angaben zur Länge und Breite von Waldlücken auch verschiedene Angaben zum Bestand, wie beispielsweise Deckungsgrad, Bestandesdichte, Durchmesserverteilung und Baumartenzusammensetzung. Zur Abschätzung der zukünftigen Entwicklung eines Bestandes werden Angaben zur Mischung, zur Bestandesstruktur und -stabilität, zur Verjüngung sowie zu Merkmalen von Einzelbäumen (z.B. Kronenlänge, Schlankheitsgrad) benötigt. Zusätzlich sind Informationen zum Standort (Bodeneigenschaften, Waldgesellschaften) erforderlich. Einige dieser Parameter werden vorzugsweise terrestrisch erhoben (z.B. Verjüngung), andere können effizienter mit Fernerkundungsmethoden (Luftbilder, Laser-Scanning LIDAR – z.B. für Lücken oder Bedeckungsgrad) erfasst werden. Bei den Standortsdaten handelt es sich grösstenteils um Ergebnisse von Modellierungen (z.B. Waldgesellschaften).

Für jeden Parameter wurden basierend auf der Wegleitung NaiS (Frehner et al 2005) Schwellenwerte festgelegt, welche es erlauben, die aktuelle Schutzwirkung sowie künftige Entwicklung mit Hilfe von LFI-Daten abzuschätzen. Auf diese Art wird es möglich sein, den Handlungsbedarf im Schweizer Schutzwald auf nationalem und regionalem Niveau zu bestimmen. Um sicherzustellen, dass der gewählte Ansatz mit LFI-Daten ähnliche Ergebnisse ergibt wie ein NaiS-Expertengutachten, wurde ein Methodentest auf LFI-Probeflächen vorbereitet.

Der Ansatz kann durch den Einbezug von zusätzlich vorhandenen Datensätzen verfeinert werden. So können beispielsweise digitale Geländemodelle (DGM) oder digitale Oberflächenmodelle (DOM) zur Präzisierung gewisser Merkmale beigezogen werden. Zusätzlich können bereits anderweitig erhobene Daten (beispielsweise Waldgesellschaften, Waldzustand oder geomorphologische Merkmale) bezüglich Naturgefahren mit terrestrischen Erhebungen verifiziert und schliesslich auch ins GIS integriert werden. Mit dieser Integration wird man der Interdisziplinarität von Schutzwald und Naturgefahren auch besser gerecht.

Ausblick

Wie die Beispiele aus den verschiedenen Ländern zeigen, sind im Management von Gebirgswäldern und insbesondere von Schutzwäldern in vielen Ländern des Alpenraums ähnliche Voraussetzungen, Probleme und Perspektiven erkennbar. Erfreulicherweise konnten in mehreren Bereichen des Schutzwaldmanagements in den letzten Jahrzehnten beträchtliche Fortschritte erzielt werden. Trotzdem ist noch einiges Verbesserungspotenzial vorhanden.

Verbesserung der Schutzwaldabgrenzung und -ausscheidung

Das bereits erwähnte Projekt SilvaProtect-CH eröffnet einen viel versprechenden Ansatz, um die Schutzwälder auf grösserer Skala objektiv abzugrenzen. So weit uns bekannt ist, wird in SilvaProtect-CH erstmals ein derart systematischer Ansatz auf nationaler Ebene angewendet. Auch wenn die so generierten Daten in der Praxis nicht direkt für die Ausscheidung der Schutzwälder verwendet werden können, bieten sie doch eine wertvolle und solide Basis für eine systematische und einheitliche Ausscheidung der Schutzwälder in der ganzen Schweiz.

In Österreich und Bayern wird momentan ein ähnlicher Ansatz wie in der Schweiz verwendet, um regionale Gefahrenhinweiskarten zu erstellen: Im EU-Projekt «Einzugsgebiete in alpinen Regionen EGAR» werden bestehende Daten analysiert, um das Gefahren- und das Schadenpotenzial zu ermitteln. Die Herleitung des Gefahrenpotenzials basiert dabei hauptsächlich auf Expertenwissen anhand von Luft-

bildanalysen. Das Schadenpotenzial wird aus Karten und Luftbildern abgeleitet. Die resultierenden Karten von Gefahren- und Schadenpotenzial im Massstab von 1:20000 werden dann verschnitten, um die möglichen Problemzonen, also diejenigen Zonen, wo Naturgefahrenprozesse auf ein relevantes Schadenpotenzial treffen, zu identifizieren. Bislang wurde etwa ein Drittel des Tirols so kartiert. Der Ansatz wurde auch in Bayern eingeführt. Der Wald ist im EGAR-Projekt zwar nicht berücksichtigt, könnte aber einfach einbezogen werden. Mit der Berücksichtigung des Waldes würde die Grundlage für eine systematische Schutzwaldausscheidung gelegt. Dabei könnte der in EGAR verfolgte Ansatz sogar noch genauere Informationen für die Entscheidungsprozesse liefern als das Projekt SilvaProtect-CH. Dies dank dem Umstand, dass in EGAR bereits einige zusätzliche Informationen integriert sind, welche bislang in SilvaProtect-CH vernachlässigt wurden (z.B. Frequenz und Intensität der Naturgefahrenprozesse, Gewichtung des Schadenpotenzials).

Verbesserung der Schutzwaldpflege

Moderne Schutzwaldpflege baut zu einem grossen Teil auf dem Potenzial von natürlichen Ökosystemen (Strukturen und Prozesse) auf und kann damit auch zur Wiederherstellung von natürlichen Ökosystemen beitragen. Da auf diese Art die Pflegemassnahmen vielfach auch an Wirksamkeit und Effizienz gewinnen, ist es nicht erstaunlich, dass in einigen Ländern finanzielle Anreize gesetzt werden, damit diese naturnahen Methoden in Schutzwäldern angewendet werden. Damit werden Waldeigentümer motiviert, das natürliche Potenzial ihrer Wälder auszunützen. Auf diese Weise wurde in der Schweiz das Grundkonzept der minimalen Pflegemassnahmen in Schutzwäldern eingeführt, und die getroffenen Massnahmen werden regelmässig auf ihre Wirksamkeit überprüft (siehe oben). Der Erfolg dieses neuen Ansatzes beruht teilweise sicher auf der Qualität der vorhandenen Richtlinien. Zusätzlich sind aber auch gezielte Bemühungen bei der Umsetzung in der Praxis nötig, indem beispielsweise Ausbildungskurse für Waldarbeiter, Forstwarte und Förster wie auch für Waldeigentümer angeboten werden.

Die momentan erhältlichen Richtlinien beruhen auf dem besten verfügbaren Wissen und sind konzeptionell ausgereift. Dennoch gibt es einige Verbesserungsmöglichkeiten. So bestehen heute noch immer Wissenslücken, was die Auswirkungen der natürlichen oder anthropogen beeinflussten Waldentwicklung auf die Bestandesstruktur anbelangt respektive auf die Schutzwirkung dieser Strukturen gegen verschiedene Naturgefahren. Darüber hinaus fehlt es bislang an ganzheitlichem Wissen zum Schutzwaldsystem. Das Schutzwaldmanagement ist interdisziplinär: So treffen biologische, forstliche, ingenieurtechnische und ökonomische Herausforderungen aufeinander (Wehrli 2005, Brang et al 2006). In Zeiten von begrenzten finanziellen Mitteln für das Schutzwaldmanagement und von erhöhten Ansprüchen an die Schutzwirkung der Wälder sollte die Wissenschaft nicht nur versuchen, auf obige Fragen Antworten zu finden, sondern auch die Möglichkeiten und Risiken, welche mit dem Verzicht auf Schutzwaldpflege verbunden sind, zu klären.

Schutzwälder sind komplexe Systeme. In ihnen treffen langsam wirkende, aufbauende Einflüsse wie die Verjüngung oder das Baumwachstum auf oftmals heftig und schnell wirkende Kräfte wie Lawinen oder Stürme, und dies über lange Zeiträume. Daher sind Schutzwälder schwierig zu untersuchen, geschweige denn zu bewirtschaften. Um diese Schwierigkeiten zu meistern, werden in neuester Zeit vermehrt Simulationsmodelle angewendet. Mit diesen wird das System untersucht und Wissen zur Verbesserung des Schutzwaldmanagements abgeleitet (siehe Dorren et al 2004, Wehrli 2005, Wehrli et al 2006, Brang et al 2007). Modelle können beispielsweise helfen, die oben beschriebenen Richtlinien respektive die darin enthaltenen Anforderungsprofile zu verbessern oder die Auswirkungen der Walddynamik auf die langfristige Schutzwirkung von Wäldern zu untersuchen (Wehrli 2005).

Verbesserung des Schutzwaldmonitorings

Wie bei der Schutzwaldpflege wurden auch beim Schutzwaldmonitoring in den letzten zwanzig Jahren laufend neue Methoden und Technologien entwickelt. So werden heute Methoden der Fernerkundung erfolgreich angewendet, und die Bildverarbeitung hat grosse Fortschritte gemacht. Die aus den verschiedenen Inventuren und anderen Monitoringansätzen generierten Daten werden mittlerweile standardmässig im GIS geführt.

Die technischen Fortschritte eröffnen auch die Möglichkeit, terrestrische Inventuren mit hoch aufgelösten Fernerkundungsdaten zu verknüpfen (z.B. Laser-Scanning LIDAR, Orthofotos und Satellitenbilder). Auf diese Weise kann die Anzahl terrestrischer Stichproben teilweise verringert werden. Die Stichprobenpunkte können als Referenzpunkte zur automatischen oder halbautomatischen Klassifikation und Analyse von multispektralen Fernerkundungsdaten und LIDAR-Oberflächenmodellen beigezogen werden. Darüber hinaus können im GIS auch bereits vorhandene Datensätze mit den Inventuren verknüpft werden, was die Informationsdichte weiter erhöht.

Hoch aufgelöste Bilder sowie LIDAR-Daten sind mittlerweile für grosse Gebiete des Alpenraums verfügbar. Aus LIDAR-Daten können digitale Geländemodelle (DGM) und digitale Oberflächenmodelle (DOM) mit einer Auflösung von etwa einem Meter abgeleitet werden. Durch den Vergleich von DGM

und DOM kann auch die Höhe der massgebenden Vegetation abgeschätzt werden. Für Nadelwälder existieren zudem mittlerweile Ansätze, um einzelne Bäume im DOM anzusprechen und somit Kennzahlen wie Bestandesdichte, Baumhöhen und Kronengrössen abzuleiten. Zusammen mit den terrestrischen Inventurdaten und passenden, praxistauglichen Vorhersagemodellen können schliesslich sogar der Holzvorrat und Merkmale zur horizontalen und vertikalen Bestandesstruktur von LIDAR-Daten abgeleitet werden (Hollaus et al 2006, Maier et al 2006). Für solche Analysen müssen aber die Koordinaten eines Aufnahmepunktes genau bestimmt sein.

Basierend auf morphometrischen Merkmalen und Vegetationstrukturen können aus LIDAR-Daten auch Hinweise zu erosions- oder rutschungsgefährdeten Zonen gewonnen werden, da die LIDAR-Technik den Blick in den Wald respektive auf den Waldboden ermöglicht.

Die Nutzung moderner Technologien war bislang mit einem höheren Kostenaufwand verbunden. Diese Zusatzkosten können aber teilweise wettgemacht werden, indem bei gleicher Resultatgüte die Anzahl terrestrischer Aufnahmepunkte reduziert und bereits existierende Daten verwendet werden. Durch eine stärkere Zusammenarbeit unter den verschiedenen Institutionen, welche Umweltdaten erheben, könnten die Kosten zusätzlich reduziert werden. Anstelle verschiedener Inventuren wäre es zweckmässiger, die vorhandenen Daten zu den verschiedensten biophysikalischen Parametern in einem Monitoringsystem zu vereinen und dieses System dann breit, allenfalls gegen Entschädigung, zugänglich zu machen.

Verbesserung der internationalen Zusammenarbeit im Schutzwaldmanagement

Ein wichtiger Schritt für eine weitere Verbesserung des Schutzwaldmanagements bietet die Verstärkung der interregionalen und internationalen Zusammenarbeit. Erfolgreiche Beispiele solcher Kooperationen sind INTERREG-Projekte. So versuchen beispielsweise im Rahmen des INTERREG III C-Projektes «Network Mountain Forest» (NMF) neun Länder (Österreich, Italien, Slowenien, Schweiz, Deutschland, Liechtenstein, Bulgarien, Slowakei und Griechenland) eine gemeinsame Strategie für Gebirgswälder zu entwickeln. Ein Ziel ist es, die Gebirgswälder auf die EU-Agenda zu bringen. Im derzeit laufenden INTERREG III B-Projekt «Naturpotenziale Alpiner Berggebiete» (NAB) arbeiten Tirol, Südtirol, Bayern, Slowenien und Piemont gemeinsam an einem Schutzwaldmanagementsystem. Dabei werden auf der Basis von Gefahrenhinweiskarten (Projekt EGAR, siehe oben) und über die Modellierung von Waldtypen Empfehlungen abgeleitet, die die Praktiker vor Ort bei der Entscheidung unterstützen sollen. Waldtypenkarten und ein Handbuch stehen mittlerweile zur Verfügung. Die Schweizerische Gebirgswaldpflegegruppe ist in beratender Funktion am Projekt beteiligt. Begleitend werden Schulungen angeboten, damit der naturnahe Waldbau stärker als bisher zum Einsatz kommt. Ähnliche Ansätze gab es im INTERREG III A-Projekt «Gestion durable des forêts de montagne à fonction de protection», in dem italienische, französische und schweizerische Waldmanagement- und Forschungsorganisationen zusammengearbeitet haben.

Um das Schutzwaldmanagement in ganz Europa noch weiter zu verbessern, wäre allerdings eine systematische und permanente Zusammenarbeit notwendig. Diese würde es erlauben, Erfahrungen und Wissen auszutauschen. ■

Literatur

AMT TIROLER LANDESREGIERUNG (2005) Tiroler Waldbericht 2005. Innsbruck: Landesforstdirektion. 46 p.

AMT TIROLER LANDESREGIERUNG (2006) Tiroler Waldbericht 2006. Innsbruck: Landesforstdirektion 25 p.

BARTELT P, STÖCKLI V (2001) The influence of tree and branch fracture, overturning and debris entrainment on snow avalanche flow. Ann Glaciol 32: 209–216.

BAYERISCHER LANDTAG (2006) Interpellation. Umsetzung der Alpenkonvention in Bayern. München: Bayer Landtag, Drucksache 15/5263.

BAYSTMELF (1982) Grundsätze für die Waldbehandlung im bayerischen Hochgebirge. München: Bayer Staatsministerium Ernährung Landwirtschaft Forsten. 71 p.

BAYSTMELF (1997) Handbuch zur Sanierung von Schutzwäldern im bayerischen Alpenraum. München: Bayer Staatsministerium Ernährung Landwirtschaft Forsten. 233 p.

BAYSTMELF (2000) Der Schutzwald in den bayerischen Alpen. Funktionen – Zustand – Sanierung. München: Bayer Staatsministerium Ernährung Landwirtschaft Forsten. 52 p.

BAYSTMELF (2005) Pressemitteilung. Fitnessprogramm für den Bergwald. Miller setzt auf Sanierung, Pflege und Jagd. München: Bayer Staatsministerium Ernährung Landwirtschaft Forsten. 2 p.

BAYSTMELF (2006) Waldzustandsbericht 2006. München: Bayer Staatsministerium Ernährung Landwirtschaft Forsten. 64 p.

BERGER F (1996) Mapping of the protective functions of the mountain's forest. In: Proc Interpraevent, Garmisch-Partenkirchen, vol 1. pp. 171–180.

BERGER F, QUETEL C, DORREN LKA (2002) Forest: a natural protection mean against rockfalls, but with which efficiency? The objectives and methodology of the rockfor project. In: Proc Interpraevent, Pacific Rim, Matsumoto (Japan). pp. 815–826.

BÖLL A, GRAF F (2001) Nachweis von Vegetationswirkungen bei oberflächennahen Bodenbewegungen – Grundlagen eines neuen Ansatzes. Schweiz Z Forstwes 152: 1–11. doi: 10.3188/szf.2001.0001

BMLUFW (2005) Nachhaltige Waldwirtschaft in Österreich – Österreichischer Waldbericht 2004. Wien: Bundesministerium Land- Forstwirtschaft Umwelt Wasserwirtschaft.

BMLUFW (2006) Waldentwicklungsplan. Richtlinie über Inhalt und Ausgestaltung. Wien: Bundesministerium Land- Forstwirtschaft Umwelt Wasserwirtschaft.

BRANG P (2001) Resistance and elasticity: promising concepts for the management of protection forests in the European Alps. For Ecol Manage 145: 107–119.

BRANG P, DUC P (2002) Zu wenig Verjüngung im Schweizer Gebirgs-Fichtenwald: Nachweis mit einem neuen Modellansatz. Schweiz Z Forstwes 153: 219–227. doi: 10.3188/szf.2002.0219

BRANG P, SCHÖNENBERGER W, OTT E, GARDNER RH (2001) Forests as protection from natural hazards. In: Evans J, editor. The forests handbook. Oxford: Blackwell, vol 2. pp. 53–81.

BRANG P, SCHÖNENBERGER W, SCHWITTER R, WASSER B, FREHNER M (2006) Management of protection forests in the European Alps: an overview. For Snow Landsc Res 80 (1): 23–44 .

BRANG P, HALLENBARTER D (2007) Bewertung von Handlungsstrategien in Schutzwäldern: Ein integraler Modellansatz. Schweiz Z Forstw 158: 176–193. doi: 10.3188/szf.2007.0176

BROSINGER F (2004) Integriertes Schutzwaldmanagement im Bayerischen Alpenraum. Konzept und Umsetzung. In: Proc Interpraevent, Riva (Trient), vol III. pp. 23–33.

BUWAL (2001) Lawinenwinter 1998/1999. Bern: Bundesamt Umwelt Wald Landschaft.

CATTIAU V, MARI E, RENAUD JP (1995) Forêt et protection contre les chutes de rochers. Ingéneries – EAI 3: 45–54.

COUVREUR S (1982) Les forêts de protection contre les risques naturels. Nancy: École Nationale du Génie Rural des Eaux et Forêts. 89 p.

DORREN LKA, BERGER F, IMESON AC, MAIER B, REY F (2004) Integrity, stability and management of protection forests in the European Alps. For Ecol Manage 195: 165–176.

DORREN LKA, BERGER F, LE HIR C, MERMIN E, TARDIF P (2005) Mechanisms, effects and management implications of rockfall in forests. For Ecol Manage 215: 183–195.

DORREN LKA ET AL (2007) State of the art in rockfall – forest interactions. Schweiz Z Forstwes 158: 128–141. doi: 10.3188/szf.2007.0128

FREHNER M, WASSER B, SCHWITTER R (2005) Nachhaltigkeit und Erfolgskontrolle im Schutzwald – Wegleitung für Pflegemassnahmen in Wäldern mit Schutzfunktion. Bern: Bundesamt Umwelt Wald Landschaft. 564 p.

FREY W, THEE P (2002) Avalanche protection of windthrow areas: A ten year comparison of cleared and uncleared starting zones. For Snow Landsc Res 77: 89–107.

GAUQUELIN X ET AL (2006) Guide des sylvicultures de montagne. Grenoble: Cemagref. 289 p.

GSTEIGER P (1993) Steinschlagschutzwald. Ein Beitrag zur Abgrenzung, Beurteilung und Bewirtschaftung. Schweiz Z Forstwes 144: 115–132.

HAMILTON LS (1992) The protective role of mountain forests. Geojournal 27: 13–22.

HEGG C, BADOUX A, WITZIG J, LÜSCHER P (2005) Forest influence on runoff generation. In: Commarmot B, Hamor F, editors. Natural forests in the temperate zone of Europe – values and utilization. Birmensdorf: Eidgenöss Forsch. anst Wald Schnee Landsch, Proc. pp. 72–79.

HOLLAUS M, WAGNER W, EBERHÖFER C, KAREL W (2006) Accuracy of large-scale canopy heights derived from LiDAR data under operational constraints in a complex alpine environment. ISPRS J Photogrammetry Remote Sensing 60: 323–338.

IN DER GAND H (1978) Verteilung und Struktur der Schneedecke unter Waldbäumen und im Hochwald. In: Mountain forests and avalanches, Proc IUFRO Working Party «Snow and Avalanches», Swiss Institute for Snow and Avalanche Research, Davos. pp. 97–122.

JAHN J (1988) Entwaldung und Steinschlag. In: Proc Interpraevent, Graz, vol 1. pp. 185–198.

KUPFERSCHMID ALBISETTI AD (2003) Succession in a protection forest after Picea abies die-back. Zürich: Eidg Techn Hochschule, PhD Thesis. 237 p.

KUPFERSCHMID ALBISETTI AD (2004) Wie gut schützen Totholzbestände vor Naturgefahren? Schutzwirkung von Gebirgsfichtenwäldern nach Buchdruckerbefall. Wald und Holz 85 (1): 33–36.

LAATSCH L, GROTTENTHALER W (1973) Labilität und Sanierung der Hänge in der Alpenregion des Landkreises Miesbach. München: Bayer Staatsministerium Ernährung Landwirtschaft Forsten. 56 p.

LAFORTUNE M, FILION L, HÉTU B (1997) Dynamique d'un front forestier sur un talus d'éboulis actif en climat tempéré froid (Gaspésie, Québec). Geogr Phys Quat 51: 1–15.

LINGUA E, COLLATIN A, HAUDEMAND JC (2003) Individuazione ed analisi delle foreste di protezione diretta (FPD) nel comune di Cogne (Valle d'Aosta). In: Proc 7th Conferenza Nazionale ASITA, l'informazione territoriale e la dimensione tempo, Verona (28–31 Oct 2003). pp. 1325–1330.

MAIER B, TIEDE D, DORREN LKA (2006) Assessing mountain forest structure using airborne laser scanning and landscape metrics. Salzburg: Int Archives Photogrammetry Remote Sensing Spatial Information Sciences XXXVI-4/C42.

MARGRETH S (2004) Die Wirkung des Waldes bei Lawinen. Birmensdorf: Eidgenöss Forsch.anst Wald Schnee Landsch, Forum für Wissen. pp. 21–26.

MAHRER F ET AL (1988) Schweizerisches Landesforstinventar: Ergebnisse der Erstaufnahme 1982–1986. Birmensdorf: Eidgenöss Forsch.anst Wald Schnee Landsch, Ber 305.

MAUSER H (2006) Überregionale Schutzwaldinventuren in Österreich. Österreichischer Walddialog – Modul I. http://www.walddialog.at/filemanager/list/16029/ (3 Apr 2007).

MELONI F, LINGUA E, MOTTA R (2005) Utilizzo di strumenti GIS per l'individuazione automatica delle foreste di protezione diretta in Valle d'Aosta. In: Proc 9th Conferenza Nazionale ASITA, Catania (15–18 Nov 2005). pp. 1499–1504.

MELONI F, LINGUA E, MOTTA R, (2006) Analisi della funzione protettiva delle foreste: l'esempio della «Carta delle foreste di protezione diretta della Valle d'Aosta». Forest@ 3: 420–425. http://www.sisef.it/ (3 Apr 2007).

MOTTA R, HAUDEMAND JC (2000) Silvicultural planning in protection forests in the European Alps: an example of planning in the Aosta Valley. Mt Res Dev 20: 74–81.

O'HARA KL (2006) Multiaged forest stands for protection forests: concepts and applications. For Snow Landsc Res 80 (1): 45–56.

OLIVER CD, LARSEN BC (1990) Forest stand dynamics. New York: McGraw-Hill. 467 p.

OMURA H, MARUMO Y (1988) An experimental study of the fence effects of protection forests on the interception of shallow mass movement. Mitt Forstl Bundesvers.anst Mariabrunn Wien 159: 139–147.

OTT E, FREHNER M, FREY HU, LÜSCHER P (1997) Gebirgsnadelwälder – Ein praxisorientierter Leitfaden für eine standortgerechte Waldbehandlung. Bern: Haupt. 287 p.

PLANAT (2005) Strategie Naturgefahren Schweiz. Synthesebericht. Bern: Bundesamt Wasser Geologie, Nationale Plattform Naturgefahren. 88 p.

PLOCHMANN R (1985) Der Bergwald in Bayern als Problemfeld der Forstpolitik. Allg Forst Jagdztg 156: 138–142.
REGIONE AUTONOMA VALLE D'AOSTA, REGIONE PIEMONTE (2006) Selvicoltura nelle foreste di protezione. Esperienze ed indirizzi gestionali in Piemonte e Valle d'Aosta. Arezzo: Compagnia delle foreste. 224 p.
RICKLI C, GRAF F, GERBER W, FREI M, BÖLL A (2004) Der Wald und seine Bedeutung bei Naturgefahren geologischen Ursprungs. Birmensdorf: Eidgenöss Forsch.anst Wald Schnee Landsch, Forum für Wissen. pp. 27–34.
RICKLI C, ZIMMERLI P, BÖLL A (2001) Effects of vegetation on shallow landslides: an analysis of the events of August 1997 in Sachseln, Switzerland. In: Kühne M et al, editors. International conference on landslide causes, impacts and countermeasures (Davos, Switzerland).
ROTTMANN M (1986) Wind- und Sturmschäden im Wald: Beiträge zur Beurteilung der Bruchgefährdung, zur Schadensvorbeugung und zur Behandlung sturmgeschädigter Nadelholzbestände. Frankfurt: Sauerländer. 128 p.
ROTTMANN M (1985) Schneebruchschäden in Nadelholzbeständen: Beiträge zur Beurteilung der Schneebruchgefährdung, zur Schadensvorbeugung und zur Behandlung schneegeschädigter Nadelholzbestände. Frankfurt: Sauerländer. 159 p.
SANDRI A (2006) Vom Nutzen des Waldes. Referat Fachtagung 200 Jahre Bergsturz von Goldau.
SCHÄRER W (2004) Der Schutzwald und seine Bedeutung in der Waldpolitik des Bundes. Birmensdorf: Eidgenöss Forsch.anst Wald Schnee Landsch, Forum für Wissen. pp. 87–90.
SCHÖNENBERGER W, BRANG P (2004) Silviculture in mountain forests. In: Burley J, Evans J, Youngquist JA, editors. Encyclopedia of forest sciences. Amsterdam: Elsevier. pp. 1085–1094.
SCHÖNENBERGER W, NOACK A, THEE P (2005) Effect of timber removal from windthrow slopes on the risk of snow avalanches and rockfall. For Ecol Manage 213: 197–208.
SONNIER J (1991) Analyse du rôle de protection des forêts domaniales de montagne. Rev for fr 43: 131–145.
WALTHERS CJ (1986) Adaptive management of renewable resources. New York: McGraw Hill. 374 p.
WILFORD DJ, SAKALS ME, INNES JL (2003) Forestry on fans: a problem analysis. For Chron 79: 291–296.
WEHRLI A (2005) Mountain forest dynamics and their impacts on the long-term protective effect against rockfall – a modelling approach. Zürich: Eidg Techn Hochschule, PhD Thesis. 180 p.
WEHRLI A ET AL (2006) Modelling the long-term effects of forest dynamics on the protective effect against rockfall. For Snow Landsc Res 80 (1): 57–76.
ZAMPA F, CIOLLI M, CANTIANI MG (2004) A GIS procedure to map forests with a particular protective function. Geomatics workbooks 3. http://geomatica.como.polimi.it (2 Apr 2007).
ZERLE A, HEIN W, BRINKMANN D, FOERST C, STÖCKEL H (2006) Forstrecht in Bayern. Kommentar. Stuttgart: Deutscher Gemeindeverlag.

Schutzwaldmanagement in den Alpen – eine Übersicht

Viele Gebirgswälder im Alpenraum schützen Siedlungen und Infrastrukturen vor Naturgefahren. Sie werden als Schutzwälder bezeichnet. Ihre Pflege wird so ausgerichtet, dass sie dauerhaft eine möglichst hohe Schutzwirkung erbringen können. Die Pflege und das Management dieser Wälder werden laufend verbessert und haben mittlerweile einen hohen Stand erreicht. Die Wirkung des Waldes gegen Naturgefahren wird immer besser verstanden. Im Moment sind im Alpenraum mehrere Projekte im Gang, mit welchen die Beurteilung der Naturgefahren und des Schadenpotenzials und darauf aufbauend die Ausscheidung von Schutzwäldern harmonisiert werden sollen. Ziel ist es, die Mittel für die Gefahrenprävention noch gezielter einzusetzen. Weiteres Verbesserungspotenzial liegt im Monitoring mit moderner Technologie (Laser-Scanning LIDAR), in der Verknüpfung von Inventurdaten aus unterschiedlichen Quellen, in Simulationsmodellen, um den Langzeitnutzen von Massnahmen im Schutzwald besser beurteilen zu können, sowie in der grenzüberschreitenden Zusammenarbeit.

Gestion des forêts protectrices dans les Alpes – un aperçu

Dans les Alpes, de nombreuses forêts protègent des localités et des infrastructures contre les dangers naturels. Elles sont désignées comme forêts protectrices. Elles sont soignées de façon à offrir durablement un effet protecteur aussi grand que possible. L'entretien et la gestion de ces forêts sont constamment améliorés et ont atteint un niveau élevé. L'effet de la forêt contre les dangers naturels est de mieux en mieux connu. Plusieurs projets sont en cours dans l'arc alpin en vue d'harmoniser l'appréciation des dangers naturels et des dommages potentiels, et, à partir de là, la délimitation des forêts protectrices. L'objectif est d'utiliser les moyens disponibles pour la prévention des dangers de manière encore plus ciblée. Les possibilités d'amélioration se situent dans le suivi au moyen de techniques modernes (Laser-Scanning LIDAR), dans la liaison avec des données d'inventaire provenant de différentes sources, dans les modèles de simulation permettant de mieux évaluer l'efficacité à long terme des mesures en forêt protectrice, ainsi que dans les collaborations transfrontalières.

> Chapter 3

A review of rockfall mechanics and modelling approaches



Progress in Physical Geography 27,1 (2003) pp. 69–87

A review of rockfall mechanics and modelling approaches

Luuk K.A. Dorren

Institute for Biodiversity and Ecosystem Dynamics, Universiteit van Amsterdam, Nieuwe Achtergracht 166, NL-1018 WV Amsterdam, the Netherlands

Abstract: Models can be useful tools to assess the risk posed by rockfall throughout relatively large mountainous areas (>500 km^2), in order to improve protection of endangered residential areas and infrastructure. Therefore the purpose of this study was to summarize existing rockfall models and to propose modifications to make them suitable for predicting rockfall at a regional scale. First, the basic mechanics of rockfall are summarized, including knowledge of the main modes of motion: falling, bouncing and rolling. Secondly, existing models are divided in three groups: (1) empirical models, (2) process-based models and (3) Geophysical Information System (GIS)-based models. For each model type its basic principles and ability to predict rockfall runout zones are summarized. The final part is a discussion of how a model for predicting rockfall runout zones at a regional scale should be developed. A GIS-based distribution model is suggested that combines a detailed process-based model and a GIS. Potential rockfall source areas and falltracks are calculated by the GIS component of the model and the rockfall runout zones are calculated by the process-based component. In addition to this model, methods for the estimation of model parameters values at a regional scale have to be developed.

Key words: distributed model, GIS, modelling, natural hazard, rockfall.

I Introduction

In mountainous areas rockfall is a daily occurrence. The unpredictability of the frequency and magnitude of rockfall potentially endangers human lives and infrastructure. There are numerous examples of infrastructure destroyed or people killed by rockfall (e.g., Porter and Orombelli, 1980; Bunce *et al.*, 1991; Badger and Lowell, 1992). To protect endangered residential areas and infrastructure, it is necessary to assess the risk posed by rockfall.

Rockfall is a relatively small landslide confined to the removal of individual and superficial rocks from a cliff face (Selby, 1982). Rockfall can generate large-scale mass

Tel., +31-20-5257420; fax, +31-20-5257431; e-mail, l.dorren@science.uva.nl

© Arnold 2003 10.1191/0309133303pp359ra

movements of rock material, but these processes are defined as rockslides or rock avalanches (see also Abele, 1994; Cruden and Varnes, 1996). Very occasionally, rockfall initiates catastrophic debris streams, which are even more dangerous (Hsü, 1975). Distinct evidences of rockfall are talus slope deposits at the foot of steep cliff faces, but rockfall also occurs on slopes covered with vegetation where evidence is less distinct.

Protective measures against rockfall can be taken by, for example, constructing catch or barrier fences and restraining nets (Hearn *et al*., 1992; Spang and Sponser, 1995; Peila *et al*., 1998), but these measures are expensive and they deteriorate with time. In some cases the maintenance of forest stands with an explicit protection function, or a protection forest, is cost-effective and more sustainable (Kienholz and Mani, 1994; Motta and Haudemand, 2000). However, in many mountainous regions it is not known whether active forest management ensures effective protection against rockfall.

One way to investigate the efficacy of a protection forest against rockfall is to carry out field experiments by throwing rocks through different types of forests and monitoring the number of rocks stopped by the forest. Unfortunately, this method is time- and labour-consuming, especially if it is required to assess the efficacy of all the protection forests throughout large mountainous areas. An alternative is to simulate falling rocks through forests using computer models. The large goal of using such modelling approaches is to predict rockfall activity and assess the function of forests for protecting human lives and infrastructure at a regional scale.

As a means of reaching this large goal the purpose of this literature study was to summarize the requirements for a model that predicts the risk posed by individual falling rocks at a regional scale. To reach this objective, three questions have to be answered. First, what are the main mechanics of rockfall? Secondly, which rockfall models have already been developed and tested? Thirdly, what are the components of existing models that predict rockfall runout zones at a regional scale? This review is structured on the basis of these three questions. Finally, the required components for a regional scale rockfall model will be discussed.

II Rockfall mechanics

1 Causes of rockfall

Rockfall starts with the detachment of rocks from bedrock slopes, which is mostly a cliff face in the case of a rockfall source area. All bedrock slopes are subject to various degrees of weathering, which may lead to fracturing, opening of joints and therefore to promotion of rockfall. The degree of rockfall promotion depends on the environmental factors causing physical and chemical weathering, and on the bedrock type (Schumm and Chorley, 1964; Day, 1997). Apart from the weathering rates, trigger mechanisms also determine whether rockfall occurs or not. In the literature, a wide range of rockfall trigger mechanics and conditions have been already described. These rockfall trigger mechanics can actually be divided into rockfall promoters and causes of the actual start of movement. However, in reality it is difficult to make a distinction between promoters and actual causes of rockfall, since often a certain process promotes weathering and causes rockfall, such as frost shattering. The slope morphology and the direct

surrounding of the potential falling rock are the most important factors determining whether a rock could fall.

A well-known promoter and cause of rockfall is frost–thaw activity (Grove, 1972; Porter and Orombelli, 1980, 1981; Coutard and Francou, 1989; McCarrol *et al*., 1998; Matsuoka and Sakai, 1999). Gardner (1983) observed rockfall in the Canadian Rocky Mountains and concluded also that rockfall occurs especially on glacially oversteepened rock slopes that are exposed to alternating freezing and thawing. These rockfalls were low magnitude, high frequency events, which is typical for rockfall in alpine areas (Matsuoka and Sakai, 1999; Hungr *et al*., 1999; Jomelli and Francou, 2000). Douglas (1980) also studied low magnitude, high frequency rockfalls in Ireland and also found strong indications of frost-induced rockfall. However, Douglas (1980) stated that geotechnical properties of the bedrock material also played an important role. This is consistent with the results of Luckman (1976), who showed that rockfall is controlled by both the morphological and geological character of the cliff and rock surface temperature fluctuations.

Zellmer (1987), Bull *et al*. (1994) and Vidrih *et al*. (2001) described another cause of rockfall. They investigated the relationship between rockfall and seismic activity and concluded that rockfall was activated by seismic activity. Wieczorek *et al*. (1995, 2000) reported that rockfalls in the Yosemite valley were caused by different factors, such as earthquakes, rain storms, rapid snow melt, freeze–thaw cycles of water in joints, root penetration and wedging, or stress relief following deglaciation. They documented about 400 slope movements, among which rockfalls and rockslides have been more numerous than other types of slope movement. In about half the reports on slope movements, the trigger was either unreported or unrecognized. The reported events show that large winter rainstorms, rapid snowmelt and earthquakes triggered more movements than did freeze–thaw conditions or human activities (Wieczorek and Jäger, 1996).

Human activities leading to decreased stability of hill slopes in hard rock are still a minor factor compared with geological factors, but locally it can be of great importance, for example undercutting of slopes during quarrying or excavations for infrastructure (Selby, 1982). In addition, animals can cause rockfall, for example chamois climbing steep cliff faces.

This overview shows that various factors were reported as causes of rockfall but, in most cases, a combination of topographical, geological and climatological factors and time determine whether rockfall occurs.

2 Modes of motion of falling rocks

After the rock has been detached and starts to move, it descends the slope in different modes of motion. These modes of motion strongly depend on the mean slope gradient (Figure 1). The three most important modes of motion are freefall through the air, bouncing on the slope surface and rolling over the slope surface. In the following sections these modes of motion will be described in detail.

a Freefall of rocks: Freefall of rocks occurs on very steep slopes. According to Ritchie (1963) freefall occurs if the slope gradient below the potential falling rocks exceeds 76°,

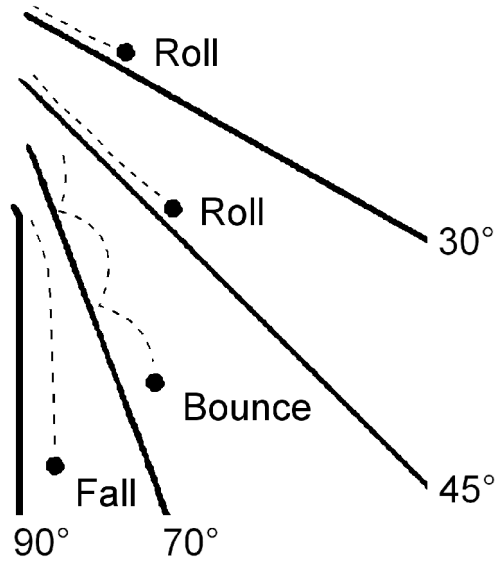


Figure 1 General modes of motion of rocks during their descent on slopes related to the mean slope gradients (modified from Ritchie, 1963 with permission of the Transport Research Board)

but in different field situations this value varies, therefore Figure 1 shows that around 70° the motion of the rock gradually transforms from bouncing to falling.

During freefall of rocks two different movements can occur. The first is translation of the centre of rock and the second is rotation of the block around its centre (Azzoni *et al.*, 1995). Translation and rotation are important, because falling rocks are hardly ever round. Following rotation in the air a rock can jump onto a different direction after impact compared with preceding directions.

Air friction influences the velocity of a freefalling rock, but according to Bozzolo and Pamini (1986) the air friction has no significant effect on the motion of the rock. Another influencing factor on freefalling rocks and their fall tracks is collision with other falling rocks, but these effects are hard to analyse during rockfall events or field investigations (Azzoni *et al.*, 1995).

b Movement at or near the slope surface: If the mean slope gradient decreases in the down-slope section, a rock collides on the slope surface after freefalling, which is defined as bouncing. During the first bounce rocks tend to break, especially incompetent rocks (Bozzolo and Pamini, 1986). Whether or not a rock breaks, 75–86% of the energy gained in the initial fall is lost in that first impact (Broilli, 1974; Evans and Hungr, 1993).

If the mean slope gradient is less than approximately 45°, a bouncing rock gradually transforms its motion to rolling because the rock gathers rotational momentum. A rolling rock is almost constantly in contact with the slope surface (Hungr and Evans, 1988). During the transition between bouncing and rolling, the rock rotates very fast and only the edges with the largest radius maintain contact with the slope. Thereby the

centre of gravity moves along an almost straight path, which is an effective mode of motion with respect to energy loss. In fact, this combination of rolling and short bounces is one of the most economic displacement mechanisms (Erismann, 1986). Sliding is another mode of motion over the slope surface, but this generally only occurs in the initial and final stages of a rockfall. If the mean slope gradient increases, a sliding rock starts falling, bouncing or rolling. If the mean slope gradient does not change while sliding, the rock usually stops because of energy loss due to friction (Bozzolo and Pamini, 1986).

c Retardation of moving rocks: After different modes of motion a moving rock stops. The velocity and therefore stopping of a falling rock mainly depends on the mean slope gradient, since falling rocks generally accelerate on steeper slopes and decelerate on flatter slopes. But apart form the mean slope gradient the velocity also depends on the size of the rock and on the material covering the slope such as soil, scree and vegetation.

Small rocks retard more easily than bigger rocks; first, because during a rockfall the total kinetic energy of small rocks is lower than that of bigger rocks, secondly large obstacles such as trees can more easily stop small rocks, thirdly, small rocks retard more easily in depressions between larger rocks on talus slopes. These are the main causes of the sorting effect on talus slopes (Kirkby and Statham, 1975; Statham, 1976; Statham and Francis, 1986). Fine material is found near the base of the rock face and down slope the average rock size increases. The biggest rocks are mostly found near the base of the talus slope (Evans and Hungr, 1993). On alpine talus slopes this sorting effect is neither linear nor fully exponential. Generally, the sorting effect only accounts for the upper part of the talus slope, since avalanches deposit boulders with variable rock sizes mainly at the base of talus slopes (Jomelli and Francou, 2000).

Stopping of rocks is an abrupt rather than a gradual process. Stopping occurs because energy is lost through collisions and friction forces that act on the rock during transport over slope surfaces. The friction force of a moving rock is not only dependent on the rock shape, but also on the surface characteristics of the slope (Statham and Francis, 1986). Slope surface characteristics can vary a lot within short distances. Therefore the friction force between a rock and the slope surface can best be characterized by a dynamic angle of friction (Kirkby and Statham, 1975). The dynamic angle of friction is related to the surface roughness (Chang, 1998), which can be defined as the variation in height perpendicular to the slope within a certain slope distance (Pfeiffer and Bowen, 1989). Kirkby and Statham (1975) defined the dynamic angle of friction for a falling rock as,

$$\tan \phi_{\mu d} = \tan \phi_0 + k * d \,/\, (2 * R) \qquad (1)$$

where, $\phi_{\mu d}$ is dynamic angle of friction (°); ϕ_0 is angle of internal friction (°) (between 20.3° and 33.8°); k is a constant (between 0.17 and 0.26); d is mean diameter of scree on the slope surface (m); R is radius of the rock (m).

With respect to scree transport on slopes, much research has been done to investigate transport mechanisms and deposition rates (Kirkby and Statham, 1975; Statham, 1976; Carson, 1977; Statham and Francis, 1986; Blijenberg, 1995; Hétu and Gray, 2000; Jomelli and Francou, 2000). However, there is little quantitative information available on the effect of forest cover on the transport of scree or large rocks.

Jahn (1988) carried out one of the few quantitative studies on the effect of forest cover

on rockfall and concluded that three to ten times as many falling rocks were stopped on forested slopes compared with similar slopes without a forest cover. Zinggeler *et al*. (1991) also investigated the importance of trees in stopping falling rocks and concluded that topography is just as important; falling rocks lose energy by colliding with tree stems, which eventually results in stopping on flatter areas in the terrain. Hétu and Gray (2000) observed the effect of forest on scree transport on slopes. They related an increased rock concentration along forest fringes on talus slopes to an increased forest density. According to them, there is a constantly ongoing battle between active talus slope development and forest colonization. The active front zone of the talus slope displaces downslope if a forest is disturbed by a large-scale mass movement or fire. This study indicated that forests cannot stop the devastating effect of large magnitude rockfall events, but for low magnitude–high frequency rockfall events forest provide effective protection. Still, much is unknown about the quantitative effect of forest cover on rockfall.

III Comparison of rockfall models

There are many different models for calculating runout zones of rockfall events. All existing rockfall models can be categorized in three main groups: (1) empirical models, (2) process-based models and (3) GIS-based models. The basic principles of each group of models and some examples will be described in this section.

1 Empirical models

Empirical rockfall models are generally based on relationships between topographical factors and the length of the runout zone of one or more rockfall events. Sometimes these models are referred to as statistical models (Keylock and Domaas, 1999). Tianchi (1983) established two relationships on the basis of recorded data from 76 major rockfalls. One relationship is an inverse logarithmic correlation between the volume of the rockfall and the ratio of the maximum vertical drop to the maximum horizontal distance travelled. The second relationship is a positive logarithmic correlation between the volume of the rockfall and the area covered by the fallen mass. On the basis of the two correlations Tianchi (1983) developed a model for a preliminary estimate of the extent of a threatening rockfall, if the volume can be estimated. Moriwaki (1987) did a comparable study and found a relationship between the angle of a line connecting the toe with the crown of the rupture and, first, the ratio of the maximum vertical drop to the maximum horizontal distance travelled and, secondly, the landslide volume.

Toppe (1987) and Evans and Hungr (1993) suggest the *Fahrböschung* principle (Heim, 1932) to predict run out zones of rockfall events. The *Fahrböschung* is the angle between a horizontal plane and a line from the top of a rockfall source scar to the stopping point for any given rockfall (Figure 2). It is important that the line follows the falltrack of the boulder. An alternative principle suggested by Evans and Hungr (1993) is the *minimum shadow angle*, following Lied (1977). This is the angle of a straight line between the highest point of the talus slope and the stopping point of the longest runout boulder for any given rockfall (Figure 2). Comparing the outcomes of several studies, the minimum

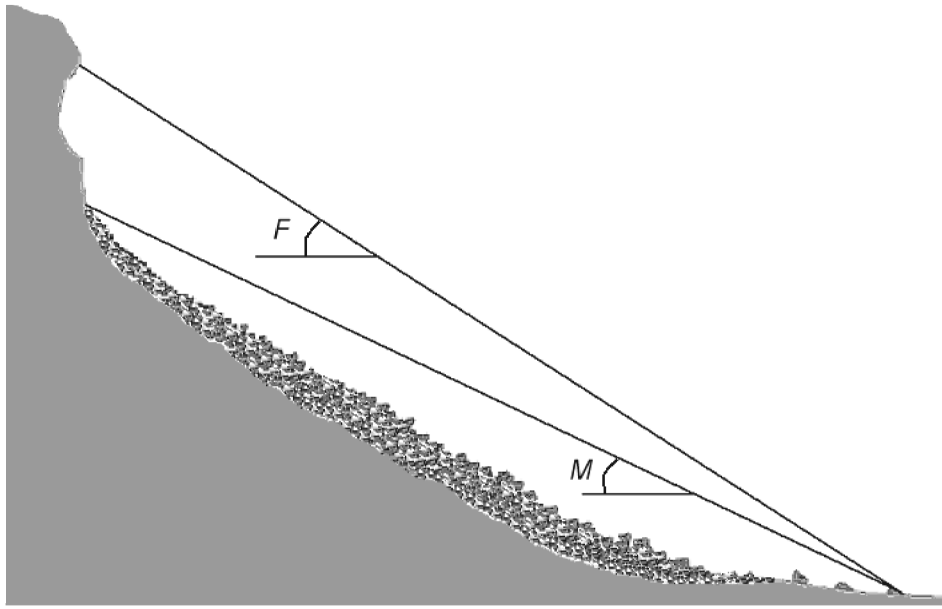


Figure 2 The *Fahrböschung* (*F*) and the *minimum shadow angle* (*M*) of a talus slope (modified from Meissl, 1998 with permission of the author)

shadow angle lies between 22° and 30° (Rapp, 1960; Govi, 1977; Lied, 1977; Hungr and Evans, 1988; Evans and Hungr, 1993). Evans and Hungr (1993) reported a *minimum shadow angle* of 27.5° after investigating 16 talus slopes in British Columbia. According to them, the *minimum shadow angle* is preferable to the *Fahrböschung*, but both should only be used for a first approximation of the length of a rockfall runout zone.

Keylock and Domaas (1999) tested three empirical models on their ability to predict the maximum length of rockfall runout zones using simple topographic parameters. The models were tested using rockfall data presented by Domaas (1994). Their first model was the *height function model*. This model assumes that the runout distance beyond the foot of the talus slope can be derived from the combined vertical height of the free rock face and the talus slope. Their second model was the α-β *model* following Heim (1932), Hsü (1975) and Körner (1976, 1980). The α-β *model* is based on the correlation between the average energy of an extreme rockfall event, where a boulder stops beyond the foot of the talus slope and the energy of an average event, where the boulder stops at the foot of the talus slope. Their third model was the *runout ratio* model, which is based on a model for estimating snow avalanche travel distance developed by McClung and Lied (1987). The *runout ratio model* describes the ratio between the horizontal length of the runout zone to the combined horizontal length of the talus slope and the free rock face. After statistical analysis of the model results and the field data on rockfall events presented by Domaas (1994), the most accurate model of the three tested by Keylock and Domaas (1999) appeared to be the *runout ratio model*.

2 Process-based models

Process-based models describe or simulate the modes of motion of falling rocks over slope surfaces. Kirkby and Statham (1975) and Statham (1976) developed a process-based rockfall model for transport of rocks over talus slopes, assuming that rocks only slide over a talus slope surface. The model results were compared with results of laboratory experiments. The model first calculated the velocity of the falling rock at the base of the cliff, following,

$$v = \sqrt{2 * g * h} \tag{2}$$

where, v is velocity (m s^{-1}); g is acceleration due to gravity (9.81) (m s^{-2}); and h is fall height (m).

On the basis of this velocity, the component of the fall velocity parallel or tangential to the slope surface was calculated, assuming that this component of the velocity is being conserved during the first impact of the rock on the slope surface. Finally the stopping position was calculated by the ratio of the fall velocity and a frictional force, which was determined by the dynamic angle of friction (see section II, 2, c).

Keylock and Domaas (1999) developed the *simple dynamics rockfall model*, which is a process-based model based on the model of Kirkby and Statham (1975). The *simple dynamics rockfall model* was tested using rockfall data presented by Domaas (1994). Their model calculated the travel distance over the slope surface on the basis of the friction force according to Kirkby and Statham (1975) and the acceleration due to gravity. On the basis of calculated exceedance probabilities of modelled rockfall travel distances, Keylock and Domaas (1999) concluded that the *simple dynamics rockfall model* did not appear to hold a significant advantage over the empirical models tested in their study.

In addition to the models of Kirkby and Statham (1975) and Keylock and Domaas (1999), there is a large group of process-based models that are rather similar (Wu, 1985; Bozzolo and Pamini, 1986; Hungr and Evans, 1988; Bozzolo *et al*., 1988; Pfeiffer and Bowen, 1989; Kobayashi *et al*., 1990; Evans and Hungr, 1993; Budetta and Santo, 1994; Chen *et al*., 1994; Azzoni *et al*., 1995, Chau *et al*., 1998). Three factors correspond in all these models. First, these process-based models are two-dimensional slope-scale models that restricted falling boulders to move in a vertical plane. Consequently, lateral movements were not simulated. Secondly, the rockfall track was defined as a composite of connected straight lines with a slope angle equal to the measured mean slope gradient on the represented segment of the rockfall track as visualized in Figure 3.

Finally, motions were simulated as a succession of flying phases and contact phases. The flying phase was simulated with a parabola equation based on the initial velocity in x and y directions and the acceleration due to gravity. The collision point of the rock on the slope surface was calculated with the intersection of the parabolic flying function and the straight slope segments.

The first difference between these two-dimensional process-based models is that some of these models considered a falling rock with its mass concentrated in one point (Wu, 1985; Hungr and Evans, 1988; Pfeiffer and Bowen, 1989; Kobayashi *et al*., 1990; Evans and Hungr, 1993), while other models considered the falling rock as an ellipsoidal body (Bozzolo and Pamini, 1986; Bozzolo *et al*., 1988; Azzoni *et al*., 1995).

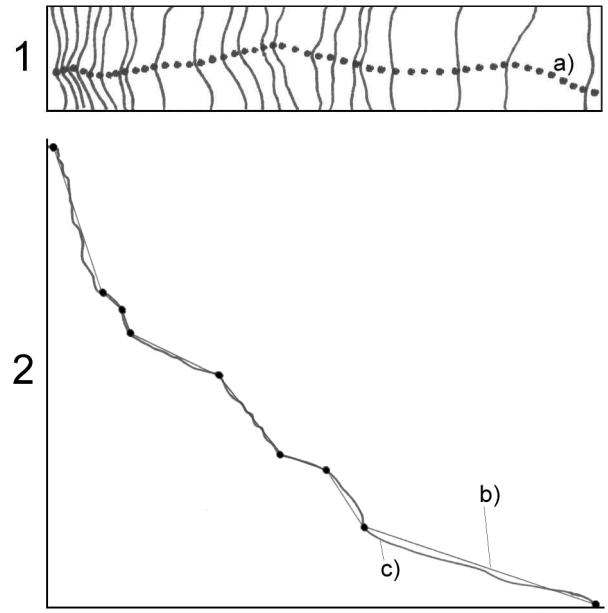


Figure 3 The upper figure (1) shows the actual rockfall path (a) projected on a contour line map. The lower figure (2) shows the slope segments (b) used in two-dimensional rockfall models representing the actual slope of the rockfall path (c)

Secondly, some models simulated the movement at or near the slope surface during a rockfall with detailed characterizations for bouncing, sliding and rolling (Bozzolo and Pamini, 1986; Kobayashi *et al*., 1990; Evans and Hungr, 1993; Azzoni *et al*., 1995), while other models considered bouncing, rolling and sliding as identical movements that can be described by a succession of impacts and bounces (Bozzolo *et al*., 1988; Pfeiffer and Bowen, 1989). Models applying specific algorithms for calculating rolling and sliding velocities mainly used Coulomb's law of friction,

$$F_f = \mu_f * m * g * \cos \beta \quad (3)$$

where, F_f is friction force (tangential to the slope surface) (kg·m s^{-2}); μ_f is coefficient of friction; m is mass of the rock (kg); g is acceleration due to gravity (9.81) (m s^{-2}); ß is mean slope gradient (°).

The calculated friction force could then be used for calculating the sliding or rolling velocity of a rock after displacement over a given distance over the slope surface (Scheidegger, 1975; Bozzolo and Pamini, 1986; Hungr and Evans 1988; van Dijke and van Westen, 1990; Kobayahi *et al*., 1990; Evans and Hungr, 1993; Azzoni *et al*., 1995; Meissl, 1998). Here, the friction coefficient is the most determining factor for the velocity.

For calculating the velocity before and after a bounce, two principle approaches used in the two-dimensional process-based models referred to above can be identified. Both approaches calculated the velocity before and after a bounce on the basis of energy loss.

However, one approach defined energy loss by a coefficient for the efficiency of collision, which is the ratio of the total kinetic energy of the rock before and after the impact. The other approach calculated energy loss on the basis of a tangential coefficient of restitution that acts in a direction parallel to the slope surface and a normal coefficient of restitution that acts in a direction perpendicular to the slope surface.

Azzoni *et al*. (1995) developed a model based on the coefficient for the efficiency of collision. Their model was designed and calibrated with the experience and data gained from several field experiments in Italy. The model considered the falling rock as an ellipsoid (Figure 4) and simulated bouncing, sliding and rolling, based on the algorithms described by Bozzolo and Pamini (1986). Energy before and after the bounce was calculated on the basis of the angular velocity.

Azzoni *et al*. (1995) concluded that their model is generally able to make correct predictions of the fall velocities, bounce height and energy during the fall. They stated that their model results for predicting runout zones were acceptable, but unfortunately no accuracy values were given. Kobayashi *et al*. (1990) developed a model that simulated the contact phases with different characterizations for bouncing and rolling. Bouncing was also based on the coefficient for the efficiency of collision. Their model results were all within the 30% range of the measured rockfall runout zones and bounce marks. Errors were caused by collision with trees, loss of mass during falling and the smooth topography that was assumed in the model. Their main conclusion was that boulder shape is important in governing the modes of motion, but variations in topography control the mode of motion.

Pfeiffer and Bowen (1989) developed a model using both a tangential and normal coefficient for the efficiency of collision. Their model considered a falling rock with its

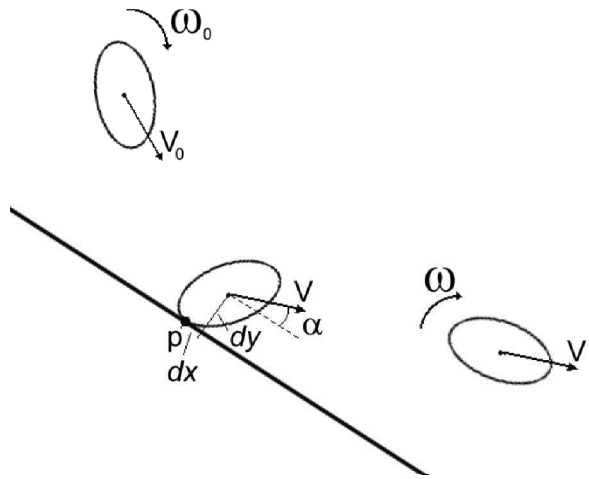


Figure 4 An ellipsoidal rock with initial angular velocity (ω_0) and initial velocity (v_0) continues its fall with angular velocity (ω) and velocity (v) after impact. The angle α is determined by the ratio of the tangential distance (dx) to the normal distance (dy) between the centre of the rock and impact point (p) (after Bozzolo and Pamini, 1986; Azzoni *et al*., 1995)

mass concentrated in one point. At each impact the incoming velocity of the rock was resolved into tangential (parallel to the slope) and normal (perpendicular to the slope) velocities. Both velocities changed because of energy loss defined by the tangential and the normal coefficient of restitution. The tangential coefficient of restitution was determined by the vegetation cover and the surface roughness. The normal coefficient of restitution was determined by elasticity of the surface material. The resultant of both outgoing velocity vectors is the velocity of the rock after bouncing on the slope surface. Rolling was simulated as a succession of impact and bouncing events.

Evans and Hungr (1993) described another example of a model that used the tangential and normal coefficient of restitution. They applied a lumped mass model to three test cases in British Columbia. In this model the rolling and the bouncing mode of motion was simulated separately. For every position on the slope the energy loss was calculated. If the ratio of the kinetic energy lost in an impact to the horizontal length of the corresponding bounce was larger than the rolling friction coefficient during three consecutive bounces, the model simulated a transition into the rolling mode, otherwise the rock continued with bouncing. The exact formula for the calculation of the rolling velocity was not given in their articles (Hungr and Evans, 1988; Evans and Hungr, 1993). Evans and Hungr (1993) concluded that their model requires much wider and thorough calibration, however, some encouraging results were already obtained.

Three-dimensional models for investigating rockfall at a slope scale were also developed (Descoudres and Zimmermann, 1987; Gascuel *et al*., 1998). Descoudres and Zimmermann's (1987) model was developed and calibrated for analysing a rockfall in Wallis, Switzerland, where large blocks were involved (1–10 m^3). The model required a high resolution Digital Elevation Model (DEM), friction coefficients and coefficients for the plasticity and elasticity of the soil. A combined algorithm calculated both the falltrack and the velocity and produced satisfactory results for the test slope. Gascuel *et al*.'s (1998) model applied a bilinear interpolation to the input data to obtain continuous data coverage. On the basis of those interpolated data the model calculated detailed falltracks and velocities using friction coefficients and stress-deformation laws of rock and soil. Since model parameter values vary over the rockfall area and were therefore not perfectly known, the values for the parameters were stochastically changed during the simulation. Again this model produced satisfactory results for the test slope.

All the above-described process-based slope-scale models did not simulate multiple falling rocks and the complex interactions between them. Over the past decade progress has been made in the development of models that identify the coordinates, velocity and angular velocity for multiple particles in a three-dimensional space. These models simulate loss and gain of kinetic energy of particles as a result of inelastic and frictional collisions with each other and with the slope surface. These models were based on Discrete Element Methods (Donzé *et al*., 1999; Okura *et al*., 2000a,b) or on Discontinuous Deformation Analysis (Koo and Chern, 1998).

3 GIS-based models

GIS-based models are those either running within a GIS environment or they are raster-based models for which input data is provided by GIS analysis. GIS-based rockfall models consist of three procedures. The first procedure identifies the rockfall source

areas in the region of interest, the second determines the falltrack and the third calculates the length of the runout zone (Hegg and Kienholz, 1995).

Meissl (1998) developed two GIS-based rockfall models using an empirical model for calculating the runout zone. The first model was *Schattenwinkel*. This model was based on the *minimum shadow angle* principle (Evans and Hungr, 1993), which is described in Section III, 1. The second model of Meissl (1998) was called *Geometrische Gefälle*. This model was based on the angle of the shortest line between the top of the rockfall source scar and the stopping point. Apart from these principles both models were identical, since both models used an identical module for calculating the falltrack and the source areas.

The falltrack module conducted a raster neighbourhood analysis using a 5×5 window. Therefore, this module was able to simulate 16 fall directions from a centre raster cell instead of eight directions (Figure 5), as in the commonly used D-8 method developed by O'Callaghan and Mark (1984). The falltrack module calculated the maximum height difference between the central raster cell and the 16 surrounding cells divided by the distance between the two cells. This analysis was referred to as the D-16 method (Meissl, 1998).

Both the *Schattenwinkel* and the *Geometrische Gefälle* model were tested on individual rockfall slopes. Only the *Schattenwinkel* model was tested for predicting rockfall runout zone at a regional scale. For this test, the rockfall source areas were derived from cliff faces on topographical maps or areas defined as endangering on geomorphological and geological maps. Unfortunately, the *Schattenwinkel* model could not handle the amount of required data (Meissl, 1998).

Other developed and tested models for rockfall hazard assessment at a regional scale were mainly GIS-based models using a process-based model for calculating the runout zone (see Van Dijke and van Westen, 1990; Meissl, 1998). These models can be defined as distributed models, since they are process-based and take into account the spatial

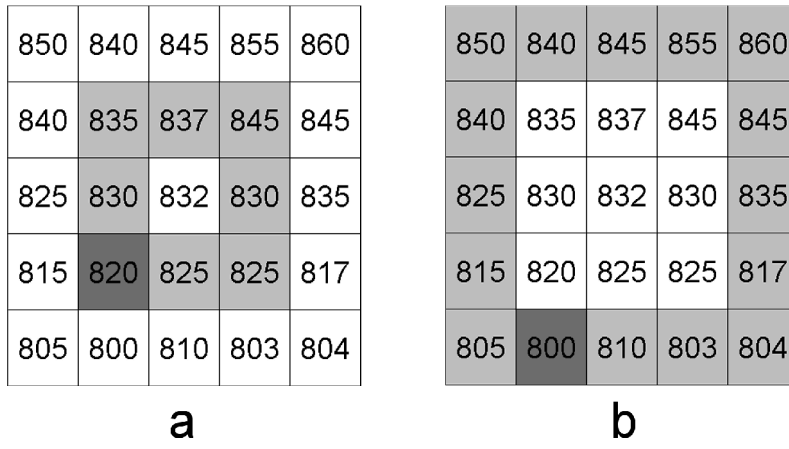


Figure 5 (a) D-8 method: fall direction from the central cell is towards the dark-grey cell if calculated with a 3×3 window. (b) Same example using a 5×5 window, which is used in the D-16 method of Meissl (1998)

variability within a certain region or catchment (Beven, 1985; Beven and Moore, 1993). In a GIS-based distributed rockfall model the terrain is represented by multiple rasters, which are derived from GIS data layers. Each raster represents a certain property of the terrain, for example, height above sea level, surface roughness, vegetation cover and geology.

Van Dijke and van Westen (1990) developed a distributed model that performs a neighbourhood analysis to a DEM derived from an isoline map with an equidistance of 20 m, representing an area of 80 km^2. A neighbourhood analysis calculated the fall direction for each raster cell. The direction was determined towards the neighbouring cell with the minimum height value. The velocity calculation of the model was based on an energy conservation principle as described by Scheidegger (1975). On the basis of this principle the velocity of the falling rock was calculated following,

$$v = \sqrt{v_0 + 2 * g * (h - \mu_f + X} \tag{4}$$

where, v is velocity of the falling rock (m s^{-1}); v_0 is initial velocity of the falling rock (m s^{-1}); g is acceleration due to gravity (9.81) (m s^{-2}); h is fall height (m); μ_f is coefficient of friction; X is distance travelled over the slope surface (m).

The velocity was calculated for each raster cell within the falltrack, starting at a potential rockfall source cell. Potential rockfall source cells were defined by the mean slope gradient (>60°). The value of the friction coefficient (μ_f) depended on the soil cover type, for example, bare rock, scree, residual soils, fluvial materials, dense forest and open forest. The model was tested for an area in the Austrian Alps by comparing the modelled results with detailed natural hazard maps of the area. The model results were compared with these maps. Van Dijke and van Westen (1990) concluded that their model was able to compute the general distributions of rockfall areas shown on their maps.

The GIS-based distributed model of Meissl (1998) was called *Sturzgeschwindigkeit*. This model simulated two different modes of motion: freefalling and sliding. The formula for the calculation of the velocity after freefalling is given in eq. (2). To account for energy loss during the first collision or bounce on the slope surface 75% of the velocity gained during the motion through the air was subtracted, following observations of Broilli (1974). In the following cells the model calculated a sliding velocity with the formula described in eq. (4).

Again, Meissl (1998) derived rockfall source areas from cliff faces on topographical maps or areas defined as endangering on geomorphological and geological maps. The falltrack was calculated with the D-16 method. *Sturzgeschwindigkeit* was tested for an alpine valley in Austria covering approximately 72 km^2. The terrain was represented using a DEM with a resolution of 50 m × 50 m. The outcomes of the model were compared with mapped rockfall patterns. From those comparisons, Meissl (1998) concluded that the simulated rockfall patterns on high altitudinal zones generally correspond with the mapped patterns, but unfortunately no model accuracies were given.

IV Synthesis: a GIS-based distributed rockfall model

As shown by many authors, models are widely used to predict the risk posed by rockfall, both at a slope scale and at a regional scale. In recent years rockfall models chiefly evolved towards three-dimensional and GIS-based models. A GIS-based model is favourable in case of predicting rockfall runout zones at a regional scale. GIS-based models require three procedures: one for identifying the rockfall source areas, the second for determining the falltrack and the third for calculating the runout zone.

A simple method for identifying rockfall source areas is defining thresholds for mean slope gradients (Toppe, 1987; van Dijke and van Westen, 1990). Another method is deriving rockfall source areas from cliff faces on topographical maps (Krummenacher, 1995; Meissl, 1998) or from areas defined as active rockfall slopes on geomorphological and geological maps (van Dijke and van Westen 1990). Another more realistic and automatic method is to identify rockfall source areas on the basis of a combined dataset in a GIS. This dataset could include: rock type, exposition, slope curvature, slope gradient and land cover.

The most common method used for determining a falltrack in GIS-based rockfall models is the D-8 method introduced by O'Callaghan and Mark (1984) or the D-16 method (Meissl, 1998). The advantage of the D-8 method is that the falltrack can be calculated cell by cell. Simultaneously the velocity of the falling block in every cell is calculated. In contrast, the D-16 method calculates the next position beyond the eighth neighbouring cells. Therefore, extra calculations have to be carried out to fill in the gaps in the raster (Meissl, 1998).

Another advantage of the D-8 method is its simplicity, which improves the speed of the computer simulation. A disadvantage of the D-8 method is the systematic error that occurs because of the restricted falltrack calculation (Figure 6), since rock movement is restricted to straight or diagonal directions. When applying the D-16 method the systematic error caused by this restriction decreases (Meissl, 1998). A point of concern for both methods is the fact that for each source cell only one direction is calculated, i.e., a rock in a given raster cell leaves by a single exit. Therefore a computer program using the D-8 or the D-16 method for determining the falltrack can never simulate the development of talus cones. The latter can be achieved by simulating lateral spreading of rocks from a single cell, using a multiple flow direction algorithm (Quinn *et al*., 1991), or variations to this algorithm as summarized by Tarboton (1997).

For calculating rockfall runout zones, empirical or process-based models can be used. An empirical model results in a first approximation of rockfall runout zones. Process-based models seem to result in more accurate predictions of runout zones. Furthermore, an advantage of process-based models is that the interaction of falling rocks with tree stems or other barriers can be simulated. The main problem of rockfall modelling is calculating the bouncing and rolling velocity. Depending on the level of detail of the input data, more or less complex algorithms can be used. One possibility is to use a single coefficient for the efficiency of collision; another is to use both a normal and a tangential coefficient of restitution. In addition, an option is to use a separate algorithm for calculating the rolling velocity or to simulate rolling by a succession of impacts and bounces.

The tangential coefficient of restitution is determined by obstacles on the slope surface and the normal coefficient of restitution is determined by the elasticity of the

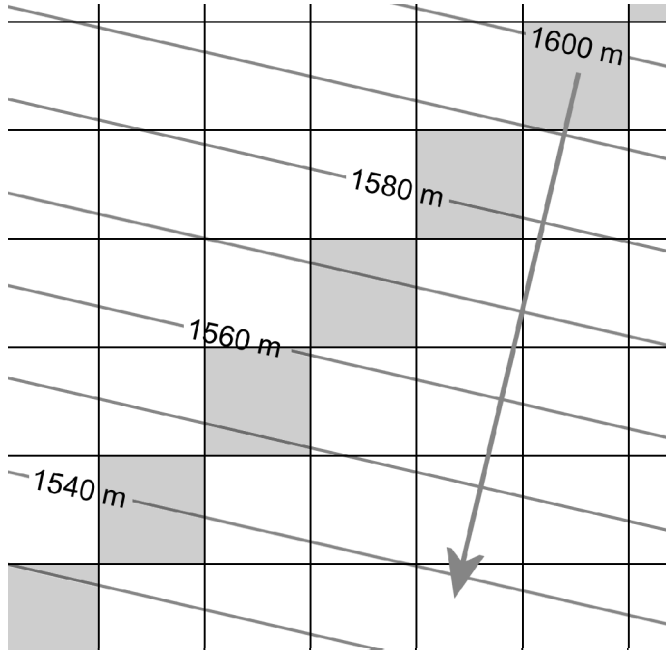


Figure 6 The arrow presents the actual falltrack on the slope depicted by the isolines. The direction deviates from the raster-based falltrack determined with the D-8 method, illustrated by the grey cells (after Meissl, 1998)

surface material. Therefore, the tangential and the normal coefficient of restitution are easier to estimate than a single coefficient for the efficiency of collision for certain slope parts. As a result the use of the tangential and the normal coefficient of restitution is preferred. Since the use of a separate algorithm for calculating the rolling velocity introduces another parameter that has to be estimated in the field (μ_f or the coefficient of friction), it is also preferred to simulate rolling by a succession of impacts and bounces. An alternative to the modelling approaches described above is to use models that are based on Discrete Element Methods (Donzé *et al.*, 1999; Okura *et al.*, 2000a,b) or on Discontinuous Deformation Analysis (Koo and Chern, 1998). However, these models require a larger amount of detailed data and are therefore not feasible for GIS-based models predicting rockfall runout zones at a regional scale.

An important condition for the calculation of rockfall runout zones using a GIS-based model is a DEM of the whole region of interest. To account for fine-scale topographic variability in the slope profiles, the preferred resolution of such a DEM is between 5 m × 5 m or 10 m × 10 m. However, a DEM for larger regions (e.g., >500 km^2) generally has a resolution of 25 m × 25 m or larger. The question is whether it is feasible to simulate freefalling, bouncing and rolling on the basis of input data with a resolution of 25 m × 25 m. With such a resolution realistic landscape details are lost, which could imply that the process is simulated accurately but the resulting pattern is not. The study by Meissl (1998) gave a preliminary answer to this question, since the GIS-based distributed model tested produced promising results. In contrast, the empirical GIS-

based model was not suitable for a regional assessment of rockfall hazard at all. Nevertheless, if input data with a resolution of 25 m × 25 m is used, the input values should be varied stochastically to account for terrain variability.

Errors observed in the outcomes of the process-based and GIS-based distributed rockfall models were mainly caused by the variability in topography and by the variability in surface characteristics (Kobayashi *et al*., 1990; Meissl, 1998). In addition, inadequate characterization of the vegetation cover explained some errors (Kobayashi *et al*., 1990). These observations indicate that more research effort is required for assessing input data parallel to the development of a GIS-based distributed model for predicting rockfall runout zones at a regional scale. Combining geomorphological and geological maps, forest inventories and remotely sensed data within a GIS could provide the required data for the terrain characterization at a regional scale.

V Conclusions

Currently, a large variety of empirical and process-based rockfall models exist. Empirical models provide a quick and simple approximation of rockfall runout zones. Process-based models produce more accurate predictions of runout zones. In addition, process-based models seem to be most suitable for application in areas other than the areas the models were developed and calibrated for. Until now many process-based models were developed for specific slopes where rockfall causes problems, but only few models were applied for predicting rockfall runout zones at a regional scale. For predicting rockfall runout zones at a regional scale, the integration of process-based models and a GIS is promising. Three procedures are crucial for this approach: first, the identification of source areas, secondly, the determination of falltracks and thirdly, the calculation of the rockfall velocity that determines the length of the runout zones. Apart from developing and testing these three procedures, research should focus on the development of methods for an accurate characterization of the terrain at a regional scale. This is required for the estimation of model parameter values and for incorporating the effect of forests on rockfall runout zones. The latter is still underdeveloped in rockfall modelling.

Acknowledgements

I wish to thank A.C. Seijmonsbergen, J. de Vente and J.H.N. Versfelt for helpful comments on the submitted manuscript.

References

Abele, G. 1994: Large rockslides: their causes and movement on internal sliding planes. *Mountain Research and Development* 14(4), 315–20.

Azzoni, A., Barbera, G.L. and **Zaninetti, A.** 1995: Analysis and prediction of rockfalls using a mathematical model. *International Journal of Rock Mechanics and Mining Science* 32, 709–24.

Badger, T.C. and **Lowell, S.M.** 1992: Rockfall control in Washington State, rockfall prediction and control and landslide case histories. *Transportation Research Record* 1343, 14–19.

Beven, K. 1985: Distributed models. In Anderson, M.G. and Burt, T.P., editors, *Hydrological Forecasting*. Chichester: John Wiley & Sons

Ltd, 405–35.
Beven, K.J. and **Moore, I.D.** 1993: *Terrain analysis and distributed modelling in hydrology*. Advances in hydrological processes. Chichester: Wiley.
Blijenberg, H.M. 1995: In-situ strength tests of coarse, cohesionless debris on scree slopes. *Engineering Geology* 39(3), 137–46.
Bozzolo, D. and **Pamini, R.** 1986: Simulation of rock falls down a valley side. *Acta Mechanica* 63, 113–30.
Bozzolo, D., Pamini, R. and **Hutter, K.** 1988: Rockfall analysis – a mathematical model and its test with field data. *Proceedings of the 5th International Symposium on Landslides in Lausanne*, Rotterdam: Balkema, 555–60.
Broilli, L. 1974: Ein Felssturz in Großversuch. *Rock Mechanics* Suppl. 3, 69–78.
Budetta, P. and **Santo, A.** 1994: Morphostructural evolution and related kinematics of rockfalls in Campania (southern Italy): a case study. *Engineering Geology* 36, 197–210.
Bull, W.B., King, J., Kong, F.C., Moutoux, T. and **Phillips, W.M.** 1994: Lichen dating of coseismic landslide hazards in alpine mountains. *Geomorphology* 10(1), 253–64.
Bunce, C.M., Cruden, D.M. and **Morgenstern, N.R.** 1991: Assessment of the hazard from rock fall on a highway. *Canadian Geotechnical Journal* 34, 344–56.

Carson, M.A. 1977: Angles of repose, angles of shearing resistance and angles of talus slopes. *Earth Surface Processes* 2, 363–80.
Chang, W.R. 1998: The effect of surface roughness on dynamic friction between neolite and quarry tile. *Safety Science* 29(2), 89–108.
Chau, K.T., Wong, R.H.C. and **Lee, C.F.** 1998: Rockfall problems in Hong Kong and some new experimental results for coefficient of restitution. *International Journal of Rock Mechanics and Mining Science* 35(4), 662–63.
Chen, H., Chen, R. and **Huang, T.** 1994: An application of an analytical model to a slope subject to rockfall. *Bulletin of the Association of Engineering Geologists* 31(4), 447–58.
Coutard, J.P. and **Francou, B.** 1989: Rock temperature measurements in two alpine environments: implications for frost shattering. *Arctic and Alpine Research* 21, 399–416.
Cruden, M.D. and **Varnes, J.D.** 1996: Landslide types and processes. In Turner, A.K. and Schuster, R.L., editors, *Landslides: investigation and mitigation*. Washington DC: Transport Research Board, 36–75.

Day, R.W. 1997: Case studies of rockfall in soft versus hard rock. *Environmental and Engineering Geoscience* 3(1): 133–40.
Descoeudres, F. and **Zimmermann, T.** 1987: Three-dimensional dynamic calculation of rockfalls, In Herget, G. and Vongpaisal, S., editors, *Proceedings of the Sixth International Congress on Rock Mechanics*. Montreal. Rotterdam: Balkema, 337–42.
Domaas, U. 1994: Geometrical methods of calculating rockfall range. *NGI Report 585910-1*. Oslo: Norwegian Geotechnical Institute.
Donzé, F., Magnier, S.A., Montani, S. and **Descoeudres, F.** 1999: Numerical study of rock block impacts on soil-covered sheds by a discrete element method, *5ème Conférence Nationale en Génie Parasismique, AFPS'99*, Cachan.
Douglas, G.R. 1980: Magnitude frequency study of rockfall in Co. Antrim, North Ireland. *Earth Surface Processes and Landforms* 5, 123–29.

Erismann, T.H. 1986: Flowing, rolling, bouncing, sliding, synopsis of basic mechanisms. *Acta Mechanica* 64, 101–10.
Evans, S.G. and **Hungr, O.** 1993: The assessment of rockfall hazard at the base of talus slopes. *Canadian Geotechnical Journal* 30, 620–36.

Gardner, J.S. 1983: Rockfall frequency and distribution in the Highwood Pass area, Canadian Rocky Mountains. *Zeitschrift für Geomorphologie* 27(3), 311–24.
Gascuel, J.-D., Cani-Gascuel, M.-P., Desbrun, M., Leroi, E. and **Mirgon, C.** 1998: Simulating landslides for natural disaster prevention. In Arnaldi, B. and Hegron, G., editors, *Computer animation and simulation '98*. Proceedings of the Eurographics Workshop, Lisbon, 31 August–1 September 1998. Springer Verlag, 1–12.
Govi, M. 1977: Photo-interpretation and mapping of the landslides triggered by the Friuli Earthquake (1976). *Bulletin of the International Association of Engineering Geology* 15, 67–72.
Grove, J.M. 1972: The incidence of landslides, avalanches and floods in western Norway during the Little Ice Age. *Arctic and Alpine Research* 4, 131–38.

Hearn, G., Barret, R.K. and **McMullen, M.L.** 1992: CDOT Flexpost rockfall fence development, testing, and analysis. Rockfall Prediction and Control and Landslide Case Histories. *Transportation research record 1343*. Washington DC: National Academy of Sciences, 23–29.
Hegg, C. and **Kienholz, H.** 1995. Determining paths of gravity-driven slope processes – the 'Vector Tree Model'. In Carrara, A. and Guzetti,

F., editors, *Geographic information systems in assessing natural hazards*. Dordrecht: Kluwer Academic Publishers, 79–92.

Heim, A. 1932: Bergsturz und Menschenleben. *Beiblatt zur Vierteljahrschrift der Naturforschenden Gesellschaft in Zürich* 77, 218 pp.

Hétu, B. and **Gray, J.T.** 2000: Effects of environmental change on scree slope development throughout the postglacial period in the Chic-Choc Mountains in the northern Gaspé Peninsula, Québec. *Geomorphology* 32(3), 335–55.

Hsü, K.J. 1975: Catastrophic debris streams (Sturzstroms) generated by rockfalls. *Geological Society of America Bulletin* 86, 129–40.

Hungr, O. and **Evans, S.G.** 1988. Engineering evaluation of fragmental rockfall hazards. *Proceedings of the 5th International Symposium on Landslides in Lausanne*. Rotterdam: Balkema, 685–90.

Hungr, O., Evans, S.G. and **Hazzard, J.** 1999: Magnitude and frequency of rock falls and rock slides along the main transportation corridors of southwestern British Columbia. *Canadian Geotechnical Journal* 36(2), 224–38.

Jahn, J. 1988: Entwaldung und Steinschlag. In *Proceedings of the International Congress Interpraevent 1988*. Bnd 1, Graz, 185–98.

Jomelli, V. and **Francou, B.** 2000: Comparing the characteristics of rockfall talus and snow avalanche landforms in an Alpine environment using a new methodological approach: Massif des Ecrins, French Alps. *Geomorphology* 35(3), 181–92.

Keylock, C. and **Domaas, U.** 1999: Evaluation of topographic models of rockfall travel distance for use in hazard applications. *Arctic, Antarctic, and Alpine Research* 31(3), 312–20.

Kienholz, H. and **Mani, P.** 1994: Assessment of geomorphic hazards and priorities for forest management on the Rigi north face, Switzerland. *Mountain Research and Development* 14(4), 321–28.

Kirkby, M.J. and **Statham, I.** 1975: Surface stone movement and scree formation. *Journal of Geology* 83, 349–62.

Kobayashi, Y., Harp, E.L. and **Kagawa, T.** 1990: Simulation of rockfalls triggered by earthquakes. *Rock Mechanics and Rock Engineering* 23, 1–20.

Koo, C.Y. and **Chern, J.C.** 1998: Modification of the DDA method for rigid block problems. *International Journal of Rock Mechanics and Mining Science* 35(6), 683–93.

Körner, H.J. 1976: Reichweite und Geschwindigkeit von Bergstürzen und Fliessschneelawinen. *Rock Mechanics* 8, 225–56.

——— 1980: The energy-line method in the mechanics of avalanches. *Journal of Glaciology* 26, 501–505.

Krummenacher, B. 1995: Modellierung der Wirkungsräume von Erd- und Felsbewegungen mit Hilfe Geographischer Informationssysteme (GIS). *Schweizerischen Zeitschrift für Forstwesen* 146, 741–61.

Lied, K. 1977: Rockfall problems in Norway. *ISMES Publication no. 90*, Bergamo, 51–53.

Luckman, B.H. 1976: Rockfalls and rockfall inventory data, some observations from Surprise valley, Jasper national park, Canada. *Earth Surface Processes* 1, 287–98.

Matsuoka, N. and **Sakai, H.** 1999: Rockfall activity from an alpine cliff during thawing periods. *Geomorphology* 28(3), 309–28.

McCarroll, D., Shakesby, R.A. and **Matthews, J.A.** 1998: Spatial and temporal patterns of late Holocene rockfall activity on a Norwegian talus slope: a lichenometric and simulation-modeling approach. *Arctic and Alpine Research* 30(1), 51–60.

McClung, D.M. and **Lied, K.** 1987: Statistical and geometrical definition of snow avalanche runout. *Cold Regions Science and Technology* 13, 107–19.

Meissl, G. 1998: Modellierung der Reichweite von Felsstürzen. Fallbeispeile zur GIS-gestützten Gefahrenbeurteilung aus dem Beierischen und Tiroler Alpenraum. Innsbrucker Geografischen Studien 28. Ph.D. Thesis, Universität Innsbruck, Innsbruck, 249 pp.

Moriwaki, H., 1987. Geomorphological prediction of the travel distance of a debris. *The China–Japan field workshop on landslide*. Xian-Lanzhou, China, 79–84.

Motta, R. and **Haudemand, J.-C.** 2000: Protective forests and silvicultural stability. An example of planning in the Aosta valley. *Mountain Research and Development* 20(2), 74–81.

O'Callaghan, J.F. and **Mark, D.M.** 1984: The extraction of drainage networks from digital elevation models. *Computer Vision, Graphics and Image Processing* 28, 323–44.

Okura, Y., Kitahara, H. and **Sammori, T.** 2000a: Fluidization in dry landslides. *Engineering Geology* 56(3), 347–60.

Okura, Y., Kitahara, H., Sammori, T. and **Kawanami, A.** 2000b: The effects of rockfall

volume on runout distance. *Engineering Geology* 58(2), 109–124.

Peila, D., Pelizza, S. and **Sassudelli, F.** 1998: Evaluation of behaviour of rockfall restraining nets by full scale tests. *Rock Mechanics and Rock Engineering* 31(1), 1–24.

Pfeiffer, T.J. and **Bowen, T.D.** 1989: Computer simulation of rockfalls. *Bulletin of the Association of Engineering Geologists* XXVI(1), 135–46.

Porter, S.C. and **Orombelli, G.** 1980: Catastrophic rockfall of September 12, 1717 on the Italian flank of the Mont Blanc Massif. *Zeitschrift für Geomorphologie N.F.* 24, 200–18.

—— 1981: Alpine rockfall hazards. *American Scientist* 69(1), 67–75.

Quinn, P., Beven, K., Chevallier, P. and **Planchon, O.** 1991: The prediction of hillslope flow paths for distributed hydrological modelling using digital terrain models. *Hydrological Processes* 5(1), 59–79.

Rapp, A. 1960: Recent development of mountain slopes in Kårkevagge and surroundings, northern Scandinavia. *Geografiska Annaler* 42, 65–200.

Ritchie, A.M. 1963: Evaluation of rockfall and its control. *Highway Research Record* 17, 13–28. Washington, DC: Highway Research Board, National Research Council.

Scheidegger, A.E. 1975: *Physical aspects of natural catastrophes*. Amsterdam / New York: Elsevier.

Schumm, S.A. and **Chorley, R.J.** 1964: The fall of endangering rock. *American Journal of Science* 262, 1041–54.

Selby, M.J. 1982: *Hillslope materials and processes*. New York: Oxford University Press.

Spang, R.M. and **Sönser, T.** 1995: Optimized rockfall protection by 'ROCKFALL'. In Fuji, T., editor, *Proceedings of the 8th International Conference on Rock Mechanics*. 25–30 September 1995. Rotterdam: A.A. Balkema, Tokyo, 1233–42.

Statham, I. 1976: A scree slope rockfall model. *Earth Surface Processes* 1, 43–62.

Statham, I. and **Francis, S.C.** 1986: Influence of scree accumulation and weathering on the development of steep mountain slopes. In Abrahams, A.D., editor, *Hillslope processes*. Winchester: Allen and Unwin Inc., 245–67.

Tarboton, D.G. 1997: A new method for the determination of flow directions and upslope areas in grid digital elevation models. *Water Resources Research* 33(2), 309–19.

Tianchi, L. 1983: A mathematical model for predicting the extent of a major rockfall. *Zeitschrift für Geomorphologie* 27(4), 473–82.

Toppe, R., 1987. Terrain models – a tool for natural hazard mapping. In Salm, B. and Gubler, H., editors, *Avalanche formation, movement and effects*. IAHS Publication no. 162, 629–38.

van Dijke, J.J. and **van Westen, C.J.** 1990: Rockfall hazard, a geomorphological application of neighbourhood analysis with ILWIS. *ITC Journal* 1, 40–44.

Vidrih, R., Ribičič, M. and **Suhadolc, P.** 2001: Seismogeological effects on rocks during the 12 April 1998 upper Soča Territory earthquake (NW Slovenia). *Tectonophysics* 330(3), 153–75.

Wieczorek, G.F. and **Jäger, S.** 1996: Triggering mechanisms and depositional rates of postglacial slope-movement processes in the Yosemite Valley, California. *Geomorphology* 15, 17–31.

Wieczorek, G.F., Nishenkod, S.P. and **Varnes, D.J.** 1995: Analysis of rockfalls in the Yosemite Valley, California. In Daemen, J.J.K. and Schultz, R.A., editors, *Rock mechanics: proceedings of the 35th US symposium*. Rotterdam: Balkema, 85–89.

Wieczorek, G.F., Snyder, J.B., Waitt, R.B., Morrissey, M.M., Uhrhammer, R.A., Harp, E.L., Norris, R.D., Bursik, M.I. and **Finewood, L.G.** 2000: Unusual July 10, 1996, rock fall at Happy Isles, Yosemite National Park, California. *Geological Society of America Bulletin* 112(1), 75–85.

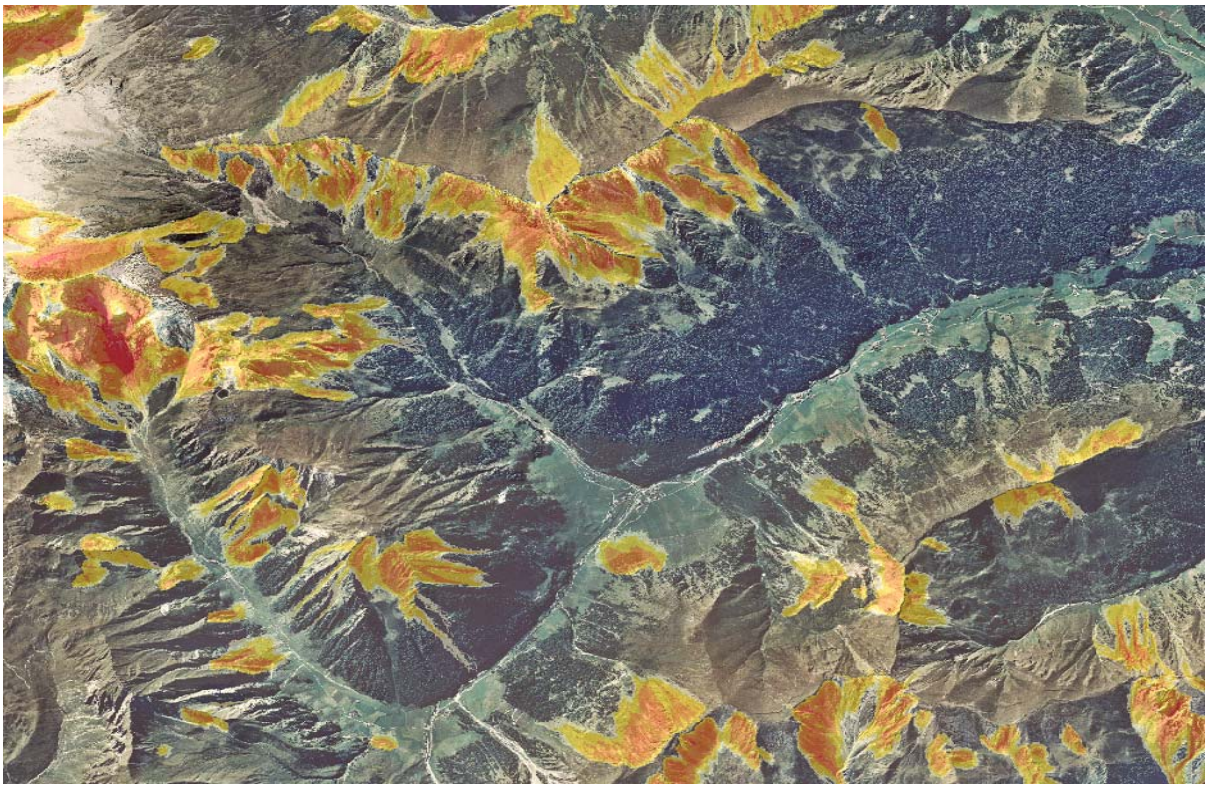
Wu, S.-S. 1985: Rockfall evaluation by computer simulation. *Transportation Research Record* 1031, 1–5.

Zellmer, J.T. 1987: The unexpected rockfall hazard. *Bulletin of the Association of Engineering Geologists* 24(2), 281–83.

Zinggeler, A., Krummenacher, B. and **Kienholz, H.** 1991: Steinschlagsimulation in Gebirgswäldern. *Berichte und Forschungen 3*. Geographisches Institut der Universität Freiburg, 61–70.

> Chapter 4

Comparison of three rockfall models at a regional scale



Available online at www.sciencedirect.com
SCIENCE DIRECT®
Geomorphology 56 (2003) 49–64
GEOMORPHOLOGY
www.elsevier.com/locate/geomorph

Comparison of three GIS-based models for predicting rockfall runout zones at a regional scale

Luuk K.A. Dorren*, Arie C. Seijmonsbergen

Institute for Biodiversity and Ecosystem Dynamics—Physical Geography, Universiteit van Amsterdam, Nieuwe Achtergracht 166, Amsterdam NL-1018WV, The Netherlands

Received 2 January 2002; received in revised form 20 December 2002; accepted 23 December 2002

Abstract

Site-specific information about the level of protection that mountain forests provide is often not available for large regions. Information regarding rockfalls is especially scarce. The most efficient way to obtain information about rockfall activity and the efficacy of protection forests at a regional scale is to use a simulation model. At present, it is still unknown which forest parameters could be incorporated best in such models. Therefore, the purpose of this study was to test and evaluate a model for rockfall assessment at a regional scale in which simple forest stand parameters, such as the number of trees per hectare and the diameter at breast height, are incorporated. Therefore, a newly developed Geographical Information System (GIS)-based distributed model is compared with two existing rockfall models. The developed model is the only model that calculates the rockfall velocity on the basis of energy loss due to collisions with trees and on the soil surface. The two existing models calculate energy loss over the distance between two cell centres, while the newly developed model is able to calculate multiple bounces within a pixel. The patterns of rockfall runout zones produced by the three models are compared with patterns of rockfall deposits derived from geomorphological field maps. Furthermore, the rockfall velocities modelled by the three models are compared. It is found that the models produced rockfall runout zone maps with rather similar accuracies. However, the developed model performs best on forested hillslopes and it also produces velocities that match best with field estimates on both forested and nonforested hillslopes irrespective of the slope gradient.
© 2003 Elsevier Science B.V. All rights reserved.

Keywords: Rockfall; GIS; Protection forest; Simulation model; Geomorphological mapping; Mountainous catchment

1. Introduction

Mountain forests provide multiple functions, of which protection against rockfall, snow avalanches, and soil erosion is increasingly considered to be the most important one (Kräuchi et al., 2000; Motta and Haudemand, 2000). However, site-specific information about the level of the protection that forests provide is often not available for large regions. Information about the level of protection that mountain forests provide against rockfall is especially scarce (Meißl, 1998). Although for some known active rockfall slopes within a forest management area some qualitative information about the efficacy of the protection forest stand might be available, forest

* Corresponding author. Tel.: +31-20-5257420; fax: +31-20-5257431.
E-mail address: l.dorren@science.uva.nl (L.K.A. Dorren).

0169-555X/$ - see front matter © 2003 Elsevier Science B.V. All rights reserved.
doi:10.1016/S0169-555X(03)00045-X

departments indicate that there is a need for information on both rockfall activity and the efficacy of protection forests for whole management areas. This is because protection forest management plans and strategies aiming at the maintenance of stable forest structures are developed for large management areas and not for individual slopes (Keller, 1994; Bebi et al., 2001).

The most efficient way to obtain information about rockfall activity and the efficacy of protection forests at a regional scale is to use a simulation model (Dorren, 2003). With respect to rockfall modelling, it is known how to simulate rockfall runout zones (in this study defined as the zone between the start and the end location for a falling rock) at a slope scale (Kirkby and Statham, 1975; Bozzolo and Pamini, 1986; Pfeiffer and Bowen, 1989; Azzoni et al., 1995; Okura et al., 2000). Some authors modelled patterns of rockfall runout zones at a regional scale (van Dijke and van Westen, 1990; Meißl, 1998, 2001). All these regional models did not, however, incorporate specific protection forests parameters. Moreover, both existing regional rockfall models use a relatively simple modelling approach. Therefore, the objective of this study was to determine if the newly developed process-based rockfall model, which incorporates protection forest parameters and the effect of forest density on the velocity of falling rocks, improves the accuracy of simulated patterns of rockfall runout zones at a regional scale. To achieve this objective, this study compared the results of the newly developed model with the outcomes of the two existing Geographical Information System (GIS)-based models. To evaluate the performance of the three models, firstly, the modelled patterns of rockfall runout zones were compared with mapped patterns. Secondly, the velocities produced by the three models were analysed. For both the pattern and the velocity analysis, a distinction was made between model performance on forested and nonforested hillslopes.

2. Study area

2.1. General description

The research area covers the Montafon region, located in the southern part of Vorarlberg, the westernmost province of Austria. The Montafon region comprises the headwaters of the river Ill and covers an area of 533 km^2 mountainous terrain. Altitudes in the Montafon region vary from 580 m a.s.l. near Lorüns up to 3312 m a.s.l. at the top of the Piz Buin, which is the highest peak in the Montafon region (Fig. 1). Within the Montafon region, 50% of the area is covered by alpine meadows, 23% are forests, 20% are alpine tundra, and 7% are agricultural and urban lands. The distribution of forest stand types at a regional scale is determined mainly by altitude, but at a slope scale, other factors such as parent material, relief, microclimate, humus forms, light, and disturbances caused by natural hazards also become important (van Noord, 1996). Generally, the canopy density decreases with increasing altitude due to the changing climatic conditions (e.g., heavier snow loads). Because uneven-aged forests predominate, tree distribution, stem density, tree height, and basal area vary strongly between forest stands. As typical for mountain forests, these varied forest stands are distributed in a patchy mosaic-like structure (Maier, 1993). Mixed forests predominate in the montane zone (500–1200 m a.s.l.) and coniferous forests (mainly *Picea abies*) in the subalpine zone (1200–1900 m a.s.l.).

The climate in the Montafon region is of the central European type with seasonal rainfall regime producing a winter minimum and a summer maximum. Since the mountainous topography determines the local climate, it may be classified as Df according to the Köppen climate system (Köppen, 1918). The average winter temperature lies between 0 and −5 °C and the average summer temperature between 7 and 17 °C. Annual precipitation varies between 1200 and 1700 mm (source: Vorarlberger Illwerke, Schruns). Both temperature and precipitation vary strongly with altitude and aspect. Föhn winds are important in the lower part of the Montafon region. The total yearly evaporation varies between 250 and 400 mm (i.e., approximately 25% of the precipitation).

2.2. Geology and geomorphology

The geological structure of the Montafon region is dominated by the Alpine orogeny, during which several large overturned folds or nappes were overthrust from a south-eastern direction. The two largest

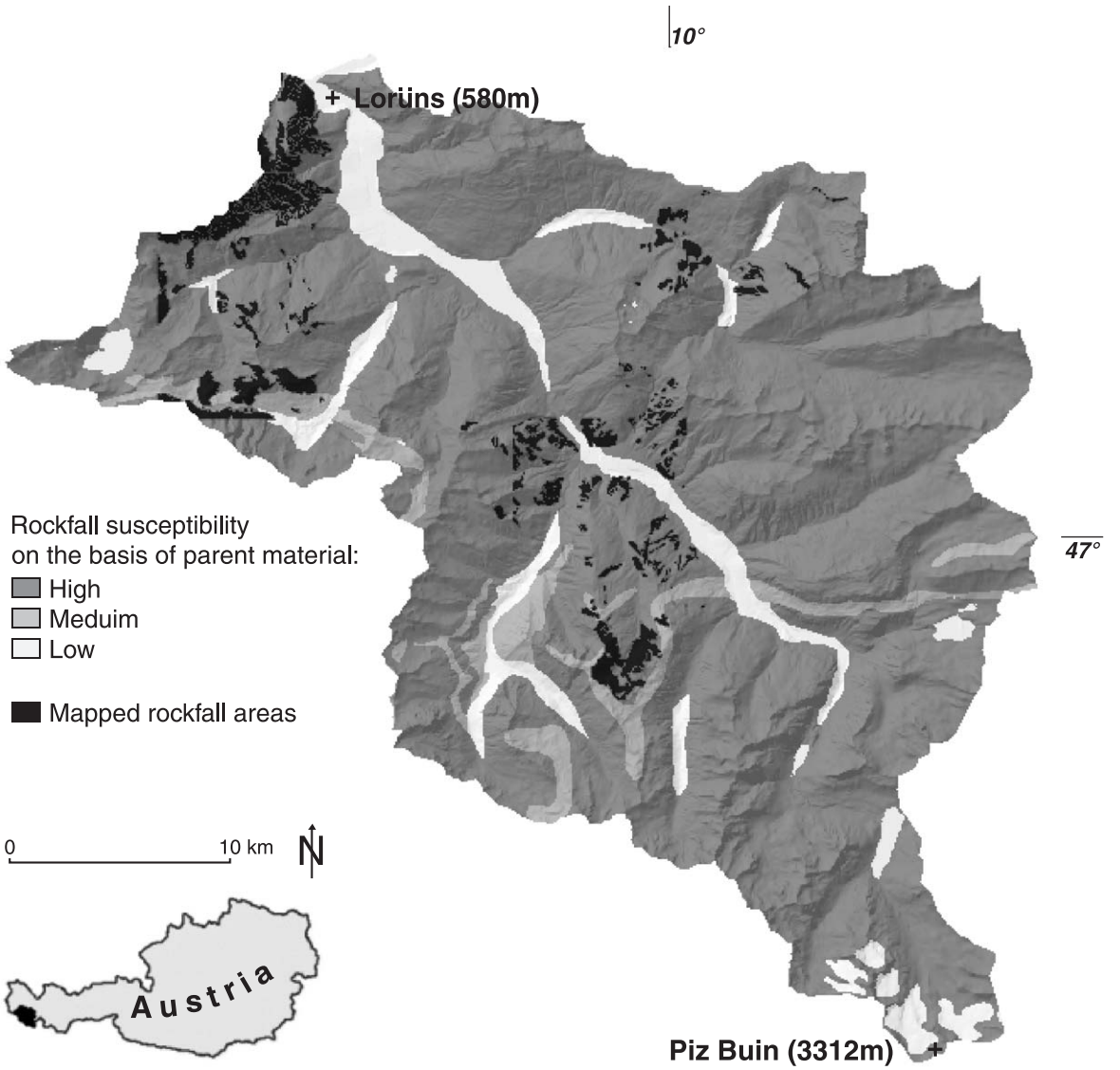


Fig. 1. Map showing the rockfall susceptibility map on the basis of parent material or bedrock type throughout the Montafon region. The black areas indicate mapped active rockfall areas.

and most important nappes are the Silvretta nappe in the southeastern and the Lechtal nappe in the northwestern part of the study area, which are both Upper East Alpine nappes (GBA, 1998). The Silvretta nappe consists of crystalline formations and the Lechtal nappe consists of resistant limestones and dolomites. The crystalline formations consist mainly of metamorphic rocks, especially paragneisses, but in the most southeastern part of the Silvretta nappe, orthogneisses and granites dominate. The transition zone between the crystalline and the sedimentary formations is known as the 'Phyllitgneis zone.'

The Pleistocene glacial and interglacial periods have had a profound impact on the landscape: firstly, in terms of the production and redistribution of loose materials, and secondly, because of pronounced glacial erosion, which resulted in oversteepened slopes. Postglacial relaxation of these slopes led to the

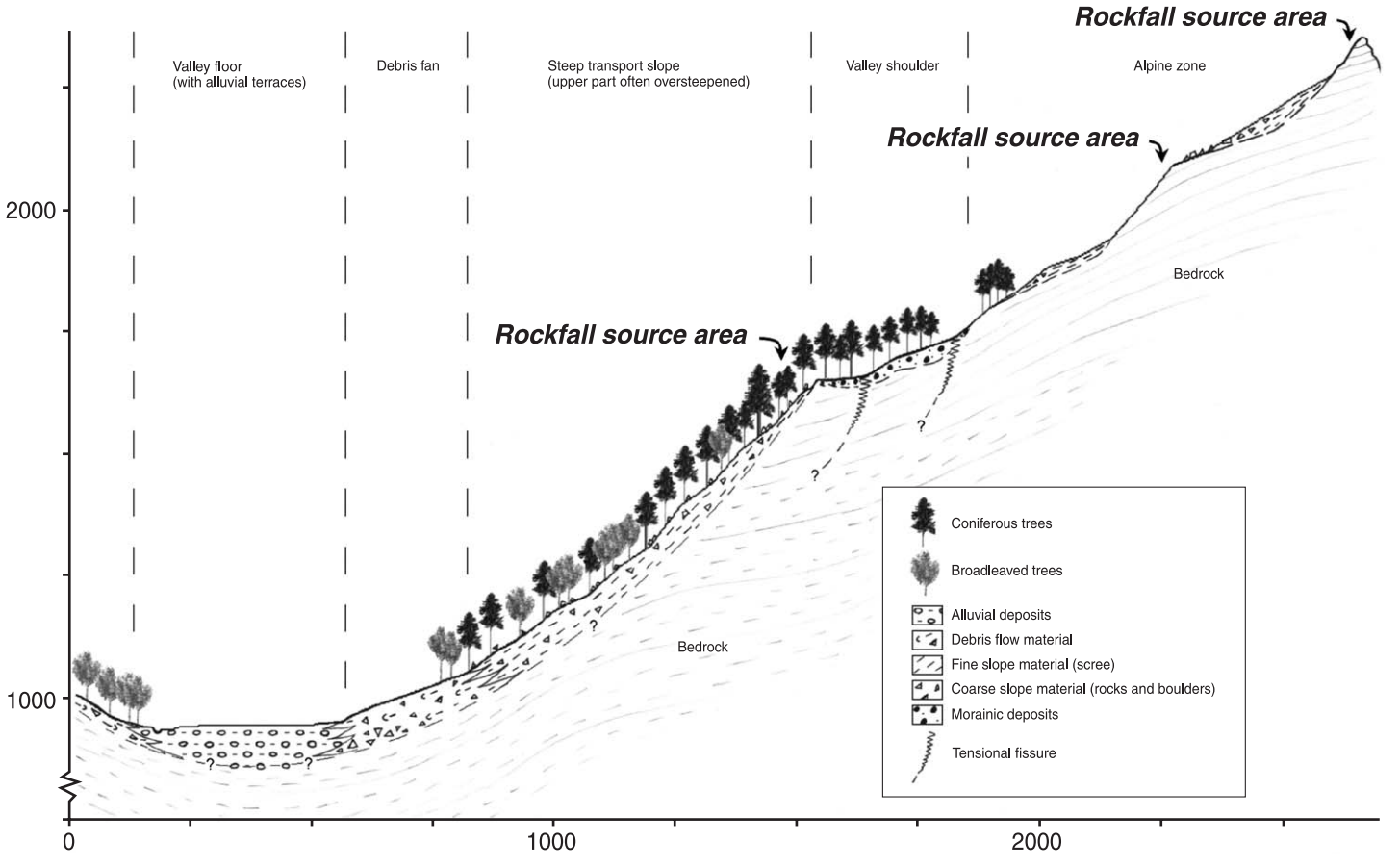


Fig. 2. General characterization of a typical slope transect in the Montafon region with deposits and rockfall source areas, showing an exaggerated vertical scale for the trees and the thickness of nonlithified materials. Question marks indicate uncertainty about the depth of boundaries or the depth of fissures. The structural layering of the bedrock is variable throughout the region (after van Noord, 1996).

development of tensional fissures and related deep-seated mass movements, bedrock toppling, as well as landsliding (van Noord, 1996). This Quaternary development, in combination with the geological structure, sets the initial conditions for the development of rockfall source areas throughout the region (Fig. 2).

In general, present rockfall source areas are found in two zones. Firstly, they are found above the steep transport slope below the valley shoulder, and secondly, in the alpine zone above the timberline (Fig. 2). Obstacles like dead wood, tree stems, shrubs, and boulders act as barriers against falling rocks on the steep transport slope. In the alpine zone, falling rocks decelerate due to the decreasing slope gradient at the bottom part of talus slopes, but also due to the increasing surface roughness produced by larger rocks (Statham and Francis, 1986).

3. Materials

A digital elevation model (DEM) produced by the National Austrian Mapping Agency was available for this study (BEV, 2001). This DEM was arranged as a regular grid of surface height measurements with a spacing of 25 m. From this DEM, a map with mean slope gradients was derived using the method of Zevenbergen and Thorne (1987). Also available were a geological map and a digital land-cover map. The 1:200,000 geological map of the Province of Vorarlberg (GBA, 1998) provided information on the main formations and tectonic units. This map was digitised, labelled, and converted to a raster with a cell size of 25×25 m (1421 rows and 1437 columns, similar to the DEM). Subsequently, the prevailing rock types and the estimated rockfall susceptibility as well as the mean rock density (GSC, 2002) were added to the geological GIS map for each formation as well (Table 1). The estimated rockfall susceptibility data have been used to create Fig. 1.

This digital land-cover map was derived from a September 1998 Landsat TM image using a maximum likelihood classification for the land-cover classes: bare, lakes, snow/ice, alpine meadows and shrubs, valley meadows, and forest. Subsequently, the forested areas have been reclassified in the classes: broadleaved forest, mixed forest, dense coniferous forest, and open coniferous forest. This was done with an object-based classification technique (see Dorren et al., in press). After classification, we refined the land-cover classes on the basis of slope classes provided by the DEM. This resulted in the final land-cover classes: cliff face (60–90°), steep bare slope (40–60°), scree slope (30–40°), bare slope (0–30°), meadow, alpine shrubs, bushes, broadleaved forest, mixed forest, dense coniferous forest, and open coniferous forest. In addition, the attributes DBH (stem diameter at breast height, normally measured at ~ 1.3 m at the upslope side) and the average number of trees per hectare were added to the forest classes in the land-cover map. These attributes were derived from the most recent regional forest inventory, which treated existing forest compartments as homogeneous (Maier,

Table 1
Data on the different rock types and materials used in the model (based on GSC, 2002)

Rock types	Formation/tectonic unit	Rock density [kg/m^3]	Rockfall susceptibility
Slate, marl, and sandstone	‘Praetigau’ flysch—‘Gempi’ slice	2400	Low
Limestone, sandstone, and schist	‘Falknis’ nappe	2600	Medium
Limestone	‘Sulzfluh’ nappe	2500	High
Chert and marl	‘Arosa’ zone	2400	Low
Limestone (Muschelkalk) and dolomite	Sediment of the ‘Geisberg’ area	2600	High
Gneiss, amphibolite, and limestone	‘Madrisa’ zone	2900	High
Dolomite and limestone	‘Lechtal’ nappe	2400	High
Amphibolite, ophiolite, and gneiss	‘Silvretta’ nappe	2950	High
Quartzite-bearing gneiss and granite gneiss	‘Silvretta’ nappe	2750	High
Mica schist	‘Silvretta’ nappe	2750	Low
Biotite-bearing gneiss	‘Silvretta’ nappe	2650	High
Serpentine, calcite, and amphibolite	Ophiolites in the Penninic zone	3000	High

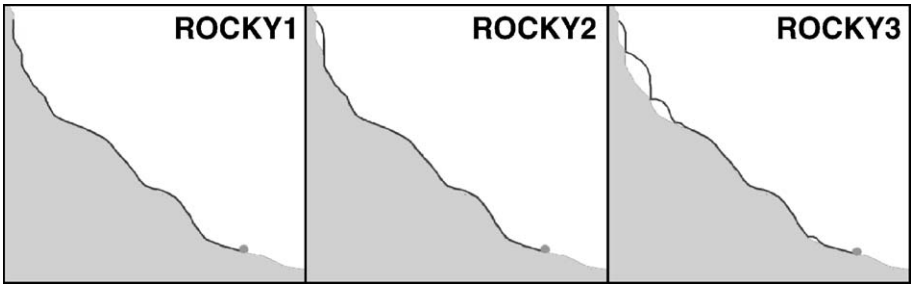


Fig. 3. Simple 2D representations of the different approaches of the three models tested: ROCKY1 only simulates sliding; ROCKY2 simulates initial freefall and then sliding; and ROCKY3 simulates sequences of bounces and motion through the air.

1993). A forest compartment is an area that is managed as a unit because of geoecological or ownership boundaries; a forest compartment may include multiple forest stands.

The dataset was completed by geomorphological raster maps, which were derived from digitised 1:10,000 geomorphological field maps (Fig. 3). The field mapping was based on a system described by De Graaff et al. (1987) and Seijmonsbergen (1992). These maps were coloured line symbol maps and incorporated information on drainage, morphography/morphometry, nonlithified materials, genesis of landforms, and current geomorphological processes (Seijmonsbergen, 1992). The information on the distribution and activity of rockfall areas in the study area derived from these maps served as a control. The rockfall areas were defined as cliff faces with scree slope below. The relative activity could be estimated by identifying the freshness of the scree. Approximately 20% of the study area was mapped using this mapping system. Some of these maps were completed recently, whereas the older ones were checked in the field on their accuracy regarding the information on distribution and activity of rockfall areas.

4. Models and methods

Three rockfall models were programmed in MATLAB 5.3 (Mathworks, 2002). Input data for the models were provided by raster analyses in the GIS Arcview 3.2 (ESRI, 2002). The first rockfall model (ROCKY1) is based on the algorithms described by Scheidegger (1975) and van Dijke and van Westen (1990). The second rockfall model (ROCKY2) forms an extended version of ROCKY1 and is based on the *Sturzgeschwindigkeit* model developed by Meißl (1998). The third rockfall model (ROCKY3) is based on algorithms modified from Pfeiffer and Bowen (1989). The main difference between ROCKY3 and the other two models is that ROCKY3 is able to simulate multiple bounces of a falling rock within a pixel. The other two models calculate the velocity of the rock on the basis of one calculation between two cell centres. The following paragraphs describe how each model calculates the source areas, the fall direction, and the runout zones of simulated falling rocks.

4.1. Source area and falltrack calculation

Potential rockfall source areas were determined on the basis of the mean slope gradient map and the geological map. Areas such as morainic and scree slopes, lake, rivers, glaciers, and floodplains were disqualified as potential rockfall source areas. Those areas or cells with both a mean slope gradient equal to or greater than 40° and which were classified as bedrock according to the geological map were considered as potential rockfall source areas or source cells. From these source cells, rocks were simulated as falling from vertical cliff faces with a height of 10 m. The initial vertical velocity of the rock was −1 m/s (negative direction is downslope) and the initial horizontal velocity was 1 m/s (positive is normal to the slope surface).

The fall direction from each raster cell is defined as the direction of the steepest descent towards a neighbouring cell. The steepest descent is calculated as the change in height between two cells divided by the distance between the cell centres. This method is

based on deriving flow direction from a DEM presented in Jenson and Domingue (1988). The three models tested all applied the above-described procedures.

4.2. Runout zone calculation

The length of each rockfall runout zone is calculated on the basis of the velocity of a falling rock. In general, a falling rock starts with acceleration on the steeper slope parts and decelerates on slope parts with lower mean slope gradient until it stops in a certain position, depending on the vegetation cover and slope surface properties.

ROCKY1 calculates the velocity on the basis of energy conservation of a mass that is considered to slide over a slope surface (Fig. 4) as defined by Scheidegger (1975). In this energy conservation approach, a friction coefficient was responsible for energy loss. For each cell in the falltrack, the velocity of the falling rock was calculated as follows:

$$V_{out} = \sqrt{V_{in}^2 + 2g(h - \mu + X)} \quad (1)$$

where: V_{out} = outgoing velocity [m/s]; V_{in} = incoming velocity [m/s]; $g = 9.81$ [m/s^2]; h = fall height [m] (height difference between two raster cells); μ = friction coefficient [−]; and X = horizontal fall distance [m].

This velocity is calculated for each cell within the falltrack, starting at the rockfall source cell. The value of the friction coefficient depends on the surface cover characteristics, including the plasticity of the material

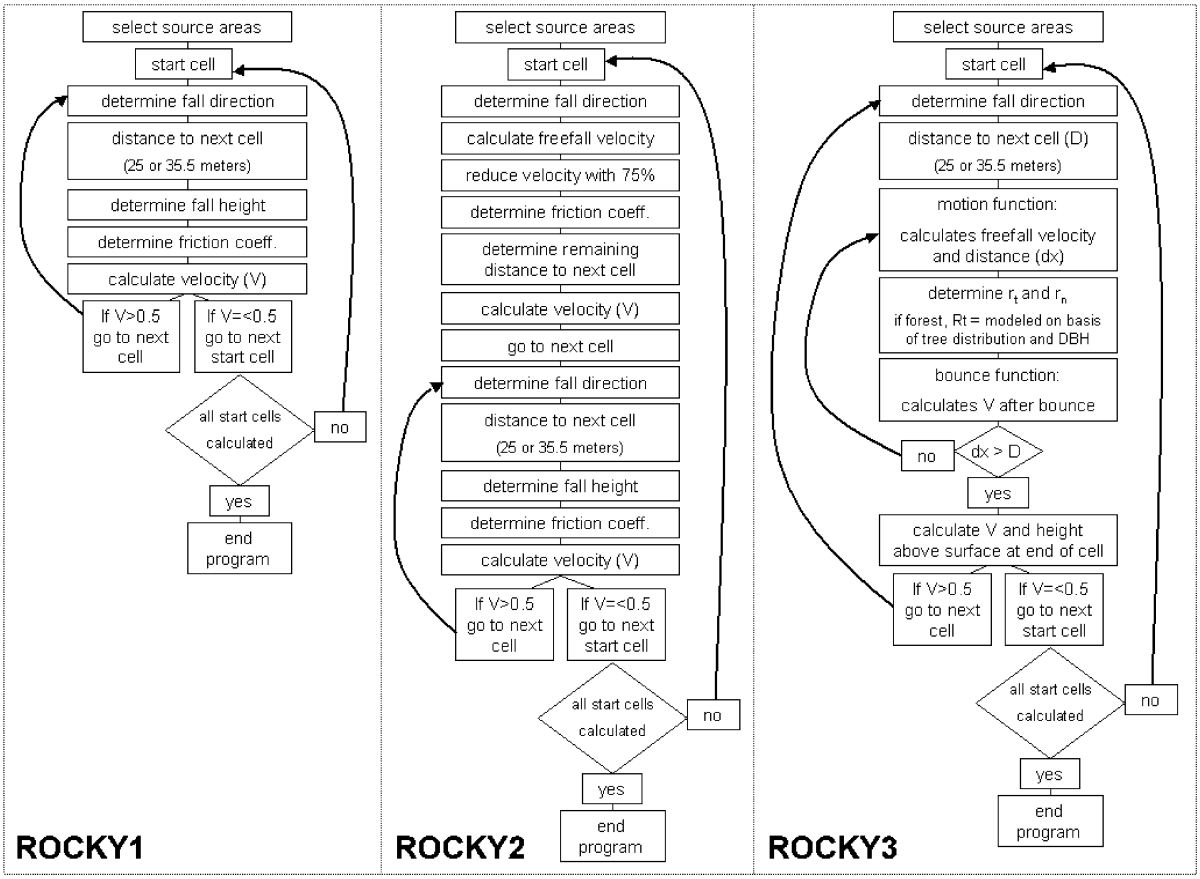


Fig. 4. Flow diagrams presenting a general overview of the three models tested.

covering the slope and the obstacles on the slope surface like vegetation, rocks, and dead wood. Values for the friction coefficient have been derived from literature (van Dijke and van Westen, 1990; Meißl, 1998) and are presented in Table 2.

ROCKY2 is quite similar to ROCKY1, except for the initial velocity calculation. In this model, the falling rock is considered to fall through the air, before it slides over the slope surface (Fig. 4). ROCKY2 calculates motion through the air with an idealized model (representing the rock as a single particle with a certain radius), and accelerates due to gravity, without incorporating the effect of air resistance. To account for energy loss during the first collision or bounce on the slope surface, 75% of the velocity gained during the motion through the air is subtracted. In the following cells, the velocity is calculated using Eq. (1).

ROCKY3 simulates a falling rock by sequences of bouncing and motions through the air (Fig. 4). Several of these sequences can occur within a pixel. The calculation of the motion through the air is similar to ROCKY2, using standard algorithms for describing a parabolic flight of a uniform accelerating particle. To calculate the velocity after the bounce, the velocity before a bounce is resolved into a tangential velocity (Vt_{in}, parallel to the slope surface) and a normal velocity (Vn_{in}, perpendicular to the slope surface).

Table 2
Tangential and normal coefficients of restitution (r_t and r_n, respectively) and the coefficient of friction (μ) used for the different land-cover types defined in this study

Land cover	r_t	r_n	μ
Cliff face (60–90°)	0.95	0.45	0.25
Steep bare slope (40–60°)	0.90	0.40	0.45
Scree slope (30–40°)	0.88	0.32	0.60
Bare slope (0–30°)	0.87	0.35	0.50
Meadow	0.87	0.30	0.55
Alpine shrubs	0.85	0.30	0.60
Bushes	0.83	0.30	0.65
Forest (200 trees per hectare average)	0.01–0.85[a] (mean 0.67)	0.28	1.00
Forest (300 trees per hectare average)	0.01–0.85[a] (mean 0.57)	0.28	1.50
Forest (500 trees per hectare average)	0.01–0.85[a] (mean 0.38)	0.28	2.00
Forest (700 trees per hectare average)	0.01–0.85[a] (mean 0.27)	0.28	2.20

[a] The distribution is dependent on the number of trees per hectare (see text for explanation).

The tangential velocity after a bounce is calculated with:

$$Vt_{out} = \sqrt{\frac{R^2(I\omega^2 + MVt_{in}^2)r_t}{(I + MR^2)}} \quad (2)$$

where: Vt_{out} = tangential velocity after the bounce [m/s]; R = radius of the falling rock [m]; I = moment of inertia = $2/5MR^2$ [kg m^2]; ω = rotational velocity [rad/s] = Vt_{out}/R; M = mass of the falling rock [kg]; Vt_{in} = tangential velocity before the bounce [m/s]; and r_t = tangential restitution coefficient determining energy loss [−].

The normal velocity after a bounce is calculated with:

$$Vn_{out} = Vn_{in}r_n \quad (3)$$

where: Vn_{out} = normal velocity after the bounce [m/s]; Vn_{in} = normal velocity before the bounce [m/s]; and r_n = normal restitution coefficient determining energy loss [−].

During every bounce within a pixel, ROCKY3 reduces the slope angle with a random value between 0° and 4°, as shown in Fig. 5. This procedure was programmed to account for the slope variability in the field, since slopes with perfectly straight slopes over a horizontal distance of 25 m hardly exist. We only allow the model to decrease the mean slope gradient during a bounce since rocks tend to bounce on the flatter parts of a scree slope. Rocks lying on the side with the two largest axes mainly form these slopes. This procedure was similar to the varying impact angle based on the surface roughness as described by Pfeiffer and Bowen (1989).

If the horizontal distance travelled by a rock between two bounces modelled in ROCKY3 is less than its diameter, the rock is considered to be rolling. Then the rock will be given a new displacement over the slope surface equal to the diameter of the rock. This prevents an infinite amount of simulated bounces per raster cell (after Pfeiffer and Bowen, 1989). Sequences of motion through the air followed by a bounce are repeated until the velocity of the falling rock is equal to or less than 0.5 m/s. This limit is also used for calculating the end location of the rockfall runout zones in ROCKY1 and ROCKY2. The flow diagrams presented in Fig. 6 visualize the different simulation steps for the tested models.

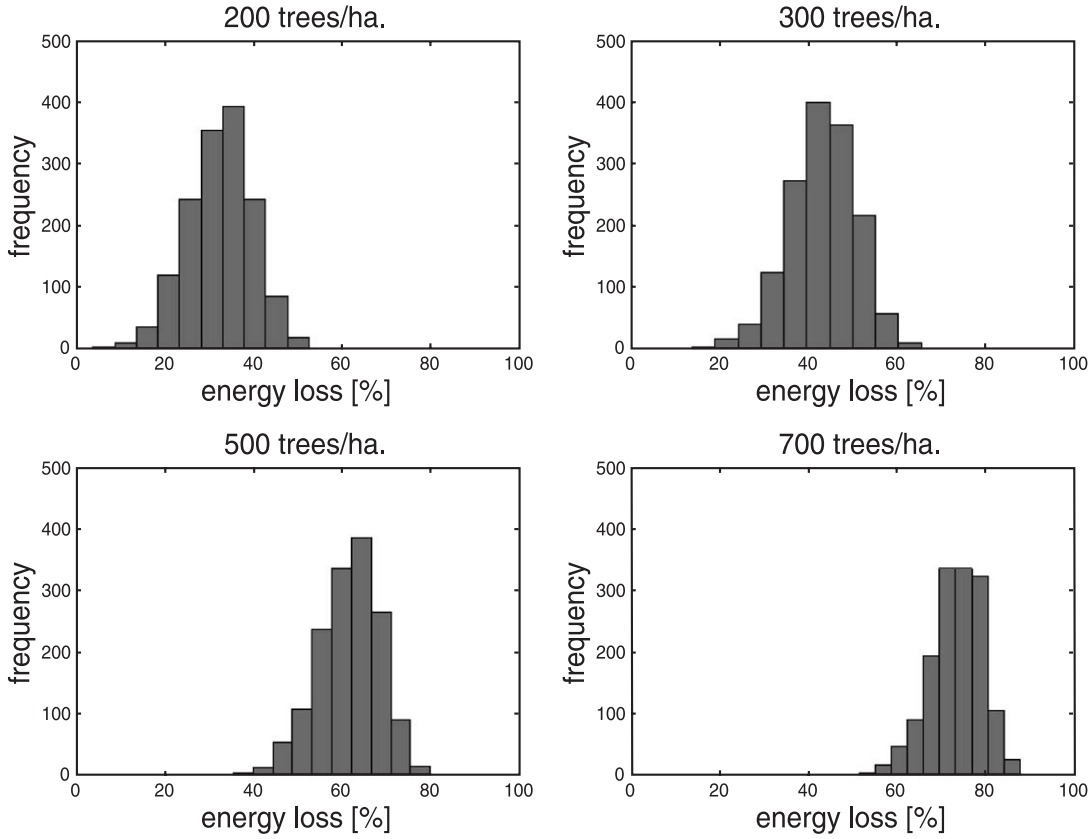


Fig. 5. Histograms of energy loss within a pixel for 200, 300, 500, and 700 trees per hectare.

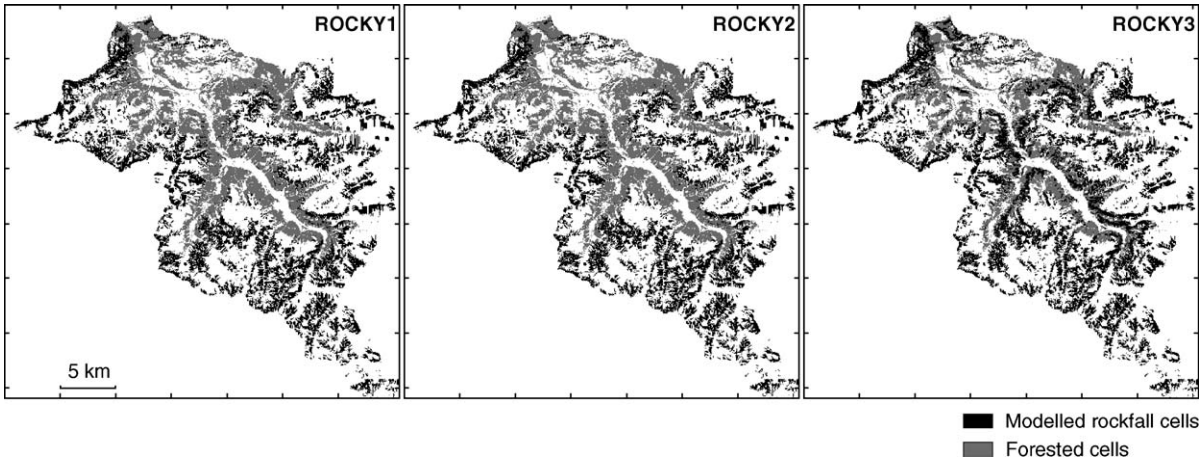


Fig. 6. Modelled patterns of rockfall runout zones within the study area produced by the three models.

4.3. Estimating input parameter values

In addition to the mean slope gradient, the determining parameter for the length of rockfall runout zones in ROCKY1 and ROCKY2 is the friction coefficient. In ROCKY3, this is the tangential and the normal restitution coefficient. These parameters represent surface cover and soil characteristics, which determine the amount of energy loss during each bounce. The friction coefficient, the tangential restitution coefficient, and the normal restitution coefficient were not calibrated on the basis of data that were measured throughout the study area. Instead, these model parameters were estimated on the basis of the land-cover map in combination with published data (Pfeiffer and Bowen, 1989; van Dijke and van Westen, 1990; Kobayashi et al., 1990; Giani, 1992; Azzoni et al., 1995; Chau et al., 1998, 2002; Meißl, 1998). The parameter values used in this study are shown in Table 2.

Estimating the tangential restitution coefficient on forested slopes was a special case. In every raster cell classified as forested, ROCKY3 simulated a forest density based on the number of trees per hectare and the DBH given for that particular cell. Within ROCKY3, a module that distributes trees randomly in a 25 × 25-m cell and calculates the energy loss as a result of different collisions with tree stems was programmed. The rock is being modelled as falling through the centreline or the diagonal of the raster cell, depending on the fall direction. In addition, the positions of the tree stems in the cell are known. This allows the model to calculate the position of the rock with respect to the tree stem during each simulation step. Since data on energy loss of falling rocks due to impacts on tree stems were not available, the following equation is used to estimate energy losses:

$$\Delta E = \sqrt{1 - \left(\frac{d}{0.5\mathrm{DBH} + R}\right)^2} \qquad (4)$$

where: ΔE = fraction of energy loss due to an impact against a tree stem [−]; d = distance between the centre of the rock and the centre of the tree stem [m]; DBH = diameter of the tree stem at breast height [m]; and R = radius of the falling rock [m].

We developed this formula assuming that a tree stem absorbs a maximum amount of kinetic energy if a central collision between a rock and a tree stem occurs. In reality, falling rocks could collide with trees at a certain height above the surface. Subsequently, a rock falls on the ground and gains new kinetic energy. This process is incorporated in the model by limiting the maximum energy loss to 99%. After the energy loss is calculated, the translation energy and the rotation energy are multiplied by the calculated fraction of energy loss. Subsequently, the resulting energies are transformed into a resultant velocity. If a rock does not collide against a tree stem, a bounce is simulated with a tangential coefficient of restitution of 0.87.

Apart from the model tests carried out with ROCKY3 for the whole study area, simulations of rocks falling through a single pixel were carried out using 1500 different tree distributions with 200, 300, and 500 trees per hectare as well as the extreme value of 700 trees per hectare. The preliminary outcomes of these simulations provided histograms of energy loss per class of number of trees per hectare (Fig. 5).

4.4. Model comparison

The radius of the simulated rocks in all the models tested was 0.25 m. This radius was used to calculate the weights of the falling rocks on the basis of the densities presented in Table 1. The modelled patterns of rockfall runout zones produced by the three models will be compared with the patterns of rockfall deposits derived from the geomorphological field maps. For this comparison, contingency tables are used. From these tables, the overall accuracies normalized for the number of mapped rockfall cells are calculated. In

Table 3
Summarized results of the tested models

	ROCKY1	ROCKY2	ROCKY3
Correctly modelled rockfall cells on forested slopes [%]	9.5	6.3	54.4
Correctly modelled rockfall cells on nonforested slopes [%]	67.4	67.4	66.8
Matches on forested slopes (nonrockfall and rockfall) [%]	53.7	52.5	66.9
Matches on nonforested slopes (nonrockfall and rockfall) [%]	75.5	75.4	75.4
Normalized overall accuracy [%]	72.1	71.5	73.5
ϕ coefficient of correspondence	0.44	0.43	0.43

Table 4
Average velocity and the standard deviation simulated by the three tested models

Slope type class	ROCKY1		ROCKY2		ROCKY3	
	Average velocity [m/s]	S.D. [m/s]	Average velocity	S.D.	Average velocity	S.D.
Forest 0–20	30.3	15.3	30.7	15.5	14.9	9.2
Nonforest 0–20	29.8	14.6	31.3	15.0	20.3	9.9
Forest 20–40	27.0	15.0	27.4	15.4	17.8	9.3
Nonforest 20–40	34.3	12.9	35.7	13.4	25.5	10.1
Forest 40–60	17.0	11.4	23.6	12.7	18.7	5.7
Nonforest 40–60	31.6	10.3	33.3	10.7	26.0	8.7
Forest 60–90	27.7	12.3	34.6	10.9	28.6	8.5
Nonforest 60–90	48.4	11.5	50.0	10.7	39.4	8.4

addition, the number of matches between mapped and modelled patterns both on forested and nonforested slopes is determined. To test for the significance of the association between the mapped and modelled patterns of rockfall runout zones, the correspondence coefficient ϕ (Burt and Barber, 1996) is calculated as well.

Furthermore, the rockfall velocities modelled by the three models are compared. For this comparison, different forested and nonforested slope classes are distinguished on the basis of the mean slope gradient.

5. Results

Fig. 6 shows an overview of the general rockfall patterns produced by the three models. They show similar results for ROCKY1 and ROCKY2, with both models producing rockfall areas in the high alpine zones, but none on the forested valley slopes. Results of ROCKY3 contrast sharply with ROCKY1 and ROCKY2 and show rockfall areas on both forested and nonforested slopes throughout the study area.

As shown in Table 3, the percentage of correctly modelled rockfall cells according to the control data varied on forested slopes and nonforested slopes for each model. Moreover, as expected, after examining the general modelled patterns in Fig. 6, there is a large difference among the results of the three models. On forested hillslopes, ROCKY3 performed best, correctly identifying 54.,4% of the mapped rockfall cells, while ROCKY1 and ROCKY2 only modelled 9.5% and 6.3%, respectively, of the mapped rockfall cells. When taking into account both mapped rockfall and nonrockfall cells, the amount of matches increased for ROCKY1 and ROCKY2 to 53.7% and 52.5%, respectively. Again, ROCKY3 performed best in this case, since 66.9% of the modelled cells matched mapped cells.

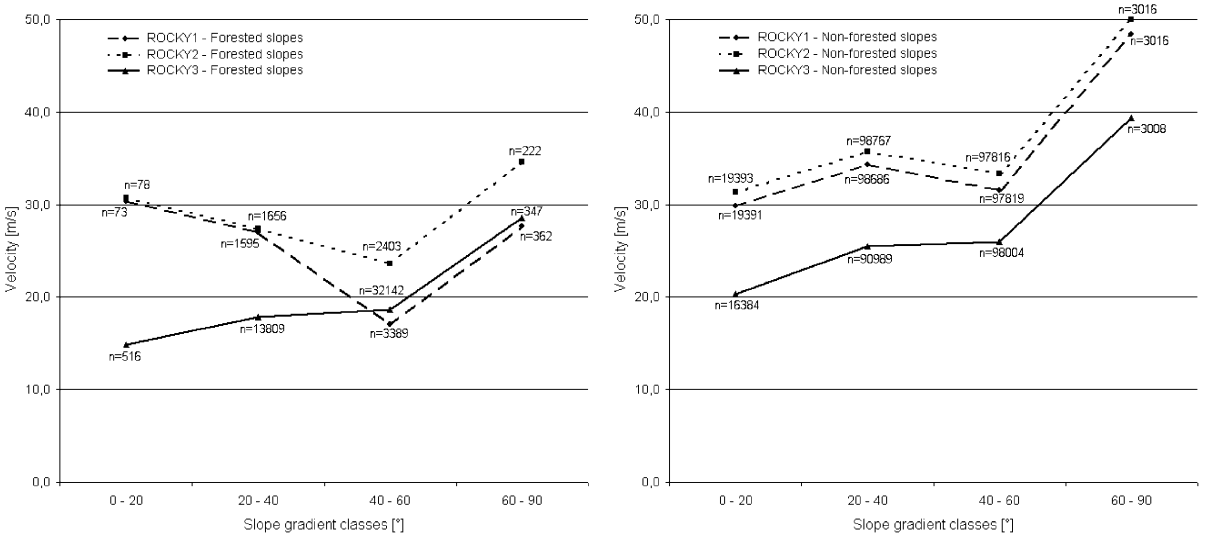


Fig. 7. Summary of the average velocities simulated by ROCKY1, ROCKY2, and ROCKY3 on different forested and nonforested slopes.

Table 5
Contingency tables of ROCKY1 presenting the number of cells and the accuracies normalized for the number of mapped cells

	Mapped as rockfall	Mapped as nonrockfall	Total
Modelled as rockfall	22,737	17,968	40,705
Modelled as nonrockfall	17,720	130,868	148,588
Total	40,457	148,836	189,293
Modelled as rockfall	0.562	0.121	0.683
Modelled as nonrockfall	0.438	0.879	1.317
Total	1.000	1.000	2.000

Table 7
Contingency tables of ROCKY3 presenting the number of cells and the accuracies normalized for the number of mapped cells

	Mapped as rockfall	Mapped as nonrockfall	Total
Modelled as rockfall	26,072	25,980	52,052
Modelled as nonrockfall	14,385	122,856	137,241
Total	40,457	148,836	189,293
Modelled as rockfall	0.644	0.175	0.819
Modelled as nonrockfall	0.356	0.825	1.181
Total	1.000	1.000	2.000

On nonforested slopes, both ROCKY1 and ROCKY2 performed slightly better than ROCKY3. The amount of correctly modelled rockfall cells was 67.4% for ROCKY1 and ROCKY2. For ROCKY3, this amount was 66.8%. Taking into account both mapped rockfall and nonrockfall cells, the produced accuracies are rather equivalent. Table 3 shows that this is also the case for the normalized overall accuracies (normalized for the number of mapped cells) produced by the three models. The highest normalized overall accuracy was, however, produced by ROCKY3 (73.5%). The association between the mapped and modelled patterns of rockfall runout zones, given by the ϕ coefficient in Table 3, is not very strong for all the three models tested ($\phi = 0.44$ or $\phi = 0.43$).

A comparison of the modelled velocities puts forward that the velocity distributions on four mean slope gradient classes, as produced by ROCKY1 and ROCKY2, are rather unrealistic, especially on the forested hillslopes (Table 4 and Fig. 7). On these hillslopes, the average velocity produced by ROCKY1 and ROCKY2 decreased from 27.0 to 17.0 m/s and from 27.4 to 23.6 m/s, respectively, while the mean gradient increased (Fig. 7). ROCKY3 was the only model that produced lower and more realistic velocities (14.9 m/s) on gentle forested hillslopes as well as higher velocities (28.6 m/s) on steep forested hillslopes. On nonforested hillslopes, all the three models produced an increase of velocity with increasing mean slope gradient. However, the velocities produced by ROCKY1 and ROCKY2 were generally 10 m/s higher than those produced by ROCKY3 (Table 4).

Table 6
Contingency tables of ROCKY2 presenting the number of cells and the accuracies normalized for the number of mapped cells

	Mapped as rockfall	Mapped as nonrockfall	Total
Modelled as rockfall	22,179	17,578	39,757
Modelled as nonrockfall	18,278	131,258	149,536
Total	40,457	148,836	189,293
Modelled as rockfall	0.548	0.118	0.666
Modelled as nonrockfall	0.452	0.882	1.334
Total	1.000	1.000	2.000

Despite the low amount of matches on forested hillslopes, ROCKY1 and ROCKY2 produced high normalized overall accuracies. As shown in the contingency tables (Tables 5–7), ROCKY1 and ROCKY2 produced fewer rockfall cells ($n = 40{,}705$ and $n = 39{,}757$, respectively) compared to ROCKY3 ($n = 52{,}052$). As a result, ROCKY1 and ROCKY2 produced more nonrockfall cells ($n = 148{,}588$ and $n = 149{,}536$, respectively) compared to ROCKY3 ($n = 137{,}241$). Therefore, ROCKY1 and ROCKY2 produced accuracies of 0.879 and 0.882 in the nonrockfall class.

The comparison of the amount of both correctly ($n = 26{,}072$) and incorrectly ($n = 25{,}980$) modelled rockfall cells produced by ROCKY3 also provides an interesting result (Table 7). Only 17.5% of all cells mapped as nonrockfall were modelled as rockfall cells. On the other hand, this amount was equal to 49.9% of all the modelled rockfall cells. For ROCKY1 and ROCKY2, this amount was 44.1% and 44.2%, respectively.

6. Discussion

The GIS-based distributed model developed for this study (ROCKY3) simulates motions of falling rocks in detail. This model also incorporates simple forest

parameters (number of trees per hectare and DBH) as well as a module that accounts both for the tree distribution and for the calculation of collisions of rocks against trees. A comparison of the modelled patterns of rockfall runout zones produced by the three models tested (ROCKY1, ROCKY2, and ROCKY3) with mapped rockfall patterns showed that ROCKY3 performed best in simulating rockfall patterns in the study area. In addition, a comparison of the velocities produced by the three models showed that ROCKY3 simulates rockfall velocities more accurately on both forested and nonforested hillslopes. Unfortunately, no data are currently available on rockfall velocities within the study area. However, during real-time rockfall experiments in the French Alps, on a nonforested avalanche track on a talus slope with a mean slope gradient of approximately 38°, falling rocks reached maximum velocities of 25 m/s (F. Berger-Cemagref Grenoble, personal communication). These slopes are typical rockfall-endangered areas that are also found in our study area. ROCKY1 and ROCKY2 generally produced higher velocities on less steep forested and nonforested hillslopes. In contrast, the velocities produced by ROCKY3 on similar hillslopes corresponded with this observation.

Although ROCKY3 provided better overall results than ROCKY1 and ROCKY2, all three models produced similar normalized overall accuracies. Since ROCKY1 and ROCKY2 simulated fewer rockfall cells than ROCKY3, the probability of cells being modelled incorrectly (mismatch with cells mapped as nonrockfall) decreased. In addition, 80% of the mapped cells are nonrockfall areas. Therefore, the amount of nonrockfall matches was very high for ROCKY1 and ROCKY2. As a consequence, the normalized overall accuracy was also high.

The three models tested encountered similar problems regarding mismatches between modelled rockfall cells and mapped nonrockfall cells (ROCKY3: 49.9%, ROCKY1: 44.1%, and ROCKY2: 44.2%). These mismatches were mainly caused by the input data, being GIS rasters with a support of 25 × 25 m. Within such rasters, fine-scale variation in the mean slope gradient and surface cover characteristics as observed in the field is lost. In addition, the topography as shown by a DEM with a support of 25 × 25 m is much smoother than the real topography (Hodgson, 1995; Walker and Willgoose, 1999; Yin and Wang, 1999; Zhang et al., 1999; Schoorl et al., 2000).

To account for this smoothing effect, starting locations in rockfall source cells are set at 10 m above the surface, since it was observed in the study area that small cliff faces with a height of 10–50 m do occur on hillslopes that are represented by raster cells with a slope gradient of 40°. Due to the use of the simple threshold value for identifying the rockfall source cells, the model produced some rockfall areas in locations where this is not the case in reality. Therefore, the model results probably improve considerably if these small cliff faces could be identified for the whole study area, which is a GIS research challenge.

The use of a mean slope gradient threshold of 40° for rockfall source areas also had a distinct effect on the modelled velocities. The velocity graph (Fig. 7) shows that the average velocities produced by the three models only increase slightly or even decrease between the slope classes 20–40° and 40–60°. This may be explained by two reasons. Firstly, since the threshold value for rockfall source areas was defined as 40°, the model started to simulate rockfall in cells with a mean slope gradient equal to or steeper than 40°. Depending on the friction or the restitution coefficients, the simulated rock stopped within the source cell, or accelerated and consequently shifted to the next cell in the falltrack. The latter generally occurred in cells with a mean slope angle much steeper than 40°. Acceleration also occurred on slopes with a mean slope gradient of 40°, but the resulting velocity in those source cells was not as high as in source cells with steeper slope gradients. Secondly, the low velocities in cells with a mean slope gradient of around 40° could be the result of falling rocks that were simulated from source cells upslope with slope gradients slightly steeper than 40°. Downslope, the velocity and the mean gradient of the slope decreased and, consequently, the rock could stop in one of the downslope cells, which could have a slope gradient of approximately 40°. High velocities on slopes with mean gradients much lower than 40° may be explained by the fact that these cells were mainly runout zones of falling rocks simulated from steep to very steep (>60°) source cells. These observations show that the threshold of 40° is a safe value to account for the smoothing effect of the 25 × 25-m

DEM, but it might also lead to incorrectly modelled patterns of rockfall runout zones.

The use of a falltrack calculation based on a multiple flow algorithm (Quinn et al., 1991; Wolock and McCabe, 1995) would improve the model as well. The currently used falltrack calculation will always generate converging rockfall runout zones instead of diverging zones (e.g., as observed on talus cones in the field). The multiple flow algorithm enables modelling of more realistic rockfall accumulation areas, which might improve the number of matches between model and map. Within this study, it was chosen to test the models with a simple falltrack procedure because this facilitated the comparison of the model results. The incorporation of the multiple flow algorithm in the three models tested would introduce a stochastic factor and therefore more difficulties for comparing the results.

The friction coefficient, the tangential restitution coefficient, and the normal restitution coefficient for different land-cover classes were estimated from literature data on the basis of the land-cover map. Firstly, this was done because field data were not available and, secondly, because simulation errors were interpreted as model errors rather than parameter estimation errors. The latter enabled us to compare the three models on their ability to predict rockfall runout zones on slopes with different characteristics throughout the study area.

As shown by the accuracy of the modelled patterns of rockfall runout zones on nonforested hillslopes as produced by the three models, the estimation of parameter values worked satisfactory. However, a more objective method for estimating these parameters at a regional scale would be preferred. Regarding the effect of forests on patterns of rockfall runout zones, different forest densities could be described reasonably well by using the number of trees per hectare and the DBH, but incorporating gaps within forest stands was not possible. Gaps in a forest are important elements of a forest structure that determine the level of protection a mountain forest provides against rockfall (Bebi et al., 2001). For rockfall modelling at a regional scale, there is thus a need for both an automated assessment and a model representation of gaps in mountain forests at a regional scale. Gaps within forests could, for example, be represented in a model by using a fractal dimension (Xu and Lanthrop, 1995). In this case, mountain forests are considered as porous systems in which the fractal dimension of the pore space represents the gap distribution. For example, such an approach has been used for describing pore structures of Swiss cheese models (Klemm et al., 1999).

7. Conclusions

From all the three models tested in this study, the combination of a GIS-based model and a process-based model, which simulates the motion of falling rocks in detail and incorporates simple forest stand parameters, was most accurate in predicting patterns of rockfall runout zones at a regional scale. Like all the models tested, this model combines three main procedures: the identification of source areas, the determination of falltracks, and the calculation of the rockfall runout zones.

Regarding the identification of source areas, the model probably improves considerably if rockfall source areas, such as small cliff faces, could be identified in detail, instead of using a mean slope gradient threshold value. With respect to determining the falltrack, the use of a multiple flow algorithm could also improve the model. The calculation of the rockfall runout zones was satisfactory. However, gaps within forest stands were not taken into account in the input data. Incorporating gaps in the forest input data might result in a better representation of the velocity development on forested slopes. Therefore, a better representation of gaps within forest stands at a regional scale is needed.

Acknowledgements

We gratefully acknowledge Bernhard Maier for providing the forest inventory data and for sharing his knowledge of mountain forest management. Furthermore, we wish to thank Ger Bergkamp and Anton Imeson for their suggestions for improvement.

References

Azzoni, A., Barbera, G.L., Zaninetti, A., 1995. Analysis and prediction of rockfalls using a mathematical model. International Journal of Rock Mechanics and Mining Science 32, 709–724.

Bebi, P., Kienast, F., Schönenberger, W., 2001. Assessing structures in mountain forests as a basis for investigating the forests' dynamics and protective function. Forest Ecology and Management 145, 3–14.

BEV, 2001. Bundesamt für Eich-und Vermessungswesen, Produktinformation zum Geländehöhenmodell. http://www.bev.gv.at/.

Bozzolo, D., Pamini, R., 1986. Simulation of rock falls down a valley side. Acta Mechanica 63, 113–130.

Burt, J.E., Barber, G.M., 1996. Elementary Statistics for Geographers. Guilford Press, New York. 640 pp.

Chau, K.T., Wong, R.H.C., Lee, C.F., 1998. Rockfall problems in Hong Kong and some new experimental results for coefficient of restitution. International Journal of Rock Mechanics and Mining Science 35 (4), 662–663.

Chau, K.T., Wong, R.H.C., Wu, J.J., 2002. Coefficient of restitution and rotational motions of rockfall impacts. International Journal of Rock Mechanics and Mining Sciences 39 (1), 69–77.

De Graaff, L.W.S., de Jong, M.G.G., Rupke, J., Verhofstad, J., 1987. A geomorphological mapping system at scale 1,10.000 for mountainous areas. Zeitschrift für Geomorphologie N.F. 31 (2), 229–242.

Dorren, L.K.A., 2003. A review of rockfall mechanics and modelling approaches. Progress in Physical Geography 27 (1), 69–87.

Dorren, L.K.A., Maier, B., Seijmonsbergen, A.C., in press. Improved Landsat-based forest mapping in steep mountainous terrain using object-based classification. Forest Ecology and Management.

ESRI, 2002. Arcview 3.2 and Spatial Analyst. Environmental Systems Research Institute. http://www.esri.com.

GBA, 1998. In: Oberhauser, R., Rataj, W. (Eds.), Geologisch-Tektonische Übersichtskarte von Vorarlberg (1,200,000) with Erläuterungen. Geological Survey of Austria, Vienna, Austria.

Giani, G.P., 1992. Rock Slope Stability Analysis. Balkema, Rotterdam. 361 pp.

GSC, 2002. GSC Atlantic Rock Properties Database. Geological Survey of Canada/Dalhousie University. http://gsca.nrcan.gc.ca/pubprod/rockprop/search_e.php.

Hodgson, M.E., 1995. What cell-size does the computed slope aspect angle represent. Photogrammetric Engineering and Remote Sensing 61 (5), 513–517.

Jenson, S.K., Domingue, J.O., 1988. Extracting topographic structure from digital elevation data for geographic information system analysis. Photogrammetric Engineering and Remote Sensing 54 (11), 1593–1600.

Keller, M., 1994. Considerations to quantify forest functions by means of a GIS. Proceedings EGIS '94, Fifth European Conference and Exhibition on Geographical Information Systems, Utrecht. EGIS Foundation, vol. 1, pp. 1676–1681.

Kirkby, M.J., Statham, I., 1975. Surface stone movement and scree formation. Journal of Geology 83, 349–362.

Klemm, A., Müller, H.-P., Kimmich, R., 1999. Evaluation of fractal parameters of percolation model objects and natural porous media by means of NMR microscopy. Physica A 266, 242–246.

Kobayashi, Y., Harp, E.L., Kagawa, T., 1990. Simulation of rockfalls triggered by earthquakes. Rock Mechanics and Rock Engineering 23, 1–20.

Köppen, W., 1918. Klassifikation der Klimate nach Temperatur, Niederschlag, und Jahreslauf. Petermann's Mitteilungen 64, 193–203.

Kräuchi, N., Brang, P., Schönenberger, W., 2000. Forests of mountainous regions, gaps in knowledge and research needs. Forest Ecology and Management 132, 73–82.

Maier, B., 1993. Forstinventur Stand Montafon. Internal Report. Stand Montafon, Schruns. 154 pp.

Mathworks, 2002. Matlab, the language of technical computing, version 5.3. The MathWorks. http//www.mathworks.com.

Meißl, G., 1998. Modellierung der Reichweite von Felsstürzen. Fallbeispeile zur GIS-gestützten Gefahrenbeurteilung aus dem Beierischen und Tiroler Alpenraum. Innsbrucker Geografischen Studien 28. PhD Thesis, Universität Innsbruck, Innsbruck, Austria. 249 pp.

Meißl, G., 2001. Modelling the runout distances of rockfalls using a geographic information system. Zeitschrift für Geomorphologie N.F. Supplementband 125, 129–137.

Motta, R., Haudemand, J.C., 2000. Protective forests and silvicultural stability—an example of planning in the Aosta Valley. Mountain Research and Development 20 (2), 180–187.

Okura, Y., Kitahara, H., Sammori, T., Kawanami, A., 2000. The effects of rockfall volume on runout distance. Engineering Geology 58 (2), 109–124.

Pfeiffer, T.J., Bowen, T.D., 1989. Computer simulation of rockfalls. Bulletin of the Association of Engineering Geologists 26 (1), 135–146.

Quinn, P., Beven, K., Chevallier, P., Planchon, O., 1991. The prediction of hillslope flow paths for distributed hydrological modelling using digital terrain models. Hydrological Processes 5, 59–79.

Scheidegger, A.E., 1975. Physical Aspects of Natural Catastrophes. Elsevier, Amsterdam.

Schoorl, J.M., Sonneveld, M.P.W., Veldkamp, A., 2000. Three-dimensional landscape process modelling: the effect of DEM resolution. Earth Surface Processes and Landforms 25, 1025–1034.

Seijmonsbergen, A.C., 1992. Geomorphological evolution of an alpine area and its application to geotechnical and natural hazard appraisal in the NW. Rätikon and S. Walgau (Vorarlberg, Austria), including map series at 1,10,000 scale. PhD Thesis, University of Amsterdam, Amsterdam, the Netherlands. 109 pp.

Statham, I., Francis, S.C., 1986. Influence of scree accumulation and weathering on the development of steep mountain slopes. In: Abrahams, A.D. (Ed.), Hillslope Processes. Allen and Unwin, Winchester, pp. 245–267.

van Dijke, J.J., van Westen, C.J., 1990. Rockfall hazard, a geomorphological application of neighbourhood analysis with ILWIS. ITC Journal 1, 40–44.

van Noord, H., 1996. The role of geomorphological information in ecological forest site typology in mountainous areas, a methodological study in the E-Rätikon and NW-Montafon mountains (Vorarlberg, Austria). PhD Thesis, University of Amsterdam, Amsterdam, the Netherlands. 185 pp.

Walker, J.P., Willgoose, G.R., 1999. On the effect of digital elevation model accuracy on hydrology and geomorphology. Water Resources Research 35 (7), 2259–2268.

Wolock, D.M., McCabe Jr., G.J., 1995. Comparison of single and

multiple flow direction algorithms for computing topographic parameters in TOPMODEL. Water Resources Research 31, 1315–1324.

Xu, J., Lanthrop, R.G., 1995. Improving simulation accuracy of spread phenomena in a raster-based Geographic Information System. International Journal of Geographical Information Systems 9 (2), 153–168.

Yin, Z.Y., Wang, X.H., 1999. A cross-scale comparison of drainage basin characteristics derived from digital elevation models. Earth Surface Processes and Landforms 24, 557–562.

Zevenbergen, L.W., Thorne, C.R., 1987. Quantitative analysis of land surface topography. Earth Surface Processes and Landforms 12, 47–56.

Zhang, X.Y., Drake, N.A., Wainwright, J., 1999. Comparison of slope estimates from low resolution DEMs: scaling issues and a fractal method for their solution. Earth Surface Processes and Landforms 24, 763–779.

> Chapter 5

Field assessment and modeling of rockfall in a protection forest



Available online at www.sciencedirect.com
SCIENCE DIRECT®
Geomorphology 57 (2004) 151–167
GEOMORPHOLOGY
www.elsevier.com/locate/geomorph

Combining field and modelling techniques to assess rockfall dynamics on a protection forest hillslope in the European Alps

Luuk K.A. Dorren[a,*], Bernhard Maier[b], Uif S. Putters[a], Arie C. Seijmonsbergen[a]

[a] *Centre for Geo-ecological Research (ICG), Institute for Biodiversity and Ecosystem Dynamics-Physical Geography, Universiteit van Amsterdam, Nieuwe Achtergracht 166, 1018 WV Amsterdam, The Netherlands*
[b] *Stand Montafon-Forstfonds, Montafonerstraße 21, A-6780 Schruns, Austria*

Received 19 June 2002; received in revised form 7 February 2003; accepted 9 February 2003

Abstract

Adequate management of a mountain forest that protects downslope areas against impacts of rockfall requires insight into the dynamics of the hillslope environment. Therefore, we applied a combined approach, using field and modelling techniques, to assess the determining factors for rockfall source areas, rockfall tracks and rockfall runout zones on a forested slope in mountainous terrain. The first objective of this study was to understand why rockfall occurs in the study area. The second objective was to translate the knowledge obtained in the field into a model that simulates rockfall dynamics on a forested slope realistically. The third objective was to assess which hillslope characteristics primarily determine the distribution of active rockfall tracks. To achieve these objectives, we made a geomorphological map of the whole study area, and we measured the major discontinuity planes in the bedrock that are exposed in the rockfall source areas. Furthermore, a test site for simulation modelling within the larger study area was defined in which both a forest and a hillslope inventory were carried out. The available data and our developed rockfall simulation model allowed us to assess the slope characteristics that mainly determine the distribution of areas affected by rockfall. We found that in decreasing order of importance, both standing and felled trees, the surface roughness and rockfall resistant shrubs primarily determine the distribution of rockfall-affected areas. Simulation tests without a forest cover produced similar rockfall runout zones as fossil rockfall events identified in the field. We believe that the combined field and modelling approach is a prerequisite for understanding how forests can protect against rockfall.
© 2003 Elsevier B.V. All rights reserved.

Keywords: Rockfall; European Alps; Hillslope

1. Introduction

Many mountain forests protect against rockfall, which might pose serious risks to local inhabitants, their houses as well as infrastructure (Jahn, 1988; Motta and Haudemand, 2000). However, it is often unknown whether the protective function of a forest covering an active rockfall slope is effective enough. The protective function of the forests could decrease as a result of the continuous disturbance caused by impacts of falling rocks. Therefore, it is difficult to predict whether the protective function of a forest covering an active rockfall slope remains effective

* Corresponding author. Tel.: +31-20-5257420; fax: +31-20-5257431.
E-mail address: l.dorren@science.uva.nl (L.K.A. Dorren).

0169-555X/$ - see front matter © 2003 Elsevier B.V. All rights reserved.
doi:10.1016/S0169-555X(03)00100-4

through time. This depends on the forest dynamics, which are strongly affected by rockfall, since the distribution as well as the frequency and magnitude of rockfall events determine the development of a forest covering the accumulation area of an active rockfall source area. At the same time, the distribution of trees on a forested rockfall slope affects the distribution, frequency and magnitude of rockfall events (Jahn, 1988). In other words, there is an interaction between rockfall and forest cover. Therefore, dynamics of a forested rockfall slope could only be studied by focusing on both forest characteristics and rockfall dynamics.

Until now, rockfall dynamics have mainly been investigated by geotechnical measurements in rockfall source areas (Wieczorek et al., 2000; Zvelebil and Moser, 2001), talus slope inventories (Statham and Francis, 1986; Evans and Hungr, 1993; Bull et al., 1994; Wieczorek and Jäger, 1996; Jomelli and Francou, 2000; Hétu and Gray, 2000), experimental tests in laboratories or on nonforested hillslopes (Kirkby and Statham, 1975; Chau et al., 1998; Okura et al., 2000a) and simulation modelling studies (Statham, 1976; Bozzolo and Pamini, 1986; Azzoni et al., 1995; Budetta and Santo, 1994; Okura et al., 2000b). Little work has been done on the interaction between rockfall and protection forests. Within this study, we applied a combined approach, using both field and modelling techniques, to assess the determining factors for rockfall source areas, their tracks and runout zones on a forested slope in mountainous terrain where rockfall is highly active. As a basis for this study, we formulated the following research questions:

1. Why do the rockfall source areas occur in the study area?
2. Could the knowledge obtained in the field be translated into a model that simulates realistic rockfall dynamics on a forested slope?
3. Which environmental characteristics primarily determine the distribution of areas affected by active rockfall?

2. Study area

The area investigated in this study was the "Außerbacher" forest, which is located near the village of Gaschurn in the Montafon region in the western part of Austria, between 47°8′ and 46°50′ latitude and 9°41′ and 10°9′ longitude. The altitude of the study area ranges from 930 m above sea level in the valley floor up to 1500 m above sea level. The forest in the area covers a south–southwest exposed slope, which may be divided in a source area, which has a mean slope gradient of 60° and an accumulation area, which has a mean slope gradient of 30°. The underlying geology, which is metamorphic bedrock, consists of amphibolites, mica schists and white/grayish ortho-(granite bearing) gneisses. The resistant amphibolites and gneisses were subject to strong glacial abrasion. Therefore, steep cliff faces developed. These faces are currently active rockfall source areas. In between the steep cliff faces, three major denudation niches are present, which are connected with distinct open tracks in the forest (Fig. 1).

The forest covering the study area is a typical mixed mountain forest, which is found on many vegetated talus/debris cones in the montane zone in the European Alps. The dominating species in the study area are primarily Norway spruce (*Picea abies*) and, to a lesser extent, sycamore (*Acer pseudoplatanus*), beech (*Fagus silvatica*) and hazel (*Corylus avellana*). The lower part of the study area is well accessible by two forest roads, which have been constructed for forest management practices (see Fig. 1).

3. Procedures

Fieldwork started with a reconnaissance and detailed geomorphological mapping on the basis of the mapping system described by De Graaff et al. (1987) and Seijmonsbergen (1992), after identifying the main landform units in the study area by interpreting false colour stereographic aerial photographs. Printed colour-infrared (CIR) orthophotos from 1996 with a resolution of 0.25 × 0.25 m, produced by the National Austrian Mapping Agency (BEV), served as a basis for mapping. The slope gradient and the exposition of the slope face as well as the dip and dip direction of the bedding planes and the most prominent joint sets were measured at 33 different locations in the rockfall source areas. These measurements were plotted in an equal area projection (Hoek and Bray, 1981) to carry out a Markland test (Markland, 1972; Hocking, 1976).

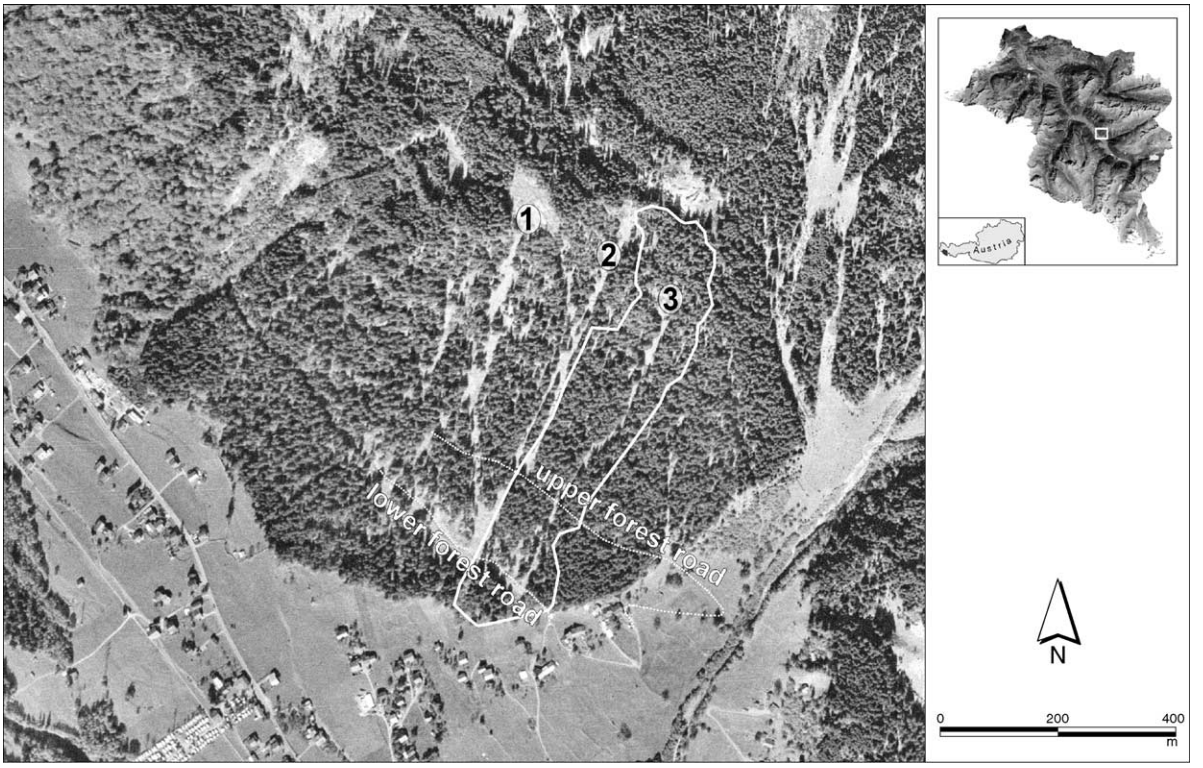


Fig. 1. Orthorectified pan-chromatic aerial photograph from 1987 showing the study area. The white outline demarcates the test site used for simulation modelling within this study. The numbers indicate the three denudation niches and the associated transport channels.

This test was done to identify potential sliding surfaces resulting from discontinuities in the bedrock in relation to the orientation of the local topography.

In addition, we carried out a field inventory to obtain a map of the spatial distribution of different hillslope characteristics that potentially affect rockfall tracks. Polygons representing terrain units with similar properties were mapped. These polygons covered an area varying from 10 to 7000 m^2, depending on the homogeneity of the terrain. For all these polygons, we estimated or measured the following parameters:

- The mean slope gradient (measured with an Abney level).
- The percentage of the surface area covered by bedrock (estimated).
- The granular composition of the material covering the surface, estimated for the top 25 cm. Percentages of contents were estimated for the following fractional classes: <5 cm, 5–20 cm and >20 cm.
- The surface roughness, classified for three transects with a length of 1, 5 and 20 m that were representative for the polygon. For all the three transects, the surface roughness was estimated as type a, b or c on the basis of Fig. 2. This resulted in three roughness values for each polygon.
- The number of barriers created by felled trees. For this, the number of felled trees, lying diagonally or perpendicular to the slope direction over a straight,

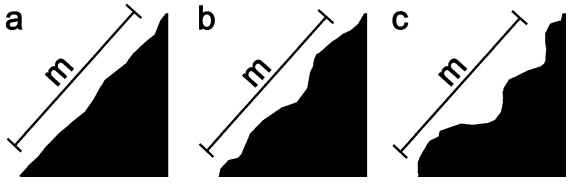


Fig. 2. Surface roughness over a transect length *m* expressed as type a, b, or c.

downslope line of 10 m that was representative for the polygon, was counted.
- The percentage of surface area covered with rockfall resistant shrubs with a height up to 5 m, such as *C. avellana*, was estimated.

Furthermore, we carried out a detailed forest inventory using the *Winkelzählprobe* (Bitterlich, 1948), which is also known as prism plot sampling or probability proportional to size sampling. Within this method, the probability of a tree being selected within a sampling plot is proportional to the basal area of a tree (Shiver and Borders, 1995). For this inventory, we used a grid with cells of 30 × 50 m. This grid almost completely covered the forested part of the test site that was used for the simulation modelling study. It is assumed that data obtained in the sampled areas in the centres of the grid cells are valid for the whole grid cell, which is justified if the *Winkelzählprobe* is used and if data values are expressed per hectare (Shiver and Borders, 1995). The inventory provided standard forest parameters such as the number of trees per hectare, the diameter at breast height (DBH), the basal area and the height of the trees, and also the number of scars on tree stems caused by heavy impacts of falling rocks and the height of these damages on the tree stems.

4. Fieldwork results

4.1. The source area

The slope gradient within the source area varies between 50° and 90°. The mean values of all the slope gradients and expositions as well as the dip and dip direction measurements of the bedding planes and the most prominent joint sets are given in Table 1. The great circles of the planes defined by the mean values given in Table 1 are shown in Fig. 3. The interior dashed circle in Fig. 3 represents the friction angle along discontinuities representative for the study area. The friction angle value of 37° was calculated using the uniaxial compressive strength (see Carson and Kirkby, 1972), which was obtained from a uniaxial compression test applied on three amphibolite samples and on one gneiss sample, in combination with the *Hoek–Brown* criterion (Hoek and Brown, 1997).

Table 1
Geological dip and dip direction measurements of the most important measured planes in the rockfall source area

Plane type	Dip (*slope gradient)	Dip direction (**exposition)
Slope face	*72 ± 14°	**187 ± 30°
Bedding planes	31 ± 12°	000 ± 18°
J1	62 ± 16°	118 ± 24°
J2	58 ± 18°	139 ± 21°

The point of intersection of the two circles for joint set 1 (J1) and joint set 2 (J2), which lies between the friction angle circle and the great circle of the slope face, indicates that these two joint planes create potential wedge failures. Especially in combination with the bedding plane that dips in opposing direction, which creates the 'roof' of potential falling rocks, wedge-shaped blocks are easily produced (Fig. 3). As shown in Table 1, the dip and dip direction values of the two major joint sets and the slope face vary considerably. This results in planar sliding at some locations because the dip and dip direction of the slope and the major joints are identical. We observed in the field that the orientation of both joint sets (J1 and J2) and the orientation of the bedding planes resulted in rocks breaking out at the bottom parts of the steep cliff face. This leads to undercutting of the slope face and subsequent migration of rockfall activity upslope. Fortunately, the joint spacing is generally small and therefore mainly small rocks are produced (largest rock diameter between 0.25 and 0.5 m).

Another factor, which also contributes to rockfall activity in the study area, is the presence of large tensional fissures in the area above the steep cliff face (Fig. 4). These fissures indicate large-scale rock creep. Parallel tensional rebound of the valley slope after glaciation during Late Glacial and Early Holocene conditions was probably the main cause of this. The effect, however, is increased by the presence of mica schist layers underneath the amphibolite and gneiss bedrock layers. The mica schist layers act as weak zones, which cause additional bulging forward and toppling of the creeping bedrock into the valley. As a consequence, the steep cliff face maintains its steepness despite active mass wasting and therefore facilitates slope failures and resulting mass wasting.

Local inhabitants informed us that rockfall generally occurs in spring and after heavy rain, which was

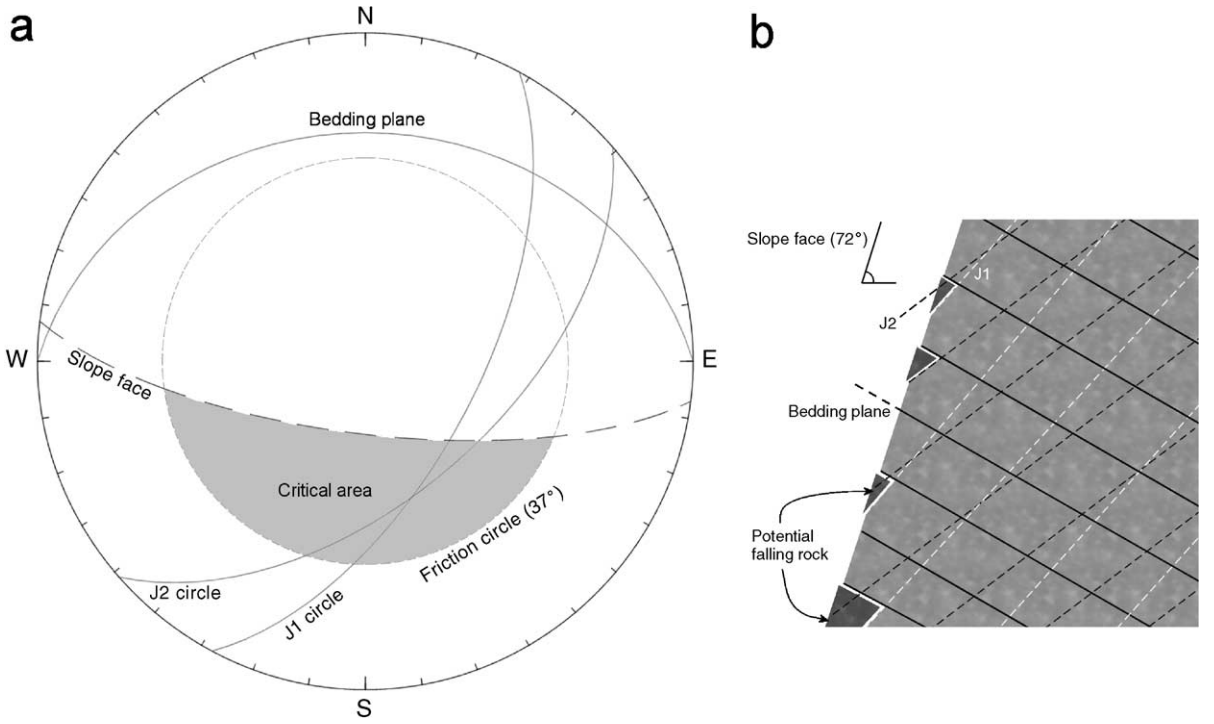


Fig. 3. (a) The lower hemisphere projection of an equal area net showing the great circles of the slope face, the bedding planes and the two most prominent joint sets (J1 and J2). (b) Two-dimensional visualisation of the effect of the intersection of the bedding planes and the joint sets in the rockfall source areas in the study area.

also observed during fieldwork. Unfortunately, the inhabitants were not able to tell which source areas particularly produce falling rocks. The transport channels visible in Fig. 1 suggest that the main rockfall activity occurs within the denudation niches upslope of the transport channels. We observed, however, that the production of potential falling rocks in the study area was not merely concentrated within the niches, but all the steep cliff faces throughout the area acted as rockfall source area. After we completed the geomorphological map, it was interesting to observe that the largest tensional fissures are aligned with the longitudinal direction of the denudation niches. This suggests that the weaker zones that are responsible for the development of the denudation niches have been predetermined by tensional fissuring.

4.2. The accumulation area

The accumulation area is a steep talus cone with a mean slope gradient of 38–40°. Distinct patterns of recent accumulation, indicated by fresh scree, were mainly found in depressions between the largest talus cones and upslope of felled trees, which were positioned diagonally on the slope to act as barriers. The size of the recent accumulated rocks, mainly consisting of amphibolites and some gneisses, generally varied between 0.2 and 0.5 m (diameter of largest rock axis). Smaller rocks and fine material were only found in the transport channels. Other than the areas with recent accumulation, a rather uniform distribution of rocks was found throughout the accumulation area, both with respect to size and inferred deposition period, which was assessed on the basis of moss cover and vegetation cover. Nevertheless, occasional groups of huge rocks (>2 m^3) and lobe-like accumulation forms consisting of nonsorted material were found. All this accumulated material was covered with moss and vegetation. These deposits indicate that both debris flows and rock avalanches do occur. We assume that the main sediment contributions to the

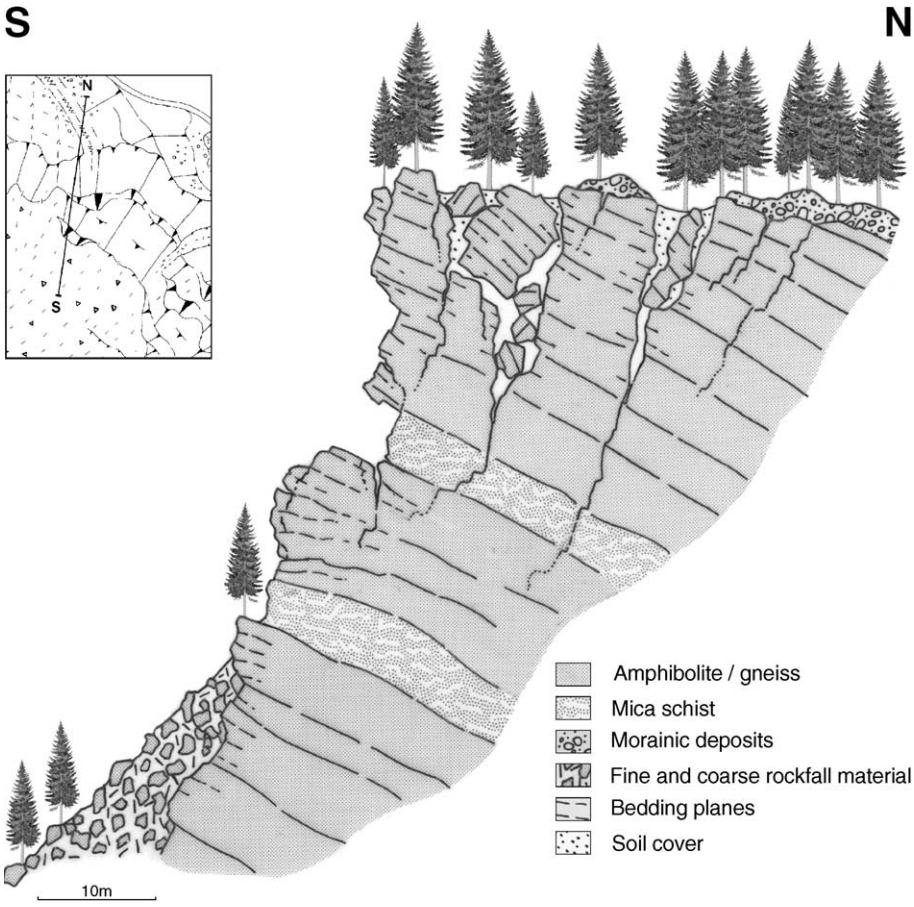


Fig. 4. Cross section showing internal rock deformation due to active large-scale tensional fissuring in the area above the steep cliff faces. The inset shows a part of the geomorphological map of the source area and the location of the cross section.

initial build up of the talus cone after deglaciation were delivered by rock avalanches and debris flows in a non- or scarcely vegetated environment.

The forest inventory was limited to an area that covered the main part of the test site that was used for simulation modelling. The composition of the forest in the test site is shown in Table 2. Although sycamores occur less frequently than Norway spruces, they are more resistant against rock impacts because they have a very good wound healing capacity. However, the number of sycamores in the area remains relatively low because Norway spruce is the dominant tree species.

A large proportion of the trees in the test site are in an ageing or even a breakdown phase, which means that most frequently quite large trees were found, but they were often old and heavily wounded by rock impacts, especially the trees in the upper part of the accumulation area. Bark and stem damage may lead to heart rot, which reduces the individual tree stability. As expected, the number of heavily damaged trees is the largest close to the rockfall source areas, and, generally, this number decreases downslope.

In relation to the ageing and breakdown phase of the forest in the test site, the lack of regeneration, indicated by the absence of seedlings, is problematic for the future protective function of the forest. This is mainly the result of hunting management. For quite a long period, hunters used the forest in the study area as a winter-feeding station for ungulates, which increased the browsing pressure considerably.

Table 2
Forest composition in the study area

Tree name	Species	Coverage in forest (%)		
Norway spruce	*Picea abies*	96		
Sycamore	*Acer pseudoplatanus*	3		
Beech	*Fagus silvatica*	<1		
Hazel	*Corylus avellana*	<1		
General information	Mean	Std. dev.	Minimum	Maximum
Number of trees/hectare	201	137	0	660
DBH (cm)	54	18	20	139

Several studies carried out in forests in the European Alps have shown that ungulate browsing decreases the regeneration of forests (Ammer, 1996; Motta, 1996). In our study area, ungulate browsing has resulted in a situation where regeneration is completely lacking.

5. GIS model development

5.1. Digital elevation model

As observed in the field, the topography determines the occurrence, the direction as well as the velocity of a falling rock. Therefore, a digital elevation model (DEM) is the most relevant dataset for simulating rockfall. We derived a DEM with a support of 2.5×2.5 m from a Triangular Irregular Network (TIN), which was produced from contour lines with an equidistance of 5 m using the TOPOGRID module in ArcInfo 7.0 (ESRI, 2003). These contour lines were created on the basis of a combined dataset consisting of slope transects measured in the field, a detailed geomorphological field map (1:2000) and existing contour lines with an interval of 20 m. Since the study area is fully covered with forest, this method was more time-efficient than using a tachymeter. In addition, the forest cover caused problems for photogrammetric height measurements using the available set of stereographic aerial photographs.

5.2. Tree distribution map

To obtain a tree distribution map, firstly, the regions of all the individual tree crowns in the study area were detected on the basis of the colour-infrared (CIR) orthophotos from 1996. In general, three different methods are described in the literature for detecting or delineating individual tree crowns from high spatial resolution aerial images (see Hill and Leckie, 1999). These are (1) detection of local intensity maximum (Blazquez, 1989; Dralle and Rudemo, 1996, 1997; Brandtberg and Walter, 1998; Uuttera et al., 1998; Wulder et al., 2000), (2) contour-based methods (Gougeon, 1995) and (3) template-based matching (Larsen and Rudemo, 1998). We firstly smoothed the orthophotos using a low pass filter. Subsequent segmentation of the image automatically delineated individual and clustered tree crowns. In addition, nonforested areas were segmented into homogenous areas. Segmentation was done in the software *eCognition* (Definiens-Imaging, 2003). Then, we used an object-based classification on the basis of membership functions related to local intensity maxima to classify all the segments in three classes, namely, tree crowns, clustered tree crowns and nontree crowns. This classification produced a tree crown map with an overall accuracy of 89.8% when compared with visually delineated tree crowns. We combined the obtained tree crown map with the forest inventory data to produce a tree distribution map, which represented the locations of trees and their DBH. The forest inventory provided data for 50 plots with a size of 30×50 m. These plots did not cover the whole test site that was used for the simulation modelling study. Therefore, the forest inventory data had to be extrapolated to obtain data for the remaining parts of the test site. For that, linear regression between the amount of raster cells classified as tree crowns in the tree crown map and the number of trees per hectare obtained from the forest inventory was used ($R^2 = 0.25$). The DBH of the trees covering the whole test site was uniformly randomly chosen between the minimum and maximum DBH that were measured in the forest inventory plots.

5.3. Rockfall simulation model

To simulate rocks that collide with tree stems, a computer model is needed that is able to calculate the motions of a falling rock realistically. Furthermore, such a simulation model should take different spatially distributed environmental characteristics into account, which influence the velocity and the direction of falling rocks. Therefore, we developed a model that combines a process-based and GIS-based model. The two main components of the model are the calculation of the falltrack of the rock and the calculation of the velocity of the falling rock. These calculations all started from predefined rockfall source areas.

Rockfall source areas were derived from the geomorphological field map. From each cell, defined as a rockfall source area, a single falling rock was simulated. The radius of this rock was 0.25 m, its initial velocity in horizontal direction (Vx) was 1 m/s and its initial velocity in vertical direction (Vy) was −1 m/s. The initial fall height in the cells that were used as rockfall start cells was set to 2 m. By doing this, we defined that the cliff faces from which rockfall start are at least 2 m high. With respect to the study area, this is a realistic value when using a grid with 2.5 × 2.5 m cells.

The mean slope gradient within each cell is derived from the DEM using the method described by Zevenbergen and Thorne (1987). Furthermore, the DEM was used for calculating the fall directions from each raster cell in the test site. For the latter, a modified multiple-flow algorithm (e.g. Quinn et al., 1991; Wolock and McCabe, 1995; Tarboton, 1997) is used, which is illustrated in Fig. 5. This method calculates the fall directions for the whole raster repeatedly for each simulation run by sampling the fall direction for each cell from a probability distribution, which is determined by the summed downslope gradient (SDG) from a central cell and the fraction of all the individual cells downslope of the central cell in the SDG. As a result, for each simulation run, falling rocks could be directed in different directions, which enables the simulation of diverging fall patterns.

The velocity of the falling rock is calculated with standard algorithms for a uniformly accelerated parabolic movement through the air and with algorithms modified from Pfeiffer and Bowen (1989) that calculate the energy balance before and after a collision (or bounce) on the slope surface. The modifications are that the factor compensating for the effect of the rockfall velocity on the elasticity of the collision is left out, since the empirical constants required for calculating this factor were not available for the study site. The model recalculates the velocity in x and y direction before a bounce into a tangential velocity (Vt_{in}), parallel to the slope surface following

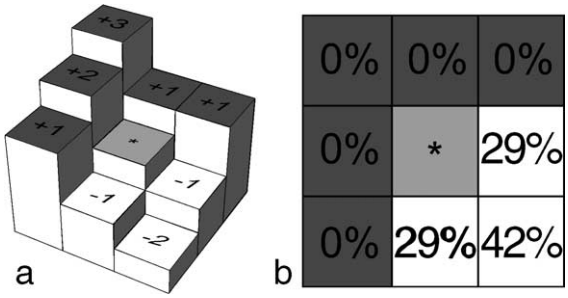


Fig. 5. (a) Example of a central cell (*) and its neighbouring cells and (b) the result of the calculation of the probabilities of the possible fall directions on the basis of the summed downslope gradient (SDG) for the example shown in (a).

$$Vt_{in} = Vy\sin(\beta) + Vx\cos(\beta) \quad (1)$$

and a normal velocity (Vn_{in}, perpendicular to the slope surface) following

$$Vn_{in} = Vy\cos(\beta) - Vx\sin(\beta) \quad (2)$$

where Vy = velocity in y direction (m/s); β = slope angle at the location of the bounce (°); and Vx = velocity in x direction (m/s). The tangential velocity after a bounce is then calculated with

$$Vt_{out} = \sqrt{\frac{(R^2(I\omega^2 + MVt_{in}^2))r_t}{(I + MR^2)}} \quad (3)$$

where Vt_{out} = tangential velocity after the bounce (m/s); R = radius of the falling rock (m); I = moment of inertia = $2/5*MR^2$ (kg m^2); ω = rotational velocity (1/s)=(Vt_{out} of the previous bounce)/R; M = mass of the falling rock (kg); Vt_{in} = tangential velocity before

the bounce (m/s); and r_t = tangential restitution coefficient determining energy loss (−), which is mainly determined by the vegetation cover and the roughness of the slope surface. The normal velocity after a bounce is calculated with

$$Vn_{out} = Vn_{in} r_n \quad (4)$$

where Vn_{out} = normal velocity after the bounce (m/s); Vn_{in} = normal velocity before the bounce (m/s); and r_n = normal restitution coefficient determining energy loss (−), which is mainly determined by the elasticity of the surface material covering the slope.

During each bounce, the slope angle at the exact location of the bounce is randomly decreased with an angle that varied between 0° and 4°. We programmed this to account for small-scale variability in the mean slope gradient, as shown in Fig. 6, which is 'smoothed-out' in the slope maps. This procedure is similar to the varying impact angle based on the surface roughness as described by Pfeiffer and Bowen (1989).

If the horizontal travelled distance of the rock between two simulated bounces is less than the diameter of the falling rock, the rock is considered to be rolling. In that case, the rock is given a new displacement over the slope surface equal to the diameter of the rock. This prevents an infinite amount of simulated bounces per raster cell (after Pfeiffer and Bowen, 1989). Sequences of motion through the air followed by a bounce are repeated until the velocity of the moving rock is equal to or less than 0.5 m/s.



Fig. 6. Photograph of the surface of a scree slope in the accumulation area of the test site, showing the small-scale variability in the mean slope gradient.

5.4. Coefficients of restitution

The slope characteristics that determine the elasticity of the surface material and thus the normal coefficient of restitution (r_n) are the composition of the material covering the surface and the vegetation cover. The slope characteristics that together determine the tangential coefficient of restitution (r_t) are the surface roughness, the vegetation cover (mainly trees and large shrubs) and the number of felled trees that are lying on the slope parallel to the contour lines that act as barriers. Another factor determining the tangential coefficient of restitution is the radius of the falling rock itself, since for larger rocks, the effective surface roughness is lower than for smaller rocks.

Standing trees affect the velocity of a falling rock as well because they act as barriers. Therefore, the model simulates collisions between falling rocks and standing trees. In case a collision occurs, this results in decrease of the kinetic energy and consequently a decrease of the velocity of the falling rock. The model is able to calculate whether these collisions occur, since the available tree distribution map defines the positions of the trees. Furthermore, the position of the falling rock is always known during simulation because the model simulated rocks as falling through the centre of the raster cells. If a collision between a rock and a tree occurs, the fraction of energy loss due to the collision is calculated on the basis of the position of the rock relative to the centre of the tree stem following

$$\Delta E = \sqrt{1 - \left(\frac{d}{0.5\mathrm{DBH} + R}\right)^2} \quad (5)$$

where ΔE = fraction of energy loss due to an impact against a tree stem (−); d = distance between the centre of the rock and the centre of the tree stem (m); DBH = diameter of the tree stem at breast height (m); and R = radius of the falling rock (m). We developed this formula assuming that a tree stem absorbs a maximum amount of kinetic energy if a

central collision between a rock and a tree stem occurs. We did not make any distinctions between the energy absorbed by different tree species because of lack of data.

In reality, falling rocks could collide with trees at a certain height above the surface. Subsequently, a rock falls on the ground and gains new kinetic energy. This process is incorporated in the model by limiting the maximum energy loss to 99%. After the energy loss is calculated, the translation and rotation energy is multiplied by the calculated fraction of energy loss. Next, the resulting energies are transformed into a resultant velocity. If a falling rock does not collide with a tree stem, energy is lost because of a bounce on the slope surface. The amount of energy loss is then defined by r_n and r_t. To analyse the effect of these parameters on the velocity before and after a bounce, a single bounce was repeatedly simulated. During these simulations, one single parameter was varied, while the other parameters involved were given a constant value. This was done for the r_n, the r_t, the radius of the rock and the mass of the rock.

The outcomes of this test showed mainly that the r_t and the radius of the rock affect the energy loss during a bounce (Fig. 7). Since the bounce is the most important part of the model that determines the energy loss, the r_t and the radius of the rock are the main parameters determining energy loss in the model. The radius of the simulated falling rocks was constant for all the model simulations ($R = 0.25$ m); therefore, the r_t is the most important parameter determining the deceleration of the simulated falling rocks. The slope gradient is the most important parameter determining the acceleration. The findings mentioned above justified the choice to estimate the r_n on the basis of the mapped slope characteristics in combination with literature data (Pfeiffer and Bowen, 1989; van Dijke and van Westen, 1990; Kobayashi et al., 1990; Giani, 1992; Azzoni et al., 1995; Chau et al., 1998, 2002; Meißl, 1998). The r_t varied between estimated minimum and maximum values, which were consistent with literature data. The actual values of r_t, however, were determined by the slope characteristics that were measured and

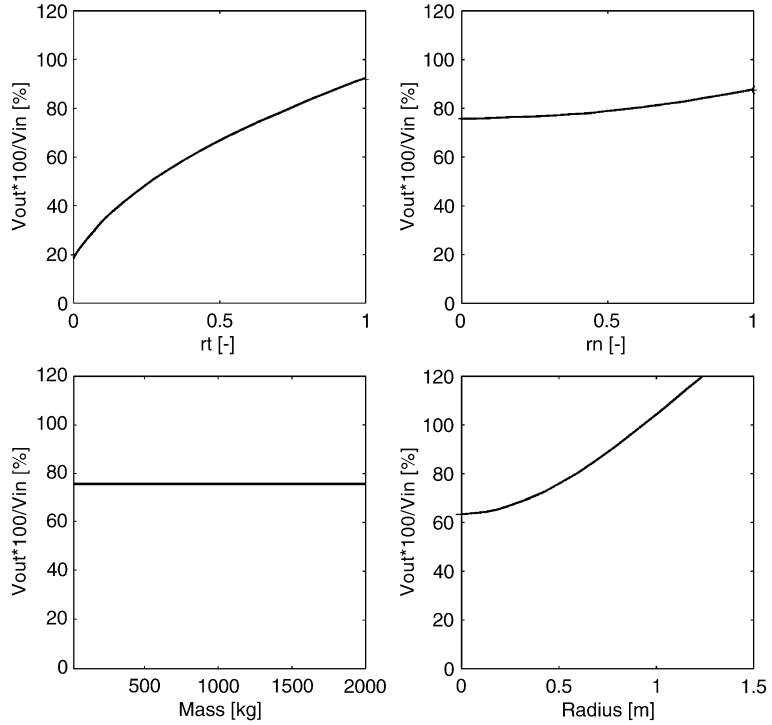


Fig. 7. The effect of the r_t, the r_n, the mass and the radius of the rock on the change of the velocity before and after a single bounce.

estimated in the field. To determine the tangential coefficient of restitution (r_t), the following formula was developed

$$r_t = \max - (\text{range}*\text{fraction}) \quad (6)$$

where max = maximum r_t value (–) = 0.95; range = range of r_t values (–) = max – min; min = minimum r_t value (–) = 0.01; and fraction = the fraction of the r_t that is attributed to the mapped slope characteristics (–). This was calculated with the following formula:

$$\text{fraction} = (SC_1 wSC_1 + SC_2 wSC_2 + \ldots + SC_i wSC_i) / (wSC_1 + wSC_2 + \ldots + wSC_i) \quad (7)$$

where SC_i = slope characteristic i and wSC_i = weight of the slope characteristic i. As shown in Table 3, different weights were addressed to each different slope characteristic. Only the extreme weight settings were tested to evaluate the effect of changing proportions of the mapped slope characteristics. One hundred simulation runs were carried out for evaluating a weight setting according to the *Monte Carlo* method (Lewis and Orav, 1989). For each simulation run, a new fall direction map was calculated using the previously mentioned modified multiple-flow algorithm. The mass and the radius of the rock and the locations of the rockfall source cells were similar for all the executed simulations. A generalised diagram of all the described model steps is presented in Fig. 8.

5.5. Validation

Data for validating the model results were both provided by the detailed forest inventory data and the geomorphological field map. Within the area covered by the forest inventory, 18 squares of 25 × 25 m were randomly selected, which were all situated within a single forest inventory grid cell. For these 18 squares, the tree volume per hectare and the number of scars per hectare caused by rock impacts were measured. These data were compared with the number of rock impacts on trees as simulated by the model. For standardisation purposes, both the validation data (observed values) and the simulated data (predicted values) within the 18 squares were expressed as percentages of the summed values within all the randomly selected squares. In detail, the observed value represented the number of scars per tree volume unit in a square expressed as percentage of the total number of scars per tree volume unit in all squares. Here, the number of scars per tree volume unit was the number of scars per hectare caused by rock impacts divided by the tree volume within the square. The predicted value represented the number of impacts in a square expressed as percentage of the summed number of impacts in all squares. For all the model

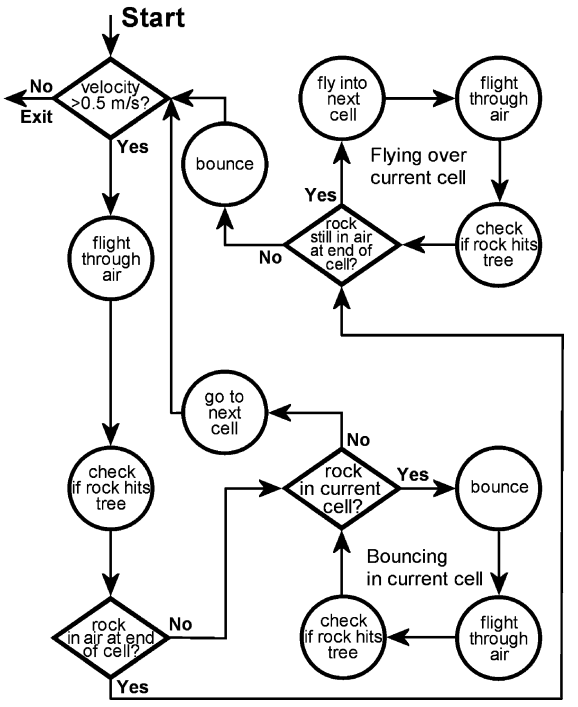


Fig. 8. Flow diagram showing the simulation of a single rock falling from a start in the developed rockfall model.

Table 3
Weight settings for the slope characteristics determining the tangential coefficient of restitution (r_t), which provided the best results

Slope characteristic	Weight	Weight range
Wooden barriers/felled trees	10	1–10
Surface roughness 1 m	3	1–10
Surface roughness 5 m	3	1–10
Surface roughness 20 m	3	1–10
Rockfall resistant shrubs	1	1–10

Table 4
Results produced by the model with optimal weight settings for the r_t as shown in Table 3

Validation data	ME	MSE	R^2
Damaged trees	0.0	0.24	–
Mapped recent rock accumulations	–	–	0.74

outcomes, the mean error (ME) and the mean squared error (MSE) were calculated following

$$\mathrm{ME} = \frac{1}{n}\sum_{i=1}^{n}(P_i - O_i) \quad (8)$$

$$\mathrm{MSE} = \frac{1}{n}\sum_{i=1}^{n}(P_i - O_i)^2 \quad (9)$$

where n is the number of observations, P_i is the modelled or predicted value in raster cell i and O_i is the observed value in raster cell i.

In addition to the size distribution of rocks throughout the test site, the geomorphological map also included the locations of recent scree and rock accumulation areas throughout the test site. This could be determined first by the absence of mosses and vegetation covering the accumulated material and second by the relative age of the deposits as inferred from the slope morphology. Within all the validation squares described in the previous paragraph, it is evaluated whether a cell modelled as an end location of a falling rock was also mapped as a recent accumulation area. This provides a Boolean dataset with a modelled and a mapped value (rockfall accumulation: value = 1, if not: value = 0) for every cell within all validation squares. On the basis of this dataset, the R^2 is calculated.

6. Simulation model results

The developed model produced rockfall runout zones that ranged from the source areas to the upper half of the accumulation area. This pattern was identical for each tested weight setting for the slope

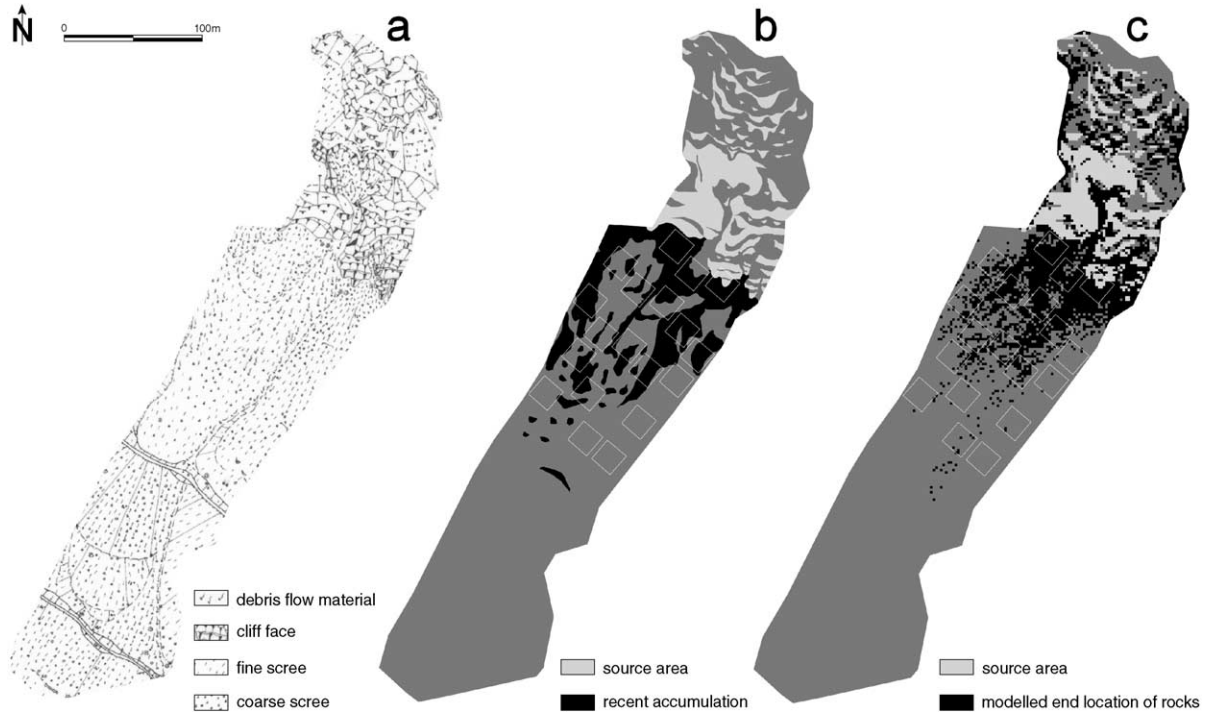


Fig. 9. (a) The geomorphological map of the test site. (b) Map showing the active or recent accumulation areas, as derived from the geomorphological map and field observations. (c) Map showing the simulated end locations or accumulation areas after 100 simulation runs using the optimal settings and a rock radius of 0.25 m. The white outlined squares are the validation squares.

characteristics determining r_t. During fieldwork, it was observed that most of the falling rocks stop within the upper part of the accumulation area. Only some rocks fall down the transport channel and reach the upper forest road. The developed model confirms this as the number of rocks reaching the upper forest road was less than 5% of the total number of falling rocks in all the simulations. In that sense, all the simulations produced comparable results. Changing the weight setting for the slope characteristics determining the r_t did, however, result in significant variation in the extent and location of local accumulation areas throughout the upper half of the accumulation area. Validation of the model results with the data on damaged trees and mapped recent rock accumulations showed that the best results were produced if the settings shown in Table 3 were used. This resulted in an R^2 of 0.74 for the correlation between the mapped and modelled accumulation areas, and this setting produced the lowest mean squared error (MSE = 0.24) between the spatial distribution of modelled impacts and the spatial distribution of the number of scars on tree stems (Table 4).

The optimal weight settings shown in Table 3 assign a high importance to the number of wooden barriers in a homogeneous terrain unit. Within this setting, wooden barriers are more than three times more important than the surface roughness measured on the 1-, 5- and 20-m transects. Different weights for these three surface roughness values were also tested, but optimal results are produced if their weights are equivalent. These results also indicate that rockfall resistant shrubs are least important for decelerating falling rocks.

Fig. 9 shows the field mapped geomorphological map of the test site (Fig. 9a), the derived recent scree accumulation map (Fig. 9b) and the result of the simulation during which the optimal weight settings were used (Fig. 9c). A black coloured cell shown in Fig. 9c indicates that, at least during one simulation, a rock stopped within that cell. Thus, it is also possible that a larger number of rocks stopped in that cell. This map only visualises the accumulation patterns, whereas the frequency map (not presented here) showed that most rocks stopped in the upper part of the accumulation area, where the dense black cloud is visible in Fig. 9c. Thus, only a few simulated rocks

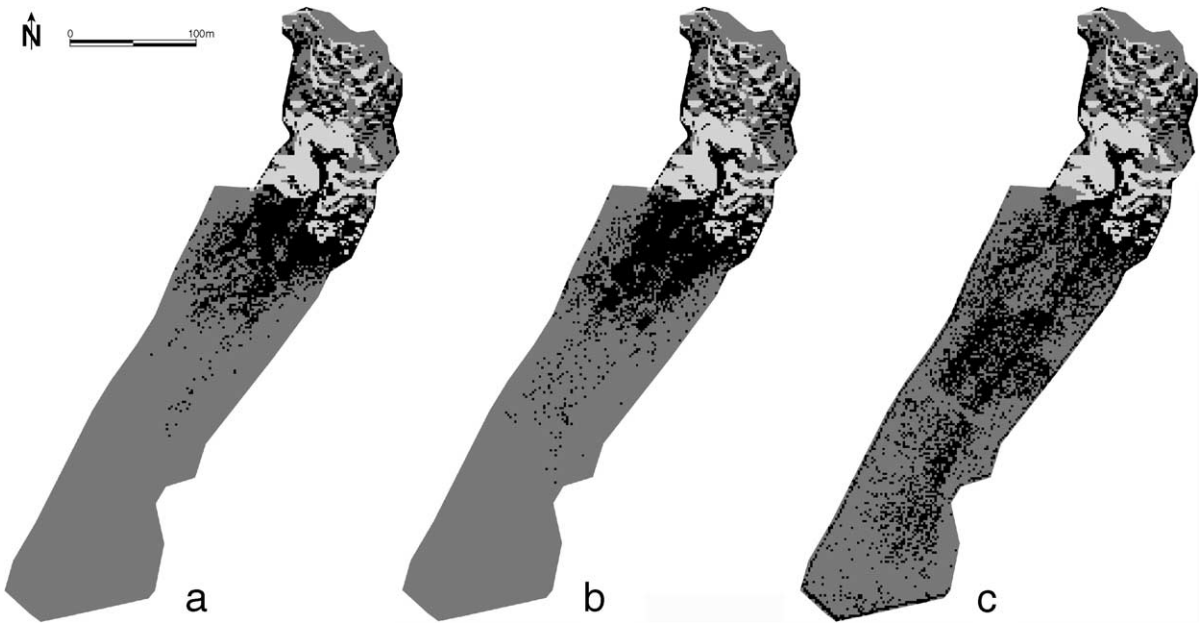


Fig. 10. (a) Map showing the simulated end locations or accumulation areas using the optimal settings, a rock radius of 0.25 m and the current forest cover; (b) idem., only with 50% less tree density; (c) same simulation, only without forest cover. All the graphs are the result of 100 simulation runs.

reached the upper forest road, which is shown in the geomorphological map (Fig. 9a).

To analyse the change of the rockfall hazard if the protection forest continues to deteriorate, the simulation model, which seemed to predict current accumulation patterns satisfactorily, was used to test scenarios with a random tree distribution with 50% fewer trees (case B) and with no trees covering the site at all (case C). The results of these simulations show that the amount of rocks reaching the valley is still zero in case B (Fig. 10b). A distinct difference is that more rocks reach the upper forest road. In case C, however, many rocks reached the lower boundary of the test site (Fig. 10c). There, the velocities of the rocks were still approximately 20 m/s.

7. Discussion

The protection forest that covers the study area is almost continuously under attack by rockfall, but especially during the spring and after heavy rain. Therefore, we consider water infiltrating in joints and frost shattering as the main trigger for rockfall in the study area. The primary cause, however, that rockfall source areas occur in the study area is because of the effect of glaciations during the Pleistocene glacial periods. Glacial erosion of competent geological formations resulted in oversteepened slopes. Postglacial relaxation of these slopes led to the development of tensional fissures and rock creep, which causes additional destabilisation of the original slopes. The steep slope gradient in combination with the unfavourable dips and dip directions of the major joint sets and the bedding planes in the study area leads to breaking out of mainly relatively small rocks (largest diameter between 0.25 and 0.5 m). Rocks in the bottom parts of the cliff face break out first; subsequently, this process slowly migrates up along the cliff face. This preferentially occurs in relation to the tensional fissures along the steep valley slopes.

At the intersection of the cliff face and the largest fissures, three major denudation niches have developed. From these niches, large amounts of detached material have been removed, deposited and consequently forming large talus slopes. In the lower zone, below the lower forest road, many fossil rock accumulations were found. This suggests that these accumulations were largely built up during a nonforested period. In the Alps, the Late Glacial or even the Early Holocene is known for its intense frost shattering, lack of forests and unstable (rock) slopes (Flint, 1971; De Graaff et al., 1989). The rock material probably moved downslope as rock avalanches, debris flows and rockfall.

The accumulation area below the denudation niches consists of large identifiable talus cones that gradually fuse into one another down the accumulation slope. At present, the rockfall activity within the denudation niches is comparable to the other steep cliff faces on the nondissected mountain face between the large denudation niches. The latter currently produce rocks that fall down and fill up local depressions between the larger talus cones in the upper part of the study area. Rocks originating from the large denudation niches fall down the slope into the forest and stop in local accumulation areas where the surface roughness is high because of previously deposited large rocks. Another observed feature is that rocks accumulate behind standing trees or felled trees that lie diagonally or perpendicular to the slope direction. Small rocks are deposited in the upper part of the accumulation area or even in the transport channel of the niches. Occasionally, rocks originating from the niches fall all the way down the existing transport channels, which have been denuded of trees by both snow avalanches and rockfalls, underneath the denudation niches.

Our simulation model, which was developed using the obtained field knowledge, confirmed the abovementioned observations for the modelling test site. This model showed that, in decreasing order of importance, firstly, standing and felled trees, secondly, the surface roughness and, thirdly, the rockfall resistant shrubs are the determining factors for the distribution of rockfall-affected areas in our test site. As mentioned before, only a relatively small number of rocks fall through the transport channel, but rocks that do so gain a high velocity because the surface roughness in the channel is low and trees or shrubs are absent. The latter is due to the fact that falling rocks destroy seedlings. In addition, snow creep and snow avalanches starting in the denudation niches also contribute to restriction of growth or even removal of seedlings. An increased tree density, both in the transport channel and in the source area, could reduce

the impact of all these disturbing processes. In short, the degradation of the protection forest in the area underneath the denudation niches is a self-reinforcing process, which needs to be reversed.

Both the simulation results and field observations showed that many falling rocks stop within the upper-forested part of the accumulation area. Though, a point of attention is the lack of regeneration of the forest, which is needed to provide backup and ensure protection in the future. If this situation does not improve and the forest continues to break down, a similar self-reinforcing process is to be expected in the whole study area as in the earlier-mentioned transport channels underneath the denudation niches. We simulated these situations by using, firstly, 50% of the current forest density and, secondly, by simulating no forest cover at all. The results showed that a reduction of the tree density by 50% increases the rockfall hazard to some extent, but an absence of the forest cover resulted in rocks reaching the main valley and thus significantly increased the rockfall hazard. Again, to prevent this situation, the primary forest management goals in the area should be to increase the regeneration and to create opportunities for trees to cover the transport channel. To achieve the latter, temporary protective measures against rockfall have to be taken in the denudation niches such as the construction of wooden barriers by placing felled trees slightly diagonal to the slope direction. By doing this, the velocity of falling rocks will be reduced, but transport will continue in a more controlled manner. This prevents accumulation of rock material on the slope, in contrast to most technical rockfall protection constructions. Another advantage is that the decaying felled trees provide excellent seedbeds for seedlings, which could stimulate regeneration. Promotion of regeneration is the second important forest management goal in the area. Hunting management has a large responsibility in this as well because this can protect seedlings against excessive browsing.

The model developed in this study simulated rockfall for a static, given situation both regarding the state of the forest and the slope characteristics. Progress could be made by coupling rockfall simulation and forest growth in a dynamic model. Such a model would be more suitable to test forest management interventions and its effect on the future protective function of the forest. The dynamic rockfall model should incorporate changes of surface characteristics due to deposition of material, like an increase in the surface roughness. Furthermore, the same model could calculate damages on trees. This could be taken into account in the dynamic forest growth model in which regeneration, growth and breakdown are simulated. This would change the initial tree distribution and therefore indirectly the distribution of active rockfall tracks. To simulate tree damages caused by rockfall impacts more accurately, a better characterisation of the mechanical behaviour of a tree after a rock impact is needed in the developed model. The experimental data required for this characterisation are currently lacking and need to be investigated.

Regarding the coefficients of restitution in our model, stochastic simulation enables us to model realistic value ranges. An example is the Monte Carlo simulation, where minimum and maximum values of the coefficients of restitution are determined by the outcome of a dynamic coupled forest growth–rockfall model, in which the spatial covariance between the surface roughness and the distribution of both standing and lying trees is represented.

8. Conclusions

The slope gradient, the various geological formations and their geotechnical properties of the bedrock are the main controlling factor for rockfall in the study area. The potential rockfall source areas were mapped at 1:2000 and used in the developed rockfall simulation model. The results showed that the current accumulation patterns throughout the study area could be modelled accurately. On the basis of a developed formula for estimating the tangential coefficient of restitution and the model tests, we conclude that, in decreasing order of importance, standing and felled lying trees, the surface roughness and rockfall resistant shrubs primarily determine the distribution of rockfall-affected areas in the test site used for simulation modelling within the study area. Deposits of older events such as rock avalanches, debris flows as well as rockfall were identified and mapped in the lowest parts of the accumulation area. Model simulation of the current field situation produced considerable shorter rockfall runout zones due to the protective function of the forest. The simulation test

without a forest cover produced rockfall similar run-out zones as the older rockfall events. The tests showed that these events occurred under different conditions than the current ones. We assume that the lowest deposits in the accumulation area are related to events that occurred in the Late Glacial or Early Holocene. Finally, we believe that a combined field research and modelling approach as applied in this study is a prerequisite for better understanding the dynamics of rockfall on a forested slope. For a better understanding of the feedbacks between rockfall and forest growth, for example, to predict the long-term effects of forest management interventions, we recommend the development of a dynamic rockfall–forest growth model.

Acknowledgements

We gratefully thank Sanneke van Asselen, Monique Blankers and Christopher Dich for their contributions to this work. Furthermore, we thank the Research Foundation for Alpine and Subalpine Environments (RFASE) and Stand Montafon Forstfonds for supporting this research.

References

Ammer, C., 1996. Impacts of ungulates on structure and dynamics of natural regeneration of mixed mountain forests in the Bavarian Alps. Forest Ecology and Management 88, 43–53.

Azzoni, A., Barbera, G.L., Zaninetti, A., 1995. Analysis and prediction of rockfalls using a mathematical model. International Journal of Rock Mechanics and Mining Science 32, 709–724.

Bitterlich, W., 1948. Die Winkelzählprobe. Allgemeine Forst- und Holzwirtschaftliche Zeitung 1, 4–5.

Blazquez, C.H., 1989. Computer-based image analysis and tree counting with aerial color infrared photography. Journal of Imaging Technology 15 (4), 163–168.

Bozzolo, D., Pamini, R., 1986. Simulation of rock falls down a valley side. Acta Mechanica 63, 113–130.

Brandtberg, T., Walter, F., 1998. Automated delineation of individual tree crowns in high spatial resolution aerial images by multiple-scale analysis. Machine Vision and Applications 11, 64–73.

Budetta, P., Santo, A., 1994. Morphostructural evolution and related kinematics of rockfalls in Campania (southern Italy): a case study. Engineering Geology 36, 197–210.

Bull, W.B., King, J., Kong, F.C., Moutoux, T., Phillips, W.M., 1994. Lichen dating of coseismic landslide hazards in alpine mountains. Geomorphology 10, 253–264.

Carson, M.A., Kirkby, M.J., 1972. Hillslope Form and Process. Cambridge Univ. Press, Cambridge. 475 pp.

Chau, K.T., Wong, R.H.C., Lee, C.F., 1998. Rockfall problems in Hong Kong and some new experimental results for coefficient of restitution. International Journal of Rock Mechanics and Mining Science 35, 662–663.

Chau, K.T., Wong, R.H.C., Wu, J.J., 2002. Coefficient of restitution and rotational motions of rockfall impacts. International Journal of Rock Mechanics and Mining Science 39, 69–77.

Definiens-Imaging, 2003. eCognition, object oriented image analysis. http://www.definiens-imaging.com/.

De Graaff, L.W.S., Jong, M.G.G.D., Rupke, J., Verhofstad, J., 1987. A geomorphological mapping system at scale 1:10,000 for mountainous areas. Zeitschrift für Geomorphologie N.F. 31, 229–242.

De Graaff, L.W.S., Kuijper, W.J., Slotboom, R.T., 1989. Die Schlussvereisung und die spätglaziale Entwicklung des Moorgebietes Gasserplatz, Feldkirch-Göfis, Vorarlberg. Jahresbericht-Geologische Bundesanstalt 132, 197–413.

Dralle, K., Rudemo, M., 1996. Stem number estimation by kernel smoothing of aerial photos. Canadian Journal of Forest Research 26, 1228–1236.

Dralle, K., Rudemo, M., 1997. Automatic estimation of individual tree positions from aerial photos. Canadian Journal of Forest Research 27, 1728–1736.

ESRI, 2003. Arcinfo. http://www.esri.com/software/arcgis/arcinfo/index.html.

Evans, S.G., Hungr, O., 1993. The assessment of rockfall hazard at the base of talus slopes. Canadian Geotechnical Journal 30, 620–636.

Flint, R.F., 1971. Glacial and Quaternary Geology. Wiley, New York.

Giani, G.P., 1992. Rock Slope Stability Analysis. Balkema, Rotterdam. 361 pp.

Gougeon, F.A., 1995. Comparison of possible classification schemes for tree crowns individually delineated on high spatial resolution MEIS images. Canadian Journal of Forest Research 21, 1–9.

Hétu, B., Gray, J.T., 2000. Effects of environmental change on scree slope development throughout the postglacial period in the Chic-Choc Mountains in the northern Gaspé Peninsula, Québec. Geomorphology 32, 335–355.

Hill, D.A., Leckie, D.G., 1999. Automated interpretation of high spatial resolution digital imagery for forestry. Proceedings International Forum, 10–12 February 1998. Natural Resources Canada, Canadian Forest Service, Victoria, British Columbia, Canada. 402 pp.

Hocking, G., 1976. A method for distinguishing between single and double plane sliding of tetrahedral wedges. International Journal of Rock Mechanics and Mining Science 13, 225–226.

Hoek, E., Bray, J.W., 1981. Rock Slope Engineering. Institution of Mining and Metallurgy, London, UK. 358 pp.

Hoek, E., Brown, E.T., 1997. Practical estimates of rock mass strength. International Journal of Rock Mechanics and Mining Science 34, 1165–1186.

Jahn, J., 1988. Entwaldung und Steinschlag. Proceedings of the International Symposium, Interpraevent, July 1988, Graz. Tagungspubl. Bd. vol. 1, pp. 185–198.

Jomelli, V., Francou, B., 2000. Comparing the characteristics of

rockfall talus and snow avalanche landforms in an Alpine environment using a new methodological approach: Massif des Ecrins, French Alps. Geomorphology 35, 181–192.

Kirkby, M.J., Statham, I., 1975. Surface stone movement and scree formation. Journal of Geology 83, 349–362.

Kobayashi, Y., Harp, E.L., Kagawa, T., 1990. Simulation of rockfalls triggered by earthquakes. Rock Mechanics and Rock Engineering 23, 1–20.

Larsen, M., Rudemo, M., 1998. Optimizing templates for finding trees in aerial photographs. Pattern Recognition Letters 19, 1153–1162.

Lewis, P.A.W., Orav, E.J., 1989. Simulation Methodology for Statisticians, Operations Analysts, and Engineers, vol. 1. Wadsworth and Brooks/Cole, Pacific Grove.

Markland, J.T., 1972. A useful technique for estimating the stability of rock slopes when the rigid wedge sliding type of failure is expected. Imperial College Rock Mechanics Research Report No. 19.

Meißl, G., 1998. Modellierung der Reichweite von Felsstürzen. Fallbeispeile zur GIS-gestützten Gefahren-beurteilung aus dem Beierischen und Tiroler Alpenraum. PhD Thesis, Universität Innsbruck, Innsbruck. 249 pp.

Motta, R., 1996. Impact of wild ungulates on forest regeneration and tree composition of mountain forests in the Western Italian Alps. Forest Ecology and Management 88, 93–98.

Motta, R., Haudemand, J.C., 2000. Protective forests and silvicultural stability—an example of planning in the Aosta Valley. Mountain Research and Development 20, 180–187.

Okura, Y., Kitahara, H., Sammori, T., Kawanami, A., 2000a. The effects of rockfall volume on runout distance. Engineering Geology 58, 109–124.

Okura, Y., Kitahara, H., Sammori, T., 2000b. Fluidization in dry landslides. Engineering Geology 56, 347–360.

Pfeiffer, T.J., Bowen, T.D., 1989. Computer simulation of rockfalls. Bulletin of the Association of Engineering Geologists XXVI, 135–146.

Quinn, P., Beven, K., Chevallier, P., Planchon, O., 1991. The prediction of hillslope flow paths for distributed hydrological modelling using digital terrain models. Hydrological Processes 5, 59–79.

Seijmonsbergen, A.C., 1992. Geomorphological evolution of an alpine area and its application to geotechnical and natural hazard appraisal in the NW. Rätikon and S. Walgau (Vorarlberg, Austria), including map series at 1:10,000 scale. PhD Thesis, University of Amsterdam, Amsterdam. 109 pp.

Shiver, B.D., Borders, B.E., 1995. Sampling Techniques for Forest Resource Inventory. Wiley, New York. 356 pp.

Statham, I., 1976. A scree slope rockfall model. Earth Surface Processes 1, 43–62.

Statham, I., Francis, S.C., 1986. Influence of scree accumulation and weathering on the development of steep mountain slopes. In: Abrahams, A.D. (Ed.), Hillslope Processes. Allen and Unwin, Winchester, pp. 245–267.

Tarboton, D.G., 1997. A new method for the determination of flow directions and upslope areas in grid digital elevation models. Water Resources Research 33, 309–319.

van Dijke, J.J., van Westen, C.J., 1990. Rockfall hazard, a geomorphological application of neighbourhood analysis with ILWIS. ITC Journal 1, 40–44.

Uuttera, J., Haara, A., Tokola, T., Maltamo, M., 1998. Determination of the spatial distribution of trees from digital aerial photographs. Forest Ecology and Management 110, 275–282.

Wieczorek, G.F., Jäger, S., 1996. Triggering mechanisms and depositional rates of postglacial slope-movement processes in the Yosemite Valley, California. Geomorphology 15, 17–31.

Wieczorek, G.F., Snyder, J.B., Waitt, R.B., Morrissey, M.M., Uhrhammer, R.A., Harp, E.L., Norris, R.D., Bursik, M.I., Finewood, L.G., 2000. Unusual July 10, 1996, rock fall at Happy Isles, Yosemite National Park, California. Geological Society of America Bulletin 112, 75–85.

Wolock, D.M., McCabe Jr., G.J., 1995. Comparison of single and multiple flow direction algorithms for computing topographic parameters in TOPMODEL. Water Resources Research 31, 1315–1324.

Wulder, M., Niemann, K.O., Goodenough, D.G., 2000. Local maximum filtering for the extraction of tree locations and basal area from high spatial resolution imagery. Remote Sensing of Environment 73, 103–114.

Zevenbergen, L.W., Thorne, C.R., 1987. Quantitative analysis of land surface topography. Earth Surface Processes and Landforms 12, 47–56.

Zvelebil, J., Moser, M., 2001. Monitoring based time-prediction of rock falls: three case-histories. Physics and Chemistry of the Earth (B) 26 (2), 159–167.

> Chapter 6

On the accuracy of the 3D rockfall model RockyFor



INT. J. GEOGRAPHICAL INFORMATION SCIENCE
VOL. 18, NO. 6, SEPTEMBER 2004, 595–609

Research Article

Effect of support size on the accuracy of a distributed rockfall model

L. K. A. DORREN
Cemagref Grenoble, 2 rue de la Papeterie, B.P. 76, F-38402 St. Martin d'Hères cedex, France; e-mail: luuk.dorren@cemagref.fr
IBED, Universiteit van Amsterdam, Amsterdam, The Netherlands

G. B. M. HEUVELINK
Laboratory of Soil Science and Geology, Wageningen University, PO Box 37, NL-6700 AA Wageningen, The Netherlands; e-mail: gerard.heuvelink@wur.nl

(*Received 3 January 2003; accepted 26 August 2003*)

Abstract. It is investigated whether a GIS-based distributed model developed for rockfall assessment at slope scale, which uses data with a support of 2.5×2.5 m, could be used for rockfall assessment at the regional scale, using input data with a support of 25×25 m and of poorer quality. It was anticipated that in the latter case the model error would increase. Three types of simulations were applied to the same model and the outcomes were validated with field data. The first simulation used input data with a support of 2.5×2.5 m and aggregated the output to a support of 25×25 m. The second simulation used the same input data as in the first simulation, but these data were aggregated to a support of 25×25 m before running the model. The third simulation used input data of poorer quality obtained at a support of 25×25 m. The results show that simulating the maximum extent of rockfall runout zones with a distributed model using data with a support of 25×25 m is realistic and feasible. This is also true for data with poorer quality as the third simulation resulted in a slightly larger mean-squared error than the first simulation. Surprisingly, it also gave a smaller error than the second simulation. We investigated the cause of the large error produced by the second simulation and concluded that this was mainly caused by the combination of a high-quality digital elevation model and the loss of spatial structure in the input data due to spatial aggregation.

1. Introduction

Geomorphological research focuses on understanding processes, patterns and landforms in geoecosystems. This type of research contributes to the basis needed for identifying, assessing and perhaps solving or preventing environmental problems such as soil erosion, flooding and rapid mass movements. Distributed models are increasingly popular tools within geomorphological research (Willgoose *et al.* 1991, Montgomery and Dietrich 1994, Tucker *et al.* 2001). They provide excellent frameworks for the conceptualization of developed theories and for simulating current or future processes and patterns in geoecosystems.

Models are simplified representations of reality and therefore model outcomes

International Journal of Geographical Information Science
ISSN 1365-8816 print/ISSN 1362-3087 online © 2004 Taylor & Francis Ltd
http://www.tandf.co.uk/journals
DOI: 10.1080/13658810410001703804

always deviate from 'the truth' to some extent and contain errors or uncertainties. These are caused partly by the model's simplification of the reality, but also because model input data are rarely known exactly and also probably contain errors (Burrough and McDonnell 1998). The degree of model simplification depends on the availability and quality of input data, which are often determined by the feasibility of measuring the inputs with sufficient detail. Clearly, it is more difficult to obtain detailed input data for a large catchment than for a small monitoring plot. Therefore, models and their input and output data are usually less detailed when moving up from a smaller to a larger spatial scale (Heuvelink 1998). Uncertainties or errors of model outcomes are thus related to spatial scale, of which one factor is the 'support' of the model input data. Here, support is defined as the largest area treated as homogenous such that an average value of the property of interest is known but not the variation within (Bierkens *et al.* 2000). Errors of model outcomes do not necessarily increase at larger supports. For example, aggregating data to large supports could decrease uncertainties about the average value in a large raster cell (Van Rompaey *et al.* 1999). On the other hand, if the model input data have a large support, errors in the model outcomes could increase due to the loss of terrain information. The input data for a model should be of sufficient detail to capture the spatial variation that is essential to describe the process or pattern being modelled (Goodchild 2001). In most cases a simpler or at least another model structure is required for modelling larger study areas, since the processes controlling changes in spatial patterns are different at different spatial scales (Bergkamp 1995). In some cases, however, the same model can be used for both a small and a large spatial scale, only the support of the input data may change.

The present paper focuses on a GIS-based distributed model developed for rockfall assessment at the slope scale, which was designed to use input data with a support of 2.5×2.5 m. The main objective was to analyse whether such a model could also be used for a larger scale (e.g. regional scale, for a study area covering 500 km^2), using input data on a support of 25×25 m. The larger support data are of poorer quality because they have less detail and involve a reduced sampling or mapping effort. It was anticipated that the model using data with a support of 25×25 m would produce a larger error than that used on a support of 2.5×2.5 m. The hypothesis was that poor data quality is the main cause of a larger model prediction error rather than the effect of simulating a similar process on a larger support. The distributed rockfall model was applied with data on a support of 2.5×2.5 m. Subsequently, the same model was applied using the same data aggregated to a support of 25×25 m. Finally, the model was applied using input data of poorer quality, which were obtained directly at a support of 25×25 m. The main objective is to determine how realistic or feasible rockfall simulation is with data on a support of 25×25 m.

2. Method and model overview

Three simulation schemes were defined to analyse the effect of input data with different aggregation levels on the accuracy of the output (figure 1). In simulation scheme 1, input data with a support of 2.5×2.5 m were used. The output was aggregated to a support of 25×25 m by averaging the outputs on the 2.5×2.5 m support. The output data were compared with validation data at the same support.

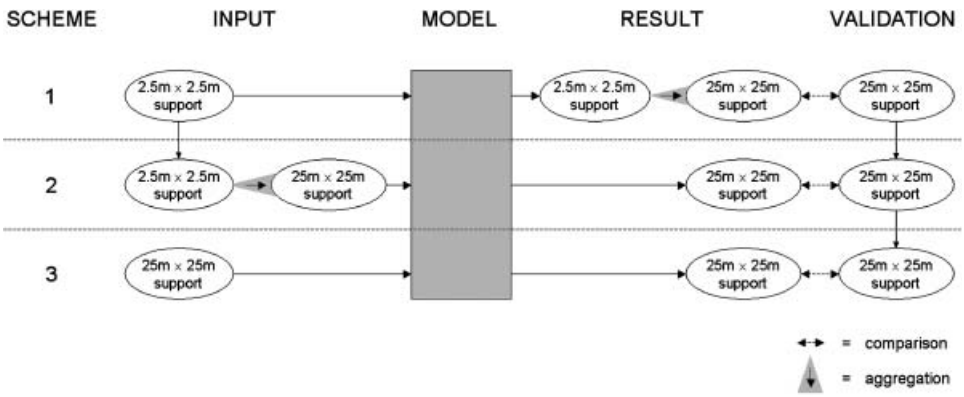


Figure 1. Three simulation schemes tested. For explanations, see the text.

In simulation scheme 2, the same input data were used as before but they were aggregated to a support of 25×25 m before running the rockfall model. In simulation scheme 3, the support of data was the same as in scheme 2, but the input data for simulation scheme 3 were obtained directly at a support of 25×25 m. Since the data used in simulation scheme 3 were obtained at the regional scale and thus less detailed than the data used in simulation schemes 1 and 2, it can be stated that the quality of these data was considerably poorer.

The same rockfall simulation model was used throughout the three simulation schemes. This model simulates a falling rock by calculating the kinetic energy balance during sequences of motion though the air and collisions on the slope surface or against trees. Start locations for the rockfall simulations were derived from field mapped rockfall source areas. From each start location, one single falling rock was simulated. For details of the used rockfall simulation program, see Dorren *et al.* (2004). A sensitivity test of the model showed that repeating the simulations 100 times using the Monte Carlo method (Lewis and Orav 1989, Mowrer 1997) produced sufficiently stable results. This number of repetitions was considered an acceptable trade off between computation time and the stability of the obtained results.

Standard algorithms for a uniform accelerated parabolic movement through the air calculated the motions through the air. Algorithms modified from Pfeiffer and Bowen (1989) calculated the energy balance before and after collisions with the slope surface and tree stems. The modifications were such that the factor compensating for the effect of the rockfall velocity on the elasticity of the collision was left out, because the empirical constants required to calculate it were not available for the study site. The algorithms for bouncing and motion through the air were combined with a procedure that calculated the fall direction based on a digital elevation model (DEM) as described in Section 3. A flow diagram of the model is given in figure 2.

The model inputs that are affected by a change of support, which were also the model inputs focused on in this study, are a DEM, the rasters containing values for the tangential and normal coefficient of restitution and the tree distribution raster, which includes both the number of trees per cell and the range of tree stem diameters. The DEM was used to determine the mean slope gradient and therefore the acceleration and deceleration of a falling block. Furthermore, the DEM

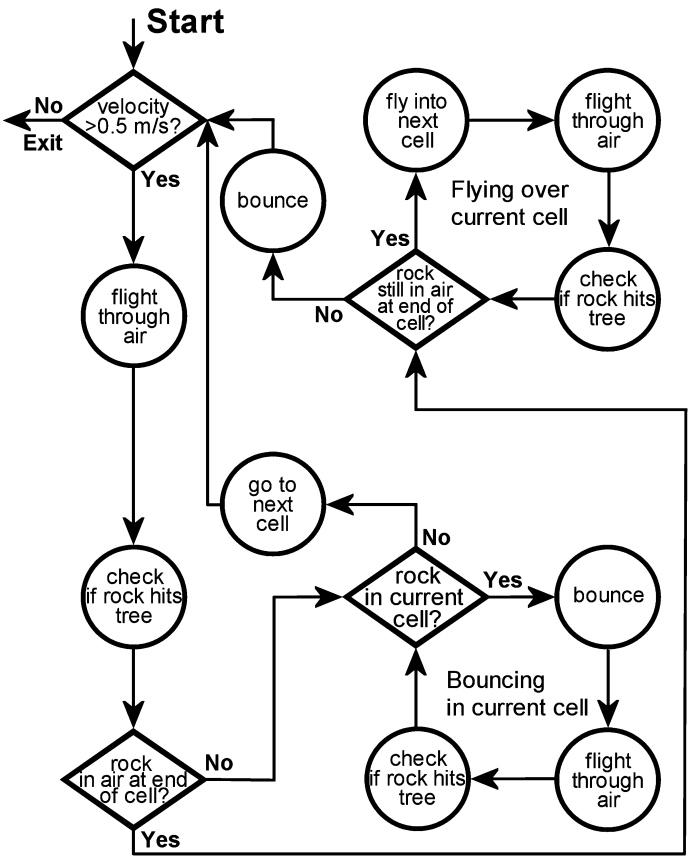


Figure 2. Flow diagram of the model used in the three simulation schemes.

determined the fall direction. The coefficients of restitution determined the amount of energy lost during a bounce, where the tangential coefficient of restitution determines energy loss parallel to the slope surface (due to surface roughness or vegetation) and the normal coefficient of restitution determines energy loss perpendicular to the slope surface (due to elasticity of the material covering the slope surface). The tree distribution determined the probability of a falling rock hitting a tree.

The outcomes produced by the three simulation schemes were compared with a validation data set on the basis of the mean error (ME) and the mean-squared error (MSE) following:

$$ME = \frac{1}{n}\sum_{i=1}^{n}(P_i - O_i) \tag{1}$$

$$MSE = \frac{1}{n}\sum_{i=1}^{n}(P_i - O_i)^2, \tag{2}$$

where n is the number of observations, P_i is the modelled or predicted value in raster cell i, and O_i is the observed value in raster cell i, which is obtained from the

validation data. The correlation coefficients between the observed and predicted values were also calculated for each simulation scheme.

3. Test site and available data

The test site was a forested, active rockfall slope in the most western part of the Austrian Alps, located at 47°00′ latitude and 10°01′ longitude. The site could be divided into two areas. The rockfall source area, which is a steep cliff face dissected by large denudation niches and an accumulation area, and a large post-glacially developed talus cone consisting mainly of rockfall scree, but also some debris flow material. The mean slope gradient in the source area was approximately 70° and in the accumulation area 38°, The slope length of the talus cone is approximately 900 m. An overview of the site is shown in figure 3.

Two DEMs were available for the site, both raster based with supports of 25×25 m (LRDEM) and 2.5×2.5 m (HRDEM). The LRDEM was created by interpolation of photogrammetric height measurements at a ground distance of 50 m, enhanced and supplemented with prominent terrain structures. The given maximum error in this DEM was 20 m (BEV 2002).

The HRDEM was derived from a TIN (Triangular Irregular Network), which was created from contour lines with an equidistance of 5 m. The contour lines were derived from a combined data set consisting of slope transects measured in the field, a detailed geomorphological field map (1:2000) and existing contour lines with an equidistance of 20 m. Since the site was fully covered with forest, we did not use a tachymeter or photogrammetric height measurements based on aerial photographs

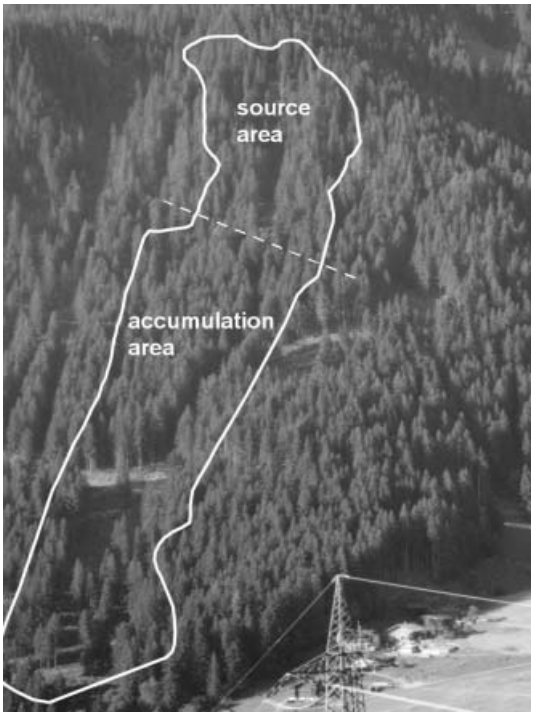


Figure 3. Part of the 'Ausserbacher' forest in the Montafon region, Austria, that served as a test site for the study. The white outline represents the test site.

to create the HRDEM. The maximum error of the HRDEM was 6 m. The main difference between the HRDEM and the LRDEM was that important terrain structures, which determine the variation in the slope gradient of the site, were well represented in the HRDEM, whereas in the LRDEM such structures were not evident at all (figure 4).

Maps of mean slope gradients were derived from both the HRDEM and the LRDEM using the method described by Zevenbergen and Thorne (1987). In addition, fall directions were calculated using a modified multiple-flow algorithm (Quinn *et al.* 1991, Wolock and McGabe 1995, Tarboton 1997). To randomize the fall direction from a central cell for each simulation run, this method calculated a fall direction raster map by sampling the fall direction for each cell randomly from a probability distribution. The latter was determined by the steepness of the mean slope gradients between the central cell and all its downslope neighbouring cells.

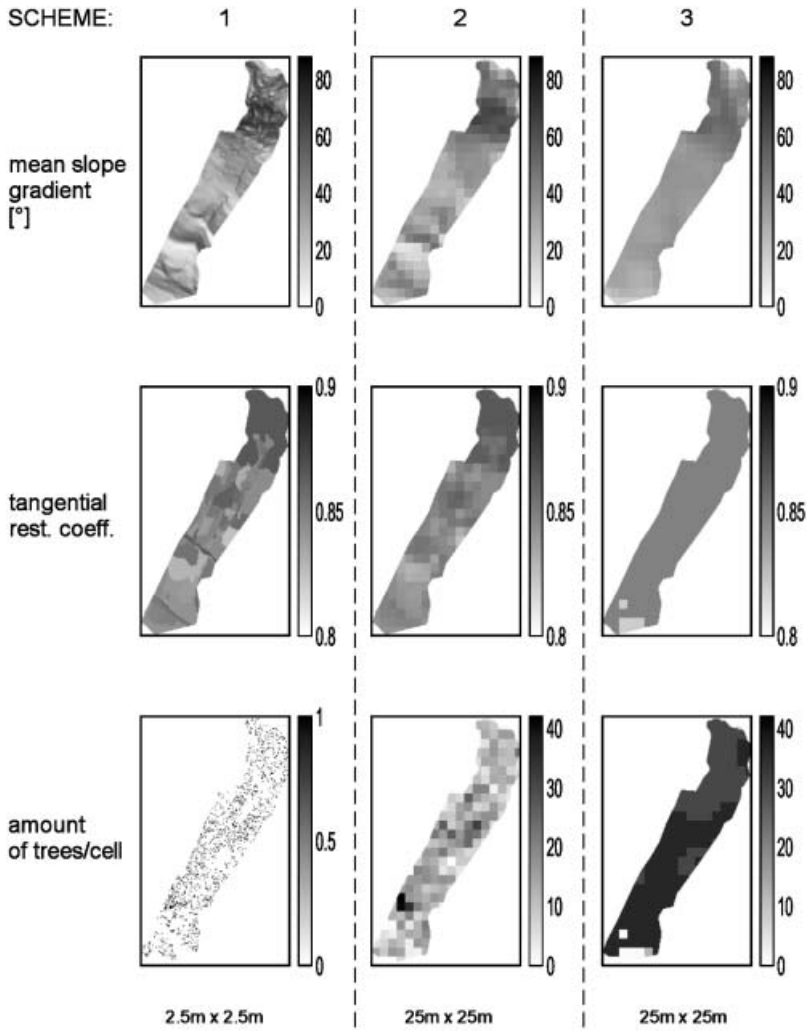


Figure 4. Slope, tangential coefficient of restitution (r_t) and number of trees per cell for simulation schemes 1–3.

The probability of a rock falling to a downslope cell was largest towards the lowest downslope cell. For details about the procedure used, see Dorren *et al.* (2004).

The tangential coefficient of restitution (r_t), the normal coefficient of restitution (r_n) and the tree distribution were represented as raster maps with a support of 25×25 m (hereafter, respectively, LRr_t, LRr_n and LRtree) and with a support of 2.5×2.5 m (hereafter HRr_t, HRr_n and HRtree). The coefficients of restitution determine the energy efficiency of a collision (Chau *et al.* 2002). The vegetation cover and the surface roughness determine the tangential coefficient of restitution. The normal coefficient of restitution is determined by the elasticity of the slope surface. The LRr_t and LRr_n were derived from data from the literature (Pfeiffer and Bowen 1989, Kobayashi *et al.* 1990, Van Dijke and Van Westen 1990, Giani 1992, Azzoni *et al.* 1995, Chau *et al.* 1998, Meißl 1998) and a land cover map, which was obtained by classifying a Landsat TM image of September 1998 (Dorren and Seijmonsbergen 2003). LRtree was also derived from this land cover map in combination with data from a regional forest inventory (Maier 1993). Both HRr_t and HRr_n were based on a detailed map (scale 1:2000) that depicted the spatial distribution of different hill-slope characteristics potentially affecting rockfall tracks (Dorren *et al.* 2004). From this map, r_t and r_n could be estimated using data from the literature (Pfeiffer and Bowen 1989, Van Dijke and Van Westen 1990, Kobayashi *et al.* 1990, Giani 1992, Azzoni *et al.* 1995, Chau *et al.* 1998, Meißl 1998). We created HRtree using a combination of a tree crown map and forest inventory data. The tree crown map was derived from an object-based classification of high-resolution digital colour-infrared (CIR) orthophotos (0.25×0.25 m) on which each individual tree crown was visible. The forest inventory, which was done with the 'Winkelzählprobe' method (Bitterlich 1948), provided additional data on the forest stands throughout the study site. This inventory method is also known as prism plot sampling or probability proportional to size sampling, i.e. the probability of a tree being selected within a sampling plot is proportional to the diameter of the tree (Shiver and Borders 1995). A grid was defined over the test site and tree stem diameters, the number of trees per ha and the rockfall damage per tree stem (number of fresh scars) were measured. From this inventory the tree volume, the number of trees and the damage per hectare were calculated for each grid cell.

HRDEM, HRr_t, HRr_n and HRtree were the input for simulation scheme 1. These data were aggregated for simulation scheme 2. LRDEM, LRr_t, LRr_n and LRtree provided input data for simulation scheme 3. A summation of all the values of the aggregated cells gave the aggregated tree map for simulation scheme 2. The input data for the three simulation schemes are given in table 1 and a flow diagram of the method is given in figure 4.

Validation data were extracted from the detailed forest inventory data. Within the grid cells covered by the forest inventory in the upper part of the accumulation area 18 squares of 25×25 m were selected randomly. We discarded the forest inventory data in the lower parts of the accumulation area because rockfall activity also originated from source areas outside the area used for this study. The size of the validation dataset is small ($n = 18$). Therefore results have to be interpreted carefully, though, these data are derived from a very large set of detailed measurements.

For these 18 squares, the tree volume and number of scars per hectare caused by

Table 1. Input data for the three simulation schemes and their origin.

Simulation scheme	Support	DEM	Tree distribution	r_t	r_n
1	2.5 × 2.5 m, HR	contour lines	orthophotos + detailed inventory	detailed field map + literature	detailed field map + literature
2	25 × 25 m, HR*	aggregated from 1	aggregated from 1	aggregated from 1	aggregated from 1
3	25 × 25 m, LR	photogrammetry	Landsat TM + regional inventory	Landsat TM + literature	Landsat TM + literature

HR, high resolution, large support; HR*, HR data aggregated to a 25 × 25 m support; LR, low resolution, small support.

rock impacts were measured. These data were compared with the number of rock impacts on trees as simulated by the model. For standardization purposes, both the validation data (observed values) and the simulated data (predicted values) in the 18 squares were expressed as percentages of the summed values of all the randomly selected squares. In other words, the observed value is the number of scars per unit tree volume in a square expressed as a percentage of the total number of scars per unit tree volume in all squares. Here, the number of scars per unit tree volume is the number of scars per hectare caused by rock impacts divided by the tree volume within the square. The predicted value represented the number of impacts in a square expressed as a percentage of the summed number of impacts in all squares.

4. Output of the three simulation schemes

Figure 5 shows the percentage of impacts in each cell for the three simulation schemes. They show a similar gradient in the number of impacts per cell. Most impacts occur in the upper right part of the area on the transition between the source area and the accumulation area. Generally, the number of impacts decreases towards the lower left, which is the accumulation area or runout zone. A notable

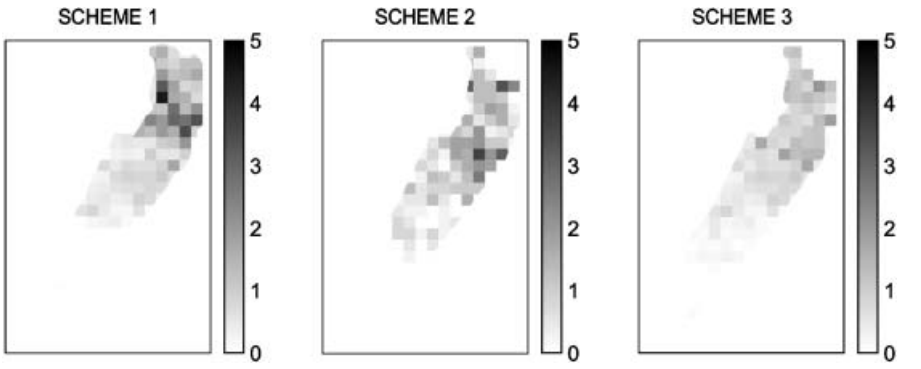


Figure 5. Produced relative numbers of impacts in a cell in percentages produced by simulation schemes 1–3.

difference between the three simulations is the location of the maximum number of impacts (figure 5). For simulation scheme 1, this is in the lower parts of the rockfall source areas, but for simulation schemes 2 and 3, it is located on the upper part of the accumulation area. However, for simulation scheme 3 the maximum number of impacts is more evenly distributed over the accumulation area.

Comparison of the simulated impacts with the number of observed scars per unit tree volume provided the results shown in figure 6. The histograms show that simulation scheme 2 produced the largest errors and simulation scheme 1 the smallest errors. In general, all errors are quite large. The scatter plots in figure 6 show the difference between each predicted and observed value for the three schemes in detail. The scatter plot of simulation scheme 1 shows that the degree of scatter between observed and predicted values is generally less than in the scatter plots of schemes 2 and 3. This is caused by a more accurate estimation of the larger observed values. Nevertheless, simulation scheme 1 also produced some considerable mismatches of the smaller observed values. The latter affects the mean-squared error considerably for simulation scheme 1 (MSE1), as shown in table 1 (MSE1 = 24.9). Simulation scheme 2 produced the largest error (MSE3 = 44.4) and simulation scheme 3 produced an intermediate one (MSE2 = 31.3). This is also indicated by the correlation coefficient (table 2). The correlation coefficient measures the strength of a linear relationship, but is not bound to the 1:1 relationship between observed and predicted values. The correlation coefficient is given here because it will indicate a systematic error in the model if both it and the MSE are large.

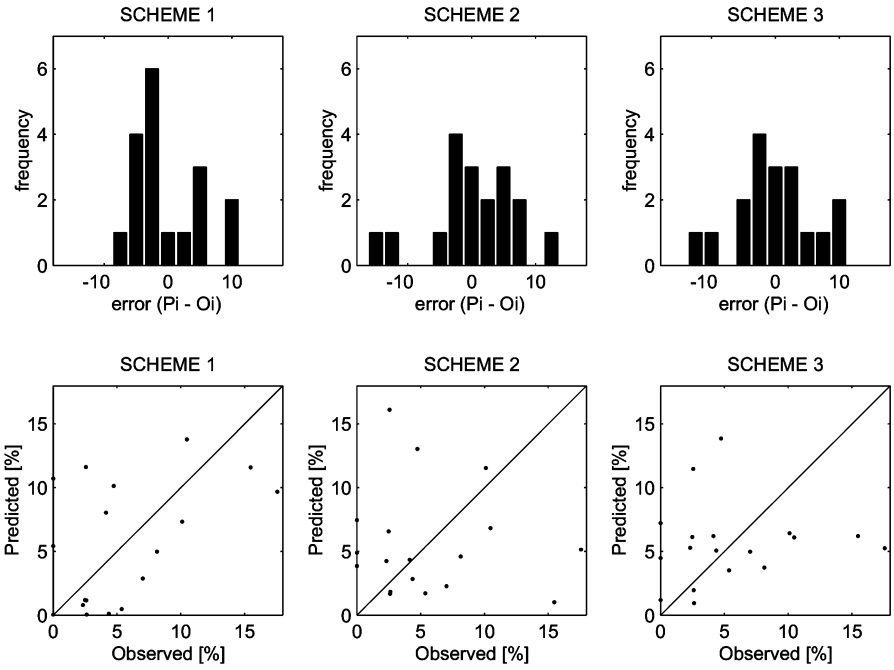


Figure 6. Histograms of the errors produced by simulation schemes 1–3 and accompanying scatter plots with observed versus predicted values.

Table 2. Mean error (ME), mean-squared error (MSE) and correlation coefficient (r) of the output of the three simulation schemes.

Simulation scheme	ME	MSE	r
1	0	24.9	0.47
2	0	44.4	0.08
3	0	31.3	0.09

5. Additional tests and discussion

5.1. *'Intermediate' simulation schemes*

We did not expect simulation scheme 3 to give a smaller MSE than scheme 2. Rather, we anticipated that scheme 3 would perform the worst, because it uses input data of the poorest quality. The only difference between simulation schemes 2 and 3 is the values for four model parameters, which have all been changed simultaneously. To assess which of these four input parameters caused a smaller MSE for simulation scheme 3, we analysed 'intermediate' simulation schemes. These 'intermediate' simulation schemes are explained in table 3.

The results presented in table 3 show that the substitution of LRtree by the aggregated HRtree (simulation scheme 7) resulted in an MSE of 29.3, which is smaller than the initial MSE for scheme 3 (figure 7a). Substitution of LRr_t by the

Table 3. Mean-squared error (MSE) of the model output produced with 'intermediate' simulation schemes 4–7 and the original schemes 2 and 3.

Simulation scheme	Used data	MSE
2	HRtree*, HRr_n*, HRr_t*, HRDEM*	44.4
3	LRtree, LRr_n, LRr_t, LRDEM	31.3
4	LRtree, LRr_n, LRr_t, HRDEM*	47.8
5	LRtree, LRr_n, HRr_t*, LRDEM	35.7
6	LRtree, HRr_n*, LRr_t, LRDEM	31.4
7	HRtree*, LRr_n, LRr_t, LRDEM	29.3

*Data aggregated to a 25×25 m support.

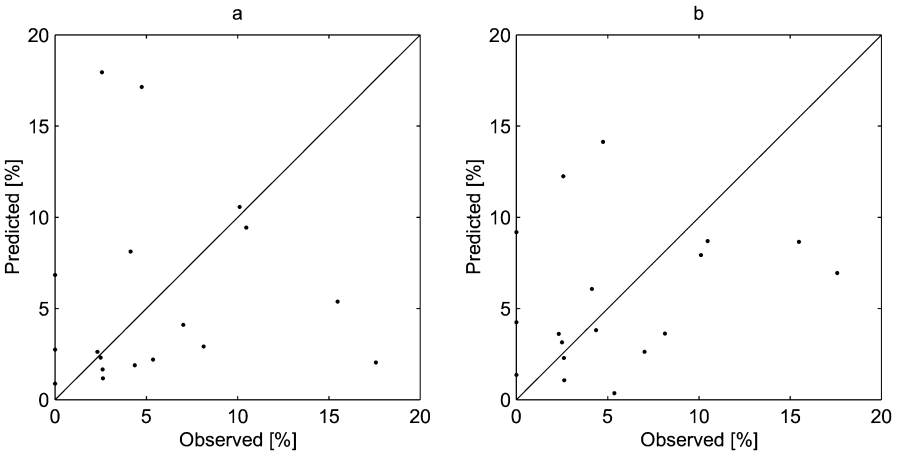


Figure 7. Scatter plots of (a) simulation scheme 7 and (b) simulation scheme 4.

aggregated HRr_t (simulation scheme 5) increased the MSE from 31.3 to 35.7. Table 2 also shows that the substitution of LRr_n by the aggregated HRr_n (simulation scheme 6) resulted in an increase of the MSE of 0.1, which indicates that the net effect of r_n on the simulation results was small.

A remarkable result is that the substitution of the LRDEM by the aggregated HRDEM (simulation scheme 4) did not decrease MSE3. On the contrary, it resulted in a large increase of the MSE from 31.3 to 47.8. The scatter plot of this simulation result is shown in figure 7b. This simulation scheme strongly overestimated the smaller observed values and strongly underestimated the larger observed values.

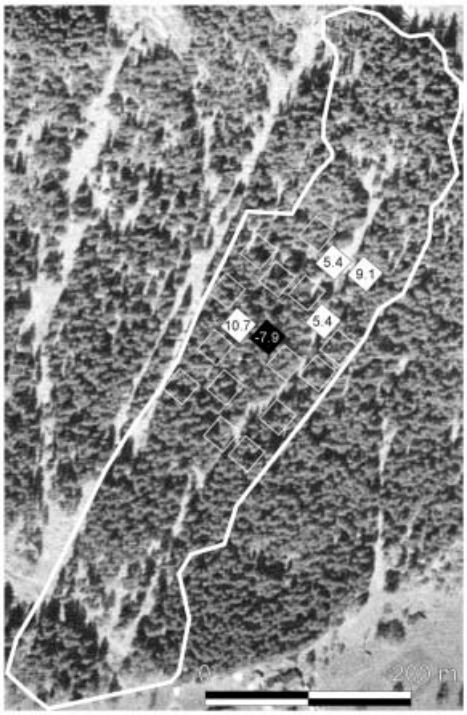
5.2. *Causes of simulation errors*

The 'intermediate' simulation scheme 4 indicated that the aggregated HRDEM was mainly responsible for the increase in error (table 2), which could be explained as follows. The transport channel shown in figure 3, which is represented in both the HRDEM and HRtree (figure 4), is averaged out to a certain extent in the aggregated HRDEM but still represented. Consequently, the fall directions calculated based on the aggregated HRDEM were generally towards this channel. This led to a concentration of falling rocks in the right side of the raster. Therefore, the number of impacts is more on that side of the area (figure 8; simulation scheme 4). This effect is reinforced by the fact that the transport channel is almost free of trees. Therefore, hardly any rock impacts against trees occur in the channel in reality. However, when using the aggregated HRtree, the forest structure in the channel as observed in the field and in HRtree is completely lost (figure 4). Consequently, the number of trees in the fall track of the simulated rocks, as represented by the aggregated HRtree, is overestimated, although the number of trees in the channel is still smaller than in the surrounding areas. As a result, the number of impacts in the channel is more strongly overestimated than in the other simulation schemes, as shown in figure 8 (simulation scheme 1–3). This error occurred to a lesser extent in simulation scheme 3, since in the LRDEM the channel was completely 'smoothed-out'. Consequently, a more uniform distribution of rock impacts was produced.

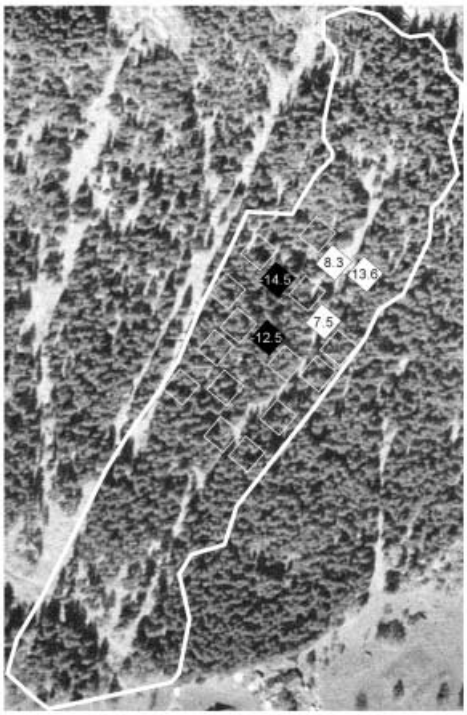
The squares with an overestimation of 10.7% and an underestimation of 7.9% in figure 8 (scheme 1) indicate a spatial mismatch between model results and field observations. Figure 8 shows that simulation schemes 2 and 3 have an underestimation only in the same area, which is about 12%. The errors in the validation squares on the lowest part of the test site show that the simulation schemes 1–3 modelled the maximum extent of rockfall runout zones quite well (figure 5), as the error values in those parts are smaller than 5%. None of the simulation schemes produced rocks at the bottom part of the hill slope, which is in agreement with reality. As mentioned before, the modelled rockfall impacts on tree stems reproduced the trend observed in reality, but were not very accurate as the MSEs of all the simulation schemes were quite high.

5.3. *Rockfall simulation at different scales*

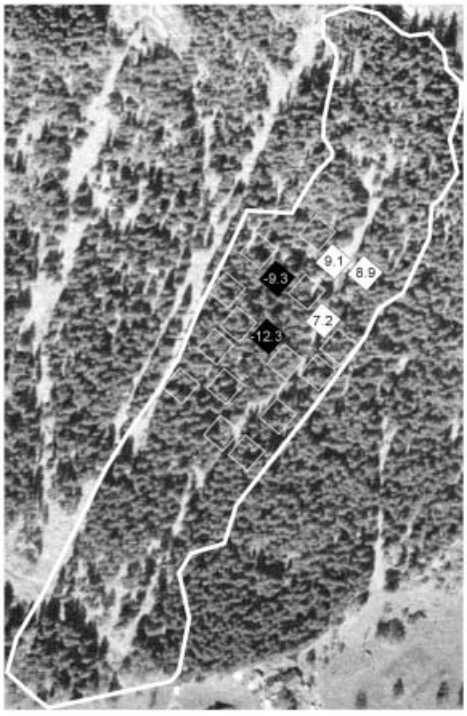
Overall, the results indicate that the GIS-based distributed model used in this study, which was developed for rockfall assessment at a slope scale, can be used for rockfall assessment at a regional scale. As expected, the simulation schemes analysed indicated that input data with a support of 25×25 m increased the MSE



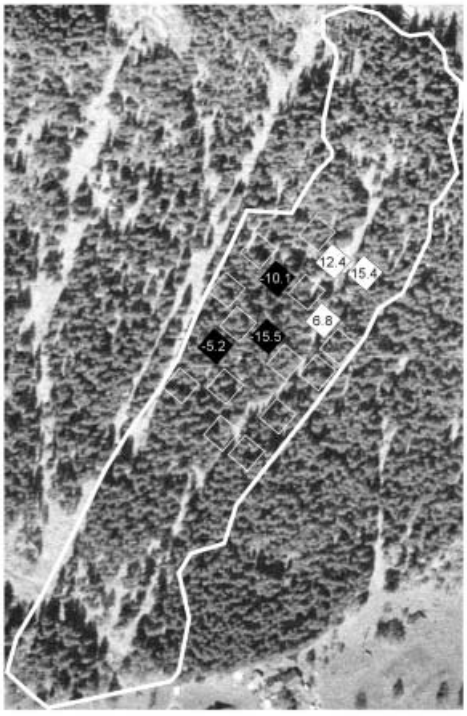
SCHEME 1



SCHEME 2



SCHEME 3



SCHEME 4

compared to input data with a support of 2.5×2.5 m. However, the simulated maximum extents of rockfall runout zones were similar for simulation schemes 1–3. In addition, these simulated maxima also corresponded with those observed in reality, which shows that modelling rockfall runout zones at the regional scale is feasible and realistic, even for forested catchments. The simulated rockfall impacts on tree stems using data with a support of 25×25 m were not accurate, as the mean-squared errors produced by simulation schemes 2 and 3 were much larger than the MSE of scheme 1. Using tree distribution data of higher quality could reduce the MSE of scheme 3 with about 2% as shown by the 'intermediate' simulation scheme 7. The accuracies of the results produced by schemes 2 and 3 indicate that simulating damage on tree stems caused by rockfall using data with a support of 25×25 m is not realistic. To assess where and how much tree stem damage will occur, high quality data with a small support are required.

6. Conclusions

This paper has investigated the relationship between the aggregation level of the input data and the accuracy of the output of a rockfall simulation model. The results showed that the simulation of rockfall with a GIS-based distributed model using data with a support of 25×25 m is feasible and realistic to simulate rockfall runout zones, but not for the simulation of tree damage caused by rockfall. The latter arose because collisions of rocks against tree stems cannot be simulated accurately where the data are of poor quality and the support is large.

As anticipated, the model using data with a support of 25×25 m produces a larger error than that using data with a support of 2.5×2.5 m. Our hypothesis was that poor data quality is a more important cause of a larger model prediction error than the effect of a larger support. This study showed that this is not necessarily true because the simulation scheme that used data of higher quality produced a larger error than the simulation scheme that used data of poorer quality. Here it was interesting to observe that the loss of important spatial structure in the input data (i.e. the rockfall channel represented in the slope map and in the tree distribution map), as caused by spatial aggregation, resulted in a larger model prediction error than the use of data that represented the landscape with less detail.

The results of this study also indicate that the use of a regional DEM of high quality requires data on forest structure of higher quality than does a regional DEM of poorer quality in case of simulating rocks falling through mountain forests. We realize that other spatial simulation models and other input data than those used in this study may well produce quite different results. However, since the forest that was chosen as a study area is representative for many forests that protect houses and infrastructure in the European Alps, we consider the outcomes also applicable for other forests in the European Alps. The main reason for this is that steep non-forested tracks, which are often preferential rockfall and also avalanche tracks, occur in many of these protection forests. The existence of such non-forested tracks was the main reason why the simulation scheme that used a DEM and tree

Figure 8. Visualization of the validation squares, where $|P_i - O_i| > 5$ for simulation schemes 1–3 as well as 'intermediate' scheme 4. The white outlined squares indicate an absolute error smaller than 5; black filled squares indicate significant underestimation by the model; white filled squares indicate significant overestimation by the model.

structure data at different supports was the most inaccurate. The same effect is likely to happen when using data from other rockfall forests. It would be interesting to aim future rockfall modelling research determining the minimum support required to obtain realistic and trustworthy modelling results for the assessment of the degree of protection provided by mountain forests against rockfall hazards in the European Alps. These assessments probably could be done using data with a support ranging from 1 to 25 m, but the question is which support would be sufficient. Goodchild (2001) stated that the input data for a model should be of sufficient detail to capture the spatial variation that is essential to describe the process or pattern being modelled. The results of this study confirm this, because it shows that to model tree damage caused by rockfall, the tree distribution must be known at a level of detail that corresponds with the physical process of rockfall.

References

AZZONI, A., BARBERA, G. L., and ZANINETTI, A., 1995, Analysis and prediction of rockfalls using a mathematical model. *International Journal of Rock Mechanics and Mining Science*, **32**, 709–724.

BERGKAMP, G., 1995, A hierarchical approach for desertification assessment. *Environmental Monitoring and Assessment*, **37**, 1–20.

BEV, 2002, Bundesamt für Eich- und Vermessungswesen, Produktinformation zum Geländehöhenmodell (available at: http://www.bev.gv.at/prodinfo/dgm/dgm_3f.htm).

BIERKENS, M. F. P., FINKE, P. A., and DE WILLIGEN, P., 2000, *Upscaling and Downscaling Methods for Environmental Research* (Dordrecht: Kluwer).

BITTERLICH, W., 1948, Die Winkelzählprobe. *Allgemeine Forst und Holzwirtschaftliche Zeitung*, **1**, 4–5.

BURROUGH, P. A., and MCDONNELL, R. A., 1998, *Principles of Geographical Information Systems* (Oxford: Oxford University Press).

CHAU, K. T., WONG, R. H. C., and LEE, C. F., 1998, Rockfall problems in Hong Kong and some new experimental results for coefficient of restitution. *International Journal of Rock Mechanics and Mining Science*, **35**, 662–663.

CHAU, K. T., WONG, R. H. C., and WU, J. J., 2002, Coefficient of restitution and rotational motions of rockfall impacts. *International Journal of Rock Mechanics and Mining Science*, **39**, 69–77.

DORREN, L. K. A., MAIER, B., PUTTERS, U. S., and SEIJMONSBERGEN, A. C., 2004, Combining field and modelling techniques to assess rockfall dynamics on a protection forest hillslope in the European Alps. *Geomorphology*, **57**, 151–167.

DORREN, L. K. A., and SEIJMONSBERGEN, A. C., 2003, Comparison of three GIS-based models for predicting rockfall runout zones at a regional scale. *Geomorphology*, **56**, 49–64.

GIANI, G. P., 1992, *Rock Slope Stability Analysis* (Rotterdam: Balkema).

GOODCHILD, M. F., 2001, Models of scale and scales of modeling. In *Modelling Scale in Geographical Information Systems*, edited by N. J. Tate and P. M. Atkinson (Chichester: Wiley), pp. 3–10.

HEUVELINK, G. B. M., 1998, Uncertainty analysis in environmental modelling under a change of spatial scale. *Nutrient Cycling in Agroecosystems*, **50**, 255–264.

KOBAYASHI, Y., HARP, E. L., and KAGAWA, T., 1990, Simulation of rockfalls triggered by earthquakes. *Rock Mechanics and Rock Engineering*, **23**, 1–20.

LEWIS, P. A. W., and ORAV, E. J., 1989, *Simulation Methodology for Statisticians, Operations Analysts, and Engineers*, Vol. 1 (Pacific Grove: Wadsworth & Brooks/Cole).

MAIER, B., 1993, Forstinventur Stand Montafon. Internal Report (Schruns, Austria: Stand Montafon).

MEIßL, G., 1998, Modellierung der Reichweite von Felsstürzen. Fallbeispeile zur GIS-gestützten Gefahrenbeurteilung aus dem Beierischen und Tiroler Alpenraum. PhD thesis, Universität Innsbruck.

MONTGOMERY, D. R., and DIETRICH, W. E., 1994, A physically-based model for the

topographic control on shallow landsliding. *Water Resources Research*, **30**, 1153–1171.

MOWRER, H. T., 1997, Propagating uncertainty through spatial estimation processes for old-growth subalpine forests using sequential Gaussian simulation in GIS. *Ecological Modelling*, **98**, 73–86.

PFEIFFER, T. J., and BOWEN, T. D., 1989, Computer simulation of rockfalls. *Bulletin of the Association of Engineering Geologists*, **26**, 135–146.

QUINN, P., BEVEN, K., CHEVALLIER, P., and PLANCHON, O., 1991, The prediction of hillslope flow paths for distributed hydrological modelling using digital terrain models. *Hydrological Processes*, **5**, 59–79.

SHIVER, B. D., and BORDERS, B. E., 1995, *Sampling Techniques for Forest Resource Inventory* (New York: Wiley).

TARBOTON, D. G., 1997, A new method for the determination of flow directions and contributing areas in grid digital elevation models. *Water Resources Research*, **33**, 309–319.

TUCKER, G. E., LANCASTER, S. T., GASPARINI, N. M., BRAS, R. L., and RYBARCZYK, S. M., 2001, An object-oriented framework for distributed hydrologic and geomorphic modeling using triangulated irregular networks. *Computers and Geosciences*, **27**, 959–973.

VAN DIJKE, J. J., and VAN WESTEN, C. J., 1990, Rockfall hazard: a geomorphological application of neighbourhood analysis with ILWIS. *ITC Journal*, **1**, 40–44.

VAN ROMPAEY, A., GOVERS, G., and BAUDET, M., 1999, A strategy for controlling error of distributed environmental models by aggregation. *International Journal of Geographical Information Science*, **13**, 577–590.

WILLGOOSE, G. R., BRAS, R. L., and RODRIGUEZ-ITURBE, I., 1991, A physically based coupled network growth and hillslope evolution model, 1, theory. *Water Resources Research*, **27**, 1671–1684.

WOLOCK, D. M., and MCCABE, G. J., JR, 1995, Comparison of single and multiple flow direction algorithms for computing topographic parameters in TOPMODEL. *Water Resources Research*, **31**, 1315–1324.

ZEVENBERGEN, L. W., and THORNE, C. R., 1987, Quantitative analysis of land surface topography. *Earth Surface Processes and Landforms*, **12**, 47–56.

> Chapter 7

Full scale rockfall experiments



Available online at www.sciencedirect.com
SCIENCE DIRECT
Forest Ecology and Management 215 (2005) 183–195
Forest Ecology and Management
www.elsevier.com/locate/foreco

Mechanisms, effects and management implications of rockfall in forests

Luuk K.A. Dorren *, Frédéric Berger, Céline le Hir, Eric Mermin, Pascal Tardif

Cemagref Grenoble, Mountain Ecosystems Research Unit 2, rue de la Papeterie, 38402 Saint Martin d'Heres Cedex, France

Received 25 November 2004; received in revised form 25 April 2005; accepted 10 May 2005

Abstract

At the scale of forest stands, there is a lack of quantitative, statistically valid data on the protective effect of forests against rockfall. Therefore, the first objective of this study was to quantify the velocities, rebound heights as well as the residual hazard of rockfall on a forested and a non-forested slope. The second objective was to evaluate existing rockfall protection forest management guidelines, as well as the underlying criteria. We carried out and analysed 100 real size rockfall experiments at a non-forested site (Site 1) and 102 identical experiments at a forested site (Site 2) on the same slope. We compared the obtained results with literature data on rockfall protection forests. At the non-forested site, results show that the mean maximum velocity is 15.4 m s^{-1} compared to 11.7 m s^{-1} at the forested site. The maximum rebound height decreases from 8 m (Site 1) to 2 m (Site 2) and the number of rocks that surpass the 223.5 m slope distance decreases from 95 out of 100 (Site 1) to 35 out of 102 (Site 2). A major effect of rockfall on a forested slope is the development of a treeless rockfall path or *couloir*, which had evolved after releasing 78 rocks at Site 2. The effect of such a *couloir* can be mitigated by cutting trees on both sides of the *couloir* and leaving the trunks on the slope, diagonally to the slope direction. This is a known and effective technique to reduce the effect of gaps in protection forests. During our experiments, none of the rocks attained their maximal velocity within the first 40 m. They did, however, attain destructive velocities (11–15 m s^{-1}) within that distance. Based on our observations, we propose a maximum gap size in the slope direction of 1.3 times the mean tree height, with a maximum of 40 m. Further, we present various findings that have direct implications for the management of rockfall protection forests. Finally, the results proved that forests can provide effective protection against rockfall.
© 2005 Elsevier B.V. All rights reserved.

Keywords: Mountain forest; Natural hazards; Protection forest; Real size experiments

1. Introduction

To sustain today's livelihoods in the European Alps, protection against natural hazards is indispensable. One of the important natural hazards is rockfall. We define rockfall as a relatively small landslide confined to the removal of individual rocks smaller than 5 m^3 from a cliff face (Selby, 1982; Berger et al., 2002). The unpredictability of rockfall potentially endangers human lives and infrastructure, as shown by the numerous examples of infrastructure destroyed or

* Corresponding author. Tel.: +33 4 76 76 28 06
E-mail address: luuk.dorren@cemagref.fr (Luuk K.A. Dorren).

0378-1127/$ – see front matter © 2005 Elsevier B.V. All rights reserved.
doi:10.1016/j.foreco.2005.05.012

people killed by rockfall (e.g., Porter and Orombelli, 1981; Bunce et al., 1991; Badger and Lowell, 1992). Although rockfall is unpredictable, it mostly occurs in spring, due to alternating freezing and thawing and after heavy rain (Erismann and Abele, 2001; Dorren, 2003; Stoffel et al., in press-a). Rockfall in the European Alps is mostly a low magnitude–high frequency event (Dussauge-Peisser et al., 2002; Hantz et al., 2003; Stoffel et al., in press-b). From the different studies on the frequency of rockfall events it is hard to give an indication how often individual rocks smaller than 5 m^3 fall throughout the European Alps. Based on data obtained in the French Alps, one could expect every year a falling rock between 0.5 and 5 m^3 20 km^{-1} cliff length, which will damage forests, roads or buildings (Dussauge-Peisser et al., 2002). Rocks smaller than 0.5 m^3 fall much more often and can cause problems to local traffic and infrastructure more continuously, but such smaller events were not recorded in the dataset used by Dussauge-Peisser et al. (2002).

To protect against rockfall, one could use technical protective measures or eco-engineering techniques (use of ecological processes, possibly combined with engineering design, to achieve physical and environmental goals, e.g., installing wooden barriers, enlarging rock piles and walls using previous rockfall deposits, but also strategic planting, cutting and positioning trunks on the slope in protection forests). An important question with respect to rockfall protective measures is how much they reduce the residual rockfall hazard, i.e., the percentage of rocks that surpasses the protective measure(s) and the kinetic energy of those rocks. Rockfall protective measures can be grouped into preventive and protective ones. The first method aims to prevent the detachment of a rock by anchoring it to a stable part of the cliff. The second is used to mitigate the hazard, either by deviating its trajectory, e.g., by using galleries, or by reducing the natural travelling distance (Heidenreich, 2004). The latter is done, for example, by constructing catch or barrier fences, rockfall dams, restraining nets and dynamic rockfall nets (Hearn et al., 1992; Spang and Sönser, 1995; Peila et al., 1998; Nicot et al., 2001). The protective effect of forests falls mainly in the second class.

Technical protective measures are expensive and they deteriorate with time. Moreover, they cannot always reduce the residual rockfall hazard completely. The latter surely accounts for protection forests as well. However, in combination with technical protective measures it is possible in many cases (Gerber, 1998). The advantage of having and maintaining a protection forest in an optimal state regarding its protective effect as well as its stability in the long term (see Dorren et al., 2004a), is that more modest or sometimes no technical protective measures at all are required, of course depending on the acceptable risk. In those cases, the maintenance of forests designated an explicit protective function is cost-efficient (Kienholz and Mani, 1994; Motta and Haudemand, 2000; Berger et al., 2002; Dorren et al., 2004a; Perret et al., 2004; Brauner et al., 2005).

Many Alpine countries in Europe are developing guidelines for maintaining rockfall protection forests (e.g., Frehner et al., in press; ONF, in preparation). For that, quantitative and statistically valid data are required. However, at the scale of forest stands, there is a lack of such data, especially for rocks with diameters larger than 0.5 m. Therefore, the objectives of this study were: (i) to quantify the velocities, rebound heights as well as the residual hazard of rockfall on a forested and a non-forested slope using real size rockfall experiments and (ii) to evaluate existing management guidelines for forests that protect against rockfall, as well as the underlying criteria, using our experimental data combined with relevant literature data.

2. Existing literature on rockfall in forests

2.1. Previous rockfall experiments in forests

Quantitative field data on rockfall in forests, obtained by rockfall experiments that are similar to ours, have been presented by Jahn (1988) and by Doche (1997). Jahn (1988) described the results of rockfall experiments that were carried out on a non-forested (NF) and a forested (F) section of a 35.5° slope between an upper and lower forest road in Liechtenstein. Section NF is about 25 m wide and 143.4 m long (distance between the starting point and the lower forest road, measured along the slope). Section F is also about 25 m wide and 161.1 m long.

Table 1
Stopping causes of falling rocks on the experimental sites of Jahn (1988)

	Non-forested site ($n = 34$) (%)	Forested site ($n = 98$) (%)
Big rocks	32	16
Trees	6	61
Tree stumps	15	1
Footpath	21	8
Forest road	15	0[a]
Cause unclear	12	13

[a] None of the rocks reached the forest road.

The forest stand consisted of *Fagus sylvatica* L., *Picea abies* (L.) Karst., *Pinus sylvestris* L. and *Fraxinus excelsior* L., with a mean stand density of 3400 trees ha^{-1} and a mean DBH of 13 cm. The mean rock diameter used on section NF was 0.26 m ($n = 34$, spherical shape) and 0.28 m ($n = 98$, spherical shape) on section F (the minimum and maximum diameter of all the used rocks were 0.13 and 0.45 m, respectively, $n = 132$). The maximum rockfall velocity measured by Jahn (1988) was 15 m s^{-1}. Higher peak velocities have been observed, but could not be measured with the chronometer. Jahn (1988) found further that 31% of all the thrown rocks reached the lower forest road on section NF, whereas 0% on section F. Specific causes for rocks to stop at the two sites are given in Table 1. On average, each rock had 0.61 frontal and 0.39 lateral impacts on section F, where 40% of the frontal impacts resulted in immediate stopping of the rocks and 27% of the rocks impacted no tree at all. Only three rocks impacted two or more trees frontally. The lateral deviation from the central fall path was about 8° (Jahn, 1988). The research of Jahn (1988) showed that a very dense forest stand, with a small mean stem diameter, can protect effectively against rocks with diameters of 0.13–0.45 m.

The report of Doche (1997) presents the set-up and the results of the rockfall experiments carried out by Cemagref Grenoble at a forested site in Vailly (France). This site has a mean slope gradient of 38°, a length of 140 m (measured along the slope) and a width of 55 m. It is covered by *P. abies* (48%), *Abies alba* Mill. (16%), *Acer pseudoplatanus* L. (16%), *F. sylvatica* (15%) and various other broad-leaved species (5%). The stand density was 485 trees ha^{-1}, the mean DBH was 28 cm (S.D. = 15 cm), the measured total basal area was 38.7 m^2. The mean diameter of the used rocks was 0.87 m (minimum = 0.65 m, maximum = 1.15 m, S.D. = 0.15 m, $n = 15$, density = 2500 kg m^{-3}, spherical shape). The mean and maximum rebound heights were 0.88 and 2.7 m, respectively. The measured mean maximum velocity was 15.0 m s^{-1}, the absolute maximum velocity measured was 19.6 m s^{-1}. These data were calculated on the basis of video recordings. Doche (1997) describes that eight rocks were stopped due to tree impacts (53.3%), five surpassed the forested zone (33.3%) and two rocks broke into pieces (13.3%) after impacting rocks that were deposited behind trees. Thus, in total, 66.6% of the rocks were stopped by the forest.

Other field research on rockfall in forests has been done by Couvreur (1982), Zinggeler (1990), Gsteiger (1993), Cattiau et al. (1995), Dorren et al. (2004a), Perret et al. (2004), Stokes et al. (in press), which mainly described retro-analyses of rockfall trajectories on forested slopes. In summary, they found that rockfall velocities on forested slopes with a mean slope gradient between 33° and 40° are in the range of 15–25 m s^{-1}, rebound heights are between 1 and 2 m.

2.2. Existing management criteria and guidelines

The potential effects of forests on the rockfall hazard act both in the rockfall source area and in the transport/accumulation area. In the rockfall source area, however, most effects are negative regarding rockfall protection. Tree roots enlarge existing joints in the bedrock and act as wedges. In addition, the presence of roots in the bedrock accelerates chemical weathering (Jahn, 1988). Finally, movement of the tree stem due to snow or wind forces can cause rockfall via the wedge effect of the roots. The positive effect is that a dense root system can hold rocks together on talus slopes (Jahn, 1988; Gerber, 1998). In practice, unstable trees on top of cliffs and trees with big roots penetrating the bedrock should be removed. In the rockfall transport and accumulation area, the effect of a forest is mostly positive, as standing trees and dead wood lying on the slope surface can act as barriers and decelerate or stop falling rocks.

To effectively stop falling rocks in the transport/accumulation area, Schwitter (1998) mentions the rule of thumb that the mean DBH of trees in a forest stand should be 1/3 of the decisive size of the falling rocks. To give an accompanying stand density is difficult,

because it depends completely on the size of the falling rock and its kinetic energy. The paradox is that the bigger the rock, the bigger the chance is that tree impacts occur, but also bigger trees are required to stop the rock. For smaller rocks, smaller trees are effective, but many more trees are required to increase the impact probability. In the minimal tending guidelines for managing rockfall forests developed by Wasser and Frehner (1996), the required stand density is independent of the size of the falling rock (400 trees ha^{-1}). Currently, this has been integrated in new guidelines, which have been developed in co-operation with Swiss forest and natural hazard specialists and our research group, in the framework of the NaIS project (in German: *Nachhaltigkeit im Schutzwald*, meaning sustainability in the protection forest, see Thormann and Schwitter, 2004; Frehner et al., in press). For a forest that has to protect against falling rocks, such as the ones we used during the experiments (mean diameter of 0.95 m), the NaiS guidelines aim at a forest consisting of at least 200 trees ha^{-1} with a mean DBH larger than 36 cm in ideal conditions and at least 150 trees ha^{-1} with the same diameters for the worst conditions.

These guidelines also mention that distances between trees in the fall direction should not exceed 20 m, because, according to Gsteiger (1993), Wasser and Frehner (1996) and Frehner et al. (in press), rocks reach their maximal speed after falling 40 m down a slope if no tree impacts occur. To estimate the mean distance between two tree impacts in a forest stand, Gsteiger (1993) proposes the concept of the mean tree free distance (MTFD), which is calculated following,

$$\mathrm{MTFD}_{\mathrm{Gsteiger}} = \frac{\mathrm{Area}}{(\mathrm{Nrstems} \times R_{\mathrm{diam}}) + \sum \mathrm{DBH}} \quad (1)$$

where Area is the evaluated area (m^2), Nrstems is the number of stems in the evaluated area, R_{diam} is the mean diameter of the rock (m) that falls in the evaluated area and ΣDBH is the sum of all the stem diameters at breast height (m) in the evaluated area. An alternative calculation is given by Perret et al. (2004):

$$\mathrm{MTFD}_{\mathrm{Perret}} = \frac{\mathrm{Area}}{\mathrm{Nrstems} \times (R_{\mathrm{diam}} + \mathrm{DBH}_m)} \quad (2)$$

where $\mathrm{DBH_m}$ is the mean DBH (m) of all the stems in the evaluated area.

A typical practice in rockfall protection forest management is to cut trees and leave the trunks lying on the slope, diagonally to the slope direction (Schwitter, 2001; Dorren et al., 2004a, 2004b; Frehner et al., in press). Such trunks prevent the development of rock accumulations and continue the rock transport in a controlled manner. Experiences in Austria show that bigger *P. abies* trees (>50 cm) can act as effective rockfall barriers for about 10 years (Dorren et al., 2004a).

A similar protective effect as obtained by lying trunks is observed in snag stands (Kupferschmid Albisetti et al., 2003) and on uncleared windthrow areas (Frey and Thee, 2002). Both latter studies report effective protection against rockfall and/or avalanches for 30 years. Cutting all the trees in a protection forest stand and leaving them lying on the slope for protection against natural hazards is, however, not a sustainable management practice. After 30 years, there will be no trees with a sufficiently large diameter to stop falling rocks with a high kinetic energy.

3. Materials and methods

3.1. Rockfall experiments

Our study area is located in the Forêt Communale de Vaujany in France (lat 45°12′, long 6°3′) and has an altitude ranging from 1200 to 1400 m above sea level. It covers a forested, northwest facing Alpine slope, which has a mean gradient of 38°. The main tree species in the study area are Silver fir (*A. alba*, 50%), Norway spruce (*P. abies*, 25%), European beech (*F. sylvatica*, 17%) and Sycamore (*A. pseudoplatanus*, 4%). Other occurring species are *Sorbus aucuparia* L., *Betula pendula* Roth, *Ulmus glabra* Huds., *Ilex aquifolium* L., *F. excelsior* L. and *Corylus avellana* L.

We defined two adjoining sites on a hillslope that is formed by a huge post-glacially developed talus cone (Fig. 1), which mainly consists of rock avalanche, snow avalanche and rockfall deposits. Site 1 is about 25 m wide and 302 m long (distance between the starting point and the lower forest road, measured along the slope). It covers an avalanche *couloir* and is, therefore, denuded of trees. Between the starting point and the lower forest road, it has the morphology of a real channel (Fig. 1). Site 2 is 53 m wide and 223.5 m

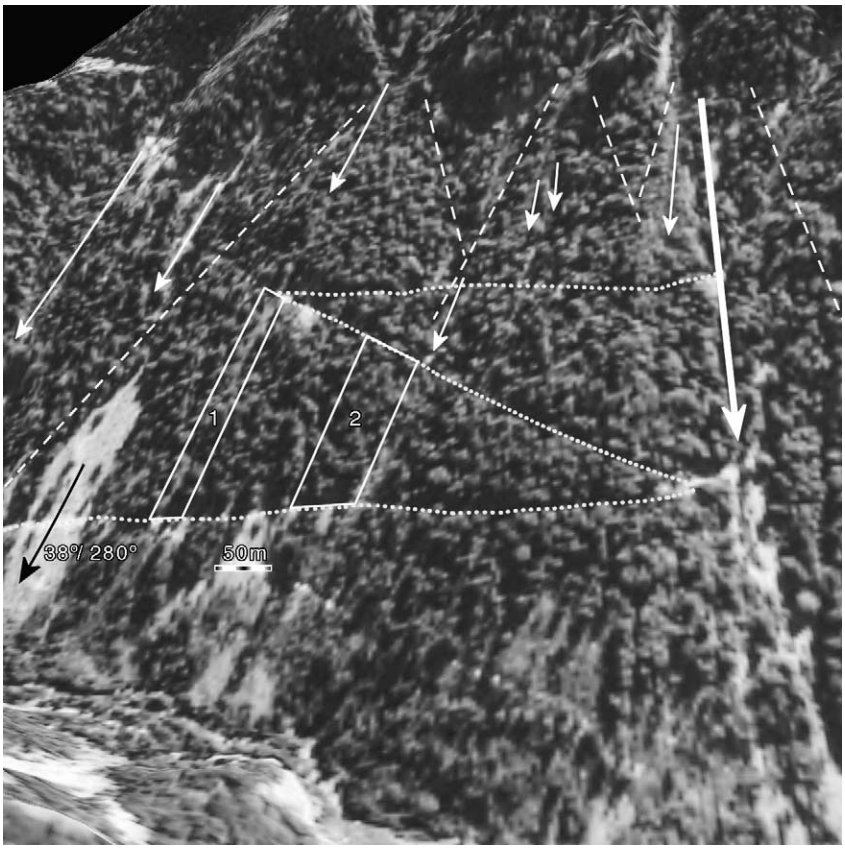


Fig. 1. A digital terrain model of the study area overlain by an orthophoto. This figure shows that the study area consists over several talus cones (dashed white lines) on which preferential rockfall and avalanche tracks exist (white arrows; the size indicates the magnitude of processes acting in the preferential track). The experimental sites are depicted by the numbers 1 and 2 in the white rectangles. The main forest road is indicated by the dotted grey line.

long and is covered by forest. In total, we measured and mapped 271 trees at Site 2, which gives a mean stand density of 290 trees ha^{-1} (planimetric). The mean DBH of all the measured trees at Site 2 was 31 cm (S.D. = 21 cm, maximum = 89 cm), the measured total basal area was 29.5 m^2 (31.6 m^2 ha^{-1}) and the mean tree height was 26 m (S.D. = 4.8 m, maximum = 36 m). There are no trees in the first 35 m of the fall line downslope of the starting point, which is necessary for the rocks to reach a velocity that is interesting for our experiments before they impact any trees. Both sites have a mean slope gradient of 38° and are easily accessible by a forest road, which was used by trucks to deliver the rocks for the experiments as well as by the caterpillar that released the rocks down the slope. The set-up of the experiments is visualized in Fig. 2. A river delimits the foot of the site, which excludes any object that could be at risk due to the experiments, and the site is representative for many active rockfall slopes in the European Alps regarding the slope surface and forest stand characteristics. It took almost three years to find and get access to a site that met all our conditions and where we were allowed to carry out the experiments.

At Site 1, the experiments have been carried out in 2001 and at site 2 they have been carried out in 2002 and 2003. Before the experiments, we installed clear warning panels to close off the complete area around the sites. We also installed five high-speed digital video cameras along the experimental sites at a height of 10 m in trees situated 30–40 m away from the



Fig. 2. (A) rocks are painted to leave marks after tree impacts or rebounds on the slope surface; (B) a caterpillar throws the rocks down the slope; (C) video cameras are installed along the slope to record the rockfall trajectories; (D) a rock accelerating in the first meters; (E) after each individual rockfall experiment, we capture its trajectory to obtain a three dimensional trajectory; (F) a sequence of movie images (each 1/4 s) taken at Site 2.

central rockfall paths of the two sites (Fig. 2C). We used the same protocol throughout all the experiments. Rocks with a mean diameter of 0.95 m were released individually, one after the other, by a caterpillar (Fig. 2B and D). The mean rock volume was 0.49 m^3 (minimum = 0.1 m^3; maximum = 1.5 m^3; S.D. = 0.3 m^3, $n = 202$) and the rock volume distribution was similar at both sites. After each rock, we surveyed its trajectory from the release to the stopping point using an Impulse LR 200 laser distance meter manufactured by Laser Technology Inc. (Centennial, Colorado, USA) (Fig. 2E). If they occurred, we measured all the damages on trees due to impacts (height and horizontal position of the impact and the size and depth of the wounds). The horizontal position of the impact on the tree stem was measured by the horizontal distance between the impact centre and the vertical central tree axis as seen from the impact direction. We painted the released rocks with biodegradable coloured powder (Fig. 2A) to facilitate the identification of the rock trajectories on the digital films and the impacts of the rocks against trees and on the ground. We neutralised impacts on the slope surface as well as on trees by leaving coloured marks in the impact craters or on the impact wounds to prevent mapping the impact twice. After finishing the trajectory survey we clambered up the slope to release the next rock. On average we managed to carry out eight rockfall experiments per day.

3.2. Data analysis

In total, we analysed the trajectories of 100 rocks at Site 1 and 102 rocks at Site 2. In total, we measured 286 rockfall impacts on tree stems. According to the position of the impact centre on the tree stem, we defined three main impact types: frontal, lateral and scratch (Fig. 3). For each impact type we determined the deviation of the fall direction after the impact with respect to the fall direction before the impact. The trajectory survey allowed us to calculate the energy line angle, which is the angle of the straight line between the starting point and the maximum stopping point (Heim, 1932; Gerber, 1998; Meißl, 1998).

We analysed the digital films of the rockfall trajectories using a free downloadable program called AviStep 2.1.1, which is developed by M. Delabaere (Saint Denis de la Réunion, France). This program allows extracting the position and the velocity of a

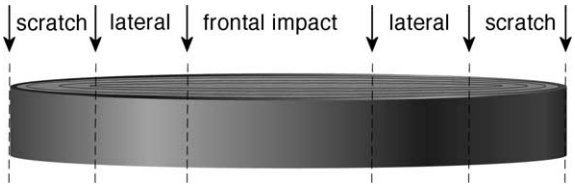


Fig. 3. Definition of the three main impact types according to the horizontal distance between the impact centre and the vertical central tree axis.

moving particle for each individual image in a digital film. The principle is as follows. Initially, each film has to be referenced in x and y direction, which means that in the first image of each film, we defined the distance in meters between two known points in the terrain, which were also clearly recognisable on the first film image. In our case, we used known distances between clearly marked trees. Then, we analysed the trajectory of each falling rock in 2D using a sequence of movie images (Fig. 2F).

We measured the rockfall velocities and the rebound heights, i.e., the maximum reached vertical height between the centre of the rock and the slope surface after each rebound on the ground. Since we used high-speed digital cameras we captured the velocities (both in x and y direction, as well as the resultant translational velocity) of each falling rock every 1/25th second. Therefore, we could accurately determine the translational velocity of a falling rock before and after tree impacts or rebounds on the slope surface. Determining the angular velocity was more difficult, as we had to determine the number of sequential images for the rock to rotate once, which was not always easy to recognise.

In addition, we calculated the mean tree free distance (MTFD) for Site 2. Since it is rather a certain surface of the tree than the tree diameter that intercepts a falling rock, we propose to calculate the MTFD using the basal area, following,

$$\mathrm{MTFD_{ba}} = \frac{\mathrm{Area}}{\mathrm{Nrstems}\left(R_{\mathrm{diam}} + \sqrt{(4G_{\mathrm{tot}})/(\pi \mathrm{Nrstems})}\right)} \quad (3)$$

where Area is the evaluated area (m^2), Nrstems is the number of stems in the evaluated area, R_{diam} is the mean diameter of the rock (m) that falls in the evaluated area G_{tot} is the total basal area in the evaluated area. In fact, here we calculate the $\mathrm{MTFD_{Perret}}$ using a mean DBH derived from the total basal area. The latter can easily and quickly be measured in the field using a relascope (Bitterlich, 1984). We calculated the $\mathrm{MTFD_{ba}}$ in many different forests where we analysed the rockfall hazard and it seems to give a more realistic value for the MTFD compared to the first two approaches. This is because the mean measured DBH tends to underestimate the total interception surface of a forest. To show the differences, we calculated $\mathrm{MTFD_{Gsteiger}}$, $\mathrm{MTFD_{Perret}}$ and $\mathrm{MTFD_{ab}}$.

4. Results

4.1. Differences in velocities and rebound heights

There is large difference between the non-forested site (Site 1) and the forested site (Site 2) regarding the rockfall velocities and the rebound heights (Table 2). The mean velocity over the whole section at Site 1 was 10.9 m s^{-1}, but this varied enormously between the upper part and the lower part. The mean of all the maximum velocities of the 100 analysed rocks was 15.4 m s^{-1} (S.D. = 3.4 m s^{-1}) and the maximum velocity measured was 30.6 m s^{-1} (attained at a distance of 184 m from the starting point, measured over the slope; the maximum translational energy was 954 kJ). On average, the rocks attained a maximum

Table 2
Summary of the observed rockfall characteristics at our experimental sites

	Site 1 non-forested (n = 100)	Site 2 forested (n = 102)
Average translation velocity (m s^{-1})	11	8
Average maximum translation velocity (m s^{-1})	15.4	11.7
Maximum translation velocity (m s^{-1})	30.6	24.2
Number of rocks stopped after 223.5 m	5	65
Number of rocks stopped on the lower forest road	15	13
Number of rocks surpassing the forested zone	n.a.	35
Mean number of tree impacts per falling rock	n.a.	2.8
Mean rebound height (m)	1.5	1
Maximum rebound height (m)	8	2 (5[a])
Number of rocks to develop a *couloir*	n.a.	72

[a] A rebound with a height of 5 m was observed after the rock hit an old tree stump that was not cut high enough, which therefore acted as a trampoline.

velocity of 11.2 m s^{-1} within the first 40 m and 15.4 m s^{-1} after 80 m. In total, 71 rocks (71%) attained a velocity higher than of 10 m s^{-1} within the first 40 m. The maximum velocity measured within the first 40 m at Site 1 was 14.8 m s^{-1}.

The mean velocity at Site 2 was 8.2 m s^{-1}, the mean maximum velocity for the 102 analysed rocks was 11.7 m s^{-1} (S.D. = 2.2 m s^{-1}) and the maximum velocity measured was 24.2 m s^{-1} (the distance from the starting point was 115 m; the maximum translational energy was 1092 kJ). On average, the maximum velocity within the first 40 m at Site 2 was 8.4 m s^{-1}. In total, 21 rocks (21%) attained a velocity higher than of 10 m s^{-1} within the first 40 m. The maximum velocity measured within the first 40 m at Site 2 was 11.6 m s^{-1}.

4.2. Rockfall trajectories, tree impacts and runout zone

Regarding the residual hazard of the forest stand at Site 2, 35 rocks (34%) surpassed the forested zone (slope length of 223.5 m), of which 13 rocks (13%) subsequently stopped on the forest road. At Site 1, we observed that 15 rocks (15%) stopped on the forest road and 11 rocks (11%) stopped before that. At Site 1, only 5 rocks (5%) stopped within the first 223.5 m, which is the length of the forested zone at Site 2. The maximal distance between the release and the stopping point (measured along the slope) was 501.3 m for Site 1, which is in the valley bottom. For Site 2, this was 324.9 m, which was below the lower forest road. Here, the forest stand characteristics were identical to the ones in the upper section. The accompanying energy line angles are 31.9° for Site 1 and 38° for Site 2.

Another observed effect of the forest cover on the rockfall trajectories is the width of the runout zone. We measured that, due to impact against trees, the falling rocks are laterally deviated from the central fall line parallel to the mean slope direction with a mean angle of 10°. At Site 1, this mean angle was less than 5°. This deviation mainly occurred as soon as the rocks passed the lower forest road at Site 1. There, their movement was no longer controlled by the channel morphology. The deviation at Site 2 is strongly determined by the different types of tree impacts: frontal, lateral and scratch. Table 3 presents the occurrence frequencies of the three main impact types, as well as the percentage of effective impacts, i.e., the tree impacts that resulted in immediate stopping of the falling rock.

Table 3
The occurrence frequency of different types of impacts (%) and their efficacy in stopping rocks, based on 286 analysed tree impacts (from Dorren and Berger, in press)

Type of impact	Occurrence (n = 286)
Frontal	63.8% (14% of these were effective[a])
Lateral	20.0% (20% of these were effective)
Scratch	16.2% (0% of these were effective)

[a] Effective means that the rock stopped immediately after the impact.

The trajectory surveys enabled us to construct 'deviation' matrices for each impact type that show the deviation in the fall direction after a tree impact (Fig. 4). In fact, the analysis of all the deviations in all the fall directions, taking into account all the tree impacts as well as all the rebounds on the ground, resulted in a deviation matrix that is equivalent to the one of the scratch impact (Fig. 4). The deviation matrix of the frontal impact shows that a large percentage (44%) of the rocks continued its fall direction straight on. This includes all the rocks that: (i) stopped behind a tree; (ii) broke or uprooted a tree and continued in the same direction; and (iii) the ones that impacted a tree and subsequently bounced a bit to the side or turned around the tree and continued more or less in the same direction.

On average, each rock had 2.8 impacts against trees (286 impacts/102 rocks), the maximum number of impacts per rock was 8 and 11 rocks (11%) impacted no tree at all (Fig. 5). The mean and maximum impact height was 0.72 and 2 m, respectively. The mean rebound height at Site 1 was 1.45 m, the maximum rebound height was 8 m. At Site 2, the mean rebound

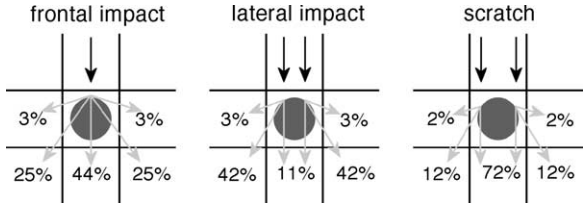


Fig. 4. Deviation matrices for the three main impact types showing the percentage of rocks that deviated from the impact direction (indicated by the downward arrow) towards the general direction indicated by the matrix cell (indicated by the grey arrow) after impacting a tree (represented as the circle).

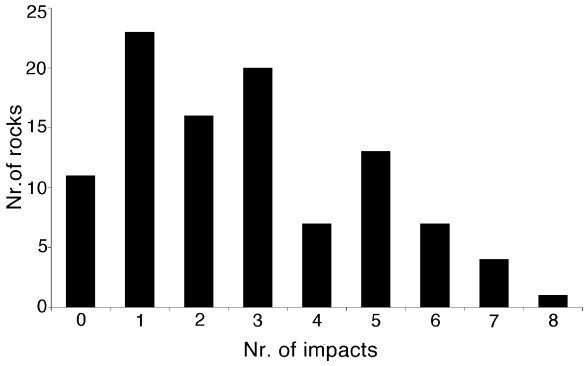


Fig. 5. Histogram of the number of tree impacts per falling rock.

height was 1.01 m, the maximum rebound height was 2 m. The $MTFD_{Gsteiger}$ for Site 2 is 34.9 m, $MTFD_{Perret}$ is 34.7 m and $MTFD_{ba}$ = 33.0 m.

Some of the impacts caused an instantaneous fracture and cutting of the tree stem. During an impact, the kinetic energy of the rock causes a displacement of the whole tree including the root system. At that moment the kinetic impact energy is transferred to the root–soil system and to the tree stem. If the tree is anchored well enough in the soil and if the stem does not break or fracture, the tree makes a hula-hoop effect and transfers the energy to the tree crown. Thereby most coniferous trees loose their top. In other cases the tree will be uprooted or broken. In fact we observed the following three main types of damage: uprooting, stem breakage and breaking of the treetop (Fig. 6). Other occurred damages were: rockfall wounds on the stem due to impacts, partial fracture of the stem and explosion of tree stems into wood sparks.

An important consequence of the cutting and uprooting of tree stems by rock impacts is the development of a rockfall path or *couloir*. This path follows the mean slope direction from the point were the rocks were released (Fig. 7). After releasing 78 rocks, such a path had evolved. After that, only four of the remaining 24 rocks followed the *couloir*, the rest was laterally deviated.

5. Discussion and conclusions

The results of this study enable us to compare the velocities, rebound heights as well as the residual hazard of rockfall on a forested and a non-forested slope. It showed that the residual rockfall hazard on a 38° slope, expressed in terms of the number of rocks that surpass a certain zone, decreases with 63% in case a forest cover is present. Not only the number of rocks

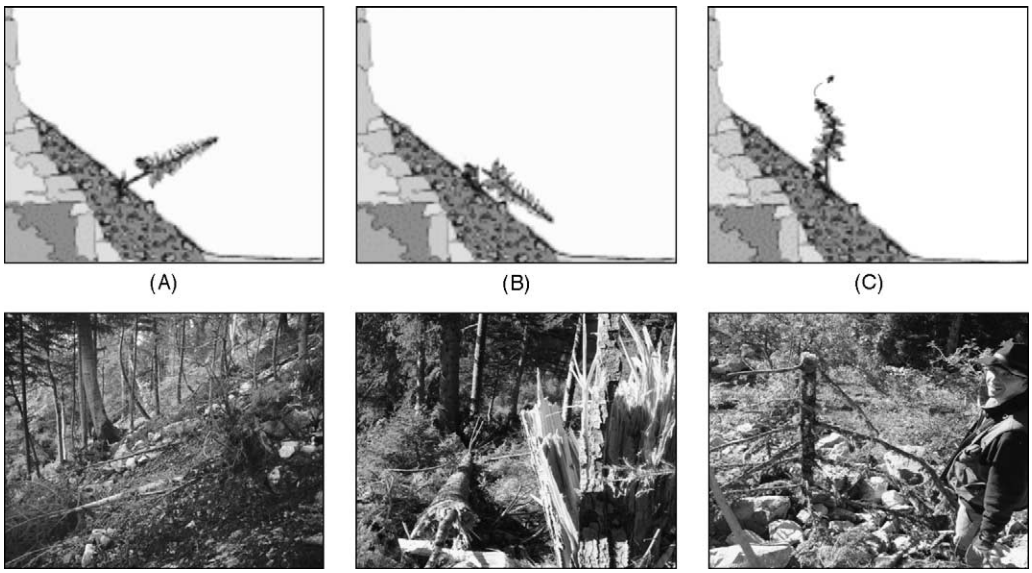


Fig. 6. Main types of tree damage observed on a forested active rockfall slope (sketch and photo of: (A) uprooting; (B) stem breakage; and (C) hula-hoop effect causing tree top break off).

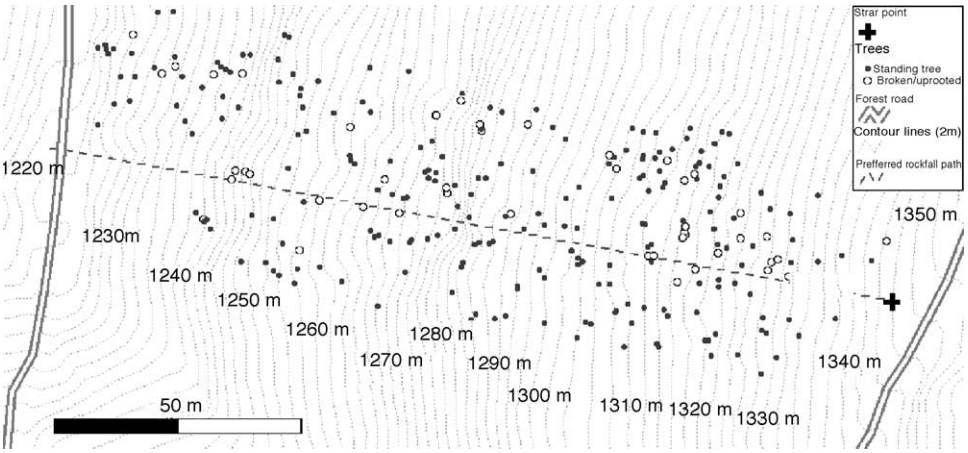


Fig. 7. Map showing all the trees at Site 2, including the ones that have been cut or uprooted by falling rocks, and the resulting rockfall *couloir*.

that stops on the slope increases on forested slopes, also the bounce height and the velocity decrease significantly. When comparing the forested with the non-forested slope, the velocities are on average reduced with 26% and the mean rebound height is reduced with 33%. These results confirm the findings of of Jahn (1988), Zinggeler (1990), Gsteiger (1993), Doche (1997), Dorren et al. (2004b) and Perret et al. (2004) that rockfall velocities on a forested slope with a mean gradient between 33 and 40° are between 15 and 25 m s^{-1} and that bounce heights are generally between 1 and 2 m. Furthermore, both our results and those of Jahn (1988) show that a forest road stops between 13 and 15% of the rocks falling on a slope with gradient between 35.5 and 38°.

The MTFD calculated with the three approaches presented in Eqs. (1)–(3) does not vary much at Site 2. We proposed the $MTFD_{ba}$ because in general it gives more realistic values and it is a good indicator for the impact probability. In combination with the mean DBH and the tree species, which are indicative for the energy dissipative capacity during rockfall impacts (Fig. 8), the efficacy of a protection forest stand can be estimated.

The obtained experimental data, combined with relevant literature data and a review of existing rockfall protection forest management guidelines, allow us to evaluate and propose management criteria. During the experiments we observed that the number of impacts against trees is more important than the efficacy of the impact expressed in the amount of dissipated energy. An enormous rock (e.g., 1.5 m^3) could be stopped by a small tree, e.g., with a DBH of 10 cm, if the rock impacted a large tree just before. Therefore, we believe that for effective protection, a large number of trees is more important than having thick trees only. Also Jahn (1988) showed that small trees could stop rocks with diameters between 0.13 and 0.45 m, if the stand is dense enough. For larger rocks, a larger mean stem diameter is required, which is clearly shown by the work of Doche (1997). An estimate of the required stand density can be calculated with the $MTFD_{ba}$, which should not be larger than 40 m, the required mean diameter can be calculated by using Fig. 8, which is based on work of Dorren and Berger (in press). The rule of thumb, mentioned by Schwitter (1998), that the mean DBH of

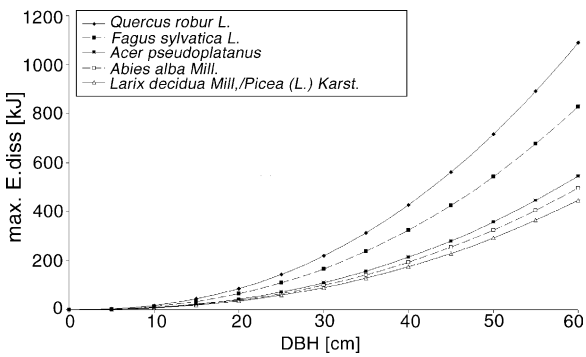


Fig. 8. Relationship between the diameter at breast height (DBH) and the maximum amount of energy that can be dissipated during a rockfall impact for six tree species (after Dorren and Berger, in press).

trees in a forest stand should be 1/3 of the decisive size of the falling rocks is valid for Site 2, but to give further characteristics of an optimal rockfall protection forests is not possible. What is very much needed is a tool that takes into account the mean diameter of the falling rock, the mean kinetic energy of the rock, the maximum length of the stopping zone and the tree species, because these parameters determine the required mean diameter and accompanying stand density.

During our experiments, none of the rocks attained their maximal velocity within the first 40 m, neither at Site 2, nor at Site 1. For that, a minimal distance of 80 m was required. However, rocks did attain destructive velocities after 40 m. Therefore, 40 m should be the maximum gap length in the slope direction in protection forests. Shorter ones are preferable, but not always realistic. We propose to use the length of an effective $MTFD_{ba}$. At site 2 this was 33 m, which was 1.3 times the mean tree height (MTH). In parallel to the maximum size of regeneration gaps in avalanche protection forests (gap length along the slope = 1.5 × MTH; gap width = 0.65 × MTH, Berger, 1997), the gap length and width in protection forests could be, respectively 1.3 × MTH and 0.5 × MTH (calculated using the lateral deviation of 10°), where the absolute maximum length and width are, respectively 40 m and 15 m, measured along the slope.

Regarding our study site, the protection provided against falling rocks with a mean diameter of 0.95 m would be sufficient if the earlier described rockfall *couloir* would not be present. The effect of the presence of such a *couloir* can be mitigated by cutting trees on both sides of the *couloir* and leaving the trunks on the slope, diagonally to the slope direction (Fig. 9). Important criteria for selecting the trees to be cut are: the position and the growth tendency with respect to the *couloir*, the DBH (thicker stems, or if possible multiple parallel trunks, are clearly more effective barriers), tree instability, the potential effect on promoting regeneration, gaps that will evolve after cutting as well as the hiding effect. That is, in protection forests, trees tend to grow behind each other, i.e., the older tree protects younger trees downslope (c.f. Gsteiger, 1993). This effect can also be seen on the map of our study site (Fig. 9). If trees with an effective diameter (>35 cm) have developed downslope of an older tree upslope, the latter could be felled.

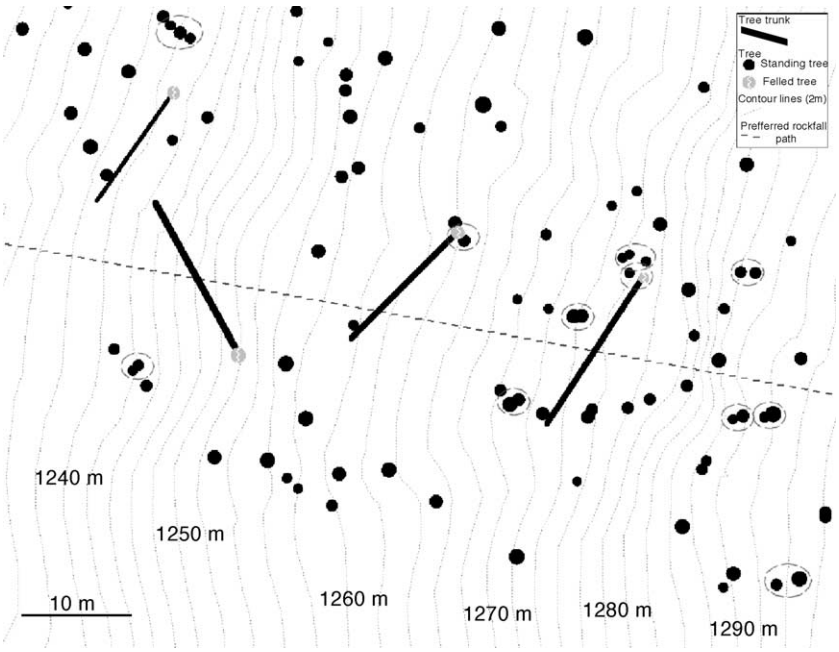


Fig. 9. Map showing a part of Site 2, including the management measures that we propose in the rockfall *couloir*. The diameter of the points represents the relative DBH of the trees and the dashed circles indicate examples of the hiding effect (see text for explanation).

Another important aspect is the direction in which the felled trunk is positioned on the slope. A choice can be made to deviate all the rocks away from a channel, preferably into areas with a high stand density or a high surface roughness (e.g., depressions where many larger rocks have been deposited). On the other hand, if the *couloir* has become a real channel, in which regeneration is impossible, all the rocks could be deviated into this channel by using accurately positioned felled trunks. A condition for the latter case would be that there is sufficient protection at the end of the *couloir*, e.g., a rockfall net or a rockfall dam.

Finally, we observed that a rotten, low cut stump acted as a trampoline for one falling rock. This resulted in a rebound height of 5 m. Consequently, trees that are to be felled in a rockfall protection forest should be cut very high (>1.3 m, if possible higher). In many places in the European Alps, rockfall nets are installed along traffic ways. Trees bordering the roads are often felled before installing these nets. Especially there it is important that those trees are cut either high enough or very low, if not, rocks can jump over the installed rockfall nets.

In some cases the selling of the felled wood could cover a large part of the forest management interventions described above, but in most cases the responsible forest management department is very much dependent on subsidies. It is for those situations that the question has to be asked whether civil engineering, protection forest management (an eco-engineering technique), or the combination of the two is most appropriate. Mountain forests in the European Alps and the protection they provide have a long and distinguished history, especially regarding protection against rockfall, snow avalanches, floods and debris flows, but active management is currently a necessity to sustain or optimise this service (Kräuchi et al., 2000; Brang, 2001; Dorren et al., 2004b). The fact that not only large stem diameters are required, allows the application of selective thinning or other minimal tending techniques that promote regeneration and ensure the forest to stay in an optimal condition regarding its protective function (Motta and Haudemand, 2000; Dorren et al., 2004b).

Unfortunately, society has nowadays often more confidence in technical protective constructions, but it turns out that they cannot always sustain the time periods that were originally planned, which results in unforeseen costs. Healthy forests at the other hand can provide long term protection, especially in combination with more modest and cheaper technical constructions that reduce the residual risk at the bottom of forested slopes. If all the services forests provide should be taken into account in the calculation of the costs of protective measures, the cost-effectiveness of protection forest management would look very different.

Acknowledgements

We thank the European Commission for the Marie Curie Fellowship (QLK5-CT-2002-51705) and for funding the ROCKFOR project (QLK5-CT-2000-01302).

References

Badger, T.C., Lowell, S.M., 1992. Rockfall control in Washington State. In: Rockfall Prediction and Control and Landslide Case Histories. Transportation Research Record 1343, National Academy of Sciences, Washington, DC, pp. 14–19.

Berger, F., 1997. Interaction forêt de montagne-risques naturels. Détermination de zones d'interventions forestières prioritaires-l'exemple du département de la Savoie, Ph.D. thesis Engref, Paris, 475 p.

Berger, F., Quetel, C., Dorren, L.K.A., 2002. Forest: a natural protection mean against rockfalls, but with which efficiency? International Congress Interpraevent 2002 in the Pacific Rim, Conference Proceedings, vol. 2, Matsumoto, Japan, pp. 815–826.

Bitterlich, W., 1984. The Relascope Idea: Relative Measurements in Forestry. Commonwealth Agricultural Bureaux. Farnham Royal, UK, 242 p.

Brang, P., 2001. Resistance and elasticity: promising concepts for the management of protection forests in the European Alps. For. Ecol. Manage. 145, 107–119.

Brauner, M., Weinmeister, W., Agner, P., Vospernik, S., Hoesle, B., 2005. Forest management decision support for evaluating forest protection effects against rockfall. For. Ecol. Manage. 207 (1–2), 75–85.

Bunce, C.M., Cruden, D.M., Morgenstern, N.R., 1991. Assessment of the hazard from rock fall on a highway. Can. Geot. J. 34, 344–356.

Cattiau, V., Mari, E., Renaud, J.P., 1995. Forêt et protection contre les chutes de rochers. Ingénieries-EAT 3, 45–54.

Couvreur, S., 1982. Les forêts de protection contre les risques naturels. École Nationale du Génie Rural des Eaux et Forêts (ENGREF), 89 p.

Doche, O., 1997. Etude expérimentale de chutes de blocs en forêt. Cemagref/Institut des Sciences et Techniques de Grenoble (ISTG), Cemagref doc. 97/0898, 130 p.

Dorren, L.K.A., 2003. A review of rockfall mechanics and modelling approaches. Prog. Phys. Geog. 27 (1), 69–87.

Dorren, L.K.A., Berger, F., in press. Stem breakage of trees and energy dissipation during rockfall impacts. Tree Phys.

Dorren, L.K.A., Berger, F., Imeson, A.C., Maier, B., Rey, F., 2004a. Integrity, stability and management of protection forests in the European Alps. For. Ecol. Manage. 195, 165–176.

Dorren, L.K.A., Maier, B., Putters, U.S., Seijmonsbergen, A.C., 2004b. Combining field and modelling techniques to assess rockfall dynamics on a protection forest hillslope in the European Alps. Geomorphology 57, 151–167.

Dussauge-Peisser, C., Helmstetter, A., Grasso, J.-R., Hantz, D., Desvarreux, P., Jeannin, M., Giraud, A., 2002. Probabilistic approach to rock fall hazard assessment: potential of historical data analysis. Nat. Haz. Earth Sys. Sci. 2 (1), 15–26.

Erismann, T.H., Abele, G., 2001. Dynamics of rockslides and rockfalls. Springer-Verlag, Berlin, 316 p.

Frehner, M., Wasser, B., Schwitter, R., in press. Nachhaltigkeit und Erfolgskontrolle im Schutzwald. Wegleitung für Pflegemassnahmen in Wäldern mit Schutzfunktion. Bundesamt für Umwelt, Wald und Landschaft (BUWAL), Bern.

Frey, W., Thee, P., 2002. Avalanche protection of windthrow areas: a 10 year comparison of cleared and uncleared starting zones. For. Snow Landsc. Res. 77 (1–2), 89–107.

Gerber, W., 1998. Waldwirkung und Steinschlag. In: R., Schwitter (Ed.), Dokumentation der 14. Arbeitstagung der Schweizerischen Gebirgswaldpflegegruppe mit der FAN 1998. Grafenort/Engelberg, pp. 1–15.

ONF, in preparation. Guide des sylvicultures de montagne. ONF/CRPF/Cemagref, France.

Gsteiger, P., 1993. Steinschlagschutzwald. Ein Beitrag zur Abgrenzung, Beurteilung und Bewirtschaftung. Schweiz. Zeit. Forstw. 144, 115–132.

Hantz, D., Vengeon, J.M., Dussauge-Peisser, C., 2003. An historical, geomechanical and probabilistic approach to rock-fall hazard assessment. Nat. Haz. Earth Syst. Sci. 3, 693–701.

Hearn, G., Barret, R.K., McMullen, M.L., 1992. CDOT Flexpost rockfall fence development, testing, and analysis. In Rockfall Prediction and Control and Landslide Case Histories. Transportation research record 1343, National Academy of Sciences, Washington, DC, pp. 23–29.

Heidenreich, B., 2004. Small- and half-scale experimental studies of rockfall impacts on sandy slopes. Ph.D. thesis, EPFL, Lausanne, 231 p.

Heim, A., 1932. Bergsturz und Menschenleben. Beiblatt zur Vierteljahrschrift der Naturforschenden Gesellschaft in Zürich 77, 218.

Jahn, J., 1988. Entwaldung und Steinschlag, International Congress Interpraevent, Graz. Conference Proceedings, vol. 1, pp. 185–198.

Kienholz, H., Mani, P., 1994. Assessment of geomorphic hazards and priorities for forest management on the Rigi north face, Switzerland. Mt. Res. Dev. 14, 321–328.

Kräuchi, N., Brang, P., Schönenberger, W., 2000. Forests of mountainous regions: gaps in knowledge and research needs. For. Ecol. Manage. 132 (1), 73–82.

Kupferschmid Albisetti, A.D., Brang, P., Schönenberger, W., Bugmann, H., 2003. Decay of *Picea abies* snag stands on steep mountain slopes. For. Chron. 79 (2), 247–252.

Meißl, G., 1998. Modellierung der Reichweite von Felsstürzen. Fallbeispeile zur GIS-gestützten Gefahrenbeurteilung aus dem Beierischen und Tiroler Alpenraum. Ph.D. thesis, Universität Innsbruck, Innsbruck, 249 p.

Motta, R., Haudemand, J.C., 2000. Protective forests and silvicultural stability—an example of planning in the Aosta Valley. Mt. Res. Dev. 20, 180–187.

Nicot, F., Cambou, B., Mazzoleni, G., 2001. Design of Rockfall restraining nets from a discrete element modelling. Int. J. Rock Mech. Min. Sci. 32 (2), 99–118.

Peila, D., Pelizza, S., Sassudelli, F., 1998. Evaluation of behaviour of rockfall restraining nets by full scale tests. Rock Mech. Rock Eng. 31, 1–24.

Perret, S., Dolf, F., Kienholz, H., 2004. Rockfalls into forests: analysis and simulation of rockfall trajectories—considerations with respect to mountainous forests in Switzerland. Landslides 1 (2), 123–130.

Porter, S.C., Orombelli, G., 1981. Alpine rockfall hazards. Am. Sci. 69, 67–75.

Schwitter, R., 2001. Zusammenfassung und Schlussfolgerungen. In: R., Schwitter (Ed.), Dokumentation der 14. Arbeitstagung der Schweizerischen Gebirgswaldpflegegruppe mit der FAN 1998. Grafenort/Engelberg, pp. 1–5.

Selby, M.J., 1982. Controls on the stability and inclinations of hillslopes formed on hard rock. Earth. Surf. Proc. 7, 449–467.

Spang, R.M., Sönser, T., 1995. Optimized rockfall protection by ''ROCKFALL''. In: T., Fuji (Ed.), Proceedings of the 8th International Conference on Rock Mechanics, 25–30 September 1995. Tokyo, Japan, pp. 1233–1242.

Stokes, A., Salin, F., Kokutse, A.D., Berthier, S., Jeannin, H., Mochan, S., Dorren, L.K.A., Kokutse, N., Ghani, M.A., Fourcaud, T., in press. Mechanical resistance of different tree species to rockfall in the French Alps. Plant Soil.

Stoffel, M., Lièvre, I., Monbaron, M., Perret, S., in press-a. Seasonal timing of rockfall activity on a forested slope at Täschgufer (Swiss Alps)—a dendrochronological approach. Zeit. Geom. N.F.

Stoffel, M., Schneuwly, D., Bollschweiler, M., Lièvre, I., Delaloye, R., Myint, M., Monbaron, M., in press-b. Analyzing rockfall activity (1600–2002) in a protection forest—a case study using dendrogeomorphology. Geomorphology.

Thormann, J.-J., Schwitter, R., 2004. Nachhaltigkeit im Schutzwald (NaiS) Nachhaltige Schutzwaldpflege und Waldbauliche Erfolgskontrolle. International Congress Interpraevent. Conference Proceedings, vol. 1 (III), Riva del Garda, pp. 331–342.

Wasser, B., Frehner, M., 1996. Minimale Pflegesmassnahmen für Wälder mit Schutzfunktion. Wegleitung. Bundesamt für Umwelt, Wald und Landschaft (BUWAL), Bern.

Zinggeler, A., 1990. Steinschlagsimulation in Gebirgswäldern: Modellierung der relevanten Teilprozesse. M.Sc. thesis, University of Bern, Bern, 116 p.

> Chapter 8

Energy dissipation by trees during rockfall impacts



Tree Physiology 26, 63–71
© 2005 Heron Publishing—Victoria, Canada

Stem breakage of trees and energy dissipation during rockfall impacts

LUUK K. A. DORREN[1,2] and FRÉDÉRIC BERGER[2]

[1] *Cemagref Grenoble, 2 rue de la Papeterie, BP 76, 38402 St. Martin d´Hères cedex, France*

[2] *Corresponding author (luuk.dorren@cemagref.fr)*

Received October 8, 2004; accepted April 9, 2005; published online October 3, 2005

Summary The capacity of individual trees to dissipate the energy released by rockfalls has previously only been quantified based on data obtained from static tree-pulling tests or from dynamic impact tests on wood samples. We predicted that these data are not representative of the maximum amount of energy that can be dissipated by living trees during rockfall impacts. To test this prediction, we carried out rockfall experiments on a forested slope in the French Alps. To calculate the rock's energy before and after impact, rockfalls were filmed digitally. The recordings of nine impacts causing instantaneous breakage of *Abies alba* Mill. trees were analyzed in detail. An exponential relationship between stem diameter at breast height (DBH) and the maximum amount of energy a tree can dissipate was highly correlated for all of our experimental data. We applied this relationship to other tree species based on published fracture energies. The relationships obtained for *Cedrus* spp., *Fagus sylvatica* L. and *Picea abies* (L.) Karst. were significantly correlated with data from other dynamic impact tests in the field and with maximum bending moments obtained from tree-pulling experiments. Multiple linear regressions showed that impact height influences the energy that will be dissipated by an *A. alba* tree, particularly for trees with a DBH less than 15 cm. For trees with a DBH greater than 15 cm, the effect of impact height was minimal up to a height of 1 m. There was a strong relationship between the amount of energy dissipated by a tree and the horizontal distance between the impact center and the vertical central axis of the tree.

Keywords: dynamic impact test, fracture energy, maximum bending moment, protection forest.

Introduction

In mountainous areas, trees can prevent snow avalanches and stop falling rocks (Brang 2001, Berger et al. 2002). The amount of energy dissipated by individual trees growing in mountain forests is determined by the species and site conditions, as well as the nature of the hazard (Kräuchi et al. 2000). Mountain forests in the European Alps have a long history of providing protection (Schönenberger 2000, Dorren et al. 2004*a*), but attempts have been made only during the last few decades to quantify this protective effect of forests. Among the tools employed in these studies, simulation models may prove to be the most useful (e.g., Dorren and Seijmonsbergen 2003).

To model protection provided by forests, it is necessary to include both forest growth and natural hazard models. This requires a detailed knowledge of how single trees function when facing natural hazards. Although some attempts have been made to assess the capacity of trees to dissipate energy, e.g., snow avalanche simulation modeling (Bartelt and Stöckli 2001), rockfall modeling (Zinggeler 1990, Dorren and Seijmonsbergen 2003, Dorren et al. 2004*b*, Perret et al. 2004), rockfall hazard assessments (Jahn 1988, Gsteiger 1993) and snow or wind damage studies (Peltola et al. 1999, Gardiner et al. 2000), there is little information on the amount of energy that can be dissipated by living trees.

There is a relatively large amount of experimental data on maximum bending moments. These data have often been obtained by static tree-pulling tests on trees with stem diameters at breast height (DBH) up to 35 cm (Petty and Swain 1985, Mizuyama and Narita 1988, Nicoll and Ray 1996, Papesch et al. 1997, Stokes 1999, Moore 2000, Peltola et al. 2000). However, these data may not be representative of trees with a large DBH (> 40 cm) or of more instantaneous impact forces, such as rockfalls or avalanches. For example, Mizuyama and Narita (1988) showed that static tests produce energy dissipation values that are about 64% ($n = 5$) lower than dynamic impact tests on the same tree species (*Cedrus* spp.).

Other data that could be used for calculating the energy dissipative capacity during dynamic impacts of tree species occurring in the European Alps, or comparable mountain ranges, are fracture energy values obtained by dynamic impact tests on wood samples (e.g., Couvreur 1982, Sell 1987, Rupé 1991, Niemz 1993). Wood samples of *Abies alba* Mill. have fracture energy values between 4 and 5.5 J cm^{-2}, whereas the fracture energy values of *Fagus sylvatica* L. samples are about twice as high. The limitation of these data is that they do not account for the behavior of the different compartments of living trees, such as the living wood, the tree crown and the root–soil system. Couvreur (1982) showed that the maximum energy dissipated by an *F. sylvatica* tree during a dynamic impact test in the field was more than 2.5 times the value derived from a dynamic impact test in the laboratory on a green, knot-free sample from a similar tree. To account for this difference, Zinggeler (1990) doubled the fracture energy value for *F. sylvatica*—obtained by Sell (1987) by impact tests on dry wood samples—in his rockfall model.

We predicted that static tree-pulling tests and dynamic impact tests on wood samples produce values that are not representative of the amount of energy that can be dissipated by liv-

ing trees during rockfall impacts or comparable dynamic impacts. Because there are no published data for living trees, our overall objective was to quantify the energy dissipative capacity during rockfall impacts of the dominating tree species in rockfall protection forests in the European Alps. Our specific aims were to: (1) develop a relationship between DBH and the maximum amount of energy that can be dissipated by an *A. alba* tree; (2) use literature data on fracture energy to establish similar relationships for other tree species; and (3) quantify the effect of the position of the impact center on the tree stem on the amount of energy that is dissipated by a tree.

Materials and methods

Rockfall experiments

The study site is in the Forêt Communale de Vaujany in France (45°12′ N, 6°3′ W, 1200–1400 m a.s.l.) and covers an area of about 0.9 ha on a forested, northwest-facing Alpine slope, with a mean gradient of 38°. The main tree species on the site are silver fir (*A. alba*, 50%), Norway spruce (*Picea abies* (L.) Karst., 25%), beech (*F. sylvatica*, 17%) and sycamore (*Acer pseudoplatanus* L., 4%). Other species present are *Sorbus aucuparia* L., *Betula pendula* Roth, *Ulmus glabra* Huds., *Ilex aquifolium* L., *Fraxinus excelsior* L. and *Corylus avellana* L. Mean stand density is 290 trees ha^{-1}. We mapped and measured all 271 trees in the study site; mean DBH was 31 ± 21 cm (± SD). During the experiments, we threw individual spherical rocks (mean diameter of 0.95 m) down the slope. The goal of the experiments was to calculate the energies of falling rocks before and after impact by capturing the rockfall event on digital film.

Before each rockfall experiment, we coated the rock with biodegradable paint, so that it left traces after impacting the tree stems. A tractor with a front end loader was used to throw the rocks down the slope. We captured the trajectory of the rock with an Impulse LR 200 laser distance meter (Laser Technology, Centennial, CO) to obtain 3D information about the rockfall trajectories. Five high-speed digital cameras installed along the experimental site provided a 2D view (Figure 1). The cameras were fixed at a height of 10 m in trees situated 30 m away from the experimental rockfall path. We also described and measured all the tree impacts and the resulting tree damage, including the size of bark wounds, the impact height, and the horizontal distance between the impact center and the vertical central tree axis (CTA) seen from the impact direction. We threw 118 rocks in total, of which 102 were analyzed. The reasons for excluding 16 of the rockfalls from analysis were: (1) they stopped within the first 10 m after sliding on the slope surface; (2) their trajectory was too far from the cameras due to lateral deviation of the falling rock; or (3) they broke into pieces during tree impact or on the slope surface. On average, we carried out eight rockfall experiments per day.

Calculation of the rockfall impact energy

We analyzed the digital films of the rockfall trajectories with the free program AviStep 2.1.1, developed by M. Delabaere (Saint Denis de la Réunion, France). This program extracts the position and velocity of a moving particle for each individual image in a digital film. The principle is as follows. First, each film has to be referenced in the *x* and *y* directions, which means that, in the first frame of each film, we defined the distance in meters between two known points in the terrain, which were clearly recognizable. In our case, we used known distances between clearly marked trees. Then, we analyzed the trajectory of each falling rock in 2D based on a sequence of movie images. Because we used high-speed digital cameras we were able to register the velocities (in both the *x* and *y* directions, as well as the resultant translational velocity) of each falling rock every 1/25th s. Therefore, we could accurately determine the translational velocity of a falling rock before and after tree impact. Determining the angular velocity was more difficult, because we had to determine the number of sequential images required for the rock to rotate once, which was not always easy to recognize.



Figure 1. A sequence of images extracted from a digital film showing a 0.95-m-diameter rock impacting an *Abies alba* tree with a stem diameter of 58 cm. The white circle indicates the position of the rock. In photograph 1, the impacted tree is hidden behind other trees. The following photographs show how the tree stem splits in two and consequently falls down.

Before each rockfall experiment, we measured the rock volume. All rocks had about the same shape (spherical), volume (0.49 m^3) and density (2800 kg m^3). With this information, we determined the mass of the rock and, therefore, the translational kinetic energy ($E_{k\text{-}trans}$), as well as the rotational energy (E_{rot}), at any point in the trajectory, provided that the rock was clearly visible in the movie images. The total kinetic energy ($E_{k\text{-}tot}$) (J) was calculated as:

$$E_{k\text{-}tot} = E_{k\text{-}trans} + E_{rot} = 0.5mv^2 + 0.5I\omega^2 \quad (1)$$

where m is the mass of the rock (kg), v is the translational velocity (m s^{-1}), I is the moment of inertia for a sphere ($0.4mr^2$, where r is the radius; kg m^2), and ω is the angular velocity (rad s^{-1}). We obtained the maximum amount of energy a tree can dissipate by calculating the difference between the kinetic energy of a rock that caused stem breakage before and after impact. We used only the total kinetic energy as the translational kinetic energy to assess whether the effect of the rotational energy could be neglected, therefore minimizing the uncertainty in our results.

Nine impacts causing instantaneous breakage of *A. alba* trees could be analyzed with sufficient detail from the film recordings. This enabled us to establish a function describing the relationship between DBH and the maximum amount of energy (J) that can be dissipated ($E_{diss,max}$) by an *A. alba* tree. We used DBH in our function because it is easy to measure in the field and because relationships between DBH and resistance to fracturing have been found by many different studies (e.g., Peltola et al. 2000, Cucchi et al. 2004). We determined a best-fit function on the basis of the coefficient of determination (R^2) and its level of significance (P), the mean error (ME) and the root mean square error (RMSE). The ME and the RMSE were calculated as:

$$\mathrm{ME} = \frac{1}{n}\sum_{i=1}^{n}\frac{100\,(C_i - O_i)}{O_i} \tag{2}$$

$$\mathrm{RMSE} = \sqrt{\frac{1}{n}\sum_{i=1}^{n}\left(\frac{100\,(C_i - O_i)}{O_i}\right)^2} \tag{3}$$

where n is number of observations, C_i is the calculated value and O_i is the observed value.

Use of literature data on fracture energy

To compare the established relationship between DBH and $E_{diss,max}$ of *A. alba* to other dominant tree species in rockfall protection forests in the European Alps, we used literature data on fracture energy values of different wood samples. These data have been obtained from dynamic impact tests in the laboratory by Couvreur (1982), Sell (1987) and Rupé (1991). The tests carried out by Rupé (1991) were identical to the laboratory tests described by Couvreur (1982), who used green, knot-free wood samples with a length of 30 cm and a height and width of 2 cm. Sell (1987) used dry, knot-free samples and reported that the mean fracture energy is 12.5% higher for *P. abies* samples (4.5 J cm^{-2}) than for *A. alba* samples (4 J cm^{-2}). Couvreur (1982) and Rupé (1991) both reported that the mean fracture energy of *P. abies* samples is 90% of the mean fracture energy of *A. alba* samples. Rupé (1991) further showed that the mean fracture energy of *Cedrus* spp. samples is 70% of the mean fracture energy of *A. alba* samples. On the basis of the mean fracture energy values reported by these authors, we calculated fracture energy ratios for different tree species (Table 1). By applying these ratios to the established $E_{diss,max}$ function for *A. alba*, we transferred our basic DBH and $E_{diss,max}$ relationship to the tree species shown in Table 1.

To assess whether the maximum bending moment (Mb), which is used in many wind-modeling studies (e.g., Peltola et al. 1999, Gardiner et al. 2000), is a good indicator of the maximum energy that can be dissipated by a tree at a rockfall impact, we compared our $E_{diss,max}$ values for *P. abies* with the Mb values. We are aware that the Mb value is not equal to the $E_{diss,max}$ value of a tree; however, to obtain energies from Mb values, the calculation described by Stokes et al. (2005) can be used.

The Mb that a tree stem can withstand at the stem base without breakage can be calculated from DBH and the modulus of rupture (MOR) of the tree (Sunley 1968, Petty and Worrell 1981, Petty and Swain 1985, Peltola et al. 1999):

$$\mathrm{Mb} = \frac{\pi \times \mathrm{MOR} \times \mathrm{DBH}^3}{32} \tag{4}$$

Here, we assume that the induced stress in the outer fibers of the tree stem is constant at all points, as first proposed by Metzger (1893) and again later by Morgan and Cannell (1994). A condition for using Equation 4 is that the tree must be well anchored in the soil. For *P. abies*, we used the mean MOR value obtained by Peltola et al. (1999, 2000) and Gardi-

Table 1. Minimum, mean and maximum fracture energies of different wood samples as obtained by Couvreur (1982) and Rupé (1991) and the mean ratio to *Abies alba* and *Fagus sylvatica*.

Tree species	Fracture energy (J cm^{-2})			Ratio to	
	Minimum	Mean	Maximum	*Abies alba*	*Fagus sylvatica*
Cedrus spp.	3.3	3.3	3.3	0.7	0.4
Picea abies	4.0	4.4	4.8	0.9	0.5
Larix decidua Mill.	4.0	4.4	4.8	0.9	0.5
Abies alba	4.3	4.9	5.5	1.0	0.6
Pinus nigra Arn.	5.5	5.5	5.5	1.1	0.7
Pinus sylvestris L.	5.5	5.5	5.5	1.1	0.7
Acer pseudoplatanus	5.5	5.5	5.5	1.1	0.7
Fraxinus excelsior L.	7.3	7.3	7.3	1.5	0.9
Fagus sylvatica	7.5	8.1	8.8	1.7	1.0
Quercus robur L.	8.8	10.6	12.5	2.2	1.3
Robinia pseudoacacia L.	11.5	13.4	15.3	2.7	1.6

ner et al. (2000), which is 32.5 MPa. Other data on the Mb of *P. abies* are presented by Stokes et al. (2005), who carried out tree-pulling tests at our study site.

Subsequently, we validated the relationship for *Cedrus* spp. with data obtained by Mizuyama and Narita (1988) from static tree-pushing tests using a bulldozer. In addition, we used data from dynamic impact tests, also carried out by Mizuyama and Narita (1988) and by Nonoda et al. (2004). During these dynamic impact tests, fracture energy was measured by impacting *Cedrus* spp. trees with a metal ball that was attached to a crane by a metal cable. Although this tree species does not occur on our study site, these data provide another possibility for validating the method of transferring the basic relationship we obtained for *A. alba* to other tree species. The relationship we obtained for *F. sylvatica* was validated with results from similar dynamic impact tests on *F. sylvatica* trees with diameters ranging from 20 to 35 cm, carried out by Couvreur (1982).

Relationship between energy dissipation and impact position

During the experiments, we registered and measured 286 tree stem impacts. Thirty-two tree impacts (16 on *A. alba* trees, 14 on *F. sylvatica* trees, and one each on an *Acer pseudoplatanus* tree and a *P. abies* tree) were captured in detail on digital film, which allowed us to establish a relationship between the energy dissipated by the tree and the horizontal distance between the impact center and the vertical CTAs, as seen from the impact direction (see Figure 2). The other 254 films could not be used, because the impact was hidden behind other trees. According to the distance between the impact center and the CTA, we defined three main impact types: frontal, lateral and scratch (Figure 2). For each impact type we determined the frequency and efficacy with which trees stopped a falling rock. In addition, we used multiple linear regression based on least squares of impact data on nine *A. alba* trees to find a relationship between observed $E_{diss,max}$ and different combinations of impact height and DBH.

Results

Energy dissipation during rockfall impacts

We observed many different rockfall impact effects, including stem bark wounds, tree uprooting, stem fracture, stem breakage and crown decapitation. We also found that translational kinetic energy could be transferred to rotational energy during a rockfall impact on a tree stem. Analyses showed that, on average, the angular velocity after tree impact is 170% of the angular velocity before the impact. Neglecting the rotational energy in the calculation of the total kinetic energy before and after an impact increased the resulting $E_{diss,max}$ values by only 0.2% on average. Therefore, we decided to use only the translational kinetic energy for all energy dissipation calculations to eliminate the uncertainty caused by errors in the angular velocity measurements.

Figure 3 shows the DBH of the nine broken *A. alba* trees and the energy that was dissipated during the impact. The line in the figure is the best-fit function ($R^2 = 0.92$, $P < 0.001$, ME = –14.1%, RMSE = 39.0%, $n = 9$). It shows that the amount of energy that can be dissipated by a living tree increases exponentially with its DBH. The best-fit function for *A. alba* has the formula:

$$E_{diss,max} = 38.7\,DBH^{2.31} \quad (5)$$

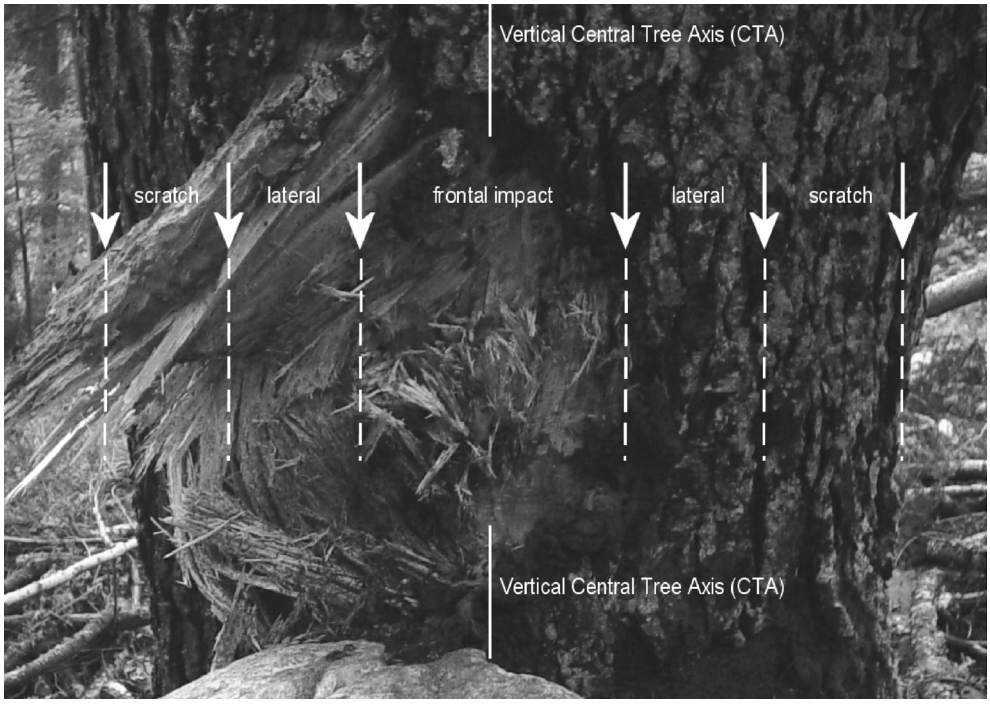


Figure 2. Three main impact types according to the horizontal distance between the impact center and the vertical central tree axis (CTA), as seen from the direction of impact.

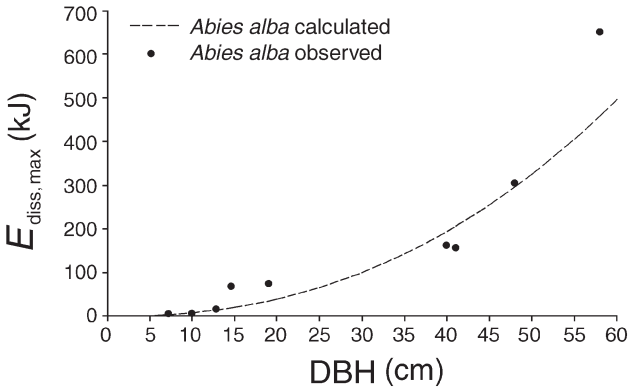


Figure 3. Relationship between the maximum amount of energy that can be dissipated by *Abies alba* ($E_{diss,max}$) and its diameter at breast height, based on nine rockfall impacts causing stem breakage.

where $E_{diss,max}$ is the maximum amount of translational kinetic energy (J) that can be dissipated by the tree during a rockfall impact.

Comparison with published fracture energy values

In our experiments, an *F. sylvatica* tree with a DBH of 34 cm resisted four frontal impacts from large, high-velocity rocks without fracturing. We also observed that *A. alba* and *P. abies* trees were generally less resistant to stem breakage than broadleaved species.

We established relationships between DBH and $E_{diss,max}$ for *P. abies*, *Cedrus* spp. and *F. sylvatica* by multiplying Equation 5 by the ratio of the species fracture energy to that of *A. alba* (see Table 1). Figure 4 shows the relationship between DBH and $E_{diss,max}$ obtained for *P. abies*, as well as the Mb values for *P. abies* based on the mean MOR value (32.5 MPa) obtained by Peltola et al. (1999, 2000) and Gardiner et al. (2000). The solid circles in Figure 4 represent the Mb values for *P. abies* obtained by Stokes et al. (2005). Figure 4 shows that, for *P. abies* with a DBH < 35 cm, our data correlate well with the data on bending moments reported by Stokes et al. (2005), Peltola et al. (1999, 2000) and Gardiner et al. (2000) (R^2 = 0.79, $P < 0.001$, $n = 12$), although our values are, on average, 1.8 times higher ($n = 12$). For larger trees, the relationship based on MOR and DBH yielded higher Mb values than our $E_{diss,max}$ values.

Figure 5 shows a similar difference between our data for *Cedrus* spp. and data obtained from static tree-pushing tests in Japan by Mizuyama and Narita (1988), with our values being on average, 2.6 times higher ($n = 7$). Figure 5 also shows the results of dynamic impact tests on *Cedrus* spp. trees carried out in the field by Mizuyama and Narita (1988) and Nonoda et al. (2004). These published data correlate well with our calculated data for *Cedrus* spp. ($R^2 = 0.62$, $P < 0.015$, $n = 9$).

Our calculated data for *F. sylvatica* correlate well ($R^2 = 0.89$, $P < 0.001$, $n = 7$) with the data obtained by Couvreur (1982), although on average, our values are 6% lower ($n = 7$) (Figure 6). Couvreur (1982) also proposed a relationship between DBH and $E_{diss,max}$ for *F. sylvatica* trees, based on the results of dynamic impact tests in the field. This relationship, designated "*F. sylvatica* fit" in Figure 6, and is similar to the relationship we found.

Figure 6 shows two additional DBH–$E_{diss,max}$ relationships that are based on laboratory impact tests ($n = 16$) conducted on *F. sylvatica* samples by Couvreur (1982) and Sell (1987). Both these relationships provided energy dissipation values that are 61% lower than the values we obtained for *F. sylvatica*.

Relationship between energy dissipation and impact position

Analysis of the translational kinetic energy before and after 32 impacts on different tree species showed that the fraction of $E_{diss,max}$ dissipated by a tree depends on the horizontal distance between the impact center and the vertical CTA. It can be calculated with the sigmoidal function (Figure 7):

$$dE = -0.046 + \frac{0.98 + 0.046}{1 + 10^{-8.007(0.58 - ((C_i - \mathrm{CTA})/0.5\,\mathrm{DBH}))}} \qquad (6)$$

where dE (%) is the fraction of $E_{diss,max}$ that is dissipated during the impact and C_i – CTA is the horizontal distance between the impact center and the vertical CTA seen from the impact direction (m), where C_i is the calculated value. This function is

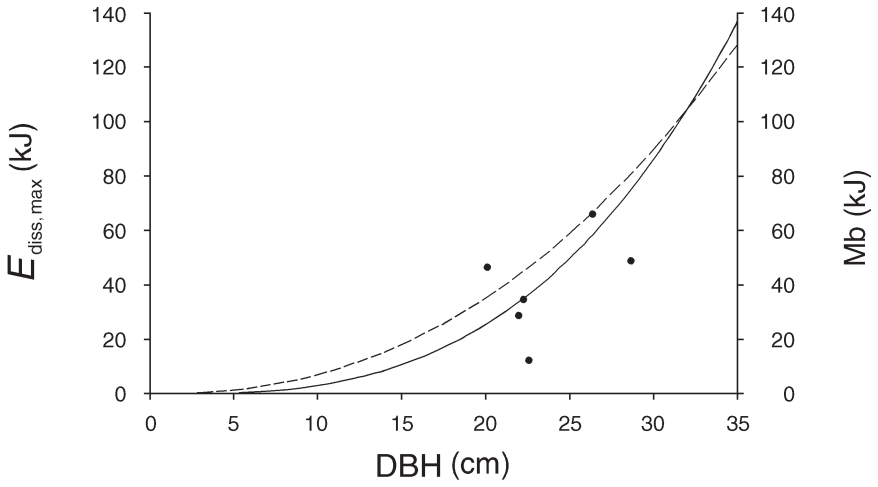


Figure 4. Relationships between stem diameter at breast height (DBH), the maximum bending moment (Mb) and the maximum amount of energy that can be dissipated by *Picea abies* ($E_{diss,max}$). The $E_{diss,max}$ of *P. abies* (calc) is the relationship calculated on the basis of our field data for *Abies alba* and the ratio presented in Table 1 (dashed line); Mb of *P. abies* (Stokes et al. 2005) are results of tree-pulling tests at our study site (●); Mb of *P. abies* (Peltola et al. 1999, 2000, Gardiner et al. 2000) are based on the relationship between the mean modulus of rupture and Mb of *P. abies* (solid line).

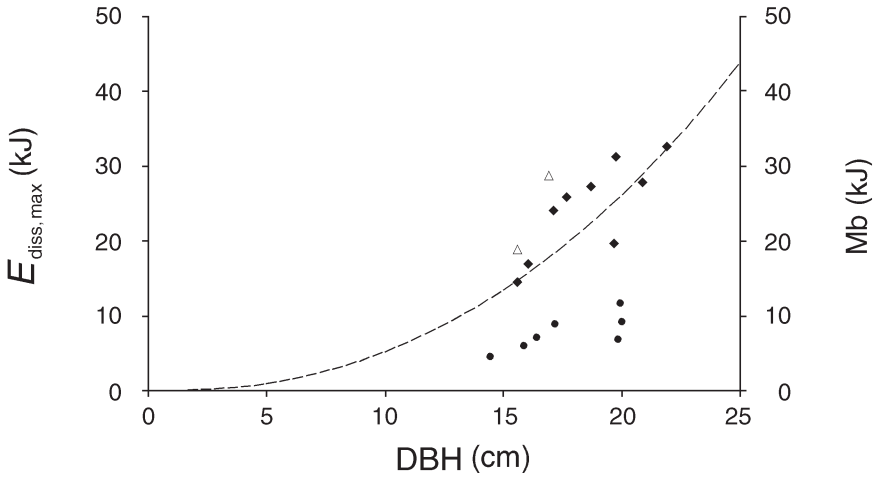


Figure 5. Relationships between diameter at breast height (DBH), the maximum bending moment (Mb) and the maximum amount of energy that can be dissipated by *Cedrus* spp. ($E_{diss,max}$). The dashed line is the relationship of *Cedrus* spp. calculated on the basis of our field data for *Abies alba* and the ratio presented in Table 1; Mb of *Cedrus* spp. (●; Mizuyama and Narita 1988, static test) are results of tree-pushing tests; *Cedrus* spp. (△; Nonoda et al. 2004, dynamic test) and *Cedrus* spp. (◆; Mizuyama and Narita 1988, dynamic test) are the results of dynamic impact tests in the field.

highly correlated to the experimental data (R^2 = 0.98, P < 0.001, ME = 4.8%, RMSE = 26.5%, n = 32).

Table 2 presents the occurrence frequencies of the three main impact types observed during the rockfall experiments (frontal, lateral and scratch), as well as the percentage of effective impacts, i.e., the tree impacts that immediately stopped the falling rock.

The maximum impact height of all 286 registered impacts was 2 m. The maximum height of the center of the 32 impacts was 1.8 m (minimum = 0.15 m, mean = 0.74 m, standard deviation (SD) = 0.42 m). The results of the multiple linear regressions between the $E_{diss,max}$ and combinations of the impact height and the DBH of the nine broken *A. alba* trees are presented in Table 3. The maximum impact height in this data set is 1 m (minimum = 0.5 m, mean = 0.77 m, SD = 0.15 m). High coefficients of determination were obtained for the regression model numbers 3, 4 and 5. With respect to ME and the RMSE, model numbers 3 and 4 gave the best results. Model 5 assumes that the higher the impact occurs on the tree stem, the greater the energy dissipated, which is not realistic. Model 4 assumes that impact height does not influence the amount of energy that will be dissipated. This leaves Model 3 as the most acceptable model, which takes into account the effect of impact height on $E_{diss,max}$. With this model, we calculated that the mean percentage of dissipated energy that is determined by impact height is 99% for trees with a DBH up to 10 cm, 23% for trees with a DBH between 10 and 15 cm and 2% for trees with a DBH > 15 cm.

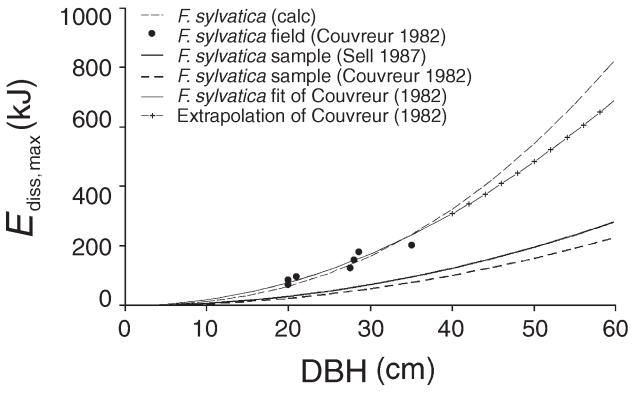


Figure 6. Relationship between the maximum amount of energy that can be dissipated by a *Fagus sylvatica* tree ($E_{diss,max}$) and its diameter at breast height (DBH). *Fagus sylvatica* (calc) is the relationship calculated on the basis of our field data for *Abies alba* and the ratio presented in Table 1; *F. sylvatica* field (Couvreur 1982) are data obtained by dynamic impact tests in the field; *F. sylvatica* sample (Sell 1987) and *F. sylvatica* sample (Couvreur 1982) are relationships calculated on the basis of dynamic impact tests on wood samples in the laboratory; and *F. sylvatica* fit and extrapolation of Couvreur (1982) is the proposed relationship based on the field data and its extrapolation for diameters larger than 40 cm.

Discussion

The overall objective of this study was to quantify the energy dissipation capacity during rockfall impacts of dominant tree species in rockfall protection forests in the European Alps. Three major findings are discussed.

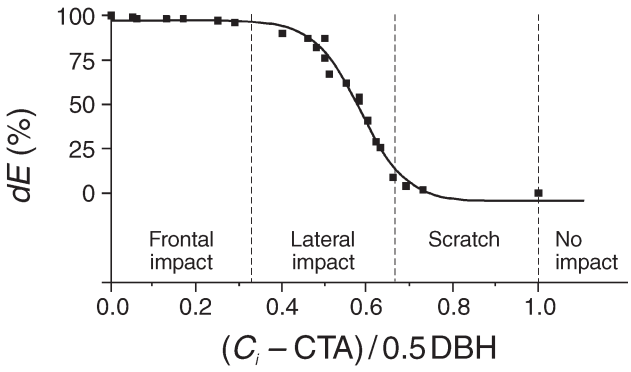


Figure 7. Sigmoidal relationship between the horizontal distance between the impact center and the vertical central tree axis (CTA) seen from the impact direction (C_i – CTA) and the fraction of the maximum amount of energy dissipated by a tree ($E_{diss,max}$). Abbreviations: dE = the fraction of $E_{diss,max}$ that is dissipated during the impact; C_i = calculated value; and DBH = diameter at breast height.

Table 2. Frequency of different types of impacts (%) and the efficacy of trees at stopping rocks, based on an analysis of 286 tree impacts.

Type of impact	Occurrence (n = 286)
Frontal	63.8% (14% of these were effective)[1]
Lateral	20.0% (20% of these were effective)
Scratch	16.2% (0% of these were effective)

[1] The rock stopped immediately after the impact.

The first major result was the empirical demonstration of an exponential relationship between DBH of *A. alba* trees and the maximum amount of energy they can dissipate ($E_{diss,max}$) during a rockfall impact. This relationship was highly correlated for all of our experimental data.

During a rockfall impact, the kinetic energy of the rock causes displacement and deformation of the tree stem as well as of the root–soil system. If the tree is anchored well enough in the soil to prevent uprooting and if the stem does not fracture or break, a sinusoidal shockwave is transferred through the stem to the tree crown. As a result, most coniferous trees start swaying and, depending on how closely the tree crown is surrounded by other stabilizing tree crowns, they lose their top. The root–soil system, the stem and the tree crown thus all play important roles in dissipating the impact energy. The volume of a tree increases exponentially with DBH (e.g., Morgan and Cannell 1994, Peltola et al. 2000), which probably explains why the energy dissipative capacity increases exponentially with increasing DBH.

To establish the relationship between DBH and $E_{diss,max}$, we used only the translational kinetic energy, instead of the total kinetic energy, before and after impact. This resulted in $E_{diss,max}$ values that were about 0.2% too high on average, but the procedure minimized the uncertainty caused by errors in the angular velocity measurements.

The second major finding was that the basic exponential relationship between DBH and $E_{diss,max}$ for *A. alba* can be transferred to other tree species by using published data on fracture energies. Validation of the relationships for *Cedrus* spp., *F. sylvatica* and *P. abies* with data from other dynamic impact tests in the field and Mb, demonstrated that the fracture energies of wood samples are good indicators of the energy dissipative capacities of different living trees. The correlations were high and significant (R^2 between 0.62 and 0.89, minimum level of significance $P < 0.015$). We now use this method to obtain relationships between DBH and $E_{diss,max}$ for different tree species in our simulation models when no other data are available.

We confirmed that broad-leaved trees are generally more resistant to breakage than conifers; however, the relationships for the tree species other than *A. alba*, *Cedrus* spp., *F. sylvatica* and *P. abies* still have to be validated by additional impact tests. Dynamic impact tests on wood samples are not suitable for this purpose, because they yield lower energy dissipation values than dynamic impact tests on living trees.

Application of the results of this study to research on rockfall protection forests depends on the development of a method for transferring the DBH–$E_{diss,max}$ function both to trees that commonly grow in clumps (e.g., *C. avellana*) and to homogeneous coppice stands. Although it is known that tree species that grow in clumps and homogeneous stands provide quite effective protection against rockfall, there are currently no available quantitative data on the energy dissipation capacity of such tree and stand structures.

The Mb obtained by tree-pulling tests correlates well with our data for trees with a DBH up to 35 cm, suggesting that it is a useful indicator of $E_{diss,max}$. For such trees, the Mb equation (Equation 4), which raises the DBH to the third power and multiplies it by MOR, works well. However, for trees with a small DBH, the Mb values are slightly lower than our $E_{diss,max}$ values, and for trees with a large DBH, they are higher. The use of a mean MOR value may be a limitation, because it is highly dependent on the shape of the tree and on wood quality (Peltola et al. 2000). Moreover, applying a bending moment invokes different mechanics than applying impact energy. Therefore, Mb values can be used only as an indicator of $E_{diss,max}$, as done in this study. To calculate the energy from an Mb value, the bending moments obtained during the tree pulling experiment should be integrated over the stem bending angles at the stem base, as described by Stokes et al. (2005). The energy values obtained by Stokes et al. (2005) are lower than our values, because only the energy dissipation of the root–soil or the stem compartment system is taken into account.

The third main result of our study is the quantification of the change in energy dissipation associated with the horizontal position of the center of the rockfall impact on the tree stem, which confirms the assumption made by Dorren and Seijmonsbergen (2003) and Dorren et al. (2004*b*) in their simulation studies. The relationship we obtained correlated highly with the experimental data.

Table 3. Regressions between the observed fraction of the maximum amount of energy dissipated by a tree ($E_{diss,max}$) and combinations of impact height (H; m) and diameter at breast height (DBH; cm) for *Abies alba* (n = 9). Abbreviations: X, b_1 and b_2 = regression variables; ME = mean error; and RMSE = root mean square error.

Variables	Model no.	X	b_1	b_2	R^2	ME (%)	RMSE (%)	P
$b_1(\mathrm{DBH})^X + b_2H$	1	1	9.035	−1.0442	0.74	−22.9	146.5	0.005
	2	2	0.1615	−0.1609	0.89	−25.7	70.6	0.0001
	3	2.31	0.048	−0.05	0.92	−13.1	48.7	0.0001
	4	2.31	0.0387	0	0.92	−14.1	39.0	0.0001
	5	3	0.003	0.1254	0.96	−15.9	67.4	0.0001

The multiple linear regressions between $E_{diss,max}$ and combinations of impact height and DBH showed that impact height influenced the energy dissipated by a tree, especially for trees with a DBH up to 15 cm. For trees with a larger DBH, we found that the effect was minimal (2%). Although these findings are based on a small data set—one tree species only, and minimum and maximum impact heights of 0.5 and 1 m, respectively—we believe that impact height also plays an important role in the case of bigger trees, because the local tree mass available to resist the impact decreases with height and the cantilever beam effect changes. We speculate that these effects probably start to play a significant role in impacts above 1.5 m. In tree-pulling studies, some work has already been done on the effect of pull height on the Mb and stem breakage (e.g., Wood 1995, Moore 2000), but it would be interesting to determine the effect of height of a dynamic impact on $E_{diss,max}$. At the experimental site, impacts did not occur above 2 m, because of the slope gradient and the absence of cliffs in the forest. In many rockfall protection forests throughout the Alps, slope gradients are 50° or more and high cliffs occur within the forests. Rockfall originating from such cliff faces often results in tree impact heights above 2 m. The highest rockfall impact on a tree stem we observed in the European Alps was at a height of 8 m and occurred after a rebound on the slope surface.

In conclusion, our results provide insight into the responses of single trees during rockfall impacts and will help improve quantification of the protective effects of forests against rockfalls. More accurate comparisons of the protection afforded by forests with civil engineering works will facilitate the combined use of silvicultural interventions and technical protective structures in rockfall protection forests.

Acknowledgments

We thank the European Commission for the Marie Curie Fellowship (QLK5-CT-2002-51705) and for funding the ROCKFOR project (QLK5-CT-2000-01302). We also thank Alexia Stokes (LRBB, FR), Thierry Fourcaud (LRBB/CIRAD, FR) and the members of the ROCKFOR consortium for fruitful discussions on the subject.

References

Bartelt, P. and V. Stöckli. 2001. The influence of tree and branch fracture, overturning and debris entrainment on snow avalanche flow. Ann. Glaciol. 32:209–216.

Berger, F., C. Quétel and L.K.A. Dorren. 2002. Forest: a natural protection mean against rockfalls, but with which efficiency? Proceedings Vol. 2. International Congress Interpraevent 2002 in the Pacific Rim, Matsumoto, Japan, pp 815–826.

Brang, P. 2001. Resistance and elasticity: promising concepts for the management of protection forests in the European Alps. For. Ecol. Manage. 145:107–119.

Couvreur, S. 1982. Les forêts de protection contre les risques naturels. École Nationale du Génie Rural des Eaux et Forêts (ENGREF), Nancy, France, 89 p.

Cucchi, V., C. Meredieu, A. Stokes, S. Berthier, D. Bert, M. Najar, A. Denis and R. Lastennet. 2004. Root anchorage of inner and edge trees in stands of Maritime pine (*Pinus pinaster* Ait.) growing in different podzolic soil conditions. Trees 18:460–466.

Dorren, L.K.A. and A.C. Seijmonsbergen. 2003. Comparison of three GIS-based models for predicting rockfall runout zones at a regional scale. Geomorphology 56:49–64.

Dorren, L.K.A, F. Berger, A.C. Imeson, B. Maier and F. Rey. 2004*a*. Integrity, stability and management of protection forests in the European Alps. For. Ecol. Manage. 195:165–176.

Dorren, L.K.A, B. Maier, U.S. Putters and A.C. Seijmonsbergen. 2004*b*. Combining field and modelling techniques to assess rockfall dynamics on a protection forest hillslope in the European Alps. Geomorphology 57:151–167.

Gardiner, B., H. Peltola and S. Kellomäki. 2000. Comparison of two models for predicting the critical wind speeds required to damage coniferous trees. Ecol. Model. 129:1–23.

Gsteiger, P. 1993. Steinschlagschutzwald. Ein Beitrag zur Abgrenzung, Beurteilung und Bewirtschaftung. Schweiz. Zeit. Forstw. 144:115–132.

Jahn, J. 1988. Entwaldung und Steinschlag. Proceedings Vol. 1. International Congress Interpraevent, Graz, Austria, pp 185–198.

Kräuchi, N., P. Brang and W. Schönenberger. 2000. Forests of mountainous regions: gaps in knowledge and research needs. For. Ecol. Manage. 132:73–82.

Metzger, K. 1893. Der Wind als massgeblicher Faktor für das Wachstum der Bäume. Mundener Forstliche Hefte 3:35–86.

Mizuyama, T. and H. Narita. 1988. Debris flow control by woods and their impact energy absorptivity. Proceedings Vol. 2. International Congress Interpraevent, Graz, Austria, pp 173–181.

Moore, J.R. 2000. Differences in maximum bending moments of *Pinus radiata* trees grown on a range of soil types. For. Ecol. Manage. 135:63–71.

Morgan, J. and G.R. Cannell. 1994. Shape of tree stems: a re-examination of the uniform stress hypothesis. Tree Physiol. 14:49–62.

Nicoll, B.C. and D. Ray. 1996. Adaptive growth of tree root systems in response to wind action and site conditions. Tree Physiol. 16: 891–898.

Niemz, P. 1993. Physik des Holzes und der Holzwerkstoffe. DRW-Verlag, Stuttgart, Germany, 243 p.

Nonoda, T., S. Hayashi, H. Kawabe and Y. Yonei. 2004. The occurring factors of standing stem breakage. Proceedings Vol. 1 (III). International Congress Interpraevent, Trento, Italy, pp 207–216.

Papesch, A.J.G., J.A. Moore and A.E. Hawke. 1997. Mechanical stability of *Pinus radiata* trees at Eyrewell Forest investigated using static tests. N.Z. J. For. Sci. 27:188–204.

Peltola, H., S. Kellomäki, H. Väisänen and V.-P. Ikonen. 1999. A mechanistic model for assessing the risk of wind and snow damage to single trees and stands of Scots pine, Norway spruce and birch. Can. J. For. Res. 29:647–661.

Peltola, H., S. Kellomäki, A. Hassinen and M. Granader. 2000. Mechanical stability of Scots pine, Norway spruce and birch: an analysis of tree-pulling experiments in Finland. For. Ecol. Manage. 135: 143–153.

Perret, S., F. Dolf and H. Kienholz. 2004. Rockfalls into forests: analysis and simulation of rockfall trajectories—considerations with respect to mountainous forests in Switzerland. Landslides 1:123–130.

Petty, J.A. and C. Swain. 1985. Factors influencing stem breakage in conifers in high winds. Forestry 58:75–84.

Petty, J.A. and R. Worrell. 1981. Stability of coniferous tree stems in relation to damage by snow. Forestry 54:115–128.

Rupé, C. 1991. Étude de peuplement forestier de protection du canton de la Saucisse, Saint-Martin le Vinoux. Cemagref, Grenoble, France, 35 p.

Schönenberger, W. 2000. Silvicultural problems in subalpine forests in the Alps. *In* Forests in Sustainable Mountain Development: A

State of Knowledge Report for 2000. Eds. M.F. Price and N. Butt. CABI Publishing, Wallingford, Oxon, U.K., pp 197–203.

Sell, J. 1987. Eigenschaften und Kenngrössen von Holzarten. Baufachverlag AG, Zürich, 80 p.

Stokes, A. 1999. Strain distribution during anchorage failure of *Pinus pinaster* Ait. at different ages and tree growth response to wind-induced root movement. Plant Soil 217:17–27.

Stokes, A., F. Salin, A.D. Kokutse et al. 2005. Mechanical resistance of different tree species to rockfall in the French Alps. Plant Soil. In press.

Sunley, J.G. 1968. Grade stresses for structural timbers. U.K. For. Prod. Res. Bull. 47:1–18.

Wood, C.J. 1995. Understanding wind forces on trees. *In* Wind and Trees. Eds. M.P. Coutts and J. Grace. Cambridge University Press, Cambridge, pp 133–146.

Zinggeler, A. 1990. Steinschlagsimulation in Gebirgswäldern: Modellierung der relevanten Teilprozesse. M.Sc. Thesis, Univ. Bern, Bern, Switzerland, 116 p.

> Chapter 9

Comparing experimental and simulated results



Natural Hazards and Earth System Sciences, 6, 145–153, 2006
SRef-ID: 1684-9981/nhess/2006-6-145
European Geosciences Union
© 2006 Author(s). This work is licensed
under a Creative Commons License.

Natural Hazards and Earth System Sciences

Real-size experiments and 3-D simulation of rockfall on forested and non-forested slopes

L. K. A. Dorren[1], **F. Berger**[1], **and U. S. Putters**[2]

[1]Cemagref Grenoble, St. Martin d'Hères cedex, France
[2]ecoRisQ, St. Martin d'Hères, France

Received: 16 September 2005 – Revised: 24 November 2005 – Accepted: 9 December 2005 – Published: 15 February 2006

Part of Special Issue "Spatial prediction modeling in natural hazards and risk"

Abstract. Only a few rockfall simulation models take into account the mitigating effect of existing forest cover. The objective of our study was to improve the generic rockfall simulation model RockyFor, which does take the effect of forest stands into account, thereby developing a clear method for quantifying and modelling slope surface characteristics based on quantitative field data. To obtain these data we carried out 218 real-size rockfall experiments on forested and non-forested sites on a mountain slope in the French Alps. On the basis of a polygon map representing different diameter classes of the material covering the slope, we determine the mean obstacle height (MOH) for each homogeneous unit at the experimental sites. We proposed an algorithm for calculating the tangential coefficient of restitution using the MOH. Comparing the simulated and observed data from the real-size rockfall experiments showed that the 3-D combined deterministic-probabilistic rockfall simulation model RockyFor accurately predicted rockfall events on a non-forested (Root Mean Square Error = 17%) and a forested site (Root Mean Square Error = 12%). We conclude that for further improvement of rockfall-forest simulation on different slope types more quantitative data is required on (1) the energy dissipative capacity of shrubs and bushes (e.g. in coppice stands), (2) the effect of the slope material, (3) the rock shape as well as the rock size, and (4) the tangential and normal coefficient of restitution. Based on the presented results we can state that the RockyFor model could contribute to better taking into account the mitigating effect of the existing forest cover when planning protective measures.

1 Introduction

To sustain and protect livelihoods in the European Alps today, forests are indispensable. They cover the steep slopes of the main valleys and protect these developed and densely populated areas against rapid mass movements that pose risks to infrastructure and inhabitants. Well-known examples are rockfall, defined in this paper as the fall of single rocks and stones with a volume smaller than $5\,m^3$ (Jahn, 1988; Gsteiger, 1993; Erismann and Abele, 2001; Berger et al., 2002), and snow avalanches (Berger, 1996; Weir, 2002). Without these forests, the costs of building and maintaining technical protective constructions would be unaffordable. This is recalled in the first paragraph of the Mountain Forest Protocol of the Alpine Convention: "mountain forests provide the most effective, the least expensive and the most aesthetic protection against natural hazards." In Austria and Switzerland alone, approximately 50 million Euros are spent yearly to maintain or improve the protection provided by mountain forests (European Observatory of Mountain Forests, 2000; Swiss Federal Statistical Office, 2002).

Forests cannot always provide sufficient protection. In the case of rockfall this is because slopes are too steep or too short, or the forest is degraded and its structure is not dense enough to stop falling rocks. In those cases protection could be provided by technical measures such as rockfall dams, nets, etc. Throughout the European Alps, rockfall simulation models are used in so-called trajectory studies, to estimate the hazard posed by rockfall to residential areas (hazard zonation) and traffic routes and to design such technical protective measures.

A wide range of models exists, varying from 2-D statistical models to 3-D deterministic models (Guzzetti et al., 2002; Dorren, 2003). With the increasing digital mapping and spatial modelling possibilities, there is a tendency towards 3-D combined deterministic – probabilistic rockfall simulation models, both at local and regional scale (e.g. Liniger, 2000; Guzzetti et al., 2002; Dorren and Seijmonsbergen, 2003; Dorren et al., 2004; Le Hir et al., 2004). The problematic part in rockfall models is the simulation of rebounds. The majority of these models calculate a rebound by means of energy loss coefficients, also called coefficients of restitution. The most widely used ones are the tangential (r_t) and the normal (r_n) coefficient of restitution (Pfeiffer

Correspondence to: L. K. A. Dorren
(luuk.dorren@cemagref.fr)

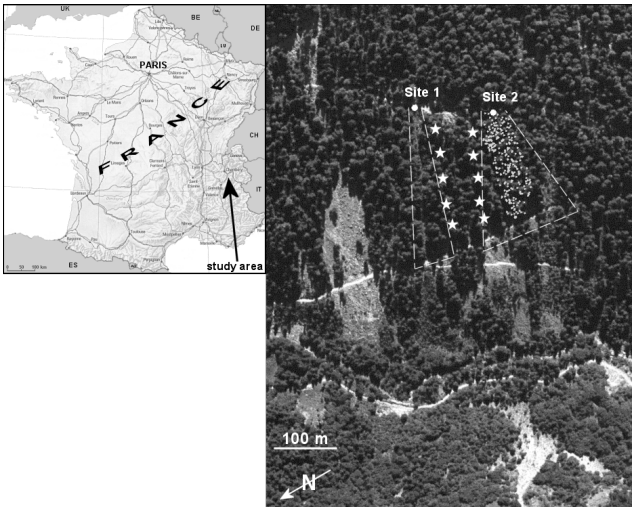


Fig. 1. An orthophoto and a map showing the study area. The two round white dots indicate the start positions of the two sites. Site 1 is an avalanche track, which is denuded of trees, Site 2 is forested. The abundant white points at Site 2 are the mapped positions of all the trees present before the experiments. The white stars indicate the camera positions on both experimental sites.

and Bowen, 1989; Budetta and Santo, 1994; Chau et al., 1998, 2002; Guzzetti et al., 2002; Agliardi and Crosta, 2003; Schweigl et al., 2003; Dorren et al., 2004). These coefficients are generally derived from literature data, whereas the difference between the characteristics of the material covering the slope surface and those of the falling rock itself are often neglected. To account for local variation, the coefficients of restitution are often randomly varied within a given distribution. For local studies, no standard methods exist for estimating the coefficients in the field. Another parameter that is often used in rockfall simulation models is the slope variation coefficient, to account for fine scale variations in the slope topography (Pfeiffer and Bowen, 1989; Spang and Krauter, 2001; Dorren et al., 2004). This coefficient is generally calculated on the basis of the rock radius and the size of the material covering the slope surface.

Only a few rockfall simulation models take into account the mitigating effect of the existing forest cover (e.g. Zinggeler et al., 1990; Liniger, 2000, Dorren and Seijmonsbergen, 2003; Dorren et al., 2004; Le Hir et al., 2004), but generally this effect is neglected. As a result, the rockfall hazard under forested slopes is often overestimated and the protective measures that are taken are too expensive. In many cases, innovative forest management could be sufficient to reach an acceptable level of safety. In the remaining cases, where technical protective measures are needed, the existing forest cover often reduces the rockfall energies and rebound heights, which would mean that more modest protective constructions would suffice.

Two steps are critical for improving the earlier mentioned rockfall hazard assessment studies in the European Alps. The first one is quantifying the effect of protection forests on rockfall hazards by using rockfall simulation models that simulate rockfall in 3-D and explicitly take the barrier effect of protection forests into account. The second step is developing a clear method for quantifying and modelling slope surface characteristics. The objective of our study was to improve the generic rockfall simulation model RockyFor developed by Dorren et al. (2004), thereby developing a clear method for quantifying and modelling slope surface characteristics based on quantitative field data. To obtain these data we carried out 218 real-size rockfall experiments on forested and non-forested sites on a mountain slope in the French Alps.

2 Materials and methods

2.1 Real-size rockfall experiments

Our study area is situated in the *Forêt Communale de Vaujany* in France (lat 45°12′, long 6°3′) and has an altitude ranging from 1200 m to 1400 m above sea level (Fig. 1). There we threw large, individual rocks (spherical shaped rocks with a mean diameter of 0.95 m) down the slope, which has a mean gradient of 38°. By using field measurements and video cameras we captured the velocity and the trajectory of the rock in 3-D. In addition we mapped and measured the size of all tree damages. We carried out these experiments on two sites, of which the central downslope axes were approximately 120 m apart from each other. Site 1 (approx. 1.1 ha) covers an avalanche track and is therefore denuded of trees (unstocked). Site 2 (approx. 0.9 ha) is covered by forest, except for the upper first 40 m, which is the distance necessary for a block of 1 m^3 to reach its maximal speed (Gsteiger, 1993; Brauner et al., 2005). The site is representative for active rockfall slopes in the European Alps. The main tree species in the study area are Silver fir (*Abies alba* – 50%), Norway spruce (*Picea abies (L.) Karst.* – 25%), beech (*Fagus sylvatica* – 17%) and Sycamore (*Acer pseudoplatanus L.* – 4%). The mean stand density on Site 2 before the experiments was 290 trees per hectare and the mean stem diameter at breast height (DBH) was 31 cm (standard deviation 21 cm).

During all the experiments the protocol was identical. Before each single rockfall experiment, we coloured the rock to be thrown with biodegradable paint, so it left traces after rebounding on the slope surface or impacting tree stems on Site 2. A caterpillar was used to throw the rocks down the slope. After each single rockfall experiment, we captured the trajectory of the rock with an Impulse LR 200 laser distance meter manufactured by Laser Technology, Inc. (Centennial, Colorado, USA) by measuring the distance and direction between each subsequent impact on the ground or against a tree. This was done to obtain information about the rockfall trajectories in 3-D, as the five digital high-speed cameras, which were installed along the experimental site, only provide a 2-D view. The cameras were fixed at a height of 10 m in trees that are situated 30 m away from the experimental

rockfall paths of the two sites. In addition, we described and measured all the tree impacts and the resulting damages on trees. In total, we captured the trajectories of 100 rocks on Site 1 and 118 rocks on Site 2. On Site 2, only 102 rocks could be used for analysis. Three reasons for not using the remaining 16 rocks were: 1) they stopped within the first ten meters after sliding on the slope surface, 2) their rockfall path was too far away from the cameras due to lateral deviation of the falling rock, or 3) they broke into pieces during impacts on trees or on the slope surface. On average we managed to carry out eight rockfall experiments per day. Additional details of the experiments are described in Dorren et al. (2005).

Before the experiments, we made a map that covered Site 2, which depicted the surface characteristics in 70 polygons with homogeneous terrain properties. The average size of these polygons was 103 m^2, the minimal size was 7 m^2. In each polygon (n=70) we measured the mean soil depth (material consisting of gravel size class and smaller), and we estimated the mean rock diameter of 70% of the rocks covering the slope surface in the polygon and the same for 20% and 10% of the surface cover. The redistribution into these three cover classes proved to work well after extensive testing in the terrain on different slope surfaces.

In parallel, we analysed the surface roughness at the positions of rock impacts on the ground by measuring the maximal height variance of the material on the ground at the impact position, which was a clear impact crater in about 20% of all cases. The latter was done to investigate if there is a relationship between the size of the material on the slope surface, the radius of the falling rock and the energy loss during a rebound on the slope surface as described by Kirkby and Statham (1975).

In addition to the surface cover map, we created a Digital Elevation Model (DEM) with a resolution of 2.5 m for the two sites. This has been done with the Inverse Distance Weighted interpolation method using on average 3 points per cell. The point data has been collected in the terrain with a detailed topographical survey using the laser distance meter and a compass.

2.2 Calculating the rockfall impact energy

We analysed the digital films of the rockfall trajectories using a free downloadable program called AviStep, which has been developed by M. Delabaere (Saint Denis de la Réunion, France). This program allows extracting the position and the velocity of a moving particle for each individual image in a digital film. The principle is as follows. First, each film has to be referenced in x and y direction, which means that in the first image of each film, we defined the distance in meters between two known points in the terrain, which were also clearly recognisable on the first film image. Then, we analysed the trajectory of each falling rock in 2-D using a sequence of movie images. Since we used high-speed digital cameras we were able to register the velocities (both in x and y direction, as well as the resultant translational velocity) of each falling rock every 1/25th second. Therefore, we could accurately determine the translational velocity of a falling rock before and after impacting a tree. Determining the angular velocity was more difficult, as we had to determine the number of sequential images for the rock to rotate once, which was not always easy to recognise.

Before each rockfall experiment we measured the volume of the rock. All rocks had approximately the same shape (spherical), volume (average 0.49 m^3 on both sites) and density (2800 $kg\,m^{-3}$). With this information we could determine the mass of the rock and therefore the translational kinetic energy ($E_{k-trans}$) as well as the rotational energy (E_{rot}) at any given point in its trajectory, given that the rock was clearly visible on the movie images.

2.3 Rockfall simulation model

Within this study we improved the rockfall model developed by Dorren et al. (2004). This model, called "RockyFor", calculates 1) runout zones of rockfall events on both forested and non-forested slopes, 2) trajectories, velocities, and translational and rotational energies of falling rocks, and 3) impacts against tree stems, potential stem breakage and the resulting energy loss. RockyFor is a process-based model that simulates rockfall in 3-D. It uses raster maps as input that describe (1) the Digital Elevation Model (DEM), (2) the rockfall source cells, (3) the elasticity of the surface material per cell, (4) the roughness of the slope surface per cell (explanation of the elasticity and the surface roughness follows), (5) the number of trees per cell, (6) the diameters of the trees in each cell, and (7) the tree species per cell. RockyFor assumes that each rockfall source cell poses the same risk and simulates, one after another, the trajectories of a given number of rocks (10...100 000) per rockfall source cell. The model accounts for flying, rolling and bouncing within a raster cell. Moreover, RockyFor can explicitly simulate rockfall impacts against individual trees, as investigated by Jahn (1988), Gsteiger (1993), Berger and Lievois (1999) and Dorren and Berger (2006). The main components of the model are (1) the calculation of the rockfall trajectory, (2) the calculation of energy loss due to impact against trees, and (3) the calculation of the velocity of the falling rock.

The trajectory of the simulated falling rock is primarily determined by the topography and is calculated by a multiple fall direction method. At every step in the simulation, the fall direction of the rock can be towards one of the downslope cells from the cell where the rock is located during that simulation step. The exact procedure is described by Dorren et al. (2004). Thus, other than the widely used water flow direction calculation methods, the model is able to produce diverging rockfall trajectories instead of converging patterns. A restriction enforced by the model is that, after a rebound on the slope surface, the rock cannot deviate more than 45° laterally from its fall direction before the rebound. Changes in the fall direction due to rebounds on the slope surface change only between two raster cells, within the raster cell the fall direction does not change unless impacts against trees occur. Observations in the field showed

Table 1. Probabilities for deviation to the left or right from the impact direction after a tree impact (for the tree impact types frontal, lateral and scratch).

Impact type	Probabilities		
	0–22.5° deviation	22.5°–67.5° deviation	67.5°–76° deviation
Frontal	44	50	6
Lateral	11	84	5
Scratch	72	24	4

that extreme deviations of rocks from principal fall lines are mainly caused by tree impacts, distinct changes in topography, or the rock shape (disc shaped rocks or other shapes differing significantly from spheres). The first two are integrated in our model, the latter is not.

2.4 Energy loss due to impact against trees

As observed during the experiments, after a tree impact the trajectory of a rock can be deviated laterally up to 76° from its fall direction before the tree impact. This accounts for the incoming and outgoing direction in a circle with a radius of 5 m around the tree. Of course, locally, meaning around the tree stem, this deviation between the fall direction before and after the impact can be even 180°. The deviation of the rock depends on the position of the rock with respect to the tree stem at the time of impact. Three main impact types have been defined (see Dorren et al., 2005). Based on these three types, the probabilities in Table 1 in combination with a uniformly distributed randomiser are used to calculate the deviation.

The impact position is also required for calculating the energy loss due to tree impacts. In addition, the diameter of the tree and the kinetic energy of the rock before the impact are needed. An input raster for the x-coordinate and one for the y-coordinate of the centre of the tree determine the tree positions. If the exact positions of the trees in the study area are not available, trees are randomly placed within each pixel, based on the number of trees assigned to each pixel (derived from the number of trees per hectare) and the diameter distribution. As the rock is modelled in 3-D, its position is known within each raster cell. If an impact takes place, the rock loses a fraction of its kinetic energy according to the following sigmoidal function:

$$\Delta E = -0.046 + \frac{0.98 + 0.046}{1 + 10^{(0.58 - ((Pi - CTA)/0.5 \times DBH)) \times (-8)}}, \quad (1)$$

where, ΔE = Percentage of maximum amount of energy that can be dissipated by the tree (%), *Pi-CTA* = horizontal distance between the impact and vertical central tree axis (m) and *DBH* = stem diameter at breast height (m).

The maximum amount that can be dissipated by a specific tree with a certain diameter is determined by the stem diameter and the tree species following:

$$\max\ E.diss. = FE_ratio \times 38.7 \times DBH^{2.31}, \quad (2)$$

where, max *E. diss.* = maximum amount of kinetic energy that can be dissipated by a tree in kJ, *FE_ratio* = the fracture energy ratio of a given tree species to *Abies alba* described by Dorren and Berger (2006) and *DBH* = stem diameter at breast height (cm).

The algorithms presented above have been developed by Dorren and Berger (2006) and are based on data obtained with the real-size rockfall experiments. By using a *FE_ratio* of 1, Eq. (2) represents the function of the maximum energy that can be dissipated by an *Abies alba* in relation to its diameter. With respect to rockfall, this tree can be considered to be representative for a tree with an average energy dissipative capacity.

2.5 Velocity of the falling rock

The velocity of the falling rock during its flight through the air is calculated with standard algorithms for a uniform accelerated parabolic movement through the air. The velocity after a rebound or bounce on the slope surface is calculated with algorithms modified from Pfeiffer and Bowen (1989), as presented in Dorren et al. (2004). During each bounce the slope angle at the exact location of the bounce is uniform randomly decreased with an angle that varied between 0 and 4°. This procedure is similar to the varying impact angle based on the surface roughness as described by Jones et al. (2000).

Energy loss is determined by the elasticity of the surface material, defined by the so-called normal coefficient of restitution (r_n) and by the roughness of the slope surface, defined by a tangential coefficient of restitution (r_t). Dorren et al. (2004) showed that the change of velocity after a rebound is mainly determined by the tangential coefficient of restitution and the slope angle at the rebound position. Both parameters are determined by the composition and size of the material covering the surface and the radius of the falling rock itself, since for larger rocks the effective surface roughness is lower than for smaller rocks, as shown by Kirkby and Statham (1975), and analogue to the principle of the slope variation coefficient used by, e.g. Pfeiffer and Bowen (1989), Spang and Krauter (2001) and Dorren et al. (2004). Therefore, we proposed the following algorithm to calculate the r_t:

$$r_t = \frac{1}{1 + (MOH/Rrock)}, \quad (3)$$

where, *MOH* is the maximum obstacle height at the slope surface (m) and *Rrock* is the radius of the falling rock (m).

In the actual calculation of the velocity after a rebound, RockyFor randomly varies the value of the r_t with 10% using a uniform distribution, to account for the local variation in the size of material covering active rockfall slopes.

The data obtained with the rockfall experiments provide the possibility to assess the validity of this algorithm. We analysed 22 rebounds on the slope surface by using the video images and calculated the tangential coefficient of restitution taking the ratio of the tangential velocity (parallel to the slope surface) of the rock before the impact and the tangential velocity after the impact. We related these data with the maximal height variance of the material on the ground at the rebound positions. To determine the strength of relationships we calculated the coefficient of determination (R^2) and its level of significance (P).

It is not possible to measure the MOH everywhere on an active rockfall slope. As it is feasible to make a polygon map with mean diameters of the material covering the surface classified in different diameter classes, it would be practical if the r_t could be estimated on the basis of such a map. We chose to map three different diameter classes that are representative for 70%, 20%, and 10% of the average diameters of the material covering the surface in a mapped polygon. To test this method, we related the measured MOH values at the rebound positions to the mean diameters of the material covering the slope as derived from our polygon map. For that, we tested two different approaches. Firstly, we calculated the mean diameter in a polygon following,

$$\overline{d} = 0.7 \times d_{70} + 0.2 \times d_{20} + 0.1 \times d_{10}\,, \tag{4}$$

where $\overline{d}$ = mean diameter of the material covering the surface in a polygon, and d_x = the mean material diameter of the 70%, 20%, or 10% class in the polygon. Subsequently, the simulated rock encountered an obstacle with a height equal to the mean diameter in the raster cell derived from the polygon map during the rebound calculations. Secondly, we made the simulation program randomly choose the MOH on the basis of the three cover classes in the polygon using a uniform distributed randomiser. Here, the probability that the simulated rock encountered an obstacle with a height equal to the mean diameter representative for the 70%, 20% and 10% cover class in the terrain was respectively 70%, 20%, and 10% during each rebound calculation. The latter method only has been applied at Site 2, because Site 1 is relatively uniform regarding the material size covering the slope surface.

2.6 Validating the model output

The primary output generated by RockyFor consists of the velocity in each cell after a given number of simulations ($\mathrm{m\,s^{-1}}$), the kinetic energy in each cell (kJ), the number of times a simulated rock passed in each cell (−), the rebound heights of the rock in normal direction to the slope surface and in the vertical direction (m), the impact height on trees in each cell (m), the number of tree impacts in each cell (−) and the number of rocks that stopped in each cell (−). The model uses many probabilistic functions. Therefore, repeating the simulations at least a 1000 times, but preferably 10 000 times per start cell produces reliable results. To validate the output of 10 000 simulation runs on Site 1 and Site 2, we compared them with the average maximum translation velocity of all the rocks ($\mathrm{m\,s^{-1}}$), the maximum translation velocity ($\mathrm{m\,s^{-1}}$), the percentage of rocks stopped after 223.5 m, the mean number of tree impacts per falling rock and the maximal vertical rebound height of rebound (m) observed at the slopes of Site 1 (non-forested) and Site 2 (forested).

In addition, to evaluate the model performance at a more detailed scale than the slope as a whole, we compared the observed and simulated translation velocity ($\mathrm{m\,s^{-1}}$), the vertical rebound height (m) and the kinetic energy (kJ) at two "evaluation screens" at Site 1. Evaluation screen 1 is located after 185 m from the starting point at Site 1, measured over the slope and evaluation screen 2 is located after 235 m.

On the basis of all the observed and simulated values we calculated Errors (E) and the Root Mean Square Errors (RMSE) following,

$$E = (C - O) * 100/O \tag{5}$$

$$\mathrm{RMSE} = \sqrt{\frac{1}{\mathrm{n}} \sum_{\mathrm{i=1}}^{\mathrm{n}} (\mathrm{E}^2)}\,, \tag{6}$$

where n is the number of observations, C is the calculated value and O is the observed value.

3 Results

3.1 Simulated and observed rockfall events

The most important results of this study are the comparison between simulated and experimentally obtained results on the non-forested and forested slope, as these indicate whether the model produces reliable results. Therefore, these results will be presented first. While presenting these results, data obtained from the real-size rockfall experiments will be presented as well. A more extensive presentation of the results of those experiments can be found in Dorren et al. (2005) and in Dorren and Berger (2006).

The comparison of the simulated data and the data observed at the slopes of Site 1 (non-forested) and Site 2 (forested), which are summarised in Table 2, show that the RockyFor model produces accurate results at the slope level RMSE Site 1 = 17%, RMSE Site 2 = 13%). The largest error is produced at Site 1 by predicting the percentage of rocks surpassing the lower forest road. In reality, we observed that 74% surpassed this road, while the model predicted that 95% would surpass it, which results in an overestimation of 28.4%.

Predicting the mean number of tree impacts that occur per falling rock resulted in the largest error at Site 2. In reality, 2.8 trees were on average impacted by each rock, while the model simulated on average 2.3 tree impacts per rock. This is an underestimation of 17.9%. Regarding the overall distribution of the number of tree impacts per rock as presented in Fig. 2, RockyFor reproduced the histogram quite well.

The number of rocks that surpassed the lower forest road on Site 2 indicates the residual hazard of the forest including

Table 2. Summary of the observed and simulated characteristics of rockfall at Site 1 (non-forested) and Site 2 (forested).

	Site 1			Site 2		
	Observed (n=100)	Simulated (n=10 000)	Error (%)	Observed (n=102)	Simulated (n=10 000)	Error (%)
Average maximum translation velocity of all the rocks (m s^{-1})	15.4	17.3	12.3%	11.7	12.8	9.4%
Maximum translation velocity observed (m s^{-1})	30.6	30.4	−0.7%	24.2	22.3	−7.9%
Percentage of rocks stopped within the first 223.5 m (%)	5	4	−20.0%	66	74	12.1%
Percentage of rocks surpassed the lower forest road (%)	74	95	28.4%	21	25	19%
Mean number of tree impacts per falling rock	n.a.	n.a.	n.a.	2.8	2.3	−17.9%
Maximal height of rebound (m)	8	7.6	−5.0%	2	2.1	5%
		RMSE	17%		RMSE	13%

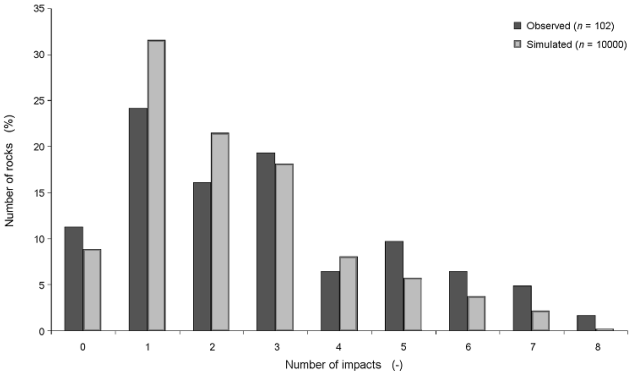


Fig. 2. Histogram showing the number of impacts against trees per rock as observed during the real-size experiments (observed) and produced by RockyFor (simulated).

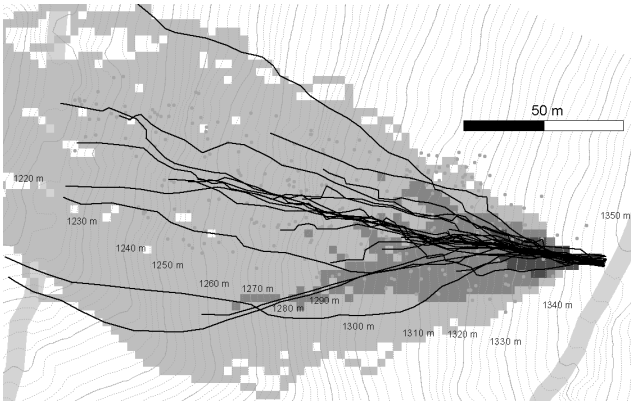


Fig. 3. Observed and simulated rockfall trajectories at the forested Site 2. Trees are indicated as grey round dots. The observed trajectories are represented by the black lines and simulated trajectories are generalised in the raster map displayed in the background. This raster map is a pass frequency map; the darker the cell the higher the simulated frequency of a rock passing through that cell.

the forest road. The model was capable to simulate this residual hazard with an error of 19%. We observed that 21% of the rocks surpassed the lower forest road at Site 2 and RockyFor predicted that 25% would surpass it. In addition, the model reproduced the spatial pattern of the observed rockfall trajectories, as presented in Fig. 3.

Looking more in detail at the velocities, kinetic energies, and rebound heights that have been observed and simulated at the two evaluation screens at Site 1, it shows that RockyFor overestimates the mean velocity, and logically also the kinetic energies, and it underestimates the rebound heights (Table 3). The RMSE is 50% at evaluation screen 1, which is 185 m from the starting point measured over the slope. At screen 2, which is 235 m from the starting point measured over the slope, the RMSE is 44%. The maximum observed values, however, are well predicted at the two screens (RMSE of 12% at screen 1 and 8% at screen 2).

3.2 Simulated and observed rebounds on the slope surface

Our analyses showed that there is no relationship between the tangential (r_t) and the normal (r_n) coefficient of restitution on forested slopes (R^2=0.06, P<0.22, n=27). The analyses of the filmed rebounds also prove that both parameters are useful, as on our test sites they seem to be independent from the velocity before the rebound of the falling rock. The key values of both coefficients as obtained by analysing the films of the real-size experiments are presented in Table 4.

The analyses also show that there is clear link between the tangential coefficient of restitution and the ratio of the MOH (in reality these consisted mainly of previously deposited rocks and stones) at the location of the impact to the radius of the rock (Fig. 4). By using Eq. (3) we are able to explain 73% of the variance in the calculated r_t values.

There is also a good relationship between the mean diameter of the surface covering the slope and the MOH as indicated by Fig. 5. By establishing the linear relationship shown in Fig. 5, we could explain 68% of the observed variance. Using this relationship to calculate the r_t on the basis of our material diameter class polygon map in our model yielded the simulation results that are presented in the first part of the results section. Using a uniform distributed randomiser that randomly chose the MOH on the basis of the three cover classes in each polygon increased the RMSE of the simulation results at Site 2 with 8%, where mainly the simulated velocity decreased.

Table 3. The observed and simulated translation velocity (v in m s^{-1}), vertical rebound height (RH in m) and kinetic energy (E_{kin} in kJ) at screen 1 (after 185 m from the starting point at Site 1, measured over the slope) and at screen 2 (after 235 m from the starting point at Site 1, measured over the slope) as well as the accompanying errors.

	Screen 1 (after 185 m)					
	Mean observed	Mean simulated	Error (%)	Max observed	Max simulated	Error (%)
v (m s^{-1})	12.5	17.1	36.8	28.1	24.1	−14.2
RH (m)	1.4	0.9	−36.5	5.0	4.2	−15.7
E_{kin} (kJ)	204.9	346.7	69.2	786.4	781.9	−0.6
		RMSE	50%		RMSE	12%
	Screen 2 (after 235 m)					
	Mean observed	Mean simulated	Error (%)	Max observed	Max simulated	Error (%)
v (m s^{-1})	13.8	17.3	25.4	28.9	26.5	−8.2
RH (m)	1.6	1.2	−27.8	6.2	5.5	−11.1
E_{kin} (kJ)	244.5	406.9	66.4	958.3	943.8	−1.5
		RMSE	44%		RMSE	8%

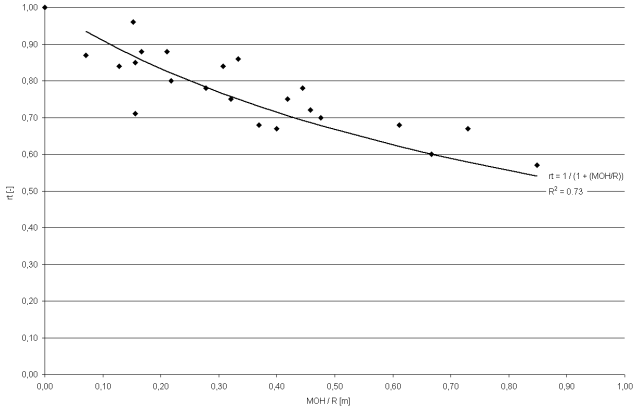


Fig. 4. The relationship between the tangential coefficient of restitution r_t and MOH/R based on analysed rebounds during the real-size rockfall experiments.

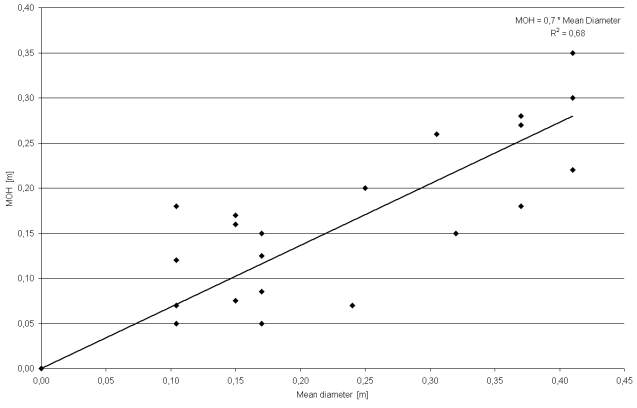


Fig. 5. The relationship between the measured MOH in the field and the mean diameter of the slope covering material as derived from the diameter classes polygon map.

4 Discussion

The objective of our study was to improve the rockfall simulation model RockyFor, thereby developing a clear method for quantifying and modelling slope surface characteristics based on quantitative field data. The results show that RockyFor is able to reproduce the observed rockfall events with errors in general between 15% and 20%. Reproduction of the characteristics of the events observed during our experiments indicates that the model is suitable for prediction as no retro-calculation or calibration on the basis of historical or recent observed events is required.

The results of the analyses at the two evaluation screens show that the model generally overestimates the observed mean values, but it reproduces the worst-case events well with a systematic underestimation of approximately 9%, on average. The mean values at the two evaluation screens are very much determined by rocks that roll or bounce down the slope slowly with relatively low bounces. These rocks are generally less spherical, with one or more relative flat sides. Such rocks, except disc shaped ones, decelerate more than round rocks during impacts and they accelerate less than round rocks because they tend to slide over the slope. Disc shaped rocks, tend to roll and bounce over the flat side and developed high rotational velocities. These rocks pose large risks as the probability that they impact trees is low, due to the small diameter. RockyFor also does not account for breaking of falling rocks. The initial rock that is simulated

Table 4. The range of values of the tangential (r_t) and normal (r_n) coefficient of restitution obtained from the real-size experiments on both sites.

	r_t		r_n	
Site	1 (non-forested)	2 (forested)	1	2
Average	0.70	0.77	0.26	0.36
Stddev.	0.12	0.10	0.09	0.13
Min.	0.50	0.57	0.11	0.21
Max.	0.95	0.96	0.41	0.68

to fall from a certain source area remains the same during the simulation. This means also that the results produced by RockyFor approach more the worst-case scenarios with high velocities, high rebounds and longer runout zones.

RockyFor predicted that the forest at Site 2 could stop 74% of all the rocks, while in reality that forest has stopped 66%. An explanation could be the fact that RockyFor does not include the quality of individual trees in the forest stand, thereby overestimating the energy that can be dissipated by a forest stand. All trees are assumed to behave "ideally" and dissipate an amount of energy determined by the stem diameter and its species. In reality, the properties that determine the amount of energy that can be dissipated by a tree vary a lot. Examples of such properties are the quality of the living wood, the size and depth of the root systems, the soil-root plate, root interactions with surrounding trees, the size and shape of the tree crown and tree diseases such as heart rot (Stokes et al., 2005; Dorren and Berger, 2006).

In relation to this, however, it is interesting to notice that the average number of tree impacts per rock was higher in reality than simulated by RockyFor. This could indicate that the problem is rather that RockyFor assumes that all rocks with a translation velocity smaller than 0.1 m/s are stopped. In reality we observed that some rocks, which were initially stopped by trees, continued to fall down the slope after approximately one second, in case they stopped in a non-stable position next to the tree. This effect could not be simulated by RockyFor, which could cause an underestimation of the number of tree impacts per simulated rock. Despite several analyses we have not been able to give a clear answer.

RockyFor predicted that only 4% more rocks surpassed the forest road that limits the foot of Site 2 (see Fig. 1) than observed in reality (simulated 25%, observed 21%, see Table 2). Looking at the number of rocks that were stopped by the forest in the simulation and reality, as given in Table 2, this means that in the simulation only 1% of the rocks stopped on the forest road but in reality 13%. This difference points out a weak point of calculating the tangential coefficient of restitution on the basis of the Maximum Obstacle Height (MOH). On undisturbed forest roads and comparable surfaces, the MOH is very low. After an impact, however, the MOH changed enormously as the rock impact created a crater in the road. In other words, on soft surfaces, such as forest roads, the rock creates a barrier for itself during the impact. Therefore, when mapping the MOH in the field, the MOH after the impact should be estimated, which makes the proposed method subjective. To avoid this in the future, we started working on a field method to estimate the MOH after an impact for different land cover types (talus slopes, talus slopes with forest soils, meadows, slopes covered by deep soils, forest roads, asphalt roads, etc.) using repeated impacts on the ground with a small granite block ($\sim$0.15 m$\times\sim$0.15 m$\times\sim$0.15 m) that can be carried in the field. In our current research we try to establish a relationship between the penetration depth of this block and the MOH for larger rocks.

Finally we would shortly like to discuss whether or not it would be wise to take into account the mitigating effect of existing forest cover in rockfall hazard assessment studies. A counter argument that is often heard is that a forest is not perennial. Generally, the same accounts for technical protective structures such as rockfall nets. According to our opinion, a site where a natural hazard poses a risk should be monitored through time, also after a hazard assessment study has been carried out and protective systems haven been installed. It reduces the probability of potential malfunctioning of the protective system, it being a technical structure, a mixed technical – ecological measure, or a pure ecological measure, such as a protection forest. In other words, monitoring a hazardous site reduces the risk, but zero risk hardly exists. In case a forest with a protective function is destroyed completely by a gale or partly by avalanches or rockfall (mostly in distinct *couloirs*), its protective function is not completely lost. Moreover, silvicultural techniques exist and are already applied in practice to maintain a large part of the level of protection before the damage occurred (see Dorren et al., 2005; Schönenberger et al., 2005). Since protection forest maintenance is cheap compared to technical protective structures and well-trained foresters are capable of safeguarding the protective function of a forest for 25 years, there is no reason why the mitigating effect of a forest should not be taken into account when planning protective measures if the potential is present on site.

5 Conclusions

Based on the presented results we conclude that the RockyFor model allows predicting the hazard posed by rockfall (velocity, kinetic energy, jump height and runout zone) accurately, both on forested as on non-forested slopes. It could thus contribute to better taking into account the mitigating effect of existing forest cover when planning protective measures. For further improvement of rockfall-forest simulation on different slopes types we conclude that more quantitative data is required on (1) the energy dissipative capacity of shrubs and bushes (e.g. in coppice stands), (2) the effect of the slope material, (3) the rock shape as well as the rock size, and (4) the tangential and normal coefficient of restitution.

Acknowledgements. We gratefully thank the European Commission for the Marie Curie Fellowship (QLK5-CT-2002-51705) and for funding the ROCKFOR project (QLK5-CT-2000-01302). We also thank G. F. Wieczorek and J. Corominas for their valuable comments on the manuscript.

Edited by: T. Glade
Reviewed by: J. Corominas, G. F. Wieczorek, and another referee

References

Agliardi, F. and Crosta, G. B.: High resolution three-dimensional numerical modelling of rockfalls, Int. J. Rock Mech. Min. Sci., 40, 455–471, 2003.

Azzoni, A. and de Freitas, M. H.: Experimentally gained parameters decisive for rock fall analysis, Rock Mech. Rock Eng., 28, 111–124, 1995.

Berger, F.: Cartographie des fonctions de protection de la forêt de montagne, International Congress Interpraevent 1996, Garmisch-Partenkirchen, Proceedings, 1, 171–180, 1996.

Berger, F. and Lievois, J.: Determination of priority forest work areas and creation of green areas in risk prevention plans – an example of researcher-specialist transfer, in: Int. Conf. Mountainous Natural Hazards, edited by: Gillet, F. and Zanolini, F., Cemagref, 12–14 April 1999, Grenoble, France, 412–416, 1999.

Berger, F., Quetel, C., and Dorren, L. K. A.: Forest: a natural protection mean against rockfalls, but with which efficiency? International Congress Interpraevent 2002 in the Pacific Rim, Matsumoto, Japan, Proceedings, 2, 815–826, 2002.

Brauner, M., Weinmeister, W., Agner, P., Vospernik, S., and Hoesle, B. : Forest management decision support for evaluating forest protection effects against rockfall, Forest Ecol. Man., 207, 75–85, 2005.

Budetta, P. and Santo, A.: Morphostructural evolution and related kinematics of rockfalls in Campania (southern Italy): A case study, Eng. Geol., 36, 197–210, 1994.

Chau, K. T., Wong, R. H. C., and Lee, C. F.: Rockfall problems in Hong Kong and some new experimental results for coefficient of restitution, Int. J. Rock Mech. Min. Sci., 35, 662–663, 1998.

Chau, K. T., Wong, R. H. C., and Wu, J. J.: Coefficient of restitution and rotational motions of rockfall impacts, Int. J. Rock Mech. Min. Sci., 39, 69–77, 2002.

Dorren, L. K. A.: A review of rockfall mechanics and modelling approaches, Prog. Phys. Geog., 27, 69–87, 2003.

Dorren, L. K. A. and Berger, F.: Stem breakage of trees and energy dissipation during rockfall impacts, Tree Phys., 26, 63–71, 2006.

Dorren, L. K. A. and Seijmonsbergen, A. C.: Comparison of three GIS-based models for predicting rockfall runout zones at a regional scale, Geomorphology, 56, 49–64, 2003.

Dorren, L. K. A., Maier, B., Putters, U. S., and Seijmonsbergen, A. C.: Combining field and modelling techniques to assess rockfall dynamics on a protection forest hillslope in the European Alps, Geomorphology, 57, 151–167, 2004.

Dorren, L. K. A., Berger, F., le Hir, C., Mermin, E., and Tardif, P.: Mechanisms, effects and management implications of rockfall in forests, Forest Ecol. Man., 215, 183–195, 2005.

Erismann, T. H. and Abele, G.: Dynamics of rockslides and rockfalls, Springer-Verlag, Berlin, 316 pp., 2001.

European Observatory of Mountain Forests: White Book 2000 on mountain forests in Europe, European Federation of Local Forest Communities, Saint Jean d'Arvey, 60 pp., 2000.

Gsteiger, P.: Steinschlagschutzwald. Ein Beitrag zur Abgrenzung, Beurteilung und Bewirtschaftung, Schweiz. Zeit. Forstw., 144, 115–132, 1993.

Guzzetti, F., Crosta, G., Detti, R., and Agliardi, F.: STONE: a computer program for the three-dimensional simulation of rock-falls, Comp. & Geosc., 28, 1079–1093, 2002.

Jahn, J.: Entwaldung und Steinschlag, International Congress Interpraevent, Graz. Proceedings, 1, 185–198, 1988.

Jones, C. L., Higgins, J. D., and Andrew, R. D.: Colorado Rockfall Simulation Program Version 4.0, Colorado Department of Transportation, Denver, CO, 127 pp., 2000.

Kirkby, M. J. and Statham, I.: Surface stone movement and scree formation, J. Geology, 83, 349–362, 1975.

Le Hir, C., Berger, F., Dorren, L. K. A., and Quétel, C.: Forest: a natural means of protection against rockfall, but how to reach sustainable mitigation? Advantages and limitations of combining rockfall models taking the forest into account, International Congress Interpraevent 2004, Riva del Garda, Italy, Proceedings, 2, 59–69, 2004.

Liniger, M.: Computersimulation von Stein- und Blockschlägen, Felsbau, 18, 64–68, 2000.

Pfeiffer, T. J. and Bowen, T. D.: Computer simulation of rockfalls, Bull. Ass. Eng. Geol., XXVI, 135–146, 1989.

Schönenberger, W., Noack, A., and Thee, P: Effect of timber removal from windthrow slopes on the risk of snow avalanches and rockfall, Forest Ecol. Man., 213, 197–208, 2005.

Schweigl, J., Ferretti, C., and Nossing, L.: Geotechnical characterization and rockfall simulation of a slope: a practical case study from South Tyrol (Italy), Eng. Geol., 67, 281–296, 2003.

Spang, R. M. and Krauter, E.: Rockfall simulation – a state of the art tool for risk assessment and dimensioning of rockfall barriers, International Conference Landslides – Causes, Impacts and Countermeasures, Davos, United Engineering Foundation, 607–613, 2001.

Stokes, A., Salin, F., Kokutse, A. D., Berthier, S., Jeannin, H., Mochan, S., Dorren, L. K. A., Kokutse, N., Ghani, M. A., and Fourcaud, T.: Mechanical resistance of different tree species to rockfall in the French Alps, Plant Soil, 278, 107–117, 2005.

Swiss Federal Statistical Office: Statistisches Jahrbuch der Schweiz 2002, Swiss Federal Statistical Office, Verlag Neue Zürcher Zeitung, 890 pp., 2002.

Weir, P.: Snow Avalanche Management in Forested Terrain, Land Management Handbook 55 British Columbia Ministry of Forests Research Branch, Victoria B.C., Canada, 190 p., 2002.

Zinggeler, A., Krummenacher, B., and Kienholz, H.: Steinschlagsimulation in Gebirgswäldern, Berichte und Forschungen der Geographisches Institut der Universität Freiburg, 3, 61–70, 1990.

> Chapter 10

Evaluating Swiss rockfall protection forests using RockyFor



Available online at www.sciencedirect.com
SCIENCE DIRECT
Forest Ecology and Management 225 (2006) 113–122
Forest Ecology and Management
www.elsevier.com/locate/foreco

Assessing the protective effect of mountain forests against rockfall using a 3D simulation model

Markus Stoffel [a,*], André Wehrli [b], Roderick Kühne [c], Luuk K.A. Dorren [d], Simone Perret [c], Hans Kienholz [c]

[a] Department of Geosciences, Geography, University of Fribourg, Pérolles, Chemin du Musée 4, CH-1700 Fribourg, Switzerland
[b] Swiss Federal Institute for Forest, Snow and Landscape Research WSL, Zürcherstrasse 111, CH-8903 Birmensdorf, Switzerland
[c] Department of Geography, University of Berne, Hallerstrasse 12, CH-3012 Berne, Switzerland
[d] Cemagref Grenoble, 2 Rue de la Papeterie, B.P. 76, F-38402 Saint Martin d'Hères Cedex, France

Received 5 April 2005; received in revised form 28 October 2005; accepted 16 December 2005

Abstract

We used one of the few rockfall models explicitly taking trees into account and compared the results obtained with the 3D simulation model RockyFor with empirical data on tree impacts at three mountain forests in Switzerland. Even though we used model input data with different resolutions at the study sites, RockyFor accurately predicted the spatial distribution of trajectory frequencies at all sites. In contrast, RockyFor underestimated mean impact heights observed on trees at the two sites where high- and medium-resolution input data were available and overestimated them at the site where input data with the lowest resolution data were used. By comparing the results of the simulation scenarios "current forest cover" and "non-forested slope", we assessed the protective effect of the current stands at all three sites. The number of rocks reaching the bottom parts of the study sites would, on average, almost triple if the "current forest cover" were absent.

We conclude that RockyFor is able to predict the spatial distribution of rockfall trajectories on forested slopes accurately, based on input data with a resolution of at least 5 m × 5 m. With the increasing availability of high-resolution data, it provides a useful tool for assessing the protective effect of mountain forests against rockfall.
© 2005 Elsevier B.V. All rights reserved.

Keywords: Protection forest; Natural hazards; RockyFor; Dendrogeomorphology; Rockfall; 3D simulation model; Swiss Alps

1. Introduction

Many mountain forests effectively protect people and their assets against natural hazards such as rockfall, snow avalanches, landslides, debris flows, soil erosion and floods (Brang et al., 2001). As a consequence, numerous settlements and transportation corridors in alpine regions directly depend on the protective effect of these forests and would – at least temporarily – become uninhabitable or inaccessible if this protection were to disappear or become inadequate (Bloetzer and Stoffel, 1998; Agliardi and Crosta, 2003).

In the Swiss Alps, rockfall and snow avalanches comprise the most common hazards, with evidence of rockfall observed in 31% and moving snow recorded in 37% of the National Forest Inventory (NFI) plots in mountain forests (Mahrer et al., 1988). While the large volumes and high energies occurring with snow avalanches often limit the protective effect of stands (Bartelt and Stöckli, 2001), the small masses that are generally involved in single rockfall events (<5 m^3; Berger et al., 2002) allow mountain forests to absorb falling rocks (Leibundgut, 1986; Lafortune et al., 1997; Hétu and Gray, 2000). On forested slopes, both living and dead trees can stop falling rocks (Cattiau et al., 1995), whereas stems lying on the ground or root plates may act as barriers to rocks moving downslope (Mössmer et al., 1994; Schönenberger et al., 2005). Taking advantage of these effects on falling rocks, forest managers repeatedly tried to optimize the protective effect of their forests by applying target values for stand parameters such as tree density, spatial tree distribution, species composition, tree conditions, diameter distribution and basal area (Chauvin et al., 1994; Wasser and Frehner, 1996; Frehner et al., 2005). While these target values undoubtedly provided a valuable tool for forest managers, they currently remain unsatisfactory, since values are predominantly based on expert knowledge rather than on empirical data.

* Corresponding author. Tel.: +41 26 300 90 15; fax: +41 26 300 97 46.
E-mail address: markus.stoffel@unifr.ch (M. Stoffel).

0378-1127/$ – see front matter © 2005 Elsevier B.V. All rights reserved.
doi:10.1016/j.foreco.2005.12.030

Empirical data are very sparse, which is why the protective effect of a stand on a given site with a given damage potential could, up to now, only be assessed with considerable uncertainty (Dorren et al., 2005). Given this lack of extensive empirical data on rockfall in mountain forests, dynamic modeling could provide a valuable tool for investigating the protective effect of different stand structures against rockfall and for improving target values for forest management.

To be useful, a model should accurately predict different patterns of rockfall processes such as the spatial envelope of rockfall trajectories, impact heights of rocks, and runout zones. Furthermore, it should be applicable under various site and stand conditions and should consider the interaction of falling rocks with trees – as investigated by Jahn (1988), Zinggeler et al. (1991), Gsteiger (1993), Krummenacher and Keusen (1996), Berger and Lievois (1999) or Dorren et al. (2005) – in sufficient detail.

The recently developed 3D rockfall model RockyFor has accurately predicted different rockfall patterns for several forested and non-forested sites in mountainous terrain (Dorren et al., in press). The model operates with high-resolution input data (2.5 m × 2.5 m) so as to obtain sound results at the forest stand level. Such data hardly exist for many areas of the Alps. The model has also been shown to predict maximal runout zones with reasonable accuracy, even if based on low-resolution input data, i.e. 25 m × 25 m (Dorren and Heuvelink, 2004). In contrast, the minimum resolution of input data required to obtain realistic simulation results for other important rockfall features characterizing the protective effect of a stand (e.g. envelope of rockfall trajectories, mean impact height, mean velocity of rocks) is not yet known. Furthermore, even if RockyFor accurately predicted rockfall runout zones and velocities at several sites in France and in Austria, it remains unknown whether it will reliably produce comprehensive results for other sites (Dorren et al., in press).

In this study, RockyFor is applied and evaluated on three different sites in the Swiss Alps with different slope and stand characteristics as well as with data sets of different qualities. The simulated rockfall patterns were then compared with empirical data obtained from the study sites. Finally, we used RockyFor to assess the protective effect of the investigated forest stands by comparing the results of simulation scenarios with and without the current forest cover.

2. Material and methods

2.1. The RockyFor model

RockyFor is a process-based rockfall simulation model that was originally developed with data obtained from field investigations in the Austrian Alps (Dorren et al., 2004). The model has since been improved and validated with data from 218 real-size rockfall experiments on forested and non-forested slopes in the French Alps (Le Hir et al., 2004; Dorren et al., 2005).

RockyFor uses raster maps as input files and simulates trajectories of falling, bouncing and rolling rocks ($\varnothing < 0.5$ m) and boulders ($\varnothing > 0.5$ m) within single raster cells. Moreover, it explicitly simulates the number of rockfall impacts against individual trees and sums them finally per raster cell. The model consists of three main modules. The first module calculates the rockfall trajectory, based on the topography of a site, which is represented by a Digital Elevation Model (DEM). At every step in the simulation, the fall direction of a rock can be towards one of the downslope cells from the cell where the rock is located during that simulation step. Hence, the model produces diverging rockfall trajectories.

The second main module calculates the energy loss due to impacts against single trees. As a result, the exact position of a falling rock and its current energy are modeled. If an impact against a tree takes place, the rock dissipates energy as a function of the relative position between rock and tree center and the stem diameter of the corresponding tree as follows:

$$\Delta E = -0.046 + \frac{0.98 + 0.046}{1 + 10^{[0.58-((P_i-\mathrm{CTA})/0.5\mathrm{DBH})-8.007]}} \quad (1)$$

where ΔE is the percentage of maximum amount of energy that can be dissipated by the tree (%); $P_i - \mathrm{CTA}$, the horizontal distance between the position of the impact and the vertical central axis of the tree as seen from the impact direction (m); DBH, the stem diameter at breast height (m). Thereby, the maximum amount of energy that can be dissipated by a tree (max. E. diss.) is a function of its DBH (m) as follows:

$$\text{max. E. diss.} = \text{FE_ratio} \times 38.7 \times \mathrm{DBH}^{2.31} \quad (2)$$

where max. E. diss. is the maximum amount of energy that can be dissipated by a tree (kJ); FE_ratio, the fracture energy ratio of a given tree species to *Abies alba* Mill. described by Dorren and Berger (2006); and DBH, the stem diameter at breast height (cm).

The third main module calculates the velocity of the falling rock after a rebound on the slope surface (for details see Dorren et al., 2004). Here, the decrease of velocity after a rebound is mainly dependent on the tangential coefficient of restitution (r_t), which is determined by the composition and size of the material covering the surface as well as the radius of the falling rock itself (Kirkby and Statham, 1975). The coefficient is calculated as a function of the radius of the rock and the mean radius of the material on the ground as follows:

$$r_t = \frac{1}{1 + (D_{\mathrm{mean}}/D_{\mathrm{rock}})} \quad (3)$$

where D_{mean} is the mean diameter of the material on the slope surface (m) and D_{rock}, the diameter of the falling rock (m). The calculated r_t is uniform randomly varied with 10% in order to take account: (i) the enormous local variation in the size of material covering rockfall slopes, as well as (ii) the geometry of the falling rock. Furthermore, its value is limited to the range (0.1, 0.99) as to avoid unrealistic energy loss (Dorren et al., 2004, in press).

2.2. Study sites

RockyFor was applied to three mountain forest sites in different areas of Switzerland. Fig. 1 gives an overview of the sites, while a summary of relevant site characteristics is presented in Table 1.

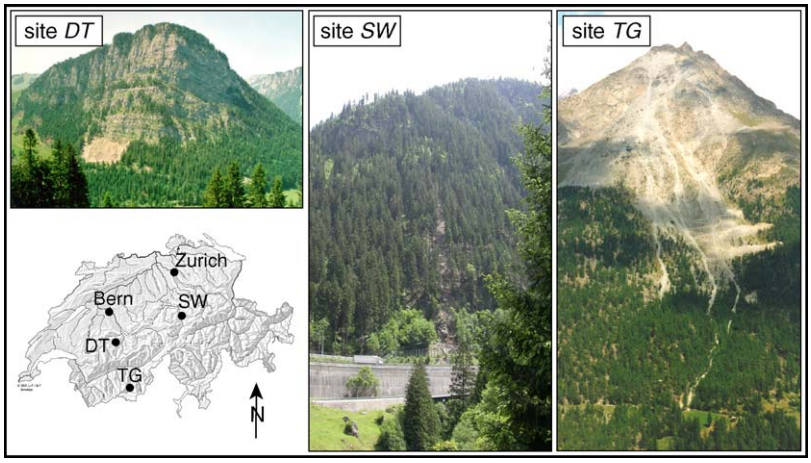


Fig. 1. Localization of the study sites Diemtigtal (site *DT*), Stotzigwald (site *SW*) and Täschgufer (site *TG*) within Switzerland.

The first site is a forest stand in the Diemtigtal (site *DT*) in the Swiss Prealps. The site lies at the foot of an approximately 400 m high limestone cliff (Fig. 1) on a southeast exposed talus slope with a mean slope gradient of 40°. The stand is dominated by *Picea abies* (L.) Karst. (77%), but other species such as *Sorbus aria* (L.) Crantz, *Sorbus aucuparia* L. or *Acer pseudoplatanus* L. occur as well (23%). The study site covers 0.3 ha, located between 1210 and 1280 m a.s.l. in the uppermost part of the talus slope. This area is in the transit zone of frequent, but mainly small falling rocks ($Ø \sim 0.2$ m). Below the study site, hiking trails and forest roads, which could be endangered by rockfall, traverse the slope.

The second site is the Stotzigwald (site *SW*), a stand in the central Swiss Alps covering a steep slope with a mean slope gradient of 45° and some interspersed cliffs (Fig. 1). This forest protects one of the most heavily used traffic routes connecting Germany and Italy. The elevation of the forest ranges from 650 to 1650 m a.s.l., but rockfall activity is mainly restricted to a zone of approximately 7.5 ha in the lower part of the forest, i.e. up to approximately 1000 m a.s.l. The stand within this zone mainly consists of *Picea abies* (83%) and *Abies alba* (13%). The slope is covered with rocks, boulders and morainic material. Bedrock consists of heavily weathered granite and gneiss. As a result, rockfall frequently occurs and rocks regularly reach the highway.

The third site is Täschgufer (site *TG*), which is located in the southern Swiss Alps (Fig. 1). Here, rockfall is frequently triggered from the heavily disintegrated paragneissic rockwalls below the Leiterspitzen summit (3214 m a.s.l.). In the upper part of the site, which covers 26 ha, mean slope gradients reach 48° and gradually decrease to 20° near the valley floor (1430 m a.s.l.). In the central area affected by rockfall, continuous forest cover reaches 1780 m a.s.l., whereas the upper part of the slope remains mostly free of vegetation. The stand predominantly consists of *Larix decidua* Mill. (95%), accompanied by single *Picea abies* and *Pinus cembra* ssp. sibirica. In the recent past, rockfall regularly reached the valley floor, causing damage to roads, hiking trails and agricultural buildings.

2.3. Model input data

For all sites, extensive data on stand structure, geomorphological characteristics and rockfall patterns were available from earlier field studies. In addition, dendrogeomorphological data on century-long fluctuations in rockfall activity exist for site *TG*. A summary of all input data used for the simulation with RockyFor is presented in Table 2.

In addition to the pre-existing data, complementary data on different site characteristics were gathered in the field (Kühne, 2005): Firstly, potential rockfall source areas were mapped, integrated into a Geographical Information System (GIS) and converted to raster maps. Secondly, terrain and vegetation parameters were mapped and polygons with homogeneous terrain characteristics described. From this data, a raster map was created for the normal coefficient of restitution (r_n; cf. Dorren and Seijmonsbergen, 2003) and for the mean diameter of the material covering the slope surface. The latter was required to calculate the tangential coefficient of restitution (r_t).

In a third step, complementary data on stand structure and empirical rockfall patterns were gathered on validation plots of approximately 225 m^2 (15 m × 15 m) at sites *SW* and *TG* so as to provide: (i) data on the tree diameter distribution and (ii) validation data for the simulation experiments. On these

Table 1
Characteristics of the three study sites

Study site (area)	Altitudinal range (m a.s.l.)	Mean slope (°)	Stand characteristics (main tree species, tree density, mean DBH)	Predominating size of rocks (mean diameter [m])
Diemtigtal (DT) 0.3 ha	1210–1280	40	*Picea abies*, 520 trees ha^{-1}, 21 cm	0.2
Stotzigwald (SW) 7.5 ha	650–1000	45	*Picea abies*, *Abies alba*, 561 trees ha^{-1}, 38 cm	0.7
Täschgufer (TG) 26 ha	1430–3214	20–48	*Larix decidua*, 150 trees ha^{-1}, 30 cm	0.9

Table 2
Data used for the simulation experiments

Feature class	Available data	Sampling method	Source	Derived model input
Stand structure	Species composition	Inventory sampling procedure on stand plots	Perret et al. (2004), Wehrli et al. (submitted), Stoffel et al. (2005a,b)	Stand raster map
	Diameter distribution	Inventory sampling procedure on stand plots	Kühne (2005), Perret et al. (2004), Wehrli et al. (submitted), Schneuwly (2003)	
	Tree density	Analysis of aerial photographs	Kühne (2005), Perret et al. (2004)	
Surface roughness	Granular composition of surface material	Estimation in five classes (<0.2 m, 0.2–0.5 m, 0.5–1 m, 1–2 m, >2 m)	Kühne (2005)	r_t-Raster map
	Vegetation cover	Estimation of proportion of bushes and shrubs	Kühne (2005)	
Subsurface damping	Damping properties of subsurface	Estimation in six classes (bedrock, scree/talus, stony soil, dry forest soil, fine humid soil)	Kühne (2005)	r_n-Raster map
DEM	Laser scan data (site DT)	Interpolation to raster using Spatial Analyst (ESRI 2005)	DTM-AV © 2004 Swisstopo (DV033531)	DEM
	Aerial photographs (sites SW & TG)	Deriving contour lines from aerial photographs and interpolation to raster using Spatial Analyst (ESRI 2005); surface points and breakline features assessed with ERDAS Stereo Analyst (Leica, 2005)	DEM © 2004 WSL, P. Thee (site SW) DEM © 2005 GIUB, R. Kühne (site TG)	
Rock properties	Rock size	Estimation of rock size description of recent accumulation (three granular classes)	Kühne (2005)	Rock size
Validation data	Number of tree impacts due to rockfall	Count of tree injuries due to rockfall in test plots	Kühne (2005), Perret et al. (2004)	Validation raster map
	Mean and max. impact heights	Assessment of h_{max}, h_{mean}	Kühne (2005), Perret et al. (2004), Schneuwly (2003), Stoffel et al. (2005a,b)	

validation plots, DBH was therefore measured for all individual trees with a DBH $\geq$ 8 cm. Rock impacts were assessed on the stem surface of trees, and the mean and maximum impact heights measured on every single tree. In order to derive forest stand maps as needed by RockyFor, field data were coupled with a tree distribution map obtained from photogrammetric analyses, where every individual tree crown was mapped on orthophotos (scale 1:9000). For site *DT*, no complementary data on stand and rockfall patterns were gathered, since data for every single tree on the site were available.

Finally, high resolution Digital Elevation Models (DEM) of 1 m × 1 m (site *DT*) and 5 m × 5 m (sites *SW* and *TG*) were produced. For site *DT*, we created a DEM by interpolating LIDAR (LIgth Detection And Ranging-Laser Scanning) point data delivered by the Swiss Topographical Service (Swisstopo, 2004) that represent the ground surface. The applied interpolation method was Ordinary Kriging using on average 12 points per raster cell. For site *SW*, the DEM was derived from contour lines (equidistance: 12.5 m) created on the basis of photogrammetric analyses realized with high quality aerial photographs (scale 1:9000). At site *TG*, in contrast, surface points and breakline features were generated from orthophotos (scale 1:9000) and coupled with 10 m contour lines digitized from a topographic map in a scale of 1:10,000.

2.4. Simulation set-up

Since RockyFor models rockfall on the basis of various stochastic algorithms, at least 100 simulation runs from each potential rockfall source cell were needed to obtain sufficiently stable results (Dorren and Heuvelink, 2004). In the first simulation run, one rock was released from each defined rockfall source cell, one after another, which means that the trajectory of each rock has been calculated individually. This process was then repeated 99 times. Thus, from a cliff that consists of 200 rockfall source cells, 20,000 rocks, and consequently different trajectories and velocities will be simulated.

To account for the varying size of falling rocks and boulders at the three sites, we simulated varying numbers of rocks for each size class (cf. Table 4). The selected number of simulations per size class was derived from estimates in the field and represents the diameter size distribution of rocks at the three sites.

The initial fall height of the rocks for the simulation experiments was set to 30 m at site *DT*, to 5 m at site *SW* and to 3 m at site *TG*. These values were determined by the morphology of the rockfall source areas and they correspond to the mean height of vertical cliff faces in the source areas of

the three sites. Simulation runs were first realized on the slopes with the ''current forest cover'', before trees were removed in the ''non-forested'' scenario and simulation runs repeated.

2.5. Assessment of model accuracy

Simulated and empirical rockfall patterns were compared on the basis of: (i) the spatial distribution of rockfall impacts on trees, which is an indicator for the spatial distribution of the rockfall trajectories and (ii) mean impact heights, which are indicators for bounce heights of rocks. To compare the simulation results with empirical values, we used the arithmetic mean per cell of the calculated variable taking into account all the simulation runs, since one simulation run cannot reproduce the data gathered in the terrain. At site *DT*, the accuracy of the model was assessed at the level of single trees, since detailed data were available (Perret et al., in press-a, in press-b). At sites *SW* and *TG*, however, the analysis was performed on validation plots of 225 m^2 (see Section 2.3). At site *TG*, simulation results were also compared with data on spatio-temporal variations in rockfall activity derived from dendrogeomorphological analysis of 129 living trees for the last 400 years (Stoffel et al., 2005b).

The number of rockfall impacts per tree was directly assessed from the empirical data for site *DT*. For sites *SW* and *TG*, a tree impact coefficient (TIC) was calculated as:

$$\mathrm{TIC} = \frac{\mathrm{TreeHits}_j}{n_{\mathrm{Trees},j}} \tag{4}$$

where $\mathrm{TreeHits}_j$ is the sum of tree impacts per validation plot j, and $n_{\mathrm{Trees},j}$, the number of trees in validation plot j. For standardization purposes, both empirical and simulated data were expressed as proportions relative to the summed values over all trees (site *DT*), and over all validation plots (sites *SW* and *TG*), respectively.

The mean impact height was calculated for every single tree (site *DT*) and for every validation plot (sites *SW* and *TG*). At site *TG*, impact heights were also integrated from century-old *Larix decidua* trees analyzed with dendrogeomorphological methods (Stoffel et al., 2005b). While tree-ring analysis yielded data on 786 rockfall impacts since 1394 AD, scars remained recognizable on the stem surface in less than 10% of all cases (Stoffel and Perret, submitted), mainly representing relatively recent or unusually large evidence of past rockfall events.

In a subsequent step, mean (ME) and root mean-squared errors (RMSE) between the predicted and the observed number of impacts and mean impact heights were calculated as follows:

$$\mathrm{ME} = \frac{1}{n}\sum_{i=1}^{n}(P_i - O_i) \tag{5}$$

$$\mathrm{RMSE} = \sqrt{\frac{1}{n}\sum_{i=1}^{n}(P_i - O_i)^2} \tag{6}$$

where n is the number of trees (site *DT*) or validation plots (sites *SW* and *TG*); P_i, the predicted (i.e. simulated) and O_i, the observed rock impacts at tree i (site *DT*) and validation plot i (sites *SW* and *TG*).

Furthermore, the proportional difference between the predicted and the observed number of impacts was calculated for each tree (site *DT*) and each validation plot (sites *SW* and *TG*), and then illustrated for deviations $\geq$2.5% and $\geq$5%. Thus, the simulated trajectories of all size classes of rocks were summed and compared with the empirical patterns.

2.6. Assessment of the protective effect of the different stands

The protective effect of the stands was then assessed at the three sites by quantifying changes in the frequency of simulated rockfall trajectories between the scenarios ''current forest cover'' and ''non-forested slope''. Differences were assessed in ''evaluation zones'' at the foot of every test slope where high damage potential exists (i.e. roads or buildings). We defined these zones in a vector map, which was subsequently transformed into a raster map. We then compared the number of rocks that entered the ''evaluation zones'' in the simulated raster maps containing the stopping positions of the rocks as produced by the two modeling scenarios. This has been done for all the simulated diameter classes. The difference between the two scenarios has been quantified by the following ratio:

$$\mathrm{RF_ratio}_i = \frac{\mathrm{PR}_{\text{non-forested_slope},i}}{\mathrm{PR}_{\text{forested_slope},i}} \tag{7}$$

where $\mathrm{PR}_{\text{non-forested_slope},i}$ and $\mathrm{PR}_{\text{forested_slope},i}$ are the number of rocks per diameter class i passing the evaluation zone on the non-forested and forested slope, respectively. Furthermore, the protective effect of the two scenarios was compared graphically after summing the simulated trajectories over all diameter classes of rocks.

Table 3
Mean (ME) and root mean-squared errors (RMSE) between observed number of tree hits and impact heights (h_{mean}) and model results obtained at study sites *DT*, *SW*, *TG* dataset 1 and *TG* dataset 2 (for explanation see text)

Site	Number of trees	Number of tree hits or TIC		Mean impact height		
		ME (%)	RMSE (%)	h_{mean} observed (m)	ME (m (%))	RMSE (m (%))
DT	138	0	0.9	0.8	−0.2 (−26)	0.4 (57)
SW	23	0	3.6	1.1	2.6 (230)	3.5 (310)
TG dataset 1	46	0	4.4	1.1	−0.6 (−59)	1.1 (96)
TG dataset 2	129/38	0	3.6	1.7	−1.4 (−85)	1.7 (101)

3. Results

3.1. Model accuracy

In general, the simulation experiments yielded very close matches between simulated and empirical spatial distributions of tree impacts on all three sites. However, for mean impact heights, the correspondence between simulated and observed data varied considerably.

At site *DT*, the simulated number of tree hits corresponds well with the empirical data, as indicated by the RMSE of 0.9% (Table 3). Fig. 2a shows that differences predominantly occur in the uppermost sector of the study site, where the model overestimates the number of hits in nine trees by +2.5 and +5%. On the southwestern edge of the study site, the model, in contrast, underestimates the number of impacts in one tree by more than −5%. For the remaining 128 trees (93%), differences between the predicted and the observed number of tree hits remain between ±2.5%. On the other hand, differences can be seen with impact heights, where RockyFor underestimates the mean impact height by −0.21 m (ME) and 0.46 m (RMSE). As can be seen from Table 3, deviations from the observed mean impact height (0.85 m), therefore, account for 26% (ME) and 57% (RMSE).

At site *SW*, the predicted tree impact coefficient (TIC) pattern matches the empirical data from the validation plots with a RMSE of 3.6% (Table 3). As illustrated in Fig. 2b, the model more commonly overestimates the number of tree hits, but underestimates occur as well. Differences exceeding ±5% are identified in four validation plots (17%) and prediction errors ranging from 2.5% to 5% are present in six plots (26%). In the other 13 validation plots (i.e. 57%), the difference between the predicted and the observed number of tree hits remains within a range of ±2.5%. As shown in Table 3, RockyFor overestimates, in contrast, mean impact heights with a ME of +2.6 m and a RMSE of 3.5 m. Compared to the mean impact height of 1.1 m observed in the field, this corresponds to an overestimation of 210% (ME) and 310% (RMSE), respectively.

At site *TG*, simulated rockfall data are compared with data gathered on 46 validation plots in the field (*TG* dataset 1) as well as with results from dendrogeomorphological reconstructions of past rockfall activity (*TG* dataset 2). As indicated in Table 3, the model again accurately predicts the empirical TIC pattern with a RMSE of 4.4% for *TG* dataset 1 and 3.6% for *TG* dataset 2. For *TG* dataset 1, underestimation occurs in eight validation plots (17%) with differences between the observed and the predicted number of tree impacts primarily remaining between −2.5% and −5%. For *TG* dataset 2, in contrast, overestimation can be observed in seven out of 129 validation plots (5%), mostly exceeding +5%, whereas underestimation can only be found in one plot (1%). Interestingly, the overestimated validation plots are concentrated along the upper fringe of the continuous forest stand and near the rockfall channel, as shown in Fig. 2c. Results also indicate that in 80% (*TG* dataset 1) and 94% (*TG* dataset 2) of the validation plots, differences between simulated and predicted TIC patterns remain within a range of ±2.5%.

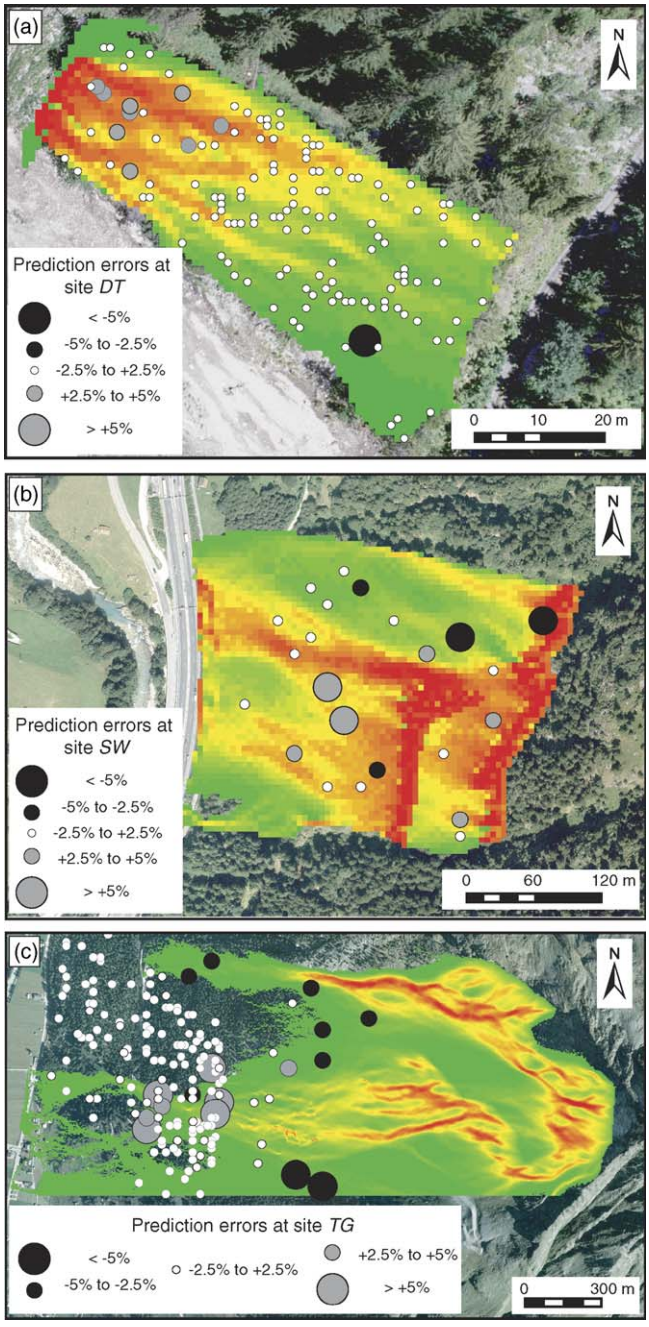


Fig. 2. Differences between simulated and observed number of rock impacts on trees or validation plots at: (a) site *DT*, (b) site *SW* and (c) site *TG*. Gray circles indicate an overestimation by the model, whereas black circles show underestimation. White circles represent trees or validation plots with a very similar number of rock impacts for simulations and observations (±2.5%) (orthophoto sources: site *DT*: © Baumgartner (2002); site *SW*: © Kanton Uri; site *TG*: © 2005 swisstopo (BA056895).

In contrast, we observed a difference between the empirical and simulated impact heights. For *TG* dataset 1, the model underestimates the mean impact height observed in the field (1.1 m) with a ME of −0.6 m and a RMSE of 1.1 m. As can be seen from Table 3, this corresponds to a relative underestimation of 59% and 96%, respectively. For *TG* dataset 2, the observed mean impact height (1.7 m) is underestimated with a ME of −1.4 m (85%) and a RMSE of 1.7 m (101%).

Table 4
Assessment of the protective effect of the investigated stands

Site start cells	Forest cover		Diameter of RF (m)											
			0.1	0.2	0.3	0.4	0.6	0.8	1	1.2	1.4	1.6	1.8	2
Site *DT* start cells 12		RF triggered	1500	2000	1500	–	–	–	–	–	–	–	–	–
	Forested	Passing RF (%)	0.7	5.2	13									
	Non-forested	Passing RF (%)	6	18.1	32.4									
		RF_ratio	8.5	3.5	2.5									
Site *SW* start cells 331		RF triggered	–	1200	–	1500	1200	1000	600	500	200	200	100	100
	Forested	Passing RF (%)		1.5		3	5.2	5.7	6.7	7.9	8.4	8.8	8.7	8.7
	Non-forested	Passing RF (%)		3.9		6.8	8.8	9.5	15.8	9.9	9.9	9.9	9.9	9.9
		RF_ratio		2.5		2.3	1.7	1.7	2.4	1.3	1.2	1.1	1.1	1.1
Site *TG* start cells 7692		RF triggered	–	1200	–	1500	1200	1100	1000	800	700	600	500	400
	Forested	passing RF (%)		0		0	0	0.001	0.002	0.003	0.006	0.011	0.035	0.057
	Non-forested	passing RF (%)		0		0	0	0.004	0.011	0.018	0.026	0.043	0.076	0.107
		RF_ratio		0		0	0	4.5	6.7	5.5	4.1	4.1	2.2	1.9

The number of rockfall fragments (RF) triggered per diameter class and start cell is given as *n*. The percentage of rocks and boulders passing the evaluation zones is given for the scenarios ''forested slope'' and ''non-forested slope'' and the differences between the two scenarios expressed with a RF_ratio (for explanation see text).

3.2. Protective effect

The comparison between the two simulation scenarios ''current forest cover'' and ''non-forested slope'' yielded significant differences for all three sites. Table 4 first of all shows that the number of rocks and boulders passing the evaluation zones was considerably higher in the ''non-forested'' scenario.

At site *DT*, the complete removal of the forest stand would result in more rocks passing the evaluation zone at the foot of the study site, as indicated by the high RF_ratios between the two scenarios. As can be seen from Table 4, this is particularly true for the smallest rock diameter class (0.1 m) used in the simulation runs, for which the RF_ratio increased by a factor of 8.5, as compared to the scenario with the ''current forest cover''. Fig. 3 gives a qualitative impression of the differences emerging between the two scenarios, indicating that the increase in the transit of rocks is most obvious in the northeastern and central parts of the study site. In contrast, negative effects appear to be less drastic in the southern half, where frequencies only slightly increased in the ''non-forested'' scenario.

At site *SW*, the number of rocks passing the evaluation zone is rather high in both scenarios. As shown in Table 4, differences between the two scenarios are most obvious for rocks and small boulders of up to 1 m in diameter, where RF_ratios varied between a factor of 1.7 and 2.5. Fig. 3 illustrates that in the ''non-forested'' scenario, a considerable increase in the number of rockfall trajectories can be observed below the subvertical cliff in the central part of the study site. Results also indicate that in the scenario with the ''current forest cover'', rocks originating from this cliff would be partly stopped through the presence of trees, whereas the absence of trees would allow most rocks and boulders to travel down the slope and reach the adjacent highway. A similar protective effect of the stand is evident for rocks originating from the uppermost cliff area.

In contrast to sites *DT* and *SW*, Table 4 indicates that the differences in the number of rocks and boulders passing through the evaluation zone at site *TG* are considerably smaller for most diameter classes. Nonetheless, significant differences arise between the two scenarios for boulders with diameters >0.8 m, as indicated by the high RF_ratios in Table 4. The qualitative comparison of the scenarios in Fig. 3 indicates a minor increase in the number of rocks passing down the slope in the rockfall channel located in the northwestern part of the study site, where the number of deposited rocks and boulders doubles in some locations. In the central part of the study site, rockfall activity increases as well, meaning that boulders would more frequently reach the main road in the valley floor (Fig. 3).

4. Discussion

4.1. Model accuracy

In the study we report here, the 3D rockfall simulation model RockyFor was tested and its capability to accurately predict rockfall patterns assessed at three forested sites in the Swiss Alps. Overall, the comparison of observed with simulated rockfall patterns yielded a high correspondence for the spatial distribution of tree impacts and a low correspondence for the mean impact heights.

The closest match between empirical and simulated distributions of tree impacts was obtained at site *DT*, where a highly resolved DEM (1 m × 1 m) allowed very accurate modeling of rockfall trajectories. At sites *SW* and *TG*, the simulation based on a 5 m × 5 m DEM derived from contour lines with an equidistance of 12.5 m (site *SW*) and 10 m (site *TG*) still yielded close matches between the empirical and predicted distribution of tree impacts with RMSE ≤4.4%. As stochastic elements are involved in rockfall processes, a complete agreement of empirical and simulated trajectories is unlikely, which is why we believe that for an accurate prediction of the spatial envelope of rockfall trajectories, a

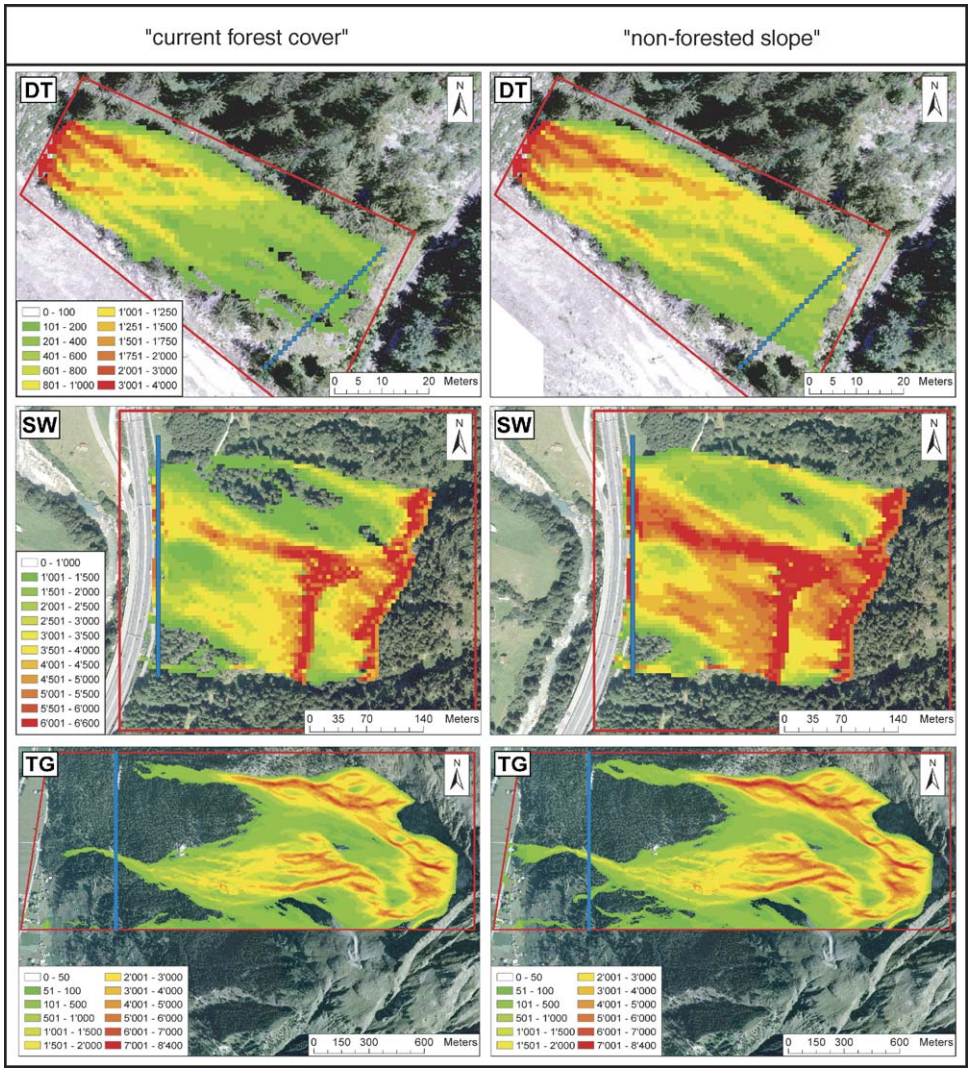


Fig. 3. Comparison of simulated rockfall trajectories for the ''current forest cover'' (left) and for the ''non-forested slope'' (right) at: (a) site *DT*, (b) site *SW* and (c) site *TG*. Evaluation zones are indicated with blue lines.

DEM with a resolution of 5 m × 5 m – as used at sites *SW* and *TG* – is largely sufficient.

In contrast to the spatial distribution of rockfall trajectories, the prediction of mean impact heights was less accurate. Even at site *DT*, predicted mean impact heights were considerably lower than the values observed in the field. This low correspondence is particularly surprising, since RockyFor produced close matches between empirical and simulated mean impact heights for a site in the French Alps, based on a DEM with a resolution of 2.5 m × 2.5 m (Dorren et al., submitted for publication). The underestimation of mean impact heights further increased at site *TG*, where the model produced a negative bias for both *TG* dataset 1 and *TG* dataset 2. In contrast, RockyFor largely overestimated mean impact heights at site *SW*.

The reasons for the poor correspondence between the predicted and the observed mean impact heights may be manifold. Since RockyFor was calibrated on the basis of more than 200 real-size experiments (Dorren et al., 2005) and different rockfall patterns, including mean impact heights accurately predicted before, we believe the main reasons for the rather low agreement between empirical and simulated mean impact heights to be model-independent rather than model-intrinsic.

A first factor that might have affected the accuracy of the simulation results is the DEM, i.e. its spatial resolution. This is particularly true for sites *SW* and *TG*, where DEMs were derived from contour lines with relatively low resolution. Consequently, micro-topographical structures are neglected in the DEM, which in turn can influence the velocity of falling rocks. For instance, huge boulders from ancient rockslide deposits could not be included in the DEM at site *TG*. These boulders may, however, cause rocks to bounce and therefore produce higher impacts than suggested by the model. At site *SW*, the rather coarse DEM was probably the main reason for the large overestimation of the mean impact height, since on this steep slope with an average inclination of 45°, the frequently occurring, abrupt changes in the slope gradient could probably not be reproduced in the DEM with sufficient accuracy. These observations are in agreement with

Agliardi and Crosta (2003), who report a decrease in bounce height in the flatter parts of the slope and an increase in bounce height on steeper slopes as soon as the resolution of support data decreases. When using a 5 m × 5 m DEM, it would, therefore, be preferable if the underlying data had a support of at least five meters as well (e.g., 1–5 m contour lines or LIDAR data), so as to take essential terrain features into account.

A second factor influencing the mean impact height in the model can be identified in the uncertainty related to the delineation of rockfall source areas and initial fall heights. Within the present study, we determined rockfall source areas based on observations and geological advisory opinions. A large number of rocks were triggered from these start cells with a given initial fall height, which again was determined based on qualitative field observations. It is, however, clear that these observations can only be seen as an approximation to reality, since precise determination of rockfall source areas and initial fall heights was rendered impossible by complex terrain features such as the 400 m high limestone cliff at site *DT*, or subvertical cliffs at site *SW*. Nonetheless, a more precise assessment of the rockfall source areas and the initial fall heights seem to be decisive for a better prediction of bounce heights of rocks and, consequently, impact heights on trees.

A third factor affecting modeled impact heights is represented by the validation datasets, which were mainly based on the assessment of impact scars visible on the stem surface of trees. As previously shown by Stoffel (2005, in press), scars as evidence of past rockfall events may become completely blurred with time and are, as a consequence, no longer visible on the stem surface. On the other hand, it is also conceivable that large scars caused by high-energy impacts at unusually high positions may persist for a long time on the stem surface, and therefore lead to an overestimation of rare impact heights. Nonetheless and as half of the scars caused through the action of large rocks (Ø 0.8 m) prove to be no longer visible on the stem surface of Larix decidua Mill. after as little as 20 years (Stoffel and Perret, submitted), we believe that our field observations of impact heights and trajectory frequencies accurately illustrate the recent rockfall activity occurring in the current forest stands. Furthermore, the accuracy of the validation datasets was also influenced by the tree species and the age of single trees. At site *TG*, for instance, the overestimated plots illustrated in Fig. 2c largely occur in areas where juvenile trees are recolonizing the slope. In contrast to their older neighbors, these trees only show a comparably low number of scars in the field, as there has not been sufficient time for scarring.

Other factors such as the small number of test plots for site *SW* or minor inaccuracies in the r_t/r_n-maps may have influenced the prediction of mean impact heights as well, but the three factors mentioned above are probably of prime importance. Nevertheless, model results clearly indicate that the 3D process-based model RockyFor is able to accurately predict the spatial envelope of rockfall trajectories based on input data with a resolution of 5 m × 5 m.

4.2. Protective effect

The second aim of this study was to assess the protective effect of the investigated stands against rockfall through a comparison of simulation scenarios with the ''current forest cover'' and on a ''non-forested slope''. This allowed quantification of the protective effect of the forest stands at the three sites, as indicated by the RF_ratios between the scenarios.

The protective effect of the stands is highest for rocks and small boulders (diameter ≤ 1 m) at sites *DT* and *SW* (cf. Table 4). Here, the number of rocks passing through the evaluation zones is between 1.7- and 8.5-times higher in the ''non-forested'' scenario, indicating an effective protective function of the current stands. At site *TG*, the stand seems, in contrast, to protect objects at risk from (large) boulders ranging from 0.8 m to 2 m in diameter rather than from smaller rocks. Even though rocks passing through the evaluation zone appear to occur much less frequently here, the protective effect of the stand should not be discounted.

We therefore think that at all three sites, the hazard potential would increase strongly without the current stands: At site *DT*, rocks would more frequently reach the forest road and endanger the nearby hiking trails, whereas at sites *SW* and *TG*, important infrastructure would be endangered (site *SW*: highway, site *TG*: main road, buildings). Given the high damage potential at sites *SW* and *TG*, several countermeasures have been taken in the recent past. At site *SW*, restraining nets have been constructed along the highway, whereas at site *TG*, seven dams have been built on the slope. As evident from our simulation results, these countermeasures are more than justified.

5. Conclusions

This study clearly showed that, based on input data with a resolution of at least 5 m × 5 m, RockyFor is able to accurately predict the spatial distribution of rockfall trajectories on forested sites with different slope and stand characteristics. In contrast, we were unable to confirm an accurate prediction of mean impact heights in the present. We believe that high-resolution input data including e.g., a laser scan based DEM, a better knowledge of rockfall source areas, and data on initial fall heights would considerably improve the quality of the predicted impact heights. In addition, the use of dendrogeomorphological analyses increases the amount and quality of validation data and should be used more systematically in rockfall forest research.

Due to its ability to accurately predict the spatial envelope of rockfall trajectories, the present version of RockyFor also provides a valuable research tool for investigating the protective effect offered by different stand structures.

Acknowledgements

We are grateful to the European Commission for the Marie Curie Fellowship (QLK5-CT-2002-51705). Additional funding was provided by the Swiss National Science Foundation (grant 4048-064409) and the Swiss Forest Agency. We kindly acknowledge Marc Baumgartner, Catherine Berger, Monika

Fässler, Connie Hett, Dominique Schneuwly and Mathias Zesiger for assistance in the field. Igor Lièvre and Patrick Thee are acknowledged for generating contour lines for sites *TG* and *SW*. We are grateful to Walter Schönenberger and Frédéric Berger for their valuable comments on a former draft and Heather Murray for improving the English of the paper. Finally, we would like to thank Swisstopo for providing the aerial photographs.

References

Agliardi, F., Crosta, G.B., 2003. High resolution three-dimensional numerical modelling of rockfalls. Int. J. Rock Mech. Mining Sci. 40, 455–471.

Bartelt, P., Stöckli, V., 2001. The influence of tree and branch fracture, overturning and debris entrainment on snow avalanche flow. Ann. Glaciol. 32, 209–216.

Baumgartner, M., 2002. Detaillierte Ersterhebungen in einem steinschlaggeschädigtem Wald im Diemtigtal. Diploma thesis. Geographisches Institut, Universität Bern, Bern.

Berger, F., Quétel, C., Dorren, L.K.A., 2002. Forest: a natural protection mean against rockfall, but with which efficiency? The objectives and methodology of the ROCKFOR project. In: Proceedings of the International Conference on Congress Interpraevent 2002 in the Pacific Rim, Matsumoto/Japan, pp. 815–826.

Berger, F., Lievois, J., 1999. Determination of priority forest work areas and creation of green areas in risk prevention plans—an example of researcher-specialist transfer. In: Gillet, F., Zanolini, F. (Eds.). In: Proceedings of the International Conference on Mountainous Natural Hazards, Grenoble, France, pp. 412–416.

Bloetzer, W., Stoffel, M., 1998. Klimawandel als Herausforderung für die Raumplanung der Vispertäler. In: Bloetzer, W., Egli, T., Petrascheck, A., Sauter, J., Stoffel, M. (Eds.), Klimaänderungen und Naturgefahren in der Raumplanung—Methodische Ansätze und Fallbeispiele. vdf Hochschulverlag AG, Zürich, pp. 127–200.

Brang, P., Schönenberger, W., Ott, E., Gardner, R.H., 2001. Forests as protection from natural hazards. In: Evans, J. (Ed.), The Forests Handbook. Blackwell Science Ltd., Oxford, pp. 53–81.

Cattiau, V., Marie, E., Renaud, J.P., 1995. Forêt et protection contre les chutes de rochers. Ingénieries Cemagref Eau-Agriculture-Territoire 3, 45–54.

Chauvin, C., Renaud, J.P., Rupé, C., 1994. Stabilité et gestion des forêts de protection. ONF Bull. Techn. 27, 37–52.

Dorren, L.K.A., Seijmonsbergen, A.C., 2003. Comparison of three GIS-based models for predicting rockfall runout zones at a regional scale. Geomorphology 56 (1–2), 49–64.

Dorren, L.K.A., Heuvelink, G., 2004. Effect of support size on the accuracy of a distributed rockfall model. Int. J. GIS 18, 595–609.

Dorren, L.K.A., Berger, F., 2006. Stem breakage of trees and energy dissipation at rockfall impacts. Tree Physiol. 26, 63–71.

Dorren, L.K.A., Maier, B., Putters, U.S., Seijmonsbergen, A.C., 2004. Combining field and modelling techniques to assess rockfall dynamics on a protection forest hillslope in the European Alps. Geomorphology 57 (3–4), 151–167.

Dorren, L.K.A., Berger, F., LeHir, C., Mermin, E., Tardif, P., 2005. Mechanisms, effects and management implications of rockfall in forests. For. Ecol. Manage. 215 (1–3), 183–195.

Dorren, L.K.A., Berger, F., Putters, U.S., in press. Real size experiments and 3D simulation of rockfall on forest slopes. Nat. Haz. Earth Syst. Sci.

Frehner, M., Wasser, B., Schwitter, R., 2005. Nachhaltigkeit und Erfolgskontrolle im Schutzwald. Wegleitung für Pflegemassnahmen in Wäldern mit Schutzfunktion. Bundesamt für Umwelt, Wald und Landschaft, Bern.

Gsteiger, P., 1993. Steinschlagschutzwald. Ein Beitrag zur Abgrenzung, Beurteilung und Bewirtschaftung. Schweiz. Z. Forstwes. 144 (2), 115–132.

Hétu, B., Gray, J.T., 2000. Effects of environmental change on scree slope development throughout the postglacial period in the Chic-Choc Mountains in the northern Gaspé Peninsula, Québec. Geomorphology 32, 335–355.

Jahn, J., 1988. Entwaldung und Steinschlag, In: Proceedings of the International Congress on Interpraevent, 1988, Graz. Band 1, pp. 185–198.

Kirkby, M.J., Statham, I., 1975. Surface stone movement and scree formation. J. Geol. 83, 349–362.

Krummenacher, B., Keusen, H.R., 1996. Rockfall simulation and hazard mapping based on digital terrain model (DTM). Eur. Geol. 12, 33–35.

Kühne, R., 2005. Steinschlagsimulation in Gebirgswäldern–Validierung und Anwendung eines 3D Modells zur Quantifizierung der Schutzwirkung von Wald. Diploma thesis. Department of Geography. University of Berne, Berne.

Lafortune, M., Filion, L., Hétu, B., 1997. Dynamique d'un front forestier sur un talus d'éboulis actif en climat tempéré froid (Gaspésie, Québec). Geogr. Phys. Quat. 51 (1), 1–15.

Le Hir, C., Berger, F., Dorren, L.K.A., Quetel, C., 2004. Forest: a natural means of protection against rockfall, but how to reach sustainable mitigation? In: Proceedings of the International Symposium Interpraevent 2004, Riva/Trient, Italy, V, pp. 59–69.

Leibundgut, H., 1986. Unsere Gebirgswälder. Paul Haupt Verlag, Bern, Stuttgart.

Mahrer, F., Bachofen, H., Brändli, U.-B., Brassel, P., Kasper, H., Lüscher, P., Riegger, W., Stierlin, H.-R., Strobel, T., Sutter, R., Wenger, C., Winzeler, K., Zingg., A., 1988. Schweizerisches Landesforstinventar: Ergebnisse der Erstaufnahme 1982–1986. Eidgenössische Forschungsanstalt für Wald, Schnee und Landschaft, Birmensdorf.

Mössmer, E.M., Ammer, U., Knoke, T., 1994. Technisch-biologische Verfahren zur Schutzwaldsanierung in den oberbayrischen Kalkalpen. Forstl. Forsch. ber. München 145: 135.

Perret, S., Baumgartner, M., Kienholz, 2004. H., Steinschlagschäden in Bergwäldern—Eine Methode zur Erhebung und Analyse. In: Proceedings of the International Symposium Interpraevent 2004, Riva/Trient, Italy, V, pp. 87–98.

Perret, S., Baumgartner, M., Kienholz, H., in press-a. Inventory and analysis of tree injuries in a rockfall-damaged forest stand. Eur. J. For. Res.

Perret, S., Stoffel, M., Kienholz, H., in press-b. Spatial and temporal rockfall activity in a forest stand in the Swiss Prealps—a dendrogeomorphological case study. Geomorphology.

Schönenberger, W., Noack, A., Thee, P., 2005. Effect of timber removal from windthrow slopes on the risk of snow avalanches and rockfall. For. Ecol. Manage. 213, 197–208.

Schneuwly, D., 2003. 500-jährige Rekonstruktion der Steinschlagfrequenz im Täschgufer anhand dendrogeomorphologischer Methoden. MSc thesis. Department of Geosciences, Geography. University of Fribourg, Fribourg.

Stoffel, M., in press. A review of studies dealing with tree rings and rockfall activity: the role of dendrogeomorphology in natural hazard research. Nat. Hazards.

Stoffel, M., 2005. Assessing the vertical distribution and visibility of rockfall scars in trees. Schweiz. Z. Forstwes. 156 (6), 195–199.

Stoffel, M., Perret, S., submitted for publication. Reconstructing past rockfall activity with tree rings: some methodological considerations. Dendrochronologia, in review.

Stoffel, M., Lièvre, I., Monbaron, M., Perret, S., 2005a. Seasonal timing of rockfall activity on a forested slope at Täschgufer (Valais, Swiss Alps)—a dendrochronological approach. Z. Geomorph. 49 (1), 89–106.

Stoffel, M., Schneuwly, D., Bollschweiler, M., Lièvre, I., Delaloye, R., Myint, M., Monbaron, M., 2005b. Analyzing rockfall activity (1600–2002) in a protection forest—a case study using dendrogeomorphology. Geomorphology 68 (3–4), 224–241.

Swisstopo, 2004. http://www.swisstopo.ch/de/vd/lwn_etat.htm (as seen on 4 March 2005).

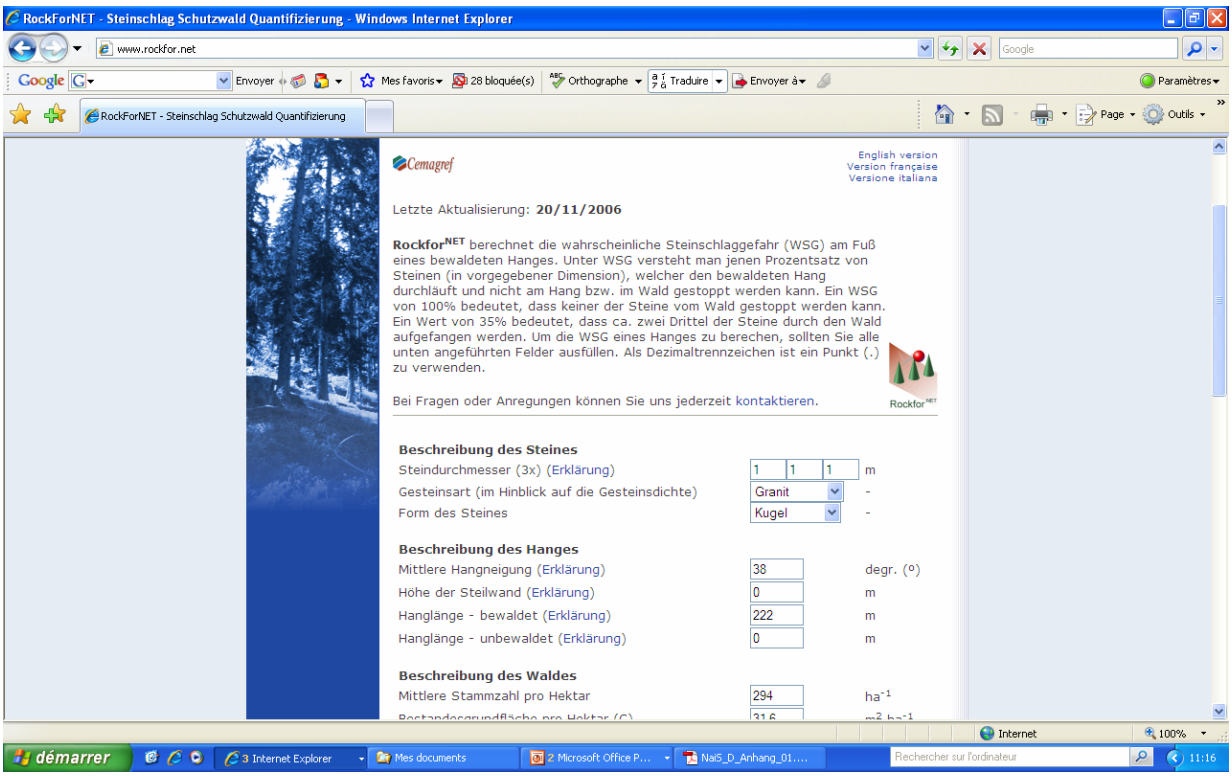
Wasser, B., Frehner, M., 1996. Minimale Pflegemassnahmen für Wälder mit Schutzfunktionen. Wegleitung. Bundesamt für Umwelt, Wald und Landschaft (BUWAL), Berne.

Wehrli, A., Weisberg, P.J., Schönenberger, W., Brang, P., Bugmann, H., submitted for publication. Improving the establishment of a forest patch model to predict the long-term protective effect of mountain forests. Eur. J. For. Res., in review.

Zinggeler, A., Krummenacher, B., Kienholz, H., 1991. Steinschlagsimulation in Gebirgswäldern. Berichte und Forschungen des Geographischen Instituts der Universität Fribourg 3, 61–70.

> Chapter 11

Principles of a simple rockfall - forest assessment tool



Principles of the tool Rockfor.net for quantifying the rockfall hazard below a protection forest

Frédéric Berger Cemagref Grenoble (FR)*
Luuk K.A. Dorren Cemagref Grenoble (FR)

Principles of the tool Rockfor.net for quantifying the rockfall hazard below a protection forest

There are presently no clear rules for determining optimal rockfall protection forests, taking into account forest and site characteristics as well as the size and energy of the falling rock. To provide a tool that meets these requirements and quantifies the protective capacity, we have developed Rockfor.net (www.rockfor.net). This paper explains the underlying principles as well as the calculation methods used. Furthermore, it presents case studies which provide validation.

Keywords: residual hazard, energy line, basal area, web-based tool
doi: 10.3188/szf.2007.0157

* 2 rue de la Papeterie, BP 76, F-38402 Saint Martin d'Hères cedex, E-Mail frederic.berger@cemagref.fr

In mountainous areas rockfall is a natural process, but due to its spontaneous release and its extreme velocities it can pose a risk for settlements and traffic routes. In this article we define rockfall as the fall of individual rocks from a cliff face (Selby 1982), where the volume of the rock can vary from one litre to several cubic meters. Rockfall occurs at all steep rock faces due to weathering and mechanical influences (Erismann & Abele 2001). At locations where hazardous rockfall events have occurred in the past, detailed studies are often carried out for risk zoning and dimensioning civil protective structures. Although civil engineering techniques developed rapidly during recent years, the possibilities for technical protection are restricted and, above all, very costly. In the European Alps, however, there are many elements that need to be protected from rockfall, as clearly indicated by the number of rocks that are stopped in forests that are upslope of many roads and settlements. Those rocks also show that forests offer an ecologically friendly and cost efficient alternative to technical protective measures against rockfall as confirmed by Jahn (1988), Gsteiger (1993), Kienholz & Mani (1994), Schwitter (1998) and Dorren et al (2005).

The forester, who is responsible for the protection provided by forests, has to be able to quantify rapidly the state of affairs regarding the protective function in a forest stand for three reasons: firstly, because a decision has to be made upon which forests require silvicultural interventions to prevent an increase of the risk posed by rockfall. Due to the natural evolution of forest stands, the protective capacity against rockfall of a forest changes over time (Ott 1978, Brang 2001). Such curative interventions prevent running behind the facts. Secondly, a quantification of the protective potential of a forest stand allows mapping forest zones where a protective function should be assigned. Thirdly, it is needed to target more detailed site investigations on local rockfall hazards as well as targeting future investments in rockfall protection using mixed civil engineering – forest management techniques.

A rapid assessment implies the calculation of the protective capacity of a forest stand using a small dataset, formalised in a user-friendly tool. The input data should give a global representation of reality and should be easy to acquire; for example, at the scale of the slope or the forest stand. Until now, an adequate tool that meets these requirements does not exist.

There are, however, guidelines for rockfall protection forests that give an idea about the required stand densities and diameters (e.g., Wasser & Frehner 1996). More recent guidelines relate required stand characteristics to the dominating rock size (e.g., Frehner et al 2005, Gauquelin et al 2006). The latter is a very important parameter, as smaller rocks have a lower impact probability, but also a low kinetic energy. Larger rocks have a higher impact prob-

ability and much more kinetic energy. In addition, the size of a rock significantly influences its modes of motion (Gerber 1998). Tools that do take the effect of the size of the falling rock into account are 2D and 3D rockfall trajectory simulation models (e.g., Zinggeler 1990, Spang & Sönser 1995, Le Hir 2005, Dorren et al 2006). However, these models require expert knowledge on modelling and on the acquisition of model parameter values in the field. As such, they are not user-friendly for forest practitioners.

One of the first concepts for quantifying the protective capacity of forests against rockfall that took the rock size into account was the «Mean Tree Free Distance» (MTFD) of Gsteiger (1993), later adapted by Perret et al (2004), Brauner et al (2005) and Dorren et al (2005). The MTFD refers to the average distance a rock travels between two tree contacts. This distance is calculated on the basis of the size of the rock, the stand density for a given planimetric area and the mean tree diameter at breast height (DBH) in that given area. Therefore, the MTFD is always expressed as a planimetric distance. Gsteiger (1993) assumed that forest stands whose MTFD exceeds 40 m cannot effectively slow down or stop falling rocks. This, however, depends on the mean slope gradient of the terrain covered by the protection forest and, more importantly, on the energy the rock develops. What is therefore very much needed is a tool that takes the slope gradient and the rock energy into account. A simple field measurement that compensates for the slope gradient is the basal area measured with a relascope (Bitterlich 1984). In addition Dorren et al (2005) state that it is a certain surface of a tree that intercepts a falling rock rather than the tree diameter. These arguments both support the development of a tool that is based on the basal area.

In summary, despite the MTFD concept and the available guidelines, there are presently no clear quantitative rules for determining the required combination of stand density and basal area, regardless of being translated into a mean DBH. This required combination should depend on the dominating rock size, its kinetic energy (to a high degree determined by the slope gradient), the length of the forested slope and the tree species present in a forest stand. To provide a tool that quantifies rapidly the protective capacity of a forest stand against rockfall, which takes into account the above mentioned parameters, we developed Rockfor.net. In this paper our first aim is to explain the underlying principles, our second is to describe the used calculation methods and our third aim is to present case studies that served for validating the tool.

Materials and methods

Real-size rockfall experiments

To calibrate the parameters used in the different calculations carried out by Rockfor.net, we carried out real-size rockfall experiments in the Forêt Communale de Vaujany in the French Alps (lat 45°12′, long 6°3′). The site (Figure 1) that has been analysed in detail for this study has an altitude ranging from ~1200 m to ~1400 m above sea level and a mean slope gradient of 38°. We released 57 individual rocks with a mean diameter of 1 m from a forest road straight down the slope, using a Caterpillar hydraulic excavator. The mean rock volume was 0.52 m^3 (min. = 0.15 m^3; max. = 1.51 m^3; stddev. = 0.32 m^3, n = 57) and the mean rock mass was 1466 kg. Additional details on the experimental protocol are presented by Dorren et al (2005). The area investigated in detail for this study covers a triangle with a base of 106 m and a height of 300 m. This corresponds to a lateral deviation from the steepest down slope descent of 10° to both sides, which covers the maximum lateral deviation of the rocks released during the experiments. The mean stand density in this area is 294 trees/ha. The total basal area measured was 31.6 m^2/ha, which gives a mean DBH of 36.9 cm. The main tree species in this area are silver fir (*Abies alba* – 57%), Norway spruce (*Picea abies* – 13%), European beech (*Fagus sylvatica* – 23%) and sycamore (*Acer pseudoplatanus* – 7%).

Basic concept of Rockfor.net

The underlying idea of the tool Rockfor.net is that the existing forest is considered as a sequence of open rockfall nets that consist of a row of trees (Figure 2). These rows are hereafter referred to as curtains. Rockfor.net begins by calculating the to-

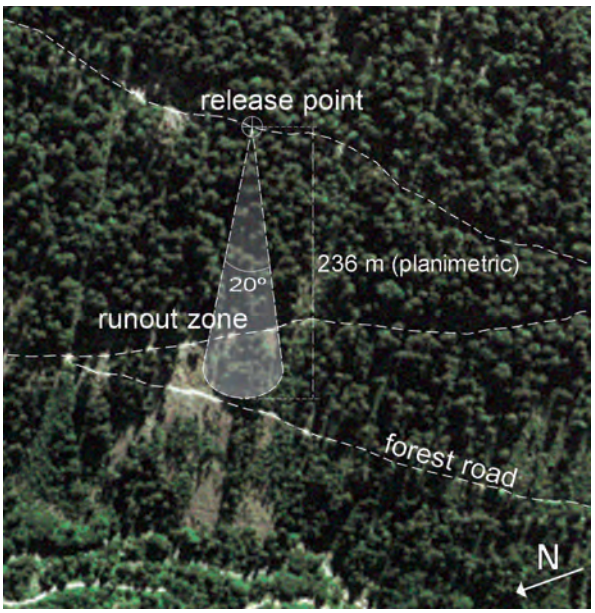


Fig 1 *Overview of the test site in Vaujany (France).*

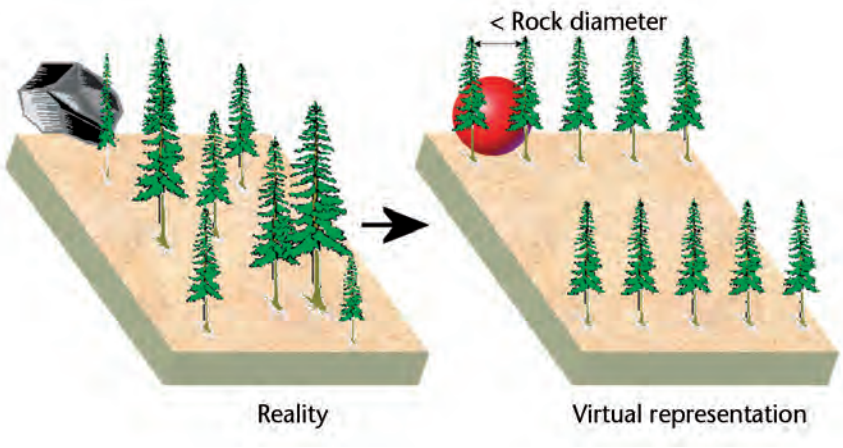


Fig 2 Explanation of the principle for expressing a real forest structure in a sequence of virtual rockfall protective tree rows (curtains).

tal energy developed by a falling rock, as calculated with the energy line principle. Then it calculates the energy dissipative capacity of each curtain and the number of curtains required for dissipating the total energy of the rock. Subsequently, the required number of curtains is converted in a required basal area using the mean DBH. Finally, Rockfor.net calculates the basal area that is theoretically encountered by the rock when it falls through the given forest. The protective role of the forest against rockfall can subsequently be quantified by comparing the required basal area with the theoretically encountered basal area. All these steps, as well as the calibration of the parameters needed for the calculations performed in these steps, will be explained in detail in the following sections.

Energy line principle

Energy loss during rebounds cannot be taken into account in a simplified tool like Rockfor.net. Therefore, the total amount of energy that has to be dissipated is calculated with the energy line angle principle as described by Heim (1932), Toppe (1987), Gerber (1998), and Meissl (1998). The energy line principle assumes that the kinetic energy of a falling rock at a given point equals the potential energy (E_{pot}) at that given point, following

$$E_{pot} = m * g * h \quad (1)$$

where m is the mass of the rock (kg), g is the acceleration due to gravity (9.81 m/s) and h is the height difference between the energy line and the terrain at a given point in m (Figure 3).

The energy line angle used in the tool Rockfor.net is 31°, which is the angle observed during the real-size rockfall experiments on a non-forested slope of 38° described by Dorren et al (2005) rounded down to the nearest integer. The restriction imposed by Rockfor.net is that the maximum velocity that can be attained by the rock (V_{max}), which is also calculated by the energy line following

$$V_{max} = \sqrt{2 * g * h} \quad (2)$$

cannot be higher than 0.64 * slope gradient (°) if the total basal area (G) of the forest is at least 10 m². Here V_{max} is given in m/s. If G is lower, or if a forest cover is absent, the maximum velocity of the rock is assumed to be 0.8 * slope gradient. The values 0.64 and 0.8 are derived from the velocities observed during the real-size experiments. The maximum velocity on the forested part was 24.3 m/s and on the non-forested part it was 30.4 m/s. Consequently, we assumed a linear relationship between the slope gradient and the maximum velocity. The condition of a minimal G of 10 m² is based on observations made by Doche (1997), who found that forests with a lower G have almost no mitigating effect on rockfall. The total amount of energy to be dissipated by the forest (E_{totd}) is calculated by Rockfor.net following

$$E_{totd} = 0.5 * m * V_{max}^2 + m * g * 0.25 * Fh \quad (3)$$

where m is the rock mass in kg, V_{max} is given in m/s, Fh is the height of the cliff or rock face and E_{totd} is given in J. The first part in equation 3 calculates the translational kinetic energy of the rock and the second part calculates an additional potential energy. Here it is assumed that 75% of the initial fall energy is dissipated during the first impact on the slope surface (Broilli 1974, Evans & Hungr 1993). The remaining 25% is considered to transform into additional kinetic energy due to rotation, which has to be dissipated by the forest as well. To evaluate the energy line principle, we compared the velocity given by the energy line principle with the absolute maximum velocity and the mean maximum velocity of all the rocks released during the experiments, which were calculated from digital films (Dorren et al 2005).

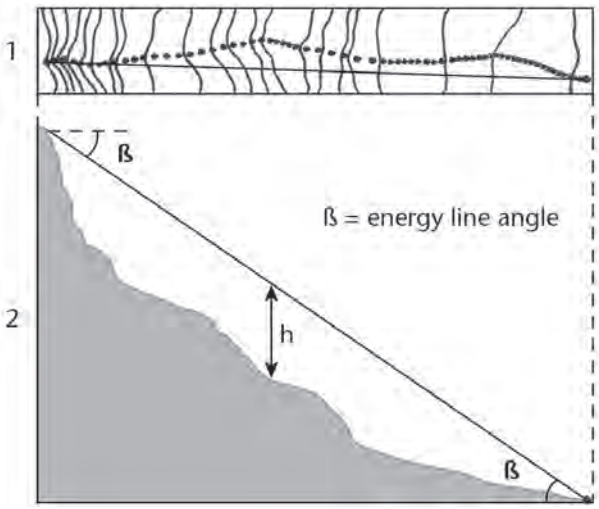


Fig 3 Explanation of the energy line principle. Scheme 1 gives a helicopter view of a slope with the rebound positions of a rockfall event; Scheme 2 shows a cross-section of the slope with the energy line of the rockfall event.

Encountered basal area

After each rock was released at the test site, we surveyed its trajectory from the release to the stopping point using an Impulse LR 200 laser distance meter manufactured by Laser Technology Inc (Centennial, Colorado, USA). If trees were impacted, we measured the basal area of the impacted tree that overlapped with the impacting rock (Figure 4). For each rock we summed to total encountered basal area (g_{en_real}) from its starting to its stopping point. Subsequently, we established a relationship between the real planimetric distance travelled and the g_{en_real} using linear regression. Next, we calculated g_{en_theo}, which is the basal area that a rock theoretically encounters after travelling a given distance through a forest with a given total basal area. This can be calculated following

$$g_{en_theo} = (d * R_{diam}) * G / 10\,000 \quad (4)$$

where g_{en_theo} is given in m², d is the travelling distance of the rock (m), R_{diam} is the diameter of the falling rock (m) and G is the total basal area of the forest (m²/ha).

To confirm the suitability of the theoretically encountered basal area (g_{en_theo}), we tested whether a significant difference exists between the linear relationship established on the basis of g_{en_real} and the g_{en_theo}, assuming a normal distribution of the estimator ($\alpha = 0.05$). In addition, we used a bootstrap analysis in which we applied 10 000 linear regressions to a dataset that was re-sampled with replacement from the original g_{en_real} data. It can then be analysed if the slope of the g_{en_theo} falls within the 95% percentile confidence interval of the regression slope distribution generated by the bootstrap.

Energy dissipation per curtain

A key parameter of Rockfor.net is the ratio of the amount of energy that is actually dissipated by one curtain to the maximum amount of energy that could be dissipated by one curtain. For further convenience this parameter is called $d_{Ecfactor}$, which is actually a measure for the efficacy of each curtain.

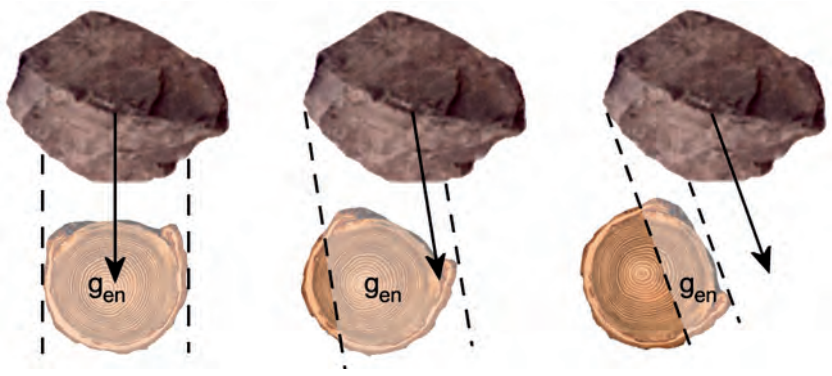


Fig 4 Basal area of the impacted tree that overlapped with the impacting rock (g_{en}). Photo of stem disc by Michelle Bollschweiler (Dendrolab, Univ. Fribourg).

Our approach for obtaining a value for this key parameter was to calculate the g_{en_theo} at the exit of the forest upslope of the middle forest road, depicted in Figure 1, which is 175 m planimetric, or 222 m measured over the slope. Hereby, we assumed that the g_{en_theo} is representative for the observed g_{en_real}. Then, on the basis of the g_{en_theo}, we calculated the mean number of tree impacts following

$$Nr_tree_impacts = (g_{en_theo} * 4) / (\pi * (DBHm)^2) \quad (5)$$

where DBHm is the mean diameter at breast height in the forest expressed in m. With the amount of energy that should have been dissipated by the forest at the point where all the rocks stopped and the calculated mean number of tree impacts, the amount of energy that is dissipated by each curtain can be calculated.

At the exit of the forest upslope of the middle forest road at the test site in Vaujany, 66% of all rocks were stopped (see also Figure 8). This means that the number of curtains required to stop all rocks (Nr_required_curtains) can be calculated with

$$Nr_required_curtains = Nr_tree_impacts * (100/66) \quad (6)$$

The virtually constructed curtains are all constituted of standardised trees. A standardised tree means that its species is a weighted mix of all occurring species in the forest (see explanation below) and that its DBH is equal to the mean DBH in the forest as derived from the G. The maximum amount of energy that could have been dissipated by one standardised tree is supposed to be given by

$$max_E_diss = FE_ratio * 38.7 * DBH^{2.31} \quad (7)$$

where max_E_diss is the maximum amount of energy that can be dissipated by one standardised tree given in J, FE_ratio is the fracture energy ratio of a given tree species to *Abies alba*. DBH is the mean stem diameter at breast height (cm). Details behind this equation are described by Dorren & Berger (2006). For example, according to Dorren & Berger (2006), the FE_ratio of *Picea abies* to *Abies alba* is 0.9. By using a FE_ratio of 1, equation 7 represents the maximum energy that can be dissipated by an *Abies alba* as a function of its diameter.

If more than one tree species occur in the forest stand, a weighted average of the FE_ratio can be calculated using the species distribution in the forest. For example, if the forest consists of 80% *Abies alba* and 20% *Picea abies*, the standardised tree has a FE_ratio of 80% * 1 + 20% * 0.9 = 0.98. By that, the energy dissipative capacity of the standardised tree is determined by a «weighted mix of all occurring species».

Multiplying this amount with the number of curtains required to stop all rocks then provides the total amount of energy dissipated by the forest. Finally, the dEc_{factor} can be calculated following

$$dEc_{factor} = E_{totd} / (Nr_required_curtains * max_E_diss) \quad (8)$$

Results

Energy line and rockfall velocity

The comparison of the velocity given by the energy line principle, using an angle of 31° with those velocities observed during the experiments (Figure 5) shows that the energy line principle slightly underestimates the absolute maximum velocity (curve a in Figure 5) and overestimates the mean maximum velocity of all the released rocks (curve c). The curve of the absolute maximum velocity (curve a) shows the upper boundary of all maximum velocities observed. The observed velocity of a sample rock (curve d), which was the rock that attained the highest velocity, shows that the energy line principle (curve b) well represents the maximum velocities of the sample rock over the distance travelled.

Using the energy line for calculating the amount of energy to be dissipated by the forest after 236 m planimetric distance, taking into account the V_{max} restriction of 24.3 m/s on a slope of 38°, an initial fall height of 0 m, and a rock mass of 1466 kg, the energy to be dissipated equals to 433 565 J.

Encountered basal area

An analysis of the residues showed that there was one outlier in the data (Figure 7), which was discarded in further analyses. These showed that there is a linear relationship between the g_{en_real} and the real planimetric distance travelled ($y = 0.003x$, $R^2 = 0.73$, $p < 0.0001$, $n = 56$), which is presented in Figure 7. There is also a good correspondence between the linear regression of g_{en_real} and the theoretical model g_{en_theo} (Root Mean Squared Error = 0.13, $n = 56$). The statistical test showed that there is no significant difference between the two ($p = 0.46$, $\alpha = 0.05$). In addition, the bootstrap analysis showed that the slope of the g_{en_theo} falls within the 95% percentile confidence interval of the generated regression slope distribution.

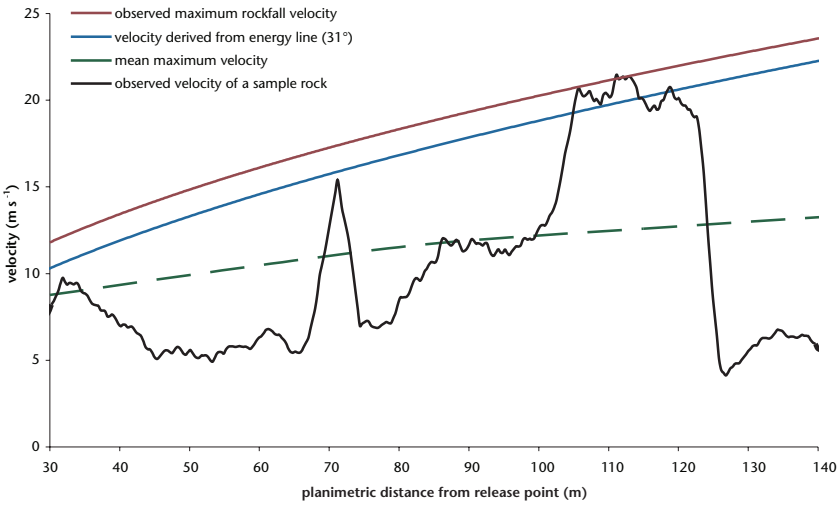


Fig 5 Observed and predicted rockfall velocities using the energy line principle with an angle of 31°.

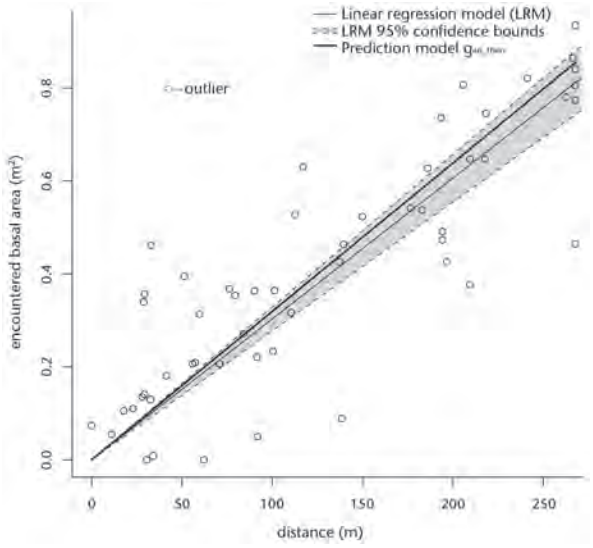


Fig 6 The cumulated real encountered basal area (g_{en_real}) from its starting to its stopping point versus the real planimetric distance travelled from the release point for each rock (depicted as black circles). The figure further presents the linear regression of g_{en_real} with the 95% confidence bounds and the predicted basal area encountered by the falling rocks.

Energy dissipation per curtain

The cumulated basal area that a rock theoretically encounters (g_{en_theo}) at the exit of the forest upslope of the middle forest road is 0.55 m². The real encountered basal area, calculated with the fitted linear relationship between the distance from the release point and the encountered basal area observed during the experiments, is 0.58 m². The g_{en_theo} of 0.55 m² equals to 5.15 tree impacts or curtains. If after 5.15 curtains 66% of the rocks are stopped, the total number or curtains required to stop all rocks equals to 7.81 (equation 6). The total amount of energy that will be dissipated by the forest equals 7.81 multiplied by the amount of energy that can be dissipated by one curtain, which are all constituted of standardised trees. The maximum amount of energy that could have been dissipated by one standardised tree with a FE_ratio of 1.15 (*Abies alba* 57% * 1 + *Picea abies* 13% * 0.9 + *Fagus sylvatica* 23% * 1.7 + *Acer pseudoplatanus* 7% * 1.1) is 186 166 J (values are published by Dorren & Berger 2006). Therefore, the final $dE_{curtain_factor}$ can be cal-

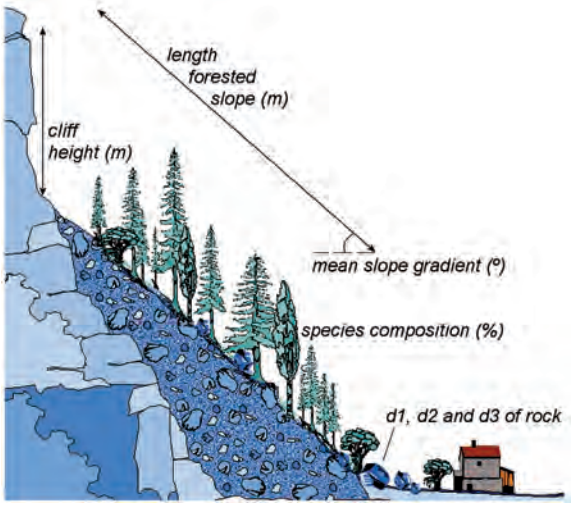


Fig 7 *Scheme showing the input parameters required for the web tool Rockfor.net.*

culated by dividing the total energy given by the energy line, being 433 565 J, by 186 166 J * 7.81 curtains, which provides 0.3. This value thus equals the efficacy of each curtain, or each impact.

Conceptualisation and creation of the tool

Rockfor.net quantifies the protective role of a forest against rockfall by comparing the energy that can be dissipated by a forest with the total energy developed by a falling rock. To do this, energies are expressed in encountered basal area. We assume that the difference between the theoretical basal area to be encountered to ($G_{required}$) stop all rocks and the available basal area ($G_{available}$) is indicative for the residual rockfall hazard, i.e., the number of rocks that surpass the forested zone on a given slope. Rockfor.net calculates the Probable Rockfall Hazard (PRH) below a forested slope following

$$PRH = 100 - (G_{available} * 100 / G_{required}) \quad (9)$$

where PRH is given in percentage

$$G_{required} = Nr_req_curtains * \pi * 0.25 * DBH^2 \quad (10)$$

$$Nr_req_curtains = E_{totd} / (max_E_diss * dEc_{factor}) \quad (11)$$

$$G_{available} = ((Rock_diameter * Slope_length)/ 10\,000) * G \quad (12)$$

where DBH is given in m, Rock_diameter is the mean rock diameter in m and Slope_length is the length of the forested slope (m).

We fixed the minimum PRH that is given by Rockfor.net at 1%, because 100% protection is virtually impossible. To calculate the PRH, the input data presented in Figure 7 are required.

In addition to the PRH, Rockfor.net provides the required stand density and the required mean DBH in order to obtain a PRH of 1%. The required mean DBH_r is calculated following

$$DBH_r = \left(\frac{E_{totd} * Curtain_{dist}}{Slope_length * FE_ratio * dE_{factor} * 38.7} \right)^{\frac{1}{2.31}} \quad (13)$$

where $Curtain_{dist}$ is the distance between two curtains, which we fixed at 30 m, a compromise between the maximum gap length in rockfall protection forests presented by Gsteiger (1993), Frehner et al (2005), Dorren et al (2005), and Gauquelin et al (2006).

The required stand density can then be calculated following

$$Rq_stand_density = (4 * G_{required}) / (\pi * DBH_r^2 / 10\,000) \quad (14)$$

To provide minimum and maximum values for the mean DBH and the density of the target stand, the free and publicly available Internet version of Rockfor.net (www.Rockfor.net), which is developed in PHP (www.php.net), calculates the required DBH and required stand density by varying the input rock diameter with ± 5%. As such, the PRH given is a result of the mean PRH calculated for the input rock diameter + 5% and the input rock diameter – 5%.

Using the parameter values presented in the previous sections and applying Rockfor.net to our test site in Vaujany, and using the input values presented in Table 1 results in a PRH of 34% after 175 m planimetric distance (middle forest road) and 11% after 236 m planimetric distance (point where all the rocks stopped).

General description	Site characteristics			Forest characteristics					Rock characteristics		Rockfall hazard	
Location	Fall height (m)	Slope gradient (°)	Length non-forested slope (m)	Length forested slope (m)	Density (stems/ha)	G (m^2/ha)	DBH (cm)	Species composition	Mean diam. (m)	Type & shape	**Observed rockfall hazard (%)**	**PRH with Rockfor.net (%)**
Vaujany	0	38	0	222 299	294	31.6	36.9	Abies alb. 57% Picea ab. 13% Fagus syl. 23% Acer ps. 7%	1	Granite, sphere	**34** **0**	**34** **11**

Tab 1 *Input and output for the test site of Vaujany (PRH = Probable Rockfall Hazard).*

General description	Site characteristics			Forest characteristics					Rock characteristics		Rockfall hazard	
Location	Fall height (m)	Slope gradient (°)	Length non-forested slope (m)	Length forested slope (m)	Density (stems/ha)	G (m^2/ha)	DBH (cm)	Species composition	Mean diam. (m)	Type & shape	**Observed rockfall hazard (%)**	**PRH with Rockfor.net (%)**
Savournon (FR) 05/04/2006	49	28	0	525	1534	29.6	16	Quercus sp. 5% Fagus syl. 95%	2.84	Limestone, rectangular	66	85
St. Martin le Vinoux (FR) 06/08/1987, (Bigot 2006)	20	35	0	270	800	16.1	16	Quercus sp. 80% Pinus ni. 20%	1	Limestone, rectangular	75	78
Lumbin (FR) 07/01/2002	50	32	0	707	1080	23.3	17	Quercus sp. 5% Acer ps. 62% Robinia ps. 8%	2.35	Limestone, rectangular	100	88
Le Fontanil (FR) 1998, (inventory; Crenn 1999)	30	32.8	0	148	2750	34.8	13	Quercus sp. 65% Fagus syl. 25% Acer ps. 10%	1.25	Limestone, rectangular	25	26
Diemtigtal (CH) 2001, (inventory; Stoffel et al 2006)	50–350	40	0	90	523	20.1	22	Picea ab. 97% Acer ps. 3% (estimated)	0.15	Limestone, rectangular	<5	4 (mean)
Vailly (FR) 1997, (experiment; Doche 1997)	0	38	0	140	485	38.7	28	Picea ab. 48% Abies alb. 16% Acer ps. 21% Fagus syl. 15%	0.87	Granite, sphere	34	35
Balzers (LI) 1987, (experiment; Jahn 1988)	0	35.5	0	161	3400	–	13	Fagus syl. 50% Picea ab. 25% Pin. sylv. 25%	0.28	Limestone, sphere	0	1

Tab 2 *Observed data, input parameters used for Rockfor.net and results of validation cases (PRH = Probable Rockfall Hazard).*

Validation

To evaluate the performance of Rockfor.net we validated the developed tool with either: 1) past rockfall events, 2) rockfall forest inventories during which the stop positions of previously fallen rocks in forests were mapped or 3) data coming from rockfall experiments other than those carried out at our test site in Vaujany. All the validation cases are summarised in Table 2, which presents a general description of the source of the data, the data observed in the terrain, the input parameters used for validating Rockfor.net and the real and calculated PRH.

Discussion

The explanation of the underlying principles of the tool Rockfor.net showed that it is strongly based on the basal area. This is well justified by the linear relationship between the encountered basal area (g_{en_real}) and the stopping distance and, therefore, indirectly with the dissipated energy of the rocks released during our experiments. The correlation between g_{en_real} and g_{en_theo} provided a good basis for predicting and quantifying the protective function of a forest against rockfall. Although the parameter values of Rockfor.net are only based on the observations at one single site, it can be concluded that the tool performs well at other sites, as shown by the validation cases. The maximum error observed in the validation cases is 19% with a Root Mean Squared Error of 9.3%. More importantly, Rockfor.net predicted satisfactorily for the validation sites whether more or less all rocks would be stopped by the forest or about 25%, 50% or more than 75% of the rocks would pass the forested zone. Consequently, we believe that the basic principles of Rockfor.net can be considered valid.

Additional strong points are that the user of the tool does not need to calibrate the tool. Only site related, global input data are required and no excessive details are required. Furthermore, the tool provides specific details on the required mean diameters and the stand density at a given site in relation to the rock size, the rockfall energy and forest characteristics.

Improvements can be made regarding the calibration and the validation of the tool. Additional real size rockfall experiments at another site would allow us to re-calibrate the tool with an additional dataset. As such, we could test the robustness of the parameter values that are currently used. An important parameter used is the $dE_{curtain_factor}$, which is currently set to 0.3. In fact, this value comes close to the probability that a rock will impact a tree frontally (P=33%), which leads to the highest energy dissipation (Dorren & Berger 2006). It would be interesting to find out whether this value changes significantly when calibrating this parameter using data from other sites.

Additional validation would allow us to test the robustness of the tool as a whole. Currently, various assumptions are included in the tool. One example is the maximum velocity restriction imposed to the energy line calculation and the underlying conditions. Another example is the assumption that the linear relationship between the g_{en_real} and the stopping distance is valid for all forest types. As for the cumulative number of rocks stopped in relation to the distance from the release point, a logarithmic function could be appropriate (Figure 8). Such a function, rather than a linear one, would increase the protective capacity of a forest stand more rapidly over the travelled distance. To better describe this function, which is of key importance for the tool Rockfor.net, additional data is needed.

Stopping reasons other than tree impacts, such as surface roughness or flat areas, are not accounted for in Rockfor.net. Due to its set-up this is impossible. However, especially smaller rocks tend to stop due to terrain features like a high surface roughness than to tree impacts. The fact that the effect of flat areas are not included explains why Rockfor.net calculated a residual rockfall hazard of 11% at the point where all the rocks actually stopped at our test site. In reality, these rocks stopped on the middle forest road (Figure 8), which is known to be a very effective protective measure (Dorren et al 2005).

Rockfor.net is currently only adapted for one typical terrain type: a cliff with a relatively straight slope covered by a rather homogeneous forest. Terrain variations, due to rock outcrops and small rock faces, or variations in the forest cover caused by local rockfall or avalanche couloirs cannot be taken into account.

Nevertheless, a basic tool is currently available that gives quite detailed information on rockfall protection forest while demanding little effort from the user. In addition, it allows the user to compare the protective capacity against rockfall of different forest stands. It provides promising first results and seems to be a valuable help for managing forests that should protect against rockfall. The tool is open for further development and validation.

Conclusions and outlook

We conclude that the basic principles of Rockfor.net can be considered as valid. Therefore, the forester currently has a tool that allows the rapid quantification of the protective function of a forest against rockfall. Priority should be given to additional validation of the tool. Further research focuses on the linkage of Rockfor.net with dynamic forest growth models, in order to test different silvicultural interventions in forest stands and their effect on the future protective capacity. ■

Acknowledgement

We thank George Kunstler, Alain Bedecarrats and Julien Pottier for helping with the statistical analysis. Christophe Bigot is acknowledged for the data acquisition in the field and Eric Mermin for testing Rockfor.net extensively.

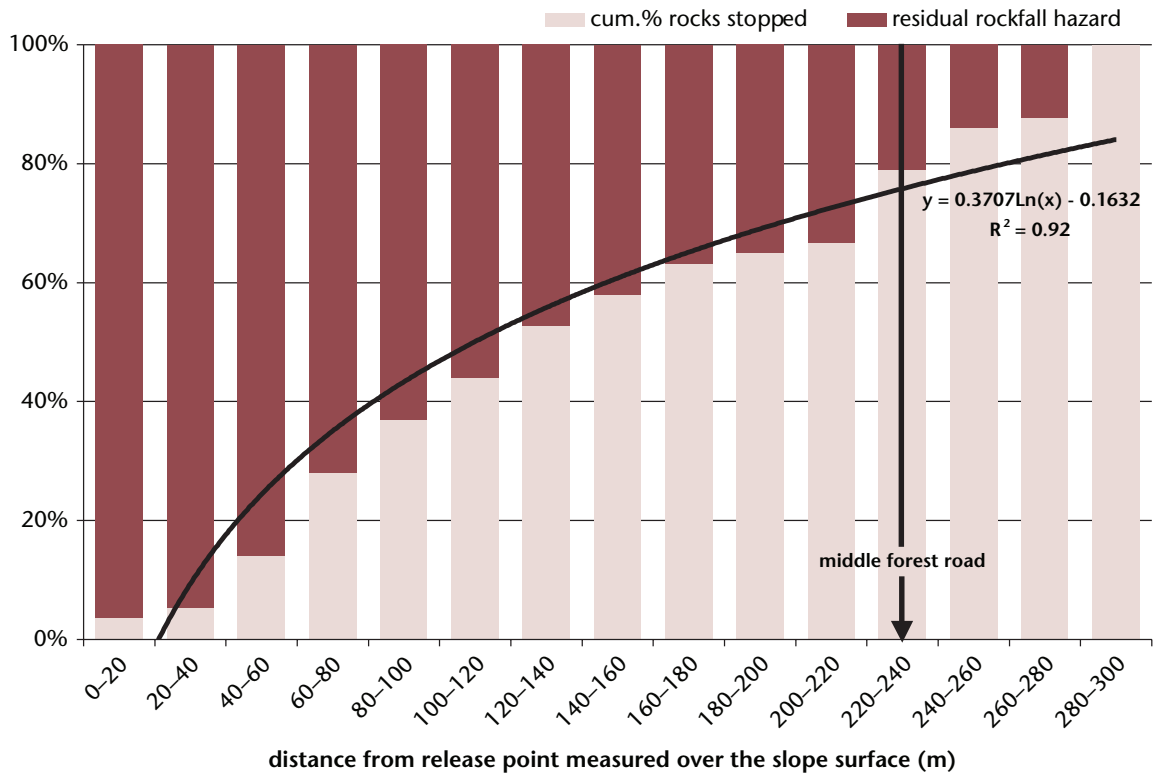


Fig 8 Cumulative percentage of rocks stopped and the residual rockfall hazard, i.e., the percentage of rocks that surpass a given point, versus the distance from the release point as observed during the real-size experiments. A logarithmic function is fitted to the cumulative percentage of stopped rocks, which is depicted as a black curve (R^2 = 0.92). The dashed white line shows the linear relationship that is currently used by Rockfor.net (R^2 = 0.98).

References

BIGOT C (2006) Regard critique sur une forêt à fonction de protection contre les chutes de blocs – Retour d'experience à St. Martin le Vinoux (Isère). Grenoble: Cemagref, MSc thesis. 78 p.

BITTERLICH W (1984) The relascope idea: relative measurements in forestry. Slough: Commonwealth Agricultural Bureaux. 242 p.

BRANG P (2001) Resistance and elasticity: promising concepts for the management of protection forests in the European Alps. For Ecol Manage 145: 107–119.

BRAUNER M, WEINMEISTER W, AGNER P, VOSPERNIK S, HOESLE B (2005) Forest management decision support for evaluating forest protection effects against rockfall. For Ecol Manage 207: 75–85.

BROILLI L (1974) Ein Felssturz in Grossversuch. Rock Mech Suppl 3: 69–78.

CRENN R (1999) Influence exercée par la forêt exploitée en taillis sur la dynamique du phénomè de chutes de pierres – analyse retrospective des traces d'un événement recent sur la commune du Fontanil-Cornillon (38). Grenoble: Cemagref, MSc thesis, unpublished. 54 p.

DOCHE O (1997) Etude expérimentale de chutes de blocs en forêt. Grenoble: Cemagref, doc 97/0898, unpublished. 130 p.

DORREN LKA, BERGER F (2006) Stem breakage of trees and energy dissipation at rockfall impacts. Tree Physiol 26: 63–71.

DORREN LKA, BERGER F, PUTTERS US (2006) Real size experiments and 3D simulation of rockfall on forest slopes. Nat Hazards Earth Syst 6: 145–153.

DORREN LKA, BERGER F, LE HIR C, MERMIN E, TARDIF P (2005) Mechanisms, effects and management implications of rockfall in forests. For Ecol Manage 215: 183–195.

ERISMANN TH, ABELE G (2001) Dynamics of rockslides and rockfalls. Berlin: Springer. 316 p.

EVANS SG, HUNGR O (1993) The assessment of rockfall hazard at the base of talus slopes. Can Geotech J 30: 620–636.

FREHNER M, WASSER B, SCHWITTER R (2005) Nachhaltigkeit und Erfolgskontrolle im Schutzwald – Wegleitung für Pflegemassnahmen in Wäldern mit Schutzfunktion. Bern: Bundesamt Umwelt Wald Landschaft. 564 p.

GAUQUELIN X ET AL (2006) Guide des sylvicultures de montagne. Grenoble: Cemagref. 289 p.

GERBER W (1998) Waldwirkung und Steinschlag. In: Proc 14. Arbeitstagung Schweizerischen Gebirgswaldpflegegruppe & FAN, Grafenort/Engelberg, unpublished report. pp. 1–15.

GSTEIGER P (1993) Steinschlagschutzwald. Ein Beitrag zur Abgrenzung, Beurteilung und Bewirtschaftung. Schweiz Z Forstwes 144: 115–132.

HEIM A (1932) Bergsturz und Menschenleben. Beiblatt Vierteljahrschr Nat.forsch Ges Zür 77: 218.

JAHN J (1988) Entwaldung und Steinschlag. In: Proc Interpraevent, Graz, vol 1. pp. 185–198.

KIENHOLZ H, MANI P (1994) Assessment of geomorphic hazards and priorities for forest management on the Rigi north face, Switzerland. Mt Res Dev 14: 321–328.

LE HIR C (2005) Forêt et chutes de blocs: méthodologie de modélisation spatialisée du rôle de protection. Marne-La-Vallée: Univ Marne-La-Vallée, PhD Thesis. 195 p.

MEISSL G (1998) Modellierung der Reichweite von Felsstürzen. Fallbeispeile zur GIS-gestützten Gefahrenbeurteilung aus dem Bayerischen und Tiroler Alpenraum. Innsbruck: Inst Geogr Univ Innsbruck, PhD Thesis. 249 p.

OTT E (1978) Zur Notwendigkeit der Pflege von Gebirgswäldern. Schweiz Z Forstwes 129: 101–116.

PERRET S, DOLF F, KIENHOLZ H (2004) Rockfalls into forests: analysis and simulation of rockfall trajectories – considerations with respect to mountainous forests in Switzerland. Landslides 1 (2): 123–130.

SCHWITTER R (1998) Zusammenfassung und Schlussfolgerungen. In: Proc 14. Arbeitstagung Schweizerischen Gebirgswaldpflegegruppe & FAN, Grafenort/Engelberg, unpublished report. pp. 1–5.

SELBY MJ (1982) Hillslope materials and processes. New York: Oxford Univ Press. 264 p.

SPANG RM, SÖNSER T (1995) Optimized rockfall protection by «ROCKFALL». In: Proc 8th Int Conf Rock Mechanics, Tokyo (25–30 Sept 1995). pp. 1233–1242.

STOFFEL M ET AL (2006) Assessing the protective effect of mountain forests against rockfall using a 3D simulation model. For Ecol Manage 225: 113–222.

TOPPE R (1987) Terrain models – a tool for natural hazard mapping. In: Salm B, Gubler H, editors. Avalanche formation, movement and effects. Wallingford: IAHS Press. pp. 629–638.

WASSER B, FREHNER M (1996) Minimale Pflegemassnahmen für Wälder mit Schutzfunktion. Wegleitung. Bern: Bundesamt Umwelt Wald Landschaft. 122 p.

ZINGGELER A (1990) Steinschlagsimulation in Gebirgswäldern: Modellierung der relevanten Teilprozesse. Bern: Univ Bern, MSc Thesis. 116 p.

Funktionsweise der Software Rockfor.net zur Bestimmung der Steinschlaggefahr unterhalb eines Schutzwaldes

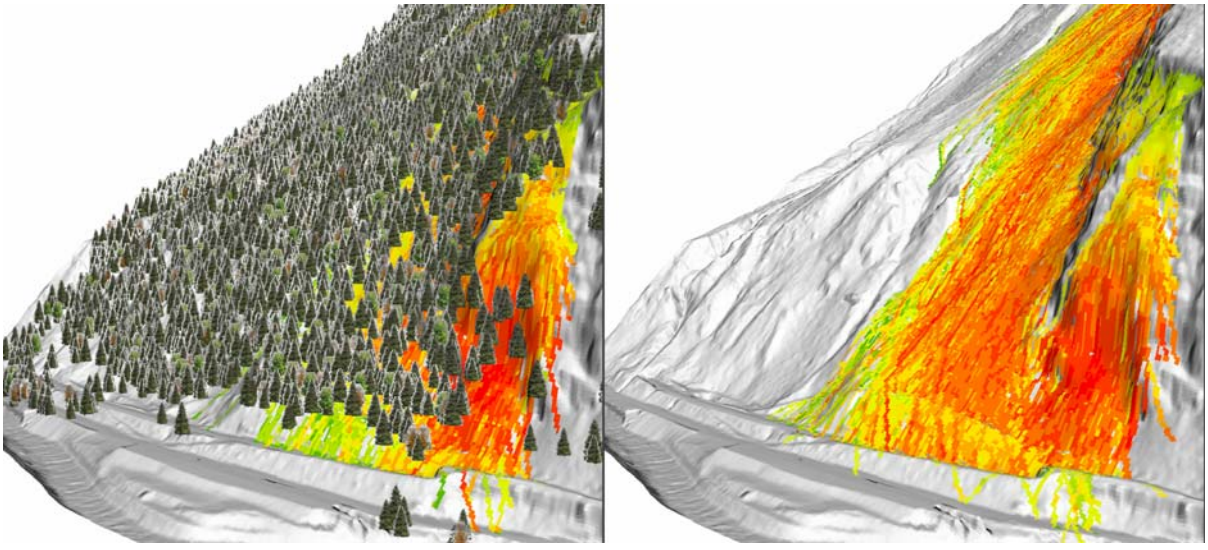
Zur Zeit bestehen keine klaren Regeln zur Bestimmung der optimalen Kriterien von Steinschlagschutzwäldern, welche auch die Wald- und Geländeeigenschaften und die Grösse und Energie der stürzenden Felsen einbeziehen. Die Software Rockfor.net (www.rockfor.net) berücksichtigt diese Anforderungen und ermöglicht es, die Schutzwirkung des Waldes zu quantifizieren. Der Aufsatz erklärt die zugrunde liegenden Prinzipien und Berechnungsmethoden und präsentiert die Fallstudien, mit welchen die Software validiert wurde.

Mode de fonctionnement du logiciel Rockfor.net permettant de déterminer le danger de chutes de pierres en aval d'une forêt protectrice

Il n'existe actuellement aucune règle claire pour définir les caractéristiques optimales des forêts de protection contre les chutes de pierres en incluant les caractéristiques de la forêt et de la topographie, de même que la grandeur et l'énergie des blocs dévalant la pente. Le logiciel Rockfor.net (www.rockfor.net) répond à ces exigences et permet de quantifier l'effet protecteur de la forêt. Le présent article présente les principes et modes de calcul à la base du logiciel, ainsi que les exemples qui ont servi à le tester.

> Chapter 12

State of the art in rockfall – forest interactions



State of the art in rockfall – forest interactions

Luuk Dorren Cemagref Grenoble (FR)*
Frédéric Berger Cemagref Grenoble (FR)
Martin Jonsson Swiss Federal Institute for Forest, Snow and Landscape Research (CH) und BergByggKonsult AB (SE)
Michael Krautblatter Geography Department, University of Bonn (DE)
Michael Mölk Geological Service, Austrian Torrent and Avalanche Control (AT)
Markus Stoffel Laboratory of Dendrogeomorphology, Department of Geosciences, University of Fribourg (CH)
André Wehrli Federal Office for the Environment (CH)

State of the art in rockfall – forest interactions

To effectively prevent rockfall related disasters below forested slopes, silvicultural, eco-engineering, civil engineering or mixed techniques can be used. To do this in a cost-efficient manner it is necessary to know the following: 1) where rockfall events occur and which magnitudes are likely, 2) to what extent the forest reduces the run-out distances, the jump heights and the energies of rocks falling downslope, and 3) how the protective function of forests could be improved. This paper gives an overview of the current scientific knowledge and methods that are applied by practitioners who deal with rockfall and forests protecting against it. Efficient ways to derive information on the probable magnitude and frequency of future rockfall events from the source and deposit area are described. Subsequently, the scientific knowledge on the energy absorption capacity of single trees and the currently available knowledge on the protective function of forest stands against rockfall are presented. Then easy-to-use tools and simulation models for rockfall hazard assessment on forested slopes are described. Finally, this paper identifies the most important challenges to be tackled in the field of integrated rockfall-forest research.

Keywords: rockfall, protection forests, review, Alps
doi: 10.3188/szf.2007.0128

* 2 rue de la Papeterie, BP 76, F-38402 St. Martin d'Hères cedex, E-Mail luuk.dorren@cemagref.fr

In March 2006, two children were killed in the French Alps by a falling rock of about 0.3 m^3 that impacted a family car. Luckily, such accidents are rare. Rockfall events, however, occur frequently in mountainous areas (Gardner 1970, Dussauge-Peisser et al 2002, Hantz et al 2003, Sass 2005). At locations where rockfall is known to pose risks to people, housing or infrastructure, protective structures have usually been put into place. In many of those cases, rockfall nets and dams are constructed upslope from houses, roads or railways (e.g., Peila et al 1998, Gerber 2001). In situations where the area between the element at risk and the cliff face is covered with mature forest, the risk is somewhat hidden. In such cases, the risk posed by rockfall is generally known only if rockfall events have reached houses or roads in the past. To effectively prevent rockfall related disasters below forested slopes, silvicultural, eco-engineering, civil engineering or mixed techniques can be used (Dorren et al 2005). Here, eco-engineering is defined as the utilisation or enhancement of biological processes in or together with engineering design. Historically, forests were relied upon for protection but with improvements in engineered materials and design there was a move toward engineered works, but these structures have generally had a shorter lifespan than originally planned.

To protect against rockfall in a cost-efficient manner it is necessary to know: 1) where and what magnitude rockfall events occur, 2) to what extent the forest may reduce the run-out distances, the jump heights and the energies of rocks falling downslope, and 3) how the protective function of forests could be improved.

Research on rockfall mechanics has been carried out since the 1920's (Smekal 1920, Lehmann 1933, Bakker & le Heux 1946, Crandell & Fahnestock 1964, Kent 1966, Broilli 1974, Bozzolo & Pamini 1986, Giani 1992, Azzoni & de Freitas 1995, Erismann & Abele 2001, Chau et al 2002). In contrast, research on the interactions between rockfall and forests was only initiated in the 1980's (Couvreur 1982, Jahn 1988). Currently, significant progress has been made in various aspects related to interactions between falling rocks and forests. The objective of this paper is to present an overview of the current scientific knowledge and methods that are used by practitioners who deal with rockfall and forests protecting against it. Finally, this paper identifies the

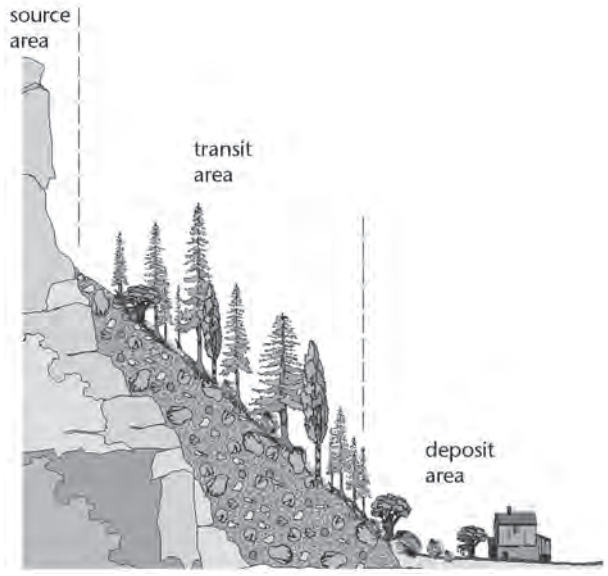


Fig 1 *Generalisation of the three main areas on an active (forested) rockfall slope.*

most important challenges that need to be met in order to improve the protection against rockfall using the natural mitigation potential of forests.

The structure of the first part of this paper follows principally the three main areas that can be distinguished on an active rockfall slope: 1) the source area, 2) the transit area, and 3) the deposit area (Figure 1). Hazardous rockfall source areas are typically characterised by steep rock faces that have unfavourable combinations of slope aspect and the dip and strike of bedding planes and the most prominent joint sets. The transit area lies between the rockfall source area and the deposit area. In this area, the rockfall velocities as well as the jump heights are maximal. Logically, the deposit area is the area where (most) rocks stop. These areas could overlap each other and boundaries between them are therefore not strict.

In all three areas, information can be obtained about the probable magnitude of future rockfall events. This is an extremely important parameter when dealing with rockfall protection. Therefore, this article pays considerable attention to the available methods in the three areas for determining the rockfall magnitude as well as the rockfall frequency. For each area we discuss the role of forests regarding rockfall protection. In the section dealing with the transit and deposit area this is done separately for individual trees and for forest stands as a whole. The subsequent sections outline management guidelines, criteria and indicators for optimal rockfall protection forests, and tools for assessing the protective function of forests against rockfall. The final section identifies challenges in integrated rockfall forest research.

Rockfall source area

In this article, we define rockfall as a relatively small landslide confined to the removal of individual rocks generally smaller than 5 m^3 from a cliff face, but singular rocks with larger volumes (e.g., 10 m^3) should not be excluded. In addition, we do not differentiate between sizes of rocks, as there are many systems to define sizes of loose rocky material. For example, the system that differentiates between cobbles (ø = 64–256 mm) and boulders (ø > 256 mm), as described by Wentworth (1922) and later adapted by others (e.g., Blair & McPherson 1999). Another system differentiates between rocks (ø < 50 cm) and blocks (ø ≥ 50 cm), as mentioned by Gerber (2001). Following the volumetric classification of Whalley (1984), the term rockfall in this paper refers mainly to debris fall (< 10 m^3), but also to boulder fall (10–100 m^3).

Locating active rockfall slopes

At the cliff face, being a potential source area for rockfalls, often a lot of information about the potential rockfall hazard can be found. The two types of parameters that can be assessed are so-called «rockfall promoters» and «rockfall triggers». Rockfall promoters are joint attitude, presence of joint infillings, open cracks, and rock strength. These parameters determine the preparation of loose rocks that eventually could fall down. Rockfall triggers are joint water pressures, freeze-thaw mechanisms, tree root growth and earthquakes, which initiate the actual rockfall (Dorren 2003, Krautblatter & Dikau 2007). Due to the complex interaction of rockfall promoters and triggers, it is difficult to provide the failure probability of a potentially falling rock as a function of a given period (Hantz et al 2003).

Quite often rockfalls occur suddenly in places with few or no prior indications of instability. Slope instability indicators include both features related to future failure, such as open cracks or rocks in limited equilibrium, and features indicating recent and past failures, such as scars in the cliff face. Generally, past rockfall activity is a good source of information if rockfall conditions in terms of magnitude and frequency of rockfall promoters and rockfall triggers have not changed significantly. Recent rockfall activity in the source areas is apparent due to the presence of «fresh» scarps, whose age can be judged according to the degree of weathering.

Future rockfall activity can be detected by comparing the geological structure of the rock mass and the topography of the slope (Hoek & Bray 1981, Goodman & Shi 1985). In this context, the size, density, orientation and continuity of rock discontinuities are of central importance. Methods for the quantitative description of discontinuities in rock masses are summarized by Barton (1978). Many

methods currently exist for estimating the probability of failure that are based on relative rock failure rating systems (Mazzoccola & Hudson 1996, Budetta, 2004, Corominas et al 2005, Jaboyedoff et al 2005). Frequently applied systems are the Slope Mass Rating by Romana (1988), the Rockfall Hazard Rating System (RHRS) developed by Pierson et al (1990) and Matterrock (Rouiller et al 1997). Such methods generally require ratings for geologic characteristics, the volume of the potentially falling rock, rockfall history, triggering factors (climate, water circulation), and in some cases estimates for future trends in the stability of a slope.

Assessing rock size

The volume of a detachable block may be estimated, as a first approximation, on the cliff face. Three parameters are considered as the most important when determining the volume of a detachable block: spacing, attitude, and persistence of discontinuities (Corominas et al 2005). Spacing of discontinuities controls the size of the individual blocks after the first impact of the fallen mass on the ground (Priest & Hudson 1976). Attitude and persistence (continuity) of joints determines the size of the largest detachable block. It is usually difficult to measure rock sizes in the rockfall source area because of limited accessibility as well as the imminent danger of rockfall. In addition, there are methodological limitations for determining joints that will finally lead to rock detachment. However, it is important to analyse both the source area and the deposit area to gain an indication of the rock size distribution (Mölk 2000). Available methods for assessing the rock size in the source area are summarised in Table 1.

Assessing rockfall frequency

In general, the frequency of rockfall events has to be assessed separately for all rock size classes as no frequency – magnitude relations have been established that covers all rock size classes (Abele 1972, Whalley 1984, Krautblatter et al 2007). Important sources for predicting rockfall frequencies are historical and present observations. Larger rockfall events are often recorded in historical descriptions, documents and maps (Morche et al 2006), but their interpretation could require experience with historical sources (Glade & Lang 2003). The prediction of future frequencies on the basis of historical rockfall events is, however, only possible if unaltered environmental conditions can be assumed (Krautblatter & Moser 2006). Therefore, such methods are generally not applicable for environments that 1) currently experience a phase transition due to climatic fluctuations (e.g., permafrost melting), 2) whose constitutional state has been altered by a preceding major event (e.g., large rockfall), 3) whose environmental setting has been changed due to anthropogenic or natural interactions (e.g., road undercutting or fluvial incision), and 4) those which are prone to be affected by future triggering situations (e.g., earthquakes, extreme rainstorm events).

For recent rockfall frequencies, institutionally organised assessments of rockfall activity are in some cases made by geological services, organisations surveying or constructing infrastructure, forest or natural hazard management services or by scientific organisations (Hungr & Evans 1988). As those surveys are not widely available, observations of local inhabitants and authorities are crucial for referring recent rockfall deposits to a certain time of collapse.

Method	Description	Advantage	Disadvantage
Visual estimation	Estimating the volumes of the joint-bordered rock-bodies visually.	Rapid method.	Unreliable, difficult to reproduce, dependent on personal experience.
Measurement of rock size (three axes) by measuring tape	Measurement of joint bordered rock-bodies by measuring tape on the rock-face.	Rock shape also captured.	Often not applicable due to difficult accessibility very time-consuming to assess a statistically reliable sample.
Tape measurement of joint distances	Measurements along a line in two directions, simplified orthogonal systems.	With the knowledge of the joint distances in two axes a calculation of rock size can be executed assuming an orthogonal joint system (e.g., BSD Ortho, Scheikl 2006). Side-result: bulking-factor (amount of opening of joints for a given measuring length).	Simplified assessment of rocks due to assumption of orthogonal rock form. Second direction of measurement often difficult to execute (working on a rope …).
Laser scanning (Fig. 2) – joint pattern/rock size distribution	Under the assumption of an orthogonal joint pattern, which has to be proved by joint analysis, a calculation of the rock size distribution can be executed. Software-tools e.g., BSD-ortho (Scheikl 2006).	Measurement of joint-orientation at their real position on the rock face enables stability analysis of e.g. wedges. Measurement without physical presence of persons on rock face possible (no rockfall hazard, no safety-equipment necessary).	Availability of technical equipment is expensive or difficult to provide. Processing can be difficult/time consuming. Software tools for analysis not commercially available. If joint orientation is unfavourable in respect to the scanner the planes might be missed.

Tab 1 *Methods for assessing rock size in a rockfall source area.*

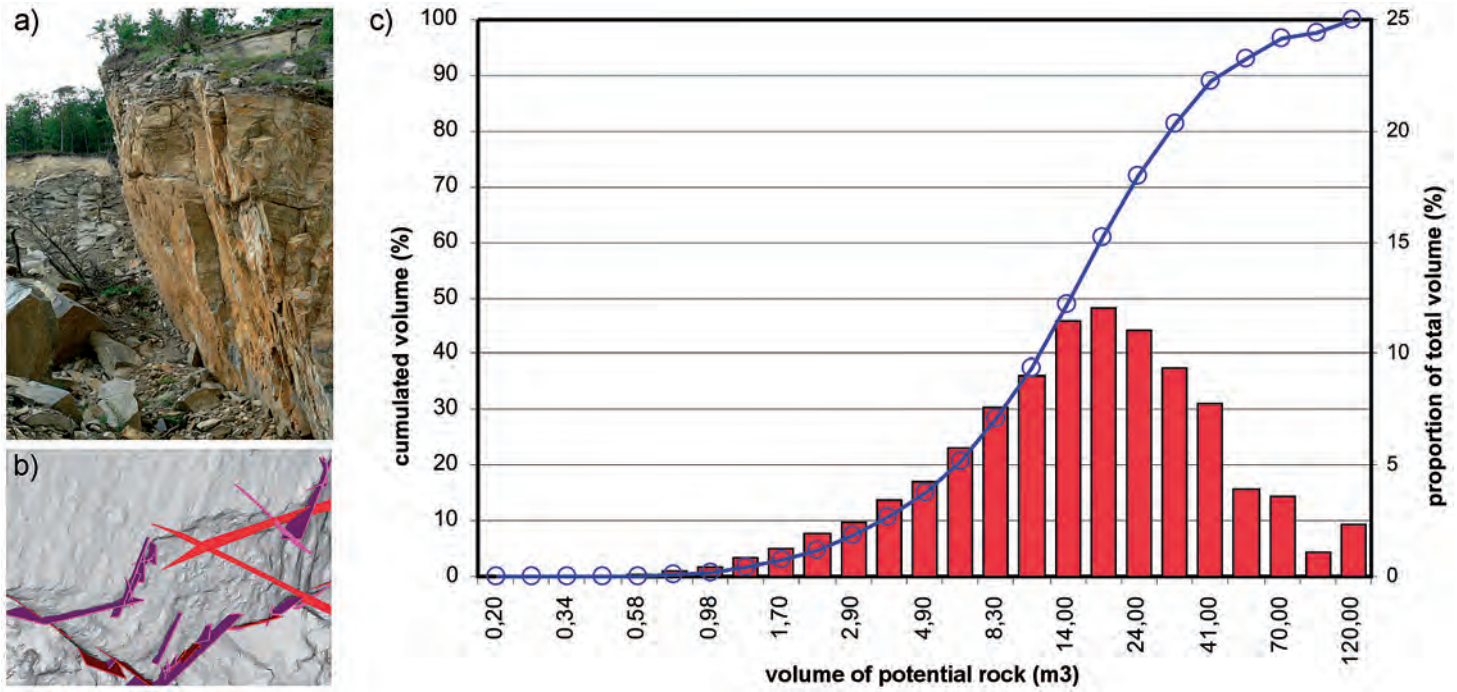


Fig 2 *Left side: photo of the demonstration site. Right side: result of the rock size analysis by using terrestrial laser scanning.* (Photo: Manfred Scheikl).

Effects of trees

In the rockfall source or detachment area, effects of trees regarding rockfall protection are generally negative. Roots of large trees can promote rockfall activity, because they generally penetrate existing joints and bedding planes in the bedrock and act as wedges. Movement of the tree stem due to snow or wind forces can cause rockfall via an additional wedge effect of the roots (Gerber 1998). In addition, the presence of roots in the bedrock accelerates chemical weathering (Jahn 1988). Therefore, in practice, unstable trees on top of cliffs and trees with large roots penetrating the bedrock should be removed. If the above described negative effects of trees are absent, the positive effect is that stable standing trees act as barriers and decelerate or stop falling rocks, even in steep source areas.

Transit and deposit area – rockfall frequency and magnitude

The easiest indicator for assessing the location of active rockfall slopes is the presence of rockfall deposits in the form of a talus slope or singular rocks deposited below a cliff face. A talus slope, also called scree slope, is a sloping mass of coarse rock fragments accumulated at the foot of a cliff or slope (Allaby & Allaby 1990). Of note, a deposit area can also act as a secondary rockfall source area.

Talus slopes document the activity of rockfall source areas over a certain span of time, e.g., a Lateglacial/Holocene (10000–15000 years) time period in Alpine environments. Therefore, they witness the historical rockfall activity. The present degree of rockfall activity is indicated by vegetation cover on talus slopes. Where rockfall is the main restricting factor for plant growth, non-vegetated talus slopes match with high rockfall activity, whereas talus slopes tend to be vegetated or even forested with decreasing rockfall activity (Gerber 1974). In situations where the slope is forested, rocks stopped by trees below a cliff face and visible rock impacts on tree stems are also good indicators of active rockfall slopes.

Assessing rock size

Deposit areas represent fragments of ancient and recent rockfall events and are therefore good sources for evaluating rock sizes. A prerequisite for assessing rock sizes on talus slopes is that rockfall conditions in terms of lithology and/or fracturing degree in the rockfall source area have not changed significantly since the initial build-up of the talus slope. Methods to assess the rock size distribution in the deposit area are summarised in Table 2.

When examining deposit areas, and especially talus slopes, it is necessary to recognise that the distribution of rock sizes is not homogeneous. Large rocks travel further (Kirkby & Staham 1975, Erismann & Abele 2001, Meissl 2001, Dorren, 2003) and are therefore concentrated at, or deposited beyond, the base of the talus slope. Secondly, over time, large rocks that are deposited on the talus slope can be covered by fine debris (small rocks). The most efficient way of finding buried rocks is ground penetrating radar (GPR) (Sass & Krautblatter 2007). Thirdly, it is necessary to recognise that the size of



Fig 3 a) Freshly detached surfaces carbonate rocks (Wetterstein limestone) can easily be distinguished optically (Reintal, Bavarian Alps). b) The freshly detached surface of a siliceous volcanic agglomerate with cm-large white inclusions is more difficult to see. The top side on the photo was exposed to weathering prior to the rockfall (Cwm Idwal, Snowdonia, North Wales).

a deposited rock may not always correspond to the original size of the falling rock, due to fracturing during downslope movement. Surfaces that have been freshly exposed due to fracturing are often visually apparent due to different weathering intensity and the lack of a biocrust, i.e., a cover with a film of bacteria (Sass et al).[1]

1 Sass O, Krautblatter M, Viles HA (2007) Quantifying and comparing present-day and long-term Holocene rockwall retreat rates in Nant Ffrancon, Snowdonia, North Wales. Earth Surf Proc Land (submitted).

Assessing rockfall frequency

If no information on the timing of the rockfall is available, a range of relative and absolute dating techniques can be utilised. Within the relative dating techniques, one of the cheapest possibilities is comparing the degree of weathering of the side of the rock that was formerly attached to the rock cliff to that which was exposed to weathering prior to the rockfall. For carbonate rocks, unweathered surfaces are often white or yellow and turn grey after some years of surface exposure (e.g. 5 years for fine-grained limestones according to Friedel 1935). For non-carbonate rocks the difference in degree of weathering is less obvious, but nevertheless apparent (Figure 3). Another indication of freshly exposed surfaces is the absence of green biocrusts. An easy measurement of the degree of weathering can be done with a Schmidt Hammer (Sass et al submitted). If needed, thin sections of weathering crusts can give final evidence for differential weathering (Trudgill & Viles 1998, Taylor & Viles 2000).

A known and suitable absolute dating technique is lichenometric dating. It is based on the assumption that the concentric growth of lichens on rocks provides an indication of the time since the rockfall event. Lichenometric dating is possible due to the regular growth rate of some species of lichen (Bull & Brandon 1998, McCarroll et al 1998, Bajgier-Kowalska 2002). Lichenometric dating is primarily applied to non-carbonate rocks, and only few stud-

Method	Description	Advantage	Disadvantage
Random estimation of block sizes	Subjective estimation of block sizes without measuring anything.	Quick and cheap.	Results are very subjective and unreliable, not reproducible.
Random tape measurement of the three axes of the rocks of a random sample	Wandering around at the deposit area and measuring block-axes randomly.	Rock form also captured.	Results very likely not reproducible due to random selection of measured blocks.
Scan-line-method	Measurement of the mean diameter of all rocks touched by a rope/measuring tape in the falling line of the slope, minimum sample 150 rocks (Fehr 1987).	Rather fast, covering the sorting effect of deposition area (downward coarsening), reproducible, statistically validated.	Simplification of block geometry and -size due to measurement of mean diameter.
Area-counting procedure	Measurement of the mean diameter of all rocks within a distinct rectangle or circle on the slope.	Reproducible, statistically validated.	Time-consuming, Simplification of block geometry and -size due to measurement of mean diameter.
Sieving	Taking a representative sample and sieving it in laboratory.	Reproducible results, given a correct sampling procedure statistically validated, standard procedure in sedimentology (laboratories mostly available).	Due to the mostly huge sample size required to get representative results, this method is very rarely applicable.
Fotosieving	By taking a photograph of a representative section of the scree slope, the rock size distribution can be determined semi automatically by support of various software (e.g., GRA-frac, Scheikl 2006).	Quick, reproducible results, statistically validated.	Often the scree material is covered with soil/vegetation and therefore only single rocks from recent events are accessible for measurement. Modern software not commercially available.

Tab 2 Methods for assessing the rock size distribution in the deposit area.

ies have succeeded in dating lichens on carbonate rocks. Growth curves of lichens must be calibrated using local inventories such as gravestones (Winchester & Chaujar 2002).

If funding is available, sophisticated absolute dating methods of deposited rocks can be applied. An overview of possible methods for dating rockfall events is given by Lang et al (1999). Frequently applied methods include dating of underlying and covering sediments using carbon content for ^{14}C-datings, or using quartz and feldspar content for luminescence dating (Schrott et al 2002). A newly introduced method is the dating of the surface exposure of rocks with cosmogenic nuclides. Surface exposure dating is possible using ^{10}Be for siliceous rocks (Ballantyne & Stone 2004) and ^{36}Cl for carbonate rocks (Desilets et al 2006). However, as the application of these methods is still very expensive, they are mostly carried out for scientific investigations. All these methods have their limitations; for example, ^{14}C-datings are generally not used for any material that is less than at least 50 years old. Moreover, there are confidence intervals that do not allow an exact date to be determined.

Another absolute dating technique is dendrogeomorphology, which studies «signatures» left in tree-ring sequences after geomorphological processes (e.g., tangential rows of traumatic resin ducts, callus overgrowing rockfall scars, reaction wood forming after tilting of the stem, sudden growth reduction as a result of breakage of the tree top). Dendrogeomorphology uses information on scars that are still visible, as well as overgrown scars that are hidden in the tree (Figure 4).

Over the last few years, dendrogeomorphology has been increasingly used in Switzerland to study past rockfall activity (Stoffel 2006, Stoffel & Perret 2006). Such studies provided reliable reconstructions of rockfall activity covering several centuries (Stoffel et al 2005a). The identification of the intra-annual position of scars together with data on the vegetation growth period even allowed determination of past rockfall activity with monthly resolution (Stoffel et al 2005b, Perret et al 2006). Dendrogeomorphology uses information on scars that are still visible, as well as overgrown scars that are hidden in the tree. For a rapid assessment of the rockfall frequencies during recent years (< 20 years depending on the size of the original scars), only the visible scars can be used (of note: the sample in Figure 4 has closed over in 5 years). For a more detailed investigation of rockfall frequencies over the several decades to centuries, a labour intensive fieldwork is required.

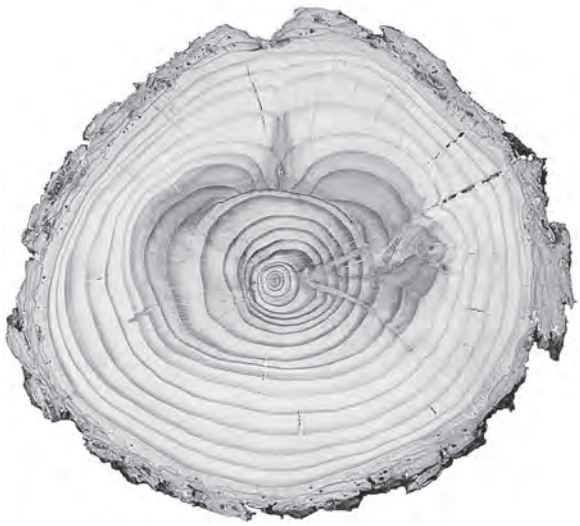


Fig 4 *Rockfall scar on a cross-section of Larix decidua Mill.*

Effects of forest in the transit and deposit area

In both the transit and the deposit areas, a protection forest stand is generally more effective in reducing the velocity and the rebound heights of falling rocks than in the source area, because the slopes are generally less steep and the forests more dense. As mentioned before, trees do have a barrier effect in the source area as well. Therefore, the following section finds its application mostly in the transit and deposit areas, but is not restricted to those two.

Energy absorption by single trees

It is often thought that only rocks with a maximum volume of approximately 2 m^3 can be stopped by single trees. There are many examples throughout the Alps of large rocks, up to 10 m^3, being stopped by trees. However, the probability that trees will be completely destroyed if impacted by such rocks is higher.

A single tree dissipates energy during a rock impact in several different ways: rotation and translation of the root system, deformation and oscillation of the tree stem, and local penetration of the rock at the impact location (Foetzki et al 2004, Brauner et al 2005). Because a single tree absorbs energy in different ways, quantification of the total amount of absorbed energy has proven to be very difficult. To quantify the energy absorption capacity, both simplified theoretical methods and results from full-scale experiments can be used. Three theoretical methods exist. The method suggested by Stokes et al (2005) uses data from static winching experiments to calculate the amount of energy required to cause a failure in the root system. The method suggested by Brauner et al (2005) assumes that the bending energy is fully developed in the whole tree stem due to the oscillation of the tree stem. This is justified by the observation that the treetops break due to a rock impact to the lower stem.

The simplest method is the one suggested by Couvreur (1982) and Zinggeler (1990), where values for the fracture energy are derived from standardized dynamic impact tests on small knot-free samples. However, recent investigations on green fresh tree stems from Norway spruce (*Picea abies* L. Karst.) trees have shown that the fracture energy per unit area increases by a factor 5 compared to small knot-free samples (Ammann 2006).

None of the theoretical methods described take into account the dynamic effects of the whole tree stem, the root-soil plate, and the surrounding soil. Therefore, real-size rockfall experiments were carried out on living trees to obtain reasonable values for the energy absorption capacity. These were performed on a forested (predominantly *Abies alba*) slope in the French Alps (Dorren & Berger 2006) and on a forested (predominantly *Picea abies*) slope in the Swiss Alps (Kalberer et al 2007). Both of these experiments are briefly discussed below.

For the experiments in the French Alps, large individual spherical rocks were released on a 38° slope and the velocity of the rocks was derived from digital video films (Dorren & Berger 2006). The translational kinetic energy was calculated before and after a tree impact that led to stem breakage, which made it possible to determine the amount of energy absorbed by the tree. On the basis of their experiments, Dorren & Berger (2006) proposed an exponential relationship between the amount of energy that can be dissipated by an *Abies alba* tree and the diameter at breast height (DBH, measured at a height of 1.3 m upslope of the tree stem). By using a scaling factor, based on previously published fracture energies, they obtained a relationship between the energy absorption capacity and the DBH for different tree species (Figure 5). They also established a relationship between the energy absorption capacity of a single tree and the degree of eccentricity of the rockfall impact on the tree stem (Figure 6). These tests and their results have been extensively reported by Dorren & Berger (2006).

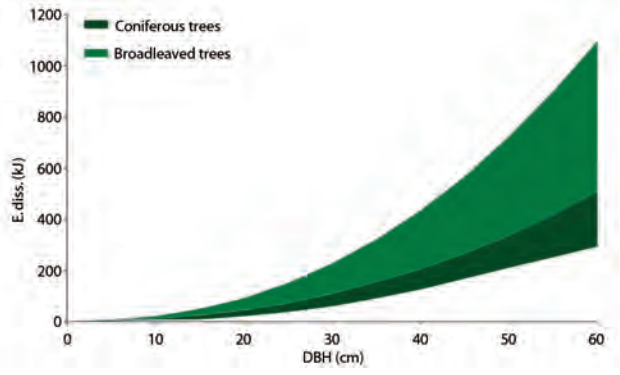


Fig 5 *General relationship between the diameter at breast height (DBH) and the range of energy that can be dissipated during a rockfall impact lower than 2 m on the tree stem for broad-leaved and coniferous species (based on data from Dorren & Berger 2006).*

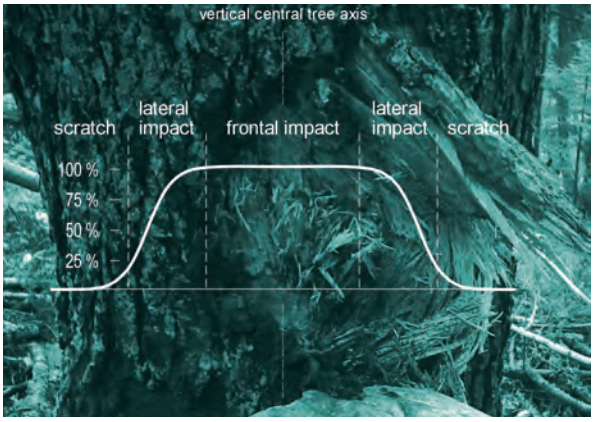


Fig 6 *Sigmoidal relationship between the horizontal position of the impact centre on the tree stem and the fraction of energy that can be dissipated by a tree (modified from Dorren & Berger 2006).*

In the Swiss Alps, the complex interaction between a rock and a tree during an impact has been investigated with a guided trolley that impacts the tree stem frontally (Kalberer et al 2007). During the impact, the response of the tree was monitored using accelerometers and high-speed cameras. Because of the accurate monitoring of the tree displacement during the rock impact, it was possible to describe where and how much energy was absorbed in the tree stem and the root-soil plate. It was observed that different processes such as stem bending, rotation, and translation of the root-soil plate absorbed the initial energy of the trolley. During these experiments it was found that a major portion of the initially absorbed energy was absorbed by the root-soil system during the rotation and translation of the root-soil plate.

When comparing the maximum energy that can be dissipated by a single Norway spruce tree with a DBH of 0.45 m as obtained by: 1) standardized dynamic impact tests on small knot free samples (used fracture energy = 5 J/cm^2), 2) static winching experiments, 3) bending energy, and 4) real size rockfall experiments, method 4 is identified as providing the highest values (Table 3).

Protective effects at the forest stand level

If the size of the dominating falling rocks as well as the rockfall frequency is known, an evaluation can be made whether an existing forest has a significant mitigation role to play or whether the chance exists that it will be destroyed by future rockfall events. Whereas rock shape is thought to have a certain influence on the rockfall process on forested slopes (Frehner et al 2005), rock size is generally the most important factor for determining the potential protective effect of a stand. It is well known that rock avalanches destroy forests that cover the transit and deposit area. Individual rocks, however,

Method	dissipated energy (kJ)
1) standardized dynamic impact tests on small knot free wood samples	8
2) static winching experiments	125
3) bending energy	184
4) real size rockfall experiments	230

Tab 3 *Maximum energy that can be dissipated by a Picea abies tree with a DBH of 0.45 m as obtained by different methods.*

can be effectively stopped by forests. This includes rocks with large volumes (Figure 7), as shown by examples from the French Southern Alps (Berger & Dorren 2007).

Rickli et al (2004) estimate that an effective mitigation of rockfall hazard by a forest stand is limited to a rock mass of approximately 10 000 kg and a velocity of approximately 20 m/s. Whereas there is no doubt that such an upper limit (i.e. a maximum rock size) exists, the values given by Rickli et al (2004) do not necessarily represent absolute limits.

Stands with high stem densities are considered to be very effective in stopping falling rocks (Omura & Marumo 1988, Cattiau et al 1995). However, uneven multilayered stands with a mosaic of all sizes and age classes are considered more suitable as regeneration is better ensured in such stands (Dorren et al 2004, O'Hara 2006).

For small rocks, stand density rather than DBH is important, since many trees are required to increase the probability of impact (Jahn 1988, Dorren et al 2005, Wehrli et al 2006). In general, the larger the moving rock, the larger the mean DBH required to stop movement. However, the required DBH to stop a falling rock depends on the tree species, because, in general, broad-leaved trees are more resistant against rockfall impacts than coniferous trees (Dorren et al 2005, Stokes et al 2005, see also Figure 5).

As a rule of thumb, Schwitter (1998) suggested that the mean DBH of trees in a stand should be approximately one-third of the decisive size of the falling rocks. This rule of thumb has been confirmed by the findings of Dorren et al (2005). Further, they found that the forest cover reduced the rockfall velocities on average by 26% and the maximum rebound heights by 75%. Their results confirm the findings of Jahn (1988) and Doche (1997), who conducted rockfall experiments on forested slopes. They concluded that rockfall velocities on a forested slope with a mean gradient between 33 and 40 degrees are between 15 and 25 m/s and that bounce heights are generally between 1 and 2 m. Other field research on rockfall in forests has been done by Couvreur (1982), Zinggeler (1990), Gsteiger (1993), Cattiau et al (1995), Perret et al (2004), and Stokes et al (2005), who mainly undertook retrospective analyses of rockfall trajectories on forested slopes. They found similar velocities and rebound heights. Tree impacts also cause lateral deviations in the rockfall trajectory. As a result, the total travelling distance of a moving rock is generally longer on forested slopes (Dorren et al 2005). As a result, the chance of the rock impacting a tree increases. However, it also results in a wider run-out area (Figure 8). A lateral deviation of 10° from the central downslope line to both sides was observed by Dorren et al (2005) and Jahn (1988).



Fig 7 *Rock with an estimated volume of 7 m³ stopped in a forest near Serres in the Southern French Alps.*

Tools for assessing the protective function of forests

The available tools for assessing or quantifying the protective function of forests against rockfall can be grouped into either 1) rapid assessment tools or 2) simulation models. Many of these tools can also be used for rockfall hazard mapping, taking the role of forests into account, or for mapping forests that currently provide effective protection against rockfall.

Rapid assessment tools

One of the first rapid assessment tools was the Mean Tree Free Distance (MTFD) calculation by Gsteiger (1993), later adapted by Perret et al (2004) and Dorren et al (2005). The MTFD basically calculates the probable mean distance between two tree impacts in a forest stand, where the forest structure is considered as a regular grid. Brauner et al (2005) also developed a tool that is based on the MTFD concept. Moreover, they added a calculation of the energy that would potentially be dissipated per tree

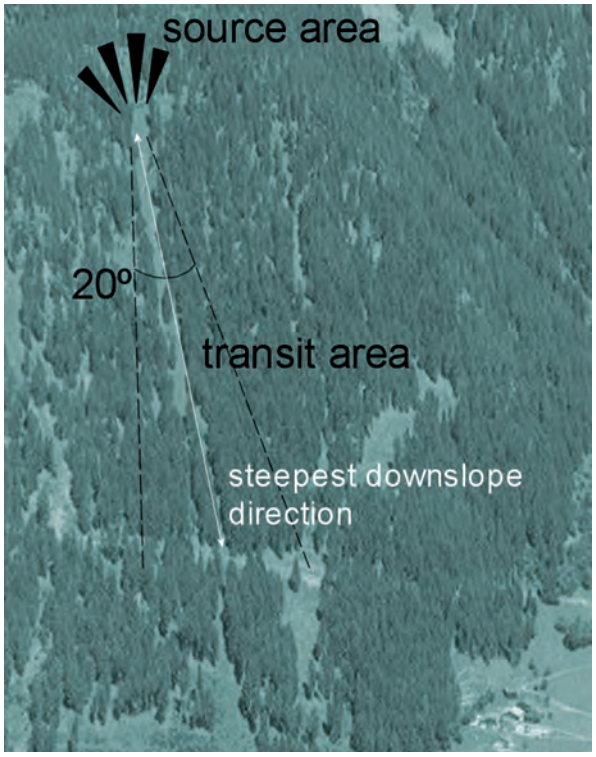


Fig 8 Tree impacts lead to lateral deviation of falling rocks. As a result, the run-out area generally equals an area covering 10° both sides from the steepest downslope direction.

impact. The latter was based on the fracture energy per unit volume wood, which was derived from laboratory bending tests of whole stems.

Another tool that combines the number of probable impacts in a forest stand with the energy dissipative capacity of trees is Rockfor.net (Berger & Dorren 2007). This tool allows a site-specific assessment of the current protective effect of a stand while taking into account forest, terrain, and rock characteristics. The basic idea of the rapid assessment tools is that a forest manager can easily assess the protective capacity of a forest stand to support decision making on required silvicultural or technical measures.

Simulation models

There is a plethora of rockfall simulation models, varying from 2D to 3D and from statistical models to deterministic models. With the increasing digital mapping and spatial modelling capabilities, there is a tendency towards 3D combined deterministic - probabilistic rockfall simulation models, both at local and regional scale (for overviews see Guzetti et al 2002, Dorren et al 2006). However, only a few rockfall simulation models take into account the mitigating effect of the existing forest cover (e.g., Zinggeler 1990, Cattiau et al 1995, Liniger 2000, Dorren & Seijmonsbergen 2003, Le Hir 2005, Dorren et al 2006, Stoffel et al 2006).

Rockfall simulation models that explicitly account for forests, include the spatial distribution of different forest stands, DBH distributions and species, assist in determining optimal combinations and locations of technical and silvicultural measures for a given site. Furthermore, they enable rockfall hazard zoning with and without taking into account the effect of forests. As such, an accurate assessment of the protective effect of a forest stand can be undertaken. Validation of these models is primarily being done by comparing simulated and mapped deposit positions of previous rockfall events or by comparing simulated rebound heights with mapped tree impact heights. The latter can be mapped directly on the tree stem or by using tree-ring data (Stoffel et al 2006).

The preparation for detailed model simulations are time and labour intensive, as many parameters require precise measurements and mapping campaigns in the field. At the same time, methods to estimate parameter values that determine the elasticity and roughness of slope surface – two very important parameters in rockfall simulation models – are still very subjective and qualitative.

Rockfall simulation models can also be coupled with forest growth simulators (Botkin et al 1972, Shugart 1984, Hasenauer et al 2000, Bugmann 2001, Courbaud et al 2001, Lexer & Hönninger 2001, Rammig et al 2006). This allows for investigation of the effect of silvicultural interventions on the future protective effect of a forest. As such, they provide solutions for dealing with uncertainties on the effect of silvicultural interventions over long periods of time, and thus address the slow rates of tree regeneration and tree growth of mountain forests. However, over long periods of time these forests may be influenced by the rapid destructive forces such as rockfall, snow avalanches, and windstorms, and, to a certain extent, ungulate browsing. To account for all these disturbances in a simulation model is almost an impossible task. Developing a coupled forest growth rockfall model, that includes the interaction between the biotic and abiotic processes (e.g., increased tree mortality due to rockfall impacts) is already challenging enough. An attempt in this direction is currently being made with the PICUS forest stand development simulation model, as described by Woltjer et al (2007). Attempts to couple forest growth with rapid rockfall assessment tools have been done by Brauner et al (2005) and Wehrli et al (2006). Currently, an attempt is being made to couple Capsis (e.g., Courbaud et al 2001) and Rockfor.net (Berger & Dorren 2007). To improve coupling of such models, more knowledge is needed on the impact of rockfall on the long term resilience and stability of forest stands; e.g., quantifying the increased mortality in the stand due to rockfall.

Finally, simulation models can be used as decision-support tools. For example, if thinning is to be carried out to promote regeneration, the protective effect is likely decreased locally and temporary. In such a case, the application of an accurate, spatially explicit rockfall model allows determining the

intensity of the intervention to prevent a significant increase in the residual rockfall hazard (i.e., number of rocks travelling through the forest).

Management of rockfall protection forests

Target values of stand parameters for effective protection have been established since the 1990's (Chauvin et al 1994, Wasser & Frehner 1996). In the minimal tending guidelines for managing rockfall forests developed by Wasser & Frehner (1996), the proposed stand density is independent of the size and energy of the falling rock (400 trees/ha). The minimal tending guidelines aim at optimising protective effects of forests with as little intervention as possible. Based on the real-size experiments, Dorren et al (2005) concluded that the number of impacts against trees were generally more important than the efficacy of a single impact expressed in the amount of energy dissipated by a single tree. For example, it is known from experience that coppice stands can be very effective in stopping small rocks (Gerber & Elsener 1998). Coppice stands have trees reproduced vegetatively from stumps or from suckering by roots. They grow faster than seedlings because they have complete root systems. Therefore, they produce «instant» and usually dense regeneration. The optimal combination of stand density and mean DBH, however, depends on the size and energy of the falling rock. Currently, the notion of rock-size dependent forest stand management has been integrated in new guidelines (Frehner et al 2005, Gauquelin et al 2006). These guidelines also provide values for maximal distances between trees in the fall direction. A limit of 20–40 m is often mentioned because, after falling 40 m down a slope without impacting trees, rocks can gain sufficient energy to destroy trees (Gsteiger 1993, Wasser & Frehner 1996, Dorren et al 2005, Gauquelin et al 2006).

In addition to the characteristics of the falling rocks and the characteristics of the stand itself, the protective effect of a forest also depends on terrain characteristics. Terrain characteristics known to significantly influence rockfall events significantly include: 1) slope angle, 2) surface roughness (structural features that influence the velocity of falling rocks, e.g., rocks and logs, and 3) surface damping (ground or soil characteristics that determine the amount of energy absorbed). Forest management can influence terrain characteristics in many ways.

The management of protection forests is to a large degree a trade-off between optimising the protective effect and assuring forest stand stability at present and over the long term (Dorren et al 2004). Since stand stability is mostly at risk in over-mature stands that lack sufficient regeneration, management interventions in rockfall protection forests often aim at thinning or creating gaps to allow more light into the forest stand. To increase terrain roughness, a common recommendation in rockfall protection forest management is to leave the trunks of cut trees lying on the slope (Figure 9), preferably diagonally to the slope direction, to create obstacles (Mössmer et al 1994, Schwitter 1998, Dorren et al 2005, Frehner et al 2005). These diagonally positioned logs prevent the development of rock accumulations and allow continued rock transport in a controlled manner. The experience in Austria is that larger *Picea abies* trees (DBH > 50 cm) can act as effective rockfall barriers for approximately ten years (Dorren et al 2005). A similar increase in terrain roughness was observed in snag stands (Kupferschmid Albisetti et al 2003, Ammann 2006) and on uncleared wind-throw areas (Frey & Thee 2002, Schönenberger et al 2005). Both latter studies have reported effective protection against rockfall and/or avalanches for 30 years. Additionally, high tree stumps (e.g., > 1.3 m) have been noted to further reduce residual rockfall hazard on a site (Dorren et al 2005, Frehner et al 2005).

Forest roads provide an example of how forest management influences terrain characteristics and, therefore, the rockfall process. Dorren et al (2005) reported that roads stopped 13-15% of the falling rocks both on forested and non-forested slopes with a gradient of 38°. A similar effect was observed at the Stotzigwald site close to Gurtnellen (Canton Uri, Switzerland) in December 2002, when a large rockslide was stopped on a forest-road, leaving a crater approximately 1 m deep.[2] Another example was observed in 2004 at the Gschösswand in the Zillertal (Austria) as shown in Figure 10.

2 M. Tschopp, Canton Uri, personal communication



Fig 9 *Rockfall protection by obstacles consisting of logs positioned on the slope (Photo: Bernhard Maier).*



Fig 10 Rock stopped on a forest road at the Gschösswand in the Zillertal in Austria.

Future challenges

One of the major future challenges in the rockfall source area is developing methods to predict when and what rock (type and size) will fall. Monitoring devices such as the terrestrial laser scanner, crack-meters or extensometers provide good opportunities for this, but methods have to be further developed. In the transit and deposit area the major challenge is to quantify the effect of different slope surfaces on the energy dissipation during a rockfall rebound and to develop objective methods for characterising the elasticity and roughness of different surface types. With respect to forest rockfall research we identified multiple challenges. The most important are:

- Obtaining knowledge on the behaviour of the root systems of trees during rock impacts as, until now, no approach exists for modelling the highly dynamic behaviour of the root-soil system during a rockfall impact.
- Obtaining quantitative information about the relationship between energy absorption capacity and DBH for multiple tree species, as well as information on how the energy absorption capacity decreases with increasing impact height on the tree stem.
- Studying the effect of the impact eccentricity, taking into account the kinetic energy of the rock, its shape and size as well as the height of the impacts using 3D information of the rock velocity.
- Gaining knowledge on the role of coppice stands in rockfall protection (energy dissipation, regeneration, etc.). The initial focus should be to determine how much energy can be absorbed by collectives of sprouts with small diameters in relation to the density and age of the coppiced trees. Rocks are sometimes trapped between branches as branches are highly flexible and therefore present different protection mechanisms than adult single trees.
- Obtaining a relationship between tree mortality and bark or tree wounds due to rock impacts and understanding mechanisms of the effects of rock impacts on mortality.
- Studying the relationship between the structural integrity or soundness of the wood (phytosanitary state) of trees and roots and their energy dissipative capacity.
- Studying the long-term effect of rockfall on the protective effect of forest stands taking into account silvicultural measures such as thinning, prevention of ungulate browsing and leaving tree trunks diagonally on the slope. This can be done by coupling rockfall and forest growth simulators, but should include field trials.
- Developing and validating easy-to-use tools for zoning the rockfall hazard in 2D with and without accounting for the effect of forests.
- Studying the effect of different forest stand structures and compositions on the protective capacity of a stand.
- Using laser scanning data for improving the digital terrain models used by rockfall simulation models and for characterising forest stand structures (stand density, spatial distribution of trees and diameter distribution derived from laser scanning data).
- Undertaking cost-benefit studies for rockfall protection using technical protective measures, protection forests or a combination of the two.
- Establishing monitoring, documentation and archiving systems for rockfall events to document and gain from the experience of practitioners in the field.
- Undertaking additional real-size rockfall experiments on sites with different terrain and forest characteristics.

Conclusions

At present, it is difficult to provide probabilities that unstable rocks will actually fall as a function of a given time period. However, currently available methods allow us to assess the frequency of historical rockfall events and the distribution of the size of the falling rocks. The latter is very important since it determines the energy of the falling rock and the tree impact probability. As such, it also determines the optimal stand structure as well as the required mean tree diameter to dissipate the energy of the falling rock. Scientific research has recently provided basic relationships to determine stand structural parameters. There are, however, many remaining research challenges to improve our knowledge of these relationships. Regarding practical aspects of rockfall protection forest management, detailed guidelines currently exist and evolve con-

stantly as new scientific knowledge becomes available. This process should be continued, but there is also a need for the development of easy-to-use tools for zoning the rockfall hazard in 2D with and without accounting for the effect of forests. ■

Acknowledgement

We thank Manfred Lexer and David Wilford for their valuable suggestions and comments, and Lakhdar Bengrine for his assistance during the final phase of the article.

References

ABELE G (1972) Kinematik und Morphologie spät- und postglazialer Bergstürze in den Alpen. Z Geomorph NF Suppl 14: 138–149.

ALLABY A, ALLABY M (1990) Oxford concise dictionary of earth sciences. New York: Oxford Univ Press. 410 p.

AMMANN M (2006) Schutzwirkung abgestorbener Bäume gegen Naturgefahren. Zürich: Eidg Techn Hochschule, PhD Thesis. 188 p.

AZZONI A, DE FREITAS MH (1995) Experimentally gained parameters decisive for rock fall analysis. Rock Mech Rock Eng 28 (2): 111–124.

BAJGIER-KOWALSKA M (2002) The application of lichenometry in the dating of landslide-rockfall slopes in the Beskid Zywiecki Mountains (Flysh Carpathians). Czasop Geogr 73: 215–230.

BAKKER JP, LE HEUX JWN (1946) Projective-geometric treatment of O. Lehmann's theory of the transformation of steep mountain slopes. Proc K Ned Akad B-PH 49: 533–547.

BALLANTYNE CK, STONE JO (2004) The Beinn Alligin rock avalanche, NW Scotland: cosmogenic ^{10}Be dating, interpretation and significance. Holocene 14: 448–453.

BARTON N, EDITOR (1978) Suggested methods for the quantitative description of discontinuities in rock masses. Int J Rock Mech Min Sc Geomech Abstr 15: 319–368.

BERGER F, DORREN LKA (2007) Principles of the tool Rockfor.net for quantifying the rockfall hazard below a protection forest. Schweiz Z Forstwes 158: 157–165. doi:10.3188/szf.2007.0157

BLAIR TC, MCPHERSON JG (1999) Grain-size and textural classification of coarse sedimentary particles. J Sediment Res 69 (1): 6–19.

BOTKIN DB, JANAK JF, WALLIS JR (1972) Some ecological consequences of a computer model of forest growth. J Ecol 60: 849–872.

BOZZOLO D, PAMINI R (1986) Simulation of rock falls down a valley side. Acta Mech 63: 113–130.

BRAUNER M, WEINMEISTER W, AGNER P, VOSPERNIK S, HOESLE B (2005) Forest management decision support for evaluating forest protection effects against rockfall. For Ecol Manage 207: 75–85.

BROILLI L (1974) Ein Felssturz in Grossversuch. Rock Mech Suppl 3: 69–78.

BUDETTA P (2004) Assessment of rockfall risk along roads. Nat Hazards Earth Sys 4: 71–81.

BUGMANN H (2001) A review of forest gap models. Clim Chang 51: 259–305.

BULL WB, BRANDON MT (1998) Lichen dating of earthquake-generated regional rockfall events, Southern Alps, New Zealand. Bull Geol Soc Am 110 (1): 60–84.

CATTIAU V, MARI E, RENAUD JP (1995) Forêt et protection contre les chutes de rochers. Ingéneries EAI 3: 45–54.

CHAU KT, WONG RHC, WU JJ (2002) Coefficient of restitution and rotational motions of rockfall impacts. Int J Rock Mech Min Sci 39 (1): 69–77.

CHAUVIN C, RENAUD JP, RUPÉ C (1994) Stabilité et gestion des forêts de protection. ONF Bull Techn 27: 37–52.

COROMINAS J ET AL (2005) Quantitative assessment of the residual risk in a rockfall protected area. Landslides 2: 343–357.

COURBAUD B, GOREAUD F, DREYFUS P, BONNET FR (2001) Evaluating thinning strategies using a tree distance dependent growth model: some examples based on the CAPSIS software «uneven-aged spruce forests» module. For Ecol Manage 145: 15–28.

COUVREUR S (1982) Les forêts de protection contre les risques naturels. Nancy: École Nationale du Génie Rural des Eaux et Forêts. 89 p.

CRANDELL DR, FAHNESTOCK RK (1964) Rock falls and avalanches, Little Tahoma Peak, Mt. Rainier, Washington. Bull US Geol Surv 1221(A): 1–30.

DESILETS D, ZREDA M, ALMASI PF, ELMORE D (2006) Determination of cosmogenic ^{36}Cl in rocks by isotope dilution: innovations, validation and error propagation. Chem Geol 233: 185–195.

DOCHE O (1997) Etude expérimentale de chutes de blocs en forêt. Grenoble: Cemagref, doc 97/0898. 130 p.

DORREN LKA (2003) A review of rockfall mechanics and modelling approaches. Progr Phys Geog 26: 69–87.

DORREN LKA, BERGER F (2006) Stem breakage of trees and energy dissipation at rockfall impacts. Tree Physiol 26: 63–71.

DORREN LKA, BERGER F, LE HIR C, MERMIN E, TARDIF P (2005) Mechanisms, effects and management implications of rockfall in forests. For Ecol Manage 215: 183–195.

DORREN LKA, BERGER F, PUTTERS US (2006) Real size experiments and 3D simulation of rockfall on forest slopes. Nat Hazards Earth Syst 6: 145–153.

DORREN LKA, BERGER F, IMESON AC, MAIER B, REY F (2004) Integrity, stability and management of protection forests in the European Alps. For Ecol Manage 195: 165–176.

DORREN LKA, SEIJMONSBERGEN AC (2003) Comparison of three GIS-based models for predicting rockfall runout zones at a regional scale. Geomorphology 56 (1–2): 49–64.

DUSSAUGE-PEISSER C ET AL (2002) Probabilistic approach to rock fall hazard assessment: potential of historical data analysis. Nat Hazards Earth Syst 2: 15–26.

ERISMANN TH, ABELE G (2001) Dynamics of rockslides and rockfalls. Berlin: Springer. 316 p.

FEHR R (1987) Einfache Bestimmung der Korngrößenverteilung von Geschiebematerial mit Hilfe der Linienzahlanalyse. Schweiz Ing Archit 138: 1104–1109.

FOETZKI A ET AL (2004) Die mechanische Stabilität von Bäumen: das Projekt Baumstabilität des FB Naturgefahren. Birmensdorf: Eidgenöss Forsch.anst Wald Schnee Landsch, Forum für Wissen. pp. 35–42.

FREHNER M, WASSER B, SCHWITTER R (2005) Nachhaltigkeit und Erfolgskontrolle im Schutzwald – Wegleitung für Pflegemassnahmen in Wäldern mit Schutzfunktion. Bern: Bundesamt Umwelt Wald Landschaft. 564 p.

FREY W, THEE P (2002) Avalanche protection of windthrow areas: A ten year comparison of cleared and uncleared starting zones. For Snow Landsc Res 77 (1–2): 89–107.

FRIEDEL H (1935) Beobachtungen an den Schutthalden der Karawanken. Carinthia II 125 (45): 21–33.

GARDNER J (1970) Rockfall: A geomorphic process in high mountain terrain. Albertan Geogr 6: 15–20.

GAUQUELIN X ET AL (2006) Guide des sylvicultures de montagne. Grenoble: Cemagref. 289 p.

GERBER E (1974) Klassifikation von Schutthalden. Geogr Helv 29: 73–82.

GERBER C, ELSENER O (1998) Niederwaldbetrieb im Steinschlaggebiet. Wald Holz 79 (14): 8–11.

GERBER W (1998) Waldwirkung und Steinschlag. In: Proc 14. Arbeitstagung Schweizerischen Gebirgswaldpflegegruppe & FAN, Grafenort/Engelberg, unpublished report. pp. 1–15.

GERBER W (2001) Guideline for the approval of rockfall protection kits. Bern: Swiss Agency Environment Forests Landscape, Environment in Practice. 39 p.

GIANI GP (1992) Rock slope stability analysis. Rotterdam: Balkema. 361 p.

GLADE T, LANG M, EDITORS (2003) Strategies and applications in natural hazard research using historical data. Nat Hazards 31 (3). 99 p.

GOODMAN RE, SHI GH (1985) Block theory and its application to rock engineering. London: Prentice-Hall. 338 p.

GSTEIGER P (1993) Steinschlagschutzwald. Ein Beitrag zur Abgrenzung, Beurteilung und Bewirtschaftung. Schweiz Z Forstwes 144: 115–132.

GUZZETTI F, CROSTA G, DETTI R, AGLIARDI F, (2002) STONE: a computer program for the three-dimensional simulation of rock-falls. Comp Geosci 28: 1079–1093.

HANTZ D, VENGEON JM, DUSSAUGE-PEISSER C (2003) An historical, geomechanical and probabilistic approach to rock-fall hazard assessment. Nat Hazards Earth Syst 3: 693–701.

HASENAUER H, BURGMANN M, LEXER MJ (2000) Konzepte der Waldökosystemmodellierung. Cent.bl gesamte Forstwes 117: 137–164.

HOEK E, BRAY JW (1981) Rock Slope Engineering. London: Institution Mining Metallurgy. 402 p.

HUNGR O, EVANS SG (1988) Engineering evaluation of fragmental rockfall hazards. In: Proc 5th Int Symp Landslides, Lausanne (10–15 Jul 1988). Rotterdam: Balkema. pp. 685–690.

JABOYEDOFF M, DUDT JP, LABIOUSE V (2005) An attempt to refine rockfall hazard zoning based on the kinetic energy, frequency and fragmentation degree. Nat Hazards Earth Syst 5: 621–632.

JAHN J (1988) Entwaldung und Steinschlag. In: Proc Interpraevent, Graz, vol 1. pp. 185–198.

KENT PE (1966) The transport mechanism in catastrophic rockfalls. J Geol 74: 79–83.

KALBERER M, AMMANN M, JONSSON M (2007) Mechanische Eigenschaften der Fichte: Experimente zur Analyse von Naturgefahren. Schweiz Z Forstwes 158 166–175 doi: 10.3188/szf.2007.0166

KIRKBY MJ, STATHAM I (1975) Surface stone movement and scree formation. J Geol 83: 349–62.

KRAUTBLATTER M, DIKAU R (2007) Towards a uniform concept for the comparison and extrapolation of rockwall retreat and rockfall supply. Geogr Ann 89A: 1–20.

KRAUTBLATTER M, MOSER M (2006) Will we face an increase in hazardous secondary rockfall events in response to global warming in the foreseeable future? In: Price MF, editor. Global Change in Mountain Regions. Duncow: Sapiens. pp. 253–254.

KRAUTBLATTER M, MOSER M, SCHROTT L, WOLF J (2007) A study on sediment yield and geomorphic work comprising all rockfall magnitudes in an Alpine Catchment (Reintal, German Alps). Geomorphology (in press).

KUPFERSCHMID ALBISETTI AD, BRANG P, SCHOENENBERGER W, BUGMANN H (2003) Decay of *Picea abies* snag stands on steep mountain slopes. For Chron 79: 247–252.

LANG A, MOYA J, COROMINAS J, SCHROTT L, DIKAU R (1999) Classic and new dating methods for assessing the temporal occurrence of mass movements. Geomorphology 30: 33–52.

LE HIR C (2005) Forêt et chutes de blocs: méthodologie de modélisation spatialisée du rôle de protection. Marne-La-Vallée: Univ Marne-La-Vallée, PhD Thesis. 195 p.

LEHMANN O (1933) Morphologische Theorie der Verwitterung von Steinschlagwänden. Vierteljahrschr Nat.forsch Ges Zür 87: 83–126.

LEXER MJ, HÖNNINGER K (2001) A modified 3D-patch model for spatially explicit simulation of vegetation composition in heterogeneous landscapes. For Ecol Manage 144: 43–65.

LINIGER M (2000) Computersimulation von Stein- und Blockschlägen. Felsbau 18 (3): 64–68.

MAZZOCCOLA DF, HUDSON, JA (1996) A comprehensive method of rock mass characterization for indicating natural slope instability, Quart J Engin Geol 29: 37–56.

MCCARROLL D, SHAKESBY RA, MATTHEWS JS (1998) Spatial and temporal patterns of Late Holocene rockfall activity on a Norwegian talus slope: lichenometry and simulation-modelling approach. Arct Alp Res 30: 51–60.

MEISSL G (2001) Modelling the runout distances of rockfall using a geographic information system. Z Geomorphol NF Suppl 125: 129–137.

MÖLK M (2000) The Kreuzlau rockfall – methodical approach for the collection of basic data aiming at the evaluation of rockfall hazards and the planning of counter-measures. Felsbau 18 (1): 47–51.

MORCHE D, KATTERFELD C, FUCHS S, SCHMIDT KH (2006) The life-span of a small high mountain lake, the Vordere Blaue Gumpe in Upper Bavaria, Germany. In: Rowan J, Duck RW, Werritty A, editors. Sediment dynamics and the hydromorphology of fluvial systems. Wallingford: IAHS Press. pp. 72–81.

MÖSSMER EM, AMMER U, KNOKE T (1994) Technisch-biologische Verfahren zur Schutzwaldsanierung in den oberbayrischen Kalkalpen. München: Bayer Landesanstalt Wald Forstwirtschaft, forstl Forsch.ber 145. 135 p.

O'HARA KL (2006) Multiaged forest stands for protection forests: concepts and applications. For Snow Landsc Res 80 (1): 45–56.

OMURA H, MARUMO Y (1988) An experimental study of the fence effects of protection forests on the interception of shallow mass movement. Mitt Forstl Bundesvers.anst Mariabrunn Wien 159: 139–147.

PEILA D, PELIZZA S, SASSUDELLI F (1998) Evaluation of behaviour of rockfall restraining nets by full scale tests. Rock Mech Rock Eng 31 (1): 1–24.

PERRET S, DOLF F, KIENHOLZ H (2004) Rockfalls into forests: Analysis and simulation of rockfall trajectories – considerations with respect to mountainous forests in Switzerland. Landslides 1: 123–130.

PERRET S, STOFFEL M, KIENHOLZ H (2006) Spatial and temporal rockfall activity in a forest stand in the Swiss Prealps – a dendrogeomorphological case study. Geomorphology 74: 219–231.

PIERSON LA, DAVIS SA, VAN VICKLE R (1990) Rockfall hazard rating system. Implementation Manual. Washington DC: Federal Highway Administration, US Dep Transp, Report FHWA-OR-EG-90–01.

PRIEST SD, HUDSON JA (1976) Discontinuity spacings in rock. Int J Rock Mech Min Sc Geomech Abstr 13: 135–148.

RAMMIG A, FAHSE L BUGMANN H, BEBI P (2006) Forest regeneration after disturbance: a modelling study for the Swiss Alps. For Ecol Manage 222: 123–136.

RICKLI C, GRAF F, GERBER W, FREI M, BÖLL A (2004) Der Wald und seine Bedeutung bei Naturgefahren geologischen Ursprungs. Birmensdorf: Eidgenöss Forsch.anst Wald Schnee Landsch, Forum für Wissen. pp. 27–34.

ROMANA M (1988) Practice of SMR classification for slope appraisal. In: Proc 5th Int Symp Landslides, Lausanne (10–15 Jul 1988). Rotterdam: Balkema. pp. 1227–1229.

ROUILLER JD, JABOYEDOFF M, MARRO C, PHLIPPOSSIAN F (1997) Matterock: méthodologie d'étude d'instabilités de falaise et d'appréciation du danger. Publ Soc Suisse Méc Sols Roches 135: 13–16.

SASS O (2005) Spatial patterns of rockfall intensity in the northern Alps. Z Geomorphol NF Suppl 138: 51–65.

SASS O, KRAUTBLATTER M (2007) Debris-flow-dominated and rockfall-dominated scree slopes: genetic models and process rates derived from GPR measurements. Geomorphology 86: 176–192. doi:10.1016/j.geomorph.2006.08.012

SCHEIKL M (2006) Risk assessment of the rockslide Spitz (Austria) based on laser scanner date, stability calculations and run-out models. In: Proc 3rd Colloquium Rock Mechanics – Theory and Practice, Vienna (Mar 2006). Vienna: Vienna University of Technology.

SCHÖNENBERGER S, NOACK A, THEE P (2005) Effect of timber removal from windthrow slopes on the risk of snow avalanches and rockfall. For Ecol Manage 213: 197–208.

SCHROTT L, NIEDERHEIDE A, HANKAMMER M, HUFSCHMIDT G, DIKAU R (2002) Sediment storage in a mountain catchment: geomorphic coupling and temporal variability (Reintal, Bavarian Alps, Germany). Z Geomorphol NF Suppl 127: 175–196.

SCHWITTER R (1998) Zusammenfassung und Schlussfolgerungen. In: Proc 14. Arbeitstagung Schweizerischen Gebirgswaldpflegegruppe & FAN, Grafenort/Engelberg, unpublished report. pp. 1–5.

SHUGART HH (1984) A theory of forest dynamics. The ecological implications of forest succession models. New York: Springer. 278 p.

SMEKAL A (1920) Über den im Hochgebirge bei Steinschlag auftretenden Geruch. Naturwissenschaften 8 (25): 496.

STOFFEL M (2006) A review of studies dealing with tree rings and rockfall activity: The role of dendrogeomorphology in natural hazard research? Nat Hazards 39 (1): 51–70.

STOFFEL M, PERRET S (2006) Reconstructing past rockfall activity with tree rings: some methodological considerations. Dendrochronologia 24 (1): 1–15.

STOFFEL M, LIÈVRE I, MONBARON M, PERRET S (2005B) Seasonal timing of rockfall activity on a forested slope at Täschgufer (Valais, Swiss Alps) – a dendrochronological approach. Z Geomorphol 49 (1): 89–106.

STOFFEL M ET AL (2005A) Analyzing rockfall activity (1600–2002) in a protection forest – a case study using dendrogeomorphology. Geomorphology 68: 224–241.

STOFFEL M ET AL (2006) Assessing the protective effect of mountain forests against rockfall using a 3D simulation model. For Ecol Manage 225: 113–122.

STOKES A ET AL (2005) Mechanical resistance of different tree species to rockfall in the French Alps. Plant Soil 278: 107–117.

TAYLOR MP, VILES HA (2000) Improving the use of microscopy in the study of weathering: sampling issues. Z Geomorphol NF Suppl 120: 145–158.

TRUDGILL ST, VILES HA (1998) Linking field and laboratory based measurements of limestone weathering rates. Q J Eng Geol 31: 333–341.

WASSER B, FREHNER M (1996) Minimale Pflegemassnahmen für Wälder mit Schutzfunktion. Wegleitung. Bern: Bundesamt Umwelt Wald Landschaft. 122 p.

WEHRLI A ET AL (2006) Modelling the long-term impacts of forest dynamics on the protective effect against rockfall. For Snow Landsc Res 80 (1): 57–76.

WENTWORTH CK (1922) A scale of grade and class terms for clastic sediments. J Geol 30: 377–392.

WHALLEY WB (1984) Rockfalls. In: Brundsden D, Prior DB, editors. Slope instability. London: Wiley. pp. 217–256.

WINCHESTER V, CHAUJAR RK (2002) Lichenometric dating of slope movements in the Nant Francon, North Wales. Geomorphology 47: 61–74.

WOLTJER M ET AL (2007) Coupling a 3D patch model and a rockfall module to assess rockfall protection in mountain forests. J Env Manage. in press. doi:10.1016/j.jenvman.2007.01.301

ZINGGELER A (1990) Steinschlagsimulation in Gebirgswäldern: Modellierung der relevanten Teilprozesse. Bern: Univ Bern, MSc Thesis. 116 p.

Stand des Wissens in den Wechselbeziehungen zwischen Steinschlag und Wald

Um Steinschlagschäden unterhalb von Wäldern zu verhindern, können waldbauliche, ingenieur-biologische, technische oder eine Kombination dieser Massnahmen zum Einsatz kommen. Für eine günstige und wirksame Ausführung ist es wichtig zu wissen, 1) wo und in welcher Grössenordnung Steinschlagereignisse auftreten, 2) um welches Ausmass der Wald die Auslaufdistanz, die Sprunghöhe und die Energie der herunterfallenden Steine oder Felsen verringert und 3) wie die Schutzwirkung des Wald verbessert werden kann. Der Aufsatz gibt einen Überblick über den heutigen Wissensstand und über die in der Praxis verwendeten Methoden. Der Beitrag benennt zudem die wichtigsten Herausforderungen, welche im Rahmen einer umfassenden Steinschlag-Wald-Forschung gelöst werden müssen.

État des connaissances sur les interactions entre les chutes de pierres et la forêt

Pour prévenir les chutes de pierres à l'aval des forêts, on peut utiliser la gestion forestière, l'ingénierie écologique ou civile, ou une combinaison de celles-ci. Pour une réalisation peu coûteuse et efficace, il faut savoir 1) où et dans quelle ampleur se produisent les chutes de pierres, 2) dans quelle mesure la forêt réduit la distance d'arrêt, la hauteur de rebond et l'énergie des pierres et des blocs en chute, et 3) comment l'effet protecteur de la forêt peut être amélioré. L'article fournit un aperçu de l'état actuel des connaissances et des méthodes utilisées dans la pratique. Il mentionne en outre les principales exigences à respecter dans le cadre d'une vaste étude sur les chutes de pierres et la forêt.

> Chapter 13

Laser scanning for characterising mountain forests



Chapter 7.2

Characterising mountain forest structure using landscape metrics on LiDAR-based canopy surface models

B. Maier[1,*], D. Tiede[2], L. Dorren[3]

[1] Stand Montafon Forstfonds, Montafonerstr. 21, 6780 Schruns, Austria, bernhard.maier@stand-montafon.at

[2] Salzburg University, Centre for Geoinformatics, Hellbrunnerstr. 34, 5020 Salzburg, Austria, dirk.tiede@sbg.ac.at

[3] Cemagref Grenoble, 2 rue de la Papeterie, BP76, 38402 St. Martin d`Heres cedex, France, luuk.dorren@cemagref.fr

KEYWORDS: protection forest, landscape ecology indices, segmentation, laser scanning, gap analysis

ABSTRACT: Forest structure is a key element to determine the capacity of mountain forests to protect people and their assets against natural hazards. LiDAR (Light Detection And Ranging) offers new ways for describing forest structure in 3D. However, mountain forest structures are complex and creative methods are therefore needed to extract reliable structural information from LiDAR. The objective of this study was to investigate if the application of landscape metrics to a normalised canopy model (nCM) allows an automatic characterisation of forest structure. We used a generic automated approach that created height class patches based on a segmented nCM. Two multi-resolution segmentations were carried

* Corresponding author

out: level 1 objects represented tree crowns and collectives of tree crowns, level 2 objects represented forest stands. Level 1 objects were classified into four height classes and subsequently overlaid with level 2 stands in order to calculate the metrics 1) canopy density and vertical layering of the forest, 2) forest gap distribution and 3) canopy roughness using the Division Index (DIVI). Canopy density values of each height class allowed the classification of the vertical layering. Distinguishing between single- and multi-layered stands, 82% of all the sample plots were correctly classified. The DIVI calculated on gaps proved to be sufficient to describe the spatial arrangement of patches and distinguish between stands with many small gaps from stands with only a few but larger gaps. Canopy roughness could not satisfactorily be described using the DIVI based on the validation plots. With the approach presented, resource and natural hazard managers can assess the structure of forest stands and as such more easily take into account the protective effect of forests.

1 Introduction

"Mountain forests provide the most effective, the least expensive and the most aesthetic protection against natural hazards" recalls the first paragraph of the Mountain Forest Protocol of the Alpine Convention. Without mountain forests, the costs of building and maintaining technical protective constructions against rapid mass movements in the Alps would be unaffordable. Forest structure is a key element that determines the protective capacity of mountain forests (Dorren et al. 2004). It can be characterised by the horizontal distribution of trees, the vertical layering and the tree species mixture.

Structures of mountain forests differ greatly from those in the lowlands. Mountain forests contain relatively few species, tend to be quite open and consist of a mosaic of tree clusters and gaps (Schönenberger 2001). In mountain forests, particularly, structure is closely related to stand stability, i.e. resistance against and resilience after disturbances such as storm and snow loads (Brang 2001). Other characteristics that determine structure are crown closure and tree density. These directly influence release probability of forest avalanches and the capacity to stop falling rocks (Dorren et al. 2005). Consequently, assessing forest structure enables forest managers and natural risk engineers to evaluate if a forest can fulfil its protective function or not. Reliable and area-extensive data on forest structure is thus a prerequisite for effective resource and risk management in mountainous regions.

Traditional methods for assessing forest structure comprise field inventories (Herold and Ulmer 2001) and aerial photo interpretation (Bebi 1999). The drawback of inventories is that they cannot provide spatially continuous information over a large area. The usefulness of photo interpretation im mountainous terrain is hampered by different illumination and shading effects. Small footprint airborne LiDAR, however, allows deriving detailed digital terrain (DTM) and surface (DSM) models. Subtracting these two models of a forested area results in a so-called normalised canopy model (nCM), which is spatially continuous and not hampered by shading effects - typical for optical remote sensing data. This facilitates assessing forest structure in 2.5D. Various studies show that it is possible to derive a variety of single structural attributes such as tree height, basal area, crown size and above-ground biomass from LiDAR data (Hyyppä et al. 2006, Hall et al. 2005, Naesset 2004, Maltamo et al. 2004, Tiede et al. 2004, Lim et al. 2003). Some studies focus on tree height variance as an indicator of vertical forest structure (Blaschke et al. 2004, Zimble et al. 2003). Until now, little attention, however, has been paid to the application of landscape metrics to LiDAR-based canopy surface models.

Landscape metrics, representing a view “from above”, allow quantifying the link between landscape structure and function. Usually, they are derived for the following three levels: 1) the patch level which corresponds to individual objects, 2) the class level, i.e., characteristics of all patches of the same type and 3) landscape level which integrates all patch types or classes across the extent of the data. For some applications a fourth level, the region level, is introduced. This level indicates a sub-area of the landscape. If we translate the landscape metrics nomenclature into the forest structure context of this study, landscape refers to the whole forest, region refers to stand, class to tree height class and patch to tree height patch. The use of landscape metrics within forests mainly focuses on forest fragmentation and biodiversity, and their changes over time (Traub & Klein 1996, Venema et al. 2005).

In this study, landscape metrics are used for another purpose, namely to describe fragmentation of the canopy surface height in terms of variability or structuring. Landscape metrics are expected to link forest structure with the protective capacity of a mountain forest. The general idea is that the use of landscape metrics leads to more objective, transparent and repeatable results compared to visual interpretation by a human interpreter. Our overall goal is to derive stand structure information as a basis for protection forest planning, management and monitoring. Therefore, the objective of this study was to investigate if the application of landscape metrics to a nCM allows an automatic characterisation of forest structure.

2 Study area and data

2.1 Study area

The study area covers 120 ha of spruce-dominated protection forest on a west facing slope near the Austrian village of Gaschurn in the Montafon valley (see Fig. 1). This forest provides essential protection against natural hazards such as landslides, avalanches and rockfall. The study area ranges from 1000 m altitude in the valley floor up to 1800 m at the tree line. The study area is dominated by steep rugged terrain with rock faces, gullies and torrents. Old-growth forests with different structure types dominate. The structural differences are due to various factors. Multi-layered structures with short-distance height variation in the canopy, so called fine-grained canopy patterns, grow on shallow soils that cover glacially eroded bedrock.

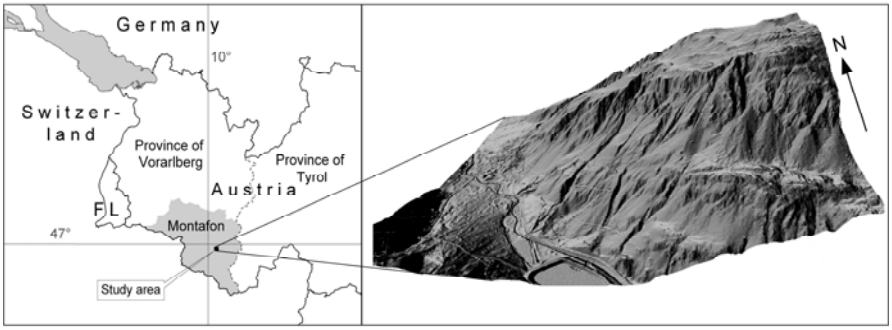


Fig. 1. Location (left) and DTM of the study area viewed from Southwest (right)

Homogenous pole stands occur in areas that used to be meadows in the lower parts of the slope. Open structures caused by windthrow are found below the rock faces in the southeastern part of the study area. Another type of open structures is found close to the tree line. These, however, consist of tree clusters (collectives), which are typical for high altitude forests. Along the avalanche tracks, tree regeneration and young stands can be found. The presence of all these different structure types makes this area well-suited for this study.

2.2 Data

The ALS data used in this study were acquired on the 10th of December 2002 under leaf-off canopy conditions. The instrument applied was a first/last pulse Airborne Laser Terrain Mapper (ALTM 1225) produced by Optech Inc. (Canada). The pulse repetition frequency of the ALTM is 25 kHz that resulted in a point density of 0.9 points m^{-2} at an average flight height of 1000 m above ground level. With a laser beam divergence of 0.3 mrad, the theoretical footprint on the ground was about 0.30 m. The average ground swath width was about 725 m, the maximum scanning angle 20º (Wagner et al. 2004).

The data obtained by the ALTM have been processed and interpolated by the TU Vienna using the *hierarchical robust filtering* approach within the SCOP++ software package (Kraus and Pfeifer 1998). As a result a DTM and a DSM, both with a resolution of 1 m × 1 m, were created. By subtracting the DTM from the DSM we obtained a nCM which describes an estimate of the forest height.

Thirty-three circular inventory plots of 314 m² served for validation. Within these plots, we recorded for each tree: diameter at breast height (1.3 m), position (azimuth and distance), height and species. In addition, we determined the vertical layering and the stand type following Maier (2007a).

3 Methodology and Implementation

3.1 Segmentation and height classification

Our method combines object-based multi-resolution segmentation and classification with GIS analyses. The rule sets for segmentation and classification are developed using CNL (Cognition Network Language), a modular programming environment available in the Definiens Developer environment. Segmentation is done using a region-based, local mutual best fitting segmentation approach. It is a pair-wise clustering process, starting with randomly selected one-cell objects. In an iterative process these objects are merged into larger ones. This segmentation process is determined by three parameters which can be set by the user. The first one is *scale* which is a stop criterion for the object growing process and thus defines the maximum segment, or object size. The other two parameters *shape (vs. colour)* and *compactness (vs. smoothness)* define the weights for the allowed heterogeneity of image values (here: height values) and shape complexity (Baatz and Schäpe 2002, Benz et al. 2004).

Segmentation was used to create two object levels which corresponded to 1) single and clustered tree crowns and to 2) forest stands. To delineate single and clustered (collectives) tree crowns the nCM was segmented into objects using a scale parameter of 5. The ancillary parameters *shape* and *compactness* were both set to 0.5. Since single tree crowns comprise different height classes, a small *scale* parameter led to onion-like concentric objects only representing parts of a tree crown. A big *scale* parameter, however, levelled out the different tree heights and resulted in a loss of structural complexity. Segmentation tests with known trees showed that a scale parameter of 5 was a good compromise. The resulting objects in this level represent homogenous tree height patches. These canopy objects were then classified according to their mean height using the height classification schema presented in Fig. 2.

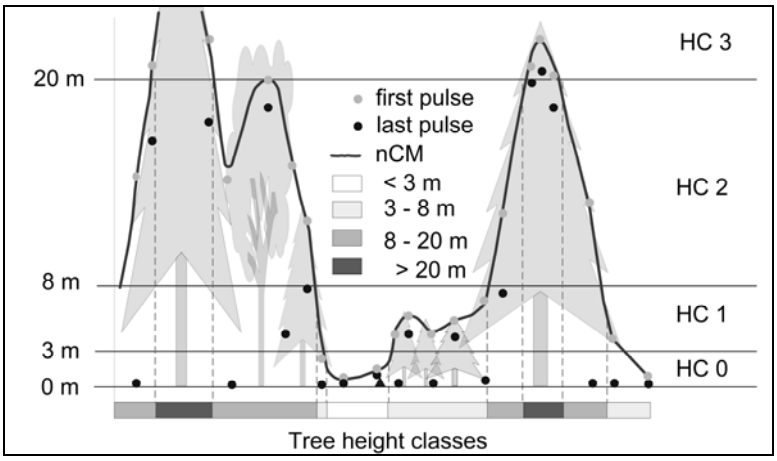


Fig. 2. Tree height classification schema

The height classification schema follows the different forest development stages that are defined in the Manual for the Aerial Photo Interpretation of the Swiss Forest Inventory (Ginzler et al. 2005). Four height classes (HC) are introduced: HC 0 comprises all segments with a mean vegetation height below 3 m. Those are regarded as unstocked as the differentiation accuracy of the laser allows no distinction between surface roughness (lying dead wood, rocks, stumps or low vegetation) and young trees. HC 1 (3-8 m) corresponds to young trees and HC 2 covers the range from 8-20 m. This class contains mainly pole forests and timber forest. HC 3 consists of tree crowns higher than 20 m, which are usually thicker trees, or old growth forest. The classified objects were subsequently dissolved into ho-

mogenous height class patches and exported into a GIS readable vector format (Polygon Shape file).

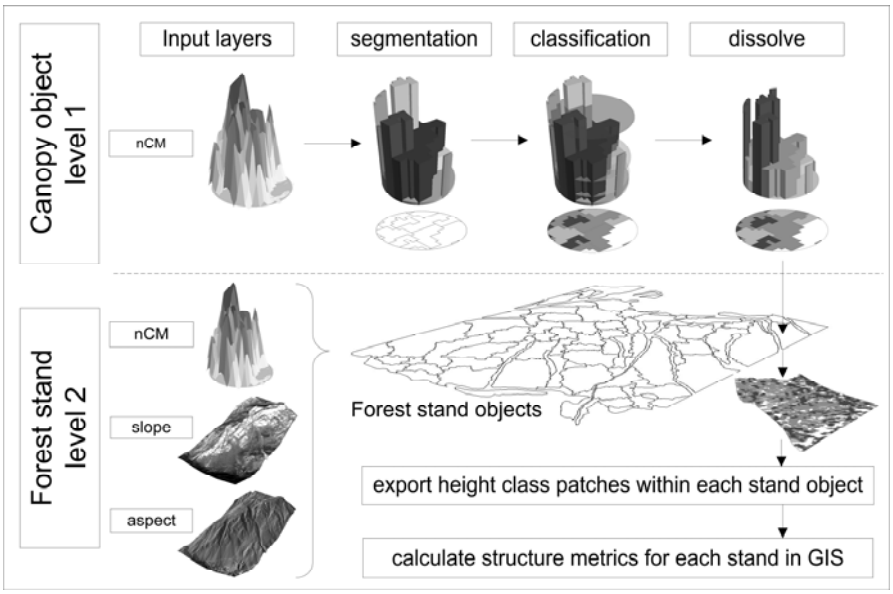


Fig. 3. Flow diagram of study methodology

To delineate forest stands, input rasters were segmented into objects using a *scale* parameter of 100, as well as a *shape* and *compactness* parameter of 0.3 and 0.4 respectively. Because terrain features strongly influence forest growth and development in relief-rich mountainous terrain, the input rasters consisted of the nCM, but also the mean slope gradient, and the aspect. We assumed that forest stands are largely homogenous in terms of age, species distribution and developmental stage and that they reflect similar physiographical conditions. The segmentation weights of the three input rasters nCM, slope and aspect were set to 1, 0.5 and 0.5 respectively. The setting of the above mentioned parameters provided the forest stand map that respected best existing stand borders observed in the field and on CIR orthophotos.

Following the segmentation and classification, a GIS was used to characterise the patch-structure (level 1) within each stand object (level 2) using landscape metrics for canopy density, vertical layering, gap distribution and canopy roughness of a forest stand. All metrics were calculated with the V-late extension for ArcGIS (Lang and Tiede 2003). Fig. 3 summarises the complete method flow of this study.

3.2 Landscape metrics calculation

The structural characteristics considered relevant for this study were: canopy density and vertical layering of the forest, forest gap distribution and canopy roughness. In the following paragraphs their calculation using landscape metrics will be explained in detail.

3.2.1 Canopy density and vertical layering of the forest

Canopy density (CD) is defined as the percentage of the area which is occupied by the horizontal projection of tree crowns. Multiple coverage in super-imposed tree layers (height classes) is not taken into account (Keller 2005). The landscape metric we used for describing CD is called CD_{total} and corresponds to the total area of all stocked height patches of HC 1, 2 and 3, in percent of the total stand area. Maier (2007b) shows that there is a good correspondence ($R^2 = 0.7$) between canopy density measured in the field by mapping crown radius and the canopy density derived from LiDAR-based canopy models.

$$CD = P_i = \frac{\sum_{j=1}^{n} a_{ij}}{A}(100) \qquad \text{(eq. 1)}$$

P_i = proportion [%] of the stand (without gaps) occupied by height class i

a_{ij} = area [m²] of patch ij

A = stand area [m²] without gaps (HC 0)

Vertical layering or stratification can be referred to as the vertical distribution of foliage (Parker and Brown 2000). When calculating CD for the three different HC (eq. 1, see McGarigal and Marks 1995), the vertical layering of the forest can be assessed. It is important to note that superimposed tree layers cannot be detected using a 2.5D nCM. Therefore, the layering assessment is restricted to the different height levels which can be seen from above. According to the Austrian Forest Inventory (AFI), a single-layered stand has only one distinct canopy layer. Two-layered structures have in addition to the dominant canopy layer a second layer, which exhibits considerable growth potential. Here, a separate forest layer needs to have a total CD of at least 30% (Schieler and Hauk 2001). According to the Swiss National Forest Inventory, single layered stands consist of one layer that covers more than 80%. Our rules for assessing the vertical layer-

ing were principally based on these guidelines, but adapted for an nCM-based analysis (Table 1).

Table 1. Rule set for vertical layering according to canopy density (CD) per height class (HC)

single-layered	one HC with CD > 60%, no other HC > 35%
two-layered	two HC with CD > 30% or one HC > 50% and one HC >20%
multi-layered	three HC with CD > 20%

For validation, we compared the vertical layering classification with the vertical structures recorded in the 33 field plots.

3.2.2 Forest gap distribution

Gaps are unstocked patches in a forest matrix. They can be formed by harvesting trees (silvicultural intervention), by natural succession or disturbances. When trees die, they create gaps that allow the sunlight reaching the ground, which could initiate forest regeneration. Windthrow, snow break and subsequent bark beetle infestations belong to the natural gap-making processes and disturbances. Small gaps are distinct and common features of mountain forests, and do not pose problems to the protective function of the forest against natural hazards. Large openings in the forest cover, however, do. They are potential avalanche release areas or can accelerate rockfall.

Therefore, the size and spatial distribution of gaps influence the protective capacity of a forest. The bigger and longer a gap is in the slope direction, the more likely forest avalanche release or falling rocks acceleration is. Gap length can be calculated by defining the longest flow path in slope direction. These values can then be compared with existing protection forest management guidelines (e.g. Frehner et al. 2005) in order to assess the need for silvicultural intervention or tending.

$$DIVI_{HC0} = 1 - \sum_{i=1}^{n} \left(\frac{a_i}{A} \right)^2 \qquad \text{(eq. 2)}$$

where a_i = area [m²] of gap patch i
A = here: total area [m²] of gaps in one stand (HC 0)

In order to assess the spatial distribution of gaps, we calculated the Division Index (DIVI, see eq. 2). The DIVI is defined as the probability that two randomly selected locations do not occur within the same patch in the forest (Jaeger 2000). Although this index originates from ecology where it

refers to the likeliness that two organisms will meet within the same patch, it can also refer to the degree of gap fragmentation, or "gappiness" of a forest stand. In other words, it expresses if gaps occur as single big unstocked areas or highly fragmented small gaps throughout the stand.

3.2.3 Canopy roughness

Finally, we tried to quantify the graininess or roughness of the forest canopy by measuring the overall fragmentation of all height classes and interpret it as a degree of structuring. This is done by calculating the Division Index on all height classes on a stand level (eq. 3). This measure of fragmentation describes if the canopy is vertically homogenous or heterogeneously structured, following McGarigal and Marks (1995), who used this index to differentiate between coarse- and fine-grained landscape structures. Within the conventional repertoire of forest inventory parameters, the parameter *StandType* (Schieler and Hauk 2001) which defines uniform, irregular and single tree structures (see Table 2) appeared the only one to represent canopy roughness (CR) as a structural parameter.

$$DIVI = 1 - \sum_{i=1}^{n} \left(\frac{a_i}{A} \right)^2 \qquad \text{(eq. 3)}$$

where a_i = area [m²] of patch i
A = here: total area [m²] of stand

Table 2. Definition of stand type according to the Austrian Forest Inventory (Schieler and Hauk 2001)

Uniform	Homogenous, more or less closed canopy with uniformly distributed trees or tree groups
Irregluar	Stands consisting of tree groups of similar height with a distinct green mantle forming inner forest edges
Single trees	Dissolved stand structure with single trees and a canopy density below 30%; trees loosely distributed over the whole area

4 Results

4.1 Canopy density and vertical layering

Canopy density results are given in Fig. 4. The stands with prevailing open or light canopy density dominate in the uppermost parts close to the tree line as well as near the valley floor (stands with $CD_{total} < 60\%$).

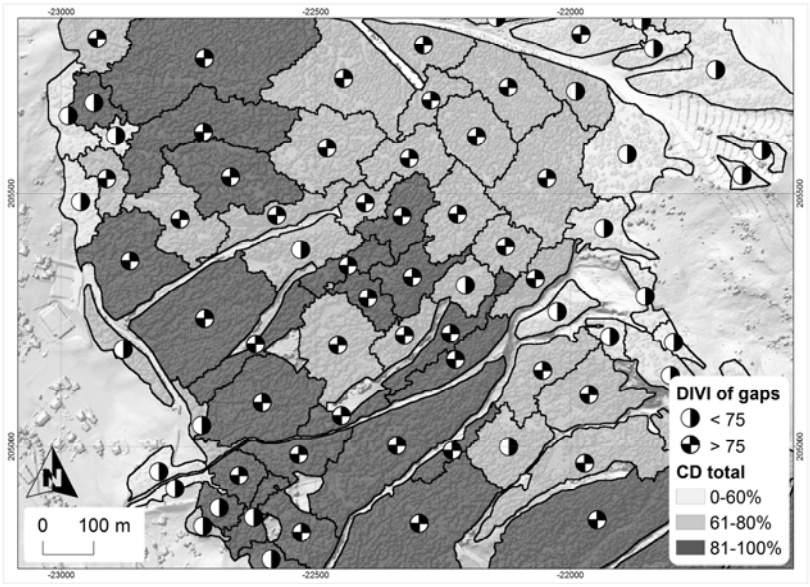


Fig. 4. Canopy density (CD_{total}) and division index (DIVI) of gaps

The latter represent the mixed and broadleaved stands which appear open due to the lack of crown reflection in the leaf-off season. The forests in the central part of the study area exhibit light structures due to the numerous rock fall channels just below the massive rock faces in that area. The open structures indicated in the upper parts correspond to a mosaic with gaps typical for high altitude forests.

Results of the layering assessment show that the homogenous pole stands in the lower part of the study area are classified as single and two-layered forests. Multi-layered structures, however, can be found in sporadic stands mainly along and in between the avalanche tracks. A comparison of the automatic layering-classification with the assessment carried out in the field results in 73% correct detections. This number increases to 82% if two- and multi-layered structures are put together into one category. Most mismatches can be found in the high-altitude forests with tree

clusters. Whilst they appear multi-layered in the field, their vertical variation falls within one height class during automatic classification. Half of the false detected sample plots are characterised by low CD values. Fig. 6 shows six examples of validation plots with layering assessments and different CD_{total}.

4.2 Gap distribution

The Division Index (DIVI) calculated on gaps (HC 0) quantifies the distribution of gaps within a stand. In order to get an idea of the total size of the unstocked area, it is necessary to combine the DIVI with the total canopy density (CD_{total}). As shown in Fig. 4 this combination very well distinguishes stands with many small gaps from others with a few large openings. In the central part of the study area a stand with a large windthrow opening is characterised by a low CD_{total} and a DIVI below 75, indicating low fragmentation. The forest stands in the northwestern part exhibit DIVI-values above 75 describing a high degree of fragmentation meaning that the unstocked area is divided into numerous small gaps.

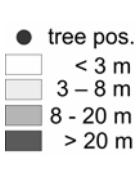
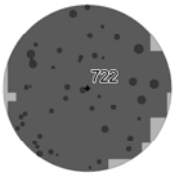
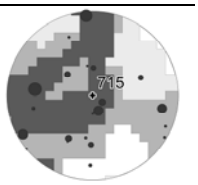
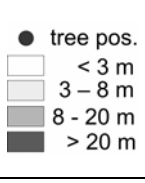
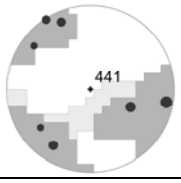
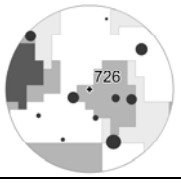
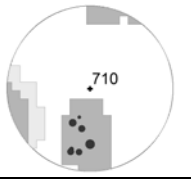
CD	Single-layered	Two-layered	Multi-layered
			
CD_{total} (valid.)	100% (correct)	87% (correct)	87% (false)
			
CD_{total} (valid.)	48% (false)	49% (false)	27% (false)

Fig. 5 Selected field validation plots (radius = 10 m) with layering and CD_{total}

The DIVI-threshold of 75 is deduced from a series of gap fragmentation patterns shown in Fig. 6. These DIVI-values are calculated on a basic gap share of 30% with increasing fragmentation.

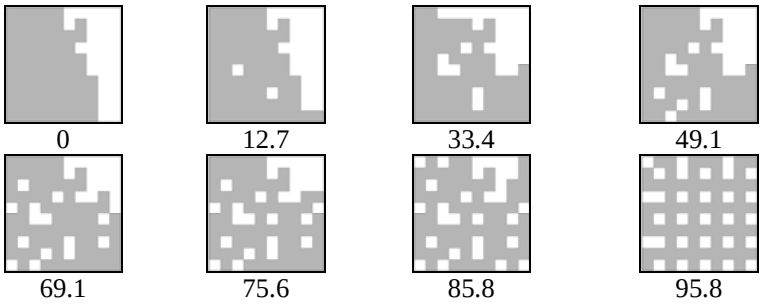


Fig. 6 Series of gap fragmentation patterns indicating the range of the Division Index (DIVI)

4.3 Canopy roughness

We regard the overall fragmentation of the height class patch mosaic as a measure for structural variability, including both the vertical as well as the horizontal structural view. Fig. 7 presents the distribution of DIVI values among the *StandType* attributes. According to a mean comparison Scheffé test (Bahrenberg et al. 1992) categories "uniform" and "irregular" are significantly different from each other (p=0.05). The category "single trees" does not significantly differ from the other two categories which may be due to the low number of samples in that class (see Fig. 7).

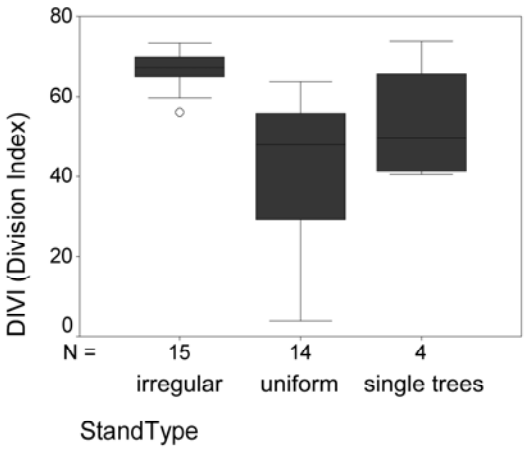


Fig. 7. Distribution of DIVI values among *StandType* categories

According to Fig. 7 we define the threshold between uniform and irregular stands at a DIVI value of 65. Using this threshold, only the open structured stands close to the tree line and the stands near the valley floor can be classified as uniform. All together only 1.5% of all stands can be classified uniform, the rest is irregularly structured.

5 Discussion

The objective of this study was to investigate if the use of landscape metrics on height class patches of the nCM allows an automatic characterisation of forest structure. For that purpose we segmented and classified the nCM and transformed it from a continuous raster surface into a polygon mosaic of vegetation height patches. This segmentation was done at the level of tree crowns and tree groups (level 1) and proved to be a straightforward way to simplify the complex canopy surface. Attempts to incorporate different morphometric derivatives such as slope and curvature of the nCM in the segmentation process did not improve the results. Thus the nCM served as the only input for that segmentation.

The segmentation of forest stands (level 2) turned out to be more difficult. It was difficult to balance the three segmentation parameters in a way that the size and shape of the resulting stand objects correlated to natural stand borders which might have appeared obvious to an expert when visually inspecting the nCM. Many stand borders looked fissured or indented, but as soon as the compactness factor was increased, narrow elongated stands (e.g. regeneration along the avalanche tracks) were dissected. Due to the iterative process the eventual parameter setting of stand segmentation must be regarded as a specific adaptation for the study area. Therefore this segmentation setting cannot be transferred to other areas.

The study showed that the automatic detection of the vertical layering corresponded fairly well with assessments in the field. If distinguishing between single- and multi-layered stands only, 82% of all the sample plots were correctly classified. Zimble et al. (2003) reached 97% correspondence between field- and LiDAR-based classification. This might be due to the fact, that they used a method based on tree-height variability and applied it to forests with canopy closures less than 60%.

As we worked with an already interpolated canopy surface model (2.5D), it was not possible to detect a forest layer which is completely covered by an dominant crown level. But because of the distinct structural characteristics of mountain forests, this restriction did not really hamper vertical layering assessment. Usually, mountain forests exhibit a relatively

open canopy and have almost no regeneration below dense layers (Ott et al. 1997). Furthermore, mountain forests are layered in tree groups, e.g. a mixture of groups with large trees and gaps filled by smaller trees. These characteristics of subalpine forersts together with the high resolution of the nCM allowed the use of already interpolated surfaces to quantify the vertical layering.

Since the perception of layering strongly depends on the scale of consideration (Parker and Brown 2000), we used forest stands as the level for detecting the vertical layering. This study showed that assessing the layering on plots with 10 m radius is possible but becomes problematic as soon as CD is very low. It turned out that the layering typology used in field inventories cannot directly be adopted to a LiDAR-nCM. The high resolution nCM we used made all the small gaps visible, which generally could not be distinguished so clearly in the field. This is why we used lower CD thresholds in our rule set for the vertical layering than suggested for field inventories.

Layering assessment very much depends on the height classification schema applied. We applied a discrete schema following the Manual for the Aerial Photo Interpretation within the Swiss Forest Inventory because it is suitable for remote-sensing based datasets and is related to practical forest management. The basic threshold of 3 m e.g. corresponds to a tree height, above which trees are regarded more stable against natural hazards and ungulate browsing. As an alternative, a height classification schema based on relative height limits for the lower, middle and upper storeys could be used. In such a schema each of the three height storeys referred to one third of the top height of a stand. By applying such a classification schema we would be able to accomodate different site and growth conditions, but at the same time it would make comparisons between stands much more complex and difficult to interpret.

The results of the study showed that forest gaps could easily be detected by means of a segmented nCM. The DIVI calculated on patches with HC 0 proved to be sufficient to describe the spatial arrangement of gaps. It was highly correlated with the distribution of gaps and helped to distinguish between stands with many small gaps and stands with only a few but larger gaps. Gap structure and distribution changes during the transition from mature to old-growth stands (Lertzmann et al. 1996). Old-growth forests are usually dominated by many small gaps and mature forests by fewer larger gaps. Generally, this developmental gap-sequence also occurs in mountain forests but is enforced by natural disturbances and the altitudinal gradient. Windthrow is the main gap-forming disturbance in mature and old-growth forests. Snowbreak mainly occurs in young pole stands. Generally, windthrow forms larger openings and snowbreak smaller gaps Gaps from both

disturbances were correctly detected in the study area. Whereas in low-altitude forests gaps occur as holes in a matrix of forest, this phenomenon reverses in high-altitude forests, where forest patches become islands in a matrix of gaps. This was also reflected in our results given in Fig. 4.

Enhancing structural diversity in mountain forests is widely recognised as a general objective of silvicultural interventions aiming at higher resistance and resilience to natural disturbances (Ott et al. 1997). In order to quantify this structural diversity or canopy roughness we used the overall DIVI on all height classes to describe if the canopy is vertically homogenous or heterogeneously structured. Whereas the concept of forest fragmentation usually implies the breakup of contiguous forest habitats by the development of settlements, roads and clearings, we were interested in the fragmentation of the nCM in terms of height variability or structuring. Within the validation plots the DIVI yielded statistically significant distinctions between uniform and irregular canopy structures. But using this threshold to distinguish between uniform and irregular types on the stand level led to almost exclusively irregular stands which did not reflect the structural reality. This might be due to the fact that the validation plots are too small to derive a suitable DIVI-threshold for stands that are on average 50 times larger than the validation plots. One would need much larger validation plots to overcome this problem.

6 Conclusions

Our object-based image analysis approach for assessing mountain forest structure confirmed the capacity of landscape metrics applied on a nCM to quantify forest structure. The selected metrics offered useful assessments of the canopy density and vertical layering as well as gap distribution and isolation. Canopy roughness could not satisfactorily be described using the DIVI based on the validation plots.

The advantage of structure assessment using landscape metrics is that it can be carried out in a transparent and easily repeatable way. But the metrics need to be calibrated with field assessments in order to link their values with local situations. Generally, this approach works particularly well in spruce-dominated mountain forests, as conifers possess well-shaped crowns and the forests are usually open and the top layer of trees is not closed. Automated structure assessment can be used in the course of protection forest planning, management and monitoring. Such an approach will and should not replace detailed field investigations, but it will help to assess structure in an area-extensive and efficient manner.

Future research will have to focus on testing different static and dynamic height classification schema. Furthermore, it might be helpful to include local maxima detection to explicitly consider tree clusters as structure types and stability features. In order to quantitatively assess the performance of such an approach, further calibration with existing structure assessments on a larger scale should be conducted. To assess scale dependency of the various metrics, corresponding sensitivity tests should be conducted prior to further application.

With this approach, resource and natural hazard managers can easily assess the structure of different forests or the same forest at different times or under different management alternatives. In the light of increasing pressure to pay attention to the protective effect of forests in natural hazard management, this forest structure assessment approach can be considered a highly valuable contribution.

References

Baatz M and Schäpe A (2000) Multiresolution segmentation—an optimization approach for high quality multi-scale image segmentation. In: Strobl J, Blaschke T, Griesebner, G. (Eds) Angewandte Geographische Informationsverarbeitung XII. Beiträge zum AGIT-Symposium Salzburg 2000, Herbert Wichmann Verlag, Kahrlsruhe, pp. 12–23.

Bahrenberg G, Giese E, Nipper J (1992) Statistische Methoden in der Geographie. Band 2 Multivariate Statistik. B.G. Teubner Stuttgart.

Bebi P (1999) Strukturen im Gebirgswald als Beurteilungsgrundlage ausgewählter Waldwirkungen. Dissertation ETH-Zürich, 125 pp.

Benz UC, Hofmann P, Willhauk G, Lingenfelder I, Heynen M (2004) Multiresolution, object-oriented fuzzy analysis of remote sensing data for GIS-ready information. ISPRS Journal of Photogrammetry & Remote Sensing 58, pp. 239-258.

Blaschke T, Tiede, D and Heurich M (2004) 3D landscape metrics to modelling forest structue and diversity based on laser scanning data. In: The International Archives of Photogrammetry, Remote Sensing and Spatial Information Sciences, vol. XXXVI-8/W2, Freiburg, pp. 129-132.

Brang P (2001) Resistance and elasticity: the management of protection forests, Forest Ecology and Management 145, pp. 107–117.

Dorren LKA, Berger F, Imeson A, Maier B and Rey F (2004) Integrity, stability and management of protection forests in the European Alps. Forest Ecology and Management 195, pp. 165-176.

Dorren LKA, Berger F, Le Hir C, Mermin E, Tardif P (2005) Mechanisms, effects and management implications of rockfall in forests. Forest Ecology and Management. 215, 1–3, pp 183–195.

Frehner M, Wasser B and Schwitter R (2005) Nachhaltigkeit und Erfolgskontrolle im Schutzwald - Wegleitung für Pflegemassnahmen in Wäldern mit Schutzfunktion. BUWAL, Bundesamt für Umwelt, Wald und Landschaft, Bern.

Ginzler C, Bärtschi H, Bedolla A, Brassel P, Hägeli Hauser M, Kamphues H, Laranjeiro L, Mathys L, Uebersax D, Weber E, Wicki P, Zulliger D (2005) Luftbildinterpretation LFI3 – Interpretationsanleitung zum dritten Landesforstinventar. Eidgenössische Forschungsanstalt für Wald, Schnee und Landschaft WSL. Birmensdorf. 87 pp.

Hall SA, Burke IC, Box DO, Kaufmann MR and Stoker JM (2005) Estimating stand structure using discrete-return lidar: an example from low density, fire prone ponderosa pine forests. Forest Ecology and Management 208, pp. 189-209.

Herold A and Ulmer U (2001) Stand stability in the Swiss National Forest Inventory: assessment technique, reproducibility and relevance. Forest Ecology and Management 145, pp. 29-42.

Hyyppä J, Yu X, Hyyppä H and Maltamo M (2006) Methods of Airborne Laser Scanning for Forest Information Extraction. In: Koukal T and Schneider W (Eds.) Proceedings of International Workshop on 3D Remote Sensing in Forestry. Vienna, pp. 63-78.

Jaeger JAG (2000) Landscape division, splitting index, and effective mesh size: new measures of landscape fragmentation. Landscape Ecology 15, pp. 115-130.

Keller M (Red) 2005 Schweizerisches Landesforstinventar. Anleitung für die Feldaufnahmen der Erhebung 2004-2007. Birmensdorf, Eidgenössische Forschungsanstalt WSL. 393 p.

Kraus K and Pfeifer N (1998) Determination of terrain models in wooded areas with airborne laser scanner data. ISPRS Journal of Photogrammetry & Remote Sensing 53, pp. 193-203.

Lang S and Tiede D (2003) vLATE Extension für ArcGIS – vektorbasiertes Tool zur quantitativen Landschaftsstrukturanalyse, ESRI Anwenderkonferenz 2003 Innsbruck. CDROM

Lertzmann KP, Sutherland GD, Inselberg, A, Saunders, SC (1996) Canopy gaps and the landscape mosaic in a coasteal temperate rain forest. Ecology 77(4) pp. 1254–1270.

Lim K, Treitz P, Wulder M, St-Onge B and Flood M (2003) LiDAR remote sensing of forest structure. Progress in Physical Geography 27, pp. 88-106.

Maier B (2007a) Zählen Messen Schätzen – Waldinventur im Standeswald. In: Malin H, Maier B, Dönz-Breuss M. (Ed.) Montafoner Standeswald – Beiträge zur Geschichte und Gegenwart eines kommunalen Forstbetriebes. Montafoner Schriftenreihe 18 pp. 43-66.

Maier B (2007b) Characterising Mountain Forest structure using Airborne Laser Scanning. Thesis. Department for Geography and Geology. Salzburg University

Maltamo H, Eerikäinen K, Pitkänen J, Hyyppä J and Vehmas M (2004) Estimation of timber volume and stem density based on scanning laser altimetry and

expected tree size distribution functions. Remote Sensing of Environment 90, pp. 319-330.

McGarigal K and Marks BJ (1995) FRAGSTATS: spatial pattern analysis program for quantifying landscape structure. USDA For. Serv. Gen. Tech. Rep. PNW-351.

Naesset E (2004) Practical Large-scale Forest Stand Inventory Using a Small-footprint Airborne Scanning Laser. Scandinavian Journal of Forest Research 19:164-179.

Ott E, Frehner M, Frey H-U, Lüscher P (1997) Gebirgsnadelwälder – Ein praxisorientierter Leitfaden für eine standortgerechte Waldbehandlung. Paul Haupt Bern.

Parker GG and Brown MJ (2000) Forest Canopy Stratification - is it Useful? The American Naturalist 155, pp. 473–484

Schieler K and Hauk E (2001) Instruktion für die Feldarbeit – Österreichische Waldinventur 2000/2002. Forstliche Bundesversuchsanstalt FBVA. Wien.

Schönenberger W (2001) Structure of mountain forests: Assessment, impacts, management, modelling. Forest Ecology and Management 145, pp. 1-2.

Tiede D, Heurich M and Blaschke T (2004) Object-based semi automatic mapping of forest stands with Laser scanner and Multi-spectral data. In: The International Archives of Photogrammetry, Remote Sensing and Spatial Information Sciences, vol. XXXVI-8W2, Freiburg, pp. 328-333.

Traub B, Klein Ch (1996) Quantitative Charakterisierung von Waldlfächenformen. Allg. Forst- u. J.-Ztg. 168(2), pp. 30-40.

Venema HD, Calamai PH, Fieguth P (2005) Forest structure optimization using evolutionalry programming and landscape ecology metrics. European Journal of Operational Research 164, pp. 423-439.

Wagner W, Eberhöfer C, Hollaus M, Summer G (2004) Robust Filtering of Airborne Laser Scanner Data for Vegetation Analysis, International Archives of Photogrammetry, Remote Sensing and Spatial Information Sciences. XXXVI (Part 8/W2), pp. 56-61.

Zimble DA, Evans DL, Carlson GC, Parker RC, Grado SC, Gerard PD (2003) Characterizing vertical forest structure using small-footprint airborne LiDAR. Remote Sensing of Environment 87, pp. 171-182.

> Other publications



Available online at www.sciencedirect.com
SCIENCE DIRECT®
Forest Ecology and Management 183 (2003) 31–46
Forest Ecology and Management
www.elsevier.com/locate/foreco

Improved Landsat-based forest mapping in steep mountainous terrain using object-based classification

Luuk K.A. Dorren[a,*], Bernhard Maier[b], Arie C. Seijmonsbergen[a]

[a]*Institute for Biodiversity and Ecosystem Dynamics—Physical Geography, Universiteit van Amsterdam, Nieuwe Achtergracht 166, NL-1018WV Amsterdam, The Netherlands*
[b]*Stand Montafon—Forstfonds, Montafonerstr. 21, A-6780 Schruns, Austria*

Received 17 December 2001; received in revised form 26 November 2002; accepted 3 February 2003

Abstract

The accuracy of forest stand type maps derived from a Landsat Thematic Mapper (Landsat TM) image of a heterogeneous forest covering rugged terrain is generally low. Therefore, the first objective of this study was to assess whether topographic correction of TM bands and adding the digital elevation model (DEM) as additional band improves the accuracy of Landsat TM-based forest stand type mapping in steep mountainous terrain. The second objective of this study was to compare object-based classification with per-pixel classification on the basis of the accuracy and the applicability of the derived forest stand type maps. To fulfil these objectives different classification schemes were applied to both topographically corrected and uncorrected Landsat TM images, both with and without the DEM as additional band. All the classification results were compared on the basis of confusion matrices and kappa statistics. It is found that both topographic correction and classification with the DEM as additional band increase the accuracy of Landsat TM-based forest stand type maps in steep mountainous terrain. Further it was found that the accuracies of per-pixel classifications were slightly higher, but object-based classification seemed to provide better overall results according to local foresters. It is concluded that Landsat TM images could provide basic information at regional scale for compiling forest stand type maps especially if they are classified with an object-based technique.
© 2003 Elsevier Science B.V. All rights reserved.

Keywords: Forest mapping; Segmentation; Landsat TM; Topographic correction; Mountain forest

1. Introduction

Intensification of land use in mountainous terrain demands integrated watershed planning, of which forest management is an important part. Forest mapping and forest ecological research form an important contribution to management strategies and plans. Since the 1970s, many authors have been investigating how remote sensing could contribute to forest mapping (Peterson et al., 1987; Ardö, 1992; Congalton et al., 1993; Gemmell, 1995; Martin et al., 1998; Kilpeläinen and Tokola, 1999; Pax-Lenney et al., 2001; Tokola et al., 2001) and to forest ecological research (Ekstrand, 1994; He et al., 1998; Lucas and Curran, 1999; Coops and Culvenor, 2000). The usefulness of Landsat TM imagery as an aid in forest management is generally agreed if TM imagery is combined with field data and high-resolution imagery (Gemmell, 1995; Trotter et al., 1997; Salvador and Pons, 1998; Kilpeläinen and Tokola, 1999; Hyyppä

* Corresponding author. Tel.: +31-20-525-7420; fax: +31-20-525-7431.
E-mail address: l.dorren@science.uva.nl (L.K.A. Dorren).

0378-1127/$ – see front matter © 2003 Elsevier Science B.V. All rights reserved.
doi:10.1016/S0378-1127(03)00113-0

et al., 2000; Bebi et al., 2001). However, the resolution of Landsat TM imagery is in many cases too low to derive forest parameters required by foresters such as timber volume, basal area and tree height. Consequently, TM imagery is generally used in forestry to provide contemporary and historic forest stand type maps (Anderson level II; see Anderson et al., 1976) and forest cover maps for larger regions. These maps could be used for assessing large-area regeneration, (re-)growth and causes of distinct changes in forests (Fiorella and Ripple, 1993).

The problem with Landsat TM-based forest stand type maps of mountainous terrain, derived with traditional per-pixel classification methods, is that the accuracy is fairly low, even if a digital elevation model (DEM) is added as extra band (Frank, 1988; Itten and Meyer, 1993). Accuracies of forest stand type maps of less-rugged or flat terrain are generally higher (see Mickelson et al., 1998). One of the reasons for this is that both land cover and topography determine the spectral values in remote sensing imagery, especially in case of steep or high relief energy areas. Strong variability in the reflectance from canopies of similar forests and direct shadows as well as cast shadows are indissoluble results of the topography in such areas, which complicate the classification. Topographic correction solves this problem according to many authors (Leprieur et al., 1988; Civco, 1989; Ekstrand, 1996; Tokola et al., 2001), although others do not agree on this (Carpenter et al., 1999). Despite topographic correction, traditional per-pixel methods still encounter problems with deriving forest stand type maps from Landsat TM images of mountainous terrain, because of the large variability in reflectance within forest stands and spectral confusion of species (Meyer et al., 1993).

Several authors have already referred to classifying segmented or merged pixels of Landsat TM images as an alternative to per-pixel methods (Ton et al., 1991; Woodcock and Harward, 1992; Stuckens et al., 2000). Image segmentation has the potential to merge pixels into objects that correspond to forest stands (Woodcock and Harward, 1992). Accordingly, this method is called object-based classification. This method could improve Landsat TM-based forest mapping in steep mountainous terrain. Therefore, the first objective of this study was to assess whether topographic correction of Landsat TM bands and adding a DEM as additional band results in improved forest stand type mapping in steep mountainous terrain. The second objective was to evaluate which classification method performed best: traditional per-pixel classification or object-based classification. These objectives raise the following research questions:

1. What is the effect of topographic correction on the accuracy of Landsat TM-based forest stand type maps?
2. Does the classification of a Landsat TM image improve when a DEM is used as additional band during the analysis?
3. Does object-based classification improve the accuracy and the applicability of Landsat TM-based forest stand type maps compared to per-pixel classification?

To answer these questions, we firstly prepared the used data, which also included the extraction of a forest mask. This mask was used for both classification methods. Subsequently, we performed the per-pixel classification and interpreted the results. After that we carried out the object-based classification and compared those results with the per-pixel classification. The set-up of this paper is identical to our research procedure, which is shown in the flow diagram in Fig. 1.

2. Materials

2.1. Study area

The Montafon region, which covers approximately 530 km^2, served as a test site for this study. It is located in the southern part of Vorarlberg, the westernmost province of Austria (between 47°80′and 46°50′ latitude and 9°41′and 10°90′ longitude, see Fig. 2). As an alpine region its altitude ranges from 600 m above sea level (a.s.l.) at the valley bottom up to over 3000 m a.s.l. The average relief energy is approximately 250 m/km^2. The geology is determined by sedimentary rocks in the northern part and by metamorphic and crystalline rocks in the southern part (GBA, 1998). The Montafon valleys are open to the northern windward side of the Alps and therefore under strong oceanic influence (mean annual temperature approximately 8 °C, mean annual precipitation at the bottom

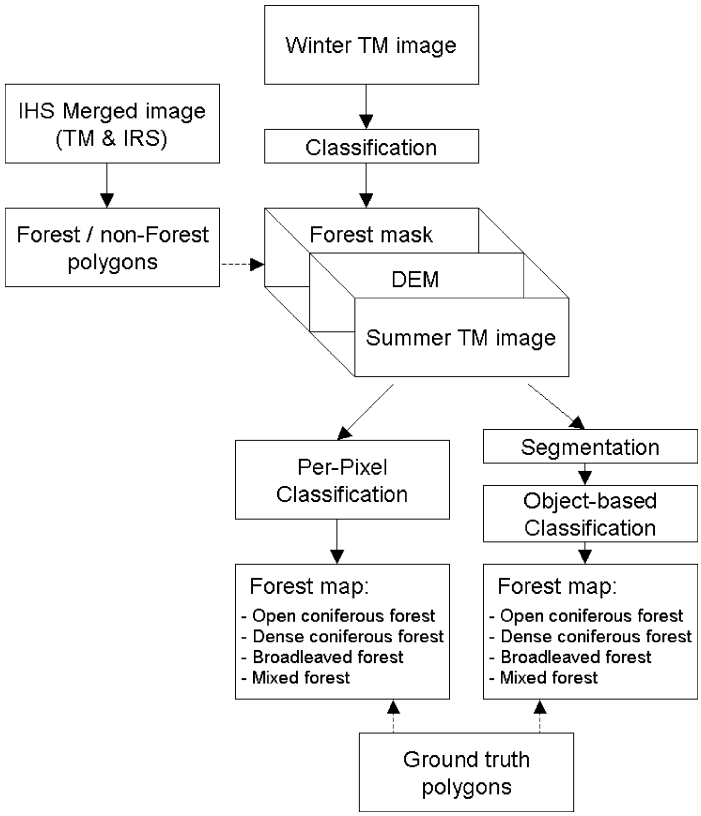


Fig. 1. Flow diagram of the research procedure (the dotted arrows refer to accuracy assessment).

of the main valley approximately 1300 mm). The forests reach up to about 1800 m a.s.l. and cover a total area of approximately 12,500 ha. Thirty-three percent of the forested area is steeper than 45°. The forests provide essential protection for villages and infrastructures against snow avalanches and rockfall. In addition, these forests are important for, amongst others, timber production and recreation. Therefore, the forests are managed in a multifunctional sustainable way. A local forest organisation is responsible for forests management in this region. For this they need information on the spatial coverage of the three main forest types: broadleaved forest, mixed forest and deciduous forest. The broadleaved (*Fagus silvatica*, *Acer pseudoplatanus*, *Tilia cordata*, *Fraxinus excelsior*) and mixed forests (*Picea abies*, *F. silvatica*, *Abies alba*) are mainly found in the valleys and up to 1000 m a.s.l. Spruce (*P. abies*) forests predominate above 1000 m a.s.l., though the mixed forests reach up to 1500 m a.s.l. *Larix decidua* and *Pinus cembra* are only found in fragmental stands close to the timberline (Maier, 1993). The distribution of forest stand types at regional scale is mainly determined by altitude, but at slope scale other factors such as parent material, relief, microclimate, humus forms, light and disturbances caused by natural hazards also become important (van Noord, 1996). Generally, the canopy density decreases with increasing altitude due to the changing climatic conditions, e.g. heavier snow loads. Because uneven-aged forests predominate, tree distribution, stem density, tree height and basal area vary strongly between forest stands. As typical for mountain forests, these varied forest stands are distributed in a patchy mosaic-like structure (Maier, 1993).

2.2. Satellite imagery and digital elevation data

A summer and a winter Landsat TM5 scene (respectively, recorded 9 September 1998 and 28 January 1998, both at 9:40 CMT) and an IRS-1C (Indian

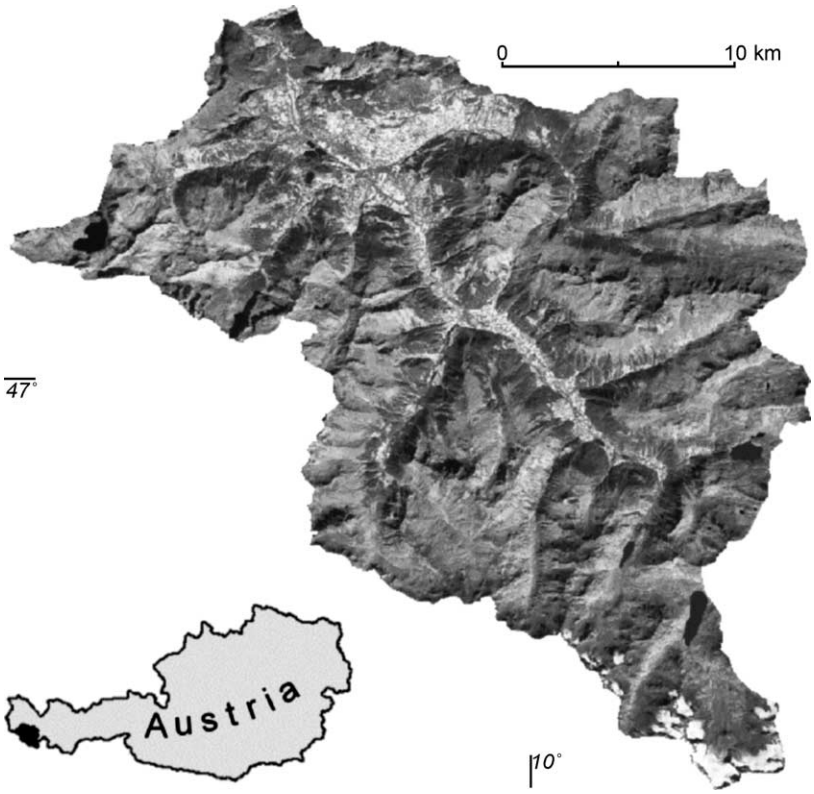


Fig. 2. Study area: the Montafon region (near-IR band of the September 1998 Landsat TM image).

Remote Sensing Satellite) panchromatic scene (recorded at 25 September 1997, 10:35 CMT) were used in this study. The resolution of a Landsat TM scene is 30 m × 30 m; the resolution of a panchromatic IRS-1C scene is 6 m × 6 m. A DEM produced by the National Austrian Mapping Agency was available for this study. This DEM is arranged as a regular grid of surface height points at 25 m spacing. According to the product information (BEV, 2001), this DEM was created by interpolation of photogrammetric height measurements at a ground distance of 50 m, enhanced and supplemented with prominent terrain structures. The modelled elevation accuracy is given as ±1 to ±3 m in open and flat land and ±5 to ±20 m in forests and high-alpine terrain.

2.3. Validation and training data

Local foresters digitised ground truth polygons on the basis of digital colour-infrared (CIR) orthophotos, which covered different areas with: open coniferous forest, dense coniferous forest, broadleaved forest and mixed forest. Mixed forests are stands where neither broadleaved nor coniferous trees account for more than 75% of the tree crown area, in accordance with the definition of UN-ECE/FAO (2000). The CIR orthophotos were taken in the period July–September 1996 and have a resolution of 0.25 m × 0.25 m. Ground truth polygons were created in areas where tree species, tree distribution and stem density were comparable in 1996 and 1998. The ground truth polygons were converted into a raster map with a cell size of 25 m × 25 m. Then, this map was randomly divided in training areas and validation areas. The validation areas were used for the accuracy assessment. The accuracies of all the classifications were assessed on the basis of confusion or error matrices (Congalton, 1991; Richards and Jia, 1999) and kappa statistics (KHAT) (Cohen, 1960; Hudson and Ramm, 1987; Congalton, 1991; Congalton and Plourde, 2000).

3. Data preparation methods

3.1. Radiometric and geometric pre-processing

Radiometric correction was applied to all the bands of the two Landsat TM scenes by multiplying by the gain and by adding the offset, which are both provided in the image header files. The images used for this study were extracted from the corrected scenes and covered approximately 35 km × 35 km. Fortunately, no detector errors or clouds were present in the used images.

The topography of mountainous terrain is responsible for geometric distortions (Itten and Meyer, 1993; Richter, 1997; Sandmeier and Itten, 1997), but in the case of steep mountainous terrain these distortions increase, therefore approximately 50 ground control points were used for orthorectifying both Landsat TM images and the IRS image. The RMS error of the rectification was 0.57 pixels (17.1 m) for the January 1998 image and 0.43 pixels (12.9 m) for the September 1998 image. Both images were resampled to 25 m× 25 m resolution using a nearest neighbour algorithm. The IRS-1C Panchromatic image was orthorectified with an RMS error of 0.26 pixels (1.56 m) and resampled to 5 m × 5 m resolution using a cubic convolution algorithm, since this image has only been used for visual interpretation and not for classification.

3.2. Extracting a forest mask

Forest masks were derived using maximum likelihood and Parallelepiped classification of the bands 1–5 of the January 1998 Landsat TM image and the bands 2, 4 and 5 of the September Landsat TM 1998 image. The January image was tested because firstly shadows are not a problem in this image, since scatter light enlightens shadowed forested areas due to the snow cover, even on steep north facing slopes, which show limited reflection in summer images. Secondly, there is no confusion between shrubs and broadleaved forests, because small shrubs are covered under a thick snow pack. For each of the classification results, confusion matrices and KHAT values were calculated on the basis of forest/non-forest polygons. These polygons were digitised on screen on the basis of a merged IRS-TM image, which was created with an Intensity-Hue-Saturation transformation (Carper et al., 1990) using the September 1998 Landsat TM image and the IRS-1C Panchromatic image. maximum likelihood classification of the bands 1–5 of the January 1998 Landsat TM image provided the most accurate forest mask (overall accuracy: 0.94, KHAT value: 0.73).

3.3. Topographic correction

To account for large variations in surface illumination that existed between areas that receive direct sunlight and areas in complete shade, the September 1998 image was corrected for topographic effects. Currently, a wide range of algorithms for topographic correction exists (Smith et al., 1980; Teillet et al., 1982; Colby, 1991; Conese et al., 1993; Meyer et al., 1993; Franklin and Giles, 1995; Sandmeier and Itten, 1997; Degui et al., 1999). The most applied algorithms are the Cosine Correction, the C-correction and the (extended) Minnaert Correction, which is based on the Minnaert constant (Minnaert, 1941) to account for non-Lambertian behaviour of vegetated surfaces (Jansa, 1998). Gu and Gillespie (1998) developed the Sun-Canopy-Sensor-correction (SCS-correction) specifically for removing topographic effects in Landsat TM images of forested areas. The SCS-correction, the Cosine Correction, the C-correction and the Minnaert Correction were evaluated by plotting reflectance values of the masked (using the forest mask) topographically corrected September 1998 TM band 4 versus the incidence angles (Meyer et al., 1993; Richter, 1998). These scatterplots indicated that the SCS-correction performed best in reducing the correlation between incidence angle and reflectance value. Therefore the SCS-correction was used in this study, of which a subset of the resulting image is shown in Fig. 3. The SCS-correction is based on the following algorithm:

$$\mathrm{DN}_{\mathrm{corr}} = \mathrm{DN}_{\mathrm{in}} \frac{\cos(\beta)\cos(\mathrm{sz})}{\cos(i)} \quad (1)$$

where $\mathrm{DN}_{\mathrm{corr}}$ is the corrected DN value, $\mathrm{DN}_{\mathrm{in}}$ the uncorrected DN value, β the slope angle (°), sz the solar zenith angle (°), i the incident angle (°), which is the angle between the direction normal to the surface and the solar beam and could be calculated following (Holben and Justice, 1980):

$$\cos(i) = \cos(\mathrm{sz})\cos(\beta) + \sin(\mathrm{sz})\sin(\beta)\cos(\mathrm{az\text{-}aspect}) \quad (2)$$

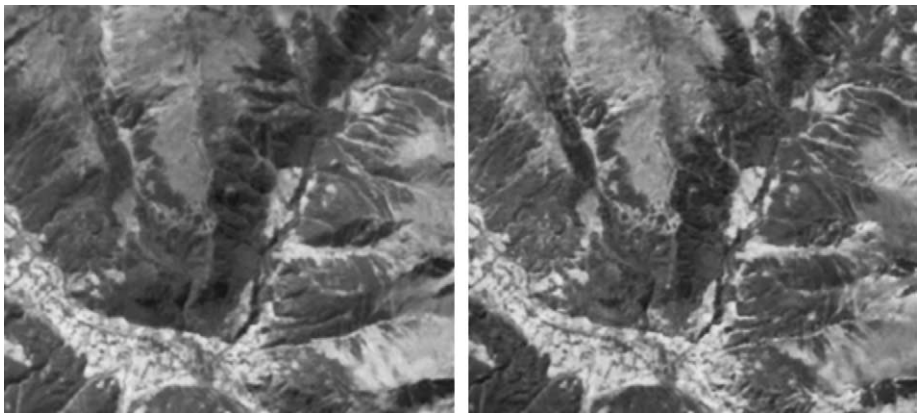


Fig. 3. Left image: subset of the raw September 1998 TM band 4; right image: subset of the topographic corrected September 1998 TM band 4 using the SCS-correction (black pixels are slopes with incidence angles larger than 90°).

where az is the solar azimuth angle (°), aspect the aspect of the slope (°).

4. Per-pixel classification methodology

After pre-processing, extracting the forest mask and applying topographic correction to the September 1998 Landsat TM image, per-pixel classifications were carried out with different datasets. All the datasets consisted of TM band 5, TM band 4 and a synthetic band (TM band 4 − TM band 2). The synthetic band was used for separating broadleaved and mixed forest (Itten et al., 1992). Spectral histograms and bi-spectral plot analyses of the signatures for the training areas indicated that the use of this combination of bands would optimise the classification since the separability of the classes was optimal within these bands.

Either topographically corrected or uncorrected TM bands were classified during each classification test. Additionally, each set of bands was classified with and without the DEM as additional band, to evaluate its effect on the classification result. This technique has been called the 'logical channel approach' (Strahler et al., 1978; Hutchinson, 1982). Here, the DEM was stretched to obtain values ranging from 0 to 255. All the different datasets were masked during classification by using the forest mask. Each classification produced four forest classes (open coniferous forest, dense coniferous forest, broadleaved forest and mixed forest) as well as a set of unclassified pixels.

It was decided to use maximum likelihood for the per-pixel classifications. The justification for this decision was based on KHAT values of preliminary results of classification tests with various unsupervised and supervised classification techniques (Richards and Jia, 1999) and additional tests with classifying principal components.

5. Per-pixel classifications: results and discussion

5.1. The effect of topographic correction

Table 1 presents the overall accuracy and the KHAT values of the different per-pixel classifications. These were calculated from the error matrices in which the classification results were compared with the validation data. This table shows that the accuracies of per-pixel classifications using topographic corrected bands are higher than those during which uncorrected bands were used. In the first case, the overall accuracy increased with 0.10 and the KHAT value increased with 0.11 when comparing classification numbers 1 and 2 (Table 1). In case of classification numbers 3 and 4, the overall accuracy increased with 0.19 and the KHAT value increased with 0.22 (Table 1). Another distinct effect of topographic correction is shown by the distribution of errors over the incidence angles (Fig. 4). This figure shows that the classification errors in the case topographic corrected images were used are more or less regularly distributed over all

Table 1
Summary of the per-pixel classification results

Classification number	Used dataset	Overall accuracy ($n = 7411$)	KHAT ($n = 7411$)
1	DEM, TM4, TM5, TM4 – TM2	0.73	0.63
2	DEM, TM4[a], TM5[a], TM4 – TM2[a]	0.63	0.52
3	TM4, TM5, TM4 – TM2	0.64	0.51
4	TM4[a], TM5[a], TM4 – TM2[a]	0.45	0.29

[a] Bands not corrected for topography.

incidence angles. In contrast, the classification errors in the case uncorrected images were used are more concentrated in faint illuminated pixels. These results show that topographic correction improves the accuracy of Landsat TM-based forest stand type maps in steep mountainous terrain. These findings agree with Meyer et al. (1993), Richter (1998) and Tokola et al. (2001).

5.2. Optimal dataset for per-pixel classification

As shown in Table 1, per-pixel classification of the topographic corrected TM bands 4, 5 and the synthetic band in combination with the DEM produced the highest overall accuracy (0.73) and KHAT value (0.63). Per-pixel classifications of the other datasets produced lower accuracies. The importance of the DEM for forest mapping in steep mountainous terrain could be explained by the fact that the distribution of forest stand types on regional scale is mainly determined by altitude. Visual evaluations of the classification results showed that classifications of TM bands without the DEM as additional band resulted in unrealistic distributions of forest stand types, such as broadleaved forests near the tree line (1800 m a.s.l.). These results show that it is necessary to use

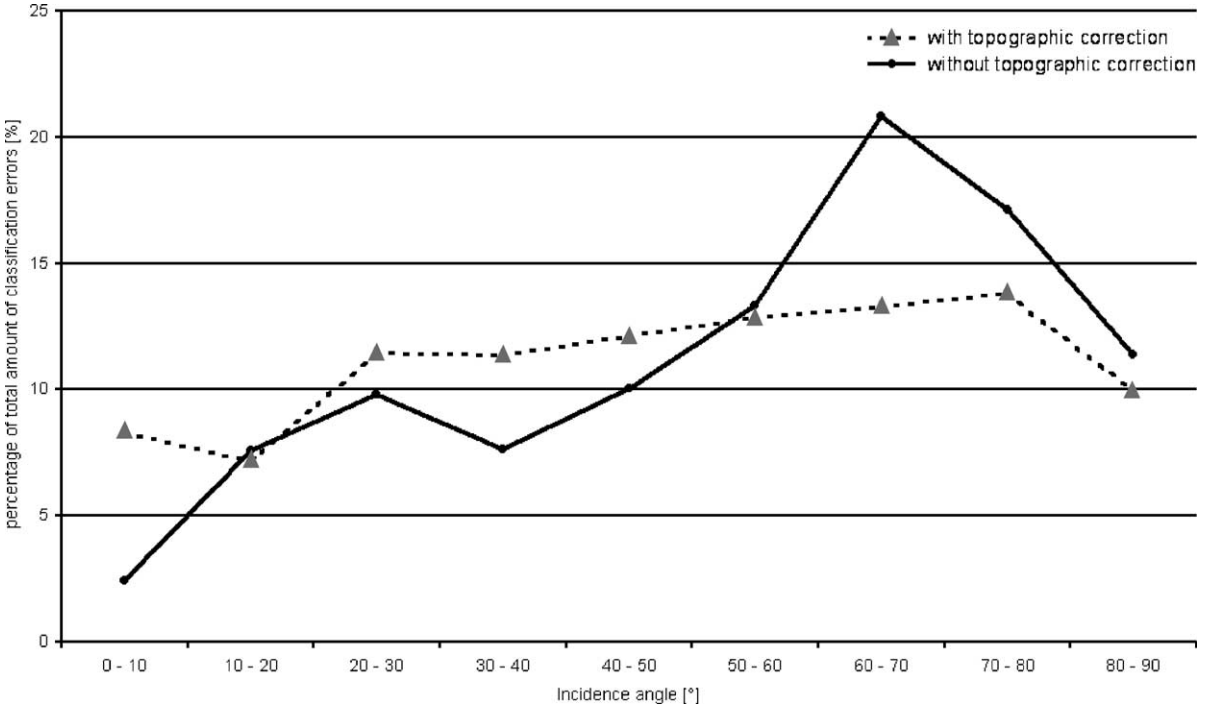


Fig. 4. The effect of topographic correction (SCS-correction) on the distribution of classification errors over different incidence angles. Percentages are normalised for the total number of pixels within each incidence angle class.

a DEM as additional band when classifying a Landsat TM image into forest stand types in steep mountainous terrain. For per-pixel classification of forest stand types in the study area, the combination of topographic corrected bands and the DEM provided the most optimal dataset tested. This dataset was also used for the object-based classification tests.

6. Object-based classification methodology

During the first step of the object-based classification method, image objects are created by means of segmentation. The segmentation process in the used software *eCognition* (Definiens-Imaging, 2001) is a bottom up region merging technique starting with randomly selected one-pixel objects, where a binary counter guarantees a regular spatial distribution and simultaneous growth of treated objects (Baatz and Schäpe, 2000). Throughout the segmentation process, an underlying optimisation procedure minimises the weighted heterogeneity ($n \times h$) of the created image objects, where n is the size of the object, defined by a scale parameter and h is a homogeneity criterion, defined by three sub-criteria: spectral heterogeneity, compactness and smoothness, which could be weighted as shown in Fig. 5. The algorithms of the segmentation process have been described in detail by Baatz and Schäpe (2000). Firstly, the forest mask, which was obtained with a supervised classification as described in Section 3.2, was segmented into forest and non-forest objects. These objects had an average size of 270 pixels. These objects were embedded in a data layer referred to as level 2. Level 2 ensured that during the eventual classification the same forest pixels according to the forest mask were classified as during the per-pixel classification. Subsequently, the large forest and non-forest objects were divided into smaller segments. The basis for this segmentation was the topographic corrected September 1998 TM band 4 and TM band 5. These smaller objects were embedded in a second data layer, hereafter referred to as level 1 (Fig. 6). Finally, all the objects in level 1 were classified using the same dataset that

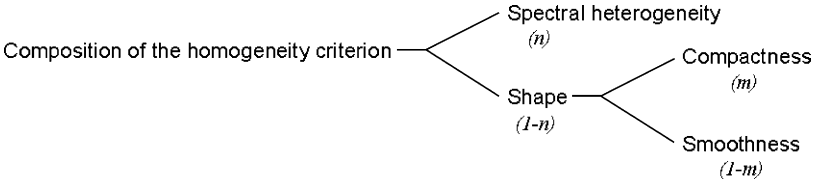


Fig. 5. Overview of the weighted sub-criteria of the homogeneity criterion, on the basis of which pixels are merged into objects.

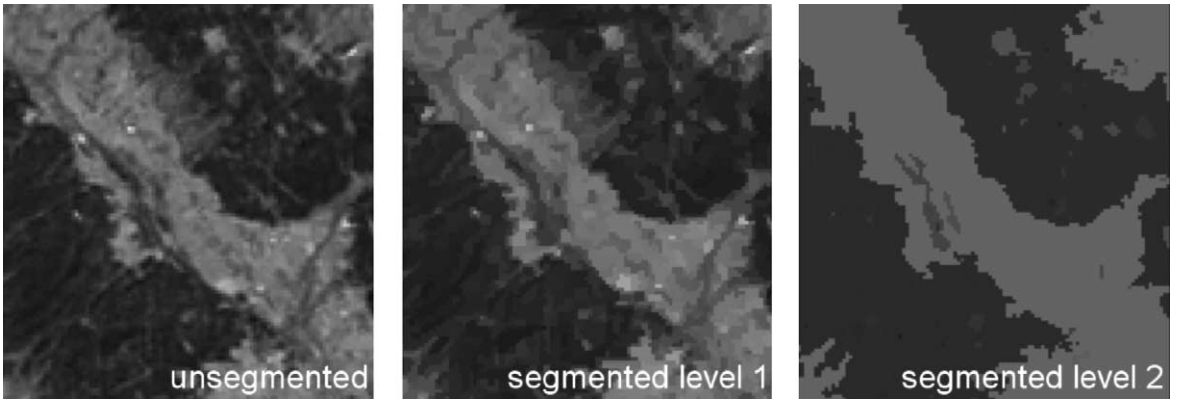


Fig. 6. Three hierarchical levels. Left image: pixel level (unsegmented TM band 4); centre image: segmented level 1 (small segmented objects, e.g. individual forest stands); right image: segmented level 2 (large forest/non-forest objects).

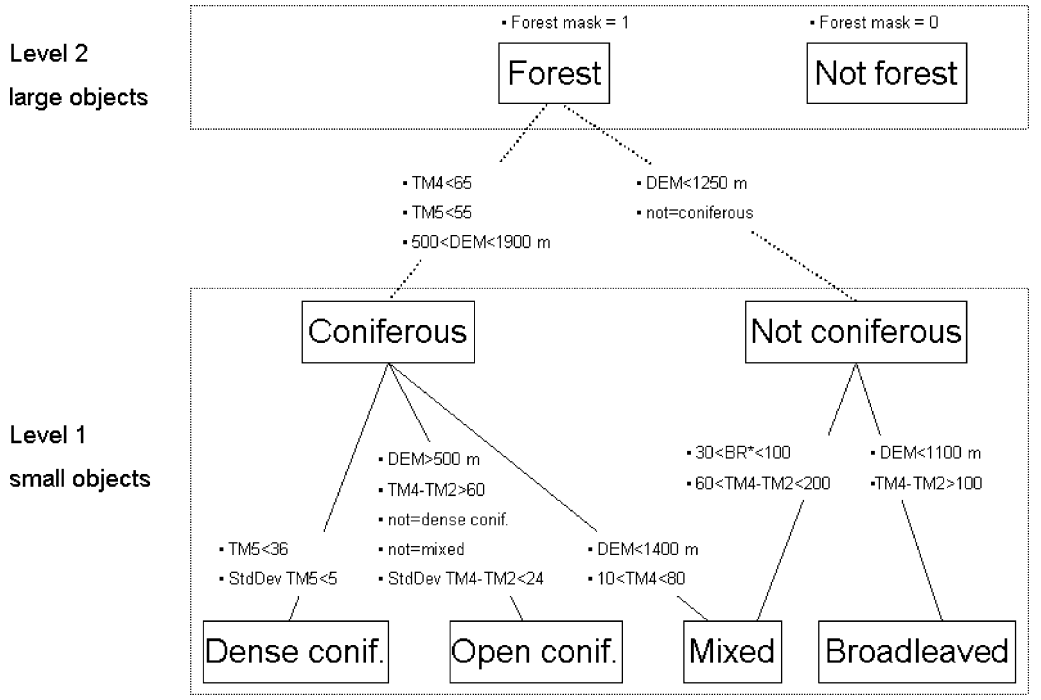


Fig. 7. Membership functions for all the classes. BR* denotes brightness = (mean TM5 + mean TM4 + mean (TM4 − TM2))/3. Objects that do not fall into any of the classes remain unclassified.

provided the best per-pixel classification result. This included TM band 4, TM band 5, the synthetic band TM4 − TM2, all corrected for topography and the DEM. The classification was based on a decision tree, which is presented in Fig. 7. This tree was built up from different membership functions for the four forest classes: mixed forest, dense coniferous forest, open coniferous forest and broadleaved forest. The membership functions for these forest classes were defined on the basis of the ground truth areas as depicted on the train map. This has effect on the portability of the developed method to other regions, since specific ground truth is needed to define the membership functions.

We tested 30 object-based classifications. For each of those different sizes of the objects in level 1 were used. The size of the objects ranged from an average object size of 2.0 pixels to 78.2 pixels. Eventually were applied. An overview of the object-based classification methodology is presented in Table 2.

Table 2
Outline of the object-based classification methodology

Step	Method	Average object size (pixels)	Used dataset	Segmentation weights
1	Segmentation of the forest mask—creation of level 2	270	Forest mask	Spectral heterogeneity: 0.6, shape: 0.4, compactness: 0.5, smoothness: 0.5
2	Creation of smaller segments—result is level 1	2.0 for the first classification to 78.2 for the last classification	TM5 and TM4	Spectral heterogeneity: 0.6, shape: 0.4, compactness: 0.5, smoothness: 0.5
3	Classification of level 1	2.0 for the first classification to 78.2 for the last classification	DEM, TM4, TM5 and TM4 − TM2	n.a.

7. Final results: object-based versus per-pixel classification

7.1. Object size and object-based classification accuracy

Fig. 8 shows the average object size versus the KHAT values and the overall accuracy of the object-based classifications. The overall accuracies and the KHAT values of the object-based classifications are dependent of the average object size. The best object-based was based on segmented objects with an average size of 21.6 pixels. The overall accuracy and the KHAT value of this classification were, respectively, 0.70 and 0.58 (Table 3). Smaller and larger objects produced lower classification accuracies. The overall accuracy and KHAT value when using smaller objects decreased to, respectively, 0.63 and 0.49 (average object size: 2.0 pixels). When using larger objects, the overall accuracy and KHAT value decreased to, respectively, 0.59 and 0.46 (average object size: 78.2 pixels).

7.2. Object-based versus per-pixel classification accuracy

Table 3 summarises the classification results of the best object-based and per-pixel classification.

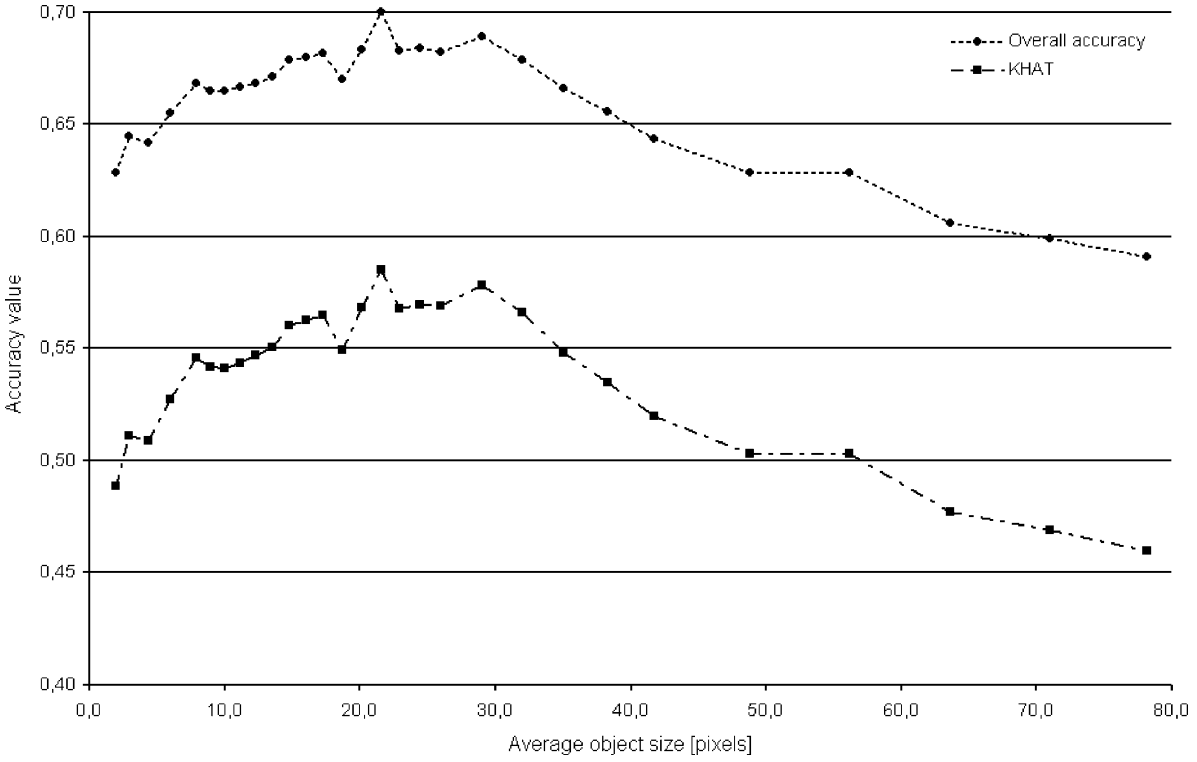


Fig. 8. Average object size versus the overall accuracy and the KHAT values of the object-based classifications.

Table 3
Summary of the best per-pixel and object-based classification results

Classification method	Average object size (pixels)	Used dataset	Overall accuracy ($n = 7411$)	KHAT ($n = 7411$)
Per-pixel	–	DEM, TM4 – TM2, TM5, TM4	0.73	0.63
Object-based	21.6	DEM, TM4 – TM2, TM5, TM4	0.70	0.58

Table 4
Confusion matrix of the best per-pixel and object-based classification, normalised for the amount of pixels within a ground truth class

	Validation/ground truth			
	Dense coniferous ($n = 2632$)	Mixed ($n = 2460$)	Broadleaved ($n = 1258$)	Open coniferous ($n = 1061$)
Per-pixel classification				
Dense coniferous	**0.814** NS[a]	0.133	0.002	0.132
Mixed	0.101	**0.720** NS	0.106	0
Broadleaved	0	0.125	**0.737** PP[b]	0
Open coniferous	0.079	0	0	**0.515** PP
Unclassified	0.006	0.022	0.155	0.353
Object-based classification				
Dense coniferous	**0.787** NS	0.103	0.006	0.155
Mixed	0.126	**0.732** NS	0.196	0.030
Broadleaved	0	0.143	**0.668** PP	0
Open coniferous	0.050	0	0	**0.415** PP
Unclassified	0.037	0.022	0.130	0.400

[a] No significant difference between both methods at the 0.01 confidence level.
[b] Per-pixel method significant better at the 0.01 confidence level.

This table shows that the overall accuracy and the KHAT value of the per-pixel classification are, respectively, 0.03 and 0.05 higher than the object-based classification. The difference in accuracy between the two methods is shown in more detail by the confusion matrices of the best per-pixel and object-based classification (Table 4). These confusion matrices tabulate the proportion of pixels matching ground truth pixels, normalised for the amount of pixels within a ground truth class. A binomial test on the class accuracies (applying normal approximation with test statistic Z) showed that no significant ($\alpha = 0.01$) differences exist between the two classification methods for the classes 'dense coniferous forest' and 'mixed forest'. The classes 'broadleaved' and 'open coniferous' were significantly better classified by the per-pixel method.

Both methods are able to classify at least 67% of the validation pixels of the classes 'dense coniferous', 'mixed' and 'broadleaved' forest correctly, but many pixels within the class 'open coniferous' could not be classified as such. This especially accounts for the object-based classification, where 40% of pixels of the class 'open coniferous' remained unclassified. Another striking difference between the two methods as shown in Table 4 is the confusion between broadleaved and mixed forest stands as classified by the object-based method, since almost 20% of the class 'broadleaved' forest has been classified as mixed forest stands.

7.3. Differences in forest stand type maps

During field visits a strong variation between open coniferous, dense coniferous, broadleaved and mixed forest stands was observed on the lower parts of the oversteepened valley slopes in the study area. Therefore, during the visual evaluation of the classification results the variation of forest stand types in this altitudinal zone was firstly evaluated. As shown in Fig. 9, the map produced by the object-based classification showed an alternation of mainly broadleaved and mixed forest stands within this zone, but also some dense and open coniferous forest stands. The per-pixel classification resulted in rather large homogeneous areas.

8. Final discussion

8.1. Accuracy and applicability of derived maps

Results in this study show that object-based classification compared to per-pixel classification does not improve the accuracy of Landsat TM derived forest stand type maps according to the overall accuracies and the KHAT values. At least, this accounts when using TM bands 4, 5, and a synthetic band (TM band 4 − TM band 2), all corrected for topography, in

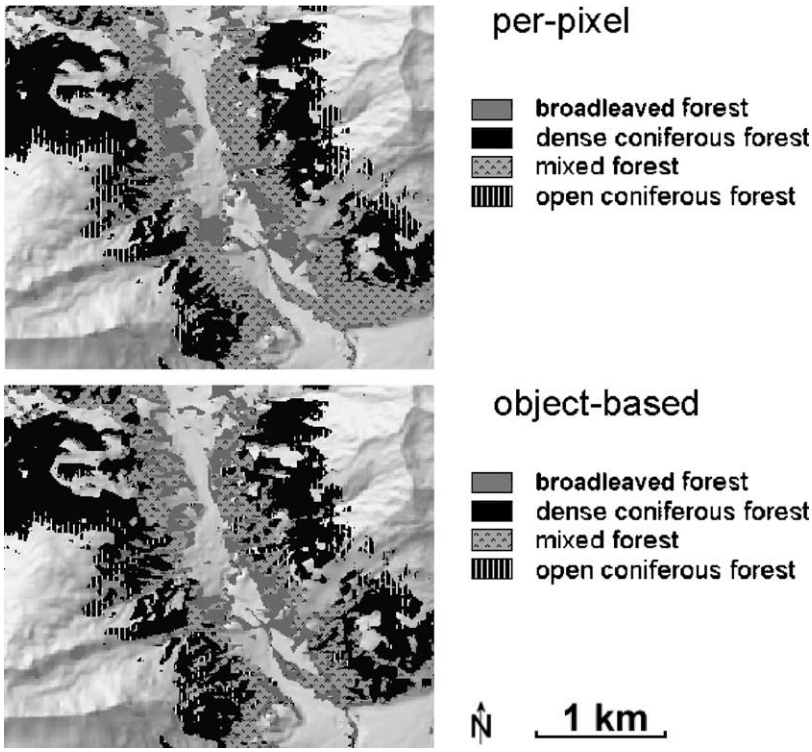


Fig. 9. Upper image: subset of the forest stand type map produced by the per-pixel classification. Lower image: subset of the forest stand type map produced by the object-based classification. The central part of the figure shows that per-pixel classification resulted in homogeneous altitudinal vegetation zones, whereas the object-based classification produced more heterogeneity, especially within the lowest forested altitudinal zone.

combination with a DEM. For forest stand type mapping in the study area using per-pixel classification, this dataset provided the most accurate results. This was not the case for object-based classification, since a large amount of open coniferous forest stands could not be classified as such (Table 4). Furthermore, the object-based classification encountered problems while separating broadleaved forest stands from mixed forest stands. This problem could probably be solved with a more specific training dataset, which is known to be required for an object-based classification as used in this study (Lobo and Chic, 1996). A specific training dataset for object-based classification might provide a better combination of TM bands and additional data. On the basis of such a dataset, the separation of the classes 'broadleaved' and 'mixed' forest could most likely be improved.

Despite lower accuracies, object-based classification compared to per-pixel classification does improve the applicability of Landsat TM-based forest stand type maps. More specifically, the forest stand type map produced by the object-based classification showed more agreement with the field situation than the map produced by the per-pixel classification. Local foresters working in the study area confirmed this. The object-based map produced a strong variation in forest stand types as observed on the lower parts of the oversteepened valley slopes in the study area. These slopes are transportation zones of snow avalanches, rockfalls, debris flows and landslides. Therefore, large variations in mixture, age and tree distribution exist (Maier, 1993; van Noord, 1996). On these slopes the per-pixel classification produced large homogeneous forested areas, which were mainly determined by altitude. The variation in forest stand types observed on the oversteepened slope in the study area was not produced.

Why, then, does object-based classification produce lower accuracies? One reason is the location of ground truth polygons in the study area. These polygons were

obtained by digitising large forest stands that are representative for each classified forest stand type. But large broadleaved forest stands are rare in the study area. Smaller broadleaved stands prevail, especially in areas where the stand type variability is high as a result of site, growth and disturbance factors. Therefore, a large set of validation data for the class 'broadleaved' was lacking. Using the DEM as additional band in the per-pixel classification resulted in a map showing strongly banded vegetation zones determined by altitude (Fig. 9). Therefore, the per-pixel classification performed very well according to the confusion matrix, since the validation pixels that were available were generally determined by altitude.

In the case of object-based classification, many different forest stand types, in particular within the lower altitudinal zones, were produced. As a result, the probability of classified forest stand objects mismatching ground truth pixels increased. It was observed that mainly the edges of delineated forest stands mismatched ground truth pixels (Fig. 10). Obviously, this led to an increase of the amount of classification errors and an according decrease of the classification accuracy. Classification errors were expressed as the amount of mismatching pixels. Instead, expressing classification errors as the amount of objects in which the majority of pixels mismatched ground truth pixels would be a more suitable method for assessing accuracy of object-based classifications. Regarding the pixel-based accuracy assessment used in this study, a random sampled ground truth set based on field inventories would probably have been better. However, in steep mountainous terrain it is very time and labour consuming to obtain such a set.

8.2. Knowledge-based classification of objects

The relation between the average object size and the accuracy of forest stand type maps derived with object-based classification, indicated that a per-pixel method is not a good basis for stand type classification. One reason is that per-pixel classification ignores the fact that there is a high probability that neighbouring pixels belong to the same class (Stuckens et al., 2000). As stated by Woodcock and Harward (1992) the ideal situation is reached when the image objects correspond with objects in the ground scene. This statement was confirmed by the results of the object-based classification of this study. These results showed that the classification accuracy decreased when using too small or too large objects. An explanation for this is that the standard deviation of objects, which was e.g. used for identifying open coniferous stands, was not suitable for classifying small objects. If objects were too large, the standard deviation within an object was too large to identify pure coniferous stands. Within this study, an average object size of 21.6 pixels resulted in the highest accuracy. This size is comparable to the average stand size in the study area, which confirms the statement of Woodcock and Harward (1992).

If segmentation provides image objects that correspond with objects in the ground scene, then an intelligent classifier should be able to classify the image objects perfectly. At present, segmentation

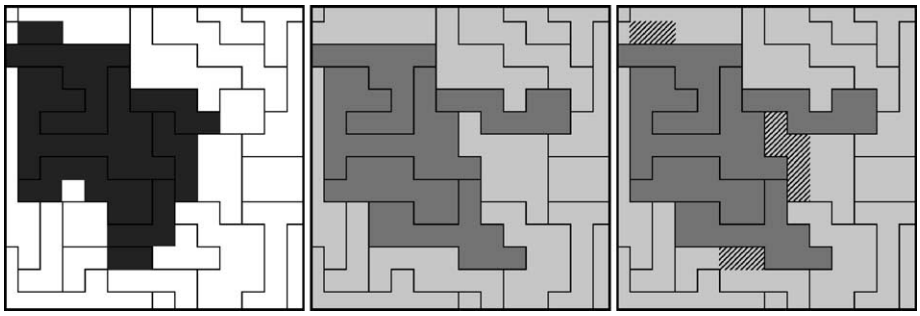


Fig. 10. Left image: hypothetical segmented image objects (black outlined) and a rasterized ground truth polygon (dark grey); centre image: hypothetical object-based classification result showing two classes (medium grey and light grey); right image: mismatched pixels (indicated with diagonal pattern) if medium grey class is identical to the ground truth class.

and object-based classification works very well for images with spatially discontinuous elements with abrupt borders such as large agricultural fields or metropolitan areas surrounded by forests (Stuckens et al., 2000). In case of segmenting Landsat TM images of steep forested mountainous terrain into forest stands, both a sophisticated segmentation procedure and an intelligent classifier are needed, since forest stands are elements with gradual and fuzzy transitions. A sophisticated segmentation procedure should be able to segment complex, gradual changing elements in images into realistic objects. Within current segmentation and pattern recognition research such procedures have already been developed and tested (Ojala and Pietikäinen, 1999). Intelligent classifiers could be based on membership functions in combination with an extensive hierarchical or multiple-scale knowledge base (Sowmya and Trinder, 2000) or on neural networks (Pax-Lenney et al., 2001).

9. Conclusions

For Landsat TM-based forest stand types mapping in the steep mountainous study area, a combination of a DEM and the TM bands 4, 5 and a synthetic band (TM band 4 − TM band 2), which were all corrected for topography, provided the most optimal dataset when using traditional per-pixel classification. Therefore, this dataset was used to compare traditional per-pixel classification with an object-based classification method. The results from this comparison suggest that an object-based approach fails to improve the accuracy of forest stand type maps in comparison with traditional per-pixel classification, according to the overall accuracies and KHAT values. Object-based classification, however, does improve the applicability of Landsat TM derived forest stand type maps. The forest stand type map derived with object-based classification agreed more with reality than the forest stand type map derived with per-pixel classification. The use of a more specific accuracy assessment method for the object-based classification could probably quantify this. Alternatively, the use of a random sampled ground truth set based on field inventories for accuracy assessment could have resulted in higher object-based classification accuracies as well. Unfortunately a random sampled ground truth set was not available, because in steep mountainous terrain it is very time and labour consuming to obtain such a set.

The relation between the average object size and the accuracy of forest stand type maps indicated that object-based classification has substantial potential for forest stand type mapping on the basis of Landsat TM. Though, techniques for segmentation and classification of spatially continuous elements with gradual transitions in images have to be improved.

Acknowledgements

This paper is a result of work carried out for the CARTESIAN project. The funding by the European Community (ENV4-CT98-0746) and the project coordination by J.C.J.H. Aerts are gratefully acknowledged. We thank Ger Bergkamp and Anton Imeson for suggestions for improvement.

References

Anderson, J.R., Hardy, E.E., Roach, J.T., Witmer, R.E., 1976. A land use and land cover classification system for use with remote sensor data. US Geological Survey, Professional Paper 964, Washington, DC, 28 pp.

Ardö, J., 1992. Volume quantification of coniferous forest compartments using spectral radiance recorded by Landsat Thematic Mapper. Int. J. Remote Sens. 13 (9), 1779–1786.

Baatz, M., Schäpe, A., 2000. Multiresolution segmentation—an optimization approach for high quality multi-scale image segmentation. In: Strobl, J., Blaschke, T., Griesebener, G. (Eds.), Angewandte Geographische Informationsverarbeitung XII. Beiträge zum AGIT-Symposium Salzburg 2000, Herbert Wichmann Verlag, Kahrlsruhe, pp. 12–23.

Bebi, P., Kienast, F., Schönenberger, W., 2001. Assessing structures in mountain forests as a basis for investigating the forests' dynamics and protective function. For. Ecol. Manage. 145 (1), 3–14.

BEV, 2001. Bundesamt für Eich- und Vermessungswesen, Produktinformation zum Geländehöhenmodell. http://www.bev.gv.at/prodinfo/dgm/dgm_3f.htm, as seen on 1 December 2001.

Carpenter, G.A., Gopal, S., Macomber, S., Martens, S., Woodcock, C.E., 1999. A neural network method for mixture estimation for vegetation mapping. Remote Sens. Environ. 70 (2), 138–152.

Carper, W.J., Lillesand, T.M., Kiefer, R.W., 1990. The use of Intensity-Hue-Saturation transformations for merging SPOT panchromatic and multispectral image data. Photogramm. Eng. Remote Sens. 56 (4), 459–467.

Civco, D.L., 1989. Topographic normalization of Landsat Thematic Mapper digital imagery. Photogramm. Eng. Remote Sens. 55 (9), 1303–1309.

Cohen, J., 1960. A coefficient of agreement of nominal scales. Educ. Psychol. Measur. 20 (1), 37–46.

Colby, J.D., 1991. Topographic normalization in rugged terrain. Photogramm. Eng. Remote Sens. 57 (5), 531–537.

Conese, C., Gilabert, M.A., Maselli, F., Bottai, L., 1993. Topographic normalization of TM scenes through the use of an atmospheric correction method and digital terrain models. Photogramm. Eng. Remote Sens. 59 (12), 1745–1753.

Congalton, R.G., 1991. A review of assessing the accuracy of classifications of remotely sensed data. Remote Sens. Environ. 37, 35–46.

Congalton, R.G., Plourde, L.C., 2000. Sampling methodology, sample placement, and other important factors in assessing the accuracy of remotely sensed maps. In: Heuvelink, G.B.M., Lemmens, M.J.P.M. (Eds.), Accuracy 2000. Delft University Press, Amsterdam, pp. 117–124.

Congalton, R.G., Green, K., Teply, J., 1993. Mapping old growth forests on national forest and park lands in the Pacific Northwest from remotely sensed data. Photogramm. Eng. Remote Sens. 59 (4), 529–535.

Coops, N., Culvenor, D., 2000. Utilizing local variance of simulated high spatial resolution imagery to predict spatial pattern of forest stands. Remote Sens. Environ. 71 (3), 248–260.

Definiens-Imaging, 2001. eCognition, object oriented image analysis. http://www.definiens-imaging.com/ecognition/index.htm, as seen on 1 December 2001.

Degui, G., Gillespie, A.R., Adams, J.B., Weeks, R., 1999. Statistical approach for topographic correction of satellite images by using spatial context information. IEEE Trans. Geosci. Remote Sens. 37 (1), 236–246.

Ekstrand, S., 1994. Assessment of forest damage with Landsat TM, correction for varying forest stand characteristics. Remote Sens. Environ. 47, 291–302.

Ekstrand, S., 1996. Landsat TM based forest damage assessment Correction for topographic effects. Photogramm. Eng. Remote Sens. 62 (2), 151–161.

Fiorella, M., Ripple, W., 1993. Analysis of conifer forest regeneration using Landsat Thematic Mapper data. Photogramm. Eng. Remote Sens. 59 (9), 1383–1388.

Frank, T., 1988. Mapping dominant vegetation communities in the Colorado Rocky Mountain front range with Landsat Thematic Mapper and digital terrain data. Photogramm. Eng. Remote Sens. 54, 1727–1734.

Franklin, S.E., Giles, P.T., 1995. Radiometric processing of aerial and satellite remote-sensing imagery. Comput. Geosci. 21 (3), 413–423.

GBA, 1998. In: Oberhauser, R., Rataj, W. (Eds.), Geologisch-Tektonische Übersichtskarte von Vorarlberg (1:200.000) mit Erläuterungen. Published by the Geological Survey of Austria.

Gemmell, F.M., 1995. Effects of forest cover, terrain, and scale on timber volume estimation with thematic mapper data in a rocky mountain site. Remote Sens. Environ. 51 (2), 291–305.

Gu, D., Gillespie, A., 1998. Topographic normalization of Landsat TM images of forest based on subpixel sun-canopy-sensor geometry. Remote Sens. Environ. 64 (2), 166–175.

He, H.S., Mladenoff, D.J., Radeloff, V.C., 1998. Integration of GIS data and classified satellite imagery for regional forest assessment and landscape modeling. Ecol. Appl. 8, 1072–1083.

Holben, B.N., Justice, C.O., 1980. The topographic effects on spectral response from nadir pointing sensors. Photogramm. Eng. Remote Sens. 46 (9), 1191–1200.

Hudson, W.D., Ramm, C.W., 1987. Correct formulation of the KHAT value of agreement. Photogramm. Eng. Remote Sens. 53 (4), 421–422.

Hutchinson, C.F., 1982. Techniques for combining Landsat and ancillary data for digital classification improvement. Photogramm. Eng. Remote Sens. 48 (1), 123–130.

Hyyppä, J., Hyyppä, H., Inkinen, M., Engdahl, M., Linko, S., Zhu, Y., 2000. Accuracy comparison of various remote sensing data sources in the retrieval of forest stand attributes. For. Ecol. Manage. 128 (1), 109–120.

Itten, K.I., Meyer, P., 1993. Geometric and radiometric correction of TM-data of mountainous forested areas. IEEE Trans. Geosci. Remote Sens. 31 (4), 764–770.

Itten, K.I., Meyer, P., Kellenberger, T., Leu, R., Sandmeier, S., Bitter, P., Seidel, K., 1992. Correction of the impact of topography and atmosphere on Landsat-TM forest mapping of Alpine regions. Remote Sensing Series 18, University of Zurich, 50 pp.

Jansa, J., 1998. A global topographic normalisation algorithm for satellite images. In: Proceedings of the ISPRS Commission VII Symposium, Budapest, Hungary. Int. Arch. Photogramm. Remote Sens. XXXII (7), 8–15.

Kilpeläinen, P., Tokola, T., 1999. Gain to be achieved from stand delineation in LANDSAT TM image-based estimates of stand volume. For. Ecol. Manage. 124, 105–111.

Leprieur, C.E., Durand, J.M., Peyron, J.L., 1988. Influence of topography on forest reflectance using Landsat thematic mapper and digital terrain data. Photogramm. Eng. Remote Sens. 54 (4), 491–496.

Lobo, A., Chic, O., 1996. Classification of Mediterranean crops with multi sensor data: per-pixel versus per-object statistics and image segmentation. Int. J. Remote Sens. 17, 2385–2400.

Lucas, N.S., Curran, P.J., 1999. Forest ecosystem simulation modelling, the role of remote sensing. Progr. Phys. Geogr. 23 (3), 391–423.

Maier, B., 1993. Forstinventur Stand Montafon. Internal Report Stand Montafon, Schruns, 154 pp.

Martin, M.E., Newman, S.D., Aber, J.D., Congalton, R.G., 1998. Determining forest species using high spectral resolution remote sensing data. Remote Sens. Environ. 65, 249–254.

Meyer, P., Itten, K.I., Kellenberger, T., Sandmeier, S., Sandmeier, R., 1993. Radiometric correction of topographically induced effects on Landsat TM data in an alpine environment. ISPRS J. Photogramm. Remote Sens. 48 (4), 17–28.

Mickelson, J.G.J., Civco, D.L., Silander, J.A.J., 1998. Delineating forest canopy species in the Northeastern United States using multi-temporal TM data and GPS referenced data. Photogramm. Eng. Remote Sens. 64, 891–907.

Minnaert, M., 1941. The reciprocity principle in lunar photometry. Astrophys. J. 93, 403–410.

Ojala, T., Pietikäinen, M., 1999. Unsupervised texture segmentation using feature distributions. Pattern Recogn. 32, 744–786.

Pax-Lenney, M., Woodcock, C.E., Macomber, S.A., Song, C., 2001. Forest mapping with a generalized classifier and Landsat TM data. Remote Sens. Environ. 77, 241–250.

Peterson, D.L., Spanner, M.A., Running, S.W., Teuber, K.B., 1987. Relationship of thematic mapper simulator data to leaf area index of temperate coniferous forest. Remote Sens. Environ. 22, 323–341.

Richards, J.A., Jia, X., 1999. Remote Sensing Digital Image Analysis, An Introduction. Springer, Berlin, 363 pp.

Richter, R., 1997. Correction of atmospheric and topographic effects for high spatial resolution satellite imagery. Int. J. Remote Sens. 18 (5), 1099–1111.

Richter, R., 1998. Correction of satellite imagery over mountainous terrain. Appl. Opt. 37 (18), 4004–4015.

Salvador, R., Pons, X., 1998. On the reliability of Landsat TM for estimating forest variables by regression techniques, a methodological analysis. IEEE Trans. Geosci. Remote Sens. 36 (6), 1888–1897.

Sandmeier, S., Itten, K.I., 1997. A physically-based model to correct atmospheric and illumination effects in optical satellite data of rugged terrain. IEEE Trans. Geosci. Remote Sens. 35 (3), 708–717.

Smith, J.A., Lin, T.L., Ranson, K.J., 1980. The Lambertian assumption and Landsat data. Photogramm. Eng. Remote Sens. 46, 1183–1189.

Sowmya, A., Trinder, J., 2000. Modelling and representation issues in automated feature extraction from aerial and satellite images. ISPRS J. Photogramm. Remote Sens. 55, 34–47.

Strahler, A.H., Logan, T.L., Bryant, N.A., 1978. Improving forest cover classification accuracy from Landsat by incorporating topographic information. In: Proceedings of the 12th International Symposium on Remote Sensing of Environment, ERIM, Ann Harbor, MI, pp. 927–942.

Stuckens, J., Coppin, P.R., Bauer, M.E., 2000. Integrating contextual information with per-pixel classification for improved land cover classification. Remote Sens. Environ. 71, 282–296.

Teillet, P.M., Guidon, B., Goodenough, D.G., 1982. On the slope-aspect correction of multispectral scanner data. Can. J. Remote Sens. 8, 84–106.

Tokola, T., Sarkeala, J., Linden, M.V.D., 2001. Use of topographic correction in Landsat TM-based forest interpretation in Nepal. Int. J. Remote Sens. 22 (4), 551–563.

Ton, J., Sticklen, J., Jain, A.K., 1991. Knowledge-based segmentation of Landsat images. IEEE Trans. Geosci. Remote Sens. 29, 222–232.

Trotter, C.M., Dymond, J.R., Goulding, C.J., 1997. Estimation of timber volume in a coniferous plantation forest using Landsat TM. Int. J. Remote Sens. 18 (10), 2209–2223.

UN-ECE/FAO, 2000. Forest Resources of Europe, CIS, North America, Australia, Japan and New Zealand (industrialized temperate/boreal countries). UN-ECE/FAO Contribution to the Global Forest Resources Assessment 2000. Geneva Timber and Forest Study Papers, No. 17, United Nations, New York and Geneva.

van Noord, H., 1996. The role of geomorphological information in ecological forest site typology in mountainous areas, a methodological study in the E-Rätikon and NW-Montafon mountains (Vorarlberg, Austria). Ph.D. Thesis. University of Amsterdam, Amsterdam, 185 pp.

Woodcock, C., Harward, V.J., 1992. Nested-hierarchical scene models and image segmentation. Int. J. Remote Sens. 13 (16), 3167–3187.

Balancing tradition and technology to sustain rockfall-protection forests in the Alps

Luuk K.A. Dorren and Frédéric Berger

Cemagref Grenoble, 2 Rue de la Papeterie, B.P. 76, F-38402 Saint Martin d'Hères Cedex, France.
luuk.dorren@cemagref.fr

Abstract
It is still uncertain what a mountain forest should look like to provide optimal protection against rockfall. Knowledge is limited due to the slow reaction of mountain forests to the rapid environmental and socio-economic changes that have occurred in the Alps over the past 100 years. Fortunately, research has progressed and an enormous amount of experiential knowledge has been gained, providing a basis for finding a balance between maintaining traditional practices and implementing new technology. This paper identifies an approach that could be used as a rough framework for managing and sustaining forests with a protective function in the Alps. Three main points are discussed: 1) evaluating traditional 'good practices' and mistakes, 2) evaluating new technologies, especially those in the field of rockfall-protection forests, and 3) merging the best of the two worlds. The evaluation of traditional ways of managing protection forests shows that the 'do nothing approach' and earlier trends in spatial planning should be avoided. In the past, people were more inclined to believe that risks were always present in mountain areas. Aware of the protective functions of forests, they did not touch forests in areas where natural hazards posed risks to settlements. Protection forests were therefore not subject to harvesting. In addition, construction did not take place in areas where natural hazards posed high risks. A review of the technologies developed during recent decades shows that we can now assess quantitatively how well different mountain forests perform in providing protection against rockfall. We show how new research tools can help in assessing the required silvicultural actions to optimise the protective function of forests.

Keywords: protection forest, traditional protection forest management, rockfall-protection forests

1 Introduction

Many livelihoods in the Alps rely heavily on mountain forests for protection against rockfall and snow avalanches. This is identified in the first paragraph of the Mountain Forest Protocol of the Alpine Convention (European Communities 1996): "mountain forests … provide the most effective, the least expensive and the most aesthetic protection against natural hazards." In Austria and Switzerland alone, approximately 50 million Euros are spent yearly to maintain or improve the protection provided by mountain forests (European Observatory of Mountain Forests 2000; Swiss Federal Statistical Office 2002). Increasingly, the protective functions of mountain forests need to be combined with other functions and uses. This is difficult as foresters and forest researchers are still determining the characteristics of a forest that provide optimal protection. Knowledge is limited due to the slow reaction of natural forests to the rapid environmental and socio-economic changes that have occurred in the Alps over the past 100 years. Fortunately, there has been considerable progress in research on protection forests. In parallel, practitioners have gained experience in managing protection forests. The combination of this knowledge and experience provides a basis for balancing tradition and technology. The aim of this paper is to review this information and

use it to develop a framework for managing and sustaining forests with a protective function in the Alps. Three main points are discussed:

1. evaluating traditional 'good practices' as well as past mistakes
2. evaluating new technologies in rockfall-protection forest studies
3. merging the best of the two worlds

This paper concentrates on these three points, particularly as they relate to rockfall.

2 Protection forests in the Alps

In the European Alps, mountain forests and the protection they provide have a long and distinguished history. However, in the last few decades, forest management has shifted its focus from timber management to multiple use and forest ecosystem management (BUTTOUD 2000; FÜHRER 2000). During this transition, there has been an increasing awareness of the need to manage the multiple functions of mountain forests. Traditionally, mountain forests have been exploited for their timber and non-timber products, with the exception of forests on slopes above residential areas that present active natural hazards. The latter type of forests were often put under a logging ban (*Bannwald* in German or *forêt mise à ban* in French), which means that the forest was and still can be classified as a reserved forest where felling is prohibited outright or selective thinning is only permitted under strict rules. In these forests, past management often consisted of 'doing nothing' (i.e. trees were rarely cut).

The main functions of forests recognised today include the production of timber and non-timber forest products, protection against natural hazards, recreation, nature conservation, watershed conservation, and sequestration of carbon dioxide (BUTTOUD 2000; FÜHRER 2000; PRICE *et al.* 2000; UN-ECE/FAO 2000). The transition in forest management has occurred due to the increasing use of mountain areas and the diversification of Alpine economies, which have evolved from agricultural to tourism-based economies. As population densities and the economic value of the main alpine valleys have increased, the protection against natural hazards provided by forests has become more important (SCHÖNENBERGER 2000). Forests traditionally designated as protection forests have now gained wider recognition due to their increasing importance as well as their direct economic and social benefits.

Protection forests are mainly designed to protect particular objects (SCHÖNENBERGER 2000). This function implies that the forest directly protects people, buildings, and infrastructure against the impact of natural hazards such as snow avalanches and rockfall (BRANG 2001). At the same time a forest provides a site-protection function, which is actually a prerequisite for the direct protective function. The site-protection function is important, as a forest stand needs to protect its site against processes such as excessive soil erosion. If the site-protection function is impaired, the forest site erodes, resulting in a loss of the forest ecosystem as a whole (DORREN *et al.* 2004a).

Unfortunately today's society has generally placed greater trust in technical protective works (e.g. engineered structures) than in protection forests. One of the reasons for this has been the lack of quantitative data on the efficacy of protection forests. Experience indicates that many of the protective works installed in the 1970s have had a shorter lifespan than originally planned. Replacement of these older structures has resulted in unforeseen expenditures. Secondly, a recent shift towards "ecological engineering" for natural hazard protec-

tion can be observed in the Alps. In addition, the knowledge and tools obtained from research during the last decade has enabled a quantitative assessment of how different mountain forests perform their protective function.

3 Good practices and mistakes in traditional protection forest management

An overview of former practices in European protection forests is provided by SUBOTSCH (1999), who compares the relevant forest laws and management strategies of Austria, France, Germany, Italy and Switzerland. The practices used in these countries to protect villages against rockfall are very similar, as they all more-or-less adopted a 'no intervention' policy in the past (18th to mid 20th century). In the surrounding or remaining forests, which mainly served for wood production, management was aimed at increasing the forest area and the standing volume (SCHÖNENBERGER 2000).

One traditional practice that was particularly useful was to allow inhabitants to carry out a basic geomorphological interpretation of the active natural hazards that posed potential direct threats. People working in the fields and forests were acutely aware of indicators of natural hazard indicators in the forests, such as the tracks or *couloirs* created by different types of mass movements (avalanche, rockfall, landslides and debris flows). By using these indicators and the experience of older generations, people could identify the types and locations of natural hazards. Evidence for this in the Alps is provided by the locations of village centres, which were generally located on the lower parts of alluvial fans from tributary valley systems, below a valley slope covered by a dense forest (Fig. 1). Such locations provided a number of advantages for villages:

– they had sufficient height above the main river to avoid flooding problems,
– they were far enough from the tributary torrential rivers to avoid damage by debris flows, and
– they were far enough from the bottom of the steep valley slopes to avoid rockfalls and avalanches that surpassed the forested zone.

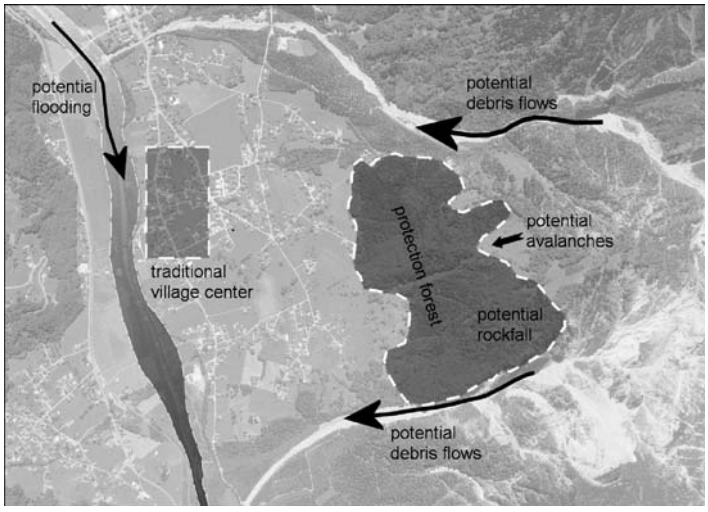


Fig. 1. Typical situation and location of a traditional village in the European Alps.

During the 19th century, mechanization was introduced and the demand for wood for industry and other uses increased. Many forests with no protective functions were cleared, leaving protection forests untouched. The only 'management' that took place in protection forests was the effect of natural disturbances (e.g. avalanches, wind throws, debris flows, and rockfalls). These processes caused the creation of couloirs and (selective) thinning. Despite these natural processes, many protection forest stands became very dense, leading to insufficient light for successful regeneration. In addition, clearcuts in the surrounding production forests, led to protection forests being used increasingly by ungulates for shelter. This, in combination with the suppression of predators by humans, led to high browsing pressures. As a consequence, regeneration was either insufficient or absent, leading to the development of even-aged, regular stands. Such stands cannot provide sufficient protection in the long term (AMMER 1996; MOTTA 1996, 2003; MOTTA and HAUDEMAND 2000). In addition, after the Second World War, the buffer zone between the traditional village centre and the foot of the forested valley slopes (Fig. 1) progressively disappeared due to housing pressures. Regional plans frequently ignored the existence of natural hazards and, as a consequence, the use of engineering works to protect villages has increased significantly since the 1970s. Protection forest restoration projects have also been initiated throughout the Alps. The 'no intervention' policy, combined with the inadequacies of recent regional planning, has created a number of problems and would be best avoided.

4 Technology for protection forest management

The forester, or any other practitioner, has to be able to quantify the state of the protective function of a forest stand for two reasons. Firstly, decisions have to be made as to which forests require silvicultural interventions to prevent an increase in the consequences of rockfall. Secondly, a quantification of the protective potential of a forest stand targets further, more detailed site investigations on the local rockfall hazard, as well as identifying future investments in rockfall-protection using combinations of civil engineering and forest management techniques. Before such an analysis can be undertaken, the location of protection forests in a management region and their current condition need to be understood. This information is required at the catchment scale, or at the scale of larger management areas (HAMILTON and BRUIJNZEEL 1997; ANDERSSON *et al.* 2000; HEROLD and ULMER 2001). Then, it is necessary to identify those forests with an impaired protective function. On the basis of these assessments, priorities for the restoration or maintenance of specific protection forest stands can be established (BERGER and RENAUD 1994; BERGER and LIEVOIS 1999). Some of the data can be collected from satellite images, orthophotos and laser scanning data. Additional stand details, such as tree diameter, species composition, structure, and stability, have to be generated through forest inventories, although a large amount of these data can be readily derived from laser scanning, albeit with less accuracy. The combination of forest inventory data and remotely sensed data in a Geographic Information System (GIS) provides a good database for forest management at both local and regional scales.

Computer simulation, spatial analysis, and GIS technology currently enable us to assess the effects of protection forests on natural hazards at the regional scale. DORREN and SEIJMONSBERGEN (2003) demonstrated how rockfall runout zones can be predicted at a regional scale, with and without taking into account the effect of protection forests. BERGER (1997) developed a method for assessing potential avalanche starting zones on forested and non-forested slopes. By combining the information on avalanche starting zones, active rock-

fall zones, a forest map, and a map with the elements at risk, a preliminary map with the locations of protection forests can be created, which will then require verification by local practitioners using orthophotos, terrain visits, and archives of historic events.

In addition to the above computer technologies, which have been adapted for regional scale analyses, technologies currently used for local scale analysis are able to account for the effects of protection forest stands and individual trees on natural hazards. Attempts have been made, for example, in snow avalanche simulation modelling (BARTELT and STÖCKLI 2001), in rockfall modelling (ZINGGELER *et al.* 1991; DORREN and SEIJMONSBERGEN 2003; DORREN *et al.* 2004b; STOFFEL *et al.* 2006) as well as in snow and wind damage studies (PELTOLA *et al.* 2000; GARDINER *et al.* 2000).

Dendrogeomorphology has been developed over the past 30 years (SHRODER 1980; STRUNK 1997). Information extracted from tree rings is being used to date, reconstruct, or map historic events. These techniques give insight into the interaction between trees and natural hazards, such as debris flows (e.g. SHRODER 1975; STRUNK 1989; WILKERSON and SCHMID 2003), rockfall (e.g STOFFEL *et al.* 2005) and avalanches (e.g. BUTLER and MALANSON 1985; SMITH *et al.* 1994).

Most forest and natural hazard studies require substantial amounts of data. Foresters need a small dataset formalized in a user-friendly tool if they are to evaluate the protective function of a forest stand rapidly and efficiently. The input data should be comprehensive and accurate, and should be easy to acquire in the field or using GIS, for example, at the scale of the slope or the forest stand. After acquiring the data, the forester needs guidelines to maintain or improve the protective function of the forest stand in question. Below, we provide examples of research and development activities in this area, and the tools that arose from them. The examples are related specifically to rockfall-protection forests.

4.1 Rockfall and forest research

The interaction between forests and falling rocks has been investigated in detail for the past 25 years (cf., COUVREUR 1982; JAHN 1988). GSTEIGER (1993) presented the concept of the "mean tree free distance" which he used to assess the protection against rockfall provided by a forest stand. This value refers to the average distance a rock travels between two tree contacts. It is assumed that forest stands whose mean tree free distance exceeds 40 meters cannot effectively slow down or stop falling rocks. Within such a distance, a rolling or bouncing rock on a 35 to 40° slope gains sufficient kinetic energy to break trees (DORREN *et al.* 2005). The protective capacity of the rockfall-protection forests is determined by the size of the falling rocks, the kinetic energy of the rocks, the stand density, and the mean tree diameter at breast height (DBH), and the tree species present. Small rocks have a lower tree contact probability than large rocks. The higher the stand density and the mean DBH, the higher the contact probability is. However, dense forest stands cannot be combined with large-diameter trees and high stability over the long-term. Juvenile forest phases generally show a high stand density with thin trees, whereas aging phases are mainly characterised by fewer and larger trees.

Several forest and rockfall experiments have been undertaken to obtain detailed information of the capacity of different trees to dissipate rockfall impact energy, to validate rockfall models, and to develop rockfall-protection forest management guidelines (e.g. COUVREUR 1982; JAHN 1988; CATTIAU *et al.* 1995; DOCHE 1997; BERGER *et al.* 2002; DORREN *et al.* 2005; STOKES *et al.* 2005). We carried out real-size rockfall experiments on forested and non-forested slopes, using high-speed digital cameras in the framework of the EU-project RockFor.

These experiments identified that mean slope gradient is the most important indicator for the possible movement of falling rocks. It is generally agreed that on slopes with a gradient greater than approximately 30° (60 %), rocks can start to roll (JOHN and SPANG 1979; JAHN 1988; GSTEIGER 1993; GERBER 1998). On shallower slopes, rolling rocks generally slow down and finally stop. Our experiments confirmed the results presented by GERBER (1998) that on slopes with a gradient of 35° (70 %) or more, rocks start to bounce. Other factors also affect a falling rock, such as its size and shape, the material covering the slope surface and the forest cover.

Our experiments clearly demonstrated that small trees are capable of stopping large rocks, given that a large portion of the kinetic energy has already been dissipated during preceding impacts. Analyses of rockfall impacts on silver fir (*Abies alba* Mill.) show that there is an exponential relationship between DBH and the maximal amount of energy that can be dissipated by a tree during a rockfall impact (DORREN and BERGER 2006). From our field observations and data analyses, we concluded that it is not only large trees that are required in a rockfall-protection forest; well-structured stands with a wide diameter distribution and a mosaic of different forest developmental phases provide the best protection. Furthermore, broadleaved trees appear to dissipate more energy during rock-tree contacts than coniferous trees. One of the better broadleaved trees regarding wound healing is the sycamore *(Acer pseudoplatanus)*. Although the wounds take longer to heal, European beech *(Fagus sylvatica)* can dissipate more rockfall impact energy, and their seedlings regenerate successfully in small openings due to their shade tolerance. Further details on the experiments and their results are described by DORREN *et al.* (2005).

4.2 A rockfall forest assessment tool

The free-of-charge and publicly accessible tool RockFor^{NET} (www.rockfor.net), developed by BERGER and DORREN (submitted), arose from our field experiments and modelling research. The model permits each user to calculate the probable residual rockfall hazard at the foot of a rockfall-protection forest. This is the percentage of rocks that pass through a forested slope and cannot be stopped in the forest stand or at the foot of the forested slope. RockFor^{NET} considers the existing forest as a spatially distributed rockfall net. It converts the existing forest structure into virtual rows of trees along the contour, with the distance between two trees in a row being equal to 90 % of the diameter of the dominant rock that falls at the site of interest. The distance between rows is 33 m. This distance has been derived from the mean tree free distance at our test site. To calculate this distance we adapted the basic concept presented by GSTEIGER (1993), in the sense that the total basal area is used as the most important parameter (DORREN *et al.* 2005). The results of our experiments demonstrated that the total basal area is an important indicator for the protective capacity of a forest stand. In addition, the basal area can be easily and quickly measured in the field using a relascope (BITTERLICH 1984).

In the model, all the trees in a row have a diameter equal to the mean DBH, which determines, in combination with the tree species, the efficacy of a tree in the energy dissipation during a rockfall impact. This follows the algorithms presented in DORREN and BERGER (2006). In order to calculate the probable rockfall hazard, RockFor^{NET} assesses how many rows are required with the mean DBH in order to protect the foot of the slope for 100 % of events, given:

– the slope length between the foot of the cliff and the foot of the forested slope,
– the height of the cliff,
– the length of the forested part of the slope,

– the rock density,
– the mean rock diameter, and
– the mean slope gradient.

These factors are required to calculate the energy to be dissipated by the forest stand. To do this, RockFor^{NET} uses the energy line angle, which is the angle of the straight line between the starting point and the maximum stopping point (HEIM 1932; TOPPE 1987; GERBER 1994). From the height difference between the energy line and the slope surface at the foot of the forested slope, the kinetic energy of the falling rock at the foot of the slope ($E_{k\text{-}foot}$) can be calculated. RockFor^{NET} assumes that the total amount of energy that has to be dissipated by the forest stand is 2.8 times the value of $E_{k\text{-}foot}$. BERGER and DORREN (submitted) found that the forest stand in which they carried out 102 real-size rockfall experiments dissipated on average 2.8 times as much as energy as the $E_{k\text{-}foot}$ calculated with the energy line. Finally, RockFor^{NET} compares the required number of trees with the existing number of trees in the stand and translates the difference between the two into a probable residual rockfall hazard (%).

The results of our experiments and of RockFor^{NET} have been formalised in silvicultural guidelines for mountain forests in France (ONF, in press) and in Switzerland (FREHNER *et al.* 2005). For the French guidelines, target values for rockfall-protection forest stands have been derived from Figure 2, which is produced by RockFor^{NET}.

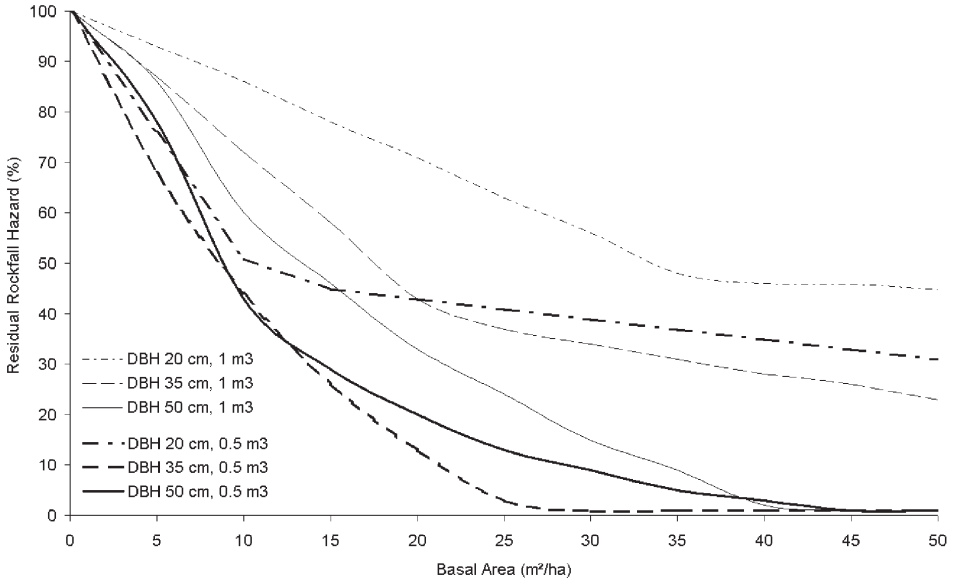


Fig. 2. Influence of the basal area of the forest stand on the residual rockfall hazard under a forested slope with a length of 500 m, a slope gradient of 38° and a rockfall source area with a of height of 10 m for different combinations of the mean tree diameter at breast height in the forest stand (DBH) and the volume of the falling rock.

5 Merging the best of two worlds: balancing tradition and technology

Taking into account the technological advances in protection forest research and management, as well as the good practices and mistakes made in the past, a useful merging of the technological and traditional world would be to take the experience of "landscape reading" (Fig. 3) and knowledge of natural hazard events of the past into account in the spatial planning and monitoring protection forests in order to assess whether there is a need for restoration or maintenance.

History has shown that doing nothing is not a sustainable practice. Forests can provide protection in the long-term only if a permanent tree cover is ensured by sufficient renewal (OTT 1978; ECKMÜLLNER 1988; KRÄUCHI *et al.* 2000; MOTTA and HAUDEMAND 2000; BRANG 2001; DORREN *et al.* 2004a). The remaining question is how much renewal would be sufficient (cf. WEHRLI *et al.* 2003) and how much removal can be accepted. Answers to these questions can be obtained by using models that simulate forest stand development to overcome the problem of the relatively slow response of forest ecosystems to 'close-to-nature' interventions. This type of intervention is currently used primarily in protection forests, which is also the result of the merging of tradition and research. Currently, these interventions are increasingly referred to as eco-engineering techniques. Examples include leaving trees diagonally on slopes in protection forests, building (temporal) protective structures, using locally felled trees and mixing silvicultural interventions with civil engineering for the time the forest needs to regenerate or restore.

Forest stand development simulation models can be used as a tool for assessing and predicting the level of protection provided by mountain forests in the future and for testing



Fig. 3. Snow avalanche track in the Montafon region (Austria), a good example of an indicator of a natural hazard (Photo L. Dorren).

silvicultural interventions (see LIU and ASHTON 1995; MLADENHOFF and BAKER 1999; PENG 2000, COURBAUD *et al.* 2001; JOHNSEN *et al.* 2001; WEHRLI 2005).

The technologies presented in this paper have been combined into a logical method for managing and sustaining protection forests (see flow diagram in Fig. 4). This method enables the identification of impaired protection forests in larger management areas and it allows for assessing where and which silvicultural interventions have to be carried out to safeguard protection against natural hazards, such as rockfall and snow avalanches. On the whole, such a method could contribute to an improvement in the management of mountain forests that protect against rockfall. This can be justified by two arguments. Firstly, the method results in better assignment of priorities for implementation of silvicultural measures at a regional scale. Secondly, silvicultural strategies within specific protection forests could be improved on the basis of the increased insight into the interaction between forest structure and rockfall as obtained by existing knowledge, local experience, and combined field and modelling studies.

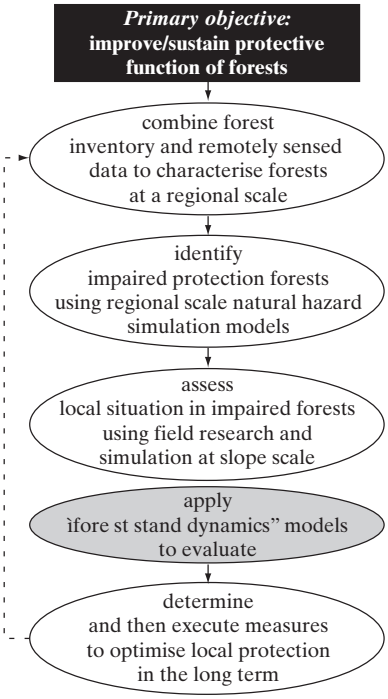


Fig. 4. Flow diagram showing how a combination of existing technologies could contribute to an improvement of the management of protection forests. The dotted arrow refers to monitoring, which focuses at a time step of five to ten years.

6 Conclusions

This paper reviews the current state-of-the-art of protection forest research and management in relation to rockfalls, focusing on traditional practices and present technologies. The traditional 'do nothing' approach is not an option for sustaining the protection provided by mountain forests. Management is needed – the question is how much.

A wide range of technologies are available to monitor, assess, simulate and assist in making decisions on specific silvicultural interventions and overall forest management. For this, the proposed general framework can assist in using the existing technologies.

Acknowledgments
We gratefully thank Bernhard Maier (Stand Montafon, Austria) and Jérôme Lievois (RTM, France) for the fruitful discussions. We also thank the European Commission for the Marie Curie Fellowship (QLK5-CT-2002-51705) and for funding the RockFor project (QLK5-CT-2000-01302). Tom Millard and an anonymous referee are thanked for their valuable comments.

7 References

AMMER, C., 1996: Impacts of ungulates on structure and dynamics of natural regeneration of mixed mountain forests in the Bavarian Alps. For. Ecol. Manage. 88: 43–53.

ANDERSSON, F.O.; FEGER, K.H.; HÜTTL, R.F.; KRÄUCHI, N.; MATTSSON, L.; SALLNÄS, O.; SJÖBERG, K., 2000: Forest ecosystem research – priorities for Europe. For. Ecol. Manage. 132: 111–119.

BARTELT, P.; STÖCKLI, V., 2001: The influence of tree and branch fracture, overturning and debris entrainment on snow avalanche flow. Ann. Glaciol. 32: 209–216.

BERGER, F., 1997: Interaction forêt de montagne – risques naturels. Détermination de zones d'interventions forestières prioritaires – l'exemple du département de la Savoie. PhD thesis Engref. Paris. 475 pp.

BERGER, F.; DORREN, L.K.A., (submitted). RockFor^{NET}: a new efficient tool for quantifying the rockfall hazard under a protection forest. Schweiz. Z. Forstwes.

BERGER, F.; LIEVOIS, J., 1999: Determination of priority forest work areas and creation of green areas in risk prevention plans – an example of researcher-specialist transfer. In: GILLET, F.; ZANOLINI, F. (eds), Int. Conf. Mountainous Natural Hazards. Cemagref, 12–14 April 1999, Grenoble, France. 412–416.

BERGER, F.; RENAUD, J.P., 1994: Stabilité et fonction de protection des forêts de montagne dans les Alpes du Nord. L'exemple de la forêt domaniale de Rioupéroux. Rev. for. fr. 46, 4: 359–374.

BERGER, F.; QUETEL, C.; DORREN, L.K.A., 2002: Forest: a natural protection mean against rockfalls, but with which efficiency? International Congress Interpraevent 2002 in the Pacific Rim, Matsumoto, Japan. Congress publication, volume 2. 815–826.

BITTERLICH, W., 1984: The relascope idea: relative measurements in forestry. Farnham Royal, Commonwealth Agricultural Bureaux. 242 p.

BRANG P., 2001: Resistance and elasticity: promising concepts for the management of protection forests in the Alps. For. Ecol. Manage. 145, 1: 107–117.

BUTLER, D.R.; MALANSON, G.P., 1985: A reconstruction of snow avalanche characteristics in Montana, U.S.A., using vegetative indicators. J. Glaciol. 31, 108: 185–187.

BUTTOUD, G., 2000: Approaches to multifunctionality in mountain forests. In: PRICE, M.F.; BUTT, N. (eds) Forests in sustainable mountain development: a state of knowledge report for 2000. IUFRO Research Series 5. Wallingford, CABI Publishing. 187–193.

CATTIAU, V.; MARI, E.; RENAUD, J.P., 1995: Forêt et protection contre les chutes de rochers. Ingénieries – EAT 1995, 3: 45–54.

COURBAUD, B.; GOREAUD, F.; DREYFUS, P.; BONNET, F.R., 2001: Evaluating thinning strategies using a tree distance dependent growth model, some examples based on the CAPSIS software "uneven-aged spruce forests" module. For. Ecol. Manage. 145, 1: 15–28.

COUVREUR, S., 1982: Les forêts de protection contre les risques naturels. École Nationale du Génie Rural des Eaux et Forêts (ENGREF). 89 p.

DOCHE, O., 1997: Etude expérimentale de chutes de blocs en forêt. Cemagref / Institut des Sciences et Techniques de Grenoble (ISTG). Cemagref doc. 97/0898, 130 p.

DORREN, L.K.A.; BERGER, F., 2006: Stem breakage of trees and energy dissipation during rockfall impacts. Tree Physiol. 26: 63–71.

DORREN, L.K.A.; SEIJMONSBERGEN, A.C., 2003: Comparison of three GIS-based models for predicting rockfall runout zones at a regional scale. Geomorphology 56, 1–2: 49–64.

DORREN, L.K.A.; BERGER, F.; IMESON, A.C.; MAIER, B.; REY, F., 2004a: Integrity, stability and management of protection forests in the Alps. For. Ecol. Manage. 195: 165–176.
DORREN, L.K.A.; MAIER, B.; PUTTERS, U.S.; SEIJMONSBERGEN, A.C., 2004b: Combining field and modelling techniques to assess rockfall dynamics on a protection forest hillslope in the Alps. Geomorphology 57, 3–4: 151–167.
DORREN, L.K.A.; BERGER, F.; LE HIR, C.; MERMIN, E.; TARDIF, P., 2005: Mechanisms, effects and management implications of rockfall in forests. For. Ecol. Manage. 215, 1–3: 183–195.
ECKMÜLLNER, O., 1988: Der österreichische Schutzwald. Cent.bl. gesamte Forstwes. 108: 187–207.
European Communities, 1996: Protokoll zur Durchführung der Alpenkonvention von 1991 im Bereich Bergwald. 12 pp.
European Observatory of Mountain Forests, 2000: White Book 2000 on mountain forests in Europe. European Federation of Local Forest Communities. Saint Jean d'Arvey. 60 pp.
FREHNER, M.; WASSER, B.; SCHWITTER, R., 2005: Nachhaltigkeit und Erfolgskontrolle im Schutzwald. Wegleitung für Pflegemassnahmen in Wäldern mit Schutzfunktion. Bern, Bundesamt für Umwelt, Wald und Landschaft. 654 pp.
FÜHRER, E., 2000: Forest functions, ecosystem stability and management. For. Ecol. Manage. 132: 29–38.
GARDINER, B.; PELTOLA, H.; KELLOMÄKI, S., 2000: Comparison of two models for predicting the critical wind speeds required to damage coniferous trees. Ecol. Model. 129: 1–23.
GERBER, W., 1994: Beurteilung des Prozesses Steinschlag, Unterlagen FAN-Kurs Oktober 1994, Poschiavo, CH. 11 pp.
GERBER, W., 1998: Waldwirkung und Steinschlag. In: SCHWITTER, R. (ed). Dokumentation der 14. Arbeitstagung der Schweizerischen Gebirgswaldpflegegruppe mit der FAN, Grafenort/ Engelberg. 15 pp.
GSTEIGER, P., 1993: Steinschlagschutzwald. Ein Beitrag zur Abgrenzung, Beurteilung und Bewirtschaftung. Schweiz. Z. Forstwes. 144: 115–132.
HAMILTON, L.S.; BRUIJNZEEL, L.A., 1997: Mountain watersheds – integrating water, soils, gravity, vegetation, and people. In: MESSERLI, B.; IVES, J. (eds) Mountains of the world. A global priority. London / New York, Parthenon. 337–370.
HEIM, A., 1932: Bergsturz und Menschenleben. Beiblatt Vierteljahrsschr. Nat.forsch. Ges. Zür. 77: 218.
HEROLD, A.; ULMER, U., 2001: Stand stability in the Swiss National Forest Inventory, assessment technique, reproducibility and relevance. For. Ecol. Manage. 145: 29–42.
JAHN, J., 1988: Entwaldung und Steinschlag, Interpraevent, Graz. Tagungspubl. Bd.1: 185–198.
JOHN, K.W.; SPANG, R.M., 1979: Steinschläge und Felsstürze. Voraussetzungen – Mechanismen – Sicherung. Tagespublikation UIC Unterausschuss K7 1979, Kandersteg.
JOHNSEN, K.; SAMUELSON, L.; TESKEY, R.; MCNULTY, S.; FOX, T., 2001: Process models as tools in forestry research and management. For. Sci. 47, 1: 2–8.
KRÄUCHI, N.; BRANG, P.; SCHÖNENBERGER, W., 2000: Forests of mountainous regions: gaps in knowledge and research needs. For. Ecol. Manage. 132, 1: 73–82.
LIU, J.; ASHTON, P.S., 1995: Individual-based simulation models for forest succession and management. For. Ecol. Manage. 73: 157–175.
MLADENOFF, D.J.; BAKER, W.L., 1999: Spatial modelling of forest landscape change. Approaches and applications. Cambridge, Cambridge University Press. 352 pp.
MOTTA, R., 1996: Impact of wild ungulates on forest regeneration and tree composition of mountain forests in the Western Italian Alps. For. Ecol. Manage. 88, 1–2: 93–98.
MOTTA, R., 2003: Ungulate impact on rowan (*Sorbus aucuparia* L.) and Norway spruce (*Picea abies* [L.] Karst.) height structure in mountain forests in the eastern Italian Alps. For. Ecol. Manage. 181, 1–2: 139–150.
MOTTA, R.; HAUDEMAND, J.C., 2000: Protective forests and silvicultural stability – An example of planning in the Aosta Valley. Mt. Res. Dev. 20, 2: 180–187.
ONF, in press. Guide des sylvicultures de montagne. ONF / CRPF / Cemagref. France.
OTT, E., 1978: Zur Notwendigkeit der Pflege von Gebirgswäldern. Schweiz. Z. Forstwes. 129, 2: 101–116.

PELTOLA, H.; KELLOMÄKI, S.; HASSINEN, A.; GRANANDER, M., 2000: Mechanical stability of Scots pine, Norway spruce and birch: an analysis of tree-pulling experiments in Finland. For. Ecol. Manage. 135, 1–3: 143–153.

PENG, C., 2000: Understanding the role of forest simulation models in sustainable forest management. Environ. Impact Assess. Rev. 20, 4: 481–501.

PRICE, M.F.; KOHLER, T.; WACHS, T., 2000: Mountains of the world; Mountain forests and sustainable development. Berne, Mountain Agenda. 42 pp.

SCHÖNENBERGER, W., 2000: Silvicultural problems in subalpine forests in the Alps. In: PRICE, M.F.; BUTT, N. (eds) Forests in sustainable mountain development: a state of knowledge report for 2000. IUFRO Research Series 5. Wallingford, CABI Publishing. 197–203.

SHRODER, J.F., 1975:. Dendrogeomorphologic analysis of mass movement. Proc. Assoc. Am. Geogr. 7: 222–226.

SHRODER, J.F., 1980: Dendrogeomorphology: review and new techniques of tree-ring dating. Prog. Phys. Geogr. 4, 2: 161–188.

SMITH, D.J.; MCCARTHY, D.P.; LUCKMAN, B.H., 1994: Snow avalanche impact pools in the Canadian Rocky Mountains. Arct. Antarc. Alp. Res. 26, 2: 116–127.

STOFFEL, M.; SCHNEUWLY, D.; BOLLSCHWEILER, M.; LIÈVRE, I.; DELALOYE, R.; MYINT, M.; MONBARON, M., 2005: Analyzing rockfall activity (1600–2002) in a protection forest – a case study using dendrogeomorphology. Geomorphology 68, 3–4: 224–241.

STOFFEL, M.; WEHRLI, A.; KÜHNE, R.; DORREN, L.K.A.; PERRET, S.; KIENHOLZ, H., 2006: Quantifying the protective effect of mountain forests against rockfall using a 3D simulation model. For. Ecol. Manage. 225, 1–3: 113–122.

STOKES, A.; SALIN, F.; KOKUTSE, A.D.; BERTHIER, S.; JEANNIN, H.; MOCHAN, S.; DORREN, L.K.A.; KOKUTSE, N.; GHANI, M.A.; FOURCAUD, T., 2005: Mechanical resistance of different tree species to rockfall in the French Alps. Plant Soil 278, 1–2: 107–117.

STRUNK, H., 1989: Dendrogeomorphology of debris flows. Dendrochronologia 7: 15–25.

STRUNK, H., 1997: Dating of geomorphological processes using dendrogeomorphological methods. Catena 31: 137–151.

SUBOTSCH, N., 1999: Comparaison des politiques de gestion des forêts à rôle de protection dans les pays alpins, signataires de la convention alpine. PhD Thesis, Grenoble, Université Joseph Fourier – Grenoble I. 485 pp.

Swiss Federal Statistical Office, 2002: Statistisches Jahrbuch der Schweiz 2002. Swiss Federal Statistical Office. Neue Zürcher Zeitung. 890 pp.

TOPPE, R., 1987: Terrain models – A tool for natural hazard mapping. In: SALM, B.; GUBLER, H. (eds) Proceedings of Avalanche formation, Movement and Effects, Davos 1986, IAHS Publication no. 162: 629–638.

UN-ECE/FAO, 2000: Forest Resources of Europe, CIS, North America, Australia, Japan and New Zealand (industrialized temperate/boreal countries). UN-ECE/FAO Contribution to the Global Forest Resources Assessment 2000. Geneva Timber and Forest Study Papers, No. 17, New York and Geneva, United Nations.

WEHRLI, A.; SCHÖNENBERGER, W.; BRANG, P., 2003: Long-term development of protection forests: Combining models of forest dynamics with models of natural hazards. European Tropical Forest Research Network Newsletter. 20–24.

WEHRLI, A.; ZINGG, A.; BUGMANN, H.; HUTH, A., 2005: Using a forest patch model to predict the dynamics of stand structure in Swiss mountain forests. For. Ecol. Manage. 205, 1–3: 149–167.

WILKERSON, F.D.; SCHMID, G.L., 2003: Debris flows in Glacier National Park, Montana: geomorphology and hazards. Geomorphology 55, 1–4: 317–328.

ZINGGELER, A.; KRUMMENACHER, B.; KIENHOLZ, H., 1991: Steinschlagsimulation in Gebirgswäldern. Berichte und Forschungen 3: Geographisches Institut der Universität Freiburg. 61–70.

Revised version accepted February 25, 2006

Available online at www.sciencedirect.com
SCIENCE DIRECT®
Forest Ecology and Management 195 (2004) 165–176
Forest Ecology and Management
www.elsevier.com/locate/foreco

Integrity, stability and management of protection forests in the European Alps

Luuk K.A. Dorren[a,*], Frédéric Berger[a], Anton C. Imeson[b], Bernhard Maier[c], Freddy Rey[a]

[a]*Cemagref Grenoble, 2 Rue de la Papeterie, B.P. 76, F-38402 Saint Martin d'Hères Cedex, France*
[b]*Institute for Biodiversity and Ecosystem Dynamics—Physical Geography, Universiteit van Amsterdam, Nieuwe Achtergracht 166, 1018 WV Amsterdam, The Netherlands*
[c]*Stand Montafon—Forstfonds, Montafonerstraße 21, A-6780 Schruns, Austria*

Received 4 March 2003; received in revised form 19 January 2004; accepted 20 February 2004

Abstract

Ecosystem management of protection forests aims at maintaining forests near a state during which effective protection is secured. As the evolution of a dynamic forest ecosystem cannot be stopped, silvicultural measures are required which aim at maintaining both the ecosystem integrity and the protective function of mountain forests. Ecosystem integrity is defined as the system's capacity to maintain structure and ecosystem functions using processes and elements characteristic for its ecoregion. Here, ecosystem functions also reflect the capability of the ecosystem to provide functions of value to humans. Ecosystem integrity of a protection forest implies that the stability (mainly the property resilience is addressed) of the forest is high, because that is required to provide a high level of protection in the long term. The main conditions promoting natural evolutionary processes and ecological stability in protection forests are: (1) a diverse composition of species; (2) sufficient natural regeneration; (3) an optimal forest structure. The first example in this chapter explains how these conditions might be achieved by silvicultural interventions in a forest that mainly protects against rockfall in the Austrian Alps. The second example deals with socio-economic aspects of ecosystem integrity of a forest that also protects against rockfall, but then in the French Alps. Both examples show that forest authorities are aware of techniques to improve the stand stability of protection forests, but the problem is that current forest management is often a kind of trial and error, because the exact consequences of interventions for forest ecosystem dynamics are not known. Therefore, it is proposed that forest ecosystem research should shift focus from protection forest dynamics to the geo-ecosystem functioning of protection forests, including the effects of natural and human disturbances. For this, the concept of panarchy may be a promising way forward.
© 2004 Elsevier B.V. All rights reserved.

Keywords: Protection forest; Ecosystem integrity; Mountain forest management; Natural hazards; Disturbance; Ecological stability; Geo-ecosystem

1. Introduction

The ultimate goal of ecosystem-based management could be summarised as 'the preservation of ecosystem integrity while satisfying human needs' (Grumbine, 1997; Yaffee, 1998; Pirot et al., 2000). Integrity in

* Corresponding author. Tel.: +33-4-76-76-28-06; fax: +33-4-76-51-38-03.
E-mail address: luuk.dorren@cemagref.fr (L.K.A. Dorren).

0378-1127/$ – see front matter © 2004 Elsevier B.V. All rights reserved.
doi:10.1016/j.foreco.2004.02.057

relation to ecosystems was first mentioned by Aldo Leopold who stated 'a thing is right when it tends to preserve integrity, stability and beauty of the biotic community. It is wrong when it tends otherwise' (Leopold, 1949).

Current ecosystem management of forests is mainly based on ecological stability in relation to disturbances. Here, stability is often, for simplicity, characterised by the two components resistance and resilience, or synonyms of these terms (Holling, 1973; Grimm et al., 1992; Larsen, 1995; Führer, 2000; Kräuchi et al., 2000; Motta and Haudemand, 2000; Brang, 2001). Increased knowledge of ecological stability in relation to disturbances and increasing labour costs resulted in a paradigm shift from forest management for timber production towards forest ecosystem management (Attiwill, 1994; Führer, 2000; Harvey et al., 2002), especially in case of management of forests that protect against natural hazards (Larsen, 1995; Brang et al., 2000; Kräuchi et al., 2000; Motta and Haudemand, 2000; Bebi et al., 2001; Brang, 2001). Parallel, it has been discussed whether forest management is necessary at all for ensuring the protective function of a mountain forest on the long term. This argument originates from the view that mountain forests are self-organising stable ecosystems (see Weiss, 2000). Yet, an increasing group of authors report that mountain forests could only fulfil their protective function on the long term if they are managed actively, since instability problems caused by overmaturity arise if silvicultural interventions are absent (Ott, 1978; Ott and Schönbächler, 1986; Führer, 2000; Kräuchi et al., 2000; Motta and Haudemand, 2000; Brang, 2001).

More 'close-to-nature' silvicultural techniques, in comparison to those applied for traditional management of timber production forests, are increasingly applied. Current examples of such methods include minimal tending and the use of stand structural types (Wasser and Frehner, 1996; Motta and Haudemand, 2000; Brang, 2001). The aim of such 'close-to-nature' silvicultural interventions in protection forests is to maintain forest stands in a stage during which effective protection is provided (Motta and Haudemand, 2000). This instantly indicates the main problem of managing protection forests, as it is impossible to stop the evolution of a forest. Therefore silvicultural measures are required, which are associated with the trend of development of the forest ecosystem and which aim at maintaining the integrity of the protection forest ecosystem. To achieve this, knowledge of ecosystem integrity of protection forests is needed. Consequently, the objective of this article is to explain the concept of ecosystem integrity with respect to protection forests and to describe how this concept could be integrated in management of protection forests. We will present two examples dealing with ecological and socio-economic aspects of ecosystem integrity of protection forests in the European Alps. Subsequently, we will discuss some research needs in order to improve ecosystem management of protection forests.

2. Protection forest: function and dynamics

First of all, we will give a short description of protection forests as defined in most alpine countries in Europe, since the term is often used for forests with different functions (Ottitsch and Weiss, 2000). Generally, a protection forest has mainly an object-protection or direct protective function (Schönenberger, 2000). At the same time a forest provides a site-protection function, which is actually a prerequisite for the direct protective function (van Noord, 1996). In addition, like all mountain forests, protection forests provide multiple functions, such as recreation, sequestration of carbon dioxide and conservation of biodiversity (Buttoud, 2000; Cattoi et al., 2000; Führer, 2000; UN-ECE/FAO, 2000).

The direct-protective function of a forest implies that the forest directly protects people, buildings and infrastructure against the impact of natural hazards such as snow avalanches and rockfall (Brang, 2001). The site-protection function is important as a forest stand needs to protect its site against processes such as excessive soil erosion and the occurrence of debris flows (Rey and Chauvin, 2001). If the site-protection function is impaired, the forest site erodes, which results in a loss of the forest ecosystem as a whole.

Mountain forests are self-organising stable ecosystems if regarded at a landscape scale, which normally do not need any silvicultural intervention for their continued existence. But people want to utilise timber as a sustainable resource and therefore need to manage forests. Furthermore, some forests have become degraded as a result of over-harvesting, heavy ungulate browsing or livestock grazing and need to be managed in order to fulfil the protective function. This means that

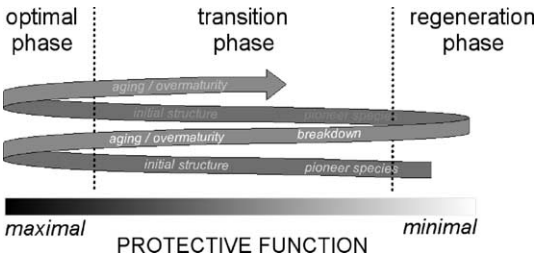


Fig. 1. Developmental phases in mountain forests in relation to the level of protection they provide.

some forests can be left untouched, others can be managed and some need to be managed.

Mountain forest stands constantly evolve from a regeneration phase to an optimal phase and back again, as illustrated in Fig. 1. During the transition phases in between the forest structure develops or breaks down. As a consequence the protective function is minimal during those phases (Motta and Haudemand, 2000), which is also indicated in Fig. 1.

The rate of transition into a next phase is not only determined by growth or ageing of individual trees, but also by the effect of disturbances on the forest ecosystem (Attiwill, 1994; Peterson et al., 2000). A disturbance is a natural or human-induced discrete event in time or space that changes physical (biotic and/or a-biotic) conditions of an ecosystem (after White and Pickett, 1985). The effect of a disturbance is determined by its magnitude and by the ecological stability of the forest stand. Throughout this article we address the property resilience of stability (Grimm and Wissel, 1997). Stability might differ a lot within a stand due to variation in stand factors such as micro-site conditions like availability of nutrients, soil moisture and light (Schönenberger, 2000). Therefore, several development phases presented in Fig. 1 may occur simultaneously within a stand. A disturbance might be 'normal' for an ecosystem. Natural disturbances in mountain forests such as snow avalanches or rockfall are important processes since they drive development and change. By doing so, these processes partly determine the integrity of a mountain forest ecosystem.

3. Forest ecosystem integrity

Theoretically, a mountain forest that goes through developmental phases without human disturbances consists of the potential natural vegetation characteristic for that ecosystem. The integrity of such an ecosystem is not necessarily high, this depends on the definition of ecosystem integrity. Many scientists discussed ecosystem integrity, especially the last decade (see Karr, 1990; Noss, 1990; Kay, 1991; Woodley et al., 1993; Westra, 1996; De Leo and Levin, 1997; Goldstein, 1998; Müller et al., 2000). Nevertheless, there is still no agreement on a uniform definition. We define ecosystem integrity as the system's capacity to maintain structure and ecosystem functions using processes and elements characteristic for its ecoregion. Here, ecosystem functions do not only refer to relations and processes that are inherently part of a dynamic, open and complex ecosystem (Pimm, 1984; O'Neill et al., 1986). Ecosystem functions also reflect the capability of the ecosystem to support goods and services of value to humans (De Leo and Levin, 1997). Examples are regulation functions, habitat functions, production functions and information functions (after de Groot, 1992). A protection forest is a good example of an ecosystem performing a regulation function.

Since our definition links ecosystem integrity to functions of value to humans, a protection forest ecosystem with a high integrity implies that the stability of the forest is also high, because that is required to provide a high level of protection in the long term. This does not account for a forest without a protective function, since the ecosystem integrity of a forest in a breakdown phase might be high, but the stability is low. A protection forest needs both ecological integrity and stability, since both determine its ecosystem integrity. Ecological integrity is needed to maintain variability in structure and functions; stability is needed to maintain the variability within a critical range. This is essential to avoid perturbation to a state in which the protective function is minimal. Here, perturbation is the change of motion, course, arrangement or structure of a whole ecosystem, caused by disturbances (after White and Pickett, 1985).

4. Ecosystem management of protection forests

Within an ecosystem, functions exist which are essential for maintaining its organisation in the face of disturbances. An ecosystem is only capable of providing functions of value to humans if these

essential functions are fulfilled. Therefore, the primary objective of management strategies is to protect, maintain and/or restore the essential ecosystem functions of forest ecosystems using processes and elements characteristic for its ecoregion (Andersson et al., 2000; Schlaepfer et al., 2002). These characteristics all are related to the ecological integrity of the system. Subsequently, stability with respect to a function of value to humans could be promoted, by e.g. applying 'close-to-nature' silvicultural techniques, to obtain high ecosystem integrity.

The main problem with protection forest management is to predict the trend of development of a forest in the face of disturbances, which could be both human and natural, but especially the natural hazard the forest should protect against. This relatively unknown factor in combination with the given fact that an ecosystem is an open, dynamic system, endorses the general rule stated by Holling and Meffe (1996) that ecosystem management should not aim at preserving something that must change. Consequently, forest ecosystem dynamics must be integrated into management strategies (Attiwill, 1994). Adaptive management is therefore a necessity. Current management of protection forests mainly tends to preserve stand stability, but the aim should be to create or maintain conditions that promote evolutionary processes while maintaining forest ecosystem integrity in relation to its assigned function. Fig. 2 shows that, before silvicultural measures are planned and executed, two important questions need to be answered. The first question is whether the ecological integrity of the protection forest is high. If this is the case, the second question is whether the ecological stability is high. If one of these conditions is not fulfilled, measures could be taken, if considered appropriate, as shown in Fig. 2.

5. Towards implementation

Conditions promoting natural evolutionary processes and ecological stability in protection forests could be categorised in three practical and general criteria (modified from Motta and Haudemand, 2000):

1. diverse composition of species;
2. sufficient natural regeneration;
3. optimal forest structure.

But before these criteria are evaluated to estimate the ecosystem integrity of a protection forest, its history must be assessed. The origin of the forest, past silvicultural treatments and evidences of natural disturbances must be known (Motta and Haudemand, 2000). The further management starts from the state defined by the criteria mentioned above, the stronger the management intervention must be (Führer, 2000), but preferably silvicultural intervention mimics

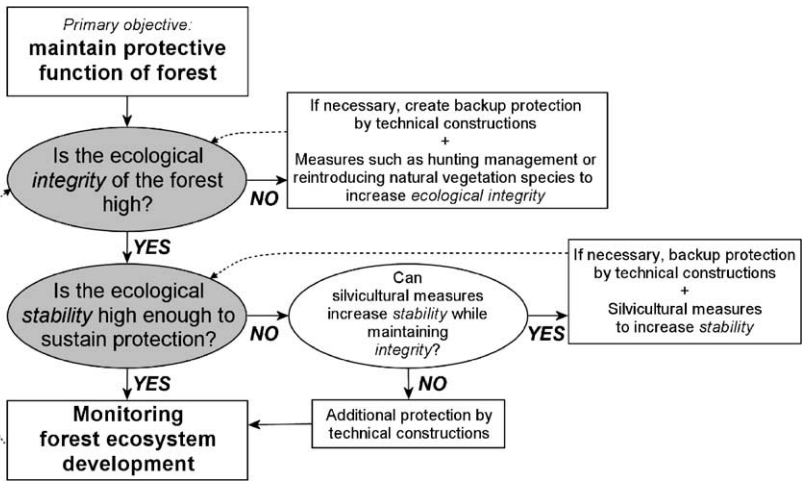


Fig. 2. Flow chart presenting essential steps in determining a management plan for protection forests. Solid arrows indicate direct actions to be taken or questions to be answered and dotted arrows indicate an intermediate time period of several years to decades.

small-scale natural disturbances (Bengtsson et al., 2000). If ecosystem dynamics tend to deviate from the course directed to fulfilment of the criteria, the suitability of the forest stand for performing a protective function might be questioned. Other protective measures, like technical constructions such as rockfall retaining nets and avalanche barriers, might be required in such a case, since management cannot push a forest ecosystem in a direction opposite to the natural one.

The composition of species should be characteristic for the ecoregion and if possible diverse (both for the trees and the understory vegetation). Diversity determines the amount of variability in the potential drivers of an ecosystem (Holling and Meffe, 1996), which are the key species and key processes in an ecosystem. It is still unclear whether a diverse composition of species increases ecosystem stability (Holling, 1973; May, 1973; Tilman and Downing, 1994; De Leo and Levin, 1997; Tilman et al., 1997; Bengtsson et al., 2000). However, there is much evidence that mixed forests are more resistant to perturbations and more resilient after disturbances than monocultures. It is also thought that they perform ecosystem functions more reliable over time (Larsen, 1995; Bengtsson et al., 2000).

Natural regeneration is equally important as the species composition, because it is the primary source for natural stand renewal. Therefore, the maintenance of a good seedling bank is required, but sufficient light, prevention of competing ground vegetation suppressing seedlings, prevention of heavy browsing by ungulates as well as suitable seedbeds are also important (Ammer, 1996; Motta, 1996; Ott et al., 1997; Fuller and Gill, 2001). Tree stems lying on the slope surface provide both good protection against rockfall and snow avalanches and they provide good seedbeds. Therefore, timber should be left in the stand unless it is too risky with respect to bark beetle infestation (Kräuchi et al., 2000).

The optimal structure of a protection forest depends on the type of natural hazards the forest is protecting against. For example, a forest protecting against rockfall should have a large number of trees, preferably with thick tree stems near the rockfall source area (Wasser and Frehner, 1996). This, however, is related to different developmental stages of a forest stand (regeneration/transtition phase and optimal phase) and therefore, difficult to achieve. The results of our rockfall experiments in a French mountain forest imply that the number of trees is more important than the diameter of the trees. At the same time a multilayered stand is needed to ensure a certain degree of protection on the long term. In the accumulation zone of a rockfall slope, a forest consisting of dense bushes and shrubs is preferred (Mani and Kläy, 1992; Gsteiger, 1993; Berger and Renaud, 1994; Berger and Rey, 2001). Generally, uneven multilayered stands with a mosaic of all sizes and age classes are the best suited for protection (Ott et al., 1997; Kräuchi et al., 2000; Motta and Haudemand, 2000). This general structure should be aimed for since protection forests mostly protect against several types of natural hazards. The cluster structure, which is characteristic for high-elevation stands, may serve as a model for the arrangement of seedlings in plantations and for silvicultural interventions in homogeneous stands aiming at the optimal structure for protection (Schönenberger, 2001b).

Ideally, a forest ecosystem that fulfils the three general criteria mentioned above enters a 'steady-state' in which small patches with alternating developmental phases provide a collective stability for the stand or forest (see Fig. 3). Führer (2000) assumes that in this state efficient mechanisms of self-regulating processes control all destabilising forces, thus keeping the destructive phases temporally and spatially within ecologically tolerable limits, which is sub-optimal for protection on the short term, but as optimal as possible on the long term.

6. A silvicultural/forest ecological example

The 'Ausserbacher' forest covers about 50 ha on a south–southwest facing slope in the Montafon region



Fig. 3. A sub-optimal protective function could be maintained by small patches in phase-shifted developmental states, which build up a collective stability for the forest stand. This approach requires that similar phases of patch dynamics are not occurring synchronically, e.g. all the patches being in a breakdown phase.

in Austria (between 46°50′ and 47°8′ latitude and 9°41′and 10°9′ longitude). The forest stretches from the valley (930 m a.s.l.), up to 1500 m a.s.l. and grows on a uniformly shaped talus slope with an average inclination of 39°. Because of its proximity to the Ausserbach hamlet this forest has always been an important resource for local inhabitants in terms of wood production and grazing livestock. Above all, the forest protects the Ausserbach hamlet against falling rocks, which originate from a cliff face, with a height up to 100 m, in the upper part of the forest hillslope. In addition, the forest prevents the release of snow avalanches on the steep parts of the hillslope.

In 1988 the protective function of the forest reached a critical level because firstly most of the trees had been damaged by rockfall while substantial regeneration was lacking and secondly, the forest was prone to wind throw. It seemed that the ecological processes could not sustain the protective function of the forest and as a result, ecosystem integrity could not be maintained. Therefore, the forest authority initiated a restoration project, which started with assessing the history of human and natural disturbances in the forest. This assessment showed that the grazing of sheep until 1960 had a long-term effect on the species composition of the forest. As they feed selectively, natural regeneration of deciduous trees and shrubs in particular, was suppressed. Indicative is that the present coverage of beech (*Fagus sylvatica*), is not more than 10%, although the potential natural forest community up to an altitude of 1050 m corresponds to a beech-dominated *Luzulo fagetum*. After 1960, two feeding stations for ungulates were installed in the forest, which resulted in an enormous browsing pressure for 20 years. This further caused a lack of natural regeneration. In addition to the direct and indirect human interference there has been a permanent impact of natural disturbances such as rockfall, snow avalanches and wind (Dorren et al., 2004).

A map of the developmental stages of the forest, carried out in 1988 according to Leibundgut (1959), showed that 84% of all the trees in the Ausserbacher forest were damaged by rockfall (Stand Montafon, 1990). About 45% of the total forest area was in a so-called ageing phase (Fig. 4), which was amongst others indicated by a low tree density of 290 trees/ha. At first sight these stands appeared stable against wind throw because of the varying horizontal and vertical structure and a well-distributed network of vital long-crowned skeleton trees (in German: *Gerüstbäume*, being trees with a stabilising function). But the high percentage of trees with heart rot reduced this apparent resistance. Crucial for the future stand development was the lack of regeneration, which would have considerably reduced the resilience of the forest in the long term.

Twenty-two percent of the forest was identified as being in an optimal phase and had an average number of 560 trees/ha. The optimal forest stands were spruce-dominated and mainly structured in homogeneous single-layers. In combination with high coefficients of slenderness (length/width ratio), short crown lengths and the high degree of trees damaged by falling rocks, the threat of wind throw would increase in these stands. Only 19% of the area could be classified as a so-called selection forest with a multi-layered structure and a mosaic of ageing, breakdown and regeneration phases. This type of forest grows mainly on steep rocky and blocky sites, because of the diversity in abiotic conditions. The unstocked (denuded of trees) stripes shown in Fig. 4 are attributable to snow gliding and intensive rockfall. In 1988, these accounted for 14% of the total area.

On the basis of all the previously described information, the forest authority regarded: (a) the reduction of ungulate population; (b) the improvement of the accessibility via forest roads; (c) the construction of avalanche barriers and rockfall nets in the major rockfall channel as urgent. These measures were a prerequisite for the implementation of the following silvicultural measures:

- small-scale felling with deposition of trees diagonal to the slope direction;
- narrow irregular stripe felling diagonal to the slope direction, using cable cranes;
- reforestation of unstocked forest land and coppicing hazel to stimulate its growth.

The forest authority aimed for a mosaic of stand patches at different developmental stages by splitting the homogeneous optimal and optimal/ageing stands into smaller patches using irregular stripe felling. Once regeneration in these felled stripes has reached a more mature stage, the mosaic-creation process will be continued by additional stripe felling. This process has to be carried out during a whole developmental

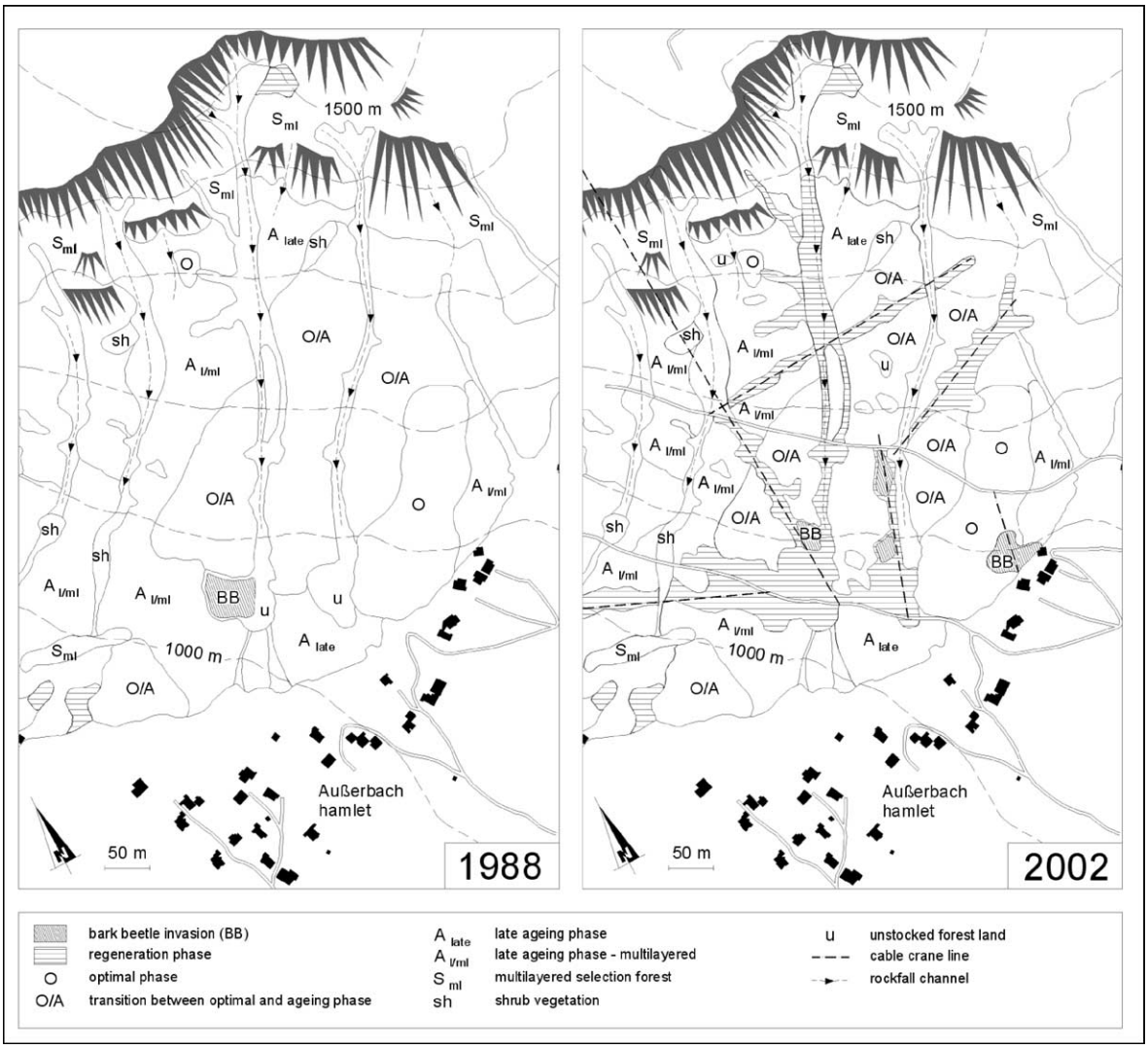


Fig. 4. Distribution of developmental phases, disturbances and silvicultural measures.

cycle of a stand, which takes about 200 years, in order to obtain phase-shifted mosaic structures (see Otto, 1994). Cut stems were left on site and deposited diagonal to the slope direction in order to decelerate and to redirect rockfall. Stems that are deposited perpendicular to the slope direction result in large rock accumulations behind them and possibly in small rock avalanches once the stems have decayed, which takes about 10 years in the study area.

The forest authority observed that in the course of felling activities the vulnerability to bark beetle infestation increased due to bark damages, sunburn on the stem, and the attraction of bark beetles by left slush timber. During warm and dry summers this indeed resulted in two subsequent bark beetle invasions (see Fig. 4), but fortunately it was observed that this contributed to the mosaic creation process. When comparing the situation of 1988 and 2002 it can be seen that 15% of the optimal phase changed into a regeneration phase. Furthermore, 32% of the unstocked forest land and areas covered with shrubs also showed regeneration (Table 1).

Table 1
The partition of the different phases in the Ausserbacher forest in 1988 and 2002

Phase	1988 (m^2)	1988 (%)	2002 (m^2)	2002 (%)
Optimal and optimal/ageing phase	85506	26	69865	21
Late ageing phase (multilayered)	101787	31	92336	28
Multilayered selection forest	92630	28	92630	28
Regeneration	2853	1	40626	12
Shrub vegetation, unstocked forest land	49284	15	36603	11
Total	332060	100	332060	100

7. A silvicultural/socio-economic example

The forest of Sainte-Foy Tarentaise (France), which covers 1130 ha, is located in the upper valley of the Isère river on steep glacially eroded valley slopes. Half of this forest covers slopes with gradients higher than 30°. The forest occupies an intermediary position between a glacier (Mont Pourri, 3780 m a.s.l.) and a valley with intense traffic. The valley road leads to the ski resorts of Tignes and Val d'Isère and traffic was estimated at 13 000 cars daily in February 1993. Especially the forest in the 'Raie' area, which covers 100 ha with mainly quasi-pure spruce stands, provides protection of roads against rockfall. This forest is located on the steepest side of a southwest oriented slope.

In April 1986, rockfall caused the death of four people, confirming the magnitude of the problem and the need for treatment. The proximity of the Olympic games in Albertville stimulated local authorities to initiate a restoration project. Moreover, the effects of the *Viviane* windstorm in 1990, which destroyed several hectares of unstable stands, stressed the need for such a project. The first step in the restoration project was an assessment of the risk posed by rockfall using a rockfall trajectory simulation program (Cattiau et al., 1995). Forestry data were derived from a study carried out by Cemagref (Renaud et al., 1994). On the basis of these data, five forest structure types were derived, which were representative for the amount of kinetic energy of falling rocks that could be absorbed by the different forest stands (Cattiau et al., 1995). The model results showed that 60–95% of all rocks starting from the top would get to the road if the forest stands were absent. The presence of trees, even scarce, reduced the rockfall hazard, either by stopping the rocks before the road or by limiting the height of the rebound, thus increasing the level of protection and reducing the cost of other measures, such as civil engineering based ones. With the forest cover present at the time of investigation, 10–15% of all the simulated falling rocks would reach the road. Subsequently, several forest cover scenarios were tested and showed that a high level of protection was provided by dense forest stands with a high basal area (>25 m^2/ha), especially if these stands were located near the top of the slope. Less dense stands, but well located in mosaics, were also providing sufficient protection, even though the average stopping distance of falling rocks was longer. In case of an absence of forest cover at the top in combination with dense forest stands at the bottom of the hillslope, most of the rocks reached the road. On the basis of these observations two silvicultural options were discussed:

- establishing relatively homogeneous and dense stands with thick tree stems (DBH of 30–40 cm) or;
- creating a structural mosaic, constituted of a regular alternation between ageing structures with initial regeneration and more dense ones with optimal growth.

The first option is very efficient in stopping rocks, but it also takes a long time, it is unstable and in the long term it needs intensive care to be maintained. The latter option, although less efficient in terms of protection, appears nonetheless better adapted and less risky in the scope of extensive management. This is because the forest structure is more stable and the continuity of functions is better guaranteed. Taking into account the local context and accompanying exploitation problems, the second option was chosen. The objective was to create structural patches of limited sizes (maximal 4–5 acres). The wood was removed by helicopter in order to avoid closing the

road and dragging wood on the ground, which might destabilise rocks. The total costs were € 21 000, the wood was sold for € 16 400 and therefore the operating loss was € 4600. The Department of Savoie, fully aware of the importance of this operation for safety, granted the owner of the forest (i.e. the local town) € 15 000. Therefore, net profit for the owner amounted to € 10 400. But, without the subsidy given by the Department of Savoie, the described operation would have been cancelled. At present, the forest provides sufficient protection against rockfall, but active management is required to maintain this level of protection. This example shows that a constant dialog between the people working in the forests, the forest managers, and forest researchers is important. In addition, efforts are needed firstly to demonstrate the wider socio-economic importance of adequate management of protection forests to local authorities/governments and secondly to involve them into the management process.

8. Synthesis: interaction between human and natural systems

Forest ecosystem integrity is rooted both in ecological as well as in social and economical aspects, as forest ecosystems are expected to provide functions of values or services to humans, which requires ecological stability. A forest is a dynamic system, continually changing in response to natural and human disturbances. Some disturbances help to maintain forest ecosystem integrity, while others threaten it. As shown by the example in the Austrian Alps, forest management interventions were required to restore the integrity of protection forests. The loss of integrity was due to the long history of direct and indirect human impact on the forest ecosystem in combination with the natural disturbances as well as the natural biotic processes. This resulted in a situation where silvicultural measures were required. This is an excellent example of a panarchy. A panarchy is a structure in which systems, including those of nature and of humans, as well as combined human–natural systems, are interlinked in continual adaptive cycles of growth, accumulation, restructuring, and renewal (Holling, 2000; Gunderson and Holling, 2002). Panarchy has evolved from hierarchy theory, firstly applied in geo-ecosystem research by Allen and Starr (1982) and O'Neill et al. (1986). They initiated an increase of theoretical understanding by viewing the landscape as a multi-scale dynamic system in which biotic and abiotic processes interact. However, both the adaptive nature of such systems, organised by periodic and transient phases of growth, conservation, collapse and reorganisation and the interaction with human systems has tended to be lost. Therefore, panarchy, a term devised to describe evolving hierarchical systems with multiple interrelated elements, offers an important new framework for understanding and resolving this dilemma. The steering variables in the panarchy of forest that protects against rockfall are the frequency and magnitude of rockfall, growth of individual trees, regeneration and breakdown of the forest as well as silvicultural interventions. These variables are all interacting. At the same time, some of them are the result of an adaptive cycle within themselves. For example, whether or not silvicultural interventions will be carried out in protection forests depends on factors acting in social, economical and to a lesser extent forest ecological systems (see also Buttoud, 2002), as shown by the example in the French Alps.

There is a need for the theoretical framework panarchy provides. The examples show that forest authorities are aware of techniques to improve the stability of protection forest ecosystems, but the problem is that current forest management is often still a kind of trial and error, because the exact consequences of interventions for forest ecosystem dynamics are not known. This accounts both for the impact of the natural hazard the forest should protect against as well as the future dynamics of the forests ecosystem. Despite this knowledge gap, which is due to the lack of research and the fact that previous disturbances affect the development of a forest for a long time, foresters are increasingly aware of the self-organising capacity of forests, which is indicated by the fact that they do take into account natural forest ecosystem processes as far as possible in the silvicultural measures taken. It is known that it is important not to try stopping the 'natural' stand development, but to exploit forest dynamics for silvicultural and overall management objectives. Especially this should be investigated more, as recognised by many authors (Attiwill, 1994; Andersson et al., 2000; Bengtsson et al., 2000; Führer, 2000; Kräuchi et al., 2000; Bebi et al.,

2001; Brang, 2001; Schönenberger, 2001a). Regarding the interaction between forests and natural hazards, research should shift focus to mountain geo-ecosystem functioning. In replication of Troll (1971), Rowe and Barnes (1994) and Huggett (1995) we prefer the term geo-ecosystem to place the emphasis not only on the biosphere, but also on the atmosphere, hydrosphere, lithosphere and pedosphere, which are dynamic and important parts of mountain forest landscapes. Understanding geo-ecosystem functioning differs from assessing how geo-ecosystem functions are performed; it is about understanding how our surrounding dynamic ecosystems, which are affected by our social and economical systems, operate. Therefore, panarchy is a promising way forward to improve ecosystem management of protection forests in mountains and to sustain ecosystem integrity in general. Because if the panarchy of a protection forest would be understood better, different silvicultural interventions could be simulated to test its effect on the integrity of the forest ecosystem. Consequently optimal silvicultural procedures could be pinpointed.

This paper presented two real world examples regarding the management of forests that protect against rockfall. In addition, the theoretical nature of the state-of-the-art concepts of ecosystem management has been described. Overall, this paper indicates a gap between the theory and practice of protection forest management. To help decrease this gap, we focus at the development of a method for obtaining more knowledge about the interaction between abiotic (rockfall) and biotic (protection forest structure) factors in a mountain geo-ecosystem. This method and the obtained knowledge will be another step towards understanding the panarchy of protection forests in mountain geo-ecosystems.

References

Attiwill, P.M., 1994. The disturbance of forest ecosystems: the ecological basis for conservative management. For. Ecol. Manage. 63 (2), 247–300.

Allen, T.F.H., Starr, T.B., 1982. Hierarchy: Perspectives for Ecological Complexity. University of Chicago Press, Chicago, p. 310.

Ammer, C., 1996. Impacts of ungulates on structure and dynamics of natural regeneration of mixed mountain forests in the Bavarian Alps. For. Ecol. Manage. 88, 43–53.

Andersson, F.O., Feger, K.H., Hüttl, R.F., Kräuchi, N., Mattsson, L., Sallnäs, O., Sjöberg, K., 2000. Forest ecosystem research—priorities for Europe. For. Ecol. Manage. 132, 111–119.

Bebi, P., Kienast, F., Schönenberger, W., 2001. Assessing structures in mountain forests as a basis for investigating the forests dynamics and protective function. For. Ecol. Manage. 145, 3–14.

Bengtsson, J., Nilsson, S.G., Franc, A., Menozzi, P., 2000. Biodiversity, disturbances, ecosystem function and management of European forests. For. Ecol. Manage. 132, 39–50.

Berger, F., Renaud, J.P., 1994. Stabilité et fonction de protection des forêts de montagne dans les Alpes du Nord. L'exemple de la forêt domaniale de Rioupéroux. Revue Forestière Française 46 (4), 359–374.

Berger, F., Rey, F., 2001. Mountain protection forests against natural hazards and risks: from research to management. In: Proceedings of the International Conference on "Forest Research: A Challenge for an Integrated European Approach". Thessaloniki, Greece, 27 August–1 September 2001, vol. I, pp. 275–280.

Brang, P., Schönenberger, W., Ott, E., 2000. Forests as Protection From Natural Hazards, The Forests Handbook, vol. 2. Blackwell Scientific, Oxford.

Brang, P., 2001. Resistance and elasticity: promising concepts for the management of protection forests in the European Alps. For. Ecol. Manage. 145, 107–117.

Buttoud, G., 2000. Approaches to multifunctionality in mountain forests. In: Price, M.F., Butt, N. (Eds.), Forests in Sustainable Mountain Development: A State of Knowledge Report for 2000. IUFRO Research Series 5. CABI Publishing, Wallingford, UK, pp. 187–193.

Buttoud, G., 2002. Multipurpose management of mountain forests: which approaches? For. Policy Econ. 4 (2), 83–87.

Cattiau, V., Marie, E., Renaud, J.P., 1995. Forêt et protection contre les chutes de rochers. Ingénieries Cemagref Eau-Agriculture-Territoire 3, 45–54.

Cattoi, S., Pollini, C., Tosi, V., 2000. Case study: multifunctionality in the fiemme valley, Italian Alps. In: Price, M.F., Butt, N. (Eds.), Forests In Sustainable Mountain Development: A State of Knowledge Report for 2000. IUFRO Research Series 5. CABI Publishing, Wallingford, UK, pp. 203–205.

De Leo, G.A., Levin, S.A., 1997. The multifaceted aspects of ecosystem integrity. Conservation Ecology 1(1). Available: as seen on December 1st 2001. http://www.consecol.org/vol1/iss1/art3.

Dorren, L.K.A., Maier, B., Putters, U.S., Seijmonsbergen, A.C., 2004. Combining field and modelling techniques to assess rockfall dynamics on a protection forest hillslope in the European Alps. Geomorphology 57 (3–4), 151–167.

Führer, E., 2000. Forest functions, ecosystem stability and management. For. Ecol. Manage. 132, 29–38.

Fuller, R.J., Gill, R.M.A., 2001. Ecological impacts of increasing numbers of deer in British woodland. Forestry 74 (3), 193–199.

Goldstein, P.Z., 1998. Functional ecosystems and biodiversity buzzwords. Conserv. Biol. 13 (2), 247–255.

Grimm, V., Schmidt, E., Wissel, C., 1992. On the application of stability concepts in ecology. Ecol. Model. 63, 143–161.

Grimm, V., Wissel, C., 1997. Babel, or the ecological stability discussions: an inventory and analysis of terminology and a guide for avoiding confusion. Oecologia 109, 323–334.

de Groot, R.S., 1992. Functions of Nature. Evaluation of Nature in Environmental Planning, Management and Decision Making. Wolters Noordhoff, Deventer, The Netherlands, p. 315.

Grumbine, R.E., 1997. Reflections on ‘‘What is ecosystem management?’’. Conserv. Biol. 11, 41–47.

Gsteiger, P., 1993. Steinschlagschutzwald, Ein Beitrag zur Abgrenzung, Beurteilung und Bewirtschaftung. Schweizerische Zeitschrift für Forstwesen 144, 115–132.

Gunderson, L.H., Holling, C.S., 2002. Panarchy: Understanding Transformations in Human and Natural Systems. Island Press, Washington, DC, pp. 507.

Harvey, B.D., Leduc, A., Gauthier, S., Bergeron, Y., 2002. Stand-landscape integration in natural disturbance-based management of the southern boreal forest. For. Ecol. Manage. 155, 369–385.

Holling, C.S., 1973. Resilience and stability of ecological systems. Ann. Rev. Ecol. Syst. 4, 1–24.

Holling, C.S., Meffe, G.K., 1996. Command and control and the pathology of natural resource management. Conserv. Biol. 10 (2), 328–337.

Holling, C.S., 2000. Theories for sustainable futures. Conserv. Ecol. 4, 7http://www.consecol.org/vol4/iss2/art7..

Huggett, R.J., 1995. Geoecology. An Evolutionary Approach. Routledge, UK, p. 320.

Karr, J.R., 1990. Biological integrity and the goal of environmental legislations: lessons for conservation biology. Conserv. Biol. 4, 244–250.

Kay, J.J., 1991. A non-equilibrium thermodynamic framework for discussing ecosystem integrity. Environ. Manage. 15 (4), 483–495.

Kräuchi, N., Brang, P., Schönenberger, W., 2000. Forests of mountainous regions: gaps in knowledge and research needs. For. Ecol. Manage. 132 (1), 73–82.

Larsen, J.B., 1995. Ecological stability of forests and sustainable silviculture. For. Ecol. Manage. 73, 85–96.

Leibundgut, H., 1959. Über Zweck und Methodik der Struktur- und Zuwachsanalyse von Urwäldern. Schweizerische Zeitschrift für Forstwesen 110, 111–124.

Leopold, A., 1949. A Sand County Almanac and Sketches Here and There. Oxford University Press, NY, p. 228.

Mani, P., Kläy, M., 1992. Naturgefahren an der Rigi-Nordlehne, Die Beurteilung von Naturgefahren als Grundlage für die waldbauliche Massnahmenplanung. Schweizerische Zeitschrift für Forstwesen 143, 131–147.

May, R.M., 1973. Stability and Complexity in Model Ecosystems. Princeton University Press, Princeton, USA.

Motta, R., 1996. Impact of wild ungulates on forest regeneration and tree composition of mountain forests in the western Italian Alps. For. Ecol. Manage. 88, 93–98.

Motta, R., Haudemand, J.C., 2000. Protective forests and silvicultural stability. An example of planning in the Aosta valley. Mountain Res. Dev. 20, 74–81.

Müller, F., Hoffmann-Kroll, R., Wiggering, H., 2000. Indicating ecosystem integrity—theoretical concepts and environmental requirements. Ecol. Model. 130, 13–23.

van Noord, H., 1996. The role of geomorphological information in ecological forest site typology in mountainous areas, a methodological study in the E-Rätikon and NW-Montafon mountains (Vorarlberg, Austria). PhD Thesis. University of Amsterdam, Amsterdam, p. 185.

Noss, R.F., 1990. Can we maintain biological and ecological integrity? Conserv. Biol. 4, 241–243.

O’Neill, R.V., DeAngelis, D.L., Waide, J.B., Allen, T.F.H., 1986. A Hierarchical Concept of Ecosystems. Princeton University Press, Princeton, New Jersey.

Ott, E., 1978. Zur Notwendigkeit der Pflege von Gebirgswäldern. Schweizerische Zeitschrift für Forstwesen 129 (2), 101–116.

Ott, E., Schönbächler, D., 1986. Die Stabilitsbeurteilung im Gebirgswald als Voraussetzung für die Schutzwald-Überwachung und—Pflege. Schweizerische Zeitschrift für Forstwesen 137 (9), 725–738.

Ott, E., Frehner, M., Frey, H., Lüscher, P., 1997. Gebirgsnadelwälder: Ein Praxisorientierter Leitfaden für eine Standortgerechte Waldbehandlung. Paul Haupt Verlag, Bern.

Ottitsch, A., Weiss, G., 2000. European mountain forest policies—a comparative analysis. In: Price, M.F., Butt, N. (Eds.), Forests in Sustainable Mountain Development: A State of Knowledge Report for 2000. IUFRO Research Series 5. CABI Publishing, Wallingford, UK, pp. 415–421.

Otto, H.J., 1994. Waldökologie. Verlag Eugen Ulmer, Stuttgart, p. 391.

Peterson, D.L., Prichard, S.J., McKenzie, D., 2000. Disturbance in mountain forests. In: Price, M.F., Butt, N. (Eds.), Forests in Sustainable Mountain Development: A State of Knowledge Report for 2000. Task Force on Forests in Sustainable Mountain Development. CABI Publishing, pp. 51–58.

Pimm, S.L., 1984. The complexity and stability of ecosystems. Nature 307, 321–326.

Pirot, J.-Y., Meynell, P.J., Elder, D., 2000. Ecosystem management: lessons from around the world. A guide for Development and Conservation Practitioners. IUCN, Gland, Switzerland and Cambridge, UK, p. 129.

Renaud, J.P., Rupe, C., Leclerc, D., 1994. Analyse des structures et diagnostic sylvicole dans une forêt à fonction de protection, Modes de gestion et stabilité. Revue Forestière Française 46 (6), 655–669.

Rey, F., Chauvin, C., 2001. Forest restoration in marly southern French Alps. In: Proceedings of the International Conference on ‘‘Forest Research: A Challenge for an Integrated European Approach’’. Thessaloniki, Greece, 27 August–1 September 2001, vol. I, pp. 365–369.

Rowe, J.S., Barnes, B.V., 1994. Geo-ecosystems and bio-ecosystems. Bull. Ecol. Soc. Am. 75, 40–41.

Schlaepfer, R., Iorgulescu, I., Glenz, C., 2002. Management of forested landscapes in mountain areas: an ecosystem-based approach. For. Policy Econ. 4 (2), 89–99.

Schönenberger, W., 2000. Silvicultural problems in subalpine forests in the Alps. In: Price, M.F., Butt, N (Eds.), Forests in Sustainable Mountain Development: A State of Knowledge Report for 2000. Task Force on Forests in Sustainable Mountain Development. CABI Publishing, pp. 197–203.

Schönenberger, W., 2001a. Trends in mountain forest management in Switzerland. Schweizerische Zeitschrift für Forstwesen 152 (4), 152–156.

Schönenberger, W., 2001b. Cluster afforestation for creating diverse mountain structures – a review. For. Ecol. Manage. 145, 121–128.

Stand Montafon, 1990. Forest Inventory Results, Internal Report. Stand Montafon Forstfonds, Schruns, Austria.

Tilman, D., Downing, J.A., 1994. Biodiversity and stability in grasslands. Nature 367, 363–365.

Tilman, D., Knops, J., Wedin, D., Reich, P., Ritchie, M., Sieman, E., 1997. The influence of functional diversity and composition on ecosystem processes. Science 277, 1300–1302.

Troll, C., 1971. Landscape ecology (geoecology) and biogeocenology—a terminology study. Geoforum 8, 43–46.

UN-ECE/FAO, 2000. Forest Resources of Europe, CIS, North America, Australia, Japan and New Zealand (industrialised temperate/boreal countries). UN-ECE/FAO Contribution to the Global Forest Resources Assessment 2000. Geneva Timber and Forest Study Papers, vol. 17. United Nations, New York and Geneva.

Wasser, B., Frehner, M., 1996. Minimale Pflegesmassnahmen für Wälder mit Schutzfunktion. Wegleitung, Bundesamt für Umwelt, Wald und Landscahft (BUWAL), Bern, p. 122.

Weiss, G., 2000. Perception of risks in mountain forests. In: Price, M.F., Butt, N. (Eds.), Forests in Sustainable Mountain Development: A State of Knowledge Report for 2000. IUFRO Research Series 5. CABI Publishing, Wallingford, UK, pp. 359–366.

Westra, L., 1996. Environmental integrity, racism and health. Sci. Total Environ. 184, 57–66.

White, P.S., Pickett, S.T.A., 1985. Natural disturbance and patch dynamics: an introduction. In: Picket, S.T.A., White, P.S. (Eds.), The Ecology of Natural Disturbance and Patch Dynamics. Academic Press, New York, pp. 3–13.

Woodley, S., Kay, J.J., Francis, G., 1993. Ecological Integrity and the Management of Ecosystems. St. Lucine Press, p. 212.

Yaffee, S.L., 1998. Three faces of ecosystem management. Conserv. Biol. 13 (4), 713–725.

Modelling long-term effects of forest dynamics on the protective effect against rockfall

André Wehrli[1,3], Luuk K.A. Dorren[2], Frédéric Berger[2], Andreas Zingg[1], Walter Schönenberger[1] and Peter Brang[1]

[1] WSL Swiss Federal Institute for Forest, Snow and Landscape Research, Zürcherstrasse 111, CH-8903 Birmensdorf, Switzerland.
andreas.zingg@wsl.ch, walter.schoenenberger@wsl.ch, brang@wsl.ch

[2] Cemagref Grenoble, 2 rue de la Papeterie, F-38402 Saint Martin d'Hères Cedex, France.
luuk.dorren@cemagref.fr, frederic.berger@cemagref.fr

[3] Current address: Federal Office for the Environment, Protective Forests and Natural Hazards, CH-3003 Berne, Switzerland. andre.wehrli@bafu.admin.ch

Abstract
Forest dynamics have long-term impacts on the effectiveness of mountain forests in providing protection against natural hazards, but these are difficult to study because of the long time periods involved. We addressed this difficulty using simulation models, combining the forest patch model ForClim with the rockfall model RockFor^{NET}, and applying the combined simulation tool to a case study. Based on empirical data, we simulated the development of three mountain forests assuming different developmental scenarios over a period of 60 years. The protective effect of the simulated stands was then assessed using a site in the Swiss Alps where data on the terrain and rock characteristics were available. This enabled us to determine the factors that are important for maintaining the long-term protective effect of a mountain forest.

The long-term protective effect of the stands against rockfall was generally high for small rocks, but limited for larger rocks (diameter >0.8 m), indicating that there is a limit to the protective potential of stands on the slope. Key factors for effective protection over the 60 years were a high initial stand density and a relatively low mortality rate. A high density of tree regeneration in the initial stand was also found to increase the long-term protective effect against small rocks, but not against larger rocks.

The modelling approach used could be improved by extending the forest dynamics model beyond 60 years and by including a more detailed representation of tree diameter distributions in the rockfall model.

Keywords: mountain forest, protection forest, stand structure, mortality, ForClim, RockFor^{NET}

1 Introduction

Many mountain forests effectively protect people and their assets against natural hazards such as rockfall, snow avalanches, landslides, debris flow, soil erosion and floods (Brang *et al.* 2001). The protective effect is mainly provided by the presence of mature trees. However, forest dynamics are constantly evolving, affecting not only stand density but also tree size and distribution. Therefore, the protective effect of a stand varies over time.

In the case of single rockfall events (<5 m^3; Berger *et al.* 2002), the focus of this study, stands with high stem density and large-diameter trees are the most effective in providing protection (Omura and Marumo 1988; Cattiau *et al.* 1995). Such stands, however, are usually susceptible to storm damage (Rottmann 1985) and snow break (Rottmann 1986; Oliver and Larsen 1990). Moreover, they cannot maintain effective long-term protection as they generally have insufficient regeneration. Sufficient regeneration is crucial as it

ensures continuous forest cover, which in turn provides the long-term protective effects. Slow tree growth in mountain forests makes a lack of renewal particularly severe (OTT *et al.* 1997), since this lack will impair the protective effect only after decades. Consequently, the loss of protection may only be recognized when it is too late to take effective ameliorative actions. However, until now, the influence of different levels of tree regeneration on the future protective effect of mountain forests has not been studied.

The protection forest system is difficult to study, let alone to manage, because the constructive forces (e.g. tree regeneration) are very slow, and the destructive forces (e.g. windstorms) are sometimes sudden and violent. This makes it difficult to quantify the influence of forest dynamics on the long-term protective function of a stand. The same is true for the impact of many of the silvicultural measures used to influence natural forest dynamics (SCHÖNENBERGER and BRANG 2004; BRANG and SCHÖNENBERGER this issue). This, in turn, makes the successful management of protection forests difficult (BRANG *et al.* 2004). Simulation models can be very valubale tools to overcome these difficulties. They enable the investigation of the long-term dynamics of the protection forest system and to gain knowledge for optimizing the management of protection forests (DORREN *et al.* 2004). In relation to the problem in hand, simulation models can be used for: 1) projecting forest dynamics (JOHNSON *et al.* 2001), and 2) for assessing the level of protection provided by different stand structures (PENG 2000).

The main idea behind this study was to combine two existing models into a simulation tool that could be used to investigate the impact of forest dynamics on the long-term protective effect of mountain forests against single rockfall events. The models had to fulfill several requirements. The forest dynamics model had to accurately project over several decades the development of the key stand characteristics that determine the protective effect of the forest. These key characteristics include tree density, diameter distribution and species composition (DORREN *et al.* 2005). Additionally, the regeneration process had to be included in sufficient detail to reflect the most important features of mountain forest regeneration (e.g. the long regeneration period at high altitudes or constraints such as the impacts of browsing by ungulates).

The rockfall model (or the model of natural hazards in general) had to provide an accurate assessment of the protective effect of a stand. For rockfall, this means that the interaction of falling rocks and trees had to be reproduced with sufficient detail and in a realistic way.

Both processes, forest dynamics and rockfall, have frequently been modelled individually. Forest dynamics, in terms of the structural forest patterns described above, have been successfully reproduced with forest patch models (cf. LINDNER *et al.* 1997; SHUGART 1998; HUTH and DITZER 2000; RISCH *et al.* 2005; WEHRLI *et al.* 2005). The regeneration process, which is usually simulated without great detail (cf. PRICE *et al.* 2001), has recently been improved in the patch model ForClim (WEHRLI *et al.* 2006), and important features of tree regeneration in mountain forests have been included (e.g., individual sapling growth, impact of browsing ungulates). The protective effect that a stand can provide against rockfall can be assessed with sufficient accuracy using recently developed rockfall models, which include the interactions of falling rocks and trees (e.g. DORREN *et al.* 2004; BRAUNER *et al.* 2005; BERGER and DORREN submitted; STOFFEL *et al.* 2006; cf. DORREN 2003 for an overview of rockfall models). Thus, there are several promising models that fulfill the needs of a combined simulation tool.

In this paper, we have combined the forest patch model ForClim (BUGMANN 1994, 1996) with the rockfall model RockFor^{NET} (BERGER and DORREN submitted). We then applied the combined simulation tool to a case study to give an example of its use in investigating a protection forest system. Based on data from three mountain forests in the Swiss Alps, we

first simulated the potential development of the initial stands under several scenarios over a period of 60 years. The protective effect of the simulated stands against rockfall was then assessed by projecting the stands onto a site that had data available for terrain and rock characteristics. Finally, the factors that are important for the long-term protective effects of a stand were identified.

2 Methods

2.1 Description of the simulation models and model combination

The forest patch model ForClim

ForClim was originally developed to assess the impacts of climatic change on the tree species composition and biomass of forests in the Swiss Alps (BUGMANN 1994, 1996). Even though ForClim was not originally designed to simulate structural forest patterns, such as diameter distributions, it has been shown to accurately reproduce such patterns in simulations over several decades (RISCH *et al.* 2005; WEHRLI *et al.* 2005). A detailed description of ForClim can be found in BUGMANN (1996). The model version used in this study, ForClim V2.9.4, is documented in detail in WEHRLI *et al.* (2006).

The rockfall model RockFor^{NET}

RockFor^{NET} was recently developed by BERGER and DORREN (submitted) to provide a tool for assessing the probable residual hazard beneath a protection forest. The residual hazard is thereby a measure of the protective effect of a stand. It is defined as the percentage of rocks passing down a forested slope (i.e. the percentage that cannot be stopped by the forest stand).

RockFor^{NET} is based on the results of more than 100 real-size rockfall experiments and has been validated at several sites (DORREN and BERGER 2006; BERGER and DORREN submitted). It enables realistic assessments of the protective effects of different stand structures. Consequently, it has been frequently applied in the assessment of the residual hazard for different sites in the European Alps.

To assess the residual hazard, RockFor^{NET} calculates the energy balance of a falling rock on a forested slope (i.e., it calculates the energy a falling rock can develop on a given slope, and compares this to the energy that can be dissipated by the stand on the slope). The model requires only a few input parameters which characterize the stand (species composition, stand density, a representative diameter at breast height (DBH), i.e. a measure of location that is representative of the DBH distribution), the terrain (cliff height, slope length between the foot of the cliff and the foot of the forested slope, slope length of the forested slope, and mean slope gradient) and the rocks (mean rock diameter and rock density).

The terrain and rock parameters are used to determine the energy developed by a falling rock. The calculation is based on the energy line angle – the angle of the straight line between the starting point and the maximum stopping point (HEIM 1932; TOPPE 1987; GERBER 1994).

The forest stands are considered as spatially-distributed "rockfall curtains" – i.e. the stand input parameters are used to generate virtual rows of trees standing next to each other (BERGER and DORREN submitted). The trees in a row have the same diameter, equal to the given representative DBH. This diameter, in combination with the tree species, determines the effectiveness of a tree row in dissipating energy during a rockfall impact.

To calculate the probable residual hazard, the model determines the number of tree rows required for full protection on the foot of the slope (i.e., 100 % of the rocks are stopped). Finally, RockFor^{NET} compares the required number of trees with the existing number of trees in the stand and translates the difference between the two into a probable residual hazard, ranging from 0 to 100 %.

Model combination

For the present study, the two models were not physically combined, but joined together by file exchange. Thus, the stand input data needed for the RockFor^{NET} model was derived from the projected stand structures simulated by ForClim.

2.2 Model input data and modelling scenarios

Stand and regeneration data

We modelled several scenarios based on empirical stand and regeneration data from three mountain forests in the Swiss Alps. The forests are dominated by Norway spruce (*Picea abies* [L.] Karst.) and silver fir (*Abies alba* Mill.) and situated between 700 and 1000 m above sea level. Figure 1 and Table 1 give an overview of the current regeneration and stand structure of the three forests.

The first stand is fairly even-aged (EA), and is referred to as the EA-stand. It consists of 561 trees ha^{-1} >4 cm DBH, and only minor timber harvesting has taken place during in recent decades. Tree regeneration (from 1 cm height and up to 3.9 cm DBH) is rather scarce, with approximately 2230 saplings ha^{-1} (Table 1). The second stand is currently being converted

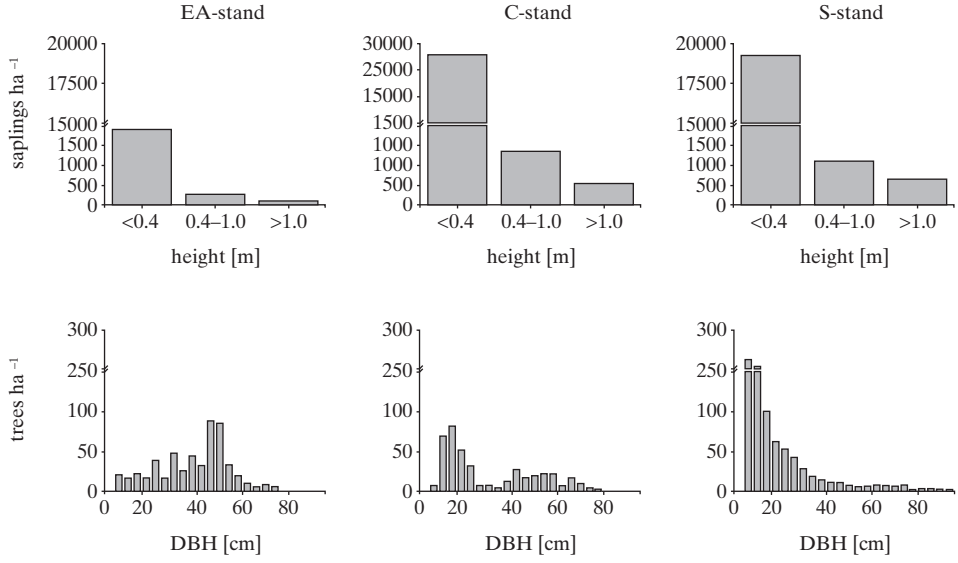


Fig. 1. Size distributions of tree regeneration (above) and DBH (below) for the three initial stands.

Table 1. Stand and regeneration characteristics of the three initial stands used in the simulation of forest dynamics.

Stand	**Stand characteristics** (main tree species, stand basal area (BA), median DBH and tree density at beginning of simulation [trees > 4 cm DBH])	**Regeneration characteristics** (main tree species, and sapling density up to 4 cm DBH at beginning of simulation)
EA-stand (even-aged stand)	Norway spruce (83 %), Silver fir (13 %) BA = 73.8 m^2 ha^{-1}, DBH_{med} = 42.3 cm, 561 trees ha^{-1}	Norway spruce (20 %), Silver fir (44 %) 2230 saplings ha^{-1}
C-stand (stand under conversion)	Norway spruce (32 %), Silver fir (62 %) BA = 44.5 m^2 ha^{-1}, DBH_{med} = 36.6 cm, 430 trees ha^{-1}	Norway spruce (42 %), Silver fir (57 %) 31 090 saplings ha^{-1}
S-stand (selection stand)	Norway spruce (43 %), Silver fir (52 %) BA = 35.1 m^2 ha^{-1}, DBH_{med} = 26.4 cm, 901 trees ha^{-1}	Norway spruce (49 %), Silver fir (51 %) 22 170 saplings ha^{-1}

into a selection forest (plentering according to SCHÜTZ 2001). It is referred to as the C-stand (stand under conversion). The stand consists of 430 trees ha^{-1} >4 cm DBH, and there is ample tree regeneration, with more than 30 000 saplings ha^{-1} (Tab. 1). The third stand has been managed as an uneven-aged selection forest for several decades. It is referred to as the S-stand. The stand consists of 901 trees ha^{-1} >4 cm DBH, and there is abundant tree regeneration, with more than 20 000 saplings ha^{-1} (Table 1).

Scenarios for the simulation of forest dynamics

The forest dynamics scenarios were based on: i) different initial stand and regeneration structures (variation of input data), and on ii) different model parameters (variation of growth constraints). An overview of the different scenarios for the simulation of the forest dynamics is given in Table 2.

We used the three initial stand and regeneration structures described above as input data. Additional scenarios for tree regeneration were included by varying sapling density and species composition in the regeneration input data. Three levels of sapling density were used, low, intermediate and high (Table 3), and species composition was varied to include the initial composition, 100 % Norway spruce regeneration, and 100 % silver fir regeneration.

The range of input data established alternative growth constraints, as stand structure strongly affects stand dynamics. Additional growth constraints were included by variation of two model parameters – browsing impact on saplings and the mortality rate of trees. Browsing impact was varied in terms of browsing intensity, which led to a species-specific reduction in sapling growth (Table 4; for details see WEHRLI *et al.* 2006). Tree mortality was varied between a standard mortality rate and an increased mortality rate. The standard mortality rate is the standard value of age-related tree mortality in patch models, which implies that 1 % of all established saplings survive to their species-specific maximum age (SHUGART 1984; BUGMANN 1994). In contrast, the increased mortality rate enables the depiction of

processes that are not explicitly modelled, such as a coarse reproduction of a thinning regime or increased tree mortality due to injuries from falling rocks. The mortality rate was thereby increased to reflect the assumption that only 0.1 % of the established saplings reach their maximum age. The same increased mortality rate was used in the study by RISCH *et al.* (2005).

Table 2. Scenarios for the simulation of forest dynamics for each initial stand.

	Species composition of tree regeneration		
	Initial composition	100 % Norway spruce	100 % silver fir
Levels of sapling density	3	3	3
Levels of browsing impact	5	2	2
Levels of mortality rate	2	2	2
Total scenarios per initial stand	*30*	*12*	*12*

Table 3. Variation of tree regeneration. Bold figures denote the initial level of tree regeneration. Regeneration levels were varied by factors of 5 (medium) and 10 (high) for the EA-stand, and by factors of 0.5 (medium) and 0.1 (low) for the C- and the S-stand, respectively.

Regeneration level	EA-stand	C-stand	S-stand
Low	**2230**	3109	2217
Medium	11150	15545	11085
High	22300	**31090**	**22170**

Table 4. Variation of browsing impact on the main tree species. Browsing impact is determined by multiplying the species-specific browsing susceptibility included in ForClim (Norway spruce = 0.25, silver fir = 0.75) by browsing intensity. Together with canopy shading, browsing impact then determines the species-specific reduction of sapling growth (reduction factor for sapling growth within a range of 0–1, whereby 0 denotes optimum height growth and 1 denotes no more height growth; for details see WEHRLI *et al.* 2006).

	Browsing intensity				
Species	0	0.67	1	1.33	2
silver fir	0	0.5	0.75	1	1
Norway spruce	0	0.166	0.25	0.333	0.5

Terrain and rock characteristics

The terrain and rock input data needed for RockFor^{NET} (Table 5) were derived from empirical terrain and rock characteristics from the site with the EA-stand. This site, called Stotzigwald, is a steep forested slope in the Swiss Alps (46°45' N and 08°39' E) with a mean slope gradient of more than 40° and multiple interspersed cliffs (THALI 1997). The forest provides protection for one of the most important highways connecting northern and southern Europe.

Scenarios for the assessment of the protective effect

The protective effect of the simulated stand structures was assessed for six different rock size classes (S1–S6), ranging from a rock diameter of 0.2 m (S1) up to 1.2 m (S6; Table 5). For each rock size class, the residual hazard of each simulated stand structure was calculated.

Table 5. Terrain and rock characteristics for the assessment of the protective effect derived from Stotzigwald site.

	Site Stotzigwald
Cliff height	40 m
Slope length between cliff and forested slope	0 m
Slope length of the forested slope	325 m
Mean slope gradient	45°
Mean rock diameters	0.2, 0.4, 0.6, 0.8, 1.0, 1.2 m
Rock density	2700 kg / m^2

2.3 Simulation set-up

Simulation of forest dynamics

Starting from one of the three initial stands, each forest scenario was simulated for a period of 60 years, which is currently considered to be the limit of accurate predictions of structural forest patterns with the ForClim model (cf. WEHRLI *et al.* 2005). Only the current tree regeneration data were used in the simulations, and additional seedling regeneration during the simulation period was excluded since data for reliable parameterizations and corroborations were not available. As evident from the study by WEHRLI *et al.* (2006), this simplification did not significantly affect the simulated stand structure after 60 years in terms of the protective effect against rockfall.

For the simulations based on the C- and S-stands, the parameterization of the tree growth module of ForClim was slightly modified because preliminary simulation runs with the standard parameterizations over-estimated tree growth compared to empirical growth data from long-term data series from these stands (Table 6). This overestimation is probably due to the parameterization of the dynamic crown structure implemented in ForClim V2.9.4, which is mainly based on data from stands that tend to be even-aged (cf. WEHRLI *et al.* 2006). We therefore introduced a correction factor in terms of a multiplier for the leaf area index for the C-stand (a correction factor of 1.2) and the S-stand (a correction factor of 1.3), which led to more realistic growth rates (Table 6).

The initialization of ForClim with stand and regeneration data was performed at the scale of individual patches, whereby the patch size was set to 225 m^2 (15 m × 15 m) for the present study. To reduce the stochastic "noise" in the simulation results, the simulation experiments were performed with numerous repetitions (n = 237–320 patches, depending on the area covered by the initial stand; cf. BUGMANN 1996; PRETZSCH and DURSKY 2001).

The input for the weather generator included in ForClim was derived from time series of monthly precipitation sums and monthly mean temperatures from the weather station at Gurtnellen (739 m a.s.l.), approximately 2.5 km from the site with the EA-stand (Stotzigwald).

Table 6. Growth rates simulated with ForClim with and without CF for the C- and S-stand, and comparison with empirical data from long-term data series for both stands. CF denotes the correction factor included in ForClim to modify the leaf area index (see text). Growth rates are measured in terms of increment of basal area ha^{-1} over 60 years. na: not available.

	empirical growth	No CF	CF 1.2	CF 1.3	CF 1.4
C-stand	42.0	50.1	42.5	na	na
S-stand	47.7	64.6	50.9	47.0	42.0

Assessment of the protective effect

For the assessment of the protective effect of the simulated stands, we only considered trees with a DBH >8 cm because the role of smaller trees in rockfall protection is unknown. Species composition and stand density were derived from the output file of ForClim and included in RockFor^{NET}. The measure of location for the DBH needed as input for RockFor^{NET} was set to the median, since most of the simulated DBH distributions were rather asymmetric. For such distributions, the median is more representative than other measures of locations (SOKAL and ROHLF 1995), and the median was therefore considered to deliver more accurate results. This assumption was confirmed by preliminary tests with other measures of location such as the mean quadratic DBH. The latter yielded poor results, with most of the scenarios for S1–S4 having no residual hazard at all. This, however, seems very unlikely on the Stotzigwald site.

2.4 Analysis of simulation results

Assessment of the residual hazard under different simulation scenarios

The protective effect provided by the different scenarios was compared graphically for all stands together and for each initial stand using boxplots (SOKAL and ROHLF 1995; SPSS Inc. 2001). The range of the residual hazards over all scenarios and the mean residual hazard over all scenarios were calculated for each rock size class. The parametric (Pearson correlation, cf. STAHEL 2000) and non-parametric (Spearman correlation, cf. STAHEL 2000) correlations between the simulated stand structures and the residual hazards were determined.

Derivation of indicators for a high long-term protective effect

We used logistic regression models to identify the most important determinants of a long-term protective effect for each rock size class. The different levels of residual hazards for each rock size class were divided into two classes, representing a high and a low protective effect, respectively, to provide the necessary binary target variable. The threshold for the allocation into these classes was fixed for each rock size class, based on qualitative observations of the frequency of rockfall events for each size class at the Stotzigwald site (Table 7). Since these events are rather frequent for smaller rocks, the thresholds for those rock size classes were set to low levels. In contrast, the threshold for S3–S6 rock classes was set to considerably higher values, to account for the lower frequency of these events.

Continuous variables (SOKAL and ROHLF 1995, p.11) were first transformed following the Tukey first aid transformations (cf. STAHEL 2000) and then included in the logistic model, whereas the categorical variables (browsing impact and mortality rate) were included as categorical co-variables based on the indicator contrast method (SPSS Inc. 2001). The most important variables for each rock size class were then determined with a backward

selection method based on Wald-values (SPSS Inc. 2001; SOKAL and ROHLF 1995). The model assumptions were verified by examining the residuals (STAHEL 2000).

In addition to the logistic models, the boxplots were examined visually and the parametric and non-parametric correlations between all variables were determined.

Table 7. Limits for the binary target variable for the logistic regression models. Stands that delivered a residual hazard up to the limit values are considered to have a high protective effect, the others are allocated to the class with a low protective effect.

	Rock size class					
	S1 (d = 0.2 m)	S2 (d = 0.4 m)	S3 (d = 0.6 m)	S4 (d = 0.8 m)	S5 (d = 1.0 m)	S6 (d = 1.2 m)
Limit	0.1 %	10 %	30 %	50 %	50 %	50 %

3 Results

3.1 Residual hazards of different stands

Residual hazard of the initial stands

The initial stands differed markedly in their protective ability against the six rock size classes (Table 8). Whereas the EA-stand, which corresponds to the current stand at the Stotzigwald site, yielded an acceptable residual hazard for all rock size classes, the performance of the C- and in particular of the S-stand were very limited for rocks with a diameter >0.2 m. From size class S4 on, the residual hazard for these two stands was >90 % – indicating that their protective effect was only marginal.

Table 8. Range of residual hazards and mean residual hazard per rock size class for all simulated stands as well as mean residual hazard and initial residual hazard per initial stand. RH: Residual hazard in %.

	All sites		EA-stand		C-stand		S-stand	
Rock size class	mean RH	range of RH	initial RH	mean RH	initial RH	mean RH	initial RH	mean RH
S1 (d = 0.2 m)	1	0–24	0	1	4	1	2	0
S2 (d = 0.4 m)	24	0–76	0	24	17	37	51	10
S3 (d = 0.6 m)	61	0–97	0	54	60	82	90	47
S4 (d = 0.8 m)	78	0–99	6	67	91	95	98	74
S5 (d = 1.0 m)	89	2–100	36	76	97	98	99	91
S6 (d = 1.2 m)	93	31–100	51	84	99	99	100	97

Residual hazards of simulated stands after 60 years

The residual hazard of the simulated stands after 60 years was low for rocks with a diameter of 0.2 m (rock size class S1, cf. Fig. 2). In most of the scenarios, the residual hazard was close to zero, but a few scenarios produced residual hazards of up to 24 % (i.e., 24 % of the rocks passed through the simulated stand) (Table 8). With increasing rock diameter, the mean residual hazard over all scenarios rapidly increased from 24 % (S2) to 61% (S3) and 78 % (S4), respectively (Table 8, Fig. 2). For the largest rock size classes (S5 and S6), the protective effect was even smaller (Table 8). Still, the range of the residual hazards for these classes

indicated that under a few scenarios, the simulated stands were able to yield a residual hazard <50 % (Fig. 2). Those scenarios only occurred in the EA-stand, and generally involved the standard mortality rate and a relatively low regeneration density.

The residual hazard under different scenarios depended strongly on the initial stand (Fig. 3). Simulations based on the EA- and S-stands generally resulted in a higher protective effect than those based on the C-stand, as shown by the mean residual hazards for each initial stand (Table 8). The latter only provided a low residual hazard for rock size class S1 (d = 0.2 m), and a rather low residual hazard for rock size class S2 (d = 0.4 m, mean residual hazard: 37 %, cf. Fig. 3 and Table 8).

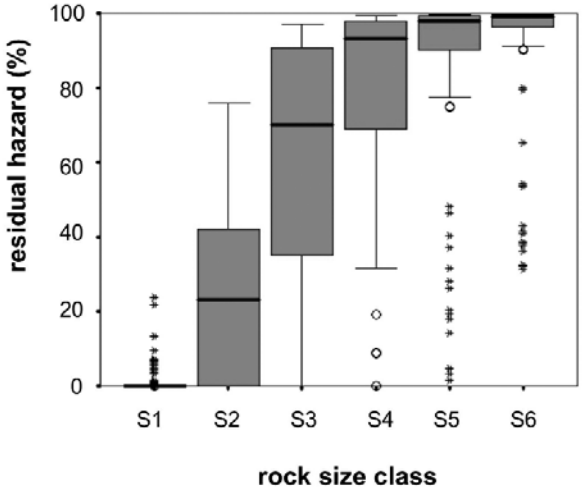


Fig. 2. Residual hazards over all scenarios for each rock size class. Circles denote outliers (1.5–3 box lengths from the end of the box), asterisks mark extremes (> 3 box lengths from the end of the box).

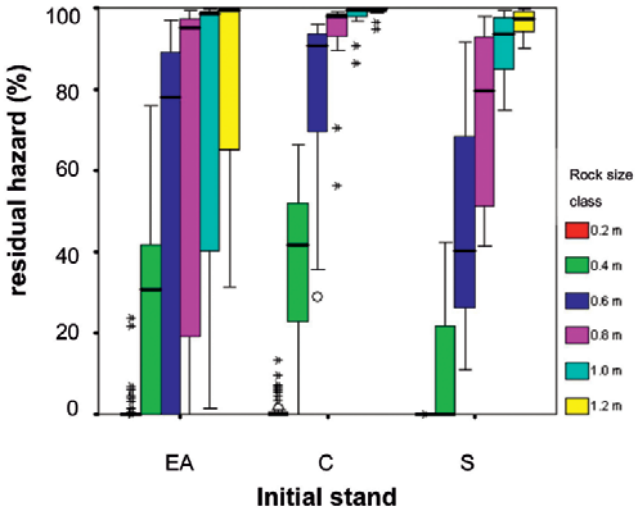


Fig. 3. Residual hazards over all scenarios for each rock size class and initial stand. Box plot symbols are explained in the legend to Figure 2.

Development of the residual hazards during the simulation period

The EA-stand, which initially provided a relatively high protective effect (Table 8), showed an increase in the residual hazard under several simulation scenarios. For the smallest rock size class, S1, 13 scenarios yielded an increase in the residual hazard when compared to the initial stand. For rock size classes S2 to S6, the residual hazards increased in 32 (S2) to 44 (S4–S6) of the 54 scenarios. Most of the scenarios leading to an increased residual hazard included an increased mortality rate.

In the scenarios based on the C-stand, which initially showed rather high residual hazards (Table 8), the residual hazard increased in comparison to the EA-stand. For S2 to S6, almost all scenarios led to an increased residual hazard compared to the initial stand. For S1, however, the residual hazard only increased under seven scenarios that had increased mortality rates.

In contrast to the C-stand, the residual hazards decreased in the S-stand, which showed relatively high residual hazards at the beginning (Table 8).

3.2 Key factors for the assessment of the residual hazard with RockFor^{NET}

The simulated stand density, and for larger rocks particularly the simulated median DBH, showed the highest correlations with the residual hazard for each rock size class, and can thus be seen as key factors for assessing the residual hazard with RockFor^{NET} (Table 9). The two key factors were negatively correlated (parametric: –0.66, non-parametric: –0.52, $p < 0.01$).

The simulated median DBH and the residual hazard were negatively correlated for all rock size classes, with very high correlations for S3 to S6 (Table 9). In contrast, the simulated stand density (stem number) and the residual hazard were only negatively correlated for rock size class S1. For all larger rocks, the correlations were found to be: i) positive, and ii) at a lower level than the correlations between the simulated median DBH and the residual hazard.

Table 9. Important correlations between simulated stand structure and residual hazard. Values denote parametric (Pearson) and non-parametric correlations (Spearman, in brackets). Negative signs indicate a negative correlation. All correlations are significant at the 0.01 level (2-tailed).

	All sites	
Rock size class	simulated median DBH	simulated density
S1 (d = 0.2 m)	–0.20 (–0.37)	–0.24 (–0.3)
S2 (d = 0.4 m)	–0.69 (–0.95)	0.46 (0.45)
S3 (d = 0.6 m)	–0.88 (–0.98)	0.62 (0.55)
S4 (d = 0.8 m)	–0.96 (–0.98)	0.61 (0.55)
S5 (d = 1.0 m)	–0.96 (–0.98)	0.56 (0.55)
S6 (d = 1.2 m)	–0.93 (–0.98)	0.52 (0.55)

3.3 Important factors for a long-term protective effect

The most important factors associated with a high long-term protective effect were determined for the rock size classes S1 to S4 using logistic regression models for each rock size class. Rock size classes S5 and S6 were excluded from these analyses because the protective effect was generally low for large rocks. An overview of the four logistic regression models is presented in Table 10. Variables with a negative B-value denote factors that helped to reduce the residual hazard, and thus to increase the protective effect.

For the rock size class S1 (d = 0.2 m), a low residual hazard was associated with high initial stand density, high regeneration density and a low mortality rate (Table 10). These findings were confirmed by boxplots for the three factors over all simulation scenarios (Fig. 4), although this is barely visible given the overall low residual hazard for S1.

For the rock size classes S2 to S4, ranging from 0.4 to 0.8 m in diameter, the same factors had a significant influence. A low residual hazard was associated with high initial stand density and a low mortality rate as for the smallest rocks, but with a low regeneration density (Table 10). Moreover, for rock size class S3, a high initial median DBH was associated with a low residual hazard (Table 10). Again, these findings were confirmed in the boxplots (Fig. 4).

Table 10. Logistic regression models for the rock size classes S1 to S4. Negative signs indicate variable that lead to a reduced residual hazard.
All variables significant at the $p < 0.01$ level. n = 162 scenarios (54 per initial stand)

		Multiple logistic regression model		
Rock size class	Parameter	limit	B-value	Wald
S1 (d = 0.2 m)	Regeneration density 2005	0.1 %	–0.023	16.3
	Initial stand density 2005		–0.821	25.4
	Standard mortality rate		–1.605	10.0
	Constant		20.034	26.3
S2 (d = 0.4 m)	Regeneration density 2005	10 %	0.022	15.0
	Initial stand density 2005		–0.824	30.7
	Standard mortality rate		–2.644	25.3
	Constant		18.751	28.9
S3 (d = 0.6 m)	Regeneration density 2005	30 %	0.029	17.9
	Initial stand density 2005		–1.114	10.6
	Initial median DBH 2005		–0.166	7.2
	Standard mortality rate		–2.284	15.6
	Constant		32.030	10.2
S4 (d = 0.8 m)	Regeneration density 2005	50 %	0.028	17.2
	Initial stand density 2005		–0.453	9.5
	Standard mortality rate		–2.076	13.1
	Constant		10.868	9.6

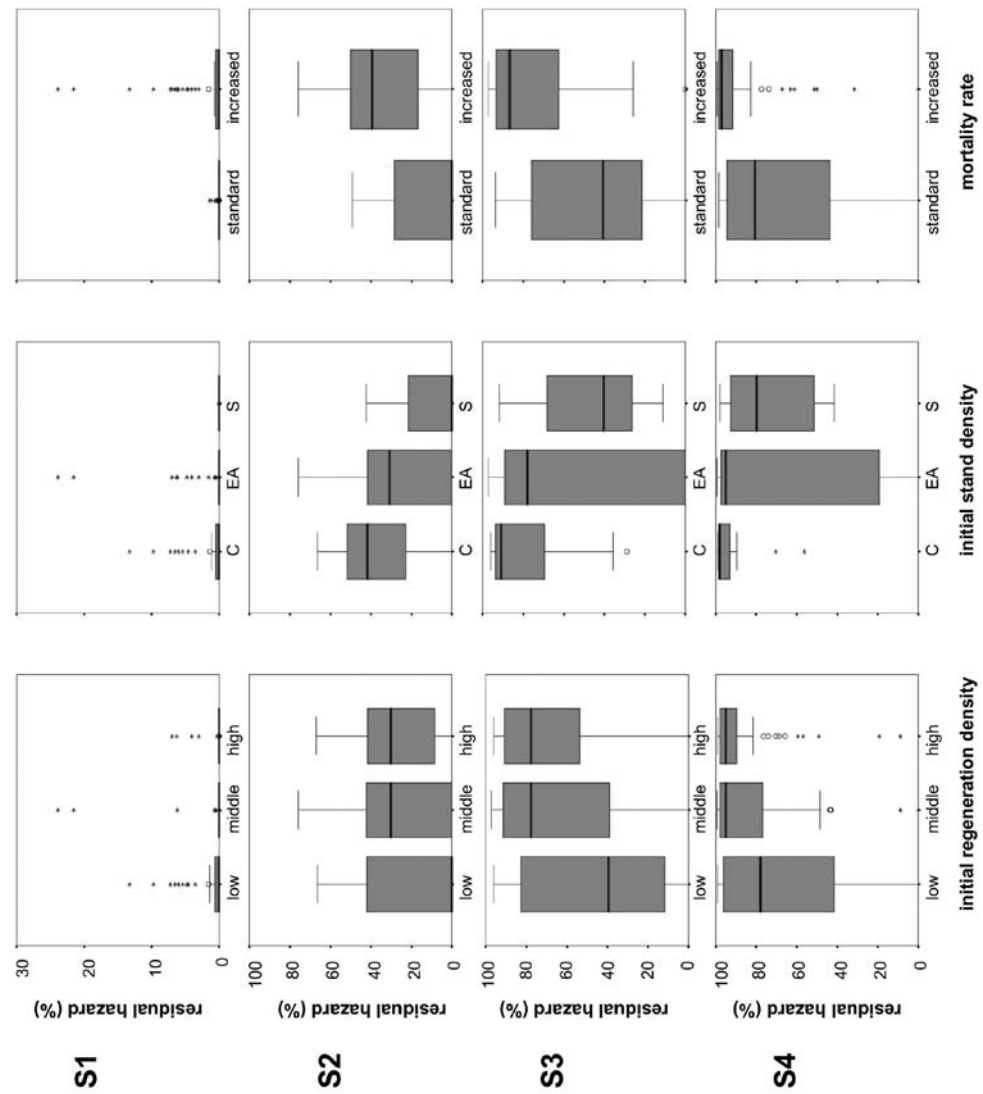


Fig. 4. Relationship between residual hazard and initial regeneration density (first column), initial stand density (second column) and mortality rate (third column) for rock size class S1 (first row), S2 (second row), S3 (third row), and S4 (fourth row). Box plot symbols are explained in the legend to Figure 2.

4 Discussion

4.1 Residual hazards of different stands

The residual hazards under the different simulation scenarios were essentially different for the six rock size classes. For the smallest rocks included in this study (S1 with d = 0.2 m), all initial stands and almost all simulated stands showed low residual hazards; they had a high protective function. Additional assessments of the protective effect against rocks smaller than S1 (d <0.2 m) always yielded a residual hazard of zero. As there is empirical evidence for very small rocks passing through the forests on the very steep slope studied, we believe that a rock diameter of about 0.2 m represents the lower boundary of the applicability of the RockFor^{NET} model. The approach of the RockFor^{NET} model, which only accounts for the forest when calculating the energy balance of a moving rock, is probably too simplistic for smaller rocks. For such rocks, factors neglected in the model (e.g. surface roughness or dampening effects of the surface) are likely to influence the energy balance of falling rocks significantly. In particular, surface roughness (e.g. woody debris, branches, shrubs, or stationary rocks) can slow down or even stop falling rocks (Jahn 1988; Meissl 1998; Dorren 2002; Schönenberger *et al.* 2005). The impact of these additional factors on the energy balance of falling rocks is very difficult to quantify, and these factors are therefore not included in RockFor^{NET}.

For rocks with d >0.8 m, our results indicate the limitations of any forest on the present, relatively short slope (325 m). On this slope, and under the given terrain characteristics, larger rocks can develop energy that cannot be dissipated by most of the simulated stand structures. This finding is in agreement with Rickli *et al.* (2004) who state that the mitigating effect of stands on rockfall is limited by the mass and velocity, and thus energy, of the falling rocks. As a consequence, technical counter-measures against large rocks are needed to reduce the residual hazard for the highway at the Stotzigwald site. Such counter-measures have indeed been installed, including restraining nets that can dissipate up to 500 kJ (Frei 2003).

For all rock size classes, the initial stand conditions had a considerable impact on the long-term protective effect. This was confirmed by the four logistic regression models. The C-stand, which is currently being converted into a selection forest, is the most limited of the three initial stands in terms of long-term protective effects. This stand only shows acceptable low residual hazards for S1- and, partially, for S2-sized rocks (Fig. 3). The reasons for this are probably: i) the low initial tree density, and ii) the initial bimodal DBH distribution, which shows a nadir between 24 to 36 cm DBH (Fig. 1). After 60 years, this initial nadir has moved to larger DBH classes, leading to a lack of such trees. Without large trees in sufficient numbers, the high-energy developed by rocks in size classes S3 to S6 cannot be dissipated sufficiently.

The S-stand which, together with the C-stand, only showed a very limited protective effect in its initial condition (see above), yields a better performance in the long term, as is evident from the development of the residual hazards compared to the initial residual hazard. This is very probably due to a considerable initial tree density with DBH <36 cm in the S-stand (Fig. 1), leading to a higher number of large trees after 60 years compared to the C-stand.

The best protective effect after 60 years, however, is generally still provided by the EA-stand, which initially shows a high number of larger trees (both > and <36 cm DBH). In the beginning, the EA-stand probably provides an almost optimal protective effect for the Stotzigwald site. Over a period of 60 years, however, the protective effect decreases slightly, as indicated by the increase of residual hazards under several simulation scenarios for all

rock size classes (see page 70). Over periods longer than 60 years, the protective effect of the EA-stand is likely to decrease further since the initial DBH distribution shows a rather low density of small trees (Fig. 1). In combination with the rather sparse level of current tree regeneration in the EA-stand (Table 1), this will probably lead to a lack of large trees in the long term, which in turn will induce an increase in the residual hazard (see page 70). Thus, when looking at a time period >60 years, the S-stand with its abundant tree regeneration and its high stand density is likely to perform better than the EA-stand. This is already indicated by the mean residual hazards for the S-stand after 60 years, which for S1 to S4 are either already lower or at least very close to the values for the EA-stand. However, these assumptions cannot reliably be verified with the present simulation tool because the accuracy of the projected stand structures obtained with the present ForClim version declines after several decades (WEHRLI *et al.* 2005). Consequently, accurate simulations with ForClim over periods longer than 60 years were not possible in this study.

4.2 Key factors for the assessment of the residual hazard with RockFor^{NET}

As can be seen from the strong correlations, the assessment of the residual hazard on a given site with RockFor^{NET} highly depends on two key factors – the simulated stand density and the simulated median DBH. The influence of these two factors on the residual hazard is closely related to rock size, and changes with increasing rock size. For small rocks, stand density and DBH reduce the residual hazard, with the influence of both factors appearing similar. This is in agreement with JAHN (1988), who reports a significant influence of both DBH and stand density on the protective effect against small rocks.

For larger rocks, the negative influence of the median DBH increases to very high values, whereas the simulated stand density is positively correlated with the residual hazard (i.e., the more trees, the higher the hazard). We think, however, that this positive correlation is not causal but mainly due to the strong negative correlation between simulated median DBH and simulated stand density (parameteric correlation of –0.66, non-parametric correlation of –0.52). A high simulated stand density is mainly caused by the recruitment of many young trees, which in turn leads to a decrease of the median DBH. This suggests a weakness in the current RockFor^{NET} version: RockFor^{NET} uses one single key indicator to represent the DBH distribution of a stand. This indicator in turn determines the energy that can be dissipated by a tree row. Therefore, the model outcome, and by this the "performance of the stand," is very sensitive to this indicator.

Nevertheless, our simulation results are in agreement with findings from empirical field studies, which report a similar change in importance of the key factors determining the protective effect of a stand against rockfall: from stand density to stem size (DBH) with the progression from small to larger rocks (DORREN *et al.* 2005; KALBERER *et al.* 2005).

4.3 Important factors for a high long-term protective effect

In all of the logistic regression models, initial stand density, regeneration density, and mortality rate had a significant influence on the long-term protective effect for rockfalls. For S3, an additional factor, the initial median DBH, also had a significant influence.

In all models, high initial stand densities as well as a relatively low mortality rate led to a high long-term protective effect. Thus, in contrast to the simulated stand density, which only had a negative influence on the residual hazard for the smallest rock size class, the initial stand density appeared to have a reducing effect on the residual hazard over all rock size

classes. This is not surprising as, after a period of 60 years, the number of surviving large trees is closely related to the initial stand density. The density of large trees however, is a key factor for the assessment of the protective effect of a stand in reality (large trees in the DBH distribution) as well as in RockFor^{NET}.

Low tree mortality is essential to maintain the protective function of a forest, and its influence is even more significant for larger rocks, as indicated by the higher B-values for S2 to S4 compared to S1 (Table 10). A stand can only maintain a high protective effect in the long term if few trees are injured by falling rocks, because such injuries are thought to increase tree mortality (Rickli *et al.* 2004). In addition tree mortality should only be moderately increased by selective cutting, and large clear cuts should certainly be avoided. However, the association of a low mortality rate with a high long-term protective effect, as shown by this study, may be slightly over-estimated. The simplistic combined simulation tool does not take into account any protective effect of dead trees because it simply eliminates such trees. In reality, dead trees (e.g. snags, Kupferschmid Albisetti 2003), and even stumps of trees felled at a height of 1.3 m or higher, can at least temporarily provide a certain protective effect and thereby reduce the residual hazard on a site (Dorren *et al.* 2005; Frehner *et al.* 2005; Schönenberger *et al.* 2005).

In contrast to the initial stand density and standard mortality rate, the influence of the regeneration density was different in the four logistic regression models. While being negative for S1, as expected (higher initial regeneration density leads to a higher stand density and thus, to a lower residual hazard), the influence was found to be positive for the other rock size classes. This positive influence is rather surprising and warrants further explanation.

One reason is the relatively short simulation period (60 years). As previously stated, ForClim currently does not allow accurate simulations over longer periods. However, a period of 60 years is apparently too short for tree saplings, growing under shelter, to become large enough to effectively dissipate energy from large falling rocks. Therefore, we could expect tree regeneration to have no significant influence on the residual hazard for larger rocks until some point beyond 60 years.

Tree regeneration was found to have a positive influence for rock sizes S2 to S4, indicating that the residual hazard increases with increasing initial regeneration density. The reason for this is likely to be the same as for the positive correlation found between simulated stand density and residual hazard. The simulated median DBH shows a significant negative correlation with the initial regeneration density (parametric: –0.39, non-parametric: –0.44, $p < 0.01$), that is, a higher initial density leads to a decrease of the median DBH due to the recruitment of more young trees. A lower median DBH in turn increases the residual hazard estimated by RockFor^{NET}. Thus, the positive influence found in the logistic regression model is probably an artefact. The median of the DBH distribution, which in this study denotes the representative DBH needed in RockFor^{NET}, is relatively sensitive to the recruitment of many young trees. The use of alternative measures of location is unlikely to improve the model performance since it would not allow a better representation of skewed DBH distributions.

Consequently, we propose that initial stand density and a relatively low mortality rate are two key factors for a high protective effect for a given rock size over a period of 60 years. In contrast to this, other variables such as browsing impact or species composition of tree regeneration did not seem to significantly influence the protective effect over the relatively short simulation period. For longer simulation periods, however, these variables, as well as the regeneration density of the initial stand, could become more important.

4.4 Modelling approach

The combined simulation tool as well as the underlying simulation models include a number of simplifications that need further investigation and could be improved in future studies.

The forest dynamics model should be improved to enable more accurate predictions of stand structures for periods exceeding 60 years. Additional data for the parameterization of the recruitment module would be necessary in order to use this module for a continuous supply of tree regeneration over the whole simulation period. Moreover, the representation of the light regime and of tree mortality would probably benefit from further investigation and improvements.

The rockfall model requires a refinement of its underlying principle – the virtual representation of stands as distributed "rockfall curtains". The representation of the DBH distribution in the model as well as the relationship between the energy which can be dissipated by the real stand and by virtual tree curtains, should be included with more detail. By doing so, RockFor^{NET} will become a more useful tool for forest managers, given that it currently performs accurate reproductions of important features of rockfall processes, and of the interaction with protection forests for certain stand structures.

Finally, the improved models for forest dynamics and rockfall could be combined physically in a single simulation tool that could be applied by forest managers. The effects of falling rocks on trees, such as injuries leading to higher mortality rates or stem breakage, could be included in the tool, as suggested by DORREN (2002).

5 Conclusions

A combination of models of forest dynamics and rockfall has been demonstrated to be useful for investigating the effect of forest dynamics on the long-term protective effect of mountain forests against rockfall. However, mountain forest dynamics are known to be slow. Our study suggests that a time period of 60 years is too short for investigating long-term effects of forest dynamics on the protective effect against rockfall.

Over a period of 60 years, initial stand density and a relatively low mortality rate are particularly important for creating effective protection. Silvicultural measures, such as selective cutting or regeneration cuts, in protection forests should therefore be moderate. To reduce the residual hazard in stands with a low tree density such as the stand undergoing conversion to an uneven-aged structure (c-stand), alternative measures might be necessary (e.g. cut trees left on the slope, diagonally to the slope direction, cf. DORREN *et al.* 2005; FREHNER *et al.* 2005).

The approach presented in this study requires further investigation and improvement. Once improved, a combined simulation tool is likely to enable the determination of the factors that are relevant to the maintenance of protective functions over 100 years or longer. Target values for these factors could eventually be delivered, which in turn could be used for the more effective and efficient management of protection forests.

Acknowledgements
This study was carried out within the framework of the National Research Programme 48 (Landscapes and Habitats of the Alps) and funded by the Swiss National Science Foundation (grant 4048-064409) and the Swiss Forest Agency. We gratefully thank the European Commission for the Marie Curie Fellowship (QLK5-CT-2002-51705) and for funding the ROCKFOR project (QLK5-CT-2000-01302). Further, we would like to express our gratitude to MeteoSchweiz for providing us with the long-term weather records. We gratefully acknowledge the constructive review comments provided by Robert Deal and Jim Schwab.

6 References

BERGER, F.; DORREN, L.K.A., submitted. Rockfor^{Net}: a new efficient tool for quantifying the rockfall hazard under a protection forest. Schweiz. Z. Forstwes.

BERGER, F.; QUÉTEL, C.; DORREN, L.K.A., 2002: Forest: A natural protection mean against rockfall, but with which efficiency? The objectives and methodology of the ROCKFOR project. Proc. Int. Congress Interpraevent 2002 in the Pacific Rim, Matsumoto/Japan. 815–826.

BRANG, P.; SCHÖNENBERGER, W.; SCHWITTER, R.; WASSER, B.; FREHNER, M., 2006: Management of protection forests in the European Alps: an overview. For. Snow Landsc. Res. 80, 1: 23–44.

BRANG, P.; SCHÖNENBERGER, W.; OTT, E.; GARDNER, R.H., 2001: Forests as Protection from Natural Hazards. In: EVANS, J. (ed) The Forests Handbook. Blackwell Science Ltd. 53–81.

BRANG, P.; SCHÖNENBERGER, W.; BACHOFEN, H.; ZINGG, A.; WEHRLI, A., 2004: Schutzwalddynamik unter Störungen und Eingriffen: Auf dem Weg zu einer systemischen Sicht. Forum für Wissen 2004: 55–66.

BRAUNER, M.; WEINMEISTER, W.; AGNER, P.; VOSPERNIK, S.; HOESLE, B., 2005: Forest management decision support for evaluating forest protection effects against rockfall. For. Ecol. Manage. 207, 1–2: 75–85.

BUGMANN, H., 1994: On the Ecology of Mountainous Forests in a Changing Climate: A Simulation Study. PhD Thesis. Zürich, Eidgenössische Technische Hochschule ETH.

BUGMANN, H., 1996: A simplified forest model to study species composition along climate gradients. Ecology 77: 2055–2074.

CATTIAU, V.; MARI, E.; RENAUD, J.P., 1995: Forêt et protection contre les chutes de rochers. Ingéneries - EAI 3: 45–54.

DORREN, L.K.A., 2002: Mountain Geoecosystems. GIS modelling of rockfall and protection forest structure. PhD Thesis. University of Amsterdam. 162 pp.

DORREN, L.K.A., 2003: A review of rockfall mechnanics and modelling approaches. Prog. Phys. Geog. 27: 69–87.

DORREN, L.K.A.; BERGER, F., 2006: Stem breakage of trees and energy dissipation during rockfall impacts. Tree Physiol. 26: 63–71.

DORREN, L.K.A.; BERGER, F.; LE HIR, C.; MERMIN, E.; TARDIF, P., 2005: Mechanisms, effects and management implications of rockfall in forests. For. Ecol. Manage. 215, 1–3: 183–195.

DORREN, L.K.A.; MAIER, B.; PUTTERS, U.S.; SEIJMONSBERGEN, A.C., 2004: Combining field and modelling techniques to assess rockfall dynamics on a protection forest hillslope in the European Alps. Geomorphology 57: 151–167.

FREHNER, M.; WASSER, B.; SCHWITTER, R., 2005: Nachhaltigkeit und Erfolgskontrolle im Schutzwald. Wegleitung für Pflegemassnahmen in Wäldern mit Schutzfunktion. Bern, Bundesamt für Umwelt, Wald und Landschaft. 564 pp.

FREI, E., 2003: Amsteg-Wassen: Gebiet "Stotzigwald". Naturgefahren aus Sicht der National- und Kantonsstrasse. Unpublished report.

GERBER, W., 1994: Beurteilung des Prozesses Steinschlag, Unterlagen FAN-Kurs Oktober 1994, Poschiavo, Switzerland. 11 pp.

HEIM, A., 1932: Bergsturz und Menschenleben. Beiblatt zur Vierteljahrsschrift der Naturforschenden Gesellschaft in Zürich. 77: 218.

HUTH, A.; DITZER, T., 2000: Simulation of the growth of a lowland dipterocarp rain forest with FORMIX3. Ecol. Model. 134: 1–25.

JAHN, J., 1988: Entwaldung und Steinschlag. Proc. Int. Congress Interpraevent 1988, Graz. Band 1: 185–198.

JOHNSEN, K., SAMUELSON, L.; TESKEY, R.; MCNULTY, S.; FOX, T., 2001: Process models as tools in forestry research and management. Forestry 47: 2–8.

KALBERER, M.; MAYER, A.C.; SPIECKER, H., 2005: The influence of various silvicultural concepts on the stability of single trees and the effectiveness of a protection forest against rockfall. Internat. For. Rev. 7, 5: 311.

KUPFERSCHMID ALBISETTI, A.D., 2003: Succession in a protection forest after *Picea abies* die-back. PhD Thesis. Zürich, Eidgenössische Technische Hochschule ETH.

LINDNER, M.; SIEVÄNEN, R.; PRETZSCH, H., 1997: Improving the simulation of stand structure in a forest gap model. For. Ecol. Manage. 95: 183–195.

MEISSL, G., 1998: Modellierung der Reichweite von Felsstürzen. Fallbeispiele zur GIS-gestützten Gefahrenbeurteilung aus dem Bayrischen und Tiroler Alpenraum. PhD Thesis. Universität Innsbruck.

OLIVER, C. D.; LARSEN, B.C., 1990: Forest stand dynamics. New York, McGraw-Hill. 467 pp.

OMURA, H.; MARUMO, Y., 1988: An experimental study of the fence effects of protection forests on the interception of shallow mass movement. Mitt. Forstl. Bundesvers. anst. Mariabrunn Wien 159: 139–147.

OTT, E.; FREHNER, M.; FREY, H.U.; LÜSCHER, P., 1997: Gebirgsnadelwälder – Ein praxisorientierter Leitfaden für eine standortgerechte Waldbehandlung. Bern, Paul Haupt. 287 pp.

PENG, C., 2000: Understanding the role of forest simulation models in sustainable forest management. Environ. Impact Assess. Rev. 20: 481–501.

PRETZSCH, H.; DURSKY, J., 2001: Evaluierung von Waldwachstumssimulatoren auf Baum- und Bestandesebene. Allg. Forst- Jagdztg. 172: 146–150.

PRICE, D.T.; ZIMMERMANN, N.E.; VAN DER MEER, P.J.; LEXER, M.J.; LEADLY, P.; JORRITSMA, I.T.M.; SCHABER, J.; CLARK, D.F.; LASCH, P.; MCNULTY, S.; WU, J.; SMITH, B., 2001: Regeneration in gap models: Priority issues for studying forest responses to climate change. Clim. Change 51: 475–508.

SPSS Inc. 2001. SPSS 11.0 for Windows. <www.spss.com/spss>

RICKLI, C.; GRAF, F.; GERBER, W.; FREI, M.; BÖLL, A., 2004: Der Wald und seine Bedeutung bei Naturgefahren geologischen Ursprungs. Forum für Wissen 2004: 27–34.

RISCH, A.C.; HEIRI, C.; BUGMANN, H., 2005: Simulating structural forest patterns with a forest gap model: a model evaluation. Ecol. Model. 181: 161–172.

ROTTMANN, M., 1985: Wind- und Sturmschäden im Wald: Beiträge zur Beurteilung der Bruchgefährdung, zur Schadensvorbeugung und zur Behandlung sturmgeschädigter Nadelholzbestände. Frankfurt a. M., Sauerländer. 128 pp.

ROTTMANN, M., 1986: Schneebruchschäden in Nadelholzbeständen: Beiträge zur Beurteilung der Schneebruchgefährdung, zur Schadensvorbeugung und zur Behandlung schneegeschädigter Nadelholzbestände. Frankfurt a. M., Sauerländer. 159 pp.

SCHÖNENBERGER, W.; BRANG, P., 2004: Silviculture in mountain forests. In: BURLEY, J.; EVANS, J.; YOUNGQUIST, J. (eds) Encyclopedia of Forest Sciences, Vol. 3., Amsterdam, Boston, Heidelberg, Elsevier Academic Press. 1085–1094.

SCHÖNENBERGER, W.; NOACK, A.; THEE, P., 2005: Timber structures against natural hazards in windthrow sites in mountain protection forests. For. Ecol. Manage. 213: 197–208.

Schütz, J.P., 2001: Opportunities and strategies of transforming regular forests to irregular forests. For. Ecol. Manage. 151: 87–94.

SHUGART, H.H., 1984: A theory of forest dynamics. The ecological implications of forest succession models. New York, Springer. 278 pp.

SHUGART, H.H., 1998: Terrestrial Ecosystems in Changing Environments. Cambridge, Cambridge University Press. 537 pp.

SOKAL, R.R.; ROHLF, F.J., 1995: Biometry: The principles and practice of statistics in biological research, 3rd edition. New York, W. H. Freeman and Company. 887 pp.

STAHEL, W.A., 2000: Statistische Datenanalyse. Braunschweig/Wiesbaden, Vieweg. 379 pp.

STOFFEL, M.; WEHRLI, A.; KÜHNE, R.; DORREN, L.K.A.; PERRET, S.; KIENHOLZ, H., 2006: Assessing the protective effect of mountain forests against rockfall using a 3D simulation model. For. Ecol. Manage. 225: 113–122.

THALI, U., 1997: Waldbauprojekt Stotzigwald, Gurtnellen. Ingenieurbüro U. Thali, Göschenen. Unpublished report.

TOPPE, R., 1987: Terrain models – A tool for natural hazard mapping. In: SALM, B.; GUBLER, H. (eds) Proceedings of Avalanche formation, Movement and Effects, Davos 1986, IAHS Publication 162: 629–638.

WEHRLI, A., WEISBERG, P.J.; SCHÖNENBERGER, W.; BRANG, P.; BUGMANN, H., 2006: Improving the establishment of a forest patch model to assess the long-term protective effect of mountain forests. Eur. J. For. Res. In press.

WEHRLI, A.; ZINGG, A.; BUGMANN, H.; HUTH, A., 2005: Using a forest patch model to predict the dynamics of stand structure in Swiss mountain forests. For. Ecol. Manage. 205: 149–167.

Revised version accepted March 16, 2006

ASSESSING PROTECTION FOREST STRUCTURE WITH AIRBORNE LASER SCANNING IN STEEP MOUNTAINOUS TERRAIN

Luuk Dorren[1], Bernhard Maier[2] and Frédéric Berger[1]

[1] *Cemagref, Mountain Ecosystems Research, St. Martin d'Hères, France; luuk.dorren@cemagref.fr*
[2] *Stand Montafon - Forstfonds, Schruns, Austria; bernhard.maier@stand-montafon.at*

ABSTRACT

Protection forest management requires reliable data on the structural characteristics of forest stands with high spatial resolution, which could be delivered by airborne laser scanning. We subtracted a digital surface model (DSM), derived from the last LiDAR pulses, from a digital terrain model (DTM), derived from the first LiDAR pulses, to obtain a "normalized crown model" (nCM). The resolution of the rasters was 1 m × 1 m. With two methods that are based on local maxima identifiers individual tree tops were detected with a mean error of 33% when comparing the number of detected trees with the measured number of trees present in the validation plot. When only taking into account the dominant and co-dominant trees, this error decreased to approx. 10%. Position errors of the trees that were automatically identified in the nCM were between 0.5 and 3.5 m, when comparing to on-site GPS measured positions. Field investigations on the causes of errors in the number of detected trees showed that they are mainly caused by trees growing in collectives. Errors in tree positions are related to tilted trees and 'missed' tree tops during scanning, as well as the cumulative errors between GPS measured positions of the base of trees and the LiDAR position. In conclusion, we are of the opinion that airborne laser scanning provides excellent data for protection forest management. It provides reliable information on the positions of individual, dominating and co-dominating trees and on the position of collectives and the tree heights. In addition, it provides excellent input data for 3D natural hazard simulation models, even in steep terrain.

Keywords: *Protection forest, local maxima, tree top identification, LiDAR*

1 INTRODUCTION

Many forests in the Alps cover steep to very steep slopes (gradients of 35 - 70 degrees) and have an important protective function against natural hazards, such as rockfall and snow avalanches. In order to sustain the protective effect of these forests, they have to be managed. This requires reliable forest data with high spatial resolution, which could be delivered by LiDAR (Lim et al. 2003). The aim was to retrieve information on the structural characteristics of a protection forest stand, especially, the tree positions and the tree height using airborne LiDAR (Light Detection And Ranging, also called laser scanning), which has been shown to be feasible in less steep terrain by Popescu et al. (2002) and Zimble et al. (2002). We specifically investigated whether reliable information of trees growing on steep slopes can easily be obtained. As most foresters use raster data in standard Geographical Information Systems (GIS) instead of 3D point clouds, we tested two methods that are based on the identification of local maxima on raster data in this study.

2 METHODS

2.1 LiDAR data

The test site for this study is the 'Schmalzberg' forest, located in the Montafon region in the western part of Austria. The forest, which is dominated by Picea abies, covers a steep slope (up to 40º) and protects residential area downslope against rockfall and snow avalanches. This site has been scanned on the 10th of December 2002. The used laser scanner was a first/last pulse Airborne Laser

Terrain Mapper (ALTM 1225) made by Optech Inc. (Canada). The pulse rate of the ALTM is 25 kHz, which resulted in a point density of 0.9 points m-2 at an average fly altitude of 1000 m above ground level. With a laser beam divergence of 0.3 mrad, the average footprint on the ground was about 0.30 m. The average ground swath width was about 725 m, the maximum scanning angle 20º (Wever 2002).

The data obtained by the ALTM have been filtered and interpolated by the TU Vienna to create a digital terrain model (DTM) and a digital surface model (DSM), both with a resolution of 1 m × 1 m and a size of 500 × 500 cells. Since most users of LiDAR data would obtain similar data, we used these two rasters as the basis data for our study. By subtracting the DTM from the DSM we obtained a "normalized crown model" (nCM), which gives an estimate of the height of vegetation or similar obstacles.

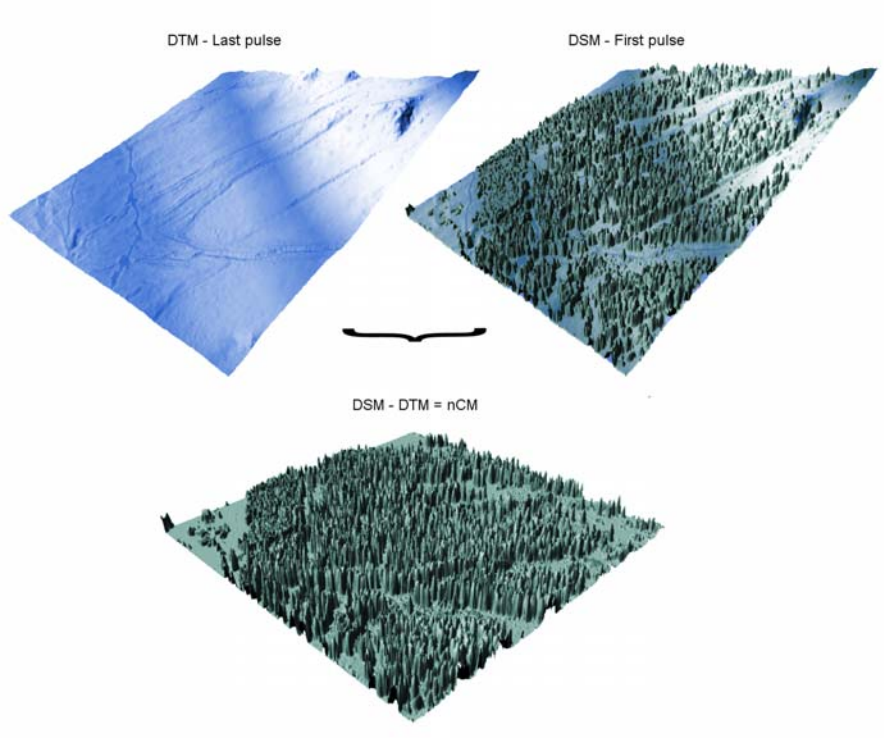


Figure 1: The 500 × 500 rasters of the study area and the creation of the normalised crown model (nCM).

2.2 Validation data

A detailed inventory within a sample plot with a 20 m radius has been carried out. Here, we measured the diameter at breast height (DBH), the tree height and the exact position of 30 trees with DBH>10 cm using a compass and an ultrasonic vertex from the sample plot centre. The position of the centre has been measured with a differential GPS. Position errors were estimated to be 0.43 m and tree height measurement errors between 0.5 and 1 m, due to the steep terrain (Maier 2005).

2.3 Tree heights and positions

To extract tree heights and positions from the nCM, we tested two methods that are based on the identification of local maxima, where those maxima are regarded as tree tops. The first method uses a variable window size (VWS) that is determined by the tree height, similar to Popescu et al. (2002). The VWS method is supported by an empirical relationship between the crown size and the tree height that is similar to Hasenauer (1997), but which is based on 500 measured tree crowns and heights in a similar forest in the area (Dünser 2002). For trees with a height up to 20 m a 1-cell window radius was used, for 20 – 30 m a 2-cell radius and for larger trees a 3-cell radius. The VWS method can be performed in a standard GIS. The second method, called Tree-top Window Analysis (TWA), is programmed in Matlab and evaluates for each cell in the nCM, which has a value larger than the defined

minimum tree height, whether it is a local maximum. Each cell is evaluated with a 3×3 window. If the evaluated cell is a local maximum, the window diameter is enlarged with two cells. Then, the evaluation is repeated. As such the method assesses the dominance of the cell over all surrounding cells. The TWA method also provides information on 'sub-maxima'. This is a cell that adjoins the local maximum with a height gradient less then 45º between the two. Condition for a sub-maximum is that all cells in the window have a lower value except for the local maximum. Such a sub-maximum could represent a tree that grows in or near a tree collective.

3 RESULTS

Figure 2 shows the sample plot with the 30 measured and all the detected tree tops. The bigger the blue in this figure dots, the larger the probability of detecting a real treetop, as calculated by the TWA method. The plot also shows the positions errors between the measured tree positions (at breast height) and the detected tree tops. Nevertheless, the heights of the detected tree tops can be used to relate them to the measured ones. The result of this comparison is given in Table 1. This shows that the TWA method detected 25 trees in the sample plot of which 21 were correct. The VWS method detected 20 trees of which 19 were correct. Position errors between the measured tree bases and the detected tree tops ranged from 0.4 – 3.5 m. The error of identifying tree tops is 33% for the TWA and 36.7% for the VWS method, when comparing with all the trees present in our validation plots. When only taking into account the dominant and co-dominant trees (non hidden trees in collectives), the mean error decreases to approx. 10%.

Table 1: Results of the comparison between measured trees and detected trees using the TWA method, the VWS method and two local maxima filters, one with a 2-cell radius and one with a 3-cell radius.

			Detected Height (m)				
Tree nr	Species	Measured height (m)	TWA	2-cell window radius (fixed)	3-cell window radius (fixed)	VWS	dH
1	Picea abies	29,0					-
2	Picea abies	35,0	35,6	35,6	35,6	35,6	-0,6
3	Picea abies	35,5	40,3	40,3	40,3	40,3	-4,8
4	Picea abies	21,0	18,7	18,7	18,7	18,7	2,3
5	Picea abies	32,0	33,2	33,2	33,2	33,2	-1,2
6	Picea abies	37,0	40,1	40,1	40,1	40,1	-3,1
7	Picea abies	15,0					-
8	Picea abies	22,5					-
9	Picea abies	36,5	31,3				5,2
10	Picea abies	32,5	33,2				-0,7
11	Picea abies	34,0	36,0	36,0	36,0	36,0	-2,0
12	Snag	22,5	35,0	35,0		35,0	-12,5
13	Snag	34,0	35,6	35,6	35,6	35,6	-1,6
14	Picea abies	30,5	34,7	34,7	34,7	34,7	-4,2
15	Picea abies	34,0	33,1	33,1	33,1	33,1	0,9
16	Snag	34,0	30,4	30,0	30,0	30,0	3,6
17	Picea abies	39,0	39,6	39,6	39,6	39,6	-0,6
18	Picea abies	32,5	34,5	34,5			-2,0
19	Picea abies	25,0					-
20	Picea abies	34,0	35,0	35,0	35,0	35,0	-1,0
21	Snag	34,0	35,9	35,8	35,8	35,8	-1,9
22	Picea abies	26,0					-
23	Picea abies	31,0	32,4	32,4	32,4	32,4	-1,4
24	Picea abies	39,5	35,7	35,7	35,7	35,7	3,8
25	Picea abies	26,0	25,0	25,0	25,0	25,0	1,0
26	Picea abies	15,0					-
27	Picea abies	34,0	33,2	33,2	33,2	33,2	0,8
28	Picea abies	8,0					-
29	Picea abies	13,5					-
30	Picea abies	27,0					-
Correctly detected			21/30	19/30	17/30	18/30	
Total trees detected (wrong ones)			25(4)	20(1)	18(1)	20(2)	

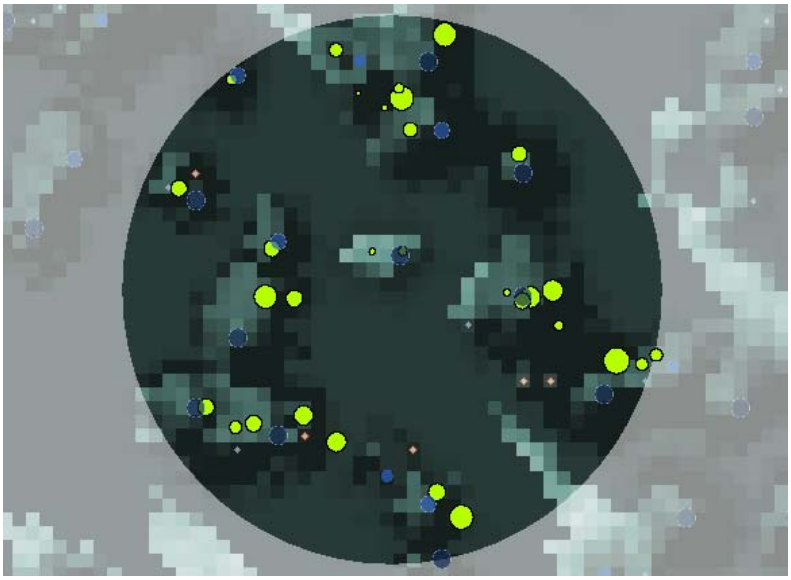


Figure 2: The sample plot with the measured trees depicted as yellow circles. The trees detected by the TWA and the VWS method are depicted as blue and small grey dots. The small white dots with the red outline were only detected by the TWA method.

4 DISCUSSION

The photos in Figure 3 illustrate examples of sources of error in LiDAR based tree detection. The detection of tree collectives (in German Rotten, see left photo) posed problems for all the methods used in this study. In collectives, trees are growing so close to each other that individual tree crowns cannot be detected, which results in one large collective tree crown after crown delineation. All the trees that were not detected by the LiDAR are growing in or near such collectives. The middle photo shows a dead standing tree (snag). Unexpectedly, all snags were detected in our sample plot, but their crowns were absent as almost no light beam is reflected by their branches. The right photo shows a tilted tree. Errors in tree positions are probably related to such tilted trees and 'missed' tree tops during scanning, as well as the cumulative errors between GPS measured positions of the base of trees and the error in the LiDAR detected tree top.



Figure 3: Examples of sources of errors in a LiDAR derived nCM (see text for explanation).

5 CONCLUSIONS

Methods based on the identification of local maxima work well for identifying the position of individual trees, as well as for determining their tree height, also in steep terrain. However, collectives consisting of multiple trees growing close to each other are detected as single tree crowns. Therefore the number of trees as detected by LiDAR in our test site is systematically underestimated. The size of the collective tree crown could probably be used as an indicator for the number of tree stems that constitute the collective in reality. Our final aim is to describe the structural characteristics of protection forest stands using LiDAR for (a) management planning, but also for (b) integrating stand characteristics (tree positions, tree heights and their DBH) in snow avalanche and rockfall simulation models (e.g., Dorren et al. 2004). Regarding tree collectives, which occur frequently in protection forests in the Alps, the problems encountered when using LiDAR can probably be solved satisfactorily by using spatial statistics and probabilistic approaches. Future research would have to focus on developing a generic and persistent method for estimating the number of trees that constitute a collective. Other solutions might be to use the raw 3D LiDAR data in combination with methods described by Zimble et al. (2003) and Maltamo et al. (2005) or the use of the full waveform LiDAR.

The DTM of steep mountainous terrain provided by LiDAR and the positions and heights of individual trees derived from the DSM have an enormous added value for natural hazard simulation models in comparison with traditional DEMs obtained from photogrammetry and tree positions derived from orthophotos. In the future we will focus on adding criteria in the TWA method to improve the estimation of the probability that a detected local maximum or sub-maximum is a real tree top. Then, the improved method should be tested and validated on a larger scale and in other types of forest than pure Picea abies stands, such as mixed montane forests and pole forests.

ACKNOWLEDGEMENTS

Markus Hollaus at the TU Vienna is acknowledged for creating the DSM and the DTM from the raw LiDAR data.

REFERENCES

Dorren, L.K.A., Maier, B, Putters, U.S. and Seijmonsbergen, A.C. (2004). Combining field and modelling techniques to assess rockfall dynamics on a protection forest hillslope in the European Alps. Geomorphology 57(3): 151-167.

Dünser, S. (2002). Ableitung von Auszeigekriterien für die Holzernte im Seilgelände auf Basis des Schutzwaldkonzepts Rellstal/Montafon (Vorarlberg). Diplomarbeit am Institut für Waldbau an der Univ. f. Bodenkultur, Wien.

Hasenauer, H. (1997). Dimensional relationships of open-grown trees in Austria. For. Ecol. Man. 96:197-206.

Lim, K., Treitz, P., Wulder, M., St-Onge, B. and Flood, M. (2003). LiDAR remote sensing of forest structure. Prog. Phys. Geog. 27:88-106.

Maier, B. (2005). Analyse von LiDAR-Baumkronen-Modellen mit Filtertechniken. SE Arbeit für Räumliche Modelle und Simulation SS 2, Institut für Geographie und Angewandte Geoinformatik, Univ. Salzburg: 20 p.

Maltamo, M., Packalén, P., Yu, X., Eerikäinen, K., Hyyppä, J. and Pitkänen, J. (2005). Identifying and quantifying structural characteristics of heterogeneous boreal forests using laser scanner data. For. Ecol. Man. 216(1-3): 41-50.

Popescu, S.C., Wynne, R.H. and Nelson, R.F. (2002). Estimating plot-level tree heights with lidar: local filtering with a canopy-height based variable window size. Comp. Elec. Agric. 37:71-95.

Wever, CH. (2002). Airborne Laser Scanning. Verfahren und Genauigkeiten. Vortrag im Rahmen des Fachforums VOGIS in Feldkirch. http://www.vorarlberg.at/pdf/vortrag_wever_23_09.pdf (27. Juli 2005).

Zimble, D.A., Evans, D.L., Carlson, G.C., Parker, R.C., Grado, S.C. and Gerard, P.D. (2003). Characterizing vertical forest structure using small-footprint airborne LiDAR. Rem. Sens. Env. 87:171-182.

Citation: Dorren, L.K.A., Maier, B. and Berger, F., 2006. Assessing protection forest structure with airborne laser scanning in steep mountainous terrain. In: T. Koukal and W Schneider (Eds.), Proceedings International Workshop 3D Remote Sensing in Forestry, 13-15 February 2006, EARSeL, Vienna: p. 238-242.

Plant and Soil (2005) 278:107–117
DOI: 10.1007/s11104-005-3899-3
© Springer 2005

Mechanical resistance of different tree species to rockfall in the French Alps

Alexia Stokes[1,5], Franck Salin[1], Adzo Dzifa Kokutse[1], Stéphane Berthier[1,2], Henri Jeannin[1], Shaun Mochan[2], Luuk Dorren[3], Nomessi Kokutse[1], Murad Abd.Ghani[1] & Thierry Fourcaud[1,4]

[1]*Laboratoire du Rhéologie du Bois de Bordeaux, (Mixed unit: CNRS/INRA/Université Bordeaux I), 69, rte d'Arcachon, 33612, Cestas cedex, France.* [2]*Forest Research, Northern Research Station, EH25 9SY, Midlothian, Scotland.* [3]*Cemagref Grenoble, 2 rue de la Papeterie, B.P. 76, 38402, St. Martin d'Hères cedex, France.* [4]*AMAP, CIRAD, TA40/PS2, Boulevard de la Lironde, 34398, Montpellier Cedex 5, France.* [5]*Corresponding author**

Received 6 October 2004. Accepted in revised form 15 March 2005

Key words: protection forest, tree stability, root anchorage, uprooting, stem breakage, scar formation

Abstract

In order to determine the mechanical resistance of several forest tree species to rockfall, an inventory of the type of damage sustained in an active rockfall corridor was carried out in the French Alps. The diameter, spatial position and type of damage incurred were measured in 423 trees. Only 5% of trees had sustained damage above a height of 1.3 m and in damaged trees, 66% of broken or uprooted trees were conifers. Larger trees were more likely to be wounded or dead than smaller trees, although the size of the wounds was relatively smaller in larger trees. The species with the least proportion of damage through stem breakage, uprooting or wounding was European beech (*Fagus sylvatica* L.). Winching tests were carried out on two conifer species, Norway spruce (*Picea abies* L.) and Silver fir (*Abies alba* Mill.), as well as European beech, in order to verify the hypothesis that beech was highly resistant to rockfall and that conifers were more susceptible to uprooting or stem breakage. Nineteen trees were winched downhill and the force necessary to cause failure was measured. The energy (E_{fail}) required to break or uproot a tree was then calculated. Most Silver fir trees failed in the stem and Norway spruce usually failed through uprooting. European beech was either uprooted or broke in the stem and was twice as resistant to failure as Silver fir, and three times more resistant than Norway spruce. E_{fail} was strongly related to stem diameter in European beech only, and was significantly higher in this species compared to Norway spruce. Results suggest that European beech would be a better species to plant with regards to protection against rockfall. Nevertheless, all types of different abiotic stresses on any particular alpine site should be considered by the forest manager, as planting only broadleaf species may compromise the protecting capacity of the forest e.g. in the case of snow avalanches.

Introduction

The use of protection forests against the impact of natural hazards e.g. rockfall and snow avalanches is becoming more and more common in Europe (Brang, 2001; Dorren and Berger, 2005; Dorren et al., 2004; Hurand and Berger, 2002; Motta and Haudemand, 2000; Ott, 1996). With the increase in catastrophic events both in the European Alps (Interreg IIIb, 2001; Sauri et al., 2003) and in mountainous regions around the

* FAX No: (+33 5) 56680713.
E-mail: stokes@lrbb3.pierroton.inra.fr

world (Tianchi et al., 2002), research into this phenomenon has accelerated. However, although it is understood that the structure of the forest plays a vital role in determining its effectiveness as a protective barrier (Jahn, 1988; Kräuchi et al., 2000), little information exists concerning the mechanical resistance of different tree species to different types of natural hazards. One particular natural hazard which has been much neglected until recent years, is that of rockfall. Not only is the movement of rocks and stones a hazard to both people and infrastructures, but rockfall safety nets are expensive and difficult to install and they deteriorate with time (Dorren, 2003). If further information on the structure of a protection forest, and the most mechanically resistant species to use against rockfall could be obtained, these data could be used as input to models of rockfall dynamics (Dorren et al., 2004) and/or fed directly into management and decision support systems (Mickovski, 2005; Stokes et al., 2004).

Even if a tree species is useful as a barrier against one particular type of hazard, the same species may not be suitable in protecting against a different type of hazard e.g. Norway spruce (*Picea abies* L.) is not especially windfirm (Stokes et al., 2000) nor resistant to rockfall (Hurand and Berger, 2002). However, in preventing snow movement, Norway spruce is highly effective in holding in place the snow mantle (Hurand and Berger, 2002). Therefore, it is necessary to determine which species is best suited to a particular function. In the case of rockfall, different types of rockfall exist, including collapsing in mass where the volume displaced is > 5.0 m^3. Individual rockfall occurs more often with smaller volumes (< 5.0 m^3) displaced (Berger et al., 2002). It is in this latter case that forests can act as a barrier and provide a protective function. When rocks impact against trees, different types of tree failure can occur, including uprooting and stem breakage (Berger et al., 2002). Certain species, particularly angiosperms, appear to be more resistant to failure than others, often sustaining wounds only (Dorren and Berger, 2005). It is not known which species are the most resistant against the impact of rocks, however, foresters have suggested from experience that broadleaf species are more resistant against rockfall impacts, although no particular reasons are given for this hypothesis. Only in the literature concerning wind damage to forests, can comparisons of different species be found with regards to their mechanical resistance (Meunier et al., 2002; Peltola et al., 2000; Stokes et al., 2000). The most common method to compare the likelihood of stem failure or uprooting, is to winch trees sideways until failure occurs (Cucchi et al., 2004; Gardiner et al., 2000; Moore, 2000; Stokes, 1999; Stokes et al., 2000). Certain species e.g. Sitka spruce (*Picea sitchensis* Bong. Carr) are more susceptible to stem breakage and uprooting than others e.g. European beech (*Fagus sylvatica* L.) (Stokes et al., 2000). Very few data exist concerning broadleaf species, primarily because conifer species are more susceptible to damage during a winter storm, and conifers are economically important timber species.

One of the most important factors governing the ability of a tree to withstand breakage or uprooting during a storm, is the morphology of the root system present (Cucchi et al., 2004; Dupuy et al., 2005; Stokes et al., 2000, 2006) Trees with deep and wide spreading root systems will be better anchored than those with superficial roots only (Stokes, 2002). The shape and size of a root system is influenced by its immediate environment as well as being inherent to a particular species (Köstler et al., 1968). Trees growing on the thin, rocky soils encountered on mountain slopes may therefore possess different rooting types depending on species. The morphology of the root system may also differ to that of the same species growing in a deep soil on flat ground (Köstler et al., 1968). Therefore, a well-anchored species growing in a particular soil type, may become highly unstable in a different environment (Dupuy et al., 2005; Moore, 2000).

In order to identify the type of tree failure which occurs in a forest subjected to rockfall, two studies were carried out on an active rockfall site in the French Alps. Initially, the position, size, species and type of damage sustained to trees growing in a mixed forest were measured. A series of winching tests were then carried out on Norway spruce, Silver fir and European beech, which enabled us to quantify the mechanical resistance of each species. The maximum energy required to cause failure was then estimated, as

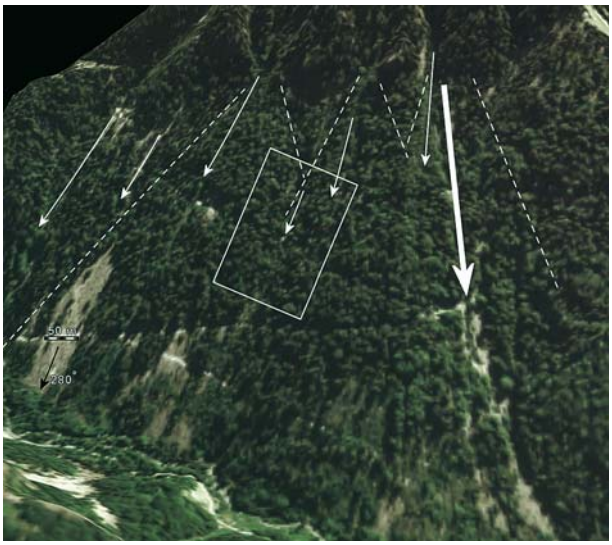


Figure 1. A digital terrain model of the study area overlain by an orthophoto. This figure shows that the site consists of several talus cones (dashed white lines) on which preferential rockfall and avalanche tracks exist (white arrows; the size indicates the magnitude of processes acting in the preferential track). The study site is depicted by the white rectangle.

during an impact between a falling rock and a tree, it is the kinetic energy of the rock which causes tree displacement. Results are discussed with regards to management strategies for protection forests.

Materials and methods

Study site

The study site was situated in the Forêt Domaniale de Vaujany, Vallée de l'Eau d'Olle, Isère (lat 45°12′, long 6°3′), France, at an altitude of 1350–1600 m. This forest is located on a northwest facing mountain side that can be divided into two areas. First, the rockfall source areas, which are a series of steep cliff faces dissected by some denudation niches occurring on top of each other. The mean slope gradient in the source area is 70° up to vertical cliffs. The second part consists of large post-glacially developed talus cones consisting mainly of rock avalanche deposits, snow avalanche deposits and rockfall scree. These large talus cones were formed after deglaciation of the main valley. The retreat of the glacier resulted in tensional rebound of the oversteepened valley slopes. This retreat led to slope instability and landsliding (mainly rock avalanches), which consequently resulted in the build up of the large talus cones (Figure 1). During the Holocene (the last 10,000 years), these talus cones have been colonised by vegetation, eventually resulting in a forest cover. Today, the dominant tree species on the site are Silver fir (*Abies alba* Mill.), Norway spruce (*Picea abies* L.), European beech (*Fagus sylvatica* L.), Sycamore (*Acer pseudoplatanus* L.), European ash (*Fraxinus excelsior* L.) and Common hazel (*Corylus avellana* L.). The forested talus cones have a slope gradient of 38–42° and act currently as rockfall transit and accumulation zones. Rocks impacting trees can cause damage and are therefore disturbing the forest ecosystem. The other major disturbances are snow creep, snow gliding, snow avalanches, ungulate browsing and wind loading. The effects of the mass movement processes are clearly reflected in the slope relief and in the vegetation as distinct preferential tracks or channels for snow transport and falling rocks. In between the preferential tracks, the forest is dominated by un-even aged Silver fir and Norway spruce and in the preferential tracks the forest is dominated by young European beech, ash and hazel trees. A storm in 1960 resulted in the loss of 2220 m^3 of timber throughout the

whole forest, of which the surface area is 818 ha (C. Bazin, pers. comm.).

Inventory of damage incurred by rockfall

In order to determine if damage by rockfall was more frequent in certain species compared to others, an inventory of trees with/without damage was carried out. A 200 × 50 m corridor was defined that covered two preferential tracks within the study site, where rockfall appeared to be the most active (Figure 1). All trees >0.1 m diameter were measured within this corridor. For each tree, the species, DBH, diameter at stem base (DSB) and type of damage were noted. Trees were noted as uprooted, broken in the stem or wounded (height and width of wound measured if below DBH).

In order to compare the extent of wound damage in trees of different sizes, the percentage of dysfunctional cambium was calculated using: (width of wound/tree basal circumference) × 100 (Guyette and Stambaugh, 2004). Analysis of variance and χ^2 tests were carried out to determine if the type of damage sustained was influenced by species and size of trees, using size parameters as covariates where necessary.

Winching tests

In order to determine the mechanical resistance of a tree to failure by rockfall, bending tests *in situ* were carried out. Trees were winched sideways until failure occurs and the force necessary to cause uprooting or stem breakage measured. Such tests were carried out on 19 adult trees. It was not possible to carry out more tests, as suitable tree material was scarce and winching tests dangerous due to the unstable, steep slope. Three species were chosen for this study, as they appeared to sustain different types of rockfall damage at the site (see results of damage mapping). These species were Silver fir, Norway spruce and European beech. Mean DBH for all trees was 0.23 ± 0.08 m and height was 14.90 ± 0.65 m (Table 1). The system employed was similar to that used by Cucchi et al. (2004), Meunier et al. (2002), Moore (2000), Peltola et al. (2000) and Stokes (1999). A motorised winch (16 kN, Hit-Trac 16B, Habegger, Switzerland) was used to winch trees sideways. For large trees, a pulley was also used which doubled the winch capacity. The winch was attached to the base of an anchoring tree at the longest possible distance to the winched tree, in order to obtain a small angle θ (Figure 2). When pulling trees downhill, a pulley was employed to deviate the force applied, so that the winch user would not be in the pathway of falling rocks or branches (Figure 2). The winch cable was attached to the test tree at a height (H_{cable}) of 4.0−8.0 m, as it was physically difficult to attach the cable any higher, due to the high number of branches encountered on most trees, which hindered climbing. The force applied was measured with a load cell (K25H-20 kN, Scaime S.A., France) and measured every second using a datalogger (Almemo 2290-8, Ahlborn, Germany). In order to measure the deflection angle, α, of the stem during winching, two inclinometers were nailed to the tree, one at cable height and the second at the stem base (Figure 2), which measured rotation of the root plate (Cucchi et al., 2004). An identical datalogger was used to record α every second during

Table 1. Means ± standard error of the parameters measured for each species tested in the winching studies and necessary for the calculation of $TM_{crit,total}$. Mean ± standard error values of the maximum energy (E_{fail}) required to cause failure in each species are also given

Variables	European beech (n = 7)	Silver fir (n = 6)	Norway spruce (n = 6)
Height (m)	17.7 ± 1.8	12.9 ± 0.8	12.7 ± 1.1
DBH (m)	0.23 ± 0.03	0.24 ± 0.02	0.24 ± 0.01
Stem weight (kg)	479.0 ± 129.0	257.5 ± 50.2	235.2 ± 42.1
Crown biomass (kg)	127.2 ± 36.8	180.4 ± 52.9	145.6 ± 28.4
Total biomass (stem + crown) (kg)	606.0 ± 161.0	437.0 ± 92.9	380.8 ± 63.6
Failure energy (kJ)	38.4 ± 12.7	22.7 ± 5.3	15.3 ± 4.7

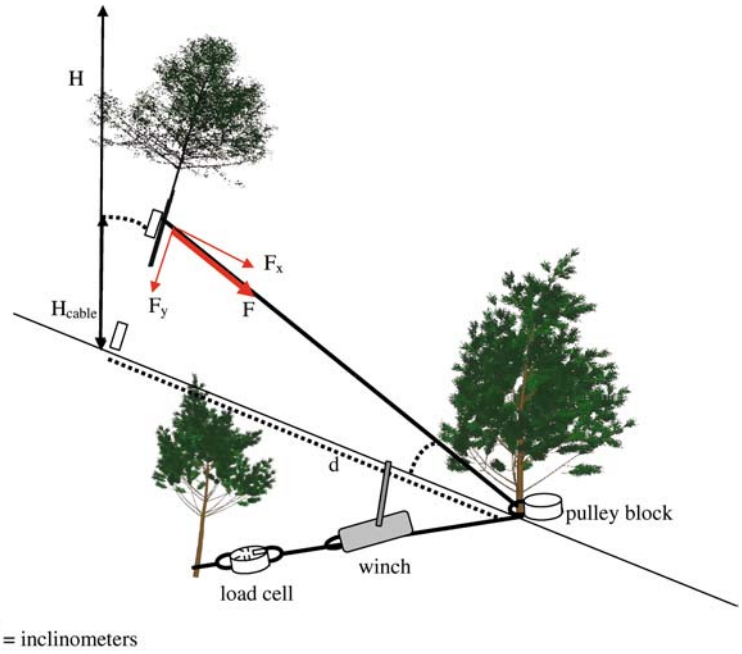


Figure 2. Trees were winched sideways and the force necessary was measured using a load cell located between the winch and anchoring tree. When winching downhill, a pulley was used to deviate the applied force around a neighbouring tree in order to prevent the tested tree or dislodged rocks from hitting the winch user. Inclinometers were attached at the stem base and at the cable attachment height (H_{cable}) in order to measure stem deflection during winching. See Methods section for an explanation of symbols.

winching. The distance between the test tree and anchorage point was also measured.

Once a tree had been winched to failure, several measurements were carried out on the stem and crown which were necessary for calculations of the total critical bending moment ($TM_{crit,total}$) (Cucchi et al., 2004). The relative crown length i.e. the distance between the first living branch and the stem apex was determined, along with the height of the first living branch. The stem circumference was measured every 1.0 m, avoiding any bulging whorls or branches. Crown biomass was measured by weighing all the live branches (Table 1). Stem green wood density (wood and bark) was calculated using (Table 1):

$$\text{Density} = \frac{\text{SectionWeight}}{\text{SectionVolume}}, \quad (1)$$

where SectionVolume is the volume of a 1.0 m long section of trunk cut from the middle of the stem volume and weighed (SectionWeight). This density was assumed to be constant throughout the stem. Total stem weight was estimated using:

$$\text{StemWeight} = \sum(\text{SectionVolume}) \times \text{Density} \quad (2)$$

As the local environment around each tree was highly variable, several measurements were made which took into account the immediate vegetation conditions. The number and species of trees within a radius of 5.0 m was recorded, along with the distance to the nearest tree. Soil moisture content was not measured, as it was considered that the large quantity of rocks and stones present would influence uprooting strength more than soil moisture.

Calculation of critical bending moment

The force required to cause failure of a tree was determined from the recorded load cell data, and associated values of σ at the time of uprooting

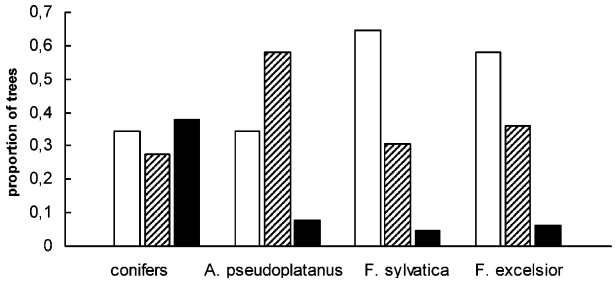


Figure 3. The proportion of healthy, wounded or dead trees were significantly different depending on species ($\chi^2 = 84.4$, $p < 0.001$). Most beech trees were healthy (white bar), whereas a high proportion of sycamore were wounded (hatched bar) and most conifers were either wounded or dead (black bar).

or stem breakage. The critical turning moment applied at the stem base was calculated using the method described in Cucchi et al. (2004):

$$\begin{aligned} \mathrm{TM}_{\mathrm{crit,applied}} = {} & F_x \times \cos\alpha \times H_{\mathrm{cable}} \\ & + F_y \times \sin\alpha \times H_{\mathrm{cable,}} \end{aligned} \quad (3)$$

where F_x is the component parallel to the soil surface and F_y the component perpendicular to the soil surface. Both are components of the maximal applied force F(N) and the deflection angle α of the trunk minus the slope angle, when the force was maximal. The tree stem was considered as a rigid cantilever beam and stem curvature was not taken into consideration. The difference between the angle of deflection measured at the stem base and at the height of the cable was therefore considered as negligible. Nevertheless, to account for any stem curvature, we used a mean of the two angles to calculate α. F_x and F_y were deducted from the value of F(N) and the cable angle θ, with regards to the soil surface. θ was derived from the distance d between the tree winched and the anchoring tree (Figure 2), as well as H_{cable}:

$$F_x = F \times \cos\theta \quad \text{and} \quad F_y = F \times \sin\theta \quad (4)$$

The total critical turning moment $\mathrm{TM}_{\mathrm{crit,total}}$ at the stem base adds the critical turning moment applied by the winch (3) to the critical turning moment $\mathrm{TM}_{\mathrm{crit,weight}}$ due to the force resulting from the overhanging weight of the leaning tree during winching. The weight of the winch and cable were neglected. $\mathrm{TM}_{\mathrm{crit,weight}}$ was calculated by resolving tree weight into stem and crown weights where the tree crown was taken as a whole and the tree stem as 1.0 m long sections stacked on top of each other.

$$\mathrm{TM}_{\mathrm{crit,weight}} = W \times G_x, \quad (5)$$

where W is the weight in N and G_x is the final horizontal position of the centre of gravity at the middle of the crown or stem section. As tree displacement was small, the horizontal component of G could be assimilated to the height of G on the stem multiplied by the sinus of the leaning angle given by the inclinometers. For the crown and stem section above the cable attachment point, this angle corresponds to the angle measured at this point. Although (3) and (4) assume the stem as a rigid cantilever, we wanted to take into account the stem lean below this point: leaning angle is an evolution in increments between the stem base angle and the attachment point angle. Stem section mass was deducted from the green wood density determined for each tree and the stem section volume assumed to be a truncated cone form. Hence, $\mathrm{TM}_{\mathrm{crit,crownweight}}$ was directly obtained and $\mathrm{TM}_{\mathrm{crit,stemweight}}$ was the sum of all the moments of tree stem sections.

Calculation of energy required to cause failure

The amount of energy (E_{fail}) required to cause tree failure was calculated by integrating numerically the total overturning moment TM, i.e. including crown and trunk weights, over the angle α of stem lean during winching (where α = the deflection angle of the trunk minus the slope angle when the force was maximal. α was

calculated as the mean of the stem two angles measured).

$$E_{\text{fail}} = \frac{1}{2}\sum_{i=1}^{n-1}(\alpha_{i+1} - \alpha_i)(\text{TM}_{i+1} + \text{TM}_i), \qquad (6)$$

where n = the number of data recorded just before tree failure, and indices i the ith record in the data base.

Data were analysed using regression analysis and relationships between a given tree parameter and $\text{TM}_{\text{crit,total}}$ or E_{fail} were compared using analysis of covariance.

Results

Inventory of damage incurred by rockfall

423 trees were measured in the active rockfall corridor. The DBH of all trees was 0.31 ± 0.10 m and DSB was 0.41 ± 0.10 m (values are means ± standard error). The percentage of conifer species on the site was low (23%), with only Norway spruce (5%) and Silver fir (17%) present. Seven broadleaf species were present, with sycamore (24%), European beech (23%) and European ash (23%) being the major species on the site. The remaining four species comprised Common aspen (*Populus tremula* L.) (3%), Silver birch (*Betula pendula* Roth.) (2%), Wych elm (*Ulmus glabra* Huds.) (1%) and European Rowan (*Sorbus aucuparia* L.) (1%). Many trees were damaged or wounded by rockfall, with 50% of broadleaf species and 65% of conifers either wounded or dead. It was not always possible to identify the broken or uprooted conifer species, which were often in an advanced state of decay, therefore both Silver fir and Norway spruce were combined for the statistical analysis. Taking into account only those species present >5% of the total percentage of trees, a higher number of dead conifers was present than either wounded or healthy conifers whereas very few dead broadleaf trees were present. Beech was the species with the highest number of healthy trees whereas sycamore was the most often wounded (Figure 3). Surprisingly, only eight trees were broken in the stem at a height >1.3 m and only 12 trees had sustained wounds above this height.

The size of the tree also appeared to influence its state. Conifers were significantly larger in diameter than broadleaf species, and ash was the species with the smallest DSB ($F_{1,386} = 3.82$, $p = 0.01$, Figure 4). In all species, the largest trees were the most susceptible to being wounded and in broadleaf species, the smallest trees were most likely to be dead ($F_{2,386} = 16.42$, $p < 0.001$, Figure 4). However, a significant negative relationship between the % dysfunctional cambium and tree DBH existed, even though variability was high ($y = -0.0593x + 39.895$, $R^2 = 0.04$, $p = 0.023$). i.e. although larger trees were more likely to sustain damage, the size of wounds were relatively smaller in larger trees. No significant differences within or between tree species were found.

The results of this inventory permitted us to choose three species for the study of tree winching. Both conifer species were chosen along with beech, in order to compare broadleaf and

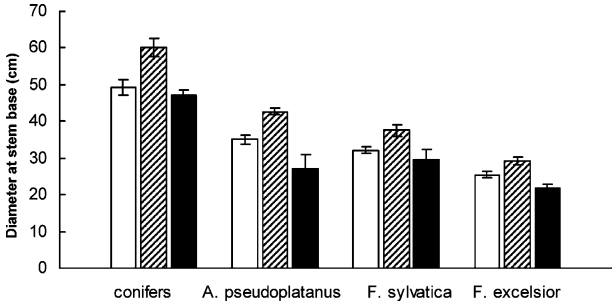


Figure 4. The diameter at stem base (DSB) influenced significantly the state of the tree. Conifers were significantly larger in diameter than broadleaf species, and ash was the species with the smallest DSB. In all species, the largest trees were the most susceptible to being wounded (hatched bar) and in broadleaf species, the smallest trees were most likely to be dead (black bar) when compared to healthy trees (white bar).

conifer species. Beech was chosen because it was the species found to have the highest proportion of undamaged trees (Figure 3).

Winching tests

Out of the 19 trees winched downhill in this study, four European beech, two Silver fir and five Norway spruce were uprooted, whilst the remaining trees all broke in the stem at a height < 1.3 m. European beech failed at a mean height of 5.9 ± 1.4%, and fir at 17.3 ± 5.0% of the total relative stem length. Out of the beeches that failed in the stem, all trees were found to be growing < 0.5 m to a large neighbouring beech tree and root grafting could be seen to occur in superficial roots of neighbouring trees when the topsoil was removed with a trowel. One beech tree was discounted from further analysis, as the base of the tree was found to be associated to a neighbouring tree and may have originated from this tree. Although the Silver fir trees were sometimes growing nearby neighbouring Silver fir and beech, no root grafting could be seen to occur. The Norway spruce which broke failed at the stem base, and was found to contain rotten wood in this area.

Linear regressions carried out between $TM_{crit,total}$ and different tree characteristics showed that the best relationship was obtained for both DBH and total biomass in European beech, and crown biomass in Silver fir (Table 2). No significant relationship was found between $TM_{crit,total}$ and any size parameter for Norway spruce. Results showed European beech was significantly more resistant to failure than Silver fir when $TM_{crit,total}$ was regressed with DBH, DBH^2 and crown biomass (Table 2). Although no significant relationship in $TM_{crit,total}$ and any size parameter was found in Norway spruce, it could be seen that $TM_{crit,total}$ was very low for this species (39.4 ± 7.6 k Nm). No significant differences in $TM_{crit,total}$ were found between uprooted and broken trees, probably due to the low number of trees tested.

Variability in E_{fail} was high both within and between species (Table 1) and significant relationships between E_{fail} and DBH or DBH^2 were found in European beech only, the best being with DBH (Figure 5). E_{fail} in European beech was significantly greater than that in Norway spruce for DBH ($F_{1,8} = 11.55$, $p = 0.009$) and DBH^2 ($F_{1,8} = 7.54$, $p = 0.025$) only.

Discussion

Although we cannot be certain that any particular tree was damaged through falling rocks, the type of damage incurred suggested that rockfall was the main abiotic stress in the corridor chosen. Nevertheless, snow or wind damage may also have resulted in uprooted or broken trees. 66% of uprooted or broken trees were conifers, but it was not always possible to determine the actual species. Only 5% of trees were broken or wounded above DBH, as the average rock rebound height was 1.0 m at this site (Dorren and Berger, 2005). Large trees were more likely to be

Table 2. Significant regression equations for $TM_{crit,total}$ and each parameter measured during the winching studies of European beech and Silver fir

	European beech			Silver fir			Comparison between species	
Variables	Regression	p	R^2	Regression	p	R^2	$F_{2,15}$	p
DBH (m)	$y = 1983690x - 307681$	0.011	0.76	$y = 1120579x - 177738$	0.017	0.80	6.73	0.008
DBH^2 (m^3)	$y = 3824259x - 67648$	0.016	0.71	$y = 2269314x - 44133$	0.010	0.84	5.42	0.017
($H \times DBH^2$) (m^3)	$y = 5881x + 130851$	0.030	0.64	$y = 130311x - 12751$	0.005	0.88	–	ns
Crown biomass (kg)	$y = 1290x - 2514$	0.027	0.66	$y = 460x + 8856$	0.002	0.92	5.44	0.017
Total biomass (stem + crown) (kg)	$y = 318x - 30875$	0.011	0.76	$y = 248x - 16879$	0.012	0.83	–	ns

Data for Norway spruce were not significant and therefore not included. Regressions between species were compared using analysis of covariance.

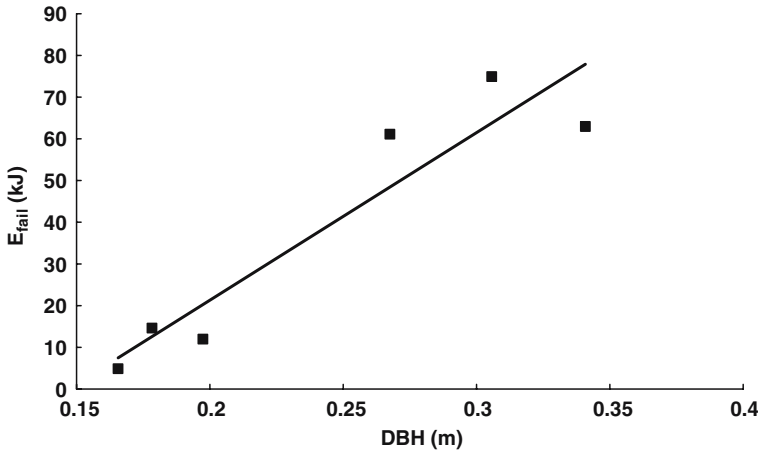


Figure 5. The amount of energy (E_{fail}) required to cause tree failure increased significantly with stem diameter at breast height (DBH) in European beech only ($y = 410.853x - 59.057$, $R^2 = 0.88$, $p = 0.006$).

wounded than smaller trees, which may be due to a decrease in rockfall activity over the last 50 years. However, smaller trees were more likely to die if damage was sustained. Small conifers were less numerous due to over browsing by ungulates in the valley (C. Bazin, pers. comm.), which will also bias the results in that small, damaged conifers were fewer due to this problem. A large amount of mosses were observed growing on the rocks along the rockfall corridor, which also suggests a decrease in rockfall activity over recent years.

The increase in the likelihood of damage with stem diameter may not only be due to a decrease in rockfall activity, but the fact that large trees are more likely to be hit by falling rocks. Whereas small trees are more likely to break and therefore die, older species will resist uprooting or breakage and sustain wounds. The larger the tree, the smaller the percentage of cambial damage that will occur. Nevertheless, certain broadleaf species are able to produce scar tissue faster than fir or spruce. This scar tissue will form around the wound and protect it from pathogen attack (Shigo, 1986). Silver fir and Norway spruce will therefore be more susceptible to infection through pathogens, leading to internal stem rot and decay, and ultimately resulting in weakened mechanical resistance to rockfall. Bark thickness was not taken into account, but is known to protect the living cambium from wounding (Guyette and Stambaugh, 2004). A future study should examine the influence of bark thickness on the percentage wound damage to a stem, for different species. Bark is usually thicker in older trees, which may be a further reason why wound size was relatively smaller in large trees.

The winching tests revealed that most Silver fir trees failed in the stem, whereas Norway spruce usually failed through uprooting. Fir trees possessed very few roots, but these roots were large and long and penetrated between the numerous rocks present in the soil (Stokes et al., 2006). Therefore, it can be considered that these trees were well anchored, as the moment required to resist overturning was greater than that needed to cause stem failure. Norway spruce possessed more superficial root systems, also with few roots (Stokes et al., 2006), and the only Norway spruce that broke in the stem was rotten at the stem base. Root systems of European beech were highly branched and deeper than spruce (Stokes et al., 2006). European beech failed several times in the stem, but only in trees which were growing nearby other beech trees. A high amount of root grafting could be seen to occur between neighbouring beech trees, which will strongly increase root anchorage. Although spruce and fir can also graft with tree roots of the same species (Bormann and Graham, 1959), no signs of root grafting were visible in the superficial surface roots of these trees.

European beech was the most resistant species to failure, and mean $TM_{crit,total}$ was nearly double that of Silver fir and was three times larger than in Norway spruce. The best correlations between $TM_{crit,total}$ and tree size parameters were found to be DBH and total biomass in beech and crown biomass in fir. In previous studies, the best correlations were usually with stem mass (Gardiner et al., 2000; Meunier et al., 2002) or $H \times DHB^2$ (Cucchi et al., 2004). It is surprising that no significant relationship was found between $TM_{crit,total}$ and any parameter measured in Norway spruce. It would probably be necessary to test a larger number of trees in order to obtain better regressions. The rocky nature of the soil also added to the variability encountered between trees. The value of $TM_{crit,total}$ was high for beech, but comparable to data for other certain species found in the literature e.g. *Pinus pinaster* Ait. (Cucchi et al., 2004) and *P. radiata* D. Don (Moore, 2000). Nevertheless, $TM_{crit,total}$ is usually much lower, and the values for fir and spruce were similar to those for *Betula* spp. and *P. sylvestris* L. (Peltola et al., 2000). Very few data exist for comparisons with broadleaf species, and none for trees growing in such conditions.

The energy (E_{fail}) required to cause tree failure was calculated from static winching data, and therefore did not take into account crown or whole stem characteristics. The effect of these components on the maximal amount of energy that can be dissipated by a tree (E_{max}) is considerable, as shown by Dorren and Berger (2005). Nevertheless, these authors obtained E_{max} values ranging from 40–115 kJ for Silver fir with a similar DBH to trees from our study. Our results showed that E_{fail} was significantly higher in European beech compared to Norway spruce, and was strongly related to stem diameter in the former species. Therefore, European beech is not only more mechanically resistant to failure, but can also resist rockfall better as stems can deflect more during an impact. These results are coherent with the results obtained by dynamic impact tests as described by Dorren and Berger (2005). Again, the lack of significant relationships between E_{fail} and stem parameters in Silver fir and Norway spruce tested in our experiments, may be due to a lack of data.

These results suggest that beech would be a better species to plant with regards to rockfall protection. Broadleaf species can also regenerate after damage, and produce large quantities of scar tissue if wounded by a falling rock. The disadvantage of broadleaf species is that they do not prevent the formation of homogeneous snow layers due to their reduced canopy surface in the winter. As a result the snow avalanche risk increases in comparison to coniferous forests. Nevertheless, more broadleaf species would need to be tested in order to determine which are the most resistant to rockfall, and thus the most useful species to plant in a rockfall protection forest. The main remaining task for protection forest managers will be to define against which natural hazard the forest has to protect. If both rockfall and snow avalanches are occurring, a mixed forest would be the most effective for protection.

Acknowledgements

Thanks are due to M. Aya, H. Bignalet, G. Cherokee, S. Daviller, M. Genet, N. Harries, B. Issenhuth, H. Lataillade, S. Mickovski, M. Sharman, (INRA), C. Quetel (Cemagref), J. Fannin (University of British Columbia, Canada) and M. Sarnatoro (University of Molise, Italy), for help with fieldwork and F. Danjon (INRA) for his critical comments on the manuscript. We thank C. Bazin (Office National des Forêts), the Marie de Vaujany and F. Berger (Cemagref) for permission to work at the study site, as well as the Hotel Cabri for their help and warm welcome over the last three years. This work was financed by the E.U. project Eco-Slopes (QLK5-2001-00289). A.D. Kokutse was funded by a Marie Curie Bursary.

References

Berger F, Quetel C and Dorren L K A 2002 Forest: a natural protection mean against rockfalls, but with which efficiency? *In* Proceedings of the International Congress. Interpravent 2002 in the Pacific Rim – Matsumoto, Japan. Vol. 2, pp. 815–826. Congress Publication.

Brang P 2001 Resistance and elasticity: promising concepts for the management of protection forests in the European Alps. Forest Ecol. Manag. 145, 107–119.

Bormann F H and Graham B F 1959 The occurrence of natural root grafting in eastern white pine *Pinus strobus* and its ecological implications. Ecology. 40, 677–691.

Corominas J 1996 The angle of reach as a mobility index for large and small landslides. Can. Geotech. J. 33, 260–271.

Cucchi V, Meredieu C, Stokes A, Berthier S, Bert D and Najar M 2004 Root anchorage of inner and edge trees of Maritime pine (*Pinus pinaster* Ait) growing in different soil podzolic conditions. Trees-Struct. Funct. 18, 460–466.

Dorren L K A 2003 A review of rockfall mechanics and modelling approaches. Prog. Phys. Geog. 27, 69–87.

Dorren L K A, Maier B, Putters U S and Seijmonsbergen A C 2004 Combining field and modelling techniques to assess rockfall dynamics on a protection forest hillslope in the European Alps. Geomorphology. 57, 151–167.

Dorren L K A and Berger F 2005. Stem breakage of trees and energy dissipation during rainfall impacts. In Press.

Dupuy L, Fourcaud T and Stokes A 2005 A numerical investigation into the influence of soil type and root architecture on tree anchorage. Plant Soil 278, 119–134.

Gardiner B A, Peltola H and Kellomaki S 2000 Comparison of two models for predicting the critical wind speeds required to damage coniferous trees. Ecol. Model. 129, 1–23.

Guyette R P and Stambaugh M C 2004 Post-oak fire scars as a function of diameter, growth, and tree age. Forest Ecol. Manag. 198, 183–192.

Hurand A and Berger F 2002 Forêts et risques naturels. Protection contre l'érosion, les mouvements de terrain et les avalanches. La Houille Blanche 3, 64–67.

Interreg III B 2001 Alpine Space Programme. General Document on the Community-Initiative Programme INTERREG III B.

Jahn J 1988 Entwaldung und Steinschlag, Interpraevent, Graz. Tagungspubl Bd.1,185–198.

Köstler J N, Brückner E, Bibelriether H (1968) Die Wurzeln der Waldbäume. Verlag Paul Parey, Hamburg & Berlin, Germany.

Kräuchi N, Brang P and Schönenberger W 2000 Forests of mountainous regions: gaps in knowledge and research needs. Forest Ecol. Manag. 132, 73–82.

Meunier S, Ruel J C, Laflamme G and Achim A 2002 Résistance comparée de l'épinette blanche et du sapin baumier au renversement. Can. J. Forest Res. 32, 642–652.

Moore J R 2000 Differences in maximum resistive bending moments of *Pinus radiata* trees grown on a range of soil types. Forest Ecol. Manag. 135, 63–71.

Motta R and Haudemand J C 2000 Protective forests and silvicultural stability. An example of planning in the Aosta Valley. Mt Res Dev. 20, 180–187.

Mickovski S B 2005 Decision support systems in eco-engineering: the case of the SDSS. *In* Eco- and Ground Bio-engineering: The Use of Vegetation to Improve Slope Stability. Eds. A Stokes, I Spanos, J E Norris and L H Cammeraat. Developments in Plant and Soil Sciences, Springer, Dordrecht. In press.

Ott E 1996 Guidelines for the protective role of forests in avalanche formation. Forstwiss Centralbl. 115, 223–230.

Peltola H, Kellomaki S, Hassinen A and Granander M 2000 Mechanical stability of Scots pine, Norway spruce and birch: an analysis of tree-pulling experiments in Finland. Forest Ecol. Manag. 135, 143–153.

Saurí D, Milego R, Canalís A, Ripoll A and Kleeschulte S 2003 Mapping the impact of recent natural disasters and technological accidents in Europe. Environmental Issue Report No. 35, European Environment Agency, Copenhagen, Denmark.

Shigo A L 1986 A new tree biology. Shigo & Tree Associates, Durham, New Hampshire, USA.

Stokes 1999 Strain distribution during anchorage failure in root systems of Maritime pine (*Pinus pinaster* Ait.) at different ages and tree growth response to wind-induced root movement. Plant Soil 217, 17–27.

Stokes A 2002 The biomechanics of tree root anchorage. *In* Plant Roots – The Hidden Half. Eds. Y Waisel, A Eshel and U Kafkaki. pp. 175–186. Plenum Publishing, New York.

Stokes A, Drexhage M and Guitard D G 2000 A method for predicting the site of failure in trees under mechanical loading. *In* The structural roots of trees and woody plants: form, function and physiology, Developments in Plant and Soil Sciences. Ed. A Stokes. pp. 279–285. Kluwer Academic Publishers, Dordrecht.

Stokes A, AbdGhani M, Salin F, Danjon F, Jeannin H, Berthier S, Kokutse A D and Frochot H 2006 Root morphology and strain distribution during overturning failure of trees on mountain slopes. *In* Eco- and Ground Bio-engineering: the Use of Vegetation to Improve Slope Stability, Developments in Plant and Soil Sciences. Eds. A Stokes, I Spanos, J E Norris and L H Cammeraat. Springer, Dordrecht. In press.

Stokes A, Mickovski S B and Thomas B R 2004 Eco-engineering for the long-term protection of unstable slopes in Europe: developing management strategies for use in legislation. *In* Landslides: Evaluation & Stabilization Vol. 2. Eds. W Lacerda, M Ehrlich, S A B Fontoura, A S F Sayao. Eds. pp. 1685–1690 A.A. Balkema Publishers, Rotterdam.

Tianchi L, Greminger P, Hofer T (2002) Hazards. Beyond The International Year of Mountains (on-line) URL: http://www.mountains2002.org/files/pdf/factsheets/Hazards-E.pdf.

Objective Comparison of Rockfall Models using Real Size Experimental Data

Frédéric Berger[1)] and Luuk Dorren[2)]
1) Cemagref Grenoble, 38402 St. Martin d'Hères, France (frederic.berger@cemagref.fr)
2) Cemagref Grenoble, 38402 St. Martin d'Hères, France (luuk.dorren@cemagref.fr)

Abstract

Consultancies using rockfall simulation software, as well as rockfall software developers, have been invited to use their simulation tools to predict the trajectories of 100 rocks in 2D or 3D using a digital elevation model of a site in the French Alps. These data have been compared with data obtained by real size rockfall experiments carried out the same site. Additional data provided to the participants were: the geographic location of the experimental site, the form and volume of the rocks used during the experiments and the locations of two calculation screens on the main path. Characterisation of the soil had to be done by the participants. At the calculation screens, each candidate had to calculate the mean and maximum velocity, kinetic energy and jump height of each rock. In addition, the stopping points of each rock had to be calculated. Eventually, 12 out of 17 candidates from 4 different countries sent back their results. Only 3 out of 12 were capable to simulate the same rockfall kinematics and trajectories with an error of ± 20%. Seven participants were capable to simulate the observed stopping distance with an error of ± 10%. The maximum errors were in the order of 400%. Among the commercial models involved, three of them were used by multiple participants. The outcomes of the test showed that two different users can obtain invalid or very accurate results with the same model. This indicates that the role of the expert is crucial in hazard expertises that use rockfall simulation models. Since this has been the first benchmarking test of its kind, the outcomes should be used with caution, as only one test site has been used. At another test site, results could be completely different. For natural hazard modelling in general, there is a need for accurate validation data.

Keywords: benchmarking, simulation model, natural hazard zoning

Introduction

In rockfall hazard prevention the use of rockfall trajectory simulation programs is common (Tianchi, 1983; Bozzolo and Pamini, 1986; Descoudres and Zimmermann, 1987; Pfeiffer and Bowen, 1989; van Dijke and van Westen, 1990; Azzoni et al., 1995; Stevens, 1998; Keylock and Domaas, 1999; Guzzetti et al., 2002; Dorren et al., 2006). Unfortunately, a wide range of model types exists, varying from 2D to 3D, statistical to deterministic based and all with different precision of the output (Dorren, 2003). This diversity, combined with the lack of precise information on the conditions of use of the different programs available, makes that the French users of trajectory studies have difficulties to identify the most adapted product to their needs. Therefore, we realised a benchmarking test of rockfall trajectory simulation programs (Berger et al., 2004). The realisation of such a blind test requires a set of reliable data.

The direction of risk and pollution prevention of the French ministry of Ecology and Sustainable Development decided to support this first benchmarking test. The data used for this test are coming from real-size rockfall experiments carried out by the Cemagref.

Objectives and public concerned

Two kinds of public are concerned by this benchmarking test:

- Research consultancies working in the field of rockfall hazard assessment using a trajectory simulation model.
- Project managers and all the other beneficiaries of expertises made with these models.

The interest of these groups is quite different. The first one wants, if the model has already been used for hazard assessment expertises, to guarantee its functioning or, if the model is under construction and not yet operational, to test it. The second group wishes to have information on the performance of currently existing models in a specified context of use for which real and reliable field data exist. The comparison of results

pp. 245–252 ©2006 by Universal Academy Press, Inc. / Tokyo, Japan

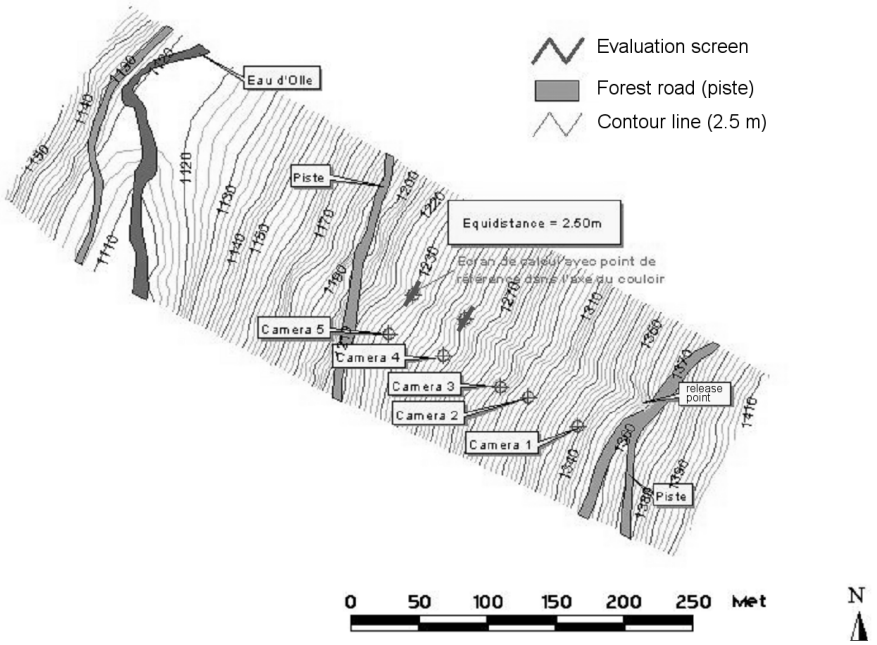


Fig. 1. Map showing the topography of the experimental site

proposed in our test has as objective to provide information to the different participants and not to provide a ranking of the results, the models used and even less to make a certification, or an agreement.

Since there is only one set of data representative for one specific site, the present test cannot, in any case, be used as a basis for a ranking of the different products. But the analysis of the results will permit to:

1. Understand the potential differences between the results coming from simulations and those measurement of real rockfall events
2. Realise a first critical analysis of a benchmarking test on trajectory models using well documented real size rockfall experiments
3. Provide the research consultancies and project managers with a first anonymous panorama on the products used and this in terms of software families and anonymous comparative information on the difference between simulation results and real data.

A future operation of model or program certification has to separate the quality of the model itself and the expertise of the model user. Both determine the accuracy of the model output. In this test we were aware of the fact that the trajectory simulation results are to a large extent determined by the operators. Therefore, this is another reason why this test cannot be used to certify or rank trajectory simulation models according to their quality or accuracy of their output.

General principle of the benchmarking test

Since 2001, the Cemagref carries out real size rockfall experiments at an experimental site, using high-speed digital video cameras to film trajectories of falling rocks that are released by a Caterpillar digger (Dorren et al., 2005). We released 100 rocks and mapped their trajectories, their deposit points and we measured their velocities as well as their passing heights. These data have been used to realise this benchmarking test.

Only the data on the location of the experimental site, its topography (in the form of a high resolution digital terrain model, as well as the contour lines with an equidistance of 2.5 m, see Fig. 1) and the characteristics of used rocks (number, volume, size, form, weight) were given to the participants (Berger et al., 2004).

The participants were supposed to characterise the soil and its energy dissipative capacity their selves (Azzoni and de Freitas, 1995; Chau et al., 2002; Dorren et al., 2004; Dorren et al., 2006). The rocks used during the experiments were all removed from their original deposit positions in order to prevent the candidates to realize retro calculations. The choice of the number of simulated rocks was left to them. After finalising the

Table 1. Values observed at the two evaluation screens.

	Rebound height (m)				Velocity (m/s)				Kinetic energy (kJ)			
	Max.	Min.	Mean	Std.	Max.	Min.	Mean	Std.	Max.	Min.	Mean	Std.
Screen 1	5,0	0,0	1,4	1,1	28,1	1,8	12,5	5,2	786,4	3,3	204,9	168,8
Screen 2	6,2	0,0	1,6	1,4	28,9	4,5	13,8	5,5	958,3	21,1	244,5	196,3
Measurement error	+/- 5%				+/- 5%				+/- 15%			

test, each participant received 1) a comparison of their own results with the real data and 2) an anonymous table showing the ranges of errors of the data simulated by all the participants.

The benchmark test consisted of 6 distinct steps:

1. Advertisement to participate at the benchmarking test
2. Application of the candidates
3. Receipt of the candidatures and transmission of the initial data to the candidates
4. Receipt of the data calculated by the participants
5. Comparison of the calculated data with the observed ones
6. Synthesising the results in a report and passing it to the participants for feedback as well as an agreement to publish the synthesised results to the ministry.

A steering committee was formed to assure a fair course of the test.

Required simulation results

The results we required from their simulations were the spatial distribution of the deposit points of all the simulated rocks and possibly the delimitation of the maximal rockfall runout area from the starting point, while explaining the extrapolation method used for delimiting this area. In this benchmarking test, this area is defines as the maximal rockfall envelope. The scale of the output map is 1: 2500. Other required data were the simulated translation velocities (m s−1), the vertical passing heights (m) and the kinetic energy (kJ) at two "evaluation screens". Evaluation screen 1 is located after 185m from the starting point, measured over the slope and evaluation screen 2 is located after 235 m. These data were compared to those obtained during the real sizes experiments. The results should be presented in a table giving the statistical distribution of the required variables (minimal value, maximal value, average value and the standard deviation), as well as a diagram showing the passing height and the velocity versus the mass of the rocks.

Comparison of simulated and real data

In total 22 candidates expressed their interest in the benchmarking test and finally 12 participants sent back their simulated results. In the following text, numbers will be used for the 12 participants to guarantee anonymity. These numbers correspond to the sequence of incoming results at our institute. Important information for interpreting the results of the test is that:

- Participant 9 and 13, participant 12 and 17 as well as participant 14 and 15 used the same commercial rockfall trajectory program.
- Participant 7, 9 and 15 used programs that they considered not to be operational.

Comparison at the two evaluation screens

Firstly, we compared the simulated data with the observed data presented in Table 1. The values observed are the values obtained with the real-size experiments. Secondly, we calculated a ratio that represents the difference between the simulated and observed value (Table 2). This ratio corresponds to: simulated value * 100 / observed value. A ratio higher than 100% represents overestimation, while a value lower than 100% represents underestimation.

Table 2. Comparison between observed and simulated values expressed in ratios

	Ratio Vmax Screen1	Ratio Vmax Screen 2	Ratio Hmax Screen 1	Ratio Hmax Screen 2	Ratio Emax Screen 1	Ratio Emax Screen 2
Part. 1	103	92	135	143	91	101
Part. 2	102	97	63	109	n.a.	n.a.
Part. 4	49	36	91	70	12	14
Part. 7	138	124	535	732	n.a.	n.a.
Part. 8	57	56	56	65	37	34
Part. 9	39	32	0	0	18	15
Part. 11	72	73	42	54	74	78
Part. 12	37	24	4	6	8	16
Part. 13	69	63	38	37	73	72
Part. 14	78	77	79	69	87	79
Part. 15	183	172	101	109	472	513
Part. 17	90	81	117	113	87	96

Comparison of the simulated trajectories

Fig. 2 presents a map with the deposit points of the 100 rocks. Basically, three main propagation axes were observed, which are presented in Fig. 3. Rock 41 (Dimensions : $120 \times 100 \times 70$ cm, 0,84 m^3, being 2350 kg) travelled the longest distance from the starting point: planimetric distance travelled was 391.20 m. It descended from 1365 m to 1119.85 m.

Regarding the stopping points the candidates expressed their results according to the altitudes or coordinates representative of a significant change of the propagation of the simulated rocks. The presentation of the data provided by the participants differed strongly from one candidate to another. Some participants gave theirs result even only on paper graphs. Therefore, to be able to compare the stopping points calculated by the candidates with those observed in reality, we presented our results and those of the candidates by altitude classes. We calculated the percentage of rocks reaching an altitude class. This calculation represents the first stage in the analysis of these data. The second stage consisted in expressing the altitude classes of in X-coordinates, in order to present the percentage of blocks reaching a given X-coordinate on the topographic profile. For that, we decided to calculate the planimetric travelled distances by projecting the stopping points on the propagation axis 2 in Fig. 3. This profile corresponds to the one that was mainly used by the candidates. From those data we could calculate and compare the distance classes of the stopping points (Table 3).

Discussion and conclusions

Regarding the degree of participation (12 participants from 4 countries) this first rockfall trajectory simulation program benchmarking test using data from real-size rockfall experiments can be considered as a success. It is important to repeat once more that the results of this test are only valid for the topographical conditions at our experimental site and the conditions of the terrain at the time of carrying out the experiments.

The steering committee of the test has decided, looking at the measurement error of the kinetic energy (+/− 15%), to fix the criteria of acceptance for the simulated values to correspond to the observed values as being those values with a ratio between 80% and 120%.

Table 4 presents the simulated results expressed in ratio differences. These values are calculated as follows: ratio difference = 100% — ratio of the participant (ratio between the simulated and observed value). The calculated values that are considered to correspond with observed values are those within the interval [−20%, 20%]. The negative values represent a n underestimation, the positive values an overestimation. To facilitate the reading of this table, we presented the results in decreasing order of the number of times a value did not fall in the interval [−20%, 20%]. This table does not represent a classification or ranking of the participants. It only provides information on how well the model performed at our experimental site.

According to this table, the general conclusions of this benchmarking test are (Berger et al., 2004):

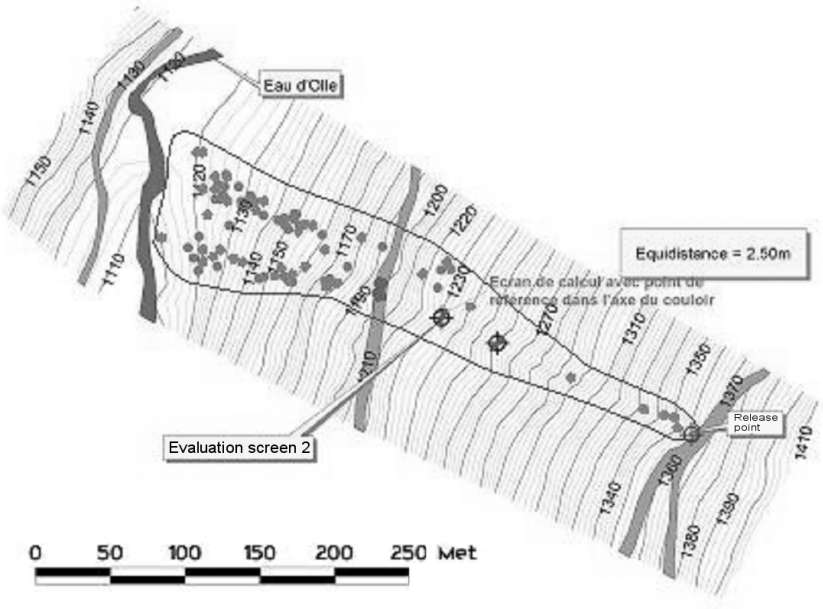


Fig. 2. Map showing the stopping points of the 100 released rocks.

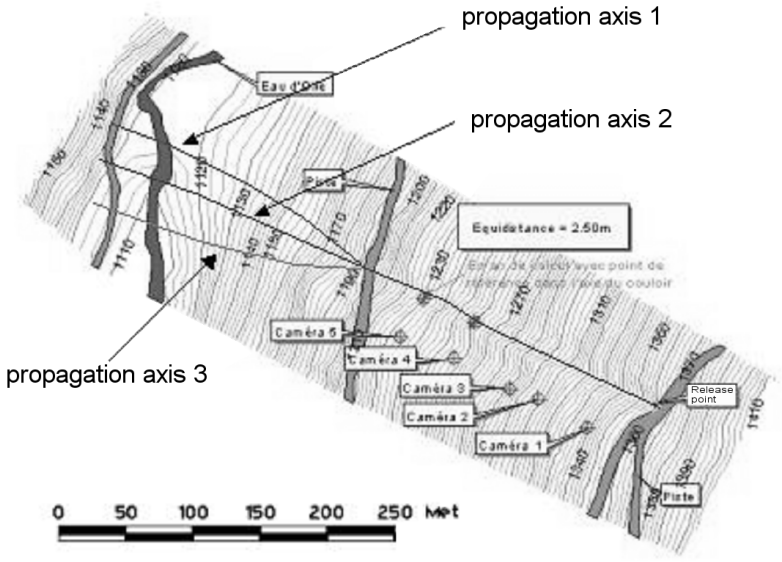


Fig. 3. Map showing the three general rockfall propagation axes.

- Concerning the calculation of rockfall kinematics: the results vary significantly. There is a global tendency to underestimate the passing height, the translational velocity and the translational kinetic energy. Regarding a rockfall protection scenario, i.e. using the data for dimensioning protective structures, only 3 participants out of the 12 have results that correspond to the experimental data (+/− 20%).
- Concerning the propagation calculation: 7 participants out of the 12 have obtained stopping distance corresponding at least to the observed one. Taking into account the protection scenario, these participants are able to propose a zoning including at least the maximal stopping distance observed.
- If we combine the kinematics and propagation calculations (disregarding the participant 2 for whom we don't have results on the energy), it appears that:
  - The participants who obtained a stopping distance in adequacy with the observed one (reaching but not over-passing the distance class of 385–400 m), have kinematic results that differ from the

Table 3. Results obtained by the participants regarding the maximal stopping point.

	Observed value		Part. 2	Part. 4	Part. 7	Part. 8	Part. 9	Part. 11	Part. 12	Part. 13	Part. 14	Part. 15	Part. 17
Max. reached distance	390		385	360	355	395	355	365	395	275	390	400	430
Simulated ñ observed distance	0		-5	-30	-35	5	-35	-25	5	-115	0	10	40
Distance Ratio (simulated/ observed	100%		99%	92%	91%	101%	91%	94%	101%	71%	100%	103%	110%
Probability of reaching 385-400 m (%)	4				0	7	0	0	20	0	2	100	11
Probability of depassing 385-400 m (%)	0	1				0			0		0	0	7
Probability ratio (simulated/ observed)	100%				0%	175%	0%	0%	500%	0%	50%	2500%	275%

ones observed. This accounts for 5 participants out of the 12.

– The opposite, i.e. propagation result different than the one observed and adequate kinematics is not verified.

  * Only, the participants having obtained a stopping distance longer than the one observed, have kinematics results that correspond most to the observed ones. This accounts for 2 participants out of the 12.
  * The participants having obtained a stopping distance shorter than the one observed (5 participants out of the 12), under-estimated the rockfall kinematics.

- Only 1 participant obtained results within the accuracy interval of −20%–20%, for the 6 kinematics parameters.
- The participants using the same commercial software obtain very different results. Consequently, we conclude that "human" expertise of the user/operator plays a substantial role.

For the 12 candidates, it showed that the trajectographic assessment performed within this test is most accurate for the calculation of the rockfall runout zone (7 participants out of 12) than for the calculation of the rockfall kinematics (3 participants out of 12).

Taking into account the dispersion of the results obtained, it's necessary that the results obtained within trajectographic studies are careful and clearly presented as only one of the elements intervening in the chain of decision-making of the expert.

This test has also allowed us to identify the weak points of the procedure that was initially established. Due to the choice to realise a blind test, the participants could not collect the whole set of the data required for a retro calculation of their trajectory simulation models. Thus, the participants were confronted with the most unfavourable situation that one could meet in reality. This underlines the difficulty of the exercise. In the future we would probably consider not carrying out the test completely blind, e.g., by leaving behind some witnesses (rock impacts, rocks at their original stopping point).

Table 4. Synthesis of the simulated results of all participants.

	ratio differences vmax Ecran1	ratio differences Vmax Ecran2	ratio differences Hmax Ecran 1	ratio differences Hmax Ecran 2	ratio differences Ecmax Ecran1	ratio differences Ecmax Ecran2	ratio differences sur la distance	Probability of reaching 385-400m	Depassing 385-400m
Part. 17	-10%	-19%	17%	13%	-18%	-4%	10%	Yes	Yes
Part. 1	3%	-8%	35%	43%	-9%	1%	4%	Yes	Yes
Part. 2	2%	-3%	-37%	9%			-1%	Yes	No
Part. 15	83%	72%	1%	9%	372%	413%	3%	Yes	No
Part. 14	-22%	-23%	-21%	-31%	-13%	-21%	0%	Yes	No
Part. 8	-43%	-44%	-44%	-35%	-63%	-66%	1%	Yes	No
Part. 12	-63%	-76%	-96%	-94%	-92%	-84%	1%	Yes	No
Part. 4	-51%	-64%	-9%	-30%	-88%	-86%	-8%	No	
Part. 11	-27%	-28%	-58%	-46%	-26%	-22%	-6%	No	
Part. 7	38%	24%	435%	632%			-9%	No	
Part. 9	-61%	-68%	-100%	-100%	-82%	-85%	-9%	No	
Part. 13	-31%	-37%	-62%	-63%	-27%	-28%	-29%	No	

Ratio difference between -20% and 20%

Ratio difference not in the interval -20% - 20%

Data not provided by the participant

If such an operation should be repeated, it will be necessary that the participants can have access to the site before and after the experiments. Consequently, the call for participation should be carried out before the realisation of the real sizes experiments.

Moreover, a preliminary meeting, associating both financiers and the participants, will be necessary to determine the protocol that has to be employed. Especially, the following should be defined:

- the data to be calculated
- the parameters describing the rocks
- the data formats
- the presentation of the results
- whether an anonymous procedure is required
- the final presentation of the outcomes of the benchmark test

This last point will optimize the phase of examination and analysis of the results.

In the future, the optimization of such operations and know-how in this field will require the (international) creation of a working group, network or association of the technical community, potential clients and scientists. This will enable exchanging data, sharing know-how and formalising technical needs, as well as scientific ones. Before doing this, we should investigate if there is a real need and willingness for such a working group, a network or association.

References

Azzoni, A. and Freitas, M.H. de, 1995. Experimentally gained parameters decisive for rock fall analysis. Rock mechanics and rock engineering, 28(2): 111–124.

Azzoni, A., Barbera, G.L. and Zaninetti, A., 1995. Analysis and prediction of rockfalls using a mathematical model. *Int. J. Rock Mech. Min. Sci.* 32:709–724.

Berger, F. et al. (2004) *Réalisation d'un test d'étalonnage des modèles de trajectographie en utilisant des données provenant d'expérimentations grandeur nature.* Cemagref:86 pp.

Bozzolo, D. and Pamini, R., 1986. Simulation of rock falls down a valley side. *Acta Mechanica* 63: 113–130.

Chau, K.T., Wong, R.H.C. and Wu, J.J., 2002. Coefficient of restitution and rotational motions of rockfall impacts. *Int. J. Rock Mech. Min. Sci.* 39(1):69–77.

Descoeudres, F. and Zimmermann, T., 1987. Three-dimensional dynamic calculation of rockfalls. In: G. Herget and S. Vongpaisal (Editors), *Proc. Sixth International Congress on Rock Mechanics.* A.A. Balkema, Rotterdam, Montréal, pp. 337–342.

Dorren, L.K.A., 2003. A review of rockfall mechanics and modelling approaches. *Prog. Phys. Geog.* 27(1): 69–87.

Dorren, L.K.A., Maier, B., Putters, U.S. and Seijmonsbergen, A.C., 2004. Combining field and modelling techniques to assess rockfall dynamics on a protection forest hillslope in the European Alps. *Geomorphology* 57(3-4): 151–167.

Dorren, L.K.A., Berger, F., LeHir, C., Mermin, E., Tardif, P. (2005) Mechanisms, effects and management implications of rockfall in forests. *For. Ecol. Manage.* 215 (1-3):183–195.

Dorren, L.K.A., Berger, F. and Putters, U.S., 2006. Real size experiments and 3D simulation of rockfall on forest slopes. *Nat. Haz. Earth Sys. Sci.* 6:145–153.

Guzzetti, F., Crosta, G., Detti, R. and Agliardi, F., 2002. STONE: a computer program for the three-dimensional simulation of rock-falls. *Comp. Geosci.* 28(9):1079–1093.

Keylock, C. and Domaas, U., 1999. Evaluation of topographic models of rockfall travel distance for use in hazard applications. *Art. Antarc. Alp. Res.* 31(3): 312–320.

Pfeiffer, T.J. and Bowen, T.D., 1989. Computer simulation of rockfalls. *Bull. Ass. Eng. Geol.* XXVI(1):135–146.

Stevens, W.D., 1998. *Rocfall: a tool for probabilistic analysis, design of remedial measures and prediction of rockfalls.* Department of Civil Engineering, University of Toronto, Ontario, Canada.

Tianchi, L., 1983. A mathematical model for predicting the extent of a major rockfall. *Zeit. Geom. N.F.* 27(4):473–482.

Van Dijke, J.J. and van Westen, C.J., 1990. Rockfall hazard: A geomorphological application of neighbourhood analysis with ILWIS. *ITC Journ.* 1: 40–44.

> Summary

Zusammenfassung / Résumé / Samenvatting



> Summary

In the Alps, a wide range of protective measures against rapid mass movements such as avalanches, rockfall and landslides, can be identified, varying from forests to different engineered structures. To fully use the potential of mountain forests to protect against natural hazards, it is critical to be able to quantify the protective function of a forest. The large goal of the last 10 years of my research has been to develop methods and tools that enable such quantification and that assess the rockfall hazard at a given site taking into account the protective effect of forests. Thereby, I used methods that focused on the rockfall process, where the forest is considered as a process constraint and methods that focused on translating forest characteristics directly into a protective capacity. This habilitation consists of 13 chapters, of which the first one presents the general framework. The following chapter gives a very general introduction in protection forests (forests that have an explicit protective function against natural hazards) in the Alps. Subsequently, the natural hazard rockfall is introduced in a literature review. The following chapter evaluates the capacity of two existing GIS-based models and a distributed, process-based model called RockyFor, developed by myself. To study the effect of the forest parameters and the slope characteristics on the rockfall process more in detail, we applied a combined approach in chapter 5, using field techniques and model simulations with RockyFor. In Chapter 6, we investigate whether the new version of RockyFor, which was further developed for rockfall assessment at slope scale, using detailed input data with a resolution of 2.5m × 2.5m, could be used for rockfall assessment at the regional scale, using low resolution input data. The results show that simulating rockfall runout zones with a distributed model using regional data is realistic and feasible. Chapter 7 then presents real size rockfall experiments and quantifies velocities, rebound heights as well as the residual hazard of rockfall on a forested and a non-forested slope. It also evaluates existing rockfall protection forest management guidelines. The next chapter presents the development of a function that describes the capacity of different tree species to dissipate the energy imposed by rockfall. After implementation of this developed function in the RockyFor model, the simulation results are being compared with the data obtained from the real size rockfall experiments in chapter 9. In addition, this chapter presents a method for quantifying and modelling slope surface characteristics based on the field measurements. Chapter 10 describes three additional tests with the RockyFor model, in which we compared the simulation results with empirical data on tree impacts from three different mountain forests in Switzerland. Chapter 11 explains the underlying principles as well as the calculation methods of a simple tool that determines the optimal density and mean DBH of a rockfall protection forest, taking into

account given forest and site characteristics, as well as the size and energy of the falling rock, and which quantifies the protective capacity of the given forest in parallel. The following chapter summarises all the previously presented and similar work in a state of the art paper on the available scientific knowledge and practical methods in the field of rockfall and protection forest. The final chapter takes up one of the research challenges mentioned in the previous review and investigates the use of LiDAR (Light Detection And Ranging, or laserscanning) data for describing forest structure in 3D. Here landscape metrics are applied to a normalised canopy model (nCM) for automatically characterising forest structure. From the work presented in this habilitation, it can be concluded that mountain forests play a very important role in protection against rockfall. Their protective effect should therefore be taken into account in all rockfall hazard analyses. From this work, I realised that without the combination of field observations, simulation models and rockfall experiments, significant progress in the following subjects would not have been possible: the realistic integration of trees in 3D models, the development of a representative and useful rockfall rebound algorithm, the further development of silvicultural guidelines for rockfall protection forests, and an improvement of the knowledge on the modes of motion on different slope gradients.

> Zusammenfassung

In den Alpen existiert eine große Auswahl an Schutzmassnahmen gegen gravitative Massenbewegungen wie Lawinen, Steinschlag und Rutschungen. Diese Auswahl reicht von Schutzwaldpflege bis zu technischen Verbauungen. Um das Schutzpotential des Waldes vollständig zu nutzen, ist es notwendig, die Schutzfunktion eines bestimmten Waldzustandes quantifizieren zu können. Das wichtigste Ziel meiner Forschungen der letzten 10 Jahre war es, Methoden und Instrumente zu entwickeln, welche diese Quantifizierung ermöglichen und welche die Steinschlaggefahr an einem Hang unter Einbezug der Schutzfunktion des Waldes beurteilen können. Dazu habe ich zwei verschiedene methodische Ansätze angewandt: Erstens, Methoden, die auf den Steinschlagprozess fokussiert sind und den Wald als eine Prozesseinschränkung miteinbeziehen. Zweitens, Methoden, welche die Waldeigenschaften direkt in eine Steinschlagschutzfunktion umsetzen. Diese Habilitation besteht aus 13 Kapiteln, von denen das erste den allgemeinen Rahmen absteckt. Das darauffolgende Kapitel führt in das Thema Schutzwald als Wald mit ausdrücklicher Schutzfunktion gegen Naturgefahren ein. Anschließend folgt eine Einführung in die Naturgefahr Steinschlag in Form einer Literatur-Review. Das nächste

Kapitel bewertet die Kapazität von zwei bestehenden regionalen, GIS-basierten Steinschlagmodellen und vergleicht diese mit einem von mir entwickelten Simulationsmodell, genannt RockyFor. Zur Untersuchung des Einflusses der Wald- und Hangeigenschaften auf den Steinschlagprozess, verwenden wir in Kapitel 5 einen kombinierten Ansatz von Geländetechniken und Modellsimulationen mit RockyFor. In Kapitel 6 untersuchen wir, ob das auf Einzelhang-Ebene weiter entwickelte Modell RockyFor, auch für eine Steinschlaganalyse auf regionaler Ebene unter Verwendung von geringer aufgelösten Daten verwendet werden kann. Die Ergebnisse zeigen, dass die Simulation der maximalen Steinschlagauslaufdistanzen mit regionalen Daten auch realistisch umsetzbar ist. Kapitel 7 präsentiert zunächst reale Steinschlagexperimente im Wald und quantifiziert Geschwindigkeiten, Sprunghöhen und Auslaufdistanzen auf einem bewaldeten und einem unbewaldeten Hang. Darüber hinaus werden bestehende Steinschlagschutzwald-Bewirtschaftungsrichtlinien analysiert und die ihnen zugrunde liegenden Kriterien bewertet. Das nächste Kapitel stellt die Entwicklung einer Funktion vor, welche die Energieaufnahmekapazität von verschiedenen Baumarten beschreibt. Nach Integration dieser Funktion im RockyFor Modell, werden in Kapitel 9 die Simulationsergebnisse mit den Daten aus den Steinschlagexperimenten verglichen. Dazu wird in diesem Kapitel eine Methode präsentiert, die es erlaubt, die Hangoberflächebeschaffenheit anhand von Geländemessungen zu quantifizieren und modellieren. Kapitel 10 präsentiert drei zusätzliche Tests mit dem RockyFor Modell, in welchen die Simulationsergebnisse mit empirischen Daten über Baumtreffer in drei verschiedenen Bergwäldern in der Schweiz verglichen werden. Kapitel 11 erklärt die zugrunde liegenden Prinzipien und die Berechnungsmethoden eines einfachen Werkzeuges, das die optimale Stammzahl und den mittleren Brusthöhendurchmesser eines Steinschlagschutzwaldes berechnet. Diese Berechnung berücksichtigt die gegebenen Wald- und Hangeigenschaften, sowie die Größe und die Energie des fallenden Blockes. Das folgende Kapitel fasst alle zuvor vorgestellten und verwandte Forschungsarbeiten in einem „State of the Art“ Artikel über die verfügbaren wissenschaftlichen Kenntnisse und praktischen Methoden im Bereich Steinschlag und Schutzwald zusammen. Das letzte Kapitel behandelt eine der im vorigem Kapitel erwähnten Forschungsherausforderungen, und untersucht die Verwendung von LIDAR (Light Detection And Ranging, oder Laserscanning) Daten für die automatische Beschreibung von Waldstrukturen. Hier werden auf Basis eines normalisierten Kronenmodells die Waldstrukturen mittels „Landscape Metrics“ automatisch berechnet. Aus den Arbeiten, welche in dieser Habilitationsschrift vorgestellt werden, lässt sich der Schluss ziehen, dass der Wald eine sehr wichtige Schutzfunktion hat. Diese Schutzwirkung soll deshalb in jeder Steinschlaggefahrenbeurteilung berücksichtigt werden. Aus dieser Arbeit ist mir klar geworden,

dass ohne die Kombination von Feldbeobachtungen, Simulationsmodellen und Steinschlag-Experimenten, folgende signifikante Fortschritte nicht möglich gewesen wären: die realistische Integration von Bäumen in 3D-Steinschlagmodellen, die Entwicklung von einem anwendbaren Steinschlag-Aufprall-Algorithmus, die Weiterentwicklung detaillierter waldbauliche Empfehlungen für Steinschlag-Schutzwälder, und das bessere Verständnis über die Art der Bewegung auf verschiedenen Hangneigungen.

> Résumé

Dans les Alpes, il existe une grande variété de mesures protectrices pour les mouvements gravitaires rapides comme des avalanches, des chutes de pierres et des glissements de terrain, allant des forêts de protection à différents ouvrages. Afin d'utiliser le potentiel des forêts de montagne de protéger contre les risques naturels, il est essentiel d'être en mesure de quantifier la fonction protectrice de la forêt. Le grand objectif des 10 dernières années de ma recherche a été de mettre au point des méthodes et des outils pour faire cela et d'évaluer les risques de chutes de pierres sur un site donné en prenant en compte de l'effet protecteur des forêts. Ainsi, j'ai utilisé des méthodes focalisées sur le processus de chutes de pierres, où la forêt est considérée comme une contrainte et j'ai utilisé des méthodes concentrées sur une traduction directe des caractéristiques des forêts en une capacité de protection. Cette habilitation est composée de 13 chapitres, dont la première présente le cadre général. Le chapitre suivant donne une introduction très générale des forêts de protection (des forêts qui ont une fonction explicite de protection contre les risques naturels) dans les Alpes. Ensuite, l'introduction du sujet de chutes de pierres est présentée dans une revue de la littérature en chapitre 3. Le chapitre suivant évalue la capacité des modèles de chutes de pierres basée sur des Systèmes d'Information Géographiques (SIG) existantes et les comparent avec un modèle de simulation de chutes de pierres développé par moi-même, nommé RockyFor. Pour étudier plus en détail l'effet de la forêt et les paramètres caractéristiques de la pente sur le processus de chutes de pierres, nous avons appliqué une approche combinée dans le chapitre 5, en utilisant les techniques de terrain et des simulations avec le modèle RockyFor. Le chapitre 6 évalue si la nouvelle version de RockyFor, qui a été développée pour l'évaluation du risque de chutes de pierres à l'échelle d'une pente et, par conséquent, en utilisant des données d'entrée avec une haute résolution, pourrait être utilisé pour une évaluation à l'échelle régionale, en utilisant des données d'entrée avec une faible résolution. Les résultats montrent que la simulation de la distance d'arrêt de chutes de pierres en utilisant des données régionales est réalisable. Le chapitre 7 présente ensuite des expériences grandeur nature

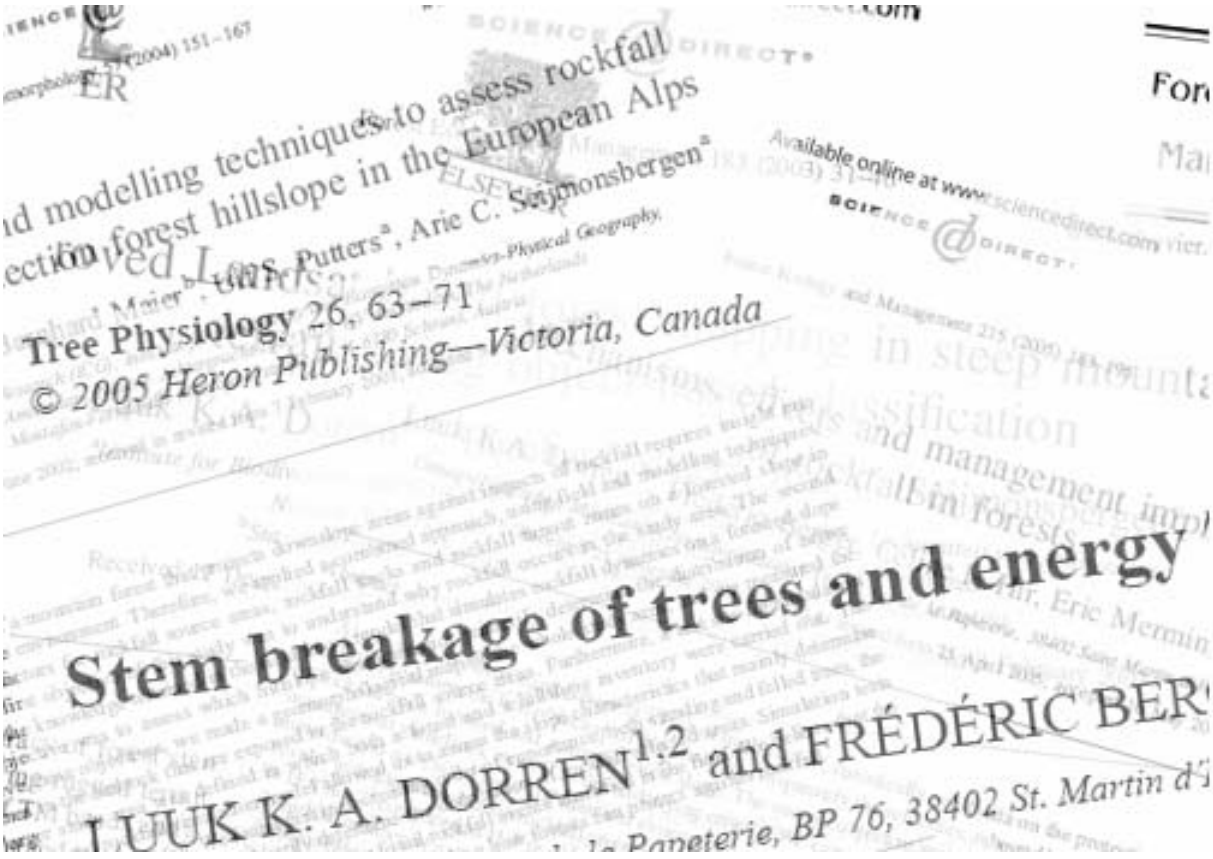
de chutes de pierres et quantifie les vitesses, les hauteurs de rebond ainsi que le risque résiduel de pierres et ce sur des sites ayant la même pente mais l'un est boisé et l'autre non. Il évalue également des recommandations de gestion des forêts de protection de chutes de pierres existantes. Le chapitre suivant présente la mise au point d'une fonction qui décrit la capacité des différentes espèces d'arbres à dissiper l'énergie imposée par pierres. Ayant développé et intégré cette fonction dans le modèle RockyFor, les résultats des simulations sont comparés avec les données obtenues à partir des expériences grandeur nature de chutes de pierres dans le chapitre 9. En outre, ce chapitre présente une méthode pour la quantification et la modélisation des caractéristiques de la surface de la pente basée sur des relevés de terrain objectifs. Le chapitre 10 présente trois essais supplémentaires avec le modèle RockyFor, dans lesquelles nous avons comparé les résultats de simulation avec des impacts sur les arbres dans trois forêts différentes en Suisse. Chapitre 11 explique les principes ainsi que les méthodes de calcul d'un outil simple qui détermine la densité optimale et le diamètre moyen à hauteur de poitrine d'une forêt de protection de chutes de pierres, en tenant compte des caractéristiques du site et de la forêt, ainsi que la taille et l'énergie des pierres. En parallèle, cet outil quantifie la capacité de protection de la forêt actuelle. Le chapitre suivant résume tous les travaux présentés précédemment ainsi que des travaux similaires dans un état de l'art des connaissances scientifiques et des méthodes pratiques disponibles dans le domaine de chutes de pierres et la forêt de protection. Le dernier chapitre reprend l'un des « challenges » de recherche mentionné dans le précédent chapitre et étudie l'usage des données LiDAR (Light Detection And Ranging, ou Laserscanning) pour décrire la structure forestière en 3D. Dans ce chapitre, des « landscape metrics » sont appliqués à un modèle normalisé de la canopée pour la caractérisation automatique de la structure forestière. A partir du des travaux présentés dans cette habilitation, il peut être conclu que les forêts de montagne ont un rôle important dans la protection vis-à-vis des chutes de pierres. C'est pourquoi l'effet des forêts devrait être prise en compte dans toutes les analyses de risques de chutes de pierres. De ce travail, je me suis rendu compte que, sans la combinaison des observations sur le terrain, des modèles de simulation et des expériences de chutes de pierres, les développements suivants n'aurait pas été possible : l'intégration réaliste des arbres dans des modèles 3D, le développement d'un algorithme de rebond, des guides des sylvicultures détaillés pour les forêts de protection de chutes de pierres, et une meilleure connaissance sur les modes de mouvements sur différents pentes.

> Samenvatting

In de Alpen vindt men een breed scala van beschermende maatregelen tegen gravitatieve massabewegingen zoals lawines, vallend gesteente (*rockfall* in het engels) en aardverschuivingen, variërend van bossen tot verschillende technische bouwwerken. Om de beschermende funkties van bergbossen tegen natuurgevaren volledig te benutten, is het essentieel om de beschermende functie van een bos te kunnen kwantificeren. Het belangrijkste doel van de laatste 10 jaar onderzoek was het ontwikkelen van methoden en instrumenten die een dergelijke kwantificering mogelijk maken en en die in staat zijn de gevaren van vallend gesteente op een bepaalde locatie in te schatten, daarbij rekening houdend met het beschermende effect van bergbossen. Daarbij gebruikte ik methoden die gericht zijn op het process van vallend gesteente zelf, waarbij het bos wordt beschouwd als een proces beperking. Daarnaast gebruikte ik methoden die gericht zijn op de directe vertaling van boskenmerken in een beschermende capaciteit. Dit habilitatieschrift bestaat uit 13 hoofdstukken, waarvan het eerste het algemeen kader presenteert. Het volgende hoofdstuk geeft een zeer algemene inleiding in "beschermbossen" (bossen met een expliciete beschermende functie tegen natuurgevaren) in de Alpen. Vervolgens wordt het natuurgevaar vallend gesteente ingeleid door middel van een literatuurstudie. Het volgende hoofdstuk evalueert de capaciteit van de bestaande Geografisch Informatie Systeem (GIS) -gebaseerde "rockfall" modellen en een proces gebaseerd simulatie model, het zogenaamde RockyFor, ontwikkeld door mijzelf. Om het effect van het bosparameters en de helling-eigenschappen op het proces vallend gesteente in detail te onderzoeken hebben we in hoofdstuk 5 gekozen voor een gecombineerde aanpak van veld technieken en simulaties met het model RockyFor. In hoofdstuk 6 onderzochten we, of de nieuwe versie van RockyFor, die werd ontwikkeld voor een gevarenanalyse op helling schaal, en dus met behulp van gedetailleerde input data, zou kunnen worden gebruikt voor een nauwkeurige analyse op regionale schaal, met behulp van input-gegevens van slechtere kwaliteit. Uit de resultaten blijkt dat dit realistisch en haalbaar is. Hoofdstuk 7 beschrijft vervolgens "rockfall" experimenten, die op ware grootte uitgevoerd zijn, en kwantificeert snelheden, spronghoogten, alsook de afgelegde afstanden van de vallende stenen op een beboste en een niet-beboste helling. Ook worden in dit hoofdstuk bestaande aanbevelingen geevalueert voor het beheer van bossen die beschermen tegen vallend gesteente. Het volgende hoofdstuk behandeld de ontwikkeling van een functie die de enerie opname capaciteit van verschillende boomsoorten beschrijft. Na de integratie van deze ontwikkelde functie in het RockyFor model, worden in hoofdstuk 9 de simulatie-uitkomsten vergeleken met de gegevens verkregen uit de vallend gesteente experimenten op ware grootte. Daarnaast beschrijft dit hoofdstuk een methode voor

het kwantificeren en modelleren van hellingoppervlakte-eigenschappen gebaseerd op veldgegevens. Hoofdstuk 10 beschrijft drie testen met het RockyFor model, waarin de simulatie-uitkomsten worden vegeleken met empirische gegevens over de boominslagen door vallende stenen in drie verschillende bergbossen in Zwitserland. In hoofdstuk 11 worden de basisprincipes en berekeningsmethoden uitgelegd van een eenvoudig instrument voor het bepalen van de optimale dichtheid en de gemiddelde diameter van bossen die beschermen tegen vallend gesteente. Hierbij wordt rekening gehouden met de kenmerken van de helling en het bos, evenals de grootte en de energie van de vallende stenen. Daarnaast kwantificeert het instrument de beschermende werking van het gegeven bos. Het volgende hoofdstuk geeft een overzicht van alle eerder gepresenteerde en soortgelijke studies in een "state of the art" artikel over de beschikbare wetenschappelijke kennis en praktische methoden op het gebied van vallend gesteente en beschermbossen. Het laatste hoofdstuk behandeld een van de onderzoeksuitdagingen die in het vorige hoofdstuk genoemd zijn en gaat over het gebruik van LiDAR (Light Detection And Ranging, ofwel laserscanning) gegevens voor het automatisch beschrijven van bosstructuren in 3D. Daartoe worden in deze studie "landscape metrics" toegepast op een genormaliseerd kronendak model. Op basis van de studies die zijn opgenomen in dit habilitatieschrift, kan worden geconcludeerd dat bossen een zeer belangrijke rol spelen in de bescherming tegen vallend gesteente en hun beschermde rol daarom in elke "rockfall" gevarenanalyse meegenomen moet worden. Door deze arbeid is het mij duidelijk geworden dat zonder de gecombineerde aanpak van veldopnamen, simulatie modellen en "rockfall" experimenten, de volgende ontwikkelingen niet mogelijk geweest zouden zijn: de realistische integratie van bomen in 3D simulatie modellen, de ontwikkeling van een representatief en objectief algoritme voor de berekening van het opspringen van vallende stenen na een inslag op de helling, de verbetering van aanbevelingen voor het beheer van bossen die beschermen tegen vallend gesteente en een betere kennis over de voortbeweging van vallende stenen op hellingen met verschillende steilheden.

> Publication list



> Articles in scientific journals (peer reviewed)

1. Bigot, C., Dorren, L.K.A., Berger, F., 2009. Quantifying the protective function of a forest against rockfall for past, present and future scenarios using two modelling approaches. Natural Hazards 49(1): 99-111.

2. Bourrier, F., Dorren, L.K.A., Nicot, F., Berger, F., Darve, 2009. Towards objective rockfall trajectory modelling using a stochastic rebound algorithm. Geomorphology (in press).

3. Jancke, O., Dorren, L.K.A., Berger, F., Fuhr, M., Köhl, M., 2009. Implications of coppice stand characteristics on the rockfall protection function. Forest Ecology and Management (in review).

4. Soutrenon, A., Tournut-Hubert, J., Berger, F., Dorren, L.K.A., 2008. Approche phytosanitaire de l'impact des blocs rocheux sur le tronc des arbres en forêts de montagne. Revue Forestière Français 60(4): 451-466.

5. Berger, F., Dorren, L.K.A., 2007. Principles of the tool Rockfor.NET for quantifying the rockfall hazard below a protection forest. Schweizerische Zeitschrift für Forstwesen 158(6): 157-165.

6. Dorren, L.K.A., Berger, F., Maier, B., 2007. Cartographier la structure de la végétation forestière avec un système lidar aéroporté en terrain montagnard, Revue Française de Photogrammétrie et de Télédétection 186: 54 – 59.

7. Dorren, L.K.A., Berger, F., Jonnson, M., Krautblatter, M., Moelk, M., Stoffel, M., Wehrli, A., 2007. State of the art in rockfall - forest interactions. Schweizerische Zeitschrift für Forstwesen 158(6): 128-141.

8. Wehrli, A., Brang, P. Maier, B., Duc, P., Binder, F., Lingua, E., Ziegner, K., Dorren, L.K.A. and Kleemayr, K., 2007. Schutzwaldmanagement in den Alpen: eine Übersicht. Schweizerische Zeitschrift für Forstwesen 158(6): 142-156.

9. Dorren, L.K.A., Berger, F., 2006. Balancing tradition and technology to sustain protection forests in the European Alps. Forest Snow Landscape Research 80(1): 87-98.

10. Dorren, L.K.A., Berger, F., Putters, U.S., 2006. Real size experiments and 3D simulation of rockfall on forested and non-forested slopes. Natural Hazards and Earth System Sciences 6: 145-153.

11. Stoffel, M., Wehrli, A., Kühne, R., Dorren, L.K.A., Perret, S., Kienholz, H., 2006. Assessing the protective effect of mountain forests against rockfall using a 3D simulation model. Forest Ecology and Management 225: 113-222.

12. Wehrli, A., Dorren, L.K.A., Berger, F., Zingg, A., Schönenberger, W., Brang, P., 2006. Modelling the long-term impacts of forest dynamics on the protective effect against rockfall. Forest Snow Landscape Research 80(1): 57-76.

13. Dorren, L.K.A., Berger, F., 2005. Stem breakage of trees and energy dissipation during rockfall impacts. Tree Physiology 26: 63-71.

14. Dorren, L.K.A., Berger, F., Le Hir, C., Mermin, E., Tardif, P., 2005. Mechanisms, effects and management implications of rockfall in forests. Forest Ecology and Management 215(1-3): 183-195.

15. Dorren, L.K.A., Imeson, A.C., 2005. Soil erosion and the adaptive cycle methaphor. Land Degradation and Development 16: 509-516.

16. Stokes, A., Salin, F., Kokutse, A.D., Berthier, S., Jeannin, H., Mochan, S., Dorren, L.K.A., Kokutse, N., Ghani, M.A., Fourcaud, T., 2005. Mechanical resistance of different tree species to rockfall in the French Alps. Plant and Soil 278 (1-2): 107-117.

17. Dorren, L.K.A., Berger, F., Imeson, A.C., Maier, B., Rey, F., 2004. Integrity, stability and management of protection forests in the European Alps. Forest Ecology and Management 195(1-2): 165-176.

18. Dorren, L.K.A., Heuvelink, G.B.M., 2004. Effect of support size on the accuracy of a distributed rockfall model. International Journal of Geographical Information Science 18: 595-609.

19. Dorren, L.K.A., Maier, B, Putters, U.S., Seijmonsbergen, A.C., 2004. Combining field and modelling techniques to assess rockfall dynamics on a protection forest hillslope in the European Alps. Geomorphology 57(3): 151-167.

20. Dorren, L.K.A., 2003. A review of rockfall mechanics and modelling approaches. Progress in Physical Geography, 27 (1): 69-87.

21. Dorren, L.K.A., Maier, B., Seijmonsbergen, A.C., 2003. Improved Landsat-based forest mapping in steep mountainous terrain using object-based classification. Forest Ecology and Management 183(1-3): 31-46.

22. Dorren, L.K.A., Seijmonsbergen, A.C., 2003. Comparison of three GIS-based models for predicting rockfall runout zones at a regional scale. Geomorphology 56(1-2): 49-64.

> Book chapters

1. Andreu, V., Khuder, H., Mickovski, S.B., Spanos, I.A., Norris, J.E., Dorren, L.K.A., Nicoll, B.C., Achim, A., Rubio, J.L., Jouneau, L., Berger, F. 2008. Ecotechnological solutions for unstable slopes: ground bio- and eco-engineering techniques and strategies. In: J.E. Norris, A. Stokes, S.B. Mickovski, E. Cammeraat, R. van Beek, B.C. Nicoll, A. Achim (Eds.). Slope stability and erosion control: ecotechnological solutions. Springer, Dordrecht, The Netherlands: pp. 211-276.

2. Van Beek, R., Cammeraat, E., Andreu, V., Mickovski, S.B., Dorren, L. 2008. Hillslope processes: mass wasting, slope stability and erosion In: J.E. Norris, A. Stokes, S.B. Mickovski, E.

Cammeraat, R. van Beek, B.C. Nicoll, A. Achim (Eds.). Slope stability and erosion control: ecotechnological solutions. Springer, Dordrecht, The Netherlands: pp. 17-64.

3. Cammeraat, L.H., Beek, R. van and Dorren, L.K.A., 2002. Ecoslopes Field Protocol, IBED – Universiteit van Amsterdam, 72 pp.

4. Maier, B., Tiede, D. and Dorren, L.K.A., 2008. Characterising mountain forest structure using landscape metrics on LiDAR-based canopy surface models. In: T. Blaschke, T., S. Lang, G. Hay (Eds.), Object-Based Image Analysis - Spatial concepts for knowledge-driven remote sensing applications. Berlin, Springer: pp. 627-645.

5. Berger, F., Dorren, L.K.A., 2006. Risques naturels : chutes de blocs & Chutes de blocs en forêt. In: X. Gauquelin, B. Courbaud (Eds.), Guide des sylvicultures de montagne - Alpes du Nord Françaises. Cemagref / CRPF Rhône-Alpes / ONF, France: pp. 34-35 & 198-201.

6. Dorren, L.K.A., Berger, F., 2006. Panarchy and sustainable risk prevention by managing protection forests in mountain areas. In: W.J. Amman, S. Dannenmann, L. Vulliet (Eds.), RISK21 - Coping with Risks due to Natural Hazards in the 21st century. Taylor and Francis, London, UK: pp. 203-213.

7. Scape, 2006. Soil conservation and protection in Europe: the way ahead. A.C. Imeson, A. Arnoldussen, D. la Rosa, L. Montanarella, L.K.A. Dorren, M. Curfs, O. Arnolds, S. van Asselen (Eds.), The SCAPE Advisory Board, EUR 22187 EN, Heiloo, The Netherlands: 139 pp.

8. Dorren, L.K.A., 2002. Littekens in het alpiene landschap. In: H. Knippenberg, M. van Schendelen (Eds.), Alles heeft zijn plaats - 125 jaar Geografie en Planologie aan de Universiteit van Amsterdam, 1877-2002: pp. 500-501.

> Conference proceedings and abstracts

1. Bourrier, F., Dorren, L.K.A., Nicot, F., Darve, F., Berger, F., 2008. Introducing an objective stochastic impact law for simulating rebounds in 3D rockfall models: simulated vs. experimental data. European Geosciences Union (EGU) - General Assembly, 14 - 18 April 2008, Wien (AT).

2. Dorren, L.K.A., Berger, F., 2008. Indicators and target values for eco-engineering in Alpine forests for optimizing protection against mass movements. Ground Bio- and Eco-engineering Conference. The Use of Vegetation to Improve Slope Stability. 14- 18 July 2008, Beijing (CN).

3. Dorren, L., Bourrier, F., Nicot, F., Berger, F., Darve, F., 2008. Towards objective rockfall trajectory modelling using a stochastic rebound algorithm. WSL Rockfall Protection Workshop. 23 - 25 June 2008, Morschach (CH).

4. Dorren, L.K.A., Moulin, J.B., 2008. Recherche et communication sur la forêt de protection. Workshop « Communication et environnement : quels produits pour des stratégies réussies ? » Congress NATUR 3/08, 22 February 2008, Basel (CH).

5. Dorren, L.K.A., Stach, N., Deshayes, M., Durrieu, S., 2008. Two remote sensing examples from the forest practice in France. Der Gepixelte Wald –Fachtagung zur Forstlichen Fernerkundung. LWF, Freising (DE): pp. 1-9.

6. Allegra, C., Dorren, L.K.A., van Beek, L.P.H., Williams, A.G., Whitehead, I.R.G., Berger, F., 2007. Assessing the stabilising effect of forest cover on landslide-prone terrain in the French Alps. EGU General Assembly, 15 – 20 April 2007, Wien (AT).

7. Berger, F., Dorren, L.K.A., 2007. Objective comparison of rockfall models using data from real size experiments. EGU General Assembly, 15 – 20 April 2007, Wien (AT).

8. Bigot, C., Dorren, L.K.A., Berger, F., 2007. Quantifying the protective function of a forest against rockfall for past, present and future scenarios using two modelling approaches. EGU General Assembly, 15 – 20 April 2007, Wien (AT).

9. Bourrier, F., Dorren, L.K.A., Berger, F., Nicot, F., Darve, F., 2007. Towards a better understanding of the coefficient of restitution of a rockfall rebound. EGU General Assembly, 15 – 20 April 2007, Wien (AT).

10. Dorren, L.K.A., 2007. Die Funktionen des Schutzwaldes bei Steinschlaggefahren - Erfahrungen aus Feldexperimenten. Expertensymposium Naturgefahren Kärnten, Gefahrenanalyse – Risikomanagement, 20 March 2007, Velden (AT).

11. Dorren, L.K.A., 2007. Impact of climate change on natural hazards and the role of forests. Key-note presentation at the IUFRO Conference Natural Hazards and Natural Disturbances in Mountain Forests, 18-21 September 2007 Trento (IT).

12. Dorren, L.K.A., Berger, F., Volkwein, A., 2007. Challenges in rockfall trajectory research. EGU General Assembly, 15 – 20 April 2007, Wien (AT).

13. Dorren, L.K.A., Berger, F., 2007. Assessment of protection forest structure with airborne laser scanning in the French Alps. FORESTSAT 2007. 5 – 7 November 2007, Montpellier (FR): pp. 1-4.

14. Rammer, W., Brauner, M., Dorren, L.K.A., Berger, F., Lexer, M.J. 2007. Validation of an integrated 3D forest - rockfall model. EGU General Assembly, 15 - 20 April 2007, Wien (AT).

15. Berger, F., Dorren, L.K.A., 2006. Objective comparison of rockfall models using real size experimental data. In: Marui, H. et al. (Eds.), Disaster mitigation of debris flows, slope failures and landslides, Universal Academy Press, Inc., Tokyo (JP): pp. 245-252.

16. Berger, F., Dorren, L.K.A., 2006. Rockfor.NET: a new efficient tool for quantifying the residual rockfall hazard of a forested slope. In: Marui, H. et al. (Eds), Disaster mitigation of debris flows, slope failures and landslides, Universal Academy Press, Inc., Tokyo (JP): pp. 229-235.

17. Buser, T., Lässig, R., Dorren, L.K.A., 2006. Knowledge transfer in the Alpine space in the eyes of the stakeholders. In: Kaennel-Dobbertin, M. (Ed.) ForestXchange. New approaches in knowledge management. International conference, 25-27 October 2006, Freiburg (DE).

18. Dorren, L.K.A., 2006. Managing ecosystems for disaster reduction services: examples from around the world. In: W.J. Amman, J. Haig, C. Huovinen and M. Stocker (Eds.), IDRC Davos 2006, Vol. 3, WSL/SLF (CH): pp. 729-731.

19. Dorren, L.K.A., Berger, F., 2006. Interactive web tool for protection forest knowledge transfer: a result from exchange between research and practice. In: Kaennel-Dobbertin, M. (Ed.) ForestXchange. New approaches in knowledge management. International conference, 25-27 October 2006, Freiburg (DE).

20. Dorren, L.K.A., Berger, F., 2006. Resistance of trees against dynamic impacts due to mass movements. In: Marui, H. et al. (Eds.), Disaster mitigation of debris flows, slope failures and landslides, Universal Academy Press, Inc., Tokyo (JP): pp. 237-243.

21. Dorren, L.K.A., Berger, F., 2006. Rockfor.NET: an efficient tool for quantifying the residual rockfall hazard of a protection forest. EGU General Assembly, 2 – 7 April, Wien (AT).

22. Dorren, L.K.A., Berger, F., Maier, B., 2006. Cartographie de la structure de la végétation forestière en montagne avec un système LiDAR aéroporté. Atelier REGLIS-LIDAR, 7-8 December 2006, Montpellier (FR).

23. Dorren, L.K.A., Berger, F., Mermin, E., Tardif, P., 2006. Results of real size rockfall experiments on forested and non-forested slopes. In: Marui, H. et al. (Eds.), Disaster mitigation of debris flows, slope failures and landslides, Universal Academy Press, Inc., Tokyo (JP): pp. 223-228.

24. Dorren, L.K.A., Maier, B., Berger, F., 2006. Assessing protection forest structure with airborne laser scanning in steep mountainous terrain. In: T. Koukal and W. Schneider (Eds.), Proceedings International Workshop 3D Remote Sensing in Forestry, 13-15 February 2006, EARSeL, Wien (AT): p. 238-242.

25. Le Hir, C., Dimnet, E., Berger, F., Dorren, L., 2006. TIN-based 3D deterministic simulation of rockfall taking trees into account. EGU General Assembly, 2 – 7 April, Wien (AT).

26. Maier, B., Tiede, D., Dorren, L., 2006. Assessing mountain forest structure using airborne laser scanning and landscape metrics. In: Lang, S., Blaschke, T. and Schöpfer, E. (Eds.), Proceedings of the 1st International Conference on Object-based Image Analysis (OBIA 2006), Salzburg (AT), ISPRS Vol. XXXVI-4/C42: 6 pp.

27. Spang, R.M., Romunde, B.J., Dorren, L.K.A., Berger, F., 2006. Rockfall mitigation effects by forests - a comparison between field tests and simulation with ROCKFALL. EGU General Assembly, 2 – 7 April, Wien (AT).

28. Berger, F, Dorren, L.K.A., 2005. RockFor.NET: the forest as rockfall net. International workshop Protection forest: science and practice. 26-28 september 2005, Vaujany (FR).

29. Berger, F., Dorren, L.K.A., Le Hir, C. 2005. State of the art in modelling rockfall-forest interactions for hazard mapping. EGU General Assembly, 25-29 april 2005, Wien (AT).

30. Dorren, L.K.A., 2005. Steinschlagmodellierung im Schutzwald. Innsbrucker Hofburg Gespräche - Naturgefahren im Dialog, 18 July 2005, Innsbruck (AT).

31. Dorren, L.K.A., 2005. Local care for soil and forest ecosystem services in mountains. Glochamore Workshop, 27-30 July 2005, Samedan (CH).

32. Dorren, L.K.A., 2005. Knowns and unknowns in rockfall simulation: examples from the RockyFor model. International workshop Protection forest: science and practice. 26-28 September 2005, Vaujany (FR).

33. Dorren, L.K.A., Berger, F., 2005. Rockyfor - 3D Steinschlag Simulation mit und ohne Wald. FAN Tagung 2005 - Modellierungen gravitativer Naturgefahrenprozess. 18 February 2005, Zürich (CH).

34. Dorren, L.K.A., Berger, F., Lievois, J., 2005. Balancing tradition and technology to sustain protection forests in the European Alps. XXII IUFRO World Congress, 8-13 August 2005, Brisbane (AU). The International Forestry Review Vol.7(5): pp. 310.

35. Stokes, A., Salin, F., Kokutse, A.D., Berthier, S., Danjon, F., Mochan, S., Dorren, L.K.A., Fourcaud, T., 2005. Mechanical resistance of different tree species to rockfall in the French Alps. XXII IUFRO World Congress, 8-13 August 2005, Brisbane (AU). The International Forestry Review Vol.7(5): pp. 313.

36. Wehrli, A., Dorren, L.K.A., Berger, F., Schönenberger, W., Brang, P. 2005. Long-term impact of forest dynamics on the protective effect of a Swiss mountain forest. XXII IUFRO World Congress, 8-13 August 2005, Brisbane (AU). The International Forestry Review Vol.7(5): pp. 313.

37. Dorren, L.K.A., Berger, F., 2004. Rockfall experiments on forested and non-forested slopes. First International Conference on "Ecoengineering: The Use of Vegetation to Improve Slope Stability" 13-17 September 2004. Thessaloniki (GR).

38. Dorren, L.K.A., 2004. Local care for natural capital in mountain ecosystems. In: S. van Asselen (Editor), Briefing Papers of the third SCAPE workshop. SCAPE, 11-13 October 2004, Schruns (AT): pp. 107-113.

39. Dorren, L., Heuvelink, G., Berger, F., 2004. Effect of support size on the accuracy of spatial models: findings of rockfall simulations on forested slopes. TIES 2004 - ACCURACY 2004 Joint Meeting, 28 June - 1 July 2004, Portland, Maine (USA): pp. 1-8.

40. Dorren, L.K.A., Maier, Seijmonsbergen, A.C., Berger, F., 2004. Rockfall, forest and human interactions in the European Alps. International Congress Interpraevent 2004, Riva del Garda (IT), vol. 2(V): pp. 13-23.

41. Dorren, L., Rey, F. 2004. A review of the effect of terracing on erosion. In: C. Boix Fayos, S. van Asselen and A.C. Imeson (Editors), Briefing Papers of the second SCAPE Workshop 13-15 April 2004, Cinque Terre (IT): pp. 97-108.

42. Le Hir, C., Berger, F., Dorren, L.K.A., Quétel, C., 2004. Forest: a natural means of protection against rockfall, but how to reach sustainable mitigation? Advantages and limitations of combining rockfall models taking the forest into account. International Congress Interpraevent 2004, Riva del Garda (IT), vol. 2(V): pp. 59-69.

43. Wits, T., Dorren, L.K.A., 2004. Morphoseries for soil monitoring in the European Alps - a case study in the Montafon, Austria. In: S. van Asselen (Editor), Briefing Papers of the third SCAPE workshop. 11-13 October 2004, Schruns (AT): pp. 97-104.

44. Dorren, L.K.A., Imeson, A.C., 2003. Soil erosion and the adaptive cycle metaphor. In: C. Boix Fayos, L.K.A. Dorren and A.C. Imeson (Editors), Briefing Papers of the first SCAPE workshop, 14-16 June 2003, Alicante (ES): pp. 31-40.

45. Berger, F., Quetel, C., Dorren, L.K.A., 2002. Forest: a natural protection mean against rockfalls, but with which efficiency?, International Congress Interpraevent 2002 in the Pacific Rim, Matsumoto (JP). Congress publication, vol. 2: pp. 815-826.

46. Van Asselen, S., Dorren, L.K.A., Seijmonsbergen, A.C., Bouten, W., 2004. Modelling self-organization of the stone size distribution on a talus zone surface. EGU General Assembly, 2004 Nice (FR). Geophysical Research Abstracts: pp. 7799.

47. Dorren, L.K.A., Maier, B., Putters, U.S., Seijmonsbergen, A.C., 2003. A field and modelling evaluation of a forest protecting against rockfall in the European Alps. EGS - AGU - EUG Joint Assembly. 6 - 11 April 2003, Nice (FR).

48. Dorren, L.K.A., 2001. GIS-based distributed modelling in geology - an example of rockfall analysis on a regional scale in Montafon, Vorarlberg. 'Modellierung & Visualisierung' workshop, Österreich - 9 November 2001., Österreichischen Geologischen Gesellschaft. 9 November 2001, Dornbirn (AT).

49. Dorren, L., Seijmonsbergen, A.C., Maier, B., 2001. Forest cover analysis in mountainous terrain; per-pixel versus object-based. AGIT Symposium 2001, Salzburg (AT).

50. Dorren, L., Seijmonsbergen, A.C., 2000. GIS-based modelling of rockfall on a broad scale using remotely sensed data and detailed geomorphological maps. AGIT Symposium 2000, Salzburg (AT).

> Technical papers

1. Dorren, L.K.A., Brang, P., 2007. Schutzwald in den Alpen – Editorial. Schweizerische Zeitschrift für Forstwesen 158(6): 127.

2. Dorren, L.K.A., Berger, F., Maier, B., 2005. Der Schutzwald als Steinschlagnetz. LWF Aktuell 50: 25-27.

3. Dorren, L.K.A., Berger, F., Metral, R., 2005. Der optimale Schutzwald gegen Steinschlag. Wald und Holz 11/05: 2-4.

4. Dorren, L.K.A., Berger, F., Metral, R., 2005. La forêt est un filet de protection naturel contre les chutes de pierres. La Forêt 12/05: 10-12.

5. Dorren, L.K.A., Maier, B., 2001. GIS basierte Felssturz-Modellierung auf regionalem Maßstab im Montafon (Vorarlberg, Össterreich). Forschen und Entdecken 9: 227-236.

6. Dorren, L.K.A., Versfelt, J.H.N., 1997. Bovenland boven water. Geografie 6(5): 36-37.

> Lebenslauf



Dr. Luuk K.A. Dorren

> Ausbildung

Dissertation zum Thema Steinschlagmodellierung und Schutzwald; Titel: *Mountain Geoecosystems – GIS modelling of rockfall and protection forest structure*; Geländearbeit im Montafon (AT)	Univ. Amsterdam (UvA) (NL)	1998-2002
BSc. und MSc. Physische Geographie; Hauptfach Alpine Geomorphologie; Diplomarbeit über Rutschungen im Widentobel (Sankt Gallen, CH)	UvA (NL)	1993-1998
Studium Technische Betriebswirtschaft	Techn. Univ. Eindhoven (NL)	1992-1993

> Berufserfahrung

Scientific officer **Bundesamt für Umwelt BAFU, Bern (CH)** **July 2008 – Heute**

- Naturgefahren – Schutzwald Experte in die Abteilung Gefahrenprävention
- Verantwortlich für die fachliche Beratung und Unterstützung des ASTRA (Bundesamt für Strassen) im schweizweiten Projekt 'Naturgefahren auf Nationalstrassen'
- Weiterentwicklung NaIS (Nachhaltigkeit im Schutzwald) – die Schweizerische Richtlinie für Schutzwaldpflegung
- Entwicklung von Protect-BIO – eine Methodik für die Miteinbeziehung der Schutzfunktion des Waldes in Naturgefahr- und Risikobeurteilungen

Senior Scientist **Cemagref, Grenoble (FR)** **September 2005 – Juni 2008**

- Initiierung, Ausführung und Begleitung von Forschungsprojekten in den Bereichen Steinschlag, Lawinen, Rutschungen, Laserscanning und Schutzwald in FR, CH, AT, DE, IT, LI und SI
- Durchführung von Naturgefahrenanalysen, Gutachten und Expertisen
- Wissens- und Erfahrungsaustausch mit Praktikern (z.B. ONF-RTM, GWG, BAFU, DDE, ASTRA, ASFINAG, SNCF), Hochschulen (z.B. SHL) und Universitäten (z.B. ENGREF, BOKU)

Post-Doktorant **Cemagref, Grenoble (FR)** **September 2003 – August 2005**

- Initiierung und Ausführung von Forschungsprojekten in den Bereichen Steinschlag und Wald in FR, CH, und AT
- Publikation von 12 Wissenschaftliche Artikel
- Erhalten eines Marie-Curie Fellowship

Naturgefahrenexperte **Ecosystem Management Commission, IUCN, Gland (CH)** **Juni 2005 – Heute**

- Expertisen im Bereich *Disaster Reduction* durch Ökosystem-Management und Wissenstransfer mit Mitgliedern der IUCN *Ecosystem Management Commission*

Arbeitsgruppenleiter **Generaldirektion Umwelt, Europäische Kommission** **Juni 2003 - Juni 2004**

- Leitung der Europäischen Arbeitsgruppe *Impacts of soil erosion* für die Bodenschutzstrategie der Europäischen Kommission

Projektmanager **UvA (NL)** **Oktober 2002 - August 2003**

- Verantwortlich für Implementierung und Management des Projektes SCAPE (*Soil Conservation And Protection for Europe*)
- Organisation internationaler Workshops in Spanien, Italien, Österreich, Norwegen und Island

Wissenschaftlicher Mitarbeiter **UvA (NL) / UNESCO - IHE (Delft, NL)** **Juni 1998 - September 2002**

- Stellvertretender Univ. Dozent im Bereich Alpine Geomorphologie, GIS und räumliche Modellierung
- Wissenschaftlicher Mitarbeiter der europäischen Projekte Cartesian (GIS Anwendungen für Skigebiets- und Naturgefahren-Management) und Ecoslopes (Eco-engineering für Prävention von Massenbewegungen)

Junior Consultant **Resource Analysis (Delft, NL)** **September 1997 - March 1998**

- Technische Unterstützung von Fernerkundungsprojekten

> Gutachten und Expertisen

Thematik	Auftraggeber	Jahr
NaIS Kurs Steinschlag – Wald in Vallorbe (CH)	Forstdienst Kanton Vaud (CH)	2008
Steinschlag-Gefahrenanalyse Schlossstrasse Vaduz (LI)	Amt für Wald, Natur und Landschaft (LI)	2008
Steinschlag-Schutzwaldanalyse Steg (LI)	Amt für Wald, Natur und Landschaft (LI)	2007
Steinschlag-Schutzwaldanalyse Plaffeien (CH)	GWG (CH)	2007
NaIS Kurs Gerinneprozesse im Schutzwald Valais	Forstdienst Kanton Valais (CH)	2007
Multi-Risiken-Analyse Tunnelportal Haiming (AT)	ASFINAG / BFW (AT)	2006
Steinschlag-Gefahrenanalyse Mont Blanc Autobahn (FR)	DDE / ONF (FR)	2005
Externer Experte Steinschlagmodellierung für SilvaProtect-CH	BUWAL (CH)	2005
Revision der Gefahrenzonenplanung Vic-sur-Cère (FR)	2G Génie Géologique (FR)	2005
Multi-Risiken-Analyse Mont Dore (FR)	Préfecture Puy de Dôme (FR)	2005

Steinschlag-Wald Modellierung Diemtigtal, Taesch und Stotzigwald (CH)	Univ. Fribourg, WSL und Univ. Bern (CH)	2005
Regionale Steinschlagmodellierung Wipptal (AT)	Wildbach- und Lawinenverbauung, Innsbruck (AT)	2004
Steinschlag-Schutzwaldanalyse Gaschurn (AT)	Stand Montafon Forstfonds (AT)	2001
Rutschungsanalyse und Gefahrenzonenplanung Malbun (LI)	Amt für Wald, Natur und Landschaft (LI)	1998

> Forschungs- und Entwicklungsprojekte

Projekttitel (Position)	**Auftraggeber**	**Periode**
PROTECT-BIO, Projekt-Leiter Teil Steinschlag	BAFU (CH)	2008 – 2009
Naturgefahren auf Nationalstrassen, Teilprojekt-Leiter	ASTRA (CH)	2008 – 2012
Forêt-LiDAR, Co-Leiter	RDT (FR)	2008 – 2009
ProAlp, WP Co-Leiter	JRC (EU)	2007 – 2008
Provialp, Co-Leiter	Interreg Alcotra (IT/FR)	2006-2007
KnowForAlp, WP-Leiter	Interreg Alpine Space Program (EU)	2005-2007
Gestion durable des forêts de montagne, Mitarbeiter	Interreg IIIa (CH/IT/FR)	2005-2007
RockFor, Mitarbeiter	DG-RTD FP5 (EU)	2001-2004
Ecoslopes, Mitarbeiter	DG-RTD FP5 (EU)	2001-2004
Cartesian, Mitarbeiter	DG-RTD FP5 (EU)	1998-2000
MEDALUS, Mitarbeiter	DG-RTD FP5 (EU)	1996 -1997

> Lehre

Postgraduat

2007: Summerschool „Eboulements, chutes de blocs – rôle de la forêt. Université d'été sur les risques naturels. Courmayeur (IT): 30 hours.

2004 – 2005: Effective oral presentation skills. Cemagref, Grenoble (FR): 24 Stunden

MSc

2008: Gastvorlesung Naturgefahrensimulation als Instrument der Gebirgswaldbewirtschaftung, BOKU Wien: 9 Stunden

2006 – 2008: Le rôle protecteur de la forêt de montagne. ENGREF/FIF (FR): 6 Stunden

2002: Summer school 'An introduction into alpine and subalpine environments in a key sector of the northern Alps'. RFASE / UNESCO – IAG, Dornbirn (AT): 4 Stunden

2001 – 2002: WLO Mountain forests and alpine geomorphology. UvA, Amsterdam (NL): 10 Stunden

1999 – 2002: Field course geo-ecological systems / alpine geomorphology. UvA, Amsterdam (NL): 48 Stunden

1998 – 1999: Interpretation of aerial photographs. UNESCO - IHE Institute for Water Education, Delft (NL): 40 Stunden

BSc

2005 – Heute: Vorlesung Steinschlag Schutzwald. SHL, Zollikofen (CH): 8 Stunden

2000: Geomorphological fieldwork Luxembourg. UvA, Amsterdam (NL): 10 Stunden

1998 – 2001: Einführung Geographische Informationssystemen und Fernerkundung. UvA (NL): 20 Stunden

Betreuung von Diplomarbeiten und Dissertationen

W. Krättli, 2008. Einfluss der Bestandesstruktur auf den Steinschlag-Rückhalt im Wald. Diplomarbeit Schweizerische Hochschule für Landwirtschaft SHL, Zollikofen.

O. Jancke, 2007 - present. Eco-engineering for rockfall protection: quantifying the function of coppice forests. Dissertation Cemagref / Univ. Hamburg.

Allegra, C., 2006. Assessing the stabilising effect of forest cover on landslide-prone terrain in the French Alps. Diplomarbeit Cemagref / Univ. Plymouth.

Bigot, C. 2006. Regard critique sur une forêt à fonction de protection contre les chutes de blocs - Retour d'experience à St. Martin le Vinoux (Isère). Diplomarbeit Cemagref / IGA-UJF.

Mwasi, B., 2004. Landscape change dynamics in a semi-arid part of Baringo District, Kenya, based on Landsat-TM-Data and GIS analysis. Dissertation UvA.

Wits, T. Assessment of an Alpine soil monitoring system for Europe - Case study in the Rellstal, Vorarlberg. Diplomarbeit UvA.

Asselen, S. van, 2003. Towards a dynamic process based model for alpine talus cone development. Diplomarbeit UvA.

Putters, U.S., 2002. Modelling rockfall on forest slopes. Diplomarbeit UvA.

Witte, A., 2002. A pixel based fractal dimension classification technique for hyperspectral image analysis. Diplomarbeit UvA.

> Andere Tätigkeiten

- Gastredakteur, Schweizerische Zeitschrift für Forstwesen, Juni 2007
- Gutachter für den Schweizerischen Nationalfonds (SNF), seit 2005
- Reviewer für verschiedene wissenschaftliche Zeitschriften (Geomorphology, For. Ecol. Manage., Comp. & Geosc., NHESS, Landslides, Nat. Hazards, Schweiz. Z. Forstw., Tree Phys., Geophys. Rev. Lett., Geotech. Geol. Eng., J. Agr. Sci. Tech., J. Env. Man.)
- Mitglied Schweizerische Gebirgswaldpflegegruppe GWG, seit 2007
- Mitglied *IUCN Ecosystem Management Commission*, seit 2005
- Mitglied Organisationskommittee *Rockfall Session* EGU General Assembly (2006 - Heute)
- Mitglied Organisationskommittee *Interpraevent Congress 2012* in Grenoble Frankreich
- Mitglied Wissenschaftlicher Beirat *2nd Int. Conference on Ground Bio- and Eco-engineering* - the use of vegetation to improve slope stability (Beijing, China *2008), WSL Rockfall Protection workshop* (Morschach, Schweiz 2008) und *IUFRO International Conference 2007: Natural Hazards and Natural Disturbances in Mountain Forests* (Trento, Italien 2007)
- Mitglied Wissenschaftlicher Beirat des Projekts *SCAPE - Soil Conservation And Protection for Europe* (2002-2005)
- Mitglied Editorial Board Schweizerische Zeitschrift f. Forstwesen (Seit 2008)
- Organisator des internationalen Symposiums *Protection forest: science and practice* (Vaujany, Frankreich 2005)
- Organisator der *Invited IUCN Session Managing ecosystems for natural disaster reduction services: examples from around the world, International Disaster Reduction Conference* (Davos, Schweiz 2006)

> Sprachen

- Verhandlungssicheres Deutsch und Französisch in Wort und Schrift
- Exzellent in Englisch, Niederländisch und Limburger Dialekt
- Basiskenntnisse des Montafoner Dialektes